ACTA CHIMICA

ACADEMIAE SCIENTIARUM HUNGARICAE

ADIUVANTIBUS

L. ERDEY, K. POLINSZKY, G. SCHAY

AC

R. BOGNÁR, GY. BRUCKNER, L. CHOLNOKY, Z. CSŰRÖS,
T. ERDEY-GRÚZ, Z. FÖLDI, M. FREUND, Á. GERECS, GY. HARDY,
Á. KISS, M. KORACH, B. LENGYEL, F. MÁRTA, J. PROSZT,
Z. SZABÓ, P. SZŐR, L. VARGHA, K. VAS

REDIGIT

S. MÜLLER

TOMUS 47. FASCICULUS 1.

AKADÉMIAI KIADÓ, BUDAPEST

1966

ACTA CHIMICA

A MAGYAR TUDOMÁNYOS AKADÉMIA KÉMIAI TUDOMÁNYOK OSZTÁLYÁNAK IDEGEN NYELVŰ KÖZLEMÉNYEI

SZERKESZTI

MÜLLER SÁNDOR

TECHNIKAI SZERKESZTŐK

DEÁK GYULA és TAKÁCS VILMOS

Az Acta Chimica német, angol, francia és orosz nyelven közöl értekezéseket a kémiai tudományok köréből.

Az Acta Chimica változó terjedelmű füzetekben jelenik meg, egy-egy kötet négy füzetből áll. Évente négy kötet jelenik meg.

A közlésre szánt kéziratok a szerkesztőség címére (Budapest 112, postafiók 39) küldendők.

Ugyanerre a címre küldendő minden szerkesztőségi levelezés. A szerkesztőség kéziratokat nem ad vissza.

Az Acta Chimica előfizetési ára kötetenként belföldre 80 Ft, külföldre 110 Ft. Megrendelhető a belföld számára az „Akadémiai Kiadó"-nál (Budapest V., Alkotmány utca 21. Bankszámla 05-915-111-46), a külföld számára pedig a „Kultúra" Könyv- és Hírlap Külkereskedelmi Vállalatnál (Budapest I., Fő utca 32. Bankszámla: 43-790-057-181) vagy annak külföldi képviseleteinél és bizományosainál.

Die Acta Chimica veröffentlichen Abhandlungen aus dem Bereiche der chemischen Wissenschaften in deutscher, englischer, französischer und russischer Sprache.

Die Acta Chimica erscheinen in Heften wechselnden Umfanges. Vier Hefte bilden einen Band. Jährlich erscheinen 4 Bände.

Die zur Veröffentlichung bestimmten Manuskripte sind an folgende Adresse zu senden:

Acta Chimica
Budapest 502, Postafiók 24.

An die gleiche Anschrift ist auch jede für die Redaktion bestimmte Korrespondenz zu richten.

Abonnementspreis pro Band: 110 Forint. Bestellbar bei dem Buch- und Zeitungs-Außenhandels-Unternehmen »*Kultúra*« (Budapest I., Fő utca 32. Bankkonto No. 43-790-057-181) oder bei seinen Auslandsvertretungen und Kommissionären.

ACTA CHIMICA

ACADEMIAE SCIENTIARUM HUNGARICAE

ADIUVANTIBUS

L. ERDEY, K. POLINSZKY, G. SCHAY

AC

R. BOGNÁR, GY. BRUCKNER, L. CHOLNOKY, Z. CSŰRÖS, T. ERDEY-GRÚZ, Z. FÖLDI, M. FREUND, Á. GERECS, GY. HARDY, Á. KISS, M. KORACH, B. LENGYEL, F. MÁRTA, J. PROSZT, Z. SZABÓ, P. SZŐR, L. VARGHA, K. VAS

REDIGIT

S. MÜLLER †

TOMUS 47

AKADÉMIAI KIADÓ, BUDAPEST

1966

INDEX

TOMUS 47

Fasciculus 1: 1966
Fasciculus 2: 1966
Fasciculus 3: 1966
Fasciculus 4: 1966

BARCZA, L.: Contributions to the Chemistry of Selenium and Selenium Compounds, XIV. Determination of Selenium in Organic Selenium Compounds 137

BARCZA, L. s. SCHULER, E. .....

BEYER, H., FEJES, P., SCHAY, G. und VARGA, K.: Neuere Untersuchungen über frontale Gaschromatographie unter Berücksichtigung der Strömungsgeschwindigkeit während der Sorption, III. Bestimmung von HTS-Werten mittels frontaler Gaschromatographie 13

BICZÓ, G. s. LADIK, J. .....

BIHARI-VARGA, M. s. NYILASY, J. .....

BILLES, F.: A New Method for the Determination of Vibrational Force Constants of Molecules 53

Book Reviews 451

BRUCKNER, V. s. SZEKERKE, M. .....

BURGER, K. s. RUFF, I. .....

Buchbesprechungen 451

CSÁSZÁR, J. and FELVÉGI, A.: Magnetic and Spectroscopic Investigation of Polynuclear Complex Cyanides 37

CSER, F. s. HARDY, GY. .....

DÉVAY, J. und MÉSZÁROS, L.: Berechnung der Korrosionswirkung des Kriechwechselstromes auf ein in einem Elektrolyten angebrachten Metall (Kurzmitteilung) 185

DOBOZY, O. s. LŐRINC, A. .....

DOLESCHALL, G., LÁNG, L. and LEMPERT, K.: Imidazoquinazolinediones, IV. Structure and Ultraviolet Spectra of Some Potentially Tautomeric Imidazoquinazolinediones and Related 4-Quinazolinones 405

FARAGÓ, T. s. SZŐKE, S. .....

FEJES, P. s. BEYER, H. .....

FEJES, P. s. VARGA, K. .....

FELVÉGI, A. s. CSÁSZÁR, J. .....

FERENCZI-GRESZ, S. s. NAGY, J. .....

FODOR-CSÁNYI, P. and LÉVAY, B.: The Significance of Phosphorescence in the Measurement of Low Energy Beta Isotopes with Liquid Scintillator and Single-Channel Counter 343

FÓTI, A., GERECS, Á. und RUFF, F.: Über die Struktur und Ringstabilität einiger O-Acetylmonose-2,4-dinitrophenylhydrazone 221

FÖLDIÁK, G. s. PAÁL, Z. .....

GÁBOR-FEHÉR, M. s. SCHULEK, E. .....

GERECS, Á. s. FÓTI, A. .....

GÖRÖG, S.: Analysis of Steroids, I. Bromometric Determination of Steroids Containing a Double Bond in Position Δ^5 1

GÖRÖG, S.: Analysis of Steroids, II. Determination of Steroids Containing an Ethynil Group 7

GÖRÖG, S. and TOMCSÁNYI, L.: Analysis of Steroids, III. Determination of Steroids Containing Isolated Carbonyl Groups 121

GYARMATI, I.: Once More on the Deduction of the Fourier Equation from the Variational Principle 63

GYARMATI, I.: Relations between the Integral Principle of Thermodynamics and the Hamilton Principle 367

H.-HANKOVSZKY, O., HIDEG, K. and MÉHES, GY.: Allylphenol and Propenylphenol Derivatives 199

HARDY, GY., NAGY, L. and CSER, F.: Investigations in the Field of Radiation-Induced Solid State Polymerization, XIV. The Radiation-initiated Polymerization of Allyl Palmitate 211

HIDEG, K. s. H.-HANKOVSZKY, O. .....

HUN, B. GY. s. TÖRÖK, F. .....

HUSZÁR, J. s. LÉGRÁDI, L. .....

ILLY, H. s. KISS, I. .....

JÁKLY, G. s. KISS, I. .....

KAJTÁR, M. T. s. SZEKERKE, M. .....

KISS, I., JÁKLY, G. and ILLY, H.: Vapour Pressure of Solid D_2O 379

KISS, I. s. RODER, M. .....

LADÁNYI, L. s. SCHULEK, E. .....

LADIK, J. and BICZÓ, G.: Investigation of the Electronic Structure of Cetalytically Active Solids. The Change of the Energy Band Structure of Infinite Ni Crystals with the Temperature 263

LÁNG, L. s. DOLESCHALL, G. .....

LEMPERT, K. and ZAUER, K.: Hydantoins, Thiohydantoins and Glycocyamidines, XXIII. Quaternization of 2,5-bis(methylthyo)-4,4-diphenyl-4*H*-imidazole and the Reaction of the Quaternary Derivative with Nucleophilic Agents 391

LEMPERT, K. s. DOLESCHALL, G. .....

LÉGRÁDI L.: p-Äthoxy-Naphtylrot, ein neuer Adsorptionsindikator 103

LÉGRÁDI, L. and HUSZÁR, J.: Oxidation Methods in Organic Analysis, I. Determination of Phenylhydrazine in the Presence of Aniline 115

LÉVAY, B. s. FODOR-CSÁNYI, P. .....

LŐRINC, A., PÉTER, F. and DOBOZY, O.: Correlation between the Paper Chromatographic R_f and R_m-values and the Structure of Azo Dyes 419

MÉHES, GY. s. H.-HANKOVSZKY, O. .....

MÉSZÁROS, L. s. DÉVAY, J. .....

MIRONOV, V. F. s. NAGY, J. .....

MONDVAI, P.: Polymerisation des Methylmethakrylats bei hohen Umsätzen, I. 281

Надь, Й., Ференци-Грес, Ш. и *Миронов, В. Ф.*: Структура связи в алкенил-кремний-органических соединений (NAGY, J., FERENCZI-GRESZ, S. and MIRONOV, V. F.: Bond Structure of Alkenyl Siliconorganic Compounds) 189

NAGY, L. s. HARDY, GY. .....

NÉMETH, A. and SZALAY, O.: New Method for the Quantitative Analysis of Combustion Processes with Toepler's Parallel Beam Schlieren Apparatus 385

NYILASI, J., BIHARI-VARGA, M. und ORSÓS, P.: Metallkomplexe der Peptide, V. 291

OPAUSZKY, I. s. RODER, M. .....

ORSÓS, P. s. NYILASI, J. .....

Пал, З. и *Фёльдиак, Г.*: О некоторых проблемах кинетики и механизма разрядно-химического окисления углеводородов в гетерогенной фазе. (PAÁL, Z. and FÖLDIÁK, G.: Some Problems in the Kinetics and Mechanism of the Oxidation of Hydrocarbons by Electric Discharge in Heterogeneous Phase) 83

PÉTER, F. s. LŐRINC, A. .....

PULAY, P. and TÖRÖK, F.: On the Parameter Form of Matrix F, II. Investigation of the Assignment with the Aid of the Parameter Form (Short communication) 273

RODER, M., OPAUSZKY, I. and KISS, I.: Thermal Stability of the Eutectic Mixture of Diphenyl and Diphenyl Methane 157

RUFF, I. and BURGER, K.: Some Theoretical and Practical Problems in the Use of Organic Reagents in Chemical Analysis, VIII. Influence of the Chelate Effect and Ring Size on the Stability of the Dioxime Complexes of Transition Metals 143
RUFF, I.: On the Role of Water in Electron Transfer Reactions, II. 241
RUFF, I.: On the Role of Water in Electron Transfer Reactions, III. 255
RUFF, F. s. FÓTI, A. .....
Sándor (Alexander) Müller, 1903—1966 101
SCHAY, G. s. BEYER, H. .....
SCHULEK, E., BARCZA, L., GÁBOR-FEHÉR, M. and LADÁNYI, L.: Reaction of Disulfur Dichloride and Sulfur Dichloride with Cyanide; their Determination through Thiocyanate 129
SOÓS, L.: New Methods of Coal Petrography, in Coal Chemistry and Coal Technology 67
SUNDARAM, K. M. S.: Surface Tension Studies of Some Binary Systems. Pyridine and Acetic Acid. (Short Communication) 167
SZALAY, O. s. NÉMETH, A. .....
SZEJTLI, J.: The Stepwise Total Hydrolysis of Alginic Acid 301
SZEKERKE, M., KAJTÁR, M. T. und BRUCKNER, V.: Synthese cyclischer N-Lostderivate aus β-substituierten Serinen, Cystein und Lysin 231
SZŐKE, S. and FARAGÓ, T.: Calculation of Force Field on Ethylene Model 173
TOMCSÁNYI, L. s. GÖRÖG, S. .....
TÓTH, B.: Untersuchung der Veränderungen von Sulfitablaugen während der Verhefung 431
TÖRÖK, F. and HUN, B. GY.: On the Vibrational Spectrum of the Trimethylsilyl Group .. 329
TÖRÖK, F. s. PULAY, P. .....
VARGA, K., FEJES, P. und BEYER, H.: Neuere Untersuchungen über frontale Gaschromatographie unter Berücksichtigung der Strömungsgeschwindigkeit während der Sorption, IV. Beurteilung chromatographischer Trennsäulen auf Grund frontalchromatographisch gemessener Transportgeschwindigkeits- und Diffusionskonstanten 23
VARGA, K. s. BEYER, H. .....
WELTNER, M.: Untersuchung der Oxydations- (Lagerungs-)vorgänge der Kohlen mit derivatographischer Methode 311
ZAUER, K. s. LEMPERT, K. .....

ANALYSIS OF STEROIDS, I

BROMOMETRIC DETERMINATION OF STEROIDS CONTAINING A DOUBLE BOND IN POSITION Δ^5

S. GÖRÖG

(Gedeon Richter Chemical Works, Budapest)

Received December 4, 1964

Among natural steroids and the intermediates of the manufacture of steroidal drugs, compounds containing a double bond in position Δ^5 occur in a great number. Consequently, determination of this double bond is frequently a task of prominent importance.

One of the methods usually applied for the determination of olefinic compounds is the measurement of the addition of bromine to the double bond. (Excellent reviews of the literature of this field are given, *e.g.* by BUDEŠINSKY [1] and STONE[2]). Most methods consist in reacting the unsaturated compound with excess bromine, followed by the back-titration of the excess bromine iodometrically. However, all these procedures have the common drawback that it is rather difficult to eliminate interfering substitution side reactions of bromine; furthermore, the methods are time-consuming, because the process is a time-reaction and back-titration is cumbersome.

In order to improve the method it was attempted to apply catalysts which accelerate the addition reaction to such an extent that direct titration became possible. In general, mercury(II) salts are used as catalysts [3]. Though these methods are rather simple and quick, several particular problems emerge concerning the adequate choice of the solvent and catalyst concentration, elimination of side reactions, and the detection of the end point for each particular group of compounds. Thus, none of the known methods can be regarded as generally applicable.

Relatively few methods have been recommended in literature for the bromometric determination of steroid compounds having a double bond. Cholesterol is, *e.g.* determined by TOMICEK and DOLEZAL [4] by titration at 60° in acetic acid solution containing sodium acetate, with a 0.1 N solution of bromine in acetic acid; potentiometric end point detection is used. According to our own experience, the uptake of bromine is rather slow under such conditions, thus the titration takes a long time. PERELMAN and GAVRILIN [5], in turn, suggest for the determination of cholesterol and β-sitosterol titration with a solution of bromine in glacial acetic acid in the presence of mercury(II) as catalyst, applying potentiometric or visual end point detection. Methods

based on iodimetric back-titration have been described by SCHWARZ and TROJANEK [6], and by TANAY [7].

The scope of our investigations was to evolve a rapid direct bromometric method for the determination of steroid compounds carrying an isolated double bond in position Δ^5. In this work, use was made of the information published in papers dealing with the analysis of other groups of compounds.

Acetic acid was chosen as the titration medium because all steroids investigated by us are satisfactorily soluble in this solvent. The titrant was a 0.1 *N* solution of bromine in acetic acid in the presence of mercury(II) chloride and sodium acetate, applied as combined catalysts. According to SCHWARZ and TROJANEK [6], sodium acetate, in addition to acting as an accelerating agent, suppresses in glacial acetic acid the enolization of the carbonyl group frequently present in steroids, and thus substitution reactions by bromine occurring in the vicinity of the carbonyl groups are slowed down. The optimum concentrations of the catalysts were established. It was found practical to use a glacial acetic acid solution which is 0.5 molar for sodium acetate and 0.08 molar for mercury(II) chloride. This solution served as the solvent in all titrations.

Under the given conditions, the titration can be conducted at room temperature at normal rate: the addition reaction takes place instantaneously. The rate of interfering substitution reactions is by an order of magnitude lower even in diffuse daylight, therefore the effect of these latter reactions can be practically completely eliminated. The end point of the titration may be detected by the appearance of the colour of bromine when it is in excess. Owing to the relatively pale tint of bromine, when this indication is used, the solution is overtitrated by about 0.5 to 1.0%. However, if the titrant is standardized in the same way, the error is eliminated. When the solution to be titrated is coloured, potentiometric end point detection is possible by using a platinum and a calomel electrode in glacial acetic acid saturated with lithium chloride; the dead-stop method may also be applied, using two smooth platinum electrodes. However, this procedure does not improve the accuracy of the method, thus instrumental end point detection is recommended for coloured solutions only.

Experimental

Solutions

0.1 *N solution of bromine in acetic acid:* 8.0 g (about 2.5 ml) of bromine is dissolved in 1000 ml of glacial acetic acid resistant to chromic acid. When kept in the dark container of an automatic burette, this titrant may be used for several months, provided its titer is established in periods of 2—3 days.

Acetic acid solution with catalyst: 68 g of crystalline sodium acetate and 21.7 g of mercury(II) chloride are dissolved in glacial acetic acid resistant to chromic acid, and the solution is made up with the solvent to exactly 1000 ml. The solution may be stored indefinitely without decomposition.

Description of the method

About 0.5 millimole of the steroid to be analyzed is weighed and dissolved in 10 ml of acetic acid solution containing the catalysts (if necessary, gentle heating may be applied). The solution is titrated at room temperature with 0.1 *N* bromine in acetic acid. At the beginning of the titration, the titrant may be added to the solution at the usual rate of titrations, under vigorous shaking. Near to the end point, the titrant should be added only so quickly that the drops may be counted. The yellow tint appearing in the end point should remain unchanged for at least 15—20 seconds.

The titrant is standardized with arsenous acid. 0.05 g of As_2O_3 is dissolved in 3 ml of 1.0 *N* sodium hydroxide, 7 ml of 20% hydrochloric acid is added, and the solution titrated with the titrant until a pale yellow tint is obtained.

The equivalent weight of the investigated steroids containing one isolated double bond was calculated as the half of the molecular weight.

The spectrophotometric measurements (see later) were carried out with an Optica Milano CF-4 spectrophotometer in anhydrous ethanol, in 1 cm quartz cuvettes.

Experimental results

The results of our model investigations with ten unsaturated steroid compounds are shown in Table I. The assays given are mean values of five parallel measurements.

The data in Table I prove that the probable error of a single measurement is less than $\pm$ 0.5%, and that the assay values are between 98 and 101%.

Table I

Diosgenin	98.5 $\pm$ 0.2%
Solasodine	100.8 $\pm$ 0.3%
O,N-Diacetylsolasodine	99.1 $\pm$ 0.3%
3 β-Acetoxy-$\Delta^{5,16}$-pregnadiene-20-one	98.8 $\pm$ 0.5%
Δ^5-Pregnene-3β-ol-20-one	100.2 $\pm$ 0.4%
16α,17α-EpoxyΔ^5-pregnene-3β-ol-20-one	101.0 $\pm$ 0.2%
Δ^5-Androstene-3β-ol-17-one	98.2 $\pm$ 0.2%
3β-Acetoxy-Δ^5-androstene-17-one	100.5 $\pm$ 0.4%
3β-Formyloxy-17α,21-diacetoxy-Δ^5-pregnene-20-one	100.3 $\pm$ 0.3%
17α-Methyl-Δ^5-androstene-3β,17β-diol	98.9 $\pm$ 0.4%

In the case of 3β-acetoxy-$\Delta^{5,16}$-pregnadiene-20-one whose molecule has two double bonds, a bromine uptake of only two equivalents was observed,

similarly to the other compounds examined. Thus, double bond Δ^5 can be selectively brominated in this substance, while double bond Δ^{16}, which is in conjugation with the carbonyl group in position 20, is left intact.

In the following, a practical application of the method is described.

Investigation of the crude products of the Oppenauer oxidation

A great majority of the compounds listed in Table I can directly be converted by Oppenauer oxidation into steroids having the Δ^4-3-carbonyl bond system; such derivatives are of great importance as drugs. Accordingly, this process represents a key step in the preparation of a number of interesting steroids.

In order to establish the optimum conditions of the oxidation process, an analytical method is necessary which lends itself to the reliable determination of the composition of the crude product of the reaction.

In first approximation it may be presumed that the components of the crude product of the Oppenauer oxidation leading to equilibrium are the pure end product and the starting material. The Δ^4-3-carbonyl bond system of the end product has an intensive and characteristic ultraviolet absorption band at about 240 nm, while the Δ^5-3-hydroxy compounds investigated by us disclose in this region a negligible slight absorption only. Consequently, the end product of the oxidation process can be determined by spectrophotometric measurements at 240 nm, while the bromometric method is suitable for the determination of the unreacted initial substance; double bond Δ^4 in conjugation with the C_3 carbonyl group does not react with bromine under the given conditions.

The correctness of the above presumption has been fully proved by our model experiments. The suitability of the method for the analysis of the crude oxidation products is demonstrated by the fact that the sum of the starting material (determined by bromometry) and the end product (established

Table II

Initial compound	Product	Specific extinction (240 ± 1 nm)
Δ^5-Pregnene-3β-ol-20-one	Progesterone	525
Δ^5-Androstene-3β-ol-17-one	Δ^4-Androstene-3,17-dione	563
3β-Formyloxy-17α,21-diacetoxy-Δ^5-pregnene-20-one	17α,21-Diacetoxy-Δ^4-pregnene-3,20-dione	395
17α-Methyl-Δ^5-androstene-3β,17β-diol	17α-Methyl-testosterone	540

by spectrophotometry) well approximated 100% in all cases, in the most various crude products.

The systems investigated by the present method are given in Table II.

The spectrophotometric data were calculated from the specific extinction values given in Table II.

The method has been successfully employed in the routine production testing of the listed compounds.

The author's thanks are due to Miss M. KAPÁS for her valuable experimental assistance.

SUMMARY

A quick direct bromometric method has been evolved for the determination of compounds having steroid skeleton and containing a double bond in position Δ^5. In the titrations, acetic acid in the presence of sodium acetate and mercury(II) chloride is used as the solvent, and the titrant is a 0.1 *N* solution of bromine in acetic acid. The probable error is less than $\pm$ 0.5%.

The suggested method is applicable in the investigation of the Oppenauer oxidation of steroids containing Δ^5-3-hydroxy bond arrangement. In the crude product of the oxidation, the quantity of unchanged starting material is determined by the present titration method, while that of the formed Δ^4-3-carbonyl compound by ultraviolet spectrophotometry.

REFERENCES

1. BUDEŠINSKY, B.: Chem. listy **53,** 997 (1959).
2. STONE, K. G.: Determination of Organic Compounds. (McGraw-Hill, New York) 1956. p. 15.
3. LUCAS, H. J., PRESSMAN, D.: Ind. Eng. Chem. Anal. Ed. **10,** 140 (1938).
4. TOMICEK, O., DOLEZAL, J.: Acta Pharm. Internat. **1,** 31 (1950).
5. PERELMAN, J. M., GAVRILIN, G. F.: Zhurn. Anal. Khim. **18,** 529 (1963).
6. SCHWARZ, V., TROJANEK, J.: Collection Czechoslov. Chem. Communs. **26,** 117 (1961).
7. TANAY, I.: Magyar Kém. Foly. **69,** 226 (1963).

Zur Analytik von Steroiden, I

Bromometrische Bestimmung der in Stellung Δ^5 eine Doppelbindung enthaltenden Steroide

S. GÖRÖG

Zusammenfassung. Zur Bestimmung von Verbindungen mit Sterangerüst, die in Stellung Δ^5 eine Doppelbindung enthalten, wurde eine rasche unmittelbare bromometrische Methode entwickelt. Bei den Titrationen diente eine Natriumacetat und Quecksilber(II)chlorid enthaltende Essigsäurelösung als Medium, während eine 0,1 n essigsaure Bromlösung als Meßlösung verwendet wurde. Die wahrscheinlichen Fehlerwerte waren geringer als $\pm$0,5%.

Die entwickelte Methode wurde bei Untersuchung der Oppenauerschen Oxydation der eine Δ^5-3-Oxybindung enthaltenden Steroide angewandt. Im Rohprodukt der Oxydation wurde die Menge der unreagierten Ausgangssubstanz mittels der beschriebenen Methode, die der entstandenen Δ^4-3-Oxoverbindung hingegen mittels ultravioletter Spektrophotometrie bestimmt.

Данные к аналитической химии соединений со стерановым скелетом, I.

Бромометрическое определение стероидов, содержащих двойную связь в положении Δ^5

Ш. ГЁРЁГ

Резюме. Был разработан быстрый прямой бромометрический метод определения соединений со стерановым скелетом, содержащих двойную связь в положении Δ^5. Титрования проводились в среде уксусной кислоты, содержащей ацетат натрия и хлорную ртуть(II), 0,1 н уксуснокислым раствором брома. Вероятная погрешность меньше $\pm$ 0,5%.

Данный метод применялся для исследования окисления по Оппенауэру стероидов, содержащих Δ^5—3-окси-связь. Количество непрореагировавшего исходного вещества в сыром продукте полученным окислением определялось вышеописанным методом, а количество образовавшегося Δ^4—3-оксо-соединения — методом ультрафиолетовой спектрофотометрии.

Dr. Sándor Görög: Budapest X. Cserkesz u. 63

ANALYSIS OF STEROIDS, II*

DETERMINATION OF STEROIDS CONTAINING AN ETHINYL GROUP

S. GÖRÖG

(Gedeon Richter Chemical Works, Budapest)

Received December 4, 1964

Ethinyl steroids, a class of compounds of great pharmaceutical importance, are usually analyzed by colorimetric methods combined with chromatographic separation [1—6], and by ultraviolet [7] as well as infrared [8, 9] spectrophotometry, similarly to the analysis of steroid compounds in general. However, most of these methods are not specific of the ethinyl group, the typical functional group of this family of compounds. The scope of the present investigations was to develop a rapid titrimetric method based on the direct measurement of the ethinyl group, and suitable for the characterization and quantitative determination of ethinyl steroids.

For the determination of monosubstituted acetylene derivatives the simplest possibility is offered by their reaction with metals, mainly with silver:

$$R-C\equiv C-H + Ag^+ \rightleftarrows R-C\equiv C-Ag + H^+ \qquad (1)$$

The principle of this method had been originally suggested by BERTHELOT [10]. Since then, a number of modifications were evolved, which are mainly based on the measurement of the formed acid. However, there is no generally accepted method in this field. The equilibrium conditions of reaction (1) and the solubility of the precipitate may be varying, depending on the nature of the compound to be determined. In certain cases the amount of nitric acid liberated by silver nitrate can be measured without any difficulty [11]. On the other hand, according to some authors, the equilibrium is shifted to the left hand side by the nitric acid produced. Therefore, instead of silver nitrate silver acetate [12] or benzoate [13] were recommended. According to some data of literature, the formed precipitate does not interfere with the end point detection of the alkaline titration. Other authors, in turn, reported interfering effects which made necessary the filtration of the solution [14] or the application of a great excess of silver. Namely, in the latter case, silver remains in solution, owing to the formation of the silver salt $R-C\equiv C-Ag \cdot 6\,AgNO_3$ [15]. In

* Part I: Acta Chim. Hung. **47**, 1 (1966).

practice, many problems may arise because of the presence of certain functional groups (such as amino, aldehyde or ester groups) which interfere with the determination. In order to eliminate this, some authors suggest the use of special reagents, such as silver ethylenediamine complex [16], or special titrants, *e.g.* tris-(hydroxymethyl)-aminomethane [17, 18]. In general, water, methanol or ethanol are used as solvents.

MIOCQUE and GAUTIER [19] employed a solution of silver nitrate in pyridine as solvent, and the liberated nitric acid was titrated with a 0.1 *N* solution of sodium hydroxide in methanol, in the presence of thymolphthalein

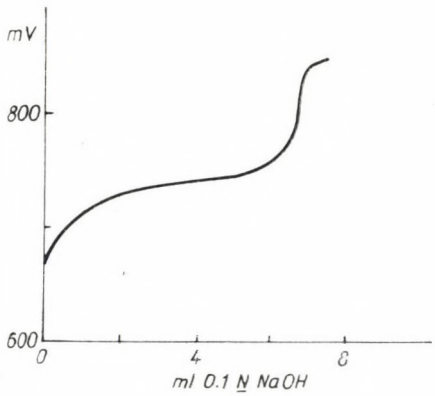

Fig. 1. Potentiometric titration curve
Titration of 19-nor-17α-pregn-5(10)-ene-20-ine-17β-ol-3-one

indicator. By the use of pyridine, this excellent method simultaneously solves the double problem of a solvent suitable for the dissolution of compounds of different types, and of a medium in which acids may be readily titrated. Furthermore, owing to the acid-binding nature of pyridine, also equilibrium (1) is shifted favourably.

Since pyridine is a good solvent also of compounds having steroid skeleton, it appeared promising to attempt the use of this solvent for our purpose. In the case of ethinyl steroids the presence of the mentioned interfering groups need not be considered. Thus, the application of a special reagent is not necessary.

It has been found that a limited amount of water does not interfere with the determination. Thus, it is possible, after dissolving the sample in pyridine, to introduce silver nitrate and sodium hydroxide in the system as aqueous solutions. In this way, the use of a methanolic solution of sodium hydroxide, which cannot be stored for long periods, can be avoided. The use of an aqueous

solution of sodium hydroxide has converted the method into a very simple procedure suitable for routine analyses.

It may be seen in Fig. 1 that under these conditions a titration curve with a sharp potential jump is obtained. The place of the jump exactly coincides with the range of colour change of thymolphthalein. The end point can be detected so well that it is possible to carry out the titration even on the 0.01 *N* scale. In this way ethinyl steroids can be determined also in pills or tablets.

The amount of pyridine applied as the solvent depends on the solubility of the steroid to be analyzed. In general, 20 ml of pyridine is satisfactory. The poor solubility of ethinyl testosterone necessitates the use of 30 ml of pyridine on the 0.1 *N* scale, or that of 10 ml on the 0.01 *N* scale.

Silver nitrate is introduced in the system as a 3.0 *N* aqueous solution. On the 0.1 *N* scale 3 ml, while on the 0.01 *N* scale only 1 ml of this solution is applied; this quantity corresponds even on the 0.1 *N* scale to a nearly tenfold excess. Such an excess is really necessary, because when less silver nitrate is used, particularly in the case of ethinyl estradiol, the large quantity of precipitate produced markedly interferes with the detectability of the end point. In the presence of a large excess of silver, complex formation observed with other solvents takes place also in pyridine [15], and thus the greatest part of the silver salt is retained in the solution.

If the titration is carried out in a flask with ground glass stopper, and the flask is kept open only for the short periods required for the addition of reagents and for the actual, not too prolonged, titration, no other measures are necessary to exclude the carbon dioxide of the atmosphere. The error committed in this way is negligible even when working on the 0.01 *N* scale.

When the end point of the titration is reached, the colourless thymolphthalein indicator turns blue or, if the solution has become yellow during titration, it shows a greenish tint.

In the analysis of pills, insoluble accompanying substances must be removed by filtration, and the filtrate is to be neutralized prior to the addition of silver nitrate.

Experimental

Reagents and instruments

Pyridine, analytical grade;

3.0 N $AgNO_3$, prepared by dissolving 51 g of silver nitrate (analytical grade) in water to give 100 ml solution;

0.1 N NaOH, aqueous solution. It is standardized with aqueous oxalic acid.

0.01 N NaOH, prepared freshly before use, by dilution of the 0.1 *N* solution;

Thymolphthalein indicator, 1% ethanolic solution.

The potentiometric titrations were carried out with a Radelkisz OP 401/1 type p_H-titrimeter, using a pair of methanolic calomel electrodes saturated with potassium chloride.

Description of the method

0.1 *N* scale

30 ml of pyridine, 3 ml of 3.0 *N* silver nitrate, and 0.2 ml of thymolphthalein indicator solution are placed in a 100 ml flask with ground glass stopper, and 0.1 *N* sodium hydroxide is added dropwise until the mixture becomes pale blue. Then about 0.3 g of the ethinyl steroid to be analyzed is added. After the sample has been completely dissolved, the solution is titrated with 0.1 *N* sodium hydroxide until a pale blue colour is obtained; if the solution was yellow, the final colour should be green.

For steroids containing one ethinyl group, the equivalent weight is equal to the molecular weight.

0.01 *N* scale

The procedure is essentially the same as described above, with the difference that 10 ml of pyridine and 1 ml of 3.0 *N* silver nitrate are used; the sample should be about 0.03 g, and the neutralization and titration are made with 0.01 *N* sodium hydroxide.

Assay of pills

The pills to be analyzed are finely powdered, and a quantity containing about 0.03 g of ethinyl steroid is shaken for 3—4 minutes with 10 ml of pyridine is a flask with a ground glass stopper. The solution is quickly filtered into another flask with ground glass stopper, and the first flask is rinsed with 3 × 5 ml of pyridine. 0.2 ml of 1% thymolphthalein is added, and the solution adjusted to a pale blue tint with 0.01 *N* sodium hydroxide. After the addition of 1 ml of 3.0 *N* silver nitrate, the solution is titrated with 0.01 *N* sodium hydroxide.

Experimental results

The results obtained in the analysis of some ethinyl steroids are summarized in the Table. The data given in the Table are mean values of 5 parallel measurements.

It is seen from the Table that when working on the 0.1 *N* scale, the probable error of a single measurement is less than $\pm$ 0.5%, and on the 0.01 *N* scale it does not exceed $\pm$ 2.0%.

Ethinyltestosterone in the Klimovan pill, and 19-nor-17α-pregn-5(10)-ene-20-ine-17β-ol-3-one in an experimental pill were determined with the present method. The essay gave 9 to 11 mg, and 4.5 to 5.5 mg, respectively, in fair accordance with the declared values of 10 and 5 mg per pill.

Table

Substance analyzed	Assay, %	
	On 0.1 *N* scale	On 0.01 *N* scale
19-nor-17α-Pregna-1,3,5(10)-triene-20-ine-3,17β-diol (ethinyl-estradiol)	99.9 ± 0.2	100.9 ± 1.3
19-nor-17α-Pregna-1,3,5(10)-triene-20-ine-3-methoxy-17β-ol	99.2 ± 0.5	100.2 ± 1.8
17α-Pregn-4-ene-20-ine-17β-ol-3-one (ethinyltestosterone)	99.1 ± 0.4	98.6 ± 1.6
19-nor-17α-Pregn-5(10)-ene-20-ine-17β-ol-3-one	99.4 ± 0.3	99.6 ± 1.7
19-nor-17α-Pregna-2,5(10)-diene-20-ine-3-methoxy-17β-ol (crude product)	97.6 ± 0.4	—
19-nor-17α-Pregn-4-ene-20-ine-17β-ol	98.9 ± 0.3	98.2 ± 1.4*

* 2 ml of 3.0 *N* silver nitrate was used.

Thanks are expressed to Miss M. KAPÁS for her useful assistance in the experimental work.

SUMMARY

The method of MIOCQUE and GAUTIER has been applied for the determination of ethinyl steroids. The reaction with silver nitrate and measurements of the liberated acid are carried out in pyridine as the solvent. The acid is liberated with an aqueous solution of silver nitrate; the titrant is an aqueous solution of sodium hydroxide.

The probable error of the method is ± 0.5% on the 0.1 *N* scale, and less than ± 2.0% on the 0.01 *N* scale.

The method also lends itself to the determination of the content of ethinyl steroids in pills.

REFERENCES

1. STENLAKE, J. B., WILLIAMS, W. D.: J. Pharm. Pharmacol. **9,** 908 (1957).
2. MCKINLEY, W. P., DEVLIN, W. F.: Canad. J. Biochem. Physiol. **35,** 699 (1957).
3. HEUSGHAM, C., JEHOTTE, J. M.: J. Pharm. Belg. **12,** 418 (1957).
4. KITAZAWA, T., NAITO, M., YOSHIDA, F., MARUYAMA, M.: J. Pharm. Soc. Japan **80,** 116 (1960).
5. KITAZAWA, T., NAITO, M., YOSHIDA, F., MARUYAMA, M.: J. Pharm. Soc. Japan **81,** 496 (1961).
6. BECKER, A., EHINGER, F.: Z. anal. Chem. **198,** 162 (1963).
7. KLEIN, S., JAMES, A. E., TUCKERMAN, M, M.: J. Am. Pharm. Assoc. Sci. Ed. **49,** 314 (1960).
8. ITO, A., AMASAKU, O.: J. Pharm. Soc. Japan **77,** 1083 (1957).
9. HAYDEN, A. L., SAMMUL, O. R.: J. Am. Pharm. Assoc. Sci. Ed. **49,** 489 (1960).
10. BERTHELOT, P. E. M.: Bull. Soc. Chim. France **5,** 176 (1866).
11. HYZER, R. E.: Anal. Chem. **24,** 1092 (1952).
12. KRESTINSKY, W., KELBOWSKAYA, M.: Ber. **64,** 2371 (1931).
13. MARSZAK, I., KOULKES, M.: Bull. Soc. Chim. France **1950,** 364.
14. HILL, A. J., TYSON, F.: J. Am. Chem. Soc. **50,** 172 (1928).
15. BARNES, L., MOLININI, L. J.: Anal. Chem. **27,** 1025 (1955).
16. KOULKES, M., MARSZAK, I.: Bull. soc. chim. France **1952,** 556.
17. BARNES, L.: Anal. Chem. **31,** 405 (1959).
18. GUTTERSON, M., MA, T. S.: Microchem. J. **5,** 601 (1961).
19. MIOCQUE, M., GAUTIER, J. A.: Bull. soc. chim. France **1958,** 467.

Zur Analytik von Steroiden, II

Bestimmung solcher Steroide, die eine Äthinylgruppe enthalten

S. GÖRÖG

Zusammenfassung. Die durch MIOCQUE und GAUTIER vorgeschlagene Methode wurde zur Bestimmung von Äthinylsteroiden angewandt. Die mit Silberionen verlaufende Reaktion bzw. die Messung der freigesetzten Säure wurde in Pyridinlösung durchgeführt. Zur Freisetzung der Säure wurde eine wässerige Silbernitratlösung, und als Meßlösung eine wässerige Natriumhydroxidlösung verwendet.

Der wahrscheinliche Fehler des Verfahrens bewegte sich im 0,1n Maß unter $\pm$ 0,5%, im 0,01n Maß hingegen unter $\pm$ 2%.

Die Methode ist auch zur Bestimmung von Äthinylsteroiden in Tabletten geeignet.

Данные к аналитической химии соединений со стерановым скелетом, II.

Определение стероидов, содержащих этинильную группу

Ш. ГЁРЁГ

Резюме. Для определения этинилстероидов применялся метод Миоск и Готие. Реакция с ионом серебра и измерение образующейся кислоты проводились в пиридиновой среде. Для выделения кислоты использовался водный раствор нитрата серебра, а затем кислота титровалась водным раствором гидрата окиси натрия.

Вероятная погрешность метода для 0,1н растворов $\pm$ 0,5%, а для 0,01н — ниже $\pm$ 2%.

Метод пригоден также и для определения этинилстероидов в таблетках.

Dr. Sándor GÖRÖG, Budapest X. Cserkesz u. 63

NEUERE UNTERSUCHUNGEN ÜBER FRONTALE GASCHROMATOGRAPHIE UNTER BERÜCKSICHTIGUNG DER STRÖMUNGSGESCHWINDIGKEIT WÄHREND DER SORPTION, III*

BESTIMMUNG VON HTS-WERTEN MITTELS FRONTALER GASCHROMATOGRAPHIE

H. BEYER, P. FEJES, G. SCHAY und K. VARGA**

(Zentralforschungsinstitut für Chemie der Ungarischen Akademie der Wissenschaften)

Eingegangen am 1. März 1965

1. *Einleitung*

In mehreren früheren Arbeiten [1, 2, 3] haben wir uns mit der Theorie der frontalen Variante der Gaschromatographie befaßt, wobei wir nur den Fall einer einzigen sorbierbaren Komponente im inerten Trägergas betrachteten und die infolge von Sorptionsvorgängen veränderliche Geschwindigkeit der Gasströmung innerhalb der Trennsäule in unsere Berechnungen einbezogen. Wir konnten zeigen und theoretisch begründen, daß infolge der gegeneinander wirkenden Effekte der endlichen Sorptionsgeschwindigkeit und Längsdiffusion in der Gasphase einerseits, und der Veränderung der Strömungsgeschwindigkeit innerhalb der Front andererseits praktisch stationäre Sorptions-, Geschwindigkeits- und Konzentrationsfronten in genügend langen Säulen auftreten können. Mit den Annahmen, wonach sich die normale Gasdiffusion nur im Zwischenkornvolumen auswirkt und die Sorptionsgeschwindigkeit mit einer linearen Kinetik beschrieben werden kann, haben wir unter Verwendung der für die frontale Variante gültigen Randbedingungen die Lösungen des den gaschromatographischen Prozeß beschreibenden Differentialgleichungssystems für stationäre Fronten entwickelt.

In der vorliegenden Arbeit wollen wir für die frontale Variante der Gaschromatographie einen Ausdruck für die Trennstufenhöhe HTS (im englischen Schrifttum mit HETP bezeichnet) ableiten und durch Vergleich mit elutionschromatographisch ermittelten HTS-Werten Schlußfolgerungen hinsichtlich der Gültigkeit und der Art der Beschränkung der gewöhnlichen HTS-Konzeption ziehen. Da wir dabei aber auf einen Teil der Ergebnisse der früheren Arbeiten aufbauen, scheint es zweckmäßig zu sein, noch einmal kurz auf die Ableitung der hier interessierenden Zusammenhänge einzugehen.

Wir konnten zeigen [3], daß der Differentialquotient der am Säulenende L gemessenen Konzentration x_L einer stationären Gasfront nach der Zeit

* Mitteilung II: Acta Chim. Hung. **43**, 221 (1965).

** Der Inhalt dieser Publikation wurde von G. SCHAY auf der Gesamtbundeskonferenz über Gaschromatographie, Mai 1964, in Moskau vorgetragen.

in guter Näherung durch folgende, nach dem kubischen Glied abgebrochene MacLaurinsche Potenzreihe beschrieben werden kann:*

$$\text{wobei} \qquad \frac{dx_L}{d\tau} = k\,(\lambda_1 x + \lambda_2 x^2 + \lambda_3 x^3), \tag{1}$$

$$\lambda_1 = \frac{1 + r\,(1 - x_0)}{2}\left\{-1 + \sqrt{1 + \frac{4\,r x_0}{[1 + r\,(1 - x_0)]^2}}\right\} \tag{2}$$

$$\lambda_2 = \frac{\lambda_1 - r\,(1 + x_0)}{3\lambda_1 + r\,(1 - x_0) + 1} \tag{3}$$

$$\lambda_3 = -\left(\frac{\lambda_1 + \lambda_2 x_0}{x_0^2}\right) \tag{4}$$

$$r \equiv \frac{q u^2}{D_{\text{eff}}\, k}$$

D_{eff} = effektiver Diffusionskoeffizient
k = Sorptionsgeschwindigkeitskonstante
q = Verteilungskoeffizient
u = Frontwanderungsgeschwindigkeit
x_0 = Ausgangskonzentration des Sorptivs in Molenbrüchen

[Wenn die Berechnungen mit experimentellen Daten zu vergleichen sind, müssen demzufolge die unmittelbar gemessenen Frontkurven $x_L(\tau)$ nach τ differenziert und die Differentialquotienten $\frac{dx_L}{d\tau}$ entsprechend (1) in Abhängigkeit von x_L aufgetragen werden.]

* Der Gang der Berechnung ist folgender: Die differentielle Bilanzgleichung für das Sorptiv und die Bruttobilanzgleichung wird nach Einführung der kombinierten Veränderlichen ψ einmal nach ψ integriert. Aus den zwei ersten Integralen wird c eliminiert. Für die (für die sorbierte Menge charakteristische dimensionslose) Größe α ergibt sich dann ein Zusammenhang folgenden Typs:

$$\alpha = \alpha\left(\frac{dx}{d\psi},\ x\right).$$

Wird dieser Zusammenhang nach ψ differenziert und mit der rechten Seite der linearen kinetischen Gleichung $\frac{d\alpha}{d\psi} = k\,(qx_L - \alpha)$, in der α durch $\alpha\left(\frac{dx_L}{d\psi}, x_L\right)$ zu ersetzen ist, gleichgesetzt, so ergibt sich für x_L eine nichtlineare gewöhnliche Differentialgleichung 2. Ordnung. Wird die Lösung in Form der Potenzreihe dritten Grades (1) gesucht, so müssen die unbekannten Koeffizienten $\lambda_i (i = 1,2,3)$ mit Hilfe der Methode des Koeffizientenvergleichs errechnet werden, wobei sich für λ_i die Ausdrücke (2)—(4) ergeben.

Die durch Koeffizientenvergleich für die Koeffizienten λ_i erhaltenen Ausdrücke (2—4) sind aber noch sehr kompliziert und in ihren Konsequenzen schwer zu übersehen. Sie lassen sich jedoch vereinfachen, wenn die Bedingung gestellt wird, daß r einen nicht zu hohen Werte annehmen darf (dies kann für ein gegebenes chromatographisches System mit einer Beschränkung des Strömungsgeschwindigkeitsbereichs durch einen noch zulässigen Maximalwert gleichgesetzt werden) und die Konzentration des in die Säule eingeführten Gasgemisches verhältnismäßig niedrig gehalten wird ($x_0 \ll 1$). In diesem Falle kann nämlich in (2) $1 - x_0 \cong 1$ gesetzt und die Reihenentwicklung des Wurzelausdrucks nach dem linearen Glied abgebrochen werden. Mit diesen Vereinfachungen erhalten wir

$$\lambda_1 = \frac{rx_0}{1 + r}. \tag{5}$$

$$\lambda_2 = \frac{\frac{rx_0}{1+r} - r(1 + x_0)}{\frac{3rx_0}{1+r} + r(1 - x_0) + 1} \cong -\frac{r(1 + r - x_0)}{3rx_0 + (1 + r)^2} \cong$$

$$\cong -\frac{r(1 + r)}{(1 + r)^2} = -\frac{r}{1 + r}. \tag{6}$$

$$\lambda_3 = 0. \tag{7}$$

Unter solchen Bedingungen* kann also die Abhängigkeit des Differentialquotienten $\frac{dx_L}{d\tau}$ von der am Säulenende gemessenen Konzentration x_L in Form einer einfachen Parabel dargestellt werden, d. h., daß die Frontkurven eine symmetrische Gestalt aufweisen.

Der Scheitelpunkt dieser einfachen Parabel bzw. die maximale Steilheit der symmetrischen Frontkurve gehört zur Konzentration $\frac{x_0}{2}$. Wird also der größte $\frac{dx_L}{d\tau}$-Wert mit φ_m bezeichnet, dann besteht für diesen der Zusammenhang

$$\frac{1}{k}\left(\frac{dx_L}{d\tau}\right)_{x_L = \frac{x_0}{2}} \equiv \frac{1}{k}\varphi_m = \lambda_1 \cdot \frac{x_0}{2} + \lambda_2 \cdot \left(\frac{x_0}{2}\right)^2.$$

* Es ist jedoch zu bemerken, daß nicht nur für $x_0 \ll 1$, sondern für jeden x_0-Wert ein endlicher r-Wert existiert, bei dem $\lambda_3 = 0$, die Frontkurve also symmetrisch ist [3]. Dieser Wert ist:

$$r = \frac{1 - \frac{x_0}{2}}{(1 - x_0)^2}.$$

Durch Kombination mit (5) und (6) und unter Berücksichtigung der Definition von r erhält man schließlich

$$\frac{x_0^2}{4\varphi_m} = \frac{D_{eff}}{qu^2} + \frac{1}{k} . \tag{8}$$

Dieser Gleichung entsprechend müssen wir eine Gerade erhalten, wenn der auf der linken Seiten stehende Ausdruck gegen $\frac{1}{qu^2}$ aufgetragen wird. Die Steigung dieser Geraden ist gleich der effektiv en Diffusionskonstante, der reziproke Ordinatenabschnitt ist der Wert der Transportgeschwindigkeitskonstante.

2. *Die frontalchromatographische HTS-Gleichung*

VAN DEEMTER und Mitarbeiter [4] haben (ausgehend vom gleichen partiellen Differentialgleichungssystem, das auch Ausgangspunkt der von uns entwickelten Theorie der frontalen Gaschromatographie ist) für die Elutionschromatographie die bekannte HTS-Beziehung abgeleitet, die mit den von uns benutzten Symbolen

$$\mathrm{HTS} = \frac{2\,D_{eff}}{c_0} + \frac{2\,q}{(1+q)^2 k}\, c_0 \tag{9}$$

lautet*. Es sei jedoch ausdrücklich vermerkt, daß die Berechnungen auf der Annahme symmetrischer Gauß-Profile der Elutionsberge basieren.

Die rechte Seite von (9) ergibt sich aber bemerkenswerterweise auch bei Umformung von (8). Hierbei hat man zu beachten, daß zwischen der linearen Einströmungsgeschwindigkeit c_0 und der Frontwanderungsgeschwindigkeit u die Beziehung $c_0 = u(1+q)$ besteht. Ersetzt man demgemäß in (8) u durch c_0 und multipliziert dann beide Seiten mit $2\,qc_0/(1+q)^2$, so werden die rechten Seiten von (8) und (9) identisch. Somit können auch die linken Seiten einander gleichgesetzt werden, wodurch man die frontalchromatographische HTS-Gleichung

$$\mathrm{HTS} = \frac{q\,c_0\,x_0^2}{2\,(1+q)^2} \cdot \frac{1}{\varphi_m} \tag{10}$$

erhält.

* Eigentlich enthält die von VAN DEEMTER angegebene Gleichung noch einen dritten. die Eddy-Diffusion im Kanalraum berücksichtigenden Summanden. Dieses sog. A-Glied der Gleichung ist jedoch, wie in zahlreichen neueren Publikationen [5, 6, 7] übereinstimmend gezeigt wird, recht fragwürdig, der Theorie nach ist es praktisch gleich Null oder sogar ein — allerdings sehr geringer — negativer Wert. Dies bestätigt die Zulässigkeit der einleitend erwähnten vereinfachenden Annahme, nach der nur die Gasdiffusion im Zwischenkornvolumen berücksichtigt wurde.

Es ist nicht sonderlich überraschend, daß die für die beiden gaschromatographischen Varianten geltenden Beziehungen (8) und (9) ineinander übergeführt werden können, wenn man bedenkt, daß sie vom gleichen partiellen Differentialgleichungssystem ausgehend und nur mit — durch die Natur der Prozesse bedingten — verschiedenartigen Nebenbedingungen abgeleitet wurden und die Analogie sich auch auf die Beschränkung ihrer Gültigkeit erstreckt, denn wie wir schon zeigten bzw. erwähnten, ist (8) bzw. (10) nur für symmetrische Frontkurven und (9) nur für Elutionsberge mit symmetrischem Gauß-Profil streng gültig.

Der Theorie nach sollte also eine Übereinstimmung der nach Gleichung (10) aus frontalchromatographischen Messungen berechneten HTS-Werte mit denjenigen zu erwarten sein, die bei gleichen Versuchsparametern aus elutionschromatographischen Daten nach der bekannten Beziehung

$$\mathrm{HST} = \left(\frac{\Delta t}{4\, t_r}\right)^2 \cdot \mathrm{L} \tag{11}$$

erhalten werden (t_r ist die unkorrigierte Gesamtretentionszeit, Δt die Basisbreite des Elutionsberges in Zeiteinheiten).

3. *Experimenteller Teil*

Es wurden jeweils Frontal- und Elutionschromatogramme von Butan in einem verhältnismäßig weiten Intervall der Strömungsgeschwindigkeit (0,2 bis 5,1 cm/s) mit den gleichen Trennsäulen aufgenommen. Als Trägergas wurde Wasserstoff und als stationäre Phase 10% bzw. 20% Squalan auf Firebrick-22 (Korngröße 0,3—0,4 mm) verwendet. Die Säulentemperatur betrug 20° C. Die Trennsäulen hatten eine Länge von 50 cm und einen inneren Durchmesser von 6 mm. Bei den Elutionsmessungen wurden 0,98 ml n-Butan dosiert, bei den frontalchromatographischen Versuchen war der Molenbruch des n-Butans in H_2 0,25. Als Detektor diente eine Wärmeleitfähigkeitsmeßzelle, zur Messung der Strömungsgeschwindigkeit ein Seifenmembranströmungsmesser.

4. *Meßergebnisse und Schlußfolgerungen*

Auf Abb. 1 sind die Ergebnisse der frontalchromatographischen Messungen entsprechend (8) aufgetragen. Die ausgezogene Kurve entspricht einer 20%igen, die unterbrochene einer 10%igen Beladung des Trägermaterials mit Squalan. Bei nicht zu großen Strömungsgeschwindigkeiten liegen die Werte der einzelnen Messungen gut auf einer Geraden. Obwohl bei unseren Experimenten die Forderung $x_0 \ll 1$ nicht erfüllt war, trat doch keine wesentliche Asymmetrie der Durchbruchskurven auf. Eine Erklärung dafür ergibt sich aus dem in der Fußnote auf S. 4 Gesagten. Die Abweichungen von der Geraden im Bereich größerer Strömungsgeschwindigkeiten finden ihre Erklärung dadurch, daß mit schneller werdender Strömung in zunehmendem Maße eine Verzerrung der Durchbruchskurven auftritt, und zwar derart, daß der Inflexionspunkt bei einer geringeren Konzentration als $\frac{x_0}{2}$ zu liegen kommt.

Der nach dem Inflexionspunkt folgende Kurvenast ist somit zeitlich weiter auseinandergezogen, als der vor der Inflexion der Kurve, so daß sich größere φ_m-Werte, also unter den Geraden liegende Punkte ergeben. Dieser Befund ist nicht überraschend, es ist sogar von vornherein zu erwarten, daß die endliche Geschwindigkeit der Sorption mit der zunehmenden Frontwanderungsgeschwindigkeit in der Gasphase zunächst noch Schritt halten kann und eine Verzögerung in erster Linie in der Nähe des Gleichgewichtes zu erwarten ist,

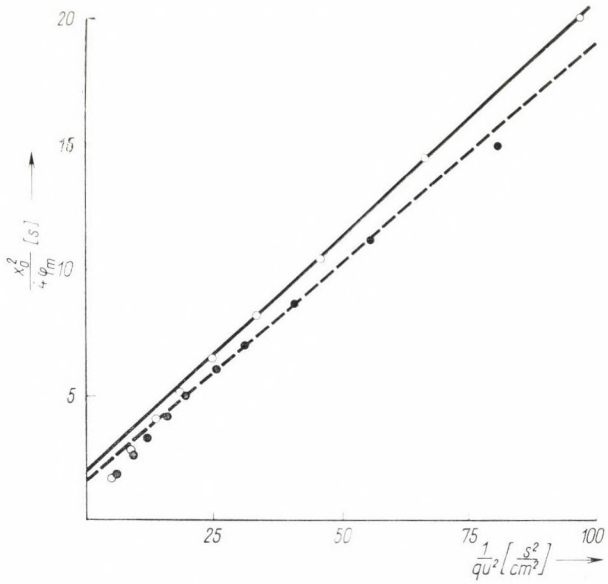

Abb. 1. 10% Squalan auf Firebrick—22

wo von Natur aus die Geschwindigkeit der Sorption wesentlich abnimmt. Die Abweichungen der Meßdaten von der nach (8) zu erwartenden Geraden sind aber z. T. wahrscheinlich auch darauf zurückzuführen, daß die verwendeten Säulen nicht lang genug waren, um auch bei sehr großen Werten der Strömungsgeschwindigkeit die Einstellung eines stationären Zustandes zu ermöglichen.

Aus den Geraden auf Abb. 1 ergeben sich für 10 bzw. 20%ige Beladung D_{eff} zu 0,174 bzw. 0,189 cm/s^2 und k zu 0,65 bzw. 0,51 s^{-1}.

Auf Abb. 2 und 3 sind für die beiden verwendeten Trennsäulen die nach (10) aus den Inflexionstangenten der frontalchromatographischen Durchbruchskurven berechneten HTS-Werte (Kurven II) und die aus (unter gleichen Versuchsbedingungen* durchgeführten) Elutionsmessungen nach (11) erhaltenen HTS-Werte (Kurven III) gegen die Lineargeschwindigkeit der Gasströmung aufgetragen.

* Die Gleichheit bezieht sich natürlich nicht auf die Konzentration.

Eine vollständige Übereinstimmung der auf verschiedene Weise erhaltenen Kurven II und III ist deshalb nicht zu erwarten, weil wegen der durch die Natur der Prozesse gegebenen unterschiedlichen Konzentrationsverhält-

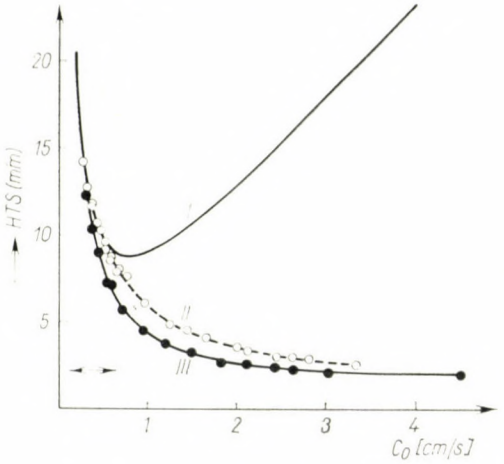

Abb. 2. 20% Squalan auf Firebrick—22

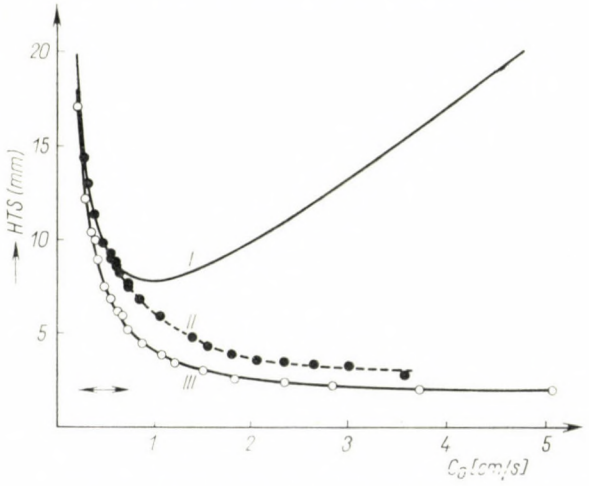

Abb. 3. □□□ 10% Squalan auf Firebrick—22
○○○ 20% Squalan auf Firebrick—22

nisse im Frontal- und Elutionsfall die für die Frontwanderung charakteristischen q-Werte nicht identisch sind, da die Sorptionsisotherme in dem betreffenden Konzentrationsbereich eine schwache Krümmung aufweist. Auf den ersten Blick ist aber zu sehen, daß der Gang der einander entsprechenden Kurven weitgehend gleich ist. Es ist also offensichtlich, daß die Berechnung

der HTS-Werte aus den Inflexionstangenten der frontalchromatographischen Durchbruckskurven und aus den Retentionszeiten und Basisbreiten von Elutionsbergen weitgehend gleichwertige Verfahren sind.

Es ist schon lange bekannt, daß die van Deemter-Gleichung — wenigstens in dieser einfachen Form — in den meisten praktischen Fällen nicht ausreicht, um die HTS-Kurven richtig wiederzugeben. Deswegen überrascht es uns auch nicht, wenn die Kurven II und III nicht den Verlauf typischer Minimumkurven zeigen, die auf Grund der van Deemter-Gleichung zu erwarten wären. Durch willkürliche Annahme von geeigneten Werten für D_{eff} und k kann man allerdings in vielen Fällen eine mehr oder weniger gute Übereinstimmung des tatsächlichen HTS-Kurvenverlaufs mit der van Deemter-Gleichung erreichen, wobei aber besonders für k meistens extrem hohe Werte angenommen werden müssen. Wir sind aber in der Lage, die tatsächlichen Werte für k und D_{eff} verhältnismäßig zuverlässig aus den Daten der bei geringeren Strömungsgeschwindigkeiten gemessenen Frontalchromatogramme auf Grund von (8) zu ermitteln und durch Einsetzen dieser Werte in (9) die HTS-Kurve zu berechnen, die sich der Theorie nach ergeben sollte.

Auf den Abb. 2 und 3 sind die HTS-Kurven mit I gekennzeichnet, die sich rechnerisch durch Einsetzen der experimentell bestimmten k- (0,65 bzw. 0,51 s^{-1}) und D_{eff}-Werte (0,174 bzw. 0,189 cm/s^2) in (9) ergeben. Ein Vergleich der Kurven I und II macht deutlich, daß nur innerhalb der durch Doppelpfeile gekennzeichneten Strömungsgeschwindigkeitsintervalle, in denen die Darstellung gemäß (8) Geraden ergibt, die Frontkurven also einen ausreichenden Symmetriegrad aufweisen, die betreffenden Kurven miteinander übereinstimmen. Bei größeren Strömungsgeschwindigkeiten wird jedoch nicht einmal der Gang der Kurven II und III annähernd richtig wiedergegeben. Die Ursachen dafür liegen auf der Hand. Die Gleichung nämlich, die die Berechnung der HTS-Werte auf Grund der Inflexionstangenten ermöglicht, gilt nur für symmetrische Durchbruchskurven und stationäre Fronten, wir haben sie aber dessen ungeachtet auch bei höheren Strömungsgeschwindigkeiten benutzt, wo in den relativ kurzen Säulen weder eine vollständige Einstellung des stationären Zustandes zu erwarten ist, noch die Durchbruchsfronten annähernd symmetrisch sind. Die Formel für die übliche HTS-Berechnung ergibt sich analog dazu nur dann, wenn angenommen wird, daß das Profil des Elutionsberges eine symmetrische Gauß-Kurve ist. Tatsächlich läßt sich aber auch bei den Elutionsbergen mit zunehmender Strömungsgeschwindigkeit des Trägergases eine immer ausgeprägter werdende Asymmetrie, das sog. »tailing« feststellen. Gleichzeitig wird die aus des Lage des Bergmaximums errechnete Retention merklich kleiner.

Es drängt sich nun die Frage auf, ob die übliche Berechnung der HTS-Werte aus den faktisch immer mehr oder weniger asymmetrischen Elutionsbergen überhaupt genügend Sinn hat. Vom praktischen Standpunkt aus steht

es außer Zweifel, daß diese Berechnungsweise, der wir eine zweite, auf frontalchromatographischen Daten beruhende Methode zur Seite gestellt haben, für die gaschromatographische Praxis, insbesondere zur Beurteilung der Trennleistungen von Säulen bei geringen Strömungsgeschwindigkeiten, von großem Nutzen ist. Theoretisch gesehen ist aber ein solches Vorgehen recht fragwürdig.

Wir sind davon überzeugt, daß ein tatsächlicher Fortschritt in der Theorie der Gaschromatographie ohne die Berücksichtigung der faktisch immer vorhandenen Asymmetrie der Frontkurve bzw. Elutionsberge nicht zu erreichen ist. Allerdings wird unseres Erachtens nicht das sich in der neueren Literatur immer mehr ausbreitende Bestreben zum Ziele führen, das darin besteht, die van Deemter-Gleichung durch weitere, theoretisch schwer zu begründende Glieder zu ergänzen. Unserer Meinung nach, müßte das Ausgangsdifferentialgleichungssystem und insbesondere die kinetische Gleichung einer kritischen Untersuchung unterzogen und derart ergänzt werden, daß es der mit steigender Strömungsgeschwindigkeit zunehmenden Asymmetrie der Durchbruchsfronten bzw. Elutionsberge Rechnung trägt. Die Weiterentwicklung der Theorie der Gaschromatographie mit gepackten Säulen müßte also hier ansetzen, wobei es sich wahrscheinlich als notwendig erweisen wird, die Definition von HTS entsprechend der erhaltenen Lösung zu revidieren. Es ist natürlich nicht ausgeschlossen, daß eine derartige Ergänzung der Theorie auf nicht voraussehbare und eventuell unüberwindbare mathematische Schwierigkeiten stößt. Trotzdem sollte aber der Ausweg in dieser Richtung gesucht werden.

ZUSAMMENFASSUNG

Auf Grund der Theorie der stationären Fronten wird eine Methode angegeben, durch die aus frontalchromatographischen Daten die effektive Diffusionskonstante in der Gasphase und die Geschwindigkeitskonstante des Sorptionsvorganges bestimmt werden können. Durch Einsetzen dieser Werte in die van Deemter-Gleichung und das Heranziehen der Inflexionstangente der durchbrechenden Frontkurve ergibt sich ein Ausdruck für HTS, der in Abhängigkeit von der Gasgeschwindigkeit denselben Gang ergibt wie die übliche Berechnung aus Retentionszeit und Basisbreite von Elutionsbergen.

LITERATUR

1. Fejes, P., Schay, G.: Acta Chim. Hung. **14,** 377 (1958).
2. Schay, G., Pethő, Á., Fejes, P.: Acta Chim. Hung. **22,** 285 (1960).
3. Fejes, P., Pethő, Á.: Acta Chim. Hung. **43,** 221 (1965).
4. van Deemter, J. J., Zuiderweg, F. J., Klinkenberg, A.: Chem. Eng. Sci. **5,** 271 (1956).
5. Giddings, J. C., Robinson, R. A.: Analyt. Chem. **34,** 885 (1962).
6. Kieselbach, R.: Analyt. Chem. **35,** 1342 (1963).
7. Knox, J. H., McLaurin, L.: Analyt. Chem. **35,** 449 (1963).

Recent Investigations on Frontal Gas Chromatography, on Taking into Account the Variations of Flow Rate during Sorption, III

Determination of HETP Values by Frontal Gas Chromatography

H. BEYER, P. FEJES, G. SCHAY and K. VARGA

Summary. On the basis of the theory of stationary fronts a new method is developed which allows to determine the effective diffusion constants in the gas phase and the mass transport velocity constants from frontal gas chromatographic data. Setting these values into the van DEEMTER equation and using the inflexion tangents of the throughbreaking front curves a new expression for HETP results. Its dependence from the gas flow rate is quite similar to the HEPT expression which results from the retention time and the basis width of elution peaks.

Новые исследования в области фронтальной газовой хроматографии с учетом изменений в скорости потока в процессе сорбции. III.

Определение величин ВЭТТ с помощью газовой хроматографии

Х. БЕЙЕР, П. ФЕЙЕШ, Г. ШАЙ и К. ВАРГА

Резюме. На основе теории стационарных фронтов авторы публикуют метод, с помощью которого, из данных по газовой хроматографии, можно определить константу эффективной диффузии и константу скорости сорбционного процесса. Подстановкой этих величин в уравнение ван Дэмтера, а также использованием изгибочной касательной пробивной фронтальной кривой, получили новое выражение для расчета ВЭТТ. Рассчитанные таким путем величины зависят от скорости газового потока точно таким же образом, как величины ВЭТТ, рассчитанные обычным путем из времени задержки и элуционного пика.

Dr. Hermann BEYER
Dr. Pál FEJES
Prof. Dr. Géza SCHAY
Károly VARGA

Budapest II. Pusztaszeri út 57/69.

NEUERE UNTERSUCHUNGEN ÜBER FRONTALE GASCHROMATOGRAPHIE, UNTER BERÜCKSICHTIGUNG DER STRÖMUNGSGESCHWINDIGKEIT WÄHREND DER SORPTION, IV*

BEURTEILUNG CHROMATOGRAPHISCHER TRENNSÄULEN AUF GRUND FRONTALCHROMATOGRAPHISCH GEMESSENER TRANSPORTGESCHWINDIGKEITS- UND DIFFUSIONSKONSTANTEN

K. VARGA, P. FEJES und H. BEYER

(Zentralforschungsinstitut für Chemie der Ungarischen Akademie der Wissenschaften, Budapest)

Eingegangen am 1. März 1965

1. Einleitung

Bei Lösung gaschromatographischer Trennaufgaben besteht der erste und wichtigste Schritt in der Auswahl der dem betreffenden Problem am besten gerecht werdenden Trennflüssigkeit. Im weiteren sind aber auch die Eigenschaften des Trägermaterials von großer Bedeutung, da die Trennflüssigkeit ihre Wirkung nur bei einer bestimmten Verteilung optimal ausüben kann, diese Verteilung aber durch die Struktur des Trägers im wesentlichen vorgegeben wird. Die Trenngüte wird — wie bekannt — neben der Qualität der Trennflüssigkeit von der Länge der Trennsäule und vom HTS-Wert, d. h. von der Trennstufenhöhe bestimmt. Es erscheint uns nun wichtig zu untersuchen, inwieweit mit Hilfe der frontalen Gaschromatographie Aufklärungen über die Beeinflußung des HTS-Wertes durch das Trägermaterial erhalten werden können, zumal wir in der III. Mitteilung dieser Reihe [1] über eine frontalchromatographische Methode berichtet haben, die es ermöglicht, die HTS-Werte und die Parameter im Ausdruck für HTS relativ einfach zu bestimmen.

Nach VAN DEEMTER hängt der HTS-Wert im wesentlichen von der linearen Geschwindigkeit c_0 der Gasströmung, vom Verteilungskoeffizienten q, von der effektiven Diffusionskonstanten D_{eff} und von der Transportgeschwindigkeitskonstante k ab. Der Verteilungskoeffizient ist für eine gegebene Substanz mit der Präparierung der Säule festgelegt. In den q-Werten kommt in erster Linie die Selektivität der Trennflüssigkeit zum Ausdruck. Unser Bestreben besteht nun darin, die chromatographische Trennsäule auf Grund der Sorptionsgeschwindigkeit und der Längsdiffusion zu bewerten und zu charakterisieren (wobei wir uns bewußt sind, daß diese beiden Faktoren nicht unabhängig von der qualitativen und quantitativen Zusammensetzung eines Probe-

* Mitteilung III: Acta Chim. Hung. **47**, 13 (1966).

gemisches sind). Deshalb werden wir unsere Untersuchungen und Betrachtungen auf diese Faktoren beschränken.

In einigen unserer Publikationen [2, 3] haben wir die effektive Diffusionskonstante folgendermaßen definiert:

$$D_{\text{eff}} = \frac{s_0}{s} \varkappa D_g \tag{1}$$

D_{eff} ist also durch die mit der Säulenfüllung gegebenen Größen s_0 und s, sowie durch die für das betreffende Trägergas und die Komponente charakteristische Diffusionskonstante D_g bestimmt.

Die Deutung der Transportgeschwindigkeitskonstante und die Auswahl der die Kinetik des Sorptionsprozesses beschreibenden kinetischen Gleichung sind ein und dasselbe Problem. In der Geschwindigkeitsgleichung sollte zum Ausdruck kommen, welcher der prinzipiell möglichen elementaren Transportprozesse für die Sorption geschwindigkeitsbestimmend ist. Diese Frage steht aber in engem Zusammenhang mit der Struktur des Trägermaterials und dem Verteilungszustand der Trennflüssigkeit. Eine solche Geschwindigkeitsgleichung, in der diese Gesichtspunkte Berücksichtigung finden, ist jedoch z. Z. nicht bekannt. Glücklicherweise können die in der gaschromatographischen Praxis vorkommenden Fälle hinsichtlich der Kinetik wenigstens in erster Näherung als Diffusionsprobleme betrachtet werden. Deshalb war es möglich, die Lösungen des mit Sorption überlagerten Diffusionsproblems in Form einer kinetischen Gleichung in der Theorie der Gaschromatographie zu verwenden. In der Praxis der Adsorptions- und Gas-Flüssigkeits-Verteilungschromatographie erwies sich z. B. die Gleichung

$$\frac{\partial a}{\partial \tau} = k\,(qx - a) \tag{2}$$

als sehr gut verwendbar, die GLUECKAUF durch Reihenentwicklung des die Porendiffusion (für größere $\varepsilon\tau$-Werte, d. h. in der Nähe des Gleichgewichtes) in kugelförmigen Teilchen beschreibenden, ziemlich komplizierten Zusammenhangs erhielt [4]. Die in (2) enthaltene Transportgeschwindigkeitskonstante wird in diesem Falle wie folgt gedeutet:

$$k = \frac{15\, D_b'}{\varrho_0^2}, \tag{3}$$

wobei

$$D_b' = D_b/A\ .$$

Der in der Theorie der Gaschromatographie als lineare kinetische Gleichung bekannte Zusammenhang (2) kann nach dem bereits Gesagten formell auch für die Beschreibung der verschiedenen elementaren Transportprozesse verwendet werden. Natürlich verändert sich dabei die Deutung von k. Ist die Sorptionsgeschwindigkeit in der stationären Phase der transportgeschwindigkeitsbestimmende Schritt, so gilt:

$$k = \frac{3\,D_f}{\gamma^2} \,. \tag{4}$$

Sind die Geschwindigkeiten der beiden erwähnten Prozesse (also Porendiffusion und Sorption in der Trennflüssigkeit) kommensurabel, dann kann k als Reziprokwert der summierten Reziprokwerte von (3) und (4) angegeben werden.

Auf Grund des oben Gesagten kann man erwarten, daß die effektive Diffusionskonstante und insbesondere die Transportgeschwindigkeitskonstante tatsächlich für die Charakterisierung gepackter chromatographischer Säulen geeignet sind, wenn man von den mit der Selektivität zusammenhängenden Faktoren absieht. Das ist besonders einleuchtend, wenn man bedenkt, daß in der Größe der Transportgeschwindigkeitskonstante und in ihrer Abhängigkeit von den Präparierungsmethoden der Säulen prinzipiell die Struktur des Trägers und die Dicke des adhärierenden Trennflüssigkeitsfilmes zum Ausdruck kommen.

2. Geeignete Methoden zur Bestimmung von k und D_{eff}

In einigen früheren Publikationen über die Theorie der frontalen Gaschromatographie [5, 6] haben wir zwei Methoden beschrieben, die für die Bestimmung der effektiven Diffusionskonstanten und der Transportgeschwindigkeitskonstanten aus frontalchromatographischen Daten geeignet sind.

Die Berechnungsweisen gelten nur für sog. stationäre Fronten (stationär werden diejenigen Fronten genannt, die mit unveränderter Gestalt und konstanter Geschwindigkeit durch die Säule schreiten). Diese Tatsache setzt aber trotzdem ihrer Verwendbarkeit keine Schranken, da die Fronten und so auch die hier zu untersuchende Konzentrationsfront in der Gasphase nach Zurücklegen einer genügend langen Strecke in der chromatographischen Trennsäule praktisch stationär werden.

Unsere weiteren Überlegungen basieren auf der kinetischen Gleichung (2), d. h. also auf der Annahme, daß die Geschwindigkeit des Massentransportes zwischen Gas- und Sorptionsphase durch einen linearen Zusammenhang zwischen den Veränderlichen x und α beschrieben werden kann.

Methode I [5]:

Im sog. kinetischen Gebiet*, d. h. bei genügend hohen Strömungsgeschwindigkeiten, bei denen die gewöhnliche Gasdiffusion in Strömungsrichtung bereits vernachlässigt werden kann, gilt für die Gasfront:

$$\ln \frac{x_L^{1-x_0}(1-x_L)^{x_0}}{x_0 - x_L} = kx_0\tau + \text{const.} \tag{5}$$

Mit Hilfe von (5) läßt sich die Größe von k aus der Linienschreiberausschlag-Zeit-Kurve errechnen, wie wir das auf Abb. 1 zeigen.

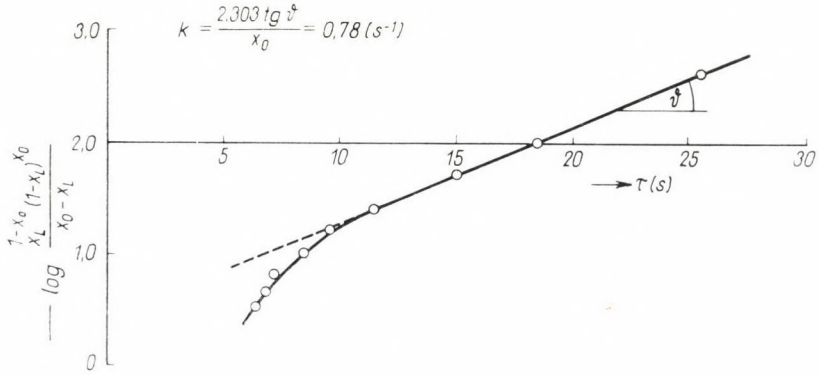

Abb. 1

Aus Abb. 1 — die aus experimentellen Daten konstruiert wurde, also keine Prinzipskizze darstellt — ist zu ersehen, daß die Meßwerte bei der Darstellung gemäß (5) bis auf die zu niedrigsten Konzentrationen gehörenden Punkte tatsächlich gut auf einer Geraden liegen. Die Abweichungen der Meßpunkte im unteren Konzentrationsbereich lassen sich dadurch erklären, daß GLUECKAUF die kinetische Gleichung für in der Nähe des Gleichgewichtes liegende Konzentrationen abgeleitet hat, ihre Verwendung für niedrigere Konzentrationen demzufolge mit ziemlich groben Fehlern verbunden ist.

Methode II [6]:

Bei mittleren Strömungsgeschwindigkeiten, im sog. Übergangsgebiet der Strömungsgeschwindigkeit (s. Fußnote S. 15), in dem der Effekt der Längsdiffusion noch nicht vernachlässigt werden kann, aber auch der Massen-

* Die genaueren Definitionen der Geschwindigkeitsbereiche haben wir schon in einer früheren Publikation [6] angegeben. Hier soll nur erwähnt werden, daß wir bei Erfüllung der Bedingung $\frac{qu^2}{k} \gg D_{\text{eff}}$ das betreffende Intervall der Strömungsgeschwindigkeit als kinetisches Gebiet, im Falle $\frac{qu^2}{k} \approx D_{\text{eff}}$ aber als Übergangsgebiet bezeichnet haben.

transport zwischen Gas- und Sorptionsphase berücksichtigt werden muß, kann ebenfalls eine die Gasfront beschreibende Gleichung abgeleitet werden. Ausgehend von dieser Frontgleichung wäre aber die Berechnung von k und D_{eff} nur schwer durchzuführen. Zu einer einfacheren und auch in der Praxis gut verwendbaren Methode gelangen wir in diesem Falle nur durch Einführung einiger weiterer Vereinfachungen.

Für Konzentrationen und Strömungsgeschwindigkeiten, die unter theoretisch wie auch experimentell mehr oder weniger gut definierbaren Schranken liegen, ergibt sich für die Gasfront die Gleichung einer symmetrischen, durch eine einzige Größe — der Wendepunktstangente φ_m der Kurve — eindeutig definierten S-Kurve. Aus einem bei einer einzigen Strömungsgeschwindigkeit gemessenen φ_m-Wert lassen sich natürlich die unbekannten Parameter D_{eff} und k mit Hilfe der Gleichung

$$\frac{x_0^2}{4\varphi_m} = \frac{D_{\text{eff}}}{qu^2} + \frac{1}{k} \tag{6}$$

(die einen Zusammenhang zwischen der Inflexionstangente und den Versuchsparametern darstellt) noch nicht errechnen. Zweckmäßigerweise verfährt man derart, daß man die bei verschiedenen Strömungsgeschwindigkeiten gemessenen φ_m-Werte in die linke Seite von (6) einsetzt und diese gegen $\frac{1}{qu^2}$ aufträgt. Die Steigung der so erhaltenen Geraden ist gleich dem effektiven Diffusionskoeffizienten, der Ordinatenabschnitt gleich dem Reziprokwert der Transportgeschwindigkeitskonstante.

Die Verwendbarkeit von (6) haben wir schon in einer früheren Veröffentlichung [6] an Hand von experimentellen Daten bewiesen. Trotzdem möchten wir hier unsere früheren Ausführungen durch einige weitere Meßergebnisse ergänzen.

Im Zusammenhang mit den oben erörterten Berechnungsmethoden sei erwähnt, daß sie manche Ähnlichkeiten aufweisen. Bei beiden Methoden wird die Stationarität der Fronten und die Gültigkeit der linearen kinetischen Gleichung vorausgesetzt. Der prinzipielle Unterschied besteht darin, daß für die Methode I die Messungen bei höheren, für die Methode II jedoch die bei mittleren Strömungsgeschwindigkeiten erforderlich sind. Wie wir bewiesen haben [6], kann man bei höheren Strömungsgeschwindigkeiten die frontverbreiternde Wirkung der Längsdiffusion außer acht lassen. Es ist deshalb selbstverständlich, daß im Prinzip und in der Praxis nur die zweite der beiden Methoden zur Bestimmung der effektiven Diffusionskonstante verwendet werden kann.

Es ist nun von Bedeutung, ob nach beiden Methoden innerhalb der experimentellen Fehlergrenzen gleiche Werte für die Transportgeschwindig-

keitskonstante erhalten werden. Wie wir im weiteren zeigen, werden die Auswertungsmethoden in dieser Hinsicht den Erwartungen tatsächlich gerecht.

3. Experimenteller Teil

Der erste Schritt der experimentellen Arbeiten bestand in der Präparierung der zu untersuchenden chromatographischen Trennsäulen. Als Trägermaterial wurden zwei feuerfeste Ziegelsteine gewählt, die in vielen Eigenschaften einander nahestehen, nämlich das ungarische Erzeugnis »Termolit« und »Firebrick 22« englischer Herkunft. Um den Vergleich der mit diesen beiden Trägern gefüllten chromatographischen Säulen auf Grund der gemessenen k- (und D_{eff}-)Werte zu erleichtern, haben wir einige physikalische Daten der Trägermaterialien bestimmt. Von diesen sollen hier die scheinbare und wahre Dichte sowie die aus den bei der Temperatur des siedenden Stickstoffs gemessenen Krypton-Adsorptionsisothermen berechneten spezifischen Oberflächen [7] hervorgehoben werden. Die Daten sind in Tab. I zusammengefaßt

Tabelle I

Physikalische Eigenschaften der Trägermaterialien

Trägermaterial	Dichte [g/cm³]		Spezifische Oberfläche [m²/g]
	scheinbare	wahre	
Termolit	0,683	2,37	4,79
Firebrick-22 ...	0,673	2,55	3,46

Nach Zerkleinerung der Trägermaterialien haben wir einige Siebfraktionen zwischen den Korngrößen von 0,2 bis 0,5 mm ausgesondert, um an Hand von Gleichung (3) zu untersuchen, ob die Eigenschaften der chromatographischen Trennsäule von der Korngröße der Säulenfüllung beeinflußt werden, d. h., ob die Porendiffusion als geschwindigkeitsbestimmender Schritt des Massentransportes betrachtet werden kann.

Als stationäre Phase diente Squalan. Es wurde, in Petroläther gelöst, auf den vorher $2-3^h$ bei 200° C im Vakuum ausgeheitzten Trägern aufgebracht. Im Hinblick auf Gleichung (4) haben wir versucht, verschiedene Schichtdicken der Trennflüssigkeit aufzubringen, indem wir die Träger mit Squalanmengen zwischen 10 und 20 Gew.-% beladen haben. In einigen Fällen haben wir — um eine einheitlichere Bedeckung zu erreichen — Firebrick-22 nach dem Ausheizen bei 80° C mit dampfförmigem Hexamethyldisilasan hydrophobiert.

Um über die Art der Benetzung etwas mehr aussagen zu können, wurde in einigen Fällen die spezifische Oberfläche der schon mit Trennflüssigkeit beladenen Träger bestimmt.* Die spezifischen Oberflächen von mit 9,99%, 14,95% und 20,0% Squalan beladenem Firebrick-22 (Korngröße 0,315—0,4 mm) ergaben sich in der gleichen Reihenfolge zu 1,65, 1,11 und 0,79 m²/g.

Die benutzten Träger wurden in 25 bzw. 50 cm lange Glassäulen mit Durchmessern von 6 bis 10 mm gefüllt. Die wichtigsten Daten der fertig präparierten Säulen sind in Tab. II zusammengefaßt.

Als Trägergas wurde Wasserstoff und als Sorptiv n-Butan in einer durch die Art der Messung gegebenen Konzentration verwendet. Die einheitliche Meßtemperatur war 20° C.

Die eigentliche Messung bestand in der Bestimmung der Kurven Konzentration-Zeit (genauer: Linienschreiberausschlag-Zeit) und der gleichzeitigen Aufnahme der Kurven $W(\tau)-\tau$ mit Hilfe des Guerinschen Seifenmembranströmungsmessers.

* Dabei konnten Lösungseffekte nur geringe Fehler verursachen, da das Squalan bei der Adsorptionstemperatur fest ist. Zwischen der Squalanoberfläche und dem gasförmigen Krypton tritt nur eine physikalische Wechselwirkung auf (die sich sicher von derjenigen zwischen der Oberfläche des Trägers und dem Sorbat unterscheidet.)

Die k- und D_{eff}-Werte wurden aus den Konzentration-Zeit Kurven errechnet. Die $W(\tau)$-τ-Kurven dienten zur Bestimmung der Sorptionskapazität der Füllung, des Totraumes, der Ausgangskonzentration des n-Butans und der Strömungsgeschwindigkeit.

Die frontalgaschromatographische Apparatur, die Messung selbst und die Ausführung der Berechnungen haben wir bereits in mehreren früheren Publikationen [8, 9] beschrieben, so daß hier auf eine Wiederholung verzichtet werden kann.

4. Meßergebnisse und ihre Bewertung

a) *Über die Zuverlässigkeit der Auswertungsmethoden*

Um die Verwendbarkeit der Auswertungsmethoden in der Praxis zur Bestimmung von k und D_{eff} zu demonstrieren, sollen einige diesbezügliche Meßergebnisse vor unseren eigentlichen Ausführungen angegeben werden.

Zuerst möchten wir zeigen, daß zwischen den Größen x_0 und φ_m tatsächlich Gleichung (6) entsprechend, eine lineare Abhängigkeit besteht. Zu diesem Zwecke formen wir (6) um in:

$$x_0^2 = \frac{4}{qu^2}\left(D_{\text{eff}} + \frac{k}{qu^2}\right) \cdot \varphi_m \tag{7}$$

Mit Hilfe dieser Gleichung kann bei Kenntnis der auf der rechten Seite stehenden Größen die Ausgangskonzentration berechnet werden. Die zur Berechnung notwendigen, von der Konzentration unabhängigen Parameter D_{eff}, k und q sind aus separaten Messungen zu entnehmen.

Die diesbezüglichen experimentellen Untersuchungen haben wir mit der Säule 3 (s. Tab. II) ausgeführt. Die Ergebnisse sind in Tab. III zusammengefaßt, in der die manometrisch eingestellte Ausgangskonzentration x_0 für die n-Butan-H_2-Gemische, die aus den Durchbruchskurven ermittelten Steigungen φ_m der Inflexionstangenten und die dazugehörigen stationären Frontwanderungsgeschwindigkeiten u sowie die mit Hilfe der Gleichung (7) unter Benutzung der Parameter $D_{\text{eff}} = 0{,}18$ cm^2/sec, $k = 0{,}38$ sec^{-1} und $q = 6{,}33$ errechneten x_0-Werte angegeben sind. In der letzten Spalte der Tab. III sind die Differenzen der Quadrate der so berechneten und der manometrisch eingestellten Ausgangskonzentrationen angeführt. Diese Differenzen sind in allen Fällen geringer als der Fehler der Methode. Die linke Seite von (6) ist — bei Beibehaltung der für die Gültigkeit dieser Gleichung notwendigen Voraussetzungen — praktisch unabhängig von der Ausgangskonzentration des Sorptivs im Trägergas.

Im Zusammenhang mit der bereits aufgeworfenen Frage der Gleichwertigkeit der beiden angegebenen Auswertungsmethoden werden in Tab. IV einige mit den Säulen 4, 5 und 7 (s. Tab. II) erhaltenen Meßergebnisse angeführt, um zu beweisen, daß die für eine gegebene Säule im kinetischen und im Übergangsgebiet der Strömungsgeschwindigkeit ermittelten k-Werte gleich sind. Es sei bemerkt, daß im Falle der Säule 5 die Abweichungen der Transport-

Tabelle II

D_{eff}-, k- und andere Kennwerte verschiedener chromatographischer Säulen

Versuchsreihe	Säulen Nr.	Träger-material	Korngröße [mm]	Squalan-gehalt [Gew.-%]	L [cm]	s [ml/cm]	m [g/cm]	$\frac{a_0}{x_0}$ [ml/g]	q	D_{eff} [cm²/s]	k [s⁻¹]
I	1	Termolit	0,2 —0,4	15,02	28,8	0,372	0,041	59,1	6,50	0,16	0,42
	2	Termolit	0,2 —0,4	15,02	28,8	0,372	0,041	57,4	6,33	0,18	0,38
	3	Termolit	0,2 —0,4	14,9	25,0	0,344	0,037	56,8	6,11	0,17	0,38
II	4	Firebrick-22	0,2 —0,25	15,05	25,0	0,367	0,031	58,83	5,02	0,16	0,77
	5	Firebrick-22	0,315—0,4	14,96	24,8	0,379	0,031	60,56	4,96	0,16	0,82
	6	Firebrick-22	0,315—0,4	14,96	49,9	0,332	0,029	57,6	5,02	0,20	0,71
	7	Firebrick-22	0,4 —0,5	15,03	25,0	0,365	0,033	58,4	5,22	0,16	0,75
III	8	Firebrick-22	0,315—0,4	9,99	49,8	0,371	0,020	58,2	3,19	0,17	0,65
	9	Firebrick-22	0,315—0,4	9,99	49,8	0,345	0,019	59,4	3,22	0,20	0,69
	10*	Firebrick-22	0,315—0,4	10,01	50,0	0,392	0,020	58,7	3,07	0,18	0,75
	5	Firebrick-22	0,315—0,4	14,96	24,8	0,379	0,031	60,56	4,96	0,16	0,82
	6	Firebrick-22	0,315—0,4	14,96	49,9	0,332	0,029	57,6	5,02	0,20	0,71
	11	Firebrick-22	0,315—0,4	20,00	25,0	0,360	0,043	57,86	6,90	0,17	0,61
	12	Firebrick-22	0,315—0,4	20,00	24,7	0,360	0,047	58,39	7,68	0,15	0,57
	13	Firebrick-22	0,315—0,4	20,00	50,0	0,342	0,045	58,78	7,68	0,19	0,51
	14*	Firebrick-22	0,315—0,4	20,01	24,7	0,336	0,046	51,20	6,97	0,19	0,64

* hydrophobierte Träger.

Tabelle III

Vergleich der aus den Inflexionstangenten der Durchbruchskurven berechneten und manometrisch eingestellten Werte der Ausgangskonzentrationen

x_0 (manometrisch)	$x_0^2 \cdot 10^2$	$\varphi_m \cdot 10^4$ [s⁻¹]	u [cm/s]	$x_{\vee,r}$ (rechnerisch)	$x_{0,r}^2 \cdot 10^2$	$\lvert x_{0,r}^2 - x_0^2 \rvert \cdot 10^2$
0,099	0,98	5,15	0,0564	0,114	1,30	0,32
0,161	2,59	8,25	0,0542	0,153	2,34	0,25
0,163	2,66	8,97	0,0570	0,173	2,99	0,33
0,207	4,28	12,14	0,0570	0,210	4,41	0,13
0,227	5,15	12,28	0,0550	0,233	5,43	0,28
0,274	7,51	15,25	0,0542	0,274	7,51	0,00
0,285	8,12	17,66	0,0546	0,293	8,58	0,46
0,322	10,32	22,40	0,0586	0,323	10,43	0,06

geschwindigkeitskonstanten von dem wahrscheinlich reellen Wert von 0,6 noch innerhalb der Meßfehler liegen.

Da es prinzipiell nicht möglich ist, effektive Diffusionskonstanten mit der Methode I zu bestimmen, werden im folgenden nur nach der Methode II erhaltene Meßergebnisse angeführt.

Tabelle IV

Vergleich der im kinetischen und Übergangsgebiet der Strömungsgeschwindigkeit gemessenen k-Werte in Abhängigkeit vom Squalangehalt des Trägers

Squalangehalt [Gew.-%]	Transportgeschwindigkeitskonstante k [s^{-1}]	
	Übergangsgebiet	Kinetisches Gebiet
10,01	0,75	0,78
14,96	0,71	0,53
20,00	0,51	0,48

b) *Untersuchung und Vergleich von chromatographischen Trennsäulen auf Grund der gemessenen k- und D_{eff}-Werte*

Nach dem in der Einleitung Gesagten ist es nicht schwer, einzusehen, daß zum Vergleich chromatographischer Trennsäulen die effektive Diffusions- und die Transportgeschwindigkeitskonstante herangezogen werden können. Im folgenden soll nun über die Meßergebnisse berichtet werden, die eine Aussage über die Struktur des Ölfilmes und den geschwindigkeitsbestimmenden Schritt der Sorption zulassen.

Wir haben für verschiedene chromatographische Säulen die k- und D_{eff}-Werte bestimmt und in Tab. II mit angegeben. In dieser Tabelle sind die Trennsäulen derart angeordnet, daß man leicht Schlüsse auf die Qualität des Trägers (Versuchsreihe I und II), auf den Einfluß der Korngröße (Versuchsreihe II) und auf die Schichtdicke der Trennflüssigkeit (Versuchsreihe III) ziehen kann.

Zuerst wollen wir uns mit der Frage befassen, ob ein merklicher Unterschied in den chromatographischen Eigenschaften der Säulen bei Verwendung von Termolit und Firebrick-22 als Träger besteht. Werden die in Tab. II für die mit Termolit (Versuchsreihe I) und Firebrick-22 (Versuchsreihe II) gefüllten Säulen gleicher Länge angegebenen Werte miteinander verglichen, so stellt man fest, daß die effektiven Diffusionskonstanten praktisch gleich sind, während der Wert der Transportgeschwindigkeitskonstanten bei Verwendung von Firebrick-22 etwa doppelt so groß wie der bei Verwendung von Termolit ist. Die Gleichheit der effektiven Diffusionskonstanten war zu erwarten und bedarf keiner weiteren Erklärung. Es ist jedoch notwendig, der Ursache für die Verschiedenheit der Transportgeschwindigkeitskonstanten weiter nachzugehen, zumal es auf den ersten Blick widersprüchlich erscheint, daß für den Träger mit größerer spezifischer Oberfläche eine geringere Transportgeschwindigkeitskonstante erhalten wird. Dieser Befund läßt sich zunächst weder mit der Annahme der Porendiffusion [Gleichung (3)] noch mit der der Sorption in der stationären Phase [Gleichung (4)] als geschwindigkeitsbestimmenden Schritt erklären.

Bevor wir versuchen, diesen Befund zu deuten, soll kurz auf den in der gaschromatographischen Praxis oft vorkommenden, sog. »Verstopfungseffekt« eingegangen werden. Die spezifischen Oberflächen der benutzten Träger (s. voranstehendes Kapitel) zeigen, daß eine bedeutende Abnahme der Oberflächengröße schon bei Beladung mit relativ geringen Squalanmengen eintritt. Dies weist darauf hin, daß schon geringste Flüssigkeitsmengen zur Verstopfung der Poren geringsten Durchmessers führen, wobei auch diejenigen mit größeren Durchmessern verschlossen werden können, die einen engeren »Eingang« aufweisen. Bringt man größere Flüssigkeitsmengen auf den Träger, so ist mit einer weiteren, aber nicht mehr so stark ausgeprägten Abnahme der Oberfläche zu rechnen. In diesem Stadium der Bedeckung sind wahrscheinlich schon alle engeren Poren des Trägers mit Flüssigkeit angefüllt.

Die Werte der spezifischen Oberflächen der beladenen Träger lassen die Schlußfolgerung zu, daß Termolit mehr, aber engere Poren als Firebrick-22 hat (s. Tab. I). Je kleiner die durchschnittliche Größe der Poren ist, mit umso größerer Wahrscheinlichkeit tritt der vorhin erwähnte Verstopfungseffekt auf. Das heißt mit anderen Worten, daß im Falle des an Mikro- und Durchgangsporen reicheren Termolits zahlenmäßig mehr Poren verstopft werden als bei Firebrick-22, daß also bei gleichen Beladungen die spezifische Oberfläche von Termolit geringer ist als die von Firebrick-22. Die unmittelbare Folge dieses Verstopfungseffektes ist aber, daß die durchschnittliche Schichtdicke der Trennflüssigkeit auf Termolit größer ist als auf Firebrick-22. Die geringeren Transportgeschwindigkeiten bei Termolit finden also ihre Erklärung, wenn man die Sorption in der flüssigen Phase nach (4) als geschwindigkeitsbestimmenden Schritt annimmt.

Im weiteren befassen wir uns ausschließlich mit dem Träger Firebrick-22. Aus Versuchsreihe II der Tab. II ist zu ersehen, daß die Streuung der Transportgeschwindigkeitskonstanten bei Verwendung von mit 15% Squalan beladenen Trägern unterschiedlicher Korngröße keinen Gang zeigt. Die k-Werte hängen also von der Korngröße nicht merklich ab. In Versuchsreihe III sind die Ergebnisse für Träger gleicher Korngröße, aber unterschiedlichem Beladungsgrad enthalten. Trotz der unregelmäßigen Streuung der Meßwerte geht daraus klar hervor, daß die Transportgeschwindigkeitskonstanten bei 20%iger Beladung am geringsten sind.

Wird für D_f ein Wert von 10^{-7} cm^2/sec angenommen, so ergibt sich mit den gemessenen Transportgeschwindigkeitskonstanten für die Schichtdicke aus (4) ein Wert von 10^{-3} cm. Dies entspricht ungefähr den Erwartungen. Eine quadratische Abhängigkeit der k-Werte von der Schichtdicke konnten wir allerdings nicht feststellen, was wohl darauf zurückzuführen ist, daß die Träger im allgemeinen nicht gleichmäßig benetzt werden [10].

Mit steigender Squalanmenge verändert sich wahrscheinlich die Schichtdicke kaum und nur die Größe der an der Oberfläche des Trägers sich ausbildenden »Flüssigkeitsinseln« bzw. Tröpfchen nimmt zu, d. h., daß die Geschwindigkeit des Transportes nicht oder nur unbedeutend beeinflußt wird. Im Zusammenhang mit dieser Frage soll noch folgendes erwähnt werden. Bei relativ geringen, auf den Träger aufgebrachten Flüssigkeitsmengen werden die Mikro- und Durchgangsporen anscheinend schon vollständig verstopft bzw.

angefüllt. Dadurch nimmt zwar, wie wir gezeigt haben, die spezifische Oberfläche der beladenen Träger bedeutend ab, das noch leere Porenvolumen ändert sich jedoch kaum, da das Volumen dieser beiden Typen von Poren nur ein Bruchteil des Gesamtporenvolumens ist. Der größte Teil der Trennflüssigkeit liegt also als Flüssigkeitsinseln bzw. Tröpfchen an den Wänden der Makroporen vor. Bringt man weitere Mengen der Trennflüssigkeit auf den Träger, so nimmt zunächst nur das Verhältnis von bedeckter zu freier Makroporenoberfläche zu. Da aber diese beschränkt ist, muß von einer mehr oder weniger gut definierten Sättigung an mit steigendem Ölgehalt auch die Filmdicke zunehmen und nach (4) zu einer Abnahme der k-Werte führen. Die für verschiedene Beladungsgrade experimentell bestimmten k-Werte (Versuchsreihe III in Tab. II) stimmen mit diesen Überlegungen überein.

In Tab. II sind auch die gemessenen effektiven Diffusionskonstanten angeführt. Bei gleichen Säulenlängen ergeben sich unabhängig von der Art, Korngröße und Beladung des Trägers praktisch gleiche Werte. Es fällt jedoch auf, daß die bei 50 cm Säulenlänge gemessenen D_{eff}-Werte größer als die bei 25 cm sind. Dieser Effekt kann teilweise dadurch eine Erklärung finden, daß bei niedrigeren Squalangehalten und den angewandten Strömungsgeschwindigkeiten die Stationarität der Fronten in kürzeren Säulen noch nicht vollständig erreicht werden kann.

Auf Grund der qualitativen Analyse der experimentell bestimmten Transportgeschwindigkeitskonstanten liegt letzten Endes die Vermutung nahe, daß die Geschwindigkeit des Massentransportes in der Gas-Flüssigkeits-Verteilungschromatographie von der Sorption in der Trennflüssigkeit als dem langsamsten Schritt bestimmt wird. Die Meßwerte weisen darauf hin, daß wahrscheinlich bei geringeren Beladungen kein zusammenhängender Film an der Oberfläche der Träger gebildet wird. Da die hydrophobierten Träger (Säulen 10 und 14 in Tab. II) praktisch die gleichen k-Werte ergeben, läßt sich eine einheitlichere Benetzung durch chemische Behandlung der Trägeroberflächen, wenigstens im Falle des Systems Squalan-Firebrick-22, nicht erzwingen.

SYMBOLE

a (z, τ) [ml/g oder n-ml/g]: in einem gegebenen Querschnitt der chromatographischen Säule auf die Mengeneinheit der aktiven Füllung bezogene durchschnittliche Gasmenge als Funktion von z und τ

a_0 [ml/g]: zur Ausgangskonzentration x_0 gehörige, auf die Mengeneinheit der aktiven Füllung (bei Adsorptionschromatographie: des Adsorbens; bei Verteilungschromatographie: der Trennflüssigkeit) bezogene sorbierte Gleichgewichtsmenge

A [ml/ml]: Steigung der linearen Sorptionsisotherme

c_0 $(\equiv v/s)$ [cm/s]: konstante lineare Geschwindigkeit der Gaszuführung

D_b [cm²/s]: Porendiffusionskonstante

D_{eff} $\left(\equiv \frac{s_0}{s} \varkappa D_g\right)$ [cm²/s]: effektive Diffusionskonstante im Gasraum der Säule

D_f [cm^2/s]: Diffusionskonstante in der Trennflüssigkeit
D_g [cm^2/s]: gewöhnliche Diffusionskonstante
k [s^{-1}]: Transportgeschwindigkeitskonstante
L [cm]: Trennsäulenlänge
m [g/cm]: Menge der aktiven Füllung pro Längeneinheit der Säule
$q \left(\equiv \frac{m}{s}\frac{a_0}{x_0}\right)$: der dimensionslose, von Temperatur und Säulenfüllung abhängige Verteilungskoeffizient der sorbierbaren Komponente
s [ml/cm]: Totraum der Säule (Porenvolumen + Kornzwischenraum) pro Längeneinheit der Säule
s_0 [ml/cm]: Kornzwischenvolumen pro Längeneinheit
u [cm/s]: Lineargeschwindigkeit der stationären Fronten
$w(z, \tau)$ [ml/s]: Volumengeschwindigkeit der Gasströmung als Funktion von z und τ
z [cm]: Längskoordinate
$x(z, \tau)$ [ml/ml]: durchschnittliche Konzentration des Sorptivs in einem gegebenen Querschnitt der Säule als Funktion von z und τ
x_0 [ml/ml]: konstante Konzentration des Sorptivs in der Gaszuführung
$\alpha \left(\equiv \frac{m}{s}a\right)$: dimensionsloser Wert für die sorbierte Menge
$\varepsilon \left(\equiv \frac{D_b}{\varrho_0^2}\right)$ [s^{-1}]: für die Geschwindigkeit des Massentransportes charakteristischer Parameter
ϱ_0 [cm]: Kornradius
$\varphi_m = \left|\left(\frac{dx}{d\tau}\right)_{\substack{z=L \\ x=x_0/2}}\right|$: Wendepunktstangente der Durchbruchskurve
ν [cm]: Schichtdicke der Trennflüssigkeit
τ [sec]: Zeitkoordinate
$\varkappa$: Labyrinthfaktor

ZUSAMMENFASSUNG

Unsere Versuchsergebnisse bestätigen die Zuverlässigkeit der schon in einer früheren Mitteilung beschriebenen Methode zur Bestimmung von effektiven Diffusionskonstanten und Transportgeschwindigkeitskonstanten aus im sog. Übergangsgebiet der Strömungsgeschwindigkeit ausgeführten frontalchromatographischen Messungen. Die auf diese Weise und aus im kinetischen Gebiet ausgeführten Messungen erhaltenen Transportgeschwindigkeitskonstanten stimmen überein.

Chromatographische Trennsäulen werden durch die Transportgeschwindigkeits- und effektiven Diffusionskonstanten bewertet und charakterisiert. Die Versuchsergebnisse lassen die Schlüsse zu, daß die Sorptionsgeschwindigkeit in der flüssigen Phase der transportgeschwindigkeitsbestimmende Schritt ist und die Trennflüssigkeit bei geringeren Beladungsgraden die Trägeroberfläche nicht gleichmäßig bedeckt, also »Flüssigkeitsinseln« vorliegen.

LITERATUR

1. Beyer, H., Fejes, P., Schay, G., Varga, K.: Acta Chim. Hung. **47,** 13 (1966).
2. Fejes, P., Fromm-Czárán, E., Schay, G.: Acta Chim. Hung. **33,** 87 (1962).
3. Fejes, P., Fromm-Czárán, E.: Acta Chim. Hung. **29,** 172 (1961).
4. Glueckauf, E.: J. chem. Soc. London **1947,** 1302.
5. Fejes, P., Schay, G.: Acta Chim. Hung. **17,** 377 (1958).
6. Fejes, P., Pethő, Á.: Acta Chim. Hung. **43,** 221 (1965).
7. Király, J.: Magy. Kém. F. **68,** 78 (1962).
8. Fejes, P., Schay, G.: Acta Chim. Hung. **14,** 439 (1958).
9. Schay, G., Fejes, P., Halász, I., Király, J.: Acta Chim. Hung. **11,** 381 (1957).
10. Schay, G., Székely, Gy., Rácz, Gy., Traply, G.: Periodica Polytechn. Budapest, Chem.-Serie, **2,** 1 (1958).

Recent Investigations on Frontal Gas Chromatography, on Taking into Account the Variations of Flow Rate during Sorption, IV

Characterization of Packed Chromatographic Columns on the Basis of Mass Transport Velocity and Diffusion Constants Measured by Frontal Gas Chromatography

K. VARGA, P. FEJES and H. BEYER

Summary. Our experimental results confirmed the reality of an earlier published method which allows to determine the effective diffusion constants and the mass transport velocity constants from frontal chromatographic data, measured in the transition region of flow rate. These mass transport velocity constants agreed with those determined by measurements in the kinetic region of flow rate.

Chromatographic columns are characterized by the effective diffusion constants and the constants of mass transport velocity. The experimental results suggest that the sorption rate in the liquid phase is the velocity-determining factor and that in the case of little low degrees of coatedness the stationary liquid is not uniformly distributed on the surfaces of the supports indicating the existence of "liquid islands".

Новые исследования в области фронтальной газовой хроматографии с учетом изменений в скорости потока в процессе сорбции. IV.

Сравнение хроматографических колони на основе величин констант скоростей транспорта и диффузии, измеренных фронтальным методом

К. ВАРГА, П. ФЕЙЕШ и Х. БЕЙЕР

Резюме. Результаты измерений доказали надежность метода, опубликованного авторами ранее. Этот метод дает возможность определения константы эффективной диффузии и константы скорости транспорта из данных фронтальной хроматографии, измеренных в переходной области скорости потока. Полученные таким путем константы хорошо согласуются с константами скорости транспорта, полученными методом, действительным в кинетической области.

Хроматографические колонны авторы характеризуют константой эффективной диффузии и константой скорости транспорта. Экспериментальные результаты показали, что сорбция, идущая в жидкой фазе, является процессом, определяющим скорость транспорта. Далее, данные показали, что в случае низкой насыщенности разделительная жидкость не равномерно распределяется по поверхности носителя, т. е. образует «островки» жидкости.

Károly VARGA
Dr. Pál FEJES
Dr. Hermann BEYER
Budapest II. Pusztaszeri út 57/69.

MAGNETIC AND SPECTROSCOPIC INVESTIGATION OF POLYNUCLEAR COMPLEX CYANIDES

J. CSÁSZÁR and A. FELVÉGI

(Institute of General and Physical Chemistry of the University, Szeged)

Received July 1, 1965

Cyanides of transition metals belong to the most stable complex molecules. Their preparation is very convenient and they have been much studied both practically and theoretically.

It is well known that $K_4[Fe(CN)_6]$ and $K_3[Fe(CN)_6]$ form nearly insoluble complexes with the ions of Cu(II), Ni(II) or Fe(III). The best known representatives of these polynuclear cyanides are the Turnbull and Prussian blue. Such complex molecules have not been studied extensively, with the exception of the mentioned iron cyanides.

The present communication reports the results of a study on the magnetic and spectroscopic properties of some double cyanides.

Experimental

Preparation of the compounds

The chemicals used in this investigation were of analytical purity. The preparation of $K_3[Co(CN)_6]$, $K_2[Ni(CN)_4]$ and $K_2[Pt(CN)_4]$ followed the procedures reported in the literature [1, 2]. The double cyanides were prepared from the aqueous solutions of the complex cyanides and metal chlorides. The nearly insoluble products were filtered off or centrifuged, washed with distilled water until free of ions, and dried over P_2O_5. The identity and purity of the dry compounds were checked by analysis of the metal content [3]. The formulas, colours and analyses of the prepared compounds are listed in Table I.

It is known [4] that mixing of equimolar amounts of, *e.g.* Fe(III) and $[Fe(CN)_6]^{4-}$ or Fe(II) and $[Fe(CN)_6]^{3-}$ gives $KFe[FeCN)_6]$ or, in the case of nickel with excess of $[Fe(CN)_6]^{3-}$, $KNi_4[Fe(CN)_6]_3$ is formed. In order to avoid every chance of uncertainty, the metallic salt was used in small excess in all cases.

Magnetic measurements

Magnetic susceptibility measurements were carried out in an inhomogeneous magnetic field with a field strength of about 7 900 Gauss, according to Gouy's method, at room temperature. For the determination of the field strength $Hg[Co(SCN)_4]$ ($\chi_M = 16.17 \cdot 10^{-6}$ [5]) and $[NiEn_3]S_2O_3$ ($\chi_M = 10.82 \cdot 10^{-6}$ [5]) were used as standards. Molar susceptibility corrections were made using the Pascal constants [6]. The calculated and measured BM values of the cyanides and of the prepared polynuclear complexes are shown in Table II.

Table I

Compounds	Colour	Metal content	
		calcd.	found
$KCo[Fe(CN)_6]$	Violet	18.0*	17.75
$KCo[Co(CN)_6]$	Pink	37.6**	37.48
$Co[Ni(CN)_4]$	Pink	26.4*	26.29
$Co[Pt(CN)_4]$	Brownish-red	16.4**	16.42
$[Co(NH_3)_6][Fe(CN)_6]$	Orange	14.9*	14.81
$[Co(En)_3][Fe(CN)_6]$***	Orange	12.6*	12.46
$[Co(NH_3)_6]_4[Fe(CN)_6]_3$	Buff	12.17*	12.08
$[Co(En)_3]_4[Fe(CN)_6]_3$***	Buff	11.2*	11.06
$Ni_3[Fe(CN)_6]_2$	Buff	29.8**	29.68
$Ni_2[Fe(CN)_6]$	Grass-green	35.6**	35,62
$KNi[Co(CN)_6]$	Light blue	18.7**	18.44
$Ni[Pt(CN)_4]$	Light blue	16.4**	16.31
$K_2Cu[Fe(CN)_6]$	Red-brown	17.9**	17.62
$KCu[Co(CN)_6]$	Greenish-blue	20.0**	19.78
$Cu[Pt(CN)_4]$	Greenish-blue	17.5**	17.38

* metal content of the complex anions
** metal content of the ionic metals
*** En = ethylenediamine

Spectroscopic investigations

The absorption spectra of the aqueous solutions of the simple cyanide complexes were measured by a Beckman DU spectrophotometer in the range of 1250 — 340 mμ at room temperature using quartz cells of 1.00, 0.1 and 0.01 cm. Reflection spectra of the polynuclear cyanides were obtained with the same instrument equipped with the standard reflection attachment, using MgO as a standard. All samples were finely ground in an agate mortar and dried prior to filling into the holder. If it was necessary to dilute the sample with MgO, n each case the validity of the Kubelka-Munk function [7, 8] was checked.

Experimental results and their interpretation

Spectrum of cations. On the basis of group-theoretical and quantum mechanical data, the magnetic and spectral properties of the Fe(III), Co(II), Ni(II) and Cu(II) ions and of their ion hydrates can be established as follows.

The spectrum of the iron(III) ($[Ar]d^5$) hexahydrate is well known [9, 10]. The ^6S ground state does not split in any case of symmetry, thus light absorption may produce electron transition only between the sextet ground term and the quartet levels with higher energy. All absorption bands must correspond therefore to spin-forbidden transitions, and this fact is reflected in the very low extinction coefficient for these bands [9]. Complexes of the

Table II

Magnetic properties of polynuclear cyanides

Compound	Hybridization in anions	No. of unpaired electrons	Calcd. spin* values	Measured BM values
$K_3[Fe(CN)_6]$	d^2sp^3	1	1.73	2.43
$K_4[Fe(CN)_6]$	d^2sp^3	0	0	0
$K_3[Co(CN)_6]$	d^2sp^3	0	0	0
$K_2[Ni(CN)_4]$	dsp^2	0	0	0
$K_2[Pt(CN)_4]$	dsp^2	0	0	0
$Fe_4[Fe(CN)_6]_3$	d^2sp^3	5	5.92	5.75
$Fe^{2+} + [Fe(CN)_6]^{3-}$	d^2sp^3	5	5.92	5.66
$[Co(NH_3)_6][Fe(CN)_6]$	d^2sp^3	1	1.73	2.48
$[Co(En)_3][Fe(CN)_6]$	d^2sp^3	1	1.73	2.43
$[Co(NH_3)_6]_4[Fe(CN)_6]_3$	d^2sp^3	0	0	0
$[Co(En)_3]_4[Fe(CN)_6]_3$	d^2sp^3	0	0	0
$KCo[Fe(CN)_6]$	d^2sp^3	4	4.90	4.61
$KCo[Co(CN)_6]$	d^2sp^3	3	3.88	4.64
$Co[Ni(CN)_4]$	dsp^2	3	3.88	3.64
$Co[Pt(CN)_4]$	dsp^2	3	3.88	3.76
$Ni_3[Fe(CN)_6]_2$	d^2sp^3	3	3.88	5.20
$Ni_2[Fe(CN)_6]$	d^2sp^3	2	2.83	3.12
$KNi[Co(CN)_6]$	d^2sp^3	2	2.83	3.08
$Ni[Pt(CN)_4]$	dsp^2	2	2.83	3.18
$K_2Cu[Fe(CN)_6]$	d^2sp^3	1	1.73	1.86
$KCu[Co(CN)_6]$	d^2sp^3	1	1.73	1.91
$Cu[Pt(CN)_4]$	dsp^2	1	1.73	1.88

* The only spin values were calculated with the equation: $\mu = \sqrt{4\,S(S+1)}$

weak- and strong-field ligands are paramagnetic with five and one electrons, respectively.

The ground state of the Fe(II) ion ($[Ar]d^6$) is ^5D. In the absorption spectrum of $[Fe(H_2O)_6]^{2+}$ a broad band of medium intensity has been found [10—12] at about 10,000 cm^{-1}, which is assigned to the transition $^5T_{2g} \rightarrow {}^5E_g$. FURLANI [11] pointed out that other Fe(II) complexes formed by ligands of weak field also have similar spectral structures. Hydrated ion and other high spin complexes are paramagnetic, with about 4.9 BM, while low spin complexes are diamagnetic.

The ground state of the Co(II) ion, having an $[Ar]d^7$ electron configuration, is ^4F. This ground term in a cubic field splits into three levels: $^4T_{1g}$, $^4T_{2g}$ and $^4A_{2g}$, therefore — taking into consideration the excited state, ^4P,

located at about 14,500 cm^{-1} — the three bands to be expected in the spectrum of $[Co(H_2O)_6]^{2+}$ may be identified with the transitions $^4T_{1g}(F) \rightarrow {}^4T_{2g}(F)$, $^4A_{2g}(F)$, $^4T_{1g}(P)$. One band can be found at 8,350 cm^{-1} and a band system at about 20,000 cm^{-1} [13—15]. Corresponding to the three unpaired electrons, the complexes of cubic symmetry have a magnetic moment of BM $\sim$ 4.8, while the tetrahedral complexes, due to changes in orbital contribution, are paramagnetic with BM 3.8.

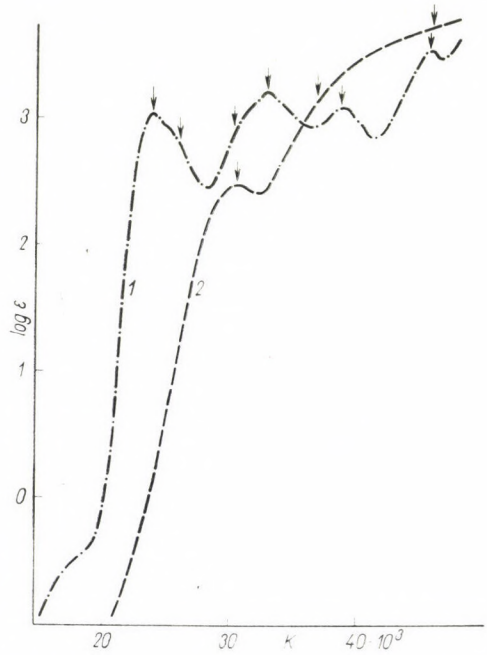

Fig. 1. Absorption spectra of $[Fe(CN)_6]^{3-}$ (—.—.—) and $[Fe(CN)_6]^{4-}$ (— — — — —) in aqueous solution

The ^3F ground state of the Ni(II) ion ($[Ar]d^8$) splits into three levels in an octahedral field. Taking into consideration the next triplet ^3P state, the three well-defined sharp bands at 8,500, 13,500 and 25,300 cm^{-1} [16—18] in the spectrum of the hydrated ion can be assigned to the transitions $^3A_{2g}(F) \rightarrow$ $\rightarrow {}^3T_{2g}(F)$, $^3T_{1g}(F)$, $^3T_{1g}(P)$. Sixfold coordinated and tetrahedral complexes are paramagnetic with a magnetic moment of about 2.9 and 4.1 BM, respectively.

The Cu(II) ion has $[Ar]d^9$ electron configuration. Its ground state (^2D) splits into two sublevels in a cubic field, thus the only complex wide band appearing in the visible spectrum of the hydrated ion can be assigned to the transition $^2E_g \rightarrow {}^2T_{2g}$ [19]. The calculated BM value is 1.73, and values measured with different compounds also vary between 1.70 and 2.1 BM.

Table III

Characteristic frequencies of mononuclear complex cyanides

Compound	Band position		Assignment
	mμ	kK	
$K_4[Fe(CN)_6]$	323	31.0	$^1A_{1g} \rightarrow {}^1T_{1g}$
	~270	~37.0	$\rightarrow {}^1T_{2g}$
	~218	~45.9	$\rightarrow {}^1T_{1u}$
$K_3[Fe(CN)_6]$	420	23.8	$^2T_{2g} \rightarrow {}^1T_{2g}$
	~384	~26.0	$\rightarrow {}^6A_1$
	~329	~30.4	$\rightarrow {}^2A_{2g}$
	302	33.1	$\rightarrow$?
	258	38.8	$\rightarrow {}^2E_g$
	214	45.7	$\rightarrow {}^2A_{1g}$
$K_3[Co(CN)_6]$	312	32.1	$^1A_{1g} \rightarrow {}^1T_{1g}$
	260	38.5	$\rightarrow {}^1T_{2g}$
	~205	~48.8	$\rightarrow {}^1T_{1u}$
$K_2[Ni(CN)_4]$	~444	~22.5	$^1A_{1g} \rightarrow {}^1A_{2g}$
	~330	~30.3	$\rightarrow {}^1B_{1g}$
	311	32.2	$\rightarrow {}^1B_u$
	284	35.2	$\rightarrow {}^1A_{2u}$
	266	37.6	$\rightarrow {}^1E_u$
$K_2[Pt(CN)_4]$	280	35.7	$^1A_{1g} \rightarrow {}^1B_{1u}$
	~258	~38.7	$\rightarrow {}^1E_u$
	255	39.2	$\rightarrow {}^1E_u$
	~242	~41.4	$\rightarrow {}^1A_{2u}$

~ shoulder

The positions of the above-discussed d—d bands are represented by arrows on the figures of the reflection spectra of the corresponding cyanides.

Spectra of the complex anions. The excitation processes of transition metal cyanides have been studied in detail by LIEHR [20], BÁN [21], BÁN and GILDE [22], Japanese authors [23], and by many others.

A detailed analysis of the spectrum of $[Fe(CN)_6]^{3-}$ has given by NAIMAN [24]. From the $^2T_{2g}$ ground state numerous transitions are possible to the neighbouring doublet, quartet and sextet states. Characteristics of the high-intensity bands to be found in the spectrum of the aqueous solutions of the complex ions (Fig. 1), as well as band assignments are summarized in Table III.

In the absorption curve of $[Fe(CN)_6]^{4-}$ (Fig. 1) two d—d bands are found at 31,000 and 37,400 cm^{-1} belonging to the transitions $^1A_{1g} \rightarrow {}^1T_{1g}$

Table IV

Compound	Band position in kK			
$[Fe(H_2O)_6]^{2+}$	~10.0[a]	—	—	—
$Fe_4[Fe(CN)_6]_3$	14.5	—	~21.0	—
$[Fe(H_2O)_6]^{3+}$[b]	—	—	—	—
$Fe^{3+} + [Fe(CN)_6]^{4-}$[c]	~11.4	13.8	~20.0	—
$[Co(H_2O)_6]^{3+}$[d]	—	16.6	—	—
$[Co(NH_3)_6]^{3+}$[d]	—	—	21.1	—
$[Co(NH_3)_6]_4\ [Fe(CN)_6]_3$	—	~15.9	23.9	—
$[Co(NH_3)_6][Fe(CN)_6]$	—	~20.1	23.6	—
$[Co(En)_3]^{3+}$[d]	—	21.3	—	—
$[Co(En)_3]_4\ [Fe(CN)_6]_3$	—	—	22.8	—
$[Co(En)_3][Fe(CN)_6]$	—	19.8	23.5	—
$[Co(H_2O)_6]^{2+}$	8.4	~17.8	20.0	—
$KCo[Fe(CN)_6]$	~10,0	18.9	~20.8	25.7
$KCo[Co(CN)_6]$	8.8	20.0	—	~26.4
$Co[Ni(CN)_4]$	9.1	15.3	20.0	—
$Co[Pt(CN)_4]$	~ 9.0	~17.4	~22.6	26.0
$[Ni(H_2O)_6]^{2+}$	8.8	14.5	25.3	—
$Ni_3[Fe(CN)_6]_2$	10.3	~19.0	25.2	—
$Ni_2[Fe(CN)_6]$	9.5	16.1	~24.6	—
$KNi[Co(CN)_6]$	10.2	16.9	27.5	—
$Ni[Pt(CN)_4]$	8.9	15.0	25.5	—
$[Cu(H_2O)_6]^{2+}$[e]	—	12.6	—	—
$K_2Cu[Fe(CN)_6]$	—	~13.6	20.2	—
$KCu[Co(CN)_6]$	~10.2	14.1	—	—
$Cu[Pt(CN)_4]$	~11.1	13.7	—	—

[a] very broad band; [b] only spin-forbidden bands of low intensity can be observed; [c] the precipitate was investigated; [d] the $^1A_1 \rightarrow {}^1T_2$ band was not determined by reflection; [e] broad complex band; ~ shoulder.

and $^1A_{1g} \rightarrow {}^1T_{2g}$, respectively, and one high charge transfer band [25] appears in the ultraviolet, at approx. 46,000 cm^{-1}. In the case of the $[Co(CN)_6]^{3-}$ complex, the same two d—d bands appear separately and at a somewhat higher frequency (Fig. 2).

The molecular orbitals of the square-planar $[Ni(CN)_4]^{2-}$ and $[Pt(CN)_4]^{2-}$ complexes have been calculated by GRAY and BALLHAUSEN [26]. The ground state is $^1A_{1g}$ in both cases. According to the calculations, three charge transfer bands appear in both complexes which overlap the d—d bands of low intensity.

GRAY and BALLHAUSEN assume that the two inflections, observed in the spectrum of the aqueous solution of the Ni(II) compounds in the visible and at the border of the ultra-violet, indicate the presence of these d—d transitions. In the case of $[Pt(CN)_4]^{2-}$ the overlapping is complete (Table III and Fig. 2).

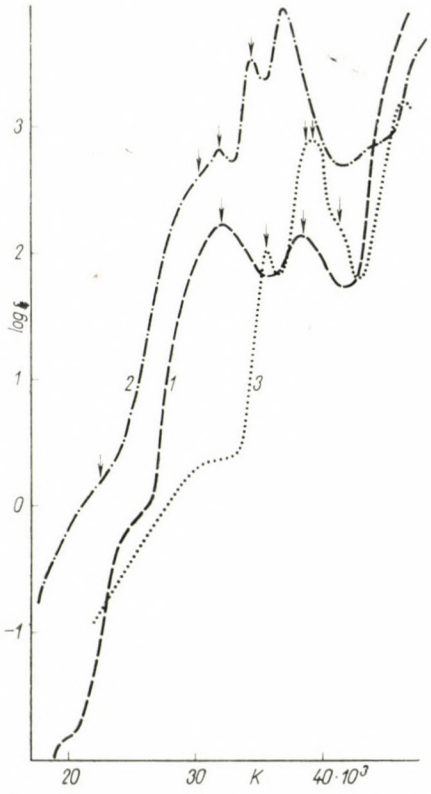

Fig. 2. Spectra of $[Co(CN)_6]^{3-}$ (— — —), $[Ni(CN)_4]^{2-}$ (— . — . — . —) and $[Pt(CN)_4]^{2-}$ (. . . . . .) in aqueous media

Investigation of polynuclear cyanides. If excess Fe(III) is reacted with $[Fe(CN)_6]^{4-}$, a very intensive blue coloured solution and precipitate is produced. The composition of the isolated compound is $Fe_4[Fe(CN)_6]_3$. In the reflection spectrum of the complex (Fig. 3) only one band system appears in the visible region, and the spectrum of a colloid solution of the solids, as well as that of a mixture made of the aqueous solutions of the two components [27] are also quite similar (Fig. 3).

Previous authors interpreted the spectrum with charge transfer processes, which occur via CN groups between the Fe(II) and Fe(III) ions situated in the lattice points:

$$- Fe^{3+} - CN^- - Fe^{2+} - + h\nu \rightarrow - Fe^{2+} - CN - Fe^{2+} -$$

and

$$- Fe^{2+} - CN - Fe^{2+} - CN^- - + h\nu \rightarrow - Fe^{3+} - CN^- - Fe^{2+} - CN^- -$$

However, ROBIN [28] has recently pointed out that the appearance of these bands and also the more intensive colour are due to a charge transfer process taking place between the Fe(III) ion and the $[Fe(CN)_6]^{4-}$ complex ion as unity.

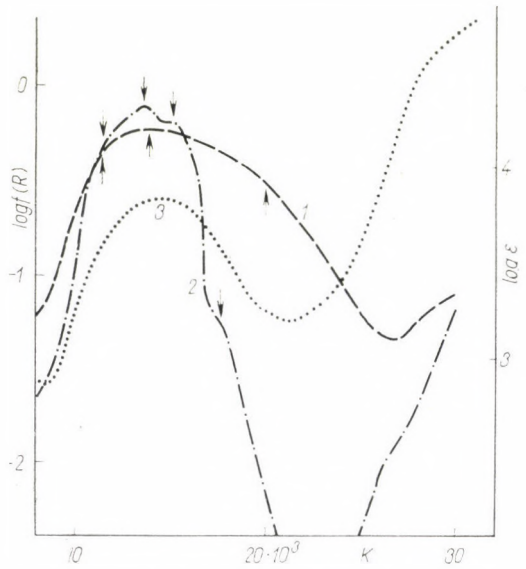

Fig. 3. $Fe_4[Fe(CN)_6]_3$: 1 (— — — — —) reflection spectrum; 2 (— . — . — . —) colloid spectrum; 3 (. . . . . .) absorption spectrum, in an aqueous solution of the system Fe^{3+} and $[Fe(CN)_6]^{4-}$

Fe(II) ion with $[Fe(CN)_6]^{3-}$ also yields an intensive blue precipitate, known as Turnbull blue; its composition has been given as $Fe_3[Fe(CN)_6]_2$. FLUCK and his coworkers [4] stated by a Mössbauer spectral investigation that the structure and the composition of Turnbull and Prussian blue are identical. The formation of the blue pigments is pictured by an oxidation-reduction reaction as the primary process:

$$Fe^{2+} + [Fe(CN)_6]^{3-} \rightarrow Fe^{3+} + [Fe(CN)_6]^{4-}$$

and the resulting Fe(III) and $[Fe(CN)_6]^{4-}$ form the blue dye.

This statement is supported by the very similar structures of the reflection and colloid spectra of both iron cyanides (Table IV and Fig. 4). The same view is confirmed by magnetic investigations according to which the BM values of the two compounds, calculated on basis of the formula

$Fe_4[Fe(CN)_6]_3$, are very similar (Table II). These values are somewhat lower than those calculated for five unpaired electrons, the difference being most probably due to metal-metal interaction.

On the basis of a Mössbauer spectrum, DUNCAN and WIGLEY [29] established that iron polynuclear cyanides are composed of spin-free cations and spin-paired anions. Indian authors [30] have also pointed out that there is not much difference between the susceptibilities of the Turnbull and Prussian blue.

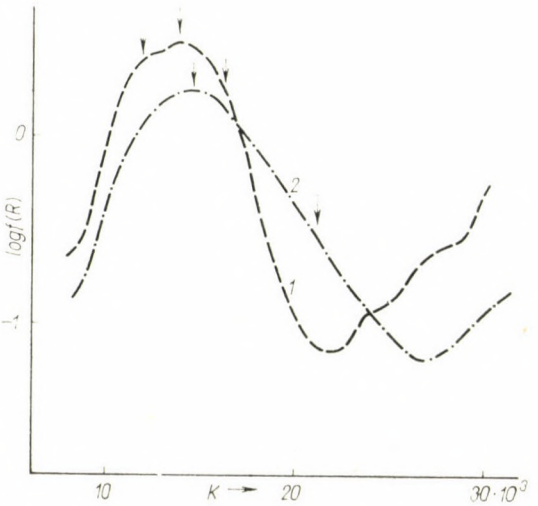

Fig. 4. System $Fe^{2+}[Fe(CN)_6]^{3-}$: 1 (— — — — —) reflection spectrum of the precipitate; 2 (— . — . — . —) colloid spectrum of the solids

Further evidence is furnished by the infrared spectrum. As is known, $[Fe(CN)_6]^{3-}$ [31] and $[Fe(CN)_6]^{4-}$ [32] complexes give the characteristic band of the C ≡ N stretching vibration at 2,125 and 2,047 cm^{-1}, respectively. We found that the infrared spectra of both polynuclear cyanides show the mentioned band at the same place, at 2,075 cm^{-1}, which cannot be interpreted on basis of different structures and compositions. Considering that in these polynuclear complexes the CN groups play, more or less, the part of bridges, such a shift of the frequencies is probable und understandable.

Very interesting are the polynuclear complexes that are formed by the coupling of two or more octahedral complex ions. The absorption and reflection spectra of the complex cations, $[CoEn_3]^{3+}$ and $[Co(NH_3)_6]^{3+}$, are well known [33—36] and their theory has also been thoroughly studied. In their solution spectra two sharp, separate bands ($^1A_1 \rightarrow {}^1T_1$ and $^1A_1 \rightarrow {}^1T_2$) can be observed (Table IV); the spectra of the aqueous solution and that of the solid samples hardly differ [37]. In the spectrum range investigated in this work, the band

corresponding only to the first transition could be found. As it is seen in Figs. 5 and 6, only one well-defined band appears between 22,800 and 23,900 cm^{-1} in the reflection spectra of the double cyanides of both Co(III) complex ions. In the descending branch of longer wavelengths several shoulders can be found (Table IV).

It is remarkable that in the spectra of compounds containing $[Fe(CN)_6]^{3-}$ the position of the main band almost coincides with that of the complex

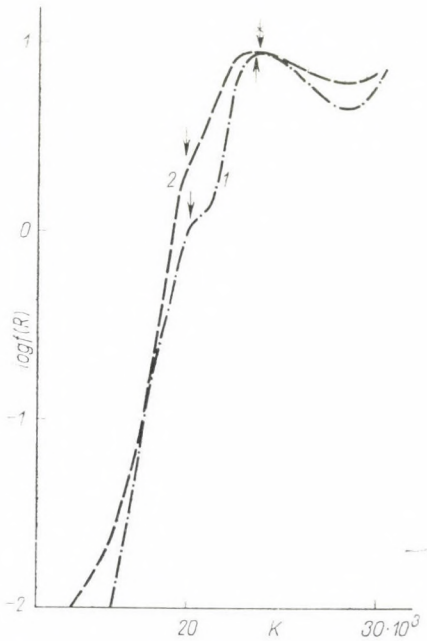

Fig. 5. Reflection curves of $[CoEn_3][Fe(CN)_6]$ (—.—.—.—) and $[Co(NH_3)_6][Fe(CN)_6]$ (— — — — —)

anion at 23,800 cm^{-1}, while the shoulders found at lower wave numbers probably indicate the presence of the d—d band of the cation. So, it may be concluded that in these polynuclear complexes both the complex anion and the complex cation are present as individual chromophores. This is in agreement with SCHILT's assumption [38] concerning $[NiPhen_3][Ni(CN)_4]$.

Magnetic properties exactly correspond to those expected. Since the complex cations are diamagnetic, in complexes containing $[Fe(CN)_6]^{4-}$ diamagnetism was found, while for those containing $[Fe(CN)_6]^{3-}$ anion 2.43 and 2.48 BM were obtained in good agreement with the 2.43 BM value measured with $K_3[Fe(CN)_6]$ [39].

The reflection spectra of the polynuclear cyanides of the Co(II) ion show two completely different structures. In the cases of the pink $KCo[Co(CN)_6]$

and $Co[Ni(CN)_4]$ the reflection spectra give almost exactly the same band positions that were measured with the hexahydrated ion (Fig. 7). Since the complex anions are diamagnetic, the expected only-spin momentum is 3.88,

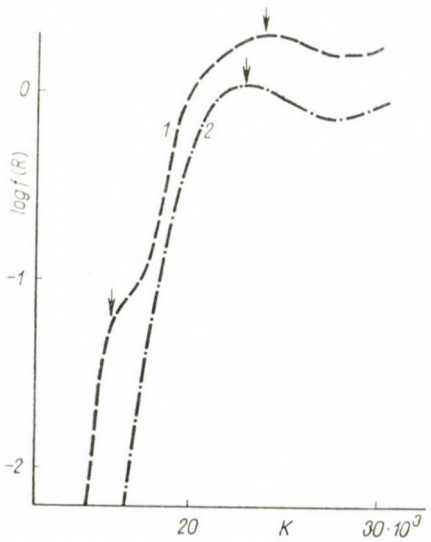

Fig. 6. Reflection spectra of $[Co(NH_3)_6]_4[Fe(CN)_6]_3$ (— — — — —) and $[CoEn_3]_4[Fe(CN)_6]_3$ (— . — . — . —)

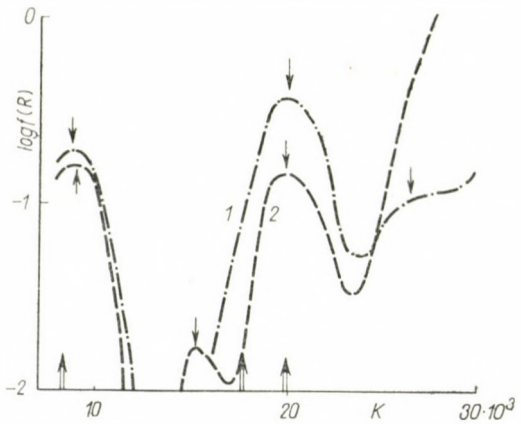

Fig. 7. Reflection spectra of $KCo[Co(CN)_6]$ (— . — . — . —) and $Co[Ni(CN)_4]$ (— — — — —)

or 5.20 BM if orbital contribution is taken into consideration. The measured BM values of the above two compounds are 4.64 and 3.64 BM, respectively. The lilac $K_2Co[Fe(CN)_6]$ and reddish-brown $Co[Pt(CN)_4]$ show reflection spectra (Fig. 8) with only indistinct inflections and flat maxima. The interpretation of these curves is difficult, though it seems probable that the

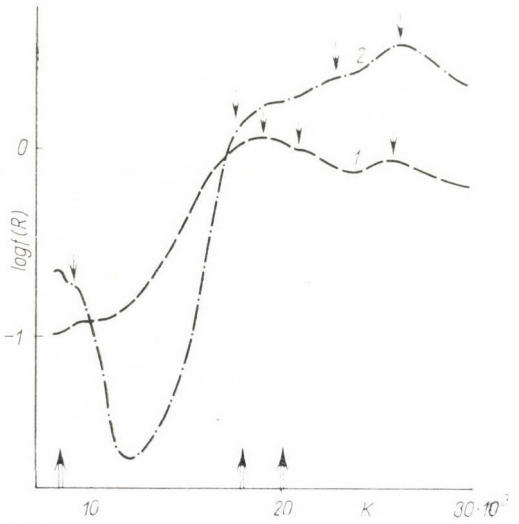

Fig. 8. Reflection curves of $K_2Co[Fe(CN)_6]$ (— — — — —) and $Co[Pt(CN)_4]$ (— . — . — . —

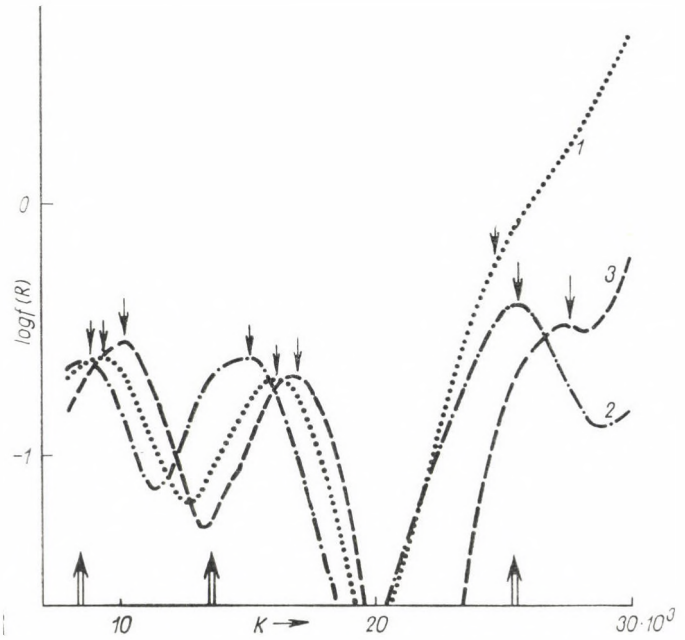

Fig. 9. Reflection spectra of $Ni_2[Fe(CN)_6]$ (. . . . .), $KNi[Co(CN)_6]$ (— . — . — . —) and $Ni[Pt(CN)_4]$ (— — — — —)

spectrum is due to the high charge transfer bands overlapping the d—d bands of the Co(II) ions. The BM values indicate the presence of three unpaired electrons.

A study of the corresponding Ni(II) compounds reveals that the spectra are identical with that of the hydrated ion (Fig. 9), with the exception of $Ni_3[Fe(CN)_6]_2$. These blue and green compounds are paramagnetic with two unpaired electrons (Table II); the value of 3.08 BM measured for $KNi[Co(CN)_6]$

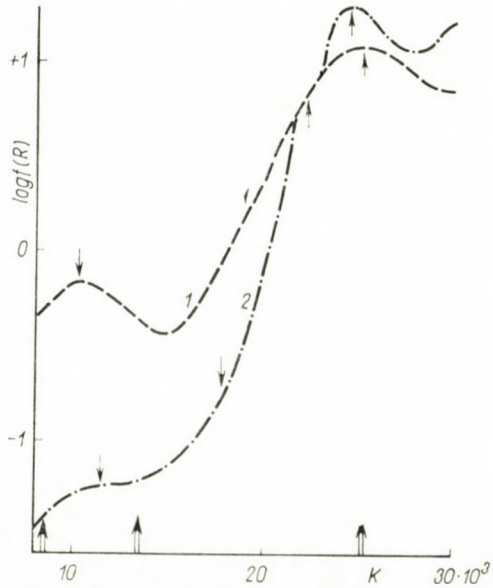

Fig. 10. $Ni_3[Fe(CN)_6]_2$: (— — — — —) reflection spectrum; (— . — . — . —) colloid spectrum in paraffin oil

is in very good agreement with 3.10 BM found by RICHARDSON and ELLIOT [40]. These susceptibility data indicate the coordination of cubic local symmetry of the Ni(II) ion. The exceptional nickel-iron(III)-cyanide is also paramagnetic, with 5.20 BM. This value approximately amounts to the total BM value of the Ni(II) ion and that of the iron(III)-cyanide anion, thus it appears that in the complex both the cation and the complex anion retain their own characteristic electron arrangements; this is influenced only to a small extent by interactions within the compound. The reflection spectrum contains one band of smaller and one of higher intensity at 10 300 and 25 200 cm^{-1}, respectively (Fig. 10); their origin is difficult to explain in any greater detail for the time being.

The reflection spectra of $KCu[Co(CN)_6]$ and $Cu[Pt(CN)_4]$ are considerably similar to the spectrum of the hydrated ion; the characteristic d—d band

appears slightly shifted towards the higher frequencies (Fig. 11). The bands here are also wide and complex. On the other hand, with $K_2Cu[Fe(CN)_6]$ one wide band of high intensity is found at about 20 000 cm^{-1} (Fig. 12),

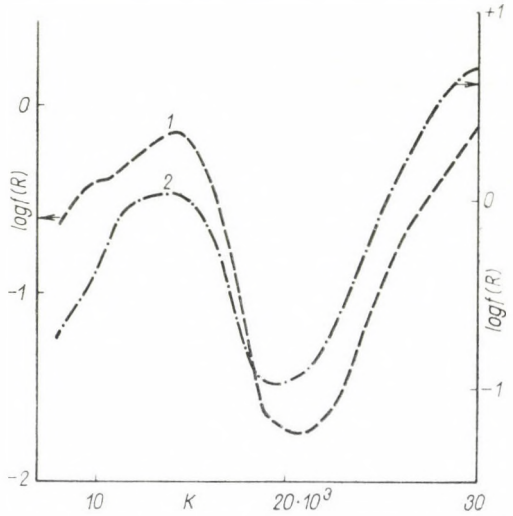

Fig. 11. Reflection spectra of $KCu[Co(CN)_6]$ (— — — — —) and $Cu[Pt(CN)_4]$ (— . — . — . —)

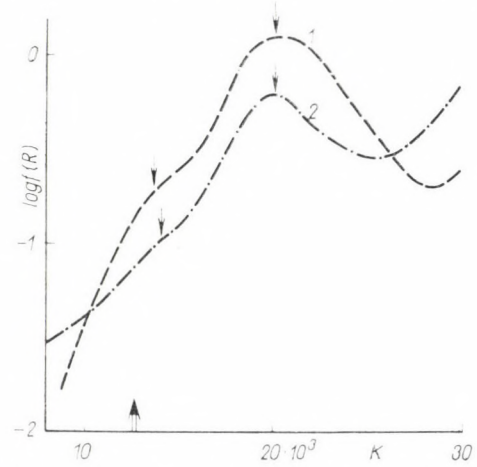

Fig. 12. $K_2Cu[Fe(CN)_6]$: (— — — — —) reflection spectrum; (— . — . — . —) colloid spectrum measured in paraffin oil

which may be considered rather as a charge transfer band. The inflection on the long wavelength side indicates the presence of the d—d band of the Cu(II) ion. Magnetic measurements suggest the presence of one unpaired electron (Table II); the results are in good agreement with those of ROLLIER and ARREGHINI [41].

SUMMARY

The magnetic properties and the reflection spectra of polynuclear cyanide complexes of transition metals have been investigated. Transition metal cations retain their own electron systems in most cases; the structures of the spectra and also magnetic properties correspond to those observed with the appropriate hydrated ions. It can be stated in all probability that the double iron cyanides, known as Turnbull and Prussian blue, have identical composition and structure. The deep colour and the bands of high intensity may be assigned to charge transfer processes.

REFERENCES

1. Fernelius, W. C., Brubage, J. J.: Inorganic Synthesis **2,** 227 (1946).
2. Bigelow, M.: Inorganic Synthesis **2,** 225 (1946).
3. Snell, F. D., Shell, C. T.: Colorimetric Methods of Analysis, Third Ed., Vol. II.
4. Fluck, E., Kerler, W., Neuwirth, W.: Z. anorg. allg. Chem. **333,** 235 (1964).
5. Král, M.: Collection Czechoslov. Chem. Commun. **29,** 2841 (1964).
6. Lewis, L., Wilkins, R. G.: Modern Coordination Chemistry (Interscience Inc., N. Y.) 1960.
7. Kubelka, P., Munk, F.: Z. techn. Physik **12,** 593 (1931).
8. Kortüm, G., Schöttler, M.: Z. Elektrochem. **57,** 353 (1953).
9. Schläfer, H. L.: Z. physik. Chem. N. F. **4,** 116 (1955).
10. Jörgensen, C. K.: Acta Chem. Scand. **8,** 1502 (1954).
11. Furlani, C.: Gazz. chim. ital. **87,** 371 (1957).
12. Cotton, F. A., Meyers, M. D.: J. Am. Chem. Soc. **82,** 5023 (1960).
13. Abragam, A., Pryce, M. H. L.: Proc. Roy. Soc. (London) **A206,** 173 (1951).
14. Holmes, O. G., McClure, D. S.: J. Phys. Chem. **26,** 1686 (1957).
15. Pappalardo, R.: Phil. Mag. **4,** 219 (1959).
16. Orgel, L. E.: J. Chem. Phys. **23,** 1004 (1955).
17. Tanabe, Y., Sugano, S.: J. Phys. Soc. Japan **9,** 766 (1954).
18. Ballhausen, C. J.: Kgl. Danske Videnskab. Selskab. Mat.-fys. Medd. **29** (8), (1955).
19. Orgel, L. E., Dunitz, J. D.: Nature **179,** 462 (1957).
20. Perumareddi, J. R., Liehr, A. D., Adamson, A. W.: J. Am. Chem. Soc. **85,** 249 (1963).
21. Bán, M. I., Horváth, E.: Acta Phys. Chem. Szeged, N. S. **5,** 34 (1959).
22. Gilde, F. J., Bán, M. I.: Acta Phys. Chem. Szeged, N. S. **3,** 42 (1957).
23. Kida, S., Fujita, J., Nakamoto, K., Tsuchida, K.: Bull. Chem. Soc. Japan **31,** 79 (1958).
24. Naiman, C. S.: J. Chem. Phys. **35,** 323 (1961).
25. Gray, H. B., Beach, N. A.: J. Am. Chem. Soc. **85,** 2922 (1963).
26. Gray, H. B., Ballhausen, C. J.: J. Am. Chem. Soc. **85,** 260 (1963).
27. Kiss, Á., Császár, J.: Z. anorg. allg. Chem. **325,** 43 (1963).
28. Robin, M. B.: Inorg. Chem. **1,** 337 (1962).
29. Duncan, J. F., Wigley, P. W. R.: J. Chem. Soc. **1963,** 1120.
30. Bhattacharya, A. K.: J. Indian Chem. Soc. **18,** 71 (1941).
31. Herrington, E. F., Kynaston, W.: J. Chem. Soc. **1955,** 3555.
32. Bonino, G. B., Salvetti, O.: Ricerca Sci. **26,** 3627 (1956).
33. Ballhausen, C. J., Asmussen, R. W.: Acta Chem. Scand. **11,** 479 (1957).
34. Griffith, J. S., Orgel, L. E.: Trans. Faraday Soc. **53,** 601 (1957).
35. Jörgensen, C. K.: Acta Chem. Scand. **8,** 1495 (1954).
36. Ballhausen, C. J.: Introduction to Ligand Field Theory (McGraw-Hill Co., N. Y.) 1962.
37. Szőke, J., Császár, J.: MTA Központi Fizikai Kutató Int. Közl. **11,** 46 (1963).
38. Schilt, A. A.: J. Am. Chem. Soc. **81,** 2966 (1959).
39. Simon, A., Knauer, H.: Z. Elektrochemie **46,** 13 (1940).
40. Richardson, J., Elliott, N.: J. Am. Chem. Soc. **62,** 3182 (1940).
41. Rollier, M. A., Arreghini, E.: Gazz. chim. ital. **69,** 499 (1939).

Magnetische und spektroskopische Untersuchung mehrkerniger komplexer Cyanide

J. CSÁSZÁR und A. FELVÉGI

Zusammenfassung. Die Reflexionsspektren und magnetischen Eigenschaften der polynuklearen Cyanidkomplexe von Übergangsmetallen wurden untersucht. Es wurde dabei festgestellt, daß die Kationen der Übergangsmetalle in der Mehrheit der Fälle ihre eigene Elektronsysteme unverändert behalten. Die Struktur und die magnetischen Eigenschaften der Spektren stimmen auch mit denen überein, die bei den hydratisierten Ionen beobachtet wurden. Es kann mit großer Wahrscheinlichkeit behauptet werden, daß die unter den Namen Turnbullsblau und Berlinerblau bekannten Eisencyanide eine identische Zusammensetzung und Struktur besitzen. Die tiefe Farbe bzw. die Banden hoher Intensität dieser Farbstoffe können den Landungsübertragungsprozessen zugeschrieben werden.

Магнитное и спектроскопическое исследование многоядерных цианид-комплексов

И. ЧАСАР и А. ФЕЛВЕГИ

Резюме. Исследовали магнитные свойства и рефлекционный спектр многоядерных цианид-комплексов ионов переходных металлов. Установили, что катионы переходных металлов в большинстве случаев сохраняют собственную электронную структуру. Структура спектров и магнитные свойства также соответствуют свойствам, наблюдаемым в случае гидратированного иона. С большой вероятностью можно установить, что известные под названием турнбуллиевая синь и берлинский голубой, цианиды железа одинаковы по своему составу и структуре. Глубокий цвет, а также полосы большой интенсивности можно приписать полосам переноса заряда.

Dr. József Császár
Anna Felvégi
Rerrich Béla tér, Szeged, Hungary.

A NEW METHOD FOR THE DETERMINATION OF VIBRATIONAL FORCE CONSTANTS OF MOLECULES

F. BILLES

(Department of Physical Chemistry, Technical University, Budapest)

Received July 8, 1965

1. Introduction

Two ways have been used so far for the calculation of Wilson's force constant matrix F.

(a) Since the number of force constants to be calculated exceeds the number of normal vibrations, the normal frequencies of molecules substituted with isotopes (usually with deuterium) are also employed in the calculation, supposing that substitution with isotopes does not change the vibrational force constants [1, 2, 3]. Writing the secular equations

$$|\mathbf{G}\mathbf{F} - \lambda\mathbf{E}| = 0 \tag{1}$$

(where $\mathbf{G}$ = the matrix of the kinetical energy constants and $\lambda = 4\pi^2\nu^2$, where ν is the vibrational frequency) by using symmetry coordinates, the number of unknowns is considerably decreased. Matrices $\mathbf{F}$ and $\mathbf{G}$, written with internal coordinates, transform in the case into step matrices. The minormatrices belong to the individual representations. If the number of normal vibrations of the molecule belonging to a representation is n, the corresponding minormatrix of $\mathbf{F}$ contains $\frac{n(n+1)}{2}$ unknowns. If n is odd, the normal frequencies of $\frac{n+1}{2}$ molecules are required; if n is even, this number is $\frac{n+2}{2}$.

The preparation of compounds with isotope substitution frequently involves considerable difficulties.

Furthermore, if n is a large number, the system of $\frac{n(n+1)}{2}$ th order equations with $\frac{n(n+1)}{2}$ unknowns, obtained by the extension of the secular equations of type (1), can hardly be solved even with the aid of electronic computers.

(b) Because of the above-mentioned difficulties, approximative methods have been recommended, where there is no need of compounds substituted

with isotopes. Such are the methods of TORKINGTON [4], SHIMANOUCHI [5], OVEREND and SCHERER [6] and LONG [7].

This paper describes a mathematically exact, i.e. not approximative method for the determination of force constants, which does not require compounds substituted with isotopes, either.

2. Theoretical

Since the calculation of the force constant matrix occurring in the secular equation (1) is facilitated introducing the symmetry coordinates S, advantages of their use are obvious.

Let n normal vibrations belong to a representation. The parts of the kinetic (T) and potential (V) energies belonging to this representation, will be:

$$2\,T = \sum_{i=1}^{n} \sum_{j=1}^{n} G_{ij}^{-1}\,\dot{S}_i\,\dot{S}_j \tag{2}$$

and

$$2\,V = \sum_{i=1}^{n} \sum_{j=1}^{n} F_{ij}\,S_i\,S_j \tag{3}$$

The symmetry coordinates belonging to this representation constitute an n-dimensional subspace of the $3\,N$-6 dimensional space of symmetry coordinates (N denotes the number of atoms in the molecule). The symmetry coordinates are orthogonal to each other).

Let us effect an optional coordinate transformation in this subspace. The new coordinates, denoted by J, are the linear combinations of the symmetry coordinates S:

$$J_i = \sum_{j=1}^{n} U_{ij}\,S_j \quad i = 1, 2, \ldots, n \tag{4}$$

where the U_{ij}-s stand for the transformational coefficients. The coordinate-differentials have to transform according to expression (4):

$$\mathrm{d}J_i = \sum_{j=i}^{n} U_{ij}\,\mathrm{d}\,S_j \quad i = 1, 2, \ldots, n \tag{5}$$

Therefore, we have

$$\dot{J}_i = \sum_{j=1}^{n} U_{ij}\,\dot{S}_j \quad i = 1, 2, \ldots, n \tag{6}$$

The values of the kinetic and potentional energies are independent of the coordinates used, hence the transformation does not affect their values: T and

V are invariant scalars. Since S_j and $\dot{S}_j$ transform like the cooordinates (i. e., like components of a vector) do, $\mathbf{G}^{-1}$ and $\mathbf{F}$ are tensors of second order in this space. If $\mathbf{G}^{-1}$ is a tensor quantity, obviously its inverse, $\mathbf{G}$ is also a tensor.

Let us choose the U_{ij} coefficients of the transformation so that matrix $\mathbf{G}^{-1}$ becomes a diagonal form Γ^{-1}:

$$\Gamma^{-1} = U' G^{-1} U \tag{7}$$

where U is the matrix of the transformational coefficients, and U' is the transposed of this matrix. The transformation is orthogonal ($U' = U^{-1}$), From (7) we have:

$$\Gamma = U' G U \tag{8}$$

The transformational matrix and the diagonal matrix may be calculated from (8), if we take into account the tensor character of G. For the principal axis transformation we have:

$$G \bar{S} = g\bar{S} \tag{9}$$

where $\bar{S}$ is the column vector formed from the coordinates S_j, and g is a component of the tensor in the direction of a principal axis. Dividing both sides by the absolute value of $\bar{S}$, we obtain the vector $\bar{e}$ lying in the direction of a principal axis, on both sides:

$$G \bar{e} = g\bar{e} \tag{10}$$

or written in another form:

$$[G - gE]\bar{e} = 0 \tag{11}$$

The system of equations (11) will have a solution other than the trivial, if

$$|G - gE| = 0 \tag{12}$$

The eigenvalues of the secular equation (12) give exactly the elements Γ_{ii} of the matrix Γ. The corresponding $\bar{e}_i$ eigenvectors give the directions of the principal axes. Their components are the direction cosines of the principal axes, i.e. the transformational coefficients U_{ij}:

$$(\bar{e}_i)_j = U_{ij} \tag{13}$$

On the basis of the transformational relation (6), the transformational coefficients diagonalizing F are the same as those diagonalizing G^{-1}. Similarly to relation (7) we have:

$$\Phi = U' F U \tag{14}$$

where Φ is the diagonalized form of F.

The expressions of the kinetic and potential energies, respectively, with the aid of equation (4), (6), (7) and (14) are:

$$2T = \sum_{i=1}^{n} \Gamma_{ii}^{-i} \dot{J}_i^2 \tag{15}$$

and

$$2V = \sum_{i=1}^{n} \Phi_{ii} J_i^2 \tag{16}$$

i. e., both are quadratic expressions. The connection of the normal coordinates Q_i with the corresponding normalizable coordinates J_i, on the basis of (15) and (16), is evidently:

$$Q_i = \sqrt{\Gamma_{ii}^{-i}}\, J_i \tag{17}$$

The equation of motion of the vibration may be written with the aid of expressions of the kinetic and potential energies (15) and (16) as follows:

$$\Gamma_{ii}^{-1} \dot{J}_i + \Phi_{ii} J_i = 0 \qquad i = 1, 2, \ldots, n \tag{18}$$

hence

$$\ddot{J}_i = -\frac{\Phi_{ii}}{\Gamma_{ii}^{-1}} J_i \qquad i = 1, 2, \ldots, n \tag{19}$$

Since this is the differential equation of harmonic vibrational motion, the relation between the constant on the right hand side and the frequency of the i-th vibration is well-known:

$$\lambda_i = \frac{\Phi_{ii}}{\Gamma_{ii}^{-i}} = \Gamma_{ii} \Phi_{ii} \tag{20}$$

where

$$\lambda_i = 4 \pi^2 \nu_i^2$$

The quantities Φ_{ii} may be calculated from (20) if the values of Γ_{ii} and λ_i are known. Then we make the inverse transformation of (14):

$$F = U \Phi U' \tag{21}$$

Thus, if the normal frequencies, n, are unknown, the elements of the matrix **F** may be calculated by taking into account the tensor properties of the matrices **G** and **F**.

The calculations made so far yield equation (1) transformed into the form:

$$\left| \Gamma \Phi - \lambda E \right| = 0 \tag{22}$$

Taking into account the transformations (8) and (14) we have:

$$\left| U' G U . U' F U - \lambda E \right| = 0 \tag{23}$$

From this

$$\left| U' G F U - U' \lambda U \right| = 0 \tag{24}$$

Factoring out the transformational matrix we have:

$$\left| U' \right| \left| G F - \lambda E \right| \left| U \right| = 0 \tag{25}$$

Since matrix **U** is orthogonal, the value of its determinant is 1, so the secular equation (1) is obtained again from (25). Therefore the spectrum of (22) agrees with that of (1).

3. The course of the calculation

The matrices G belonging to the individual respresentations are calculated from the geometrical data of the molecule and the atomic weights [1]. Then the characteristic determinant of the matrix **G** is to be found, and the corresponding eigenvectors are calculated. In this way the eigenvalues g_k and matrix **U** are obtained.

The normal frequencies observed in the spectrum are assigned to the normalizable coordinates (see the example), then the individual eigenvalues g_k are assigned to the J_i coordinates so that the difference $\left| G_{jj} - g_k \right|$ ($k = 1, 2, \ldots, n$) should be minimum. S_j is the coordinate with the greatest coefficient, U_{ij}, occurring in expression (4). In this way the matrix Γ is obtained. With the aid of the Γ_{ii}-s and λ_i-s the elements of the matrix Φ are calculated from (20), then matrix **F** is determined by the transformation (21).

4. Example

The matrix **F** of ethylene has been calculated with the above-mentioned tensor method. The ethylene molecule belongs to the point group V_h. The geometrical data of the molecule are as follows [8] (see also Fig. 1):

$$l = 1.071 \pm 0.01 \text{ A}$$
$$k = 1.353 \pm 0.01 \text{ Å}$$
$$\beta = 119.9° \pm 0.5°$$

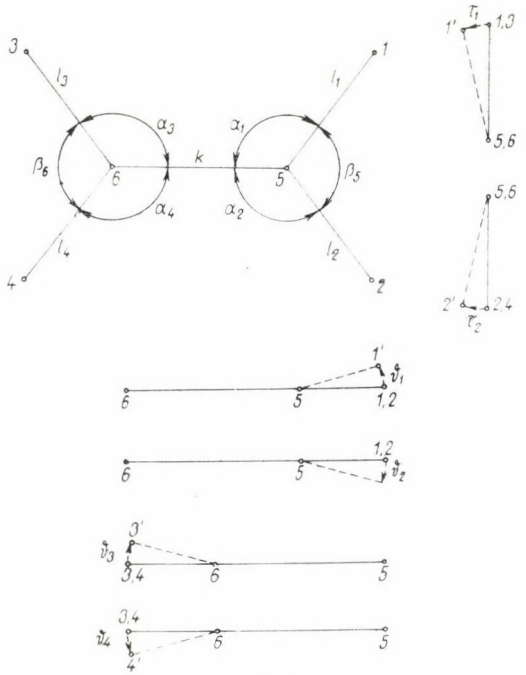

Fig. 1

The values of the normal frequencies are taken from the paper of CRAWFORD, LANCASTER and INSKEEP [9].

The tables below show the assignments of the normal frequencies, the starting matrices **G**, as well as the calculated matrices Γ, **U**, Φ and **F**. The frequencies calculated with the aid of matrices **F** correspond exactly to the experimentally observed frequencies.

Representation A_g

$\nu_1 = 3019.3 \text{ cm}^{-1}$ $\quad S_1 = 1/2\ (l_1 + l_2 + l_3 + l_4)$
$\nu_2 = 1623.3 \text{ cm}^{-1}$ $\quad S_2 = k$
$\nu_3 = 1342.4 \text{ cm}^{-1}$ $\quad S_3 = 1\ (\alpha_1 + \alpha_2 + \alpha_3 + \alpha_4)$

$$\mathbf{G} = \begin{bmatrix} 1.1169 & 0.1441 & -0.0674 \\ 0.1441 & 0.1665 & -0.0779 \\ -0.0674 & -0.0779 & 0.9013 \end{bmatrix} \text{(gmole)}^{-1}$$

$$\mathbf{\Gamma} = \begin{bmatrix} 1.1620 & 0 & 0 \\ 0 & 0.1392 & 0 \\ 0 & 0 & 0.8835 \end{bmatrix} \text{(gmole)}^{-1}$$

$$\mathbf{\Phi} = \begin{bmatrix} 4.6211 & 0 & 0 \\ 0 & 11.1529 & 0 \\ 0 & 0 & 1.2015 \end{bmatrix} \text{mdyne/Å}$$

$$\mathbf{F} = \begin{bmatrix} 4.4395 & -0.8731 & -1.0877 \\ -0.8731 & 10.9690 & 0.7121 \\ -1.0877 & 0.7121 & 1.4999 \end{bmatrix} \text{mdyne/Å}$$

$$\mathbf{U} = \begin{bmatrix} 0.9436 & -0.1412 & 0.2916 \\ 0.1594 & 0.9863 & -0.0414 \\ -0.2915 & 0.0884 & 0.9214 \end{bmatrix}$$

Representation A_u

$\nu_4 = 1027\ \text{cm}^{-1}$ $\qquad S_4 = \frac{1}{\sqrt{2}}(\tau_1 + \tau_2)$

$\mathbf{G} = \mathbf{\Gamma} = [2.3088]\ \text{(gmole)}^{-1}$
$\mathbf{F} = \mathbf{\Phi} = [2.6910]\ \text{mdyne/Å}$
$\mathbf{U} = [1.0000]$

Representation B_{1g}

$\nu_5 = 3075\ \text{cm}^{-1}$ $\qquad S_5 = \frac{1}{2}(l_1 - l_2 - l_3 - l_4)$

$\nu_6 = 1236\ \text{cm}^{-1}$ $\qquad S_6 = \frac{1}{2}(\alpha_1 - \alpha_2 - \alpha_3 + \alpha_4)$

$$\mathbf{G} = \begin{bmatrix} 1.0338 & -0.0559 \\ -0.0559 & 0.9397 \end{bmatrix} \text{(gmole)}^{-1}$$

$$\mathbf{\Gamma} = \begin{bmatrix} 1.0690 & 0 \\ 0 & 0.9045 \end{bmatrix} \text{(gmole)}^{-1}$$

$$\mathbf{\Phi} = \begin{bmatrix} 5.2104 & 0 \\ 0 & 0.9948 \end{bmatrix} \text{mdyne/Å}$$

$$\mathbf{F} = \begin{bmatrix} 4.4963 & -1.6326 \\ -1.6326 & 1.7439 \end{bmatrix} \text{mdyne/Å}$$

$$\mathbf{U} = \begin{bmatrix} 0.9068 & 0.4216 \\ -0.4216 & 0.9068 \end{bmatrix}$$

Representation B_{1u}

$\nu_7 = 949.2\ \text{cm}^{-1}$ $\qquad S_7 = \frac{1}{2}(\vartheta_1 + \vartheta_2 + \vartheta_3 + \vartheta_4)$

$\mathbf{G} = \mathbf{\Gamma} = [4.0403]\ \text{(gmole)}^{-1}$
$\mathbf{F} = \mathbf{\Phi} = [1.3135]\ \text{mdyne/Å}$
$\mathbf{U} = [1.0000]$

Representation B_{2g}

$\nu_8 = 943\ \text{cm}^{-1}$ $\qquad S_8 = \frac{1}{2}(\vartheta_1 + \vartheta_2 - \vartheta_3 - \vartheta_4)$

$\mathbf{G} = \mathbf{\Gamma} = [3.7701]\ (\text{gmole})^{-1}$
$\mathbf{F} = \mathbf{\Phi} = [1.3874]\ \text{mdyne/Å}$
$\mathbf{U} = [1.0000]$

Representation B_{2u}

$\nu_9 = 3105.5\ \text{cm}^{-1}$ $\qquad S_9 = \frac{1}{2}(l_1 - l_2 + l_3 - l_4)$

$\nu_{10} = 810.3\ \text{cm}^{-1}$ $\qquad S_{10} = \frac{1}{2}(\alpha_1 - \alpha_2 + \alpha_3 - \alpha_4)$

$$\mathbf{G} = \begin{bmatrix} 1.0338 & 0.0674 \\ 0.0674 & 0.9737 \end{bmatrix}\ (\text{gmole})^{-1}$$

$$\mathbf{\Gamma} = \begin{bmatrix} 1.0776 & 0 \\ 0 & 0.9300 \end{bmatrix}\ (\text{gmole})^{-1}$$

$$\mathbf{\Phi} = \begin{bmatrix} 5.2719 & 0 \\ 0 & 0.4159 \end{bmatrix}\ \text{mdyne/Å}$$

$$\mathbf{F} = \begin{bmatrix} 3.8336 & 2.2171 \\ 2.2171 & 1.8542 \end{bmatrix}\ \text{mdyne/Å}$$

$$\mathbf{U} = \begin{bmatrix} 0.8389 & -0.5442 \\ 0.5442 & 0.8389 \end{bmatrix}$$

Representation B_{3u}

$\nu_{11} = 2989.5\ \text{cm}^{-1}$ $\qquad S_{11} = \frac{1}{2}(l_1 + l_2 - l_3 - l_4)$

$\nu_{12} = 1443.5\ \text{cm}^{-1}$ $\qquad S_{12} = \frac{1}{2}(\alpha_1 + \alpha_2 - \alpha_3 - \alpha_4)$

$$\mathbf{G} = \begin{bmatrix} 1.1169 & -0.0674 \\ -0.0674 & 0.9013 \end{bmatrix}\ (\text{gmole})^{-1}$$

$$\mathbf{\Gamma} = \begin{bmatrix} 1.1362 & 0 \\ 0 & 0.8820 \end{bmatrix}\ (\text{gmole})^{-1}$$

$$\mathbf{\Phi} = \begin{bmatrix} 4.6333 & 0 \\ 0 & 1.3916 \end{bmatrix}\ \text{mdyne/Å}$$

$$\mathbf{F} = \begin{bmatrix} 4.3867 & 0.8594 \\ 0.8594 & 1.6382 \end{bmatrix}\ \text{mdyne/Å}$$

$$\mathbf{U} = \begin{bmatrix} 0.9612 & -0.2758 \\ 0.2758 & 0.9612 \end{bmatrix}$$

SUMMARY

A new method of calculation of force constants has been evolved, where Wilson's matrices **G** and **F** are regarded as tensors of an *n*-dimensional space. This method is exact, not approximative. In spite of this fact, it does not require use of the normal frequencies of compounds substituted with isotopes. The method has been applied to the ethylene molecule.

REFERENCES

1. Wilson, E. B., Decius, J. C., Cross, P. C.: Molecular Vibrations (McGraw Hill, London, 1955).
2. Urey, H. C., Bradley, C. A.: Phys. Rev. **38,** 1969 (1931).
3. Shimanouchi, T.: J. Chem. Phys. **17,** 245, 734, 848 (1949).
4. Torkington, P.: J. Chem. Phys. **17,** 1026 (1949).
5. Mann, D. E., Shimanouchi, T., Meal, J. H., Fano, L.: J. Chem. Phys. **27,** 43, 51 (1957); Shimanouchi, T., Suzuki, T.: J. Mol. Spectroscopy **6,** 227 (1961).
6. Overend, J., Scherer, J. R.: J. Chem. Phys. **32,** 1289, 1720 (1960); **33,** 1681 (1960).
7. Long, D. A., Gravenor, R. B., Woodger, M.: Spectrochimica Acta **19,** 937 (1963).
8. Tables of Interatomic Distances and Configuration in Molecules and Ions (The Chemical Society, London, 1958), p. 129.
9. Crawford, B. L., Lancaster, J. E., Inskeep, R. G.: J. Chem. Phys. **21,** 678 (1953).

Einen neue Methode zur Bestimmung der Schwingungskraftkonstanten von Molekülen

F. BILLES

Zusammenfassung. Durch Betrachtung der Wilsonschen **G** und **F** Matrixen als Tensore eines Raums von der Dimension *n* gelang es eine neue Methode zur Berechnung der Kraftkonstanten zu entwickeln. Dieses Verfahren ist keine Annäherungsmethode, sondern eine exakte Methode. Trotzdem sind die Normalfrequenzen der mit Isotopen substituierten Verbindungen dazu nicht benötigt. Die neue Methode wurde bei dem Äthylenmolekül angewendet.

Новый метод определения колебательных силовых постоянных молекул

Ф. БИЛЛЕШ

Резюме. Принимая **G** и **F** матрицы Вильсона за тензоры n-размерного поля, удалось разработать новый метод расчета силовых постоянных. Этот метод, математически является точным, а не приближенным методом. В противоположность этому, в случае данного метода нет надобности в нормальных частотах изотоп-замещенных соединений. Метод был применен в случае молекулы этилена.

Dr. Ferenc Billes; Budapest XI. Budafoki út 8.

ONCE MORE ON THE DEDUCTION OF THE FOURIER EQUATION FROM THE VARIATIONAL PRINCIPLE

(SHORT COMMUNICATION)

I. GYARMATI

(Department for Physical Chemistry, Polytechnical University, Budapest)

Received October 26, 1965

In two earlier papers the variational principles of thermodynamics have been discussed in detail [1, 2]. Among others the Fourier equation has been derived from a new representation of the principle of least dissipation of energy, then a thermodynamic integral principle was formulated. Unfortunately, in the derivation of the Fourier equation we were insisting too strictly upon the direct determination of the original form of the equation, and owing to this fact a non-desirable modification was carried out on the variational principle. Evidently it was such a procedure (and on the other hand an unnecessary one), when the local extremum principle was multiplied by T^2 (see formula (4.9) in [2]). We show now, that in the case of a rigorous entropy representation, the equation of heat conduction can be deduced in exact manner in every respect.

Let us start from the well-known entropy balance

$$\varrho\dot{s} + \nabla \cdot \mathbf{J}_s = \mathbf{J}_q \cdot \mathbf{X}_q = \sigma_q \tag{1}$$

where

$$\mathbf{J}_s = T^{-1}\mathbf{J}_q\,, \qquad \mathbf{X}_q = \nabla \mathbf{T}^{-1} \tag{2}$$

The form of the linear law (differing from that used in [1, 2]) is:

$$\mathbf{J}_q = L_{qq}\nabla T^{-1} = -\lambda \nabla T \tag{3}$$

where $\lambda = T^{-2}L_{qq}$ is the heat conductivity coefficient in the Fourier picture. The dissipation function (T^{-1} times the one used in [1, 2]), will be:

$$\psi_q \equiv \frac{L_{qq}}{2}(\nabla T^{-1})^2\,. \tag{4}$$

Now, using (3) and (4) for the local extremum principle, we get:

$$[\varrho\dot{s} + \nabla \cdot \mathbf{J}_s - \psi]_{\mathbf{J}_s} = \left[\varrho\dot{s} + \nabla \cdot (T^{-1}\mathbf{J}_q) - \frac{L_{qq}}{2}(\nabla T^{-1})^2\right]_{\mathbf{J}_q} = \text{maximum.} \tag{5}$$

Considering that the relation is valid for solid bodies

$$\frac{\mathrm{d}s}{\mathrm{d}t} = T^{-1}\frac{\mathrm{d}u}{\mathrm{d}t} = T^{-1}\frac{\partial u}{\partial t} \tag{6}$$

which follows from the general forms of the Gibbs relation

$$\mathrm{d}s = \frac{1}{T}\,\mathrm{d}u + \frac{p}{T}\,\mathrm{d}v - \sum_{k=1}^{k}\frac{\mu_k}{T}\,\mathrm{d}c_k\,, \tag{7}$$

and making use of the vector analytical identity

$$\nabla\cdot(T^{-1}\mathbf{J}_q) = \nabla T^{-1}\cdot\mathbf{J}_q + T^{-1}\nabla\mathbf{J}_q\,, \tag{8}$$

we may write (5) in the following global form:

$$L = \int_V \left[\varrho T^{-1}\frac{\partial u}{\partial t} + \nabla T^{-1}\cdot\mathbf{J}_q + T^{-1}\nabla\mathbf{J}_q - \frac{L_{qq}}{2}(\nabla T^{-1})^2\right]_{\mathbf{J}_q}\mathrm{d}V = \text{maximum} \tag{9}$$

If we wish here to vary T^{-1} alone at fixed $\mathbf{J}_q$ and $\dfrac{\partial u}{\partial t}$, we get:

$$\delta L = \int_V \left[\left(\varrho\frac{\partial u}{\partial t} + \nabla\cdot\mathbf{J}_q\right)\delta T^{-1} + (\mathbf{J}_q - L_{qq}\nabla T^{-1})\cdot\nabla\delta T^{-1}\right]\mathrm{d}V = 0\,. \tag{10}$$

This extremum condition leads, with the linear law (3) and with the relation $\dfrac{\partial u}{\partial t} = c_v\dfrac{\partial T}{\partial t}$ valid in case of a solid body, to

$$\delta L = \int_V \left[\varrho c_v\frac{\partial T}{\partial t} + \nabla\cdot(L_{qq}\nabla T^{-1})\right]\delta T^{-1}\,\mathrm{d}V = 0\,, \tag{11}$$

from which it follows:

$$\varrho c_v\frac{\partial T}{\partial t} + \nabla\cdot(L_{qq}\nabla T^{-1}) = 0. \tag{12}$$

This differential equation can be written with the aid of (3) into the well-known form of the Fourier equation, hence (12) is equivalent to it. We wish to emphasize that though the results given in the papers [1, 2] and those published here are practically equivalent, our present deduction is more logical and can be theoretically easily generalized. Our previous derivation (which led directly to the traditional form of the Fourier equation) was based upon the theoretically most unfortunate representation, on the Fourier picture. This picture cannot be extended in the direction of general non-isotherm problems (thermodiffusion, etc.), and can, on the other hand, easily be misleading. Indeed, if in the frame of our present and in every respect exact

method we find the Lagrange function (more exactly the Lagrangian density) corresponding to (11), we get:

$$\mathscr{L}_q = \varrho c_v T^{-1} \frac{\partial T}{\partial t} - \frac{L_{qq}}{2} (\nabla T^{-1})^2 \tag{13}$$

and thus the Euler—Lagrange equations of our variational problem are:

$$\frac{\partial \mathscr{L}_q}{\partial T^{-1}} - \sum_{\alpha=1}^{3} \frac{\partial}{\partial x_\alpha} \frac{\partial \mathscr{L}_q}{\partial \left(\frac{\partial T^{-1}}{\partial x_\alpha} \right)} = 0, \tag{14}$$

which are equivalent to (12). Since the Lagrangian density as expressed in (13) is identical with (5) (without the divergency member, which means that $\mathbf{J}_s$, or T^{-1} and $\mathbf{J}_q$ are prescribed on the boundaries), it is possible to write:

$$\mathscr{L}_q = \varrho \dot{s} - \psi_q . \tag{15}$$

This Lagrangian density differs not only by the very undesirable factor T^2 from the one determined in the case of using the Fourier picture, but also with respect to the sign of the dissipation function. This means, that the thermodynamic Lagrangian density has to be written generally in the form

$$\mathscr{L} = \varrho \dot{s} - \psi (\mathbf{X}, \mathbf{X}) . \tag{16}$$

Thus it can be said, that the thermodynamic Lagrangian density must always be given as the difference of the kinetic part containing the time derivative $\dot{s}$, and the potential part determined by the dissipation function ψ. Our recent investigations which are concerned with the deduction of the total system of transport equations from the thermodynamic integral principle developed by us, show without any doubt that (16) is the correct and in every respect general thermodynamic Lagrangian density. For that one is the integral principle given in [2] valid (see formulae (5.11) and (5.12) in [2]).

SUMMARY

From the new representation of the principle of least dissipation of energy developed by us earlier, the Fourier equation of heat conduction has been derived. Differing from the previously used Fourier picture in the course of our present derivation, we confined ourselves rigorously to the entropy representation. It is shown that the Lagrangian density of thermodynamics is in our particular case, as well as in general, of the form $\mathscr{L} = \varrho \dot{s} - \psi$.

REFERENCES

1. GYARMATI, I.: Zsurn. Fiz. Khim. (Moscow) **39**, 1489 (1965).
2. GYARMATI, I.: Acta Chim. Hung. **43**, 353 (1965).

Dr. István GYARMATI, Budapest XI. Budafoki út 8.

NEW METHODS OF COAL PETROGRAPHY IN COAL CHEMISTRY AND COAL TECHNOLOGY*

L. Soós

(Research Laboratory for Geochemistry of the Hungarian Academy of Sciences, Budapest)

Received July 3, 1964

A question frequently raised in former times and still raised sometimes today is whether coal petrography can be of real assistance to coal mining and the coalutilizing industries, that is, whether it is a branch of science of practical applications, or just a theoretical discipline apt to solve first and foremost the problems of coal genesis. In discussions concerning this point some have spoken for, some against coal petrography. This diversity of judgment can be traced back to several causes, the first of which is that some of those who work in practice insufficiently know and misinterpret, or sometimes do not know at all the perspectives opened by the application of coal petrographic methods. Consequently, they do not realize the use of coal petrography, or if they do, their views may easily be erroneous.

The second cause follows from the first: many people expect from coal petrography the solution of problems which cannot possibly be solved by the experts of coal petrography alone, but require the cooperation of chemists, physico-chemists or technologists. On the other hand, often problems are not recognized whose solution would be available by coal petrographic methods alone. Therefore, the questions are often stated and the tasks outlined in a way that frustrates success in advance.

It is, of course, justified to ask whether the specialists of coal petrography have done all to sufficiently develop and emphasize the practical aspects of this branch of science.

Before this question is answered a slight detour is necessary. The beginning of practical applications of coal petrography dates back to about 1930. It is well known that coal petrography has acquired considerable merits, practical as well as purely scientific, particularly on the territory of investigation of coal genesis, by developing the moor-system. However, it must be admitted that for a time this branch of science did not take part in the solu-

*Lecture delivered before the Coal Symposium organized by the Petroleum, Coal and Gas Technology Committee of the Department of Chemical Sciences of the Hungarian Academy of Sciences and the Coal Chemistry Group of the Hungarian Chemical Society, Budapest, February 14, 1964.

tion of practical problems as much as it was expected by the workers in practice. It is easy to see the reasons why such an activity was impossible. The explanation is that coal mining and the coal-utilizing industries had begun to develop earlier and at a quicker pace than theoretical research on coal. Practice thus got considerably ahead of theory. The limited volume of theoretical knowledge concerning coal and the resulting imperfections of the methods of investigation, reacting upon coal petrography, for a while handicapped but eventually provoked and fostered its development.

However, if the achievements of the last 20 years are considered, it is apparent that coal petrography, after having disposed of its initial, mainly methodological difficulties (that is, since 1940 and particularly 1945) has attained results worthy of attention and of considerable profit to practice. It is quite another matter how far these results, of which the latest shall be treated in the present paper, have been or are being put to practical use by mining and coal utilization.

It is well known and obvious even to the naked eye that coal is not a homogeneous organic substance of a fixed chemical composition; on the contrary, under the microscope it is seen to consist of a considerable number of organic as well as of a few inorganic constituents. Consequently, the chemical and physico-chemical methods usually employed to characterize well-defined organic compounds are unsuited to give a satisfactory description of coal. Coal, particularly its more thoroughly coalified varieties, cannot be dissolved without destroying the original structure, at most a few constituents may be extracted; therefore, the classical methods of structure study are very seldom if at all applicable to the problem. The common shortcoming of the usual chemical and technological methods of coal chemistry is that they furnish only the mean properties of the studied material, but fail to reveal which of the organic components (macerals) are responsible and in what measure for one or another property of coal.

Nor did the study of the four band types, fusain, clarain, vitrain and durain give satisfactory results, because the investigation of these inhomogeneous band types consisting of several organic and inorganic minerals by the usual methods of chemistry and technology could furnish again mean values only. It has to be pointed out in this respect that the various band types possess different and approximately determinable technological properties, the study of which affords much more useful information to the man of practice than a study of coal as a whole. It is, however, sufficiently proved by what has been said above that the satisfactory knowledge of the constitution, structure and technological properties of coal cannot be acquired except by a comprehensive complex study of its individual constituents.

The sudden development of coal petrography has been started indeed by the recognition of these facts, followed by the distinguishing and characteriz-

ing of the coal macerals, subsequently the separation of the individual macerals from the coal, their physico-chemical study and systematizing. Consequential studies into this field were initiated about 1945 and have led to valuable information. To this also the workers of th's country have appreciably contributed: I am referring in the first place to the results concerning the separation, characterization and systematization of homogeneous coal macerals achieved by SZÁDECZKY-KARDOSS [10].

Our task is to deal here briefly with some problems of interest to coal mining, processing and utilization, which have been solved or are significantly promoted on the way of solution by the results of applied coal petrography, at home or abroad.

The scope of this paper is, of course, insufficient to treat more than the problems which the author considers to be the most important; a discussion of all methods of coal petrography would require by now a complete book.

The topics briefly introduced here will be the following:

I. questions of mining and sampling of coal in the mine;

II. coal petrographic aspects of the study of coking coals and the composition of coal mixtures.

I. Questions of mining and sampling of coal in the mine

I. Thorough knowledge of the materials constituting the disclosed coal seam is of considerable importance to coal mining, for two reasons:

1. It is essential to know the macro- and microstructure of the seam, since this is the best basis for a prognosis of the quality of coal in the as yet undisclosed parts of the seam. This group of problems includes in the first place the questions of seam identification and parallelization.

2. The exact knowledge of the materials of the seam under exploitation makes possible to forecast the working costs and to decide the most advantageous utilization of the coal, furthermore it provides information concerning mine safety and health. I am referring here to problems such as dust formation, the composition of dust and spontaneous ignition.

The methods of coal petrography, especially the microscopic methods, are ideally suitable for and indispensable in the study of these factors.

ad 1. Just like in any other kind of coal analysis, the first step of a coal petrographic study is *sampling*, necessarily performed on the basis of macropetrographic differences. The correct execution of sampling in order to characterize a given coal seam has obviously a decisive influence on the correctness of the results. The difficulties inherent in sampling in the mine are, however, considerable owing to poor lighting, the wetness of the coal face, etc. It is sometimes practically impossible to detect any macroscopic difference between

parts of a seam whose chemical and technological properties turn out to be markedly different.

In order to improve the examination in the mine of lignites and to eliminate the factors that may lead to incorrect sampling, we have developed a new field method that has been found most useful in practice. It is known that the coal macerals bituminites (liptinites) give a relatively strong greenish-yellowish luminescence when exposed to ultraviolet radiation. Making use of some microscopic studies in the laboratory, luminescence investigations were initiated in the mine, on the standing coal face.

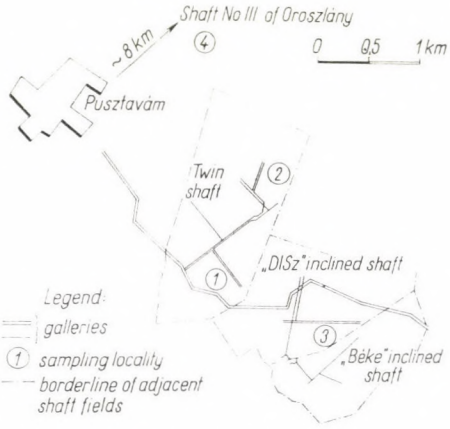

Fig. 1. Sketch map of the localities mentioned in the text

The luminescence studies first carried out in the mines between Pusztavám and Oroszlány yielded interesting and important results which we should like to discuss here briefly, as a preliminary report.

In the Pusztavám-Oroszlány coal-field, the Lower Eocene coal bed consists of two fairly uncontaminated seams numbered at present I and II and of an underlying clayey seam complex. At the time of our studies the lowermost clayey seam was not yet adequately disclosed. Our studies had therefore to be restricted to several points of Seams I and II in the Pusztavám mine, and to Seam II, being exploited in the No. 3 Shaft of Oroszlány (Fig. 1).

For the purpose of these studies a portable luminescence apparatus of about 120 Watt output was constructed, equipped with a Type HQV 125 quartz lamp and an UG 1 ultraviolet filter. Since this filter also transmits some visible light, we have used spectacles made of appropriate barrier filter glass to eliminate any violet or bluish light reflected from the coal wall. The peak output of the quartz lamp employed is at 3650 Å.

The studies carried out in the mine have revealed the following.

Proceeding downwards from the roof, the first 20 centimetres of Seam I of Pusztavám (total thickness 120 cm) did not respond by any luminescence to ultraviolet excitation. This part of the seam thus appears black, with minute scattered resin particles. The next 20 cm was brown in colour, containing 1 to 2 mm thick bands emitting a bright yellow luminescence. The matrix of the underlying 35-cm layer was light greyish yellow, finely striped with 1 to 0.1 mm

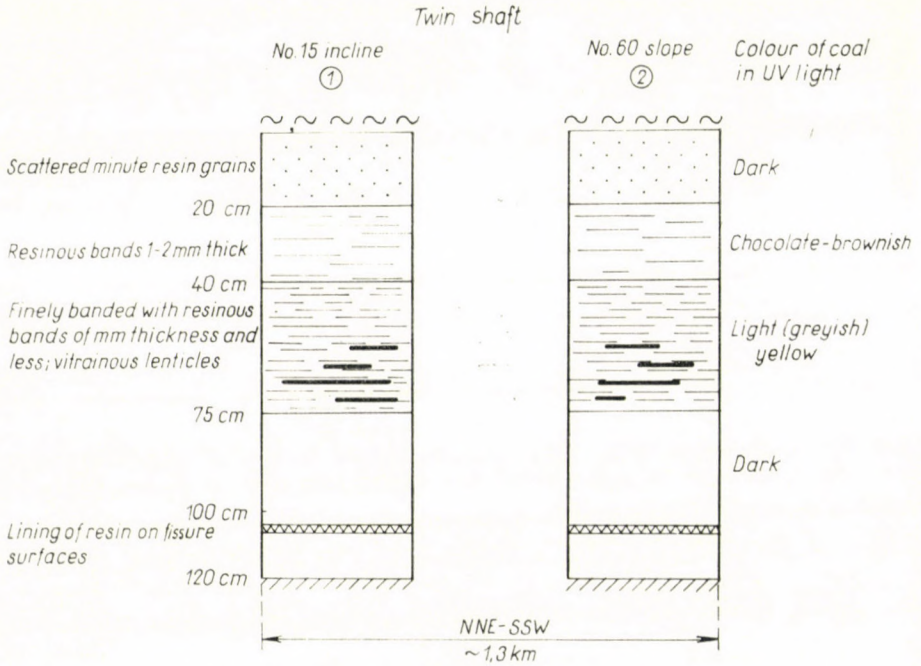

Fig. 2. Luminescence of Seam No. I of Pusztavám

thick bands showing bright yellow luminescence. Small lenticles of vitrain are present in this part of the seam which do not emit any luminescence, appearing consequently black under ultraviolet radiation. The next 25 cm exhibited no luminescence except for some rather scarce strings of resin. Some 20 centimetres above the floor, the faces of the joints exhibited a resinous lining of yellowish-reddish luminescence. The luminescence properties of Seam I are summarized in Fig. 2.

It is very remarkable that in the No. 15 incline and in the No. 60 slope as well as in the DISZ inclined shaft, Seam I had almost to the centimetre the same sequence of properties at points of observation 1.3 to 1.8 km apart.

Seam II, of 220 to 280 cm thickness, was studied in the twin shaft of Pusztavám at the aforementioned two points, as well as in the DISZ inclined shaft and in the No. 3 shaft of Oroszlány. The study of this seam gave even more

remarkable results. Seam II invariably exhibits five distinct resinous bands of bright yellow luminescence, present at all points examined. These persistent resinous bands are not visible in the usual lighting of the mine or the laboratory; they can be detected only by their luminescence. Their thickness varies between 1 and 20 mm, and can be traced from Pusztavám to Oroszlány, through some 8 kilometres. The luminescent resinous bands of Seam II of Pusztavám

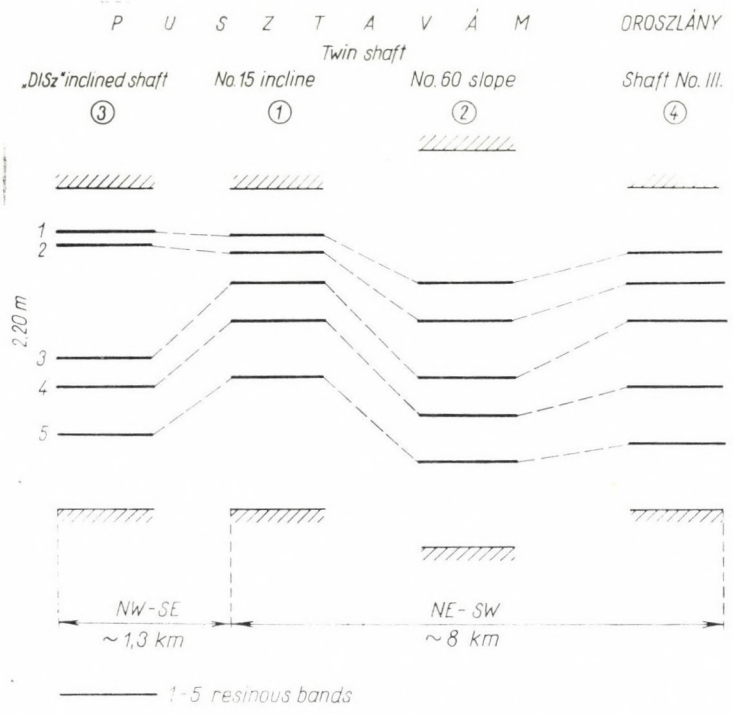

Fig. 3. The luminescent resinous bands of the Seam No. II of Pusztavám and Oroszlány

and Oroszlány are shown in Fig. 3. The total thickness of the bands in Seam II is between 25 and 55 mm. Along a fault displacing the seam at one of the working faces of No. III Shaft of Oroszlány, even the dislocation of the resinous bands together with the seam could be observed.

In connection with this method it has to be noted that the luminescent macerals are excellently visible, aglow, as it were, against the black coal wall.

From what has been said above, it is evident that the method may have two principal possibilities of application:

(a) In the course of sampling, changes in the seam may be detected that would pass otherwise unnoticed; this fact permits suitable selection of samples. We mean here in the first place the thin but persistent resin bands

previously unobserved, which could get into the sample only by accident, and then only in a quantity that could hardly influence the properties of the sample as a whole.

(b) From the point of view of mining, the method is an excellent, reliable, rapid and cheap means of seam identification. It is unnecessary to dwell any further on the importance of this fact.

It is obvious that the outlined method based on the luminescence of the bituminites is of no use beyond the coalification break, as the bituminites turn into non-luminescent huminites at this stage. Consequently, our new method is best suited, as proved also by theoretical considerations outlined in another paper [8], to the study of Eocene lignites containing some bituminite, or liptobiolitic formations of other periods. The results of similar studies on the Upper Cretaceous coal of Ajka, as well as their genetic, geologic, palaeogeographic and microtectonic relations and their significance in the estimation of reserves and in coal processing will be reported in a separate paper. The extension of the luminescence investigations to the Mecsek Mountains Jurassic coal basin is planned; in that region, however, the luminescence of the inorganic constituents may be expected to play a predominant or exclusive role.

ad 2. A widely studied important problem of mine health is pneumoconiosis and silicosis afflicting the underground personnel of the mine, due to the presence of silica or quartz. Since these sicknesses do not depend on dust concentration only but also on mineral composition, it is an important and responsible task of petrography to determine the often exceedingly fine (0.5 to 8 μ) inorganic mineral particles not only in a quantitative manner but also by qualitative analysis. Thus it is frequently necessary to distinguish quartz, illite, kaolinite, mica, sulfides and carbonates, a task that is performed by microscopy on polished powder surfaces by the phase contrast technique or in a dark field. Clay minerals, noxious in a way not yet fully understood, may be identified by dyeing, DTA, X-ray and electron microscopic methods.

A further problem of equal importance to mine safety and health is the study of the causes of mine fires and spontaneous ignition. In respect of this problem the task of coal petrography is to detect, mainly by microscopic investigations the macerals which are the first to suffer oxidation producing heat; so these points of the coal seam may be located. Petrographic studies of this problem [9, 7] have detected the *principal cause* of spontaneous ignition to be the oxidation of finely distributed huminite particles of large specific surface, promoted eventually by certain chemical and physical factors, such as increase of the surface owing to geological conditions. SZÁDECZKY-KARDOSS [9] succeeded in proving that on the exposed surface of the coal and along the joints thin oxidized layers are formed that protect the coal from further oxidation. If the coal suffers no further breaking up after the development of

the oxidized protective layers, then oxidation is stopped and the danger of spontaneous ignition is practically eliminated. If, on the other hand, such layers are continuously removed, *e.g.* by factors bringing about the comminution of the coal, oxidation may proceed to a degree where spontaneous ignition sets in.

II. Coal petrographic problems connected with coking coals

It is known that the volatile content of a coal permits conclusions concerning the degree of coalification; it is also one of the parameters of the coking properties of the coal. However, in studying coking coals or their mixtures, determination of the volatile content yields but a mean value; the problem as to what coals or coal macerals of what degree of coalification or what volatile content are responsible for this mean value cannot be solved except by coal petrographic methods, such as analysis and physical investigations (*e.g.* measuring of light reflectance). Thus coking coals cannot be characterized by their volatile content alone; the well-known three parameters are required. In the study of coking coals the knowledge of the quantitative composition of the rock is also very important, though insufficient in itself, because the percentual distribution of the macerals does not permit conclusions about the volatile content, *i.e.* the degree of coalification, or such inferences are very vague.

Coking coal consists of several macerals of different chemical, physical and technological properties, such as vitrinite, the principal carrier of coking capacity, bituminites, usually present in moderate amounts, and inert macerals such as fusinite, and micrinite. Of these macerals, the inert ones are unfavourable to coking. From the point of view of coking, an ideal coal should consist of pure vitrain, without any detrimental macerals. However, it must be noted at once that even the vitrain of such an ideal coal would not necessarily have uniform composition, because it may be composed of more and less coalified vitrinites, that is, of particles of higher or lower volatile content. This is, *e.g.* the case with the Komló coal.

It is also known that the light reflectance of the individual organic coal macerals increases with the progress of coalification, that is, with the decrease of their volatile content. [2]. Microscopy is therefore suitable to distinguish vitrinites in the various stages of coalification, or inert substances of considerably higher reflectance can be quantitatively determined. The only adequate method known so far for determining the distribution of the macerals according to their volatile content is the direct determination of their reflectance distribution under the microscope.

Reflectance, a clue to the fine structural properties of the coal macerals, is a dynamic factor well suited to characterize certain petrographic and chemical-technological properties of coal, such as its degree of coalification, coking

capacity, etc.; the rapid and accurate determination of reflectance is the aim of an increasing volume of research. Reflectance data of the coal macerals may be used to investigate the following important problems:

— the determination of the degree of coalification, that is, the numerical characterization of the degree of metamorphism;

— from the absorption coefficient and refractive index, calculated from the reflectance the degree of condensation and or aromaticy of the carbon atoms may be determined;

— characterization of the technological properties *(e.g.* as mentioned, the coking capacity) and the correlation of the seams may become possible in a manner much less time-consuming than the procedures employed so far.

An accurate determination of reflectance is essential in cases where its value changes parallel to the continuous variation of the chemical structure of the substance investigated. In such cases reflectance defines the degree of the gradual change of the lattice structure or of the metamorphism. With the exception of a single maceral group this applies to the case of coal macerals, of which vitrinite and the oxinites (inert substances) exhibit a reflectance dependent in a continuous manner on coalification up to the anthracite stage. The exceptional group is that of the bituminites; their coalification is continuous up to the coalification break observable in the fat coal stage; at this break abrupt vitrainization takes place. After this break, the vitrainized bituminites change again continuously.

Such considerations have induced us to investigate the physical properties of coal macerals, first of all their optical properties, and to develop a method of reflectance determination providing the possibility of numerical determination of the optical properties of the individual, mostly minute microscopic macerals.

In the case of perpendicular incidence, the reflectance of an isotropic, transparent medium depends solely on the relative refractive index, in an isotropic absorbing medium, such as coal, also on the absorptive index, given by the *Beer* formula:

In air:

$$R = \frac{(n-1)^2 + n^2 \varkappa^2}{(n+1)^2 + n^2 \varkappa^2} \tag{1}$$

In oil immersion:

$$R' = \frac{(n-n')^2 + n^2 \varkappa^2}{(n+n')^2 + n^2 \varkappa^2} \tag{2}$$

where

R = reflectance measured in air, R' = reflectance measured in oil immersion, n = refractive index of the absorbing medium (coal, in the present case), n' = refractive index of the immersion liquid, $\varkappa$ = absorptive index of the absorbing medium.

The two equations readily yield the refractive index. The adsorptive index can be obtained from the first equation.

The refractive index is

$$n = \frac{1}{2} \frac{n'^2 - 1}{n' \frac{(1+R')}{(1-R')} - \frac{1+R}{1-R}} \tag{3}$$

and for the absorptive index we have

$$\varkappa = \frac{1}{n} \sqrt{\frac{(n+1)^2 R - (n-1)^2}{1-R}} \tag{4}$$

The two values of reflectance used for calculating the refractive index must be very accurate, otherwise the results will be useless.

Measurements of the reflectance of vitrinites was initiated in 1932 by HOFFMANN and JENKNER [2]; these authors used the Berek slit microphotometer. This long used method is subjective: the result depends on a visual comparison of light intensities instead of using an instrument, and a great deal of uncertainty is involved even if the operator is highly skilled. This method only yields the mean reflectance of the whole field of vision, and it cannot afford data accurate enough for calculating the refractive index and absorptive index.

In order to eliminate possible errors introduced by subjective measurements, several workers [6, 1, 11] have adopted the technique which employs a photocell; though this is more accurate than the Berek method, it still does not furnish satisfactory results. Both the Berek slit microphotometer and the photocell require intense light, so in either case it is impossible to narrow down the field of vision sufficiently to exclude all but a single homogeneous maceral, which has as a rule the diameter of a few microns only. Neither method permits the utilization of monochromatic light, unless broadband filters of poor selectivity and low absorption are used. In view of the fact that both the refractive index and absorptive index depend on the wavelength, the determination of the reflectance should naturally be performed in monochromatic light.

Considering that the vitrinite of a gas coal has about 1% reflectance measured in oil immersion, the use of a usual microscope lamp of 30 watts results in a light intensity between $3 \cdot 10^{-10}$ and $2 \cdot 10^{-7}$ lumens for a vitrinite grain

of a few microns diameter, according to KÖTTER [3]. Insertion of an interference filter in order to produce monochromatic light results in a further decrease by about one order of magnitude. Owing to this small value, the only device suited to the direct determination of light intensity is the photomultiplier, where amplification is considerably higher than with a photocell. The first to use the multiplier were MCCARTNEY and HOFER [5], later on KÖTTER [3].

The above considerations have led also the present author to develop a photomultiplier method that permits determination of the reflectance and optical parameters of coal macerals of 1.5 to 5 μ size in a much shorter time and with considerably greater accuracy than can be attained by either the Berek or the photocell method. The absolute error of our measurements is between 0.24 and 0.4%, whereas that of the Berek method is between 3 and 5%, and that of the photocell method about 1%.

The method and apparatus that have been in use to satisfaction for more than a year is described below.

The microscope is a type Zetopan-Pol of Reichert make, provided with a phototube. The light falling perpendicularly upon the polished surface and reflected from here can be projected through a prism either into the eyepiece or into the phototube. The principle of this apparatus employed to measure the intensity of the reflected light is as follows:

A fixed diaphragm placed in the image plane of the eyepiece of the phototube (measuring diaphragm) ensures that only a detail of given size of the field of vision may reach the cathode of the multiplier mounted upon the phototube. The photocurrent, whose intensity depends on the reflectance of the substance, is measured by a mirror galvanometer of a sensitivity of $5.45 \cdot 10^{-10}$ A/mm. The smallest particle size that can be measured by this apparatus is, as already mentioned, 1.5 to 5 μ depending on the magnification employed. The measurements are carried out in monochromatic light produced by an interference filter.

The trajectory of the light rays in the apparatus is shown in Fig. 4 (p. 78).

The photomultiplier employed was a type 1P 28 of RCA make; the light source was a low-voltage bulb of 30 Watts. Both the multiplier and the lamp were fed from a stabilized power supply unit.

The complete apparatus is presented in Fig. 5. The dark current of the photomultiplier as well as the reflection of the objective lenses have been determined and compensated on the galvanometer.

Contrary to other authors, we employed as a reflectance standard a prism of heavy flint glass whose reflectance in oil immersion as calculated from its refractive index was 0.793% at 5470 Å.

In connexion with the measurements of reflectance, the following important results are worth mentioning.

With the purpose of studying the relationships between the degree of coalification, volatile content and reflectance, respectively, we have investigated the reflectance of vitrinites. The samples studied were of coals of low ash content, the volatile content of which had been determined by the usual method. Fragments of the sample broken down to about 1 mm size were

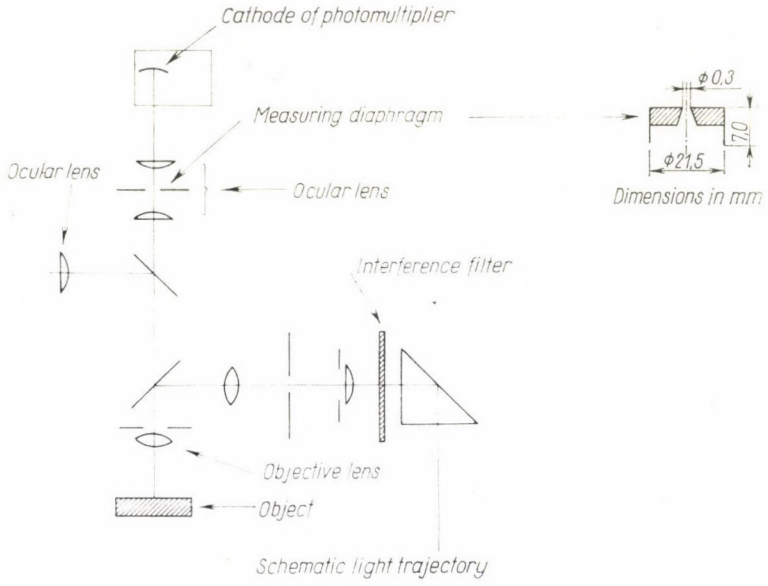

Fig. 4

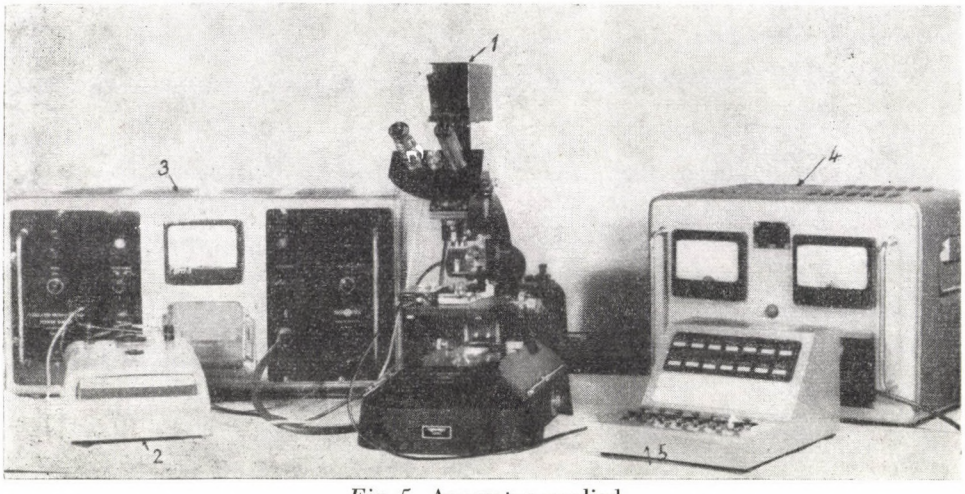

Fig. 5. Apparatus applied
1: multiplier, 2: galvanometer, 3: d.c. power supply, 4. a.c. stabilizer, 5: point counter

embedded in an epoxy resin and the surfaces were polished. The average reflectance of the sample was determined by measuring the reflectance at 5470 Å in oil immersion of at least fifty grains of vitrinite per preparate, chosen randomly all over the sample. The diagram in Fig. 6 permits the rapid determination of the degree of coalification and the volatile content on the basis of the measured reflectance.

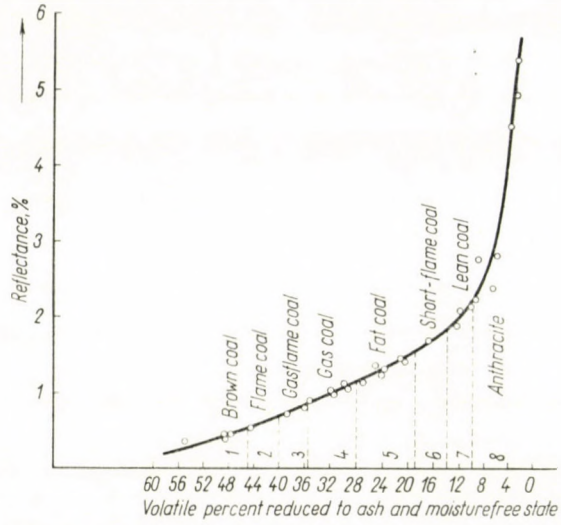

Fig. 6. Reflectance vs. volatile content as measured under oil immersion at a wave-length of 5470 Å

We have determined and/or calculated the refractive indices of several coal macerals. We shall not deal with this topic here in any detail, except for mentioning that an investigation of the well-known relationship between the refractive index and the dielectric constant of coals may produce interesting and useful results.

The reflectance of grains of vitrinite was studied in a coal containing over 50% of ash, which occurs at Nagybátony, close to an andesite contact. From the results and by establishing the volatile content with the aid of Fig. 6, the degree of metamorphism has been estimated. This technique opens up the way of characterizing in this respect also such high-ash clayey coals where determination of the volatile content was bound to yield wholly illusory values.

We have determined on a polished surface the reflection spectrum of some coal macerals. Microspectrophotometric measurements have been carried out in thin sections on xanthoresinite, huminite and melanoresinite. Both the measurements of reflection and absorption were carried out in the visible range transmitted by the optics of the microscope. The results will be reported in a separate paper.

The described method has rendered accessible the study and eventual solution of the following other problems:

(1) Compilation of reflectance statistics of coking coals and coking coal mixtures.

We have already remarked that determination of the volatile content furnishes but mean values, and that the problem of allocating the volatiles to well-defined coal macerals of known degree of coalification and volatile content as well as of well-defined technological properties can only be achieved by reflectance measurements. Thus, for instance, according to KÖTTER and LANGNER [4] 25% volatile content can be due to 100% fat coal, but just as well to a mixture consisting of 21% gasflame, 18% gas, 32% fat, and 29% short-flame coal, or to a mixture of 16% gasflame, 31% gas, 20% short-flame, and 33% fat coal. This is why the swelling index is 9 in the first case, 4.5 in the second, and 1 in the third. By reflectance statistics, that is, by determining the distribution of the macerals according to volatile content, the problem can be readily and unequivocally numerical decided by measuring a single parameter. That makes possible to adjust the composition of coal mixtures prepared for coking in the most favourable manner, by determining the proper mixing rates in advance.

(2) The apparatus just described allows the rapid determination of bituminites. Let us restrict ourselves here to the remark that of the coal macerals it is only the bituminites that exhibit any luminescence.

As it is revealed by what has been said in this paper, the methods of coal petrography have indeed undergone considerable development. Of course, the present paper is no attempt at a comprehensive review because, as already mentioned, the number of coal petrographic methods is very large.

SUMMARY

Possible applications of coal petrography in the fields of mining, coal chemistry and coal technology are reviewed.

A new method of seam parallelization and of sampling in the mine is given and the coal petrographic aspects of spontaneous ignition are briefly discussed. The latest and most important achievements of coal petrography in facilitating the solution of several technological problems are dealt with. A method for the objective characterization of the degree of coalification on the basis of the reflectance of the macerals, the determination of the optic parameters of coal macerals and a way of rating coking coal mixtures on the basis of reflectance statistics are described. The quantitative determination of bituminites by their luminescence is outlined.

REFERENCES

1. DAHME, A., MACKOWSKY, M. Th.: Brennstoff-Chemie **31,** 129 (1950); **32,** 175 (1951).
2. HOFFMANN, E., JENKNER, A.: Glückauf **68,** 81 (1932).
3. KÖTTER, K.: Brennstoff-Chemie **41,** 263 (1960).
4. KÖTTER, K., LANGNER, W. D.: Brennstoff-Chemie **42,** 380 (1961).
5. MCCARTNEY, J. T., HOFER, L. J. E.: Anal. Chemistry **27,** 1320 (1955).

6. ORCEL, M. J.: Bull. Soc. Franc. Min. **53,** 301 (1930).
7. Soós, L.: Földtani Közlöny **93,** 173 (1963).
8. Soós, L.: A melanorezinit szénkémiai és szénkőzettani vizsgálata. (Chemical and petrological study of melanoresinite.) Kőszén- és kőolaj anyagismereti monográfiai sorozat. Vol. 2. (Publishing House of the Hungarian Academy of Sciences, Budapest) 1964.
9. SZÁDECZKY-KARDOSS, E.: Bányászati és Kohászati Lapok **77,** 241 (1944).
10. SZÁDECZKY-KARDOSS, E.: Bánya és Kohómérnöki Oszt. Közl. **17,** 176 (1948—49).
11. WEGE, E.: Brennstoff-Chemie **35,** 1, 33 (1954).

Über neue quantitative kohlenpetrographische Methoden auf dem Gebiet der Kohlenchemie und Kohlentechnologie

L. SOÓS

Zusammenfassung. Eine Übersicht über die Anwendungsmöglichkeiten der Kohlenpetrographie auf dem Gebiet des Bergbaus, der Kohlenchemie und Kohlentechnologie wird vorgelegt.

Die neuen Methoden der Flözkorrelierung und Probeentnahme im Bergwerk, und die petrographischen Beziehungen der Selbstentzündung werden besprochen. Jene neueste und wichtigste petrographische Verfahren, mittels welcher man verschiedene technologische Probleme leichter lösen kann, werden kritisch behandelt. Das Problem der objektiven Bestimmung des Inkohlungsgrades auf Grund des Reflexionsvermögens, der Ermittlung der optischen Kennwerte der einzelnen Kohlenbestandteile, und der Auswertung der Kokskohle auf Grund einer Reflexionsstatistik wird besprochen. Die Möglichkeiten der quantitativen Bestimmung der bituminitischen Kohlenbestandteile durch Lumineszenzmessung werden erwähnt.

Новые количественные методы петрографии угля в области химии и технологии угля

Л. ШОШ

Резюме. Дается обзор о возможности применения петрографии угля в области горного дела химии и технологии угля.

Коротко рассматривается идентификация пластов и отбор горных проб с помощью нового метода, кроме этого автор занимается петрографическими вопросами самовоспламенения. Обсуждаются те новейшие и наиболее важные петрографические методы, с помощью которых некоторые технологические задачи становятся более легко разрешимыми. Автор занимается вопросом объективного определения степени обуглероживания, основанной на отражательной способности, определением оптических параметров отдельных мацералов угля, а также оценкой коксового угля на основе статистики отражательной способности. Обсуждается возможность количественного определения битуминитов на основе люминисценции.

Dr. László Soós; Budapest VIII. Múzeum körút 4/a.

О НЕКОТОРЫХ ПРОБЛЕМАХ КИНЕТИКИ И МЕХАНИЗМА РАЗРЯДНО-ХИМИЧЕСКОГО ОКИСЛЕНИЯ УГЛЕВОДОРОДОВ В ГЕТЕРОГЕННОЙ ФАЗЕ

З. ПАЛ и Г. ФЁЛЬДИАК

(Научно-исследовательский институт нефти и природного газа, Веспрем—Будапешт)

Поступило 30. янв. 1965 г.

В течение последнего десятилетия развивалось массовое производство жирных кислот путем окисления парафина [1]. Так как при этом оказывается недостатком необходимость очищения продукта от соединений марганца, использованных как катализатор, достойны внимания стремления к замещению катализатора ироникающими излучениями.

Бах и сотр. показали [2], что в радиационно-химическом окислении парафиновых углеводородов при температурах до 60° С наблюдаются практически все продукты термического окисления. На основе небольшого энергетического выхода ($G = 1—6$ молекул на 100 эв) и некоторых особенностей реакции предполагали, что элементарные акты реакции произошли непосредственно за счет энергии «горячих» частиц (радикалов, ионов, и т. п.), образующихся под влиянием излучения, значит, окисление имеет нецепный характер. Однако, при повышении температуры окисления выше 100° С, выходы резко увеличивались [3].

По наблюдению *Эмануеля* [7] в процессе окисления парафина при 127° С поглощение доз уже в 70 р оказалось достаточным к тому, чтобы начинался процесс, после индукционного периода нескольких часов, вместо несколько сотен часов, со скоростью, равной скорости термического окисления. [7]

В случае увеличения поглощенной дозы до примерно 10^5 р, после окончания облучения но не переставая вводить кислород, скорость последующего окисления сохранялась на уровне радиационно-химического процесса который превышал скорость термической, некаталитической реакции [6, 8]. Эти факты дают возможность окислять технический парафин или цетан без применения катализатора, со скоростью, необходимой в промышленных процессах [4—6].

Инициирование цепных реакций, происходящих в последних случаях обеспечивается в первую очередь за счет реакционно-способных радикалов, образующихся при взаимодействии с излучением, а дальнейшие ступени с меньшей энергией активации происходят более или менее независимо от облучения, за счет термической энергии молекул.

В литературе пока не выяснен окончательно вопрос о различии или идентичности цепных реакций, протекающих в термическом и радиационно-химическом окислении [3]. В пользу различия говорит наблюдение о большей чистоте и яркости продукта радиационно-химического окисления, а также меньшее содержание гидроксикислот и кетокислот в продукте, облученном до конца опыта в сравнении с оксидатом, в случае которого облучение было прервано во время реакции [9].

По мнению авторов реакции, происходящие в тихом электрическом разряде представляют специальную область радиационной химии в широком смысле. Недавно и экспериментально послучилось показать практическую идентичность химического влияния тихого электрического разряда и проникающих излучений и найти количественную связь между ними [10]. Однако, в случае конденсированных фаз распределение энергии разряда из-за небольшой глубины проникновения частиц, как и в случае мягких β-лучей, чрезвычайно неоднородно.

В настоящей работе исследована применимость разрядно-химической методики, использованной до сих пор главным образом в реакциях гомогенных разложений, в процессе, протекающем в гетерогенной фазе, между двумя участниками реакции. При этом целью работы являлось определение сохранности или изменения закономерностей радиационно-химического окисления в реакции, происходящей под влиянием тихого электрического разряда; как зависит характер реакции от температуры и установление различий или подобностей между общем протеканием, кинетикой и механизмом термического и разрядно-химического окисления.

Экспериментальная часть

Вместо стеклянных приборов с электролитическими обкладками, распространенных в разрядной химии, была изготовлена установка (автоклав), пригодная для изучения разрядно-химических реакций при повышенных температурах и при высоких давлениях [11].

Напряжение с частотой 600 гц было предоставлено с помощью питательного блока с предохранителем замыкания и защитой от прикосновения, составляющего из осциллятора звуковой частоты, усилителя с мощностью 100 вт и трансформатора высокого напряжения. Во время опыта измерялись напряжение (6—8 кв), сила тока (5—10 ма) и количество перешедшего электрического заряда. Общий расход мощности составлял 30—80 вт, доля безваттного и потерянного тока точно не определялась.

Разряд имел место в пространствах между концентрическими рубашками цилиндра, расстояние которых было 2—3 мм. В этих пространствах находилась воздушно—масляная пена, поверхность которой во время опыта постоянно возобновлялась вследствие барботирования воздуха.

В качестве исходного вещества использовалось парафиновое масло. Это — смесь различных парафинистых соединений, главним образом с разветвленными цепями, практически не содержащая ароматики; оно в температурном интервале опытов (20—150° С) жидко и имеет небольшую упругость пара. Так как с точки зрения окисления третичные углеродные атомы имеют наибольшую реакционную способность, легко понять, что длительность индукционного периода при термическом окислении парафинового масла, содержащего разветвленные углеводороды составляет несколько часов в отличии от

твердых парафинов, содержащих главным образом углеводороды с нормальными цепями, в случае которых длительность индукционного периода может достигать несколько сотен часов. [12] Характеристика исходного вещества приведена в табл. I.

Табл. I

Некоторые характерные данные исходного парафинового масла

Плотность 20° C	0,8812
Средний молекулярный вес	385
Содержание кислорода	0,0%
Кислотное число	< 0,1 мг KOH/г
Эфирное число	< 0,1 мг KOH/г
Карбонильное число	< 0,2 мг KOH/г
Содержание перекисей	0,0 мг экв/г·10^{-2}
Иодбромное число	0,06 мг J_2/100 мг

По опыту использовалось 100 мл (~ 85 г) парафинового масла. Автоклав нагревался с помощью газовой горелки до желаемой температуры, измеренной с помощью платинового термометра сопротивления с точностью ± 1° C. Количество продуваемого воздуха измерялось газовыми часами, включенными в систему после автоклава.

Оксидат, отобранный после охлаждения автоклава был более или менее темноватый и имел острый запах. Так как исходное вещество являлось многокомпонентной смесью, характеризуемой только общими нефтяными показателями, оказалось целесообразным характеризовать и продукт количеством кислородсодержащих функциональных групп. Затем определялось кислотное, эфирное, карбонильное, в некоторых случаях и гидроксильное число, а также содержания перекисей. Содержание кислорода в продукте определялось методикой поглощения β-излучения [13].*

В некоторых случаях, простая алгебраическая функция, описывающая взаимосвязь между показателями оксидата и экспериментальными параметрами, аппроксимировалась хорошо с помощью линеарной регрессии, использованной в математической статистике, хотя число точек измерений было небольшое.

Результаты опытов

Для установления оптимальной скорости потока воздуха проводились опыты с применением скоростей в пределах 25—200 лит/час. Величина показателей, кроме содержания перекисей, была приближенно прямо пропорциональна скорости воздуха. Однако, увеличение скоростей окисления путем ускорения подачи воздуха ограничивалось тем фактом, что выше скорости 100 лит/час часть масла выпенивалась из реактора. Чтобы избежать этого, величина скорости потока воздуха в большинстве опытов составляла 75 лит/час.

Под влиянием тихого электрического разряда и при комнатной температуре начиналось окисление, но продукт содержал только небольшое количество кислородсодержащих веществ. Влияние температуры на про-

* Авторы благодарят за определения старшего научного сотрудника, *Т. Балинта*.

цесс исследовано в интервале 25 и 150° С, в опытах, длительностью 4 часа. При повышении температуры до 80—90° С, степень окисления существенно не росла. Приблизительно около 100° С скорость окисления увеличивалась почти на порядок, а потом при 135—140° С повышалась еще в 4—5 раз. Относительное ускоряющее реакцию влияние разряда было самым оптимальным между 100—120° С, так как выше 120° С скорость наступающего термического окисления все более приближалась к скорости разрядно-химического процесса и примерно при 150° С достигла ее.

Количество предполагаемых первичных продуктов — перекисей — достигло своего максимума при 120—130° С и в разрядно-химических и в термических опытах, а выше этой температуры — вне зависимости от применения разряда — понизилось до очень маленькой величины. Выше 135—140° С и величина кислотного числа понижалась; вместе с этим в продукте наблюдалось нерастворимое, илистое, темное вещество.

В целях чтобы сравнить влияния разряда и катализитора, оказывавшие на окисление, проводились сравнительные опыты в присутствии примерно 6% вес $KMnO_4$ с применением и без применения разряда, впрочем при одинаковых условиях. Оксидат, очищенный от твердого остатка катализатора (состоящий из Mn^{IV} и Mn^{VI}) был подвергнут анализу. Данные, приведенные

Табл. II

Сопоставление термического катало,итического и разрядно-химического окисления
Длительность опыта 4 часа
Скорость воздуха 25 лит/час

а) Температура: 115 ±3° С

Режим окисления	Кислотное	Эфирное	Карбониль-ное	Перекиси
	число	в мг КОН/г	оксидат	мг экв/г · 10^{-2}
Термический	0	—	0	0
Каталитический	1,6	3,1	10,6	0,4
Разрядно-химический	2,5	5,4	23,6	20

б) Температура: 125 ±3° С

Термический	0,5	0,7	12,3	10,3
Каталитический	1,5	3,4	10,7	0,8
Разрядно-химический	2,2	2,9	21,0	19,3
Разрядно-химический с катализатором	3,4	4,0	11,6	0,5

в табл. II показывают, что разряд и катализатор ускоряли окисление примерно в одинаковой мере. Так как перманганат калия благоприятствовал главным образом разложению перекисей [14], концентрация их в конечном продукте была незначительна. Совместное действие катализатора и разряда не представляло качественно новый эффект, ускоряющий реакцию на порядок.

В температурной области, в которой скорости разрядно-химического и термического окисления были соравномерными, проводились более под-

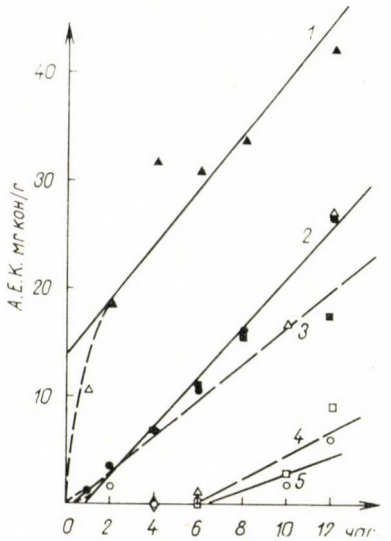

Рис. 1. Кинетика оксления при 120° С

Скорость воздуха: 75 лит. в час; ●, ○ — кислотное число; ■, □ — эфирное число, ▲, △ — карбонильное число в мг КОН/г оксидат; полные знаки обозначают разрядно-химические, пустые знаки термические опыты. Сокращения: Р — разрядно-химический; Т — термический; А — кислотное число; Е — эфирное число; К — карбонильное число; t — время реакции (час).

1 : $K_P = 2{,}57\,t + 13{,}8$; 2 : $A_P = 2{,}31\,t - 2{,}0$; 3 : $E_P = 1{,}70\,t - 0{,}55$; 4 : E_T; 5 : A_T

робные исследования насчет кинетики образования отдельных продуктов. Результаты опытов, проведенных при 120, 125 и 130° С показаны на рис. 1, 2 и 3. В случае применения разряда реакция немедленно начиналась; величины кислотного, эфирного и карбонильного числа были прямо пропорциональны длительности опыта. В контрольных опытах, без применения разряда после индукционного периода, длительность которого была обратно пропорциональна температуре, зависимость вышеупомянутых показателей от времени также удовлетворительно описывалась с помощью линеарной регрессионной функции.

Более подробное исследование кинетики образования и разложения перекисей, считаемых первичными продуктами реакции, было проведено

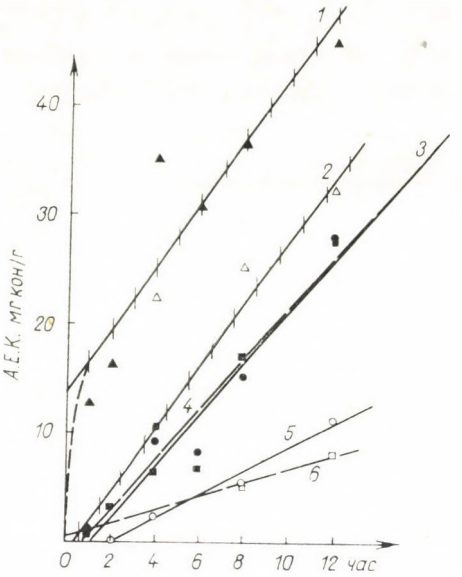

Рис. 2. Кинетика окисления при 125° С
Объяснение обозначений см. на рис. 1.
$1 : K_P = 2{,}92 + 13{,}5$; $2 : K_T = 2{,}90\,t - 0{,}7$; $3 : E_P = 2{,}32\,t - 1{,}8$; $\mathbf{4 : A_P = 2{,}37\,t - 2{,}4}$;
$5 : A_T = 1{,}08\,t - 2{,}2$; $6 : E_T = 0{,}63\,t = 0{,}63\,t + 0{,}7$

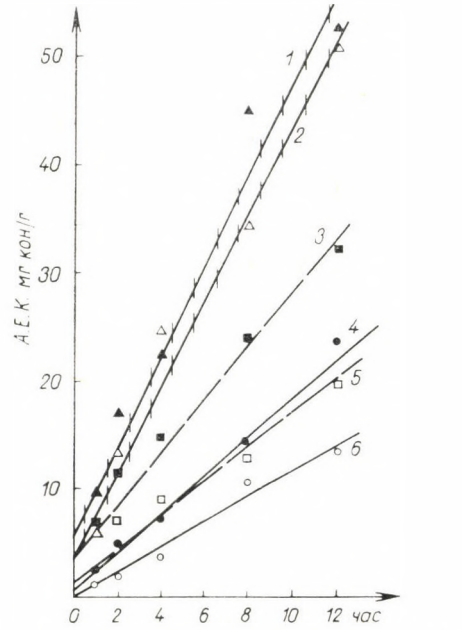

Рис. 3. Кинетика окисления при 130° С
Объяснение обозначений см. на рис. 1.

$1 : K_P = 4{,}24\,t + 5{,}4$; $2 : K_T = 4{,}05 + 3{,}4$; $3 : E_P = 2{,}48\,t + 3{,}6$; $\mathbf{4 : A_P = 1{,}80\,t + 0{,}4}$;
$5 : E_T = 1{,}56 + 1{,}3$; $6 : A_T = 1{,}20\,t - 0{,}2$

из образцов, отобранных из реакционной смеси во время опытов (через трубку для введения воздуха). Было установлено, что содержание перекисей в продукте снижалось до 20—60% от исходного во время медленного охлаждения в автоклаве; этот факт объясняет большой разброс данных, полученных при анализе образцов, отобранных за 24 часа после окончания опыта. Содержание перекисей имело максимум в зависимости от времени (рис. 4). Применение электрического поля и повышение температуры ускоряли до-

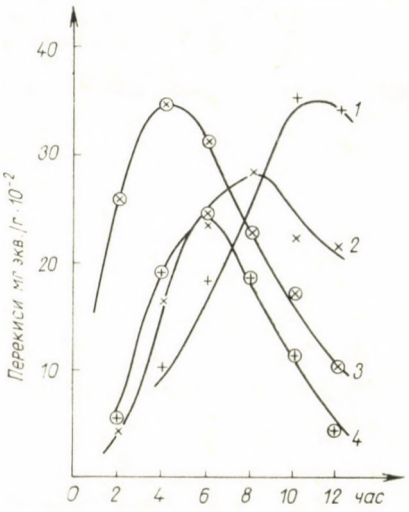

Рис. 4. Кинетика образования и разложения перекисей
× — разрядно-химический, 120° C; + — термический, 120° C; ⊗ — разрядно-химический, 130° C; ⊕ — термический, 130° C; остальные те же самые как на рис. 1

стижение максимума. Разбросы в условиях отбора пробы и в результатах анализа не позволяли делать количественные выводы из численных величин максимума или точек кривых.

В случае применения разряда только в начальном периоде реакции, скорость окисления после выключения электрического поля отставала от скорости разрядно-химического процесса, но превышала скорости термической реакции.

Что касается подробных экспериментальных результатов см. статью, опубликованную раньше [15].

Обсуждение результатов

На основании результатов можно делать вывод, что тихий электрический разряд является эффективным способом ускорения реакции и в гетерогенной фазе, аналогичным с проникающими излучениями. Оказалось

невозможным определять величины G или аналогичные величины в ходе реакции, потому что нельзя было точно измерять долю электрической энергии, прошедшую через само пространство реакции. Было показано раньше, что мощность данной установки в газовой фазе с химической точки зрения соответствует мощности дозы примерно 10^8 рад в час [16]. На основе этих данных, учитывая величину кислотного числа $\sim$ 10 мг KOH/г оксидат, образующегося в течении 4 часов, по грубому первому приближению $G_{кисл}$ находится в порядке 10 молекул на 100 эв. Эта величина непротиворечит данным радиационно-химической реакции. Общая глубина окисления была в таком же порядке, как по данным *Проскурнина* и *Хмельницкого* [5,8], пользовавшихся γ-излучением.

Первичные эффекты разряда следующие:

а) В газовой фазе образуются реакционноспособные молекулы озона, возбужденного кислорода (—O—O—), которые могут реагировать с молекулами углеводородов.

б) Ускоренные электроны и возбужденные или ионизированные частицы азота ударяются о молекулах углеводородов, находящихся на поверхности, в результате чего образуются реакционно-способные радикалы, реагирующие с присутствующими невозбужденными молекулами кислорода.

Таким образом разряд обеспечивает инициирование независимое от термической энергии, имеющее поэтому более или менее постоянную интенсивность.

Общий характер окисления в конце концов зависит от роли термических реакций, зависимых от температуры и разрядно-химических реакций, которые в первом приближении происходят вне зависимости от температуры. На основании результатов — по аналогии выводов о цепных реакциях радиационно-химического крекинга [17] — различались три температурных области окисления. Существование таких температурных областей кажется характерным для радиационно-термических цепных реакций.

1. При комнатных температурах окисление не является цепной реакцией. Первичные продукты, образовавшиеся при разрядно-химическом инициировании, рекомбинируются с большой вероятностью. Окисление продолжается только в том случае, если прореагированная молекула сохранила какое-то количество избытка энергии, приобретанного в разряде, или при столкновении с другой частицей, происходящей из разряда. Так как вероятность этих процессов невелика, количество продуктов относительно мало.

2. При повышении температуры достигается предельная температура, называемая ϑ_{ox}, выше которой режим имеет достаточную термическую энергию для того, чтобы разрядно-химическое инициирование было последовано термическим продолжением цепи. Хотя скорость термического инициирования незначительна, количество продуктов все-таки существенно растет. Эта предельная температура в нашем случае находится около 100° C, выше

этого уже характерны *разрядно-термические процессы.* Предельные температуры, обнаруженные в работе *Баха* и *Тун Тянь-Чженя* [3], применявших γ-излучение, выше которых выход тех или иных продуктов резко увеличивался, считаются по существу также ϑ_{ox}.

Величина предельной температуры начала радиационно-термических цепных реакций в случае крекинга была 250° C [17]. По представлению, разъясненному в [17], величина ϑ определяется главным образом энергией активации продолжения цепи (если разница в предэкспоненциальном множителе пренебрегаема). Величины энергий активации продолжения цепной реакции у крекинга $E_{пр} \approx 15$ ккал/моль, и у окисления $E_{пр} \approx 7—11$ ккал/мол [14, 17], а соответствующие предельные температуры в согласии с этим $\vartheta = 250°$ C, и $\vartheta_{ox} = 100°$ C. В работе *Баха* [3] также наблюдается симбатность между величинами ϑ_{ox} и энергии активации соответствующего процесса.

3. Температура, выше ϑ, соответствующая началу термического инициирования реакционных цепей с заметной скоростью, обозначалась Θ в случае крекинга [17]. При температурах выше Θ, скорость термических инициирований все более и более растет. В то же время роль радиационно-химического инициирования, независимого от температуры падает, и на несколько градусов выше Θ уже незаметна.

Наличие аналогичной предельной температуры наблюдается и в случае окисления углеводородов (Θ_{ox}), но его понятие и величина не так однозначны, как в случае крекинга, так как процесс окисления отличается индукционным периодом. Во время индукционного периода сами реакции инициирования играют главную роль, а потом — реакции разветвления цепи. Определения Θ и Θ_{ox}, соответственно, связывается с реакцией, происхождение которой считается более важным. Если Θ_{ox} определяется, как минимальная температура, при которой термический процесс происходит только после очень продолжительного (в крайнем случае бесконечного) индукционного периода, тогда Θ_{ox} определяется по развлетвлению цепи. А в случае определения Θ_{ox} температурой термического окисления с коротким (в крайнем случае ничтожным) индукционным периодом, признаком начала термической реакции считается реакция инициирования с заметной скоростью.

В данном случае по аналогии крекинга, Θ_{ox} определялась по-последнему, причем индукционный период короче часа практически пренебрегался. По такому счету величина Θ_{ox} получилась 130—135° C.

Кинетика инициирования окисления — принимая предположения литературы, по которому инициирование является реакцией между молекулами кислорода и углеводорода [14, 18] — описывается формально по-следующему:

а) В случае термической реакции:

$$-\frac{d[RH]}{dt} = k_t [RH] [O_2] \qquad (1)$$

б) В случае разрядно-химической (радиационно-химической) реакции:

$$-\frac{d[RH]}{dt} = k_t [RH] [O_2] + k_I f(I) [RH] \qquad (2)$$

где k_t — константа скорости термической реакции (по Аррениусу) [моль$^{-1}$. литер. сек$^{-1}$]; k_I — константа скорости радиационно-химической реакции, независимая от температуры [моль$^{-1}$. литер. сек$^{-1}$]; I — мощность дозы [эрг. сек$^{-1}$]; $f(I)$ — функция, определяющая зависимость между мощностью дозы и скоростью инициирования; в большинстве случаев $f(I) = I^{1/2}$. Однако, не было возможности определения численных величин этих констант. Непосредственным доказательством эффекта разряда на инициирование является наблюдение об увеличении скорости образования первичных продуктов — перекисей — под влиянием разряда.

Кроме этого разряд влияет и на остальные продукты реакции. Это влияние — не имея абсолютных величин G и констант скоростей — характеризовалось соотношением аналогичных продуктов, образующихся в термических и разрядно-химических опытах, проведенных впрочем при одинаковых условиях. Из данных, приведенных на рисунках 1—3 и в табл. III.

Табл. III

Скорость образования отдельных продуктов и их соотношение в разрядно-химических и термических опытах
(на основании средних опытов длительностью 1—12 часов)

Температура °C		Скорость образования в ммоль/час, от целого количества оксидата			Соотношение скоростей образования (термических: разрядно-химических)		
		кислот	эфиров	карбонильных соединений	кислот	эфиров	карбонильных соединений
117*	P	1,14	1,09	3,48	0,12	0,22	0,64
	T	0,14	0,24	2,20			
120	P	3,50	2,58	3,90			
	T						
125	P	3,60	3,52	4,44	0,45	0,37	0,99
	T	1,64	0,96	4,37			
130	P	2,74	3,76	6,44	0,67	0,63	0,96
	T	1,82	2,37	6,15			
150**					0,91	1,28	1,02

На основании тангенса угла регрессионных функций, исключая:
* На основании опыта длительностью 12 часов
** На основании опыта длительностью 4 часа

хорошо видно, что применение разряда ускоряло образование кислот в большой, эфиров в меньшей мере, и почти не влияло на скорость образования карбонильных соединений. При изменении температуры скорость образования отдельных продуктов не изменялась одинаково даже в разрядно-химических опытах, этот факт отражается изменением их соотношений (табл. IV). (Следует отметить, что при 130° С уже наблюдается небольшое понижение и абсолютной величины кислотного числа по сравнению с величиной, измеренной при 125° С.)

Так как глубина проникновения энергичных частиц разряда не превышает толщины слоя поверхностных двух-трех молекул, эффект разряда, ускоряющий реакцию наблюдается на границе фаз. Поэтому увеличение скорости воздуха (повышающее величину границы фаз в среднем за срок опыта) ускоряет окисление в случае применения разряда в гораздо большей мере, чем в термических опытах [15]. Кроме этого при этом также наблюдается изменение состава продукта в направлении больших количеств соединений с высшей степенью окисления, показывающее повышенную роль разрядно-химических реакций при больших скоростях воздуха (табл. IV).

Табл. IV

Влияние температуры (а) и скорости воздуха (б) на соотношение отдельных продуктов разрядно-химического окисления

а) Скорость воздуха 75 лит/час.
Длительность опытов 1—12 часов (средние по тангенсу угла регрессионных функций).

Температура °С	Соотношение продуктов		
	карбонилы/кислоты	эфиры/кислоты	карбонилы/эфиры
120	1,11	0,73	1,5
125	1,23	1,00	1,2
130	2,36	2,06	1,7

б) Температура: 128 ±2° С
Длительность опытов: 4 часа

Скорость воздуха лит/час	Соотношение продуктов		
	карбонилы/кислоты	эфиры/кислоты	карбонилы/эфиры
25	11	1,35	8,2
50	6,2	1,5	4,1
100	3,2	1,2	2,6
165	2,1	1,0	2,0

Так как образующиеся на поверхности реакционно-способные частицы не сохраняются долго, скорость окисления падает после прекращения разряда в ходе опыта. Если доля срока включения разряда понижается в целом сроке опыта, состав продукта приближается к составу, характерному на термический процесс (табл. V). Как известно [6,8], в радиационно-химическом окислении, сохранение скорости в последующем окислении обеспе-

Табл. V

Количество кислородсодержащих продуктов в зависимости от длительности разряда

Длительность опытов: 12 часов
Скорость воздуха: 75 лит. в час
Температура: 125° C

Длительность разряда час	Относительная доля* разряда, в %	Кислотное число		Эфирное число		Карбонильное число	
		мг KOH/г	доля*	мг KOH/г	доля*	мг KOH/г	доля*
0	0	11,1	39,2	8	29,0	32,2	70,0
2	16,7	19,3	69,0	16,7	60,5	38,3	83,0
6	50	21,3	76,0	22,5	81,5	41,9	91,0
12	100	28,0	100,0	27,6	100,0	46,0	100,0

* «Доля» значит процентную долю показателя от величины, измеренной в опыте, проведенном под влиянием разряда от начала до конца (12 часов).

чивается реакционно-способными частицами, образующимися под влиянием проникающего излучения в объем жидкости.

Эти факты указывают на то, что в области разрядно-термических реакций влияние разряда не ограничивается ускорением инициирования, но появляется и в дальнейших реакциях и благоприятствует в первую очередь образованию кислот. По литературе, в термическом окислении кислоты образуются в консекутивных реакциях, через карбонильные соединения [14, 18]. Так как количество карбонильных соединений было примерно одинаково в разрядно-химических и термических опытах, образование повышенного количества кислот объясняется другими реакциями. С одной стороны под влиянием разряда процесс протекает при более низких температурах (120—130° C), при которых скорость реакций, ведущих к уменшению кислот (декарбоксилирование, этерификация), еще незначительна, в согласии с промышленным опытом, по которому в термическом окислении более низкие температуры благоприятствуют образованию кислот. С другой стороны — в согласии с литературными данными — результаты указывают на протекание разрядно-химических реакций, представляющих собой пути образования кислот, отличающиеся от вышеупомянутых.

а) Из молекул углеводородов образуются промежуточные продукты, отличающиеся от гидроперекисей, разлагающиеся непосредственно в кислоты. *Бах* предполагала образование таких промежуточных продуктов в ходе радиационно-химического окисления углеводородов при комнатной температуре [4,5].

б) Возможно, что молекулы перекисей, образовавшиеся обычным путем, вступают в дальнейшие разрядно-химические реакции, ведущие к образованию кислот:

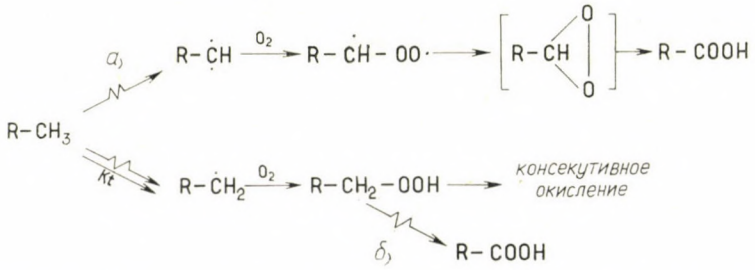

Относительная роль механизма *б)* уменьшается тем обстоятельством, что концентрация гидроперекисей на 1—2 порядка меньше, чем концентрация углеводородов, поэтому вероятность столкновения энергичных частиц разряда с неизменной молекулой углеводорода бóльшая. Но сдвиг максимума кривых, описывающих зависимость концентрации перекисей от времени, под влиянием разряда в направлении более коротких сроков при сохранности формы кривых указывает на то, что разряд влияет на образование и разложение перекисей примерно в одинаковой мере (рис. 4). Вероятно, что фактически происходят оба процесса, но на основание результатов не могли обсуждать их роль в точном механизме реакции.

На основании результатов очевидно, что в разрядно-термической области влияние разряда не ограничивается на ускорение инициирования аддитивным путем, а фактически участвует в целом ходе реакции, в тесной связи с самыми термическими элементарными актами, вследствие чего его влияние в принципе не описывается путем вычитания количества продуктов, образовавшихся в термических опытах из количества продуктов разрядно-химических опытов, проведенных впрочем при одинаковых условиях [19].

Авторы выражают искреннюю благодарность академику, профессору *Михаю Фройнду*, директору Венгерского Научно-исследовательского института нефти и природного газа за действительную поддержку этой работы.

РЕЗЮМЕ

Было показано, что тихий электрический разряд и проникающие излучения имеют аналогичные влияния в ускорении химических реакций не только в гомогенной газовой фазе, но и в случае гетерогенных процессов. Вследствие малой глубины проникновения

энергичных частиц, ускоренных в разряде, это влияние обнаруживается только на границе фаз. В разрядно-химическом окислении парафинового масла отличаются три температурные области реакции: ниже $\vartheta_{ox} \approx 100°$ С имеет место нецепное окисление, выше этой предельной температуры после разрядно-химического инициирования следует термическое продолжение реакционной цепи, а выше $\Theta_{ox} = 130-135°$ С основную роль начинают играть термические инициирования. На основе сопоставления настоящей и ранних работ авторов, а также литературных данных, наличие таких температурных областей считается общехарактерным для радиационно-химических цепных реакций. В средней, разрядно-химической области температуры, ускорение инициирования сопровождается повышением количества продуктов с высшей степенью окисления, что указывает на изменение общего механизма окисления под влиянием разряда.

ЛИТЕРАТУРА

1. Prückner, H.: Chem. Technik **4,** 193 (1952).
2. *Бах, Н. А.:* Сборник работ по радиационной химии, (Изд. АН СССР, Москва) 1955, стр. 145.
3. *Бах, Н. А., Тун Тянь Чжень:* Докл. АН СССР **129**, 604 (1959).
4. Montarnal, R.: Énérgie Nucléaire **1,** 282 (1959).
5. *Проскурнин, М. А., Хмельницкий, Ю. Л.* и др.: Докл. АН СССР **112,** 886 (1957).
6. Dragut, A., Ioanid, G. *et al.:* Revista de Chimie, **11,** 270 (1960).
7. *Эмануель, Н. М.:* Докл. АН СССР **111**, 1286 (1956).
8. *Хмельницкий, Ю. Л., Мелехонова, И. И., Нестеровский, В. В.:* Нефтехимия **2**, 368 (1962).
9. *Проскурнин, М. А.:* Личное сообщение, 1960.
10. Földiák, G., Paál, Z.: Magyar Kémikusok Lapja **18,** 573 (1963).
11. Földiák, G.: Chem. Technik **13,** 749 (1961).
12. *Хмельницкий, Ю. Л.:* Личное сообщение, 1962.
13. Bálint, T.: MÁFKI Közlemények **1,** 5 (1959).
14. *Семенов, Н. Н.:* Некоторые проблемы химической кинетики и реакционной способности, (Изд. АН СССР, Москва) 1958
15. Paál, Z.: MÁFKI Közlemények **4,** 128 (1964); дисс., 1962.
16. Paál, Z., Földiák, G.: Radiation Chemistry. Proc. of the 1962 Tihany Symposium (Akadémiai Kiadó, Budapest) 1962, p. 445.
17. Földiák, G., Paál, Z.: Acta Chim. Hung. **42,** 421 (1964).
18. *Кнорре, Д. Г., Майзус, З. К.* и др.: Успехи химии **26**, 416 (1957).
19. *Топчиев, А. В., Полак, Л. С., Тимофеев, В. Д.:* Нефтехимия **3**, 114 (1963).

Über einige Probleme der Kinetik und des Mechanismus der elektrischen entladungschemischen Kohlenwasserstoffoxydation in heterogener Phase

Z. PAÁL and G. FÖLDIÁK

Zusammenfassung. Es wurde festgestellt, daß eine stille elektrische Entladung nicht nur bei Reaktionen in homogener Gasphase, sondern auch bei Oberflächenreaktionen in heterogener Phase fähig ist, eine reaktionsbeschleunigende Wirkung derselben Natur wie die der Hochenergiestrahlungen auszuüben. Nachdem der Wirkungsabstand der Entladung nur bis zur Oberflächenschicht reicht, spielt die Phasengrenze bei solchen Reaktionen eine wichtige Rolle.

Bei der auf Einwirkung einer stillen elektrischen Entladung stattfindenden Oxydation der Paraffinöle können drei Temperaturbereiche unterschieden werden, u. zw.:

a) unterhalb $\vartheta_{ox} = 100$ °C ist die Oxydation keine Kettenreaktion;

b) oberhalb der Grenztemperatur ϑ_{ox} folgen der temperaturabhängigen entladungschemischen Initiierung verschiedene thermische Kettenvorgänge: die Reaktion ist von entladungschemisch-thermischer Natur;

c) definitionsmäßig wurde jene Temperatur (130—135°) als Grenztemperatur der thermischen Initiierung Θ_{ox} betrachtet, oberhalb welcher die Induktionsperiode der thermischen

Oxydation kürzer als eine Stunde war. Über der Grenztemperatur Θ_{ox} wurde die thermische Initiierung der geschwindigkeitsbestimmende Vorgang.

Auf Grund des Vergleichs der Angaben vorliegender Versuche, unserer früheren Versuche und der Literaturdaten wird die Existenz dieser Temperaturbereiche als eine allgemein kennzeichnende Eigenschaft strahlungschemischer Kettenreaktionen betrachtet.

Es wurde festgestellt, daß das Produkt der entladungschemischen Oxydation — abweichend vom Produkt der thermischen Oxydation — an Verbindungen höheren Oxydationsgrades reicher ist. Zur Erklärung dieser Beobachtung wurde angenommen, daß sich der Mechanismus der Reaktion auf Einwirkung der Entladung ändert, und sich entladungschemische Vorgänge abspielen die zur Bildung von Säuren führen.

Some Problems in the Reaction Kinetics and Mechanism of Hydrocarbon Oxidation Promoted by Electric Discharge in Heterogeneous Phase

Z. PAÁL and G. FÖLDIÁK

Summary. It was found that a silent electric discharge and high energy radiations have an analogous effect in promoting chemical reactions not only in homogeneous gas phase, but in heterogeneous surface reactions, too. Since the penetration of the discharge extends only to the surface layer phase boundaries play an important role in such reactions.

In paraffin oil oxidation taking place under the effect of a silent electric discharge, three temperature ranges can be distinguished:

a) below temperatures of $\vartheta_{ox} \approx 100°$ C, the oxidation process has no chain character;

b) above the limiting temperature ϑ_{ox} the discharge-chemical initiations are independent of the temperature and are followed by thermal chain propagations: the reaction has a combined discharge-chemical-thermal nature;

c) the limiting temperature of thermal initiations Θ_{ox} was defined as the temperature above which the induction period of thermal oxidation was shorter than one hour (130—135°). Above the limiting temperature Θ_{ox}, the reaction rate is determined by thermal initiations.

Comparing our present and previous results with literature data, the existence of such temperature ranges is to be considered as a general characteristic feature of radiation chemical chain reactions.

The product formed in discharge chemical oxidation was shown to contain compounds of higher oxidation state in greater percentage than that of the thermal process. In order to interpret this phenomenon an alteration in reaction mechanism caused by the discharge is suggested: discharge-chemical reactions leading to the formation of acids are supposed.

Dr. Zoltán PAÁL
Dr. Gábor FÖLDIÁK } Budapest XII. Konkoly Thege út

Printed in Hungary

A kiadásért felel az Akadémiai Kiadó igazgatója — Műszaki szerkesztő: Farkas Sándor

A kézirat a nyomdába érkezett: 1965. X. 20. — Terjedelem: 8,75 (A/5) ív. 28 ábra

66. 61489 Akadémiai Nyomda, Budapest — Felelős vezető: Bernát György

Zeitschrift für anorganische und allgemeine Chemie

Gegründet 1892 von G. KRÜSS
erweitert von G. TAMMANN
unter Mitwirkung von zahlreichen Fachgelehrten und unter ständiger Mitarbeit von Prof. Dr. W. KLEMM, Münster i. W. und Prof. Dr. J. GOUBEAU, Stuttgart, herausgegeben von Prof. Dr. G. RIENÄCKER, Berlin
Jährlich etwa 8 Bände mit je 6 Heften. Bezugspreis je Band 24, — MDN
Im Jahre 1966 erscheinen die Bände 342—349

Die »Zeitschrift für anorganische und allgemeine Chemie« ist die maßgebende literarische Sammelstelle für die wissenschaftlichen Abhandlungen auf dem Gebiete der anorganischen Chemie. Viele Probleme, die heute technische Selbstverständlichkeiten sind, wurden hier zum ersten Male erörtert.

Journal für praktische Chemie

Gegründet 1828 von Otto LINNE ERDMANN
fortgesetzt von H. KOLBE, E. v. MEYER, B. RASSOW und H. STAUDINGER
unter ständiger Mitarbeit von H. BERTSCH, Berlin, J. GOUBEAU, Stuttgart, H. MEERWEIN, Marburg/L., E. WICKE, Münster i. W., G. WITTIG, Heidelberg, im Auftrage der Chemischen Gesellschaft in der Deutschen Demokratischen Republik herausgegeben von Prof. Dr. B. HELFERICH, Bonn, Prof. Dr. Ing. E. LEIBNITZ, Leipzig, Prof. Dr. E. THILO, Berlin
Jährlich etwa 4 Bände mit je 6 Heften. Bezugspreis je Band 24,— MDN
Im Jahre 1966 erscheinen die Bände 31—34

Im »Journal für praktische Chemie« werden experimental-Arbeiten, die präparativ, analytisch oder überhaupt von Bedeutung sind und nicht vorwiegend theoretisches Interesse haben, veröffentlicht.

Zeitschrift für wissenschaftliche Photographie, Photophysik und Photochemie

Gegründet 1903
Unter Mitwirkung von zahlreichen Fachgelehrten herausgegeben von Dr. H. ARENS, Dessau und Prof. Dr. H. FRIESER, München
Jährlich 1 Band mit 12 Heften. Bezugspreis je Band 28,— MDN
Im Jahre 1966 erscheint der Band 60

Als einzige wissenschaftliche Photozeitschrift Deutschlands findet sie im Ausland besondere Beachtung.

JOHANN AMBROSIUS BARTH · LEIPZIG

INDEX

ANORGANISCHE UND ANALYTISCHE CHEMIE — INORGANIC AND ANALYTICAL CHEMISTRY — НЕОРГАНИЧЕСКАЯ И АНАЛИТИЧЕСКАЯ ХИМИЯ

GÖRÖG, S.: Analysis of Steroids, I. Bromometric Determination of Steroids Containing a Double Bond in Position Δ^5 1

GÖRÖG, S.: Analysis of Steroids, II. Determination of Steroids Containing an Ethinyl Group 7

PHYSIKALISCHE CHEMIE — PHYSICAL CHEMISTRY — ФИЗИЧЕСКАЯ ХИМИЯ

BEYER, H., FEJES, P., SCHAY, G. und VARGA, K.: Neuere Untersuchungen über frontale Gaschromatographie unter Berücksichtigung der Strömungsgeschwindigkeit während der Sorption, III. Bestimmung von HTS-Werten mittels frontaler Gaschromatographie 13

VARGA, K., FEJES, P. und BEYER, H.: Neuere Untersuchungen über frontale Gaschromatographie unter Berücksichtigung der Strömungsgeschwindigkeit während der Sorption, IV. Beurteilung chromatographischer Trennsäulen auf Grund frontalchromatographisch gemessener Transportgeschwindigkeits- und Diffusionskonstanten 23

CSÁSZÁR, J. and FELVÉGI, A.: Magnetic and Spectroscopic Investigation of Polynuclear Complex Cyanides 37

BILLES, F.: A New Method for the Determination of Vibrational Force Constants of Molecules 53

GYARMATI, I.: Once More on the Deduction of the Fourier Equation from the Variational Principle. (Short Communication) 63

CHEMISCHE TECHNOLOGIE — CHEMICAL TECHNOLOGY — ХИМИЧЕСКАЯ ТЕХНОЛОГИЯ

SOÓS, L.: New Methods of Coal Petrography in Coal Chemistry and Coal Technology 67

Пал, З. и *Фёльдиак, Г.:* О некоторых проблемах кинетики и механизма разрядно-химического окисления углеводородов в гетерогенной фазе. (PAÁL, Z. and FÖLDIÁK, G.: Some Problems in the Reaction Kinetics and Mechanism of Hydrocarbon Oxidation by Electric Discharge in Heterogeneous Phase) 83

The Acta Chimica publish papers on chemistry, in English, German, French and Russian.

The Acta Chimica appear in volumes consisting of four parts of varying size, 4 volumes being published a year.

Manuscripts should be addressed to

Acta Chimica
Budapest 502, Postafiók 24.

Correspondence with the editors should be sent to the same address.

The subscription rate is 110 forints a volume. Orders may be placed with "*Kultúra*" Foreign Trade Company for Books and Newspapers (Budapest I., Fő utca 32. Account No. 43-790-057-181) or with representatives abroad.

Les Acta Chimica paraissent en français, allemand, anglais et russe et publient des mémoires du domaine des sciences chimiques.

Les Acta Chimica sont publiés sous forme de fascicules. Quatre fascicules seront réunis en un volume (4 volumes par an).

On est prié d'envoyer les manuscrits destinés à la rédaction à l'adresse suivante:

Acta Chimica
Budapest 502, Postafiók 24.

Toute correspondance doit être envoyée à cette même adresse.

Le prix de l'abonnement est de 110 forints par volume.

On peut s'abonner à l'Entreprise pour le Commerce Extérieur de Livres et Journaux «*Kultúra*» (Budapest I., Fő utca 32. Compte-courant No. 43-790-057-181) ou à l'étranger chez tous les représentants ou dépositaires.

«*Acta Chimica*» издают трактаты из области химической науки на русском, французском, английском и немецком языках.

«*Acta Chimica*» выходят отдельными выпусками разного объема. 4 выпуска составляют один том. 4 тома публикуются в год.

Предназначенные для публикации рукописи следует направлять по адресу:

Acta Chimica
Budapest 502, Postafiók 24.

По этому же адресу направлять всякую корреспонденцию для редакции.

Подписная цена «*Acta Chimica*» — 110 форинтов за том. Заказы принимает предприятие по внешней торговле книг и газет «*Kultúra*» (Budapest I., Fő utca 32. Текущий счет № 43-790-057-181) или его заграничные представительства и уполномоченные.

25,— Ft

All the reviews of the Hungarian Academy of Sciences may be obtained among others from the following bookshops:

ALBANIA
Ndermarja Shtetnore e Botimeve
Tirana

AUSTRALIA
A. Keesing
Box 4886, GPO
Sidney

AUSTRIA
Globus Buchvertrieb
Salzgries 16
Wien I.

BELGIUM
Office International de Librairie
30, Avenue Marnix
Bruxelles 5
Du Monde Entier
5, Place St. Jean
Bruxelles

BULGARIA
Raznoiznos
1Tzar Assen
Sofia

CANADA
Pannonia Books
2 Spadina Road
Toronto 4, Ont.

CHINA
Waiwen Shudian
Peking
P. O. B. Nr. 88.

CZECHOSLOVAKIA
Artia A. G.
Ve Smeckách 30
Praha II.
Postova Novinova Sluzba
Dovoz tisku
Vinohradska 46
Praha 2
Postova Novinova Sluzba
Dovoz tlace
Leningradska 14
Bratislava

DENMARK
Ejnar Munksgaard
Nörregade 6
Kopenhagen

FINLAND
Akateeminen Kirjakauppa
Keskuskatu 2
Helsinki

FRANCE
Office International de Documentation et Librairie
48, rue Gay Lussac
Paris 5

GERMAN DEMOCRATIC REPUBLIC
Deutscher Buch-Export und Import
Leninstraße 16.
Leipzig C. I.
Zeitungsvertriebsamt
Clara Zetkin Straße 62.
Berlin N. W.

GERMAN FEDERAL REPUBLIC
Kunst und Wissen
Erich Bieber
Postfach 46
7 Stuttgart S.

GREAT BRITAIN
Collet's' Subscription Dept.
44—45 Museum Street
London W. C. I.
Robert Maxwell and Co. Ltd.
Waynflete Bldg. The Plain
Oxford

HOLLAND
Swetz and Zeitlinger
Keizersgracht 471—487
Amsterdam C.
Martinus Nijhof
Lange Voorhout 9
The Hague

INDIA
Current Technical Literature
Co. Private Ltd.
Head Office:
India House OPP.
GPO Post Box 1374
Bombay I.

ITALY
Santo Vanasia
71 Via M. Macchi
Milano
Libreria Commissionaria Sansoni
Via La Marmora 45
Firenze

JAPAN
Nauka Ltd.
2 Kanada-Zimbocho 2-chome
Chiyoda-ku
Tokyo
Maruzen and Co. Ltd.
P. O. Box 605
Tokyo
Far Eastern Booksellers
Kanada P. O. Box 72
Tokyo

KOREA
Chulpanmul
Korejskoje Obshchestvo po Exportu i Importu Proizvedenij Pechati
Phenjan

NORWAY
Johan Grundt Tanum
Karl Johansgatan 43
Oslo

POLAND
Export und Import Unternehmen RUCH
ul. Wilcza 46.
Warszawa

ROUMANIA
Cartimex
Str. Aristide Briand 14—18.
Bucuresti

SOVIET UNION
Mezhdunarodnala Kniga
Moscow
G—200

SWEDEN
Almquist and Wiksell
Gamla Brogatan 26
Stockholm

USA
Stechert Hafner Inc.
31 East 10th Street
New York 3 N. Y.
Walter J. Johnson
111 Fifth Avenue
New York 3. N. Y.

VIETNAM
Xunhasaba
Service d'Export et d'Import des Livres et Périodiques
19, Tran Quoc Toan
Hanoi

YUGOSLAVIA
Forum
Vojvode Misica broj 1.
Novi Sad
Jugoslovenska Kniga
Terazije 27.
Beograd

15. 1. 1966 Index: 26.007

ACTA CHIMICA

ACADEMIAE SCIENTIARUM HUNGARICAE

ADIUVANTIBUS

L. ERDEY, K. POLINSZKY, G. SCHAY

AC

R. BOGNÁR, GY. BRUCKNER, L. CHOLNOKY, Z. CSŰRÖS,
T. ERDEY-GRŰZ, Z. FÖLDI, M. FREUND, Á. GERECS, GY. HARDY,
Á. KISS, M. KORACH, F. MÁRTA, J. PROSZT, Z. SZABÓ,
P. SZŐR, L. VARGHA, K. VAS

REDIGIT

B. LENGYEL

TOMUS 47. FASCICULUS 2.

AKADÉMIAI KIADÓ, BUDAPEST

1966

ACTA CHIM. HUNG.

ACTA CHIMICA

A MAGYAR TUDOMÁNYOS AKADÉMIA KÉMIAI TUDOMÁNYOK OSZTÁLYÁNAK IDEGEN NYELVŰ KÖZLEMÉNYEI

SZERKESZTI

LENGYEL BÉLA

TECHNIKAI SZERKESZTŐK

DEÁK GYULA és TAKÁCS VILMOS

Az Acta Chimica német, angol, francia és orosz nyelven közöl értekezéseket a kémiai tudományok köréből.

Az Acta Chimica változó terjedelmű füzetekben jelenik meg, egy-egy kötet négy füzetből áll. Évente átlag négy kötet jelenik meg.

A közlésre szánt kéziratok a szerkesztőség címére (Budapest 502, postafiók 32) küldendők.

Ugyanerre a címre küldendő minden szerkesztőségi levelezés. A szerkesztőség kéziratokat nem ad vissza.

Az Acta Chimica előfizetési ára kötetenként belföldre 80 Ft, külföldre 110 Ft. Megrendelhető a belföld számára az „Akadémiai Kiadó"-nál (Budapest V., Alkotmány utca 21. Bankszámla 05-915-111-46), a külföld számára pedig a „Kultúra" Könyv- és Hírlap Külkereskedelmi Vállalatnál (Budapest I., Fő utca 32. Bankszámla: 43-790-057-181) vagy annak külföldi képviseleteinél és bizományosainál.

Die Acta Chimica veröffentlichen Abhandlungen aus dem Bereiche der chemischen Wissenschaften in deutscher, englischer, französischer und russischer Sprache.

Die Acta Chimica erscheinen in Heften wechselnden Umfanges. Vier Hefte bilden einen Band. Jährlich erscheinen 4 Bände.

Die zur Veröffentlichung bestimmten Manuskripte sind an folgende Adresse zu senden:

Acta Chimica
Budapest 502, Postafiók 32.

An die gleiche Anschrift ist auch jede für die Redaktion bestimmte Korrespondenz zu richten.

Abonnementspreis pro Band: 110 Forint. Bestellbar bei dem Buch- und Zeitungs-Außenhandels-Unternehmen »*Kultúra*« (Budapest I., Fő utca 32. Bankkonto No. 43-790-057-181) oder bei seinen Auslandsvertretungen und Kommissionären.

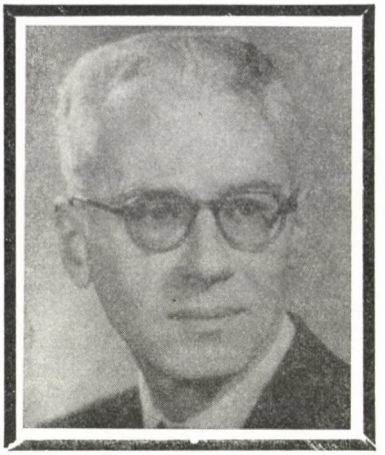

Es ist eine traurige Pflicht des Redaktionskomitees von Acta Chimica Academiae Scientiarum Hungaricae zu melden, daß

Dr. SÁNDOR (ALEXANDER) MÜLLER

Chefredakteur dieser Zeitschrift, korrespondierendes Mitglied der Ungarischen Akademie der Wissenschaften, Professor der L. Eötvös Universität, Budapest, ein weitbekannter Forscher der theoretischen und experimentellen organischen Chemie, in seinem 63ten Lebensjahre am 21. Januar 1966 nach kurzer Krankheit hingeschieden ist.

Wir werden des Verstorbenen stets in Verehrung gedenken.

p-ÄTHOXY-α-NAPHTHYLROT, EIN NEUER ADSORPTIONSINDIKATOR

L. LÉGRÁDI

(Industriewerke Nitrokémia, Fűzfő, Ungarn)

Eingegangen am 24. Juli 1964

Der Säure-Basen-Indikator α-Naphthylrot ist in Wasser nur spärlich löslich und wird daher in wäßrigem Medium nur selten angewandt. Als Adsorptionsindikator eignet sich die Verbindung zur titrimetrischen Bestimmung von Bromid, Jodid und Rhodanid [1]. Mit dem Einbau verschiedener Substituenten in das Molekül können die Eigenschaften desselben tiefgreifend verändert werden. In einer früheren Mitteilung habe ich über die Darstellung des o-Äthylderivates des α-Naphthylrots berichtet [2]; auf diese Weise konnte der p_H-Bereich des Farbumschlages in Richtung niedrigerer p_H-Werte verschoben werden, und die Verbindung ließ sich als Adsorptionsindikator zur Titration von Chlorid in alkoholischem Medium anwenden [3].

Es wurde nun versucht, durch Einbau neuer Substituenten einen solchen Säure-Basen-Indikator herzustellen, der auch als Adsorptionsindikator verwendet werden kann. Die Einführung einer p-Äthoxygruppe in das α-Naphthylrot-Molekül schien auch deshalb zweckmäßig zu sein, weil die p-Alkoxygruppen den Säure-Basen-Indikatoren bekanntlich günstige Eigenschaften verleihen. Auf solche Weise konnte aus dem Chrysoidin, welches als Säure-Basen-Indikator keine besonders günstigen Eigenschaften besitzt, durch Einbau der p-Äthoxygruppe ein sehr guter Säure-Basen-Indikator erhalten werden.

Durch Diazotieren von p-Phenetidin und Koppeln mit α-Naphthylaminhydrochlorid ist es mir gelungen, einen Säure-Basen- und Adsorptionsindikator mit vorteilhaften Eigenschaften herzustellen.

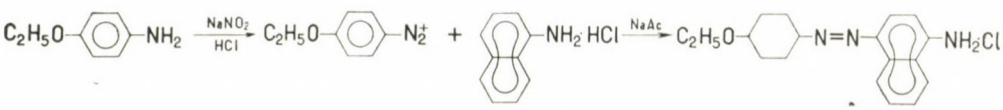

Sämtliche Ausgangsprodukte werden technisch hergestellt und sind daher leicht zugänglich. Der Einbau der Äthoxygruppe verleiht dem Indikator die folgenden günstigen Eigenschaften: Als Säure-Basen-Indikator besitzt er eine lebhaftere Farbe, der Farbumschlag ist besser und als Adsorptionsindikator kann er auch zur Titration des Cyanidions angewandt werden.

Experimenteller Teil

Das p-Äthoxy-α-naphthylrot wurde in erster Linie als Adsorptionsindikator untersucht. Hierzu mußten vor allem die Farbumschläge bei den verschiedenen p_H-Werten festgestellt werden. Der Anzeigebereich des Indikators reicht von p_H 3,2 bis p_H 4,4. In Tab. I sind die Farbveränderungen bei den einzelnen p_H-Werten zusammengestellt.

Tabelle I

Farbveränderungen des Indikators

pH	Farbe
1—3	dunkelviolett
3—3,2	violett
3,2—3,5	violettrot
3,5—3,6	rot
3,6—3,7	orangerot
3,7—4	kastanienbraun
4,0—4,5	orange
4,5—12,0	gelb

Mit dem Indikator p-Äthoxy-α-naphthylrot wurden verschiedene Niederschlagstitrationen durchgeführt um zu entscheiden, welche Ionen mit Hilfe dieses Indikators bestimmt werden können. Zuerst wurden verschiedene Anionen mit Silbernitrat in einem Ausgangsvolumen von 50 ml titriert. Der Indikator wurde in 0,25%iger äthanolischer Lösung angewandt. Die Lösung wurde nicht angesäuert, sondern stellte man eine saure Indikatorlösung aus einem Teil Eisessig und einem Teil der 0,25%igen äthanolischen Indikatorlösung her und säuerte die Prüflösung nötigenfalls mit diesem Gemisch an. Die Ergebnisse der Titrationen wurden mit potentiometrischen Titrationsresultaten verglichen, die man gleichfalls in einem Ausgangsvolumen von 50 ml mit 0,1 n Meßlösung durchführte. Die Elektroden waren Silber und eine gesättigte Kalomelelektrode. Die Ergebnisse der Bestimmung der Anionen sind in Tab. II zusammengefaßt. Bei den Aniontitrationen ist die Farbe der Ausgangslösung orange oder gelb. Auf Wirkung des Silbernitrats geht die Farbe in gelb und sodann in violett über; am Äquivalenzpunkt tritt ein Farbumschlag auf gelb, bei Bromid und Rhodanid auf orange ein. Bei der Bestimmung von Cyanidionen ist die Lösung anfangs gelb, während der Titration wird sie rot, später violett und blau, um am Äquivalenzpunkt in grauviolett umzuschlagen. Die noch titrierbare kleinste Lösungsmenge ist bei Jodid und Bromid 0,2 ml 0,01 n

Tabelle II

Titration von Anionen mit Silbernitrat

Ion	Meßlösung Silbernitrat	Angewandte saureund neutrale Indikatorlösung	Verbrauch an Meßlösung, ml		Abweichung vom Äquivalenzpunkt	
			Potentiom.	Indik.	ml	%
Jodid	0,1n	8 Tropfen 0,25%ige + 1 Tropfen saure Ind.-lösung p_H = 3,8—5,5	5,13 5,14 5,14 5,14 5,14	5,14 5,14 5,13 5,13 5,14	0,00	0,00
Jodid	0,01n	8 Tropfen 0,25%ige + 1 Tropfen saure Ind.-lösung p_H = 3,8—5,5	5,14 5,14	5,16 5,18 5,18 5,18 5,18	0,04	0,78
Jodid	0,01n	8 Tropfen 0,25%ige + 1 Tropfen saure Ind.-lösung p_H = 3,8—5,5	2,03 2,03	2,02 2,02 2,04 2,02 2,01	0,01	0,50
Bromid	0,1n	8 Tropfen 0,25%ige + 1 Tropfen saure Ind.-lösung p_H = 3,8—5,5	5,15 5,15 5,16 5,15 5,15	5,15 5,14 5,14 5,13 5,15	0,01	0,20
Bromid	0,01n	4 Tropfen 0,25%ige + 0,5 Tropfen saure Ind.-lösung p_H = 4,5—5,5	5,15 5,15	5,22 5,24 5,24 5,24 5,25	0,09	1,75
Cyanid	0,1n	8 Tropfen 0,25%ige + 2 Tropfen saure Ind.-lösung p_H =3,5—4,5	5,00 5,01 5,01 5,00 5,01	5,00 5,01 5,01 5,00 5,01	0,00	0,00
Rhodanid	0,1n	8 Tropfen 0,25%ige Ind.-lösung p_H = 5—5,5	5,50 5,51 5,52 5,51 5,52	5,50 5,51 5,52 5,51 5,52	0,00	0,00

Lösung, in einem Volumen von 50 ml, in Gegenwart von einem Tropfen der sauren und einen Tropfen der neutralen Indikatorlösung. Beim Rhodanid erhält man beim Titrieren mit 0,01n Meßlösung einen unscharfen und beim Cyanid überhaupt keinen Endpunkt bzw. Farbumschlag.

Die Titrationen wurden auch in umgekehrter Richtung, nämlich durch Titration von Silbernitratlösung mit Anionen durchgeführt. Die Ergebnisse sind in Tab. III zusammengefaßt. Die Versuchsbedingungen waren die gleichen, wie bei der Titration der Anionen. Beim Titrieren der Silberionen ist die Ausgangslösung violett oder rot, sie wird dann während der Titration orange oder gelb und am Äquivalenzpunkt erfolgt der Farbumschlag auf violett, beim Jodid auf bläulichgrau und beim Rhodanid auf bläulichviolett. Die niedrigsten, noch titrierbaren Silberionenkonzentrationen sind bei Anwendung von 0,01n Meßlösung und in einem Ausgangsvolumen von 50 ml folgende: Titration von

Tabelle III

Titration von Silberionen mit Anionen

Meßlösung	Angewandte saure und neutrale Indikatorlösung	Verbrauch an Meßlösung, ml		Abweichung vom Äquivalenzpunkt	
		Potentiom.	Indik.	ml	%
0,1n Kaliumjodid	8 Tropfen saure Ind.-lösung $p_H = 2{,}6-3{,}3$	5,14 5,14 5,15 5,14 5,15	5,14 5,14 5,15 5,14 5,15	0,00	0,00
0,01n Kaliumjodid	3 Tropfen 0,25%ige + 3 Tropfen saure Ind.-lösung $p_H = 3-3{,}6$	5,15 5,15	5,13 5,14 5,13 5,14 5,16	0,01	0,10
0,01n Kaliumjodid	1 Tropfen 0,25%ige + 2 Tropfen saure Ind.-lösung $p_H = 3-3{,}6$	1,03 1,03	1,00 1,01 1,00 1,01 1,01	0,02	1,94
0,1n Kaliumbromid	7 Tropfen saure Ind.-lösung $p_H = 2{,}6-3{,}3$	5,08 5,08 5,05 5,08 5,09	5,08 5,07 5,05 5,08 5,08	0,01	0,20
0,01n Kaliumbromid	3 Tropfen 0,25%ige + 3 Tropfen saure Ind.-lösung $p_H = 3-3{,}6$	5,08 5,08	4,97 4,99 4,99 5,02 4,97	0,09	1,77
0,1n Ammonium-rhodanid	10 Tropfen saure Ind.-lösung $p_H = 2{,}8-3{,}4$	4,74 4,73 4,72 4,72 4,71	4,74 4,73 4,74 4,72 4,71	0,00	0,00
0,01n Ammonium-rhodanid	3 Tropfen 0,25%ige + 3 Tropfen saure Ind.-lösung $p_H = 3-3{,}6$	4,73 4,73	4,75 4,80 4,80 4,80 4,80	0,07	1,48

0,2 ml 0,01n Silbernitrat mit Kaliumjodid, 0,5 ml 0,01n Silbernitrat mit Kaliumbromid und 5 ml 0,01n Silbernitrat mit Ammoniumrhodanid. Der relative Fehler betrug bei 0,1n Meßlösung $\pm$ 0,02%, bei 0,01n Meßlösung $\pm$ 0,04%.

Wirkungsmechanismus des Adsorptionsindikators p-Äthoxy-α-naphthylrot

Im Sinne der Theorie von PUNGOR und SCHULEK über die Wirkungsweise der Adsorptionsindikatoren [4] hängt die Indikation unmittelbar mit den Veränderungen der physikalischen Eigenschaften des adsorbierten Farbstoffes zusammen. Um also den Indikationsmechanismus des p-Äthoxy-α-naphthylrots aufklären zu können, müssen die Änderungen der physikalischen Konstanten des adsorbierten Farbstoffes gemessen werden. Da das p-Äthoxy-α-

naphthylrot ein Säure-Basen-Indikator ist und mit keiner der Meßlösungen einen Niederschlag gibt, scheint eine Oberflächen-Säure-Basen-Indikation wahrscheinlich zu sein.

Auf Grund der Experimente von SCHULEK und PUNGOR kann die Oberflächen-Säure-Basen-Indikation durch Messung der p_H-Änderung während der Titration sowie durch Bestimmung der Änderung der Dissoziationskonstante des Farbstoffadsorbats auf Wirkung eines Eigenionüberschusses nachgewiesen werden [5]. Außerdem läßt sich die Oberflächen-Säure-Basen-Indikation auch mit Hilfe von Adsorptionsmessungen nachweisen [6].

1. Bestimmung der p_H-Änderung während der Titration

100 ml einer 0,001n Prüflösung wurden in Gegenwart von 8 Tropfen 0,25%iger Indikatorlösung mit 0,01n Meßlösung unter gleichzeitiger Registrierung der Änderungen des p_H-Wertes titriert. Die Ergebnisse sind in Tab. IV gezeigt.

Wird das Anion mit Silbernitrat titriert, so kommt es zu Beginn der Titration, in Gegenwart des Anionenüberschusses zur Protonaufnahme durch den Indikator, daher nimmt das p_H der Lösung zu. In der Nähe des Äquivalenzpunktes nimmt der negative Ionenüberschuß stark ab, es setzt Protonenverlust des Indikators ein, und der p_H-Wert der Lösung beginnt abzunehmen. Diese Abnahme hält am Äquivalenzpunkt noch an, da der Indikator sein Proton nur auf Wirkung eines positiven Ionenüberschusses vollkommen verliert. Die am Äquivalenzpunkt eintretende p_H-Abnahme ist beim Jodid am stärksten, beim Bromid ist sie geringer und beim Rhodanid am geringsten, während das p_H beim Chlorid überhaupt nicht abnimmt.

Tabelle IV

Änderung des p_H-Wertes während der Titration

Meßlösung Äquiv.%	Titration von				Titration von $AgNO_3$ mit			
	KJ	KBr	NH_4SCN	NaCl	KJ	KBr	NH_4SCN	NaCl
0	6,65	5,20	4,95	5,20	6,60	4,72	4,93	4,60
20	6,69	5,30	5,05	5,28	6,59	4,72	4,94	4,60
40	6,70	5,36	5,09	5,30	6,58	4,76	4,95	4,60
60	6,72	5,36	5,09	5,32	6,57	4,78	4,96	4,60
80	6,72	5,35	5,09	5,34	6,55	4,80	4,99	4,61
90	6,73	5,30	5,05	5,35	6,60	4,81	5,00	4,61
98	6,73	5,28	5,02	5,35	6,65	4,95	5,04	4,62
100	6,60	5,25	4,96	5,35	6,85	5,00	5,08	4,62
110	6,50	5,20	4,95	5,35	—	5,10	5,15	4,63

Werden Silberionen mit Anionen titriert, so nimmt der Indikator am Äquivalenzpunkt, auf Wirkung des negativen Ionenüberschusses, ein Proton auf, das p_H der Lösung steigt an. Die Reihenfolge der Größe der p_H-Änderung ist die gleiche wie bei der Titration der Anionen.

2. *Bestimmung der Änderung der Dissoziationskonstante des Farbstoffadsorbats*

Den zweiten Beweis der Oberflächen-Säure-Basen-Indikation lieferte die Bestimmung der Änderung der Dissoziationskonstante des Farbstoffadsorbats auf Wirkung verschiedener Eigenionüberschüsse. Die Dissoziationskonstante des adsorbierten Farbstoffes nimmt nämlich bei Kationenüberschuß zu und bei Anionenüberschuß ab; am Äquivalenzpunkt ist diese Änderung sprunghaft [5]. Die Ergebnisse dieser Messungen zeigt Tab. V.

Die Bestimmungen wurden auf folgende Weise durchgeführt: Zu 10 ml 0,01n Silbernitratlösung wurden 5, 9, 10, 11, und 15 ml 0,01n Anionenlösung,

Tabelle V

Farbstoffadsorbat als Säure-Basen-Indikator

Adsorbent: 4-(4'-Äthoxy-phenylazo)-1-naphthylamin-hydrochlorid

Adsorbens	Eigenionüberschuß Äquiv.	Umschlagbereich	Dissoziations-konst. K	Farbumschlag
Silberjodid	50% Ag^+	2,8—3,3	$8{,}91 \cdot 10^{-4}$	violett-gelb
	10% Ag^+	2,9—3,3	$7{,}94 \cdot 10^{-4}$	schwer feststellbar
	Äqu.-Punkt	4,5—6,3	$3{,}98 \cdot 10^{-6}$	schwer feststellbar
	10% J^-	5,4—7,2	$5{,}01 \cdot 10^{-7}$	gut sichtbar
	50% J^-	5,7—7,5	$2{,}51 \cdot 10^{-7}$	gut sichtbar
Silberbromid	50% Ag^+	2,8—3,3	$8{,}91 \cdot 10^{-4}$	rot-gelb
	10% Ag^+	2,9—3,3	$7{,}94 \cdot 10^{-4}$	schwer feststellbar
	Äqu.-Punkt	3,6—4,6	$7{,}94 \cdot 10^{-5}$	schwer feststellbar
	10% Br^-	4,4—6,5	$3{,}54 \cdot 10^{-6}$	gut sichtbar
	50% Br^-	4,7—7,0	$1{,}41 \cdot 10^{-6}$	gut sichtbar
Silberrhodanid	50% Ag^+	2,7—3,1	$1{,}25 \cdot 10^{-3}$	rot-gelb
	10% Ag^+	2,8—3,2	$1{,}00 \cdot 10^{-3}$	schwer feststellbar
	Äqu.-Punkt	2,9—3,6	$5{,}62 \cdot 10^{-4}$	schwer feststellbar
	10% SCN^-	3,5—5,2	$4{,}46 \cdot 10^{-5}$	schwer feststellbar
	50% SCN^-	3,7—5,3	$3{,}16 \cdot 10^{-5}$	schwer feststellbar
Silberchlorid	50% Ag^+	4,7—5,9	$5{,}01 \cdot 10^{-6}$	rotviolett-gelb
	10% Ag^+	4,6—5,8	$6{,}31 \cdot 10^{-6}$	gut sichtbar
	Äqu.-Punkt	4,6—5,8	$6{,}31 \cdot 10^{-6}$	Farbumschlag
	10% Cl^-	4,8—6,0	$3{,}98 \cdot 10^{-6}$	
	50% Cl^-	4,8—6,0	$3{,}98 \cdot 10^{-6}$	
Silbercyanid	50% Ag^+	2,7—3,6	$7{,}08 \cdot 10^{-4}$	bläulichviolett-braun
	10% Ag^+	2,7—3,6	$7{,}08 \cdot 10^{-4}$	gut sichtbarer
	Äqu.-Punkt	2,7—3,6	$7{,}08 \cdot 10^{-4}$	Farbumschlag
	10% CN^-	3,2—4,6	$1{,}25 \cdot 10^{-4}$	
	50% CN^-	3,6—4,8	$6{,}31 \cdot 10^{-5}$	farblose Lösung

sowie 5 Tropfen der 0,25%igen Indikatorlösung gegeben, das Gemisch wurde mit 0,5%iger Salpetersäure auf ca. $p_H = 2{,}8$ angesäuert und mit 0,1n Natriumhydroxidlösung titriert. In die Lösung war eine Glas- und eine Kalomelelektrode getaucht, die mit einem p_H-Meßgerät verbunden waren. Der Umschlags-p_H-Wert des Indikators wurde bei Titration mit 0,1n Natriumhydroxidlösung bzw. 0,1n Salpetersäure bestimmt. Im Interesse der besseren Feststellbarkeit des Farbumschlages wurden die Bestimmungen beim Silbercyanid in 0,1n Konzentration, bei vollständiger Adsorption durchgeführt. Beim Jodid und Bromid ist der Farbumschlag hingegen im 0,1n Maßstab, in Gegenwart von Silberüberschuß infolge des Ablaufes von chemischen Reaktionen nicht sichtbar. Beim Bromid und Rhodanid ist die Änderung der Dissoziationskonstante in Gegenwart von Silberüberschuß gering, die Titration kann jedoch in beiden Richtungen durchgeführt werden. Auf Grund dieses Umstandes bzw. der mit dem Indikator 4-(2'-Äthyl-phenylazo)-1-naphthylamin-hydrochlorid gemachten Erfahrungen ist es wahrscheinlich, daß in Gegenwart von Silberionen ein chemischer Prozeß abläuft. Dies bestätigt auch das beim Chlorid erhaltene negative Ergebnis. Das beim Cyanid in Anwesenheit eines Überschusses von Silberionen erhaltene negative Ergebnis deutet entweder auf den Ablauf eines chemischen Prozesses oder darauf, daß die Protonaufnahme bzw. -abgabe des Indikators durch die Silberionen nicht beeinflußt wird.

3. Adsorptionsmessungen

Um die noch offenen Fragen beantworten zu können, wurden auch Adsorptionsmessungen durchgeführt, deren Methode in einer früheren Arbeit bereits beschrieben wurde [6]. Zuerst wurde die Anfangsadsorption bestimmt. Zu diesem Zweck wird das Adsorbens mit dem Adsorptivum in saurem Medium, in Gegenwart eines Silberionüberschusses titriert. Die Werte der Anfangsadsorption sind in Tab. VI zusammengestellt. Die Anfangsadsorption ist beim Silberchlorid am geringsten, sie nimmt beim Bromid zu und erreicht beim Jodid bereits einen beträchtlichen Wert. Im Falle des Silberrhodanids und Silbercyanids haben wir es mit einer echten Adsorption zu tun, der violette Farbstoff wird mit blaßvioletter Farbe adsorbiert.

Wie aus der Tabelle VI hervorgeht, nimmt die Menge des adsorbierten Farbstoffes in folgender Reihenfolge ab: $AgJ > AgBr > AgSCN > AgCN > AgCl$. Die Reihenfolge ist die gleiche, wie beim 4(-2'-Äthyl-phenylazo)-1-naphthylamin-hydrochlorid, die Werte sind jedoch um 50—100% höher.

Um ein vollständiges Bild über das Verhalten des Indikators zu gewinnen, wurde auch die Menge des nach 30 Minuten dauerndem Rühren adsorbierten Farbstoffes bestimmt und zwar auf einem Niederschlag mit positiver Ladung in saurem und neutralem Medium, auf einem Niederschlag mit negativer Ladung in saurem und neutralem Medium und ebenso auf einem neutralen

Niederschlag. Die ml-Zahl der durch einen aus 10 ml 0,1n Silberionenlösung gebildeten Silberhaloidniederschlag nach 30 Minuten dauerndem Rühren adsorbierten 0,01%igen Farbstofflösung ist in Tab. VII gezeigt. Außer der Menge des adsorbierten Indikators ist auch die Farbe der Niederschläge nach 30 Minuten dauerndem Rühren angegeben, während das Zeichen *S* bzw. *A* über den Zahlen anzeigt, ob der Indikator als Säure-Basen- oder als Adsorp-

Tabelle VI

Anfangsadsorption

Adsorbens aus 10 ml 0,1 n Ag^+	Verbrauch an 0,01%igem Indikator, ml	Verhältniszahl	Farbe des Niederschlages	Farbe der Lösung	Bemerkung
AgCl	0,10	1	weiß	blaßviolett	
AgBr	0,30	3	graugelb	blaßviolett	
AgJ	1,00	10	graugelb	blaßviolett	
AgSCN	0,25	2,5	blaßviolett	farblos	echte Ads.
AgCN	0,20	2	blaßviolett	farblos	echte Ads.

tionsindikator angewandt werden kann. Der kleingeschriebene Buchstabe bedeutet, daß die Indikatorwirkung nur schwierig beobachtet werden kann. Die Umrahmung mit ausgezogener Linie zeigt an, daß während der 30 Minuten dauernden Adsorption keine Veränderung eintritt, während sich die Farbe außerhalb der Umrahmung während des Prozesses ändert.

Aus der Tabelle VII geht hervor, daß sich ein chemischer Prozeß bei jedem Adsorbens abspielt, im Gegensatz zum 4-(2'-Äthyl-phenylazo)-1-naphthylamin-hydrochlorid, bei welchem im Falle des Silberrhodanids der Ablauf eines chemischen Prozesses nicht festgestellt werden konnte. Die Menge des adsorbierten Farbstoffes ist auf jedem Adsorbens genügend groß und beträgt in den meisten Fällen mehr als das Doppelte des beim 4-(2'-Äthyl-phenylazo)-1-naphthylamin-hydrochlorid gemessenen Wertes.

Beim Silberchlorid läßt sich am neutralen und negativen Niederschlag in saurem Medium auch eine Wirkung des Adsorptionsindikators feststellen, obzwar die Titration nicht durchgeführt werden kann. Die beobachtete Adsorptionswirkung ist jedoch nicht äquivalent, da sich beim Silberion nur auf Wirkung eines großen Überschusses ein Farbumschlag einstellt. In neutralem Medium geht die Farbe des Indikators am Silberchloridniederschlag, nach längerem Rühren — hauptsächlich bei Silberüberschuß — von gelb in rot über. Dieses rote Indikatoradsorbat nimmt auf Wirkung von Lauge eine gelbe Farbe an, demnach kommt es also während der Adsorption, in Gegenwart eines Silberionüberschusses zu einer Protonaufnahme. Dies beweist, daß das

Silberion keinen Einfluß auf den vom Niederschlag adsorbierten Farbstoff ausübt. Beim Silberchlorid kann der Ablauf eines chemischen Prozesses nicht mit Sicherheit festgestellt werden. Der Farbumschlag wird auch in neutralem Medium durch Protonaufnahme verursacht.

Beim Silberbromid und Silberjodid spielt sich während der Adsorption ein chemischer Prozeß ab, seine Folge ist, daß der adsorbierte Indikator grau wird, und auch seine Indikatorwirkung verliert. Auch beim Silberrhodanid kann der Ablauf eines chemischen Prozesses beobachtet werden, jedoch tritt hier Braunfärbung ein.

Das Cyanidion kann mit p-Äthoxy-α-naphthylrot titriert werden, der Farbumschlag ist jedoch nicht reversibel. Nach der Zugabe von 20% der

Tabelle VII

Grad der Adsorption

Adsorbens	Verbrauch an 0,01%iger Indikatorlösung in ml					
	Positiver Niederschlag		Neutraler Niederschlag		Negativer Niederschlag	
	sauer	neutral	sauer	neutral	sauer	neutral
Silberchlorid	S 5,00 violett	S 5,00 rot	S A 3,00 violett	S 4,00 orange-rot	S A 14,00 violett	S 5,00 orange-braun
Silberbromid	3,75 grau	6,50 grau	S A 7,00 violett	s 7,00 grau	S A 18,00 bräunl.-violett	S 26,00 bräunl.-violett
Silberjodid	a 9,00 grau	s a 10,50 grau	s A 14,00 grau	S 22,00 bräunl.-grau	S A 54,00 violett-blau	S A 54,00 bräunl.-grau
Silberrhodanid	S A 4,00 rosa	S A 4,00 orange	S A 11,50 hell-violett	S 12,00 gelb	S A 36,00 violett	S 26,00 orange-braun
Silbercyanid	S 3,50 dunkel-violett	23,00 bräunl.-grau	S 7,00 blau-violett	S 6,00 gelb		

äquivalenten Ionenmenge ist eine schwache Farbveränderung auch bei der Titration des Silberions mit Cyanidionen zu beobachten. Der Fehler dürfte in der schwachen Wirkung des Silberions liegen, was auch durch das bei der Bestimmung der Dissoziationskonstante des Farbstoffadsorbats erhaltene Ergebnis bekräftigt wird. Ein chemischer Prozeß spielt sich auch beim Cyanid ab, in erster Linie auf positivem Niederschlag in neutralem Medium, in welchem

das Farbstoffadsorbat eine bräunlichgraue Farbe annimmt, und die Indikatorwirkung vollkommen aufhört. In saurem Medium, in Gegenwart von Silberionen, wird der Farbstoff mit dunkelvioletter Farbe adsorbiert. Dies bedeutet, daß die positive Ladung des Niederschlages auf den adsorbierten Farbstoff keine Wirkung ausübt, da er mit unveränderter Farbe gebunden wurde, obzwar zu erwarten gewesen wäre, daß die positive Ladung des Niederschlags eine Protonabgabe des Indikators bewirkt und die violette Farbe eine hellere Tönung annimmt.

Besprechung der Ergebnisse

Es gelang, den Säure-Basen-Indikator α-Naphthylrot durch Einführung einer Äthoxygruppe in para-Stellung in einen Säure-Basen- und Adsorptionsindikator mit günstigeren Eigenschaften umzuwandeln. Das p-Äthoxy-α-naphthylrot kann aus p-Phenetidin und α-Naphthylamin leicht hergestellt werden. Der neue Säure-Basen-Indikator läßt sich bei argentometrischen Titrationen vorteilhaft anwenden, so zur Bestimmung von Bromid, Jodid, Rhodanid und Cyanid. Seine günstigen Eigenschaften verdankt er der Äthoxygruppe in para-Stellung, mit dem das Molekül außer der Aminogruppe über noch einen Substituenten mit positiver Mesomerwirkung verfügt.

Den Funktionsmechanismus des Adsorptionsindikators p-Äthoxy-α-naphthylrot konnte ich auf Grund der Versuche von PUNGOR und SCHULEK nachweisen. Hierzu bestimmte ich einesteils jene p_H-Änderung, die durch die Funktion des Indikators am Äquivalenzpunkt verursacht wird, anderenteils die auf Wirkung des Eigenionüberschusses des Farbstoffadsorbats eintretende Änderung seiner Dissoziationskonstante. Mit diesen Messungen konnte die Oberflächen-Säure-Basen-Wirkung bei der Adsorptionsindikation des p-Äthoxy-α-naphthylrots nachgewiesen werden. Die am Äquivalenzpunkt eintretende p_H-Änderung war beim Jodid, Bromid und Rhodanid meßbar, im Falle des Chlorids änderte sich das p_H nicht. Daraus folgt, daß das Chlorid in Gegenwart von p-Äthoxy-α-naphthylrot als Indikator nicht titriert werden kann.

Die auf Wirkung des Eigenionüberschusses in beiden Richtungen eintretende Änderung der Dissoziationskonstante des Farbstoffadsorbats war beim Jodid, Bromid und Rhodanid meßbar. Beim Chlorid trat keine Veränderung ein, während sich die Dissoziationskonstante beim Cyanid nur in einer Richtung änderte. Dies steht auch mit jenem Ergebnis im Einklang, wonach das Chlorid in Gegenwart von p-Äthoxy-α-naphthylrot als Indikator weder in der einen noch in der anderen Richtung titriert werden kann, während sich das Cyanidion mit Silberionen titrieren läßt, umgekehrt jedoch nicht. Beim Rhodanid ändert sich die Dissoziationskonstante in geringerem Maße, als beim Jodid und Bromid, daher ist der Farbumschlag bei der Bestimmung

des Rhodanids mit 0,01n Meßlösung — im Gegensatz zum Bromid und Jodid — nicht mehr genügend scharf.

Mit dem p-Äthoxy-α-naphthylrot wurden auch Adsorptionsmessungen durchgeführt. Zu diesem Zweck titrierte man das Adsorbens zur Bestimmung der Anfangsadsorption in Gegenwart eines Silberionüberschusses, in saurem Medium mit der verdünnten Indikatorlösung. Außerdem bestimmte man die Menge des adsorbierten Farbstoffes auch nach 30 Minuten dauerndem Rühren. Die Ergebnisse dieser Untersuchungen zeigten, daß die Menge des adsorbierten Farbstoffes beim p-Äthoxy-α-naphthylrot ungefähr zweimal so viel oder noch mehr beträgt, als beim 4-(2'-Äthyl-phenylazo)-1-naphthylamin-hydrochlorid. Hieraus kann gefolgert werden, daß bei der Adsorption bzw. in der Wechselwirkung zwischen Farbstoff und Adsorbens die positive mesomere Wirkung der in para-Stellung zur Azogruppe eingeführten Substituenten eine wesentliche Rolle spielt. Die Anfangsadsorption war nur im Falle des Silberrhodanids und Silbercyanids eine echte Adsorption, während der violettgefärbte Indikator beim Jodid und Bromid mit graugelber Farbe an den Niederschlag gebunden wurde, was auf den Ablauf eines chemischen Prozesses schließen läßt. Noch deutlicher zeigte sich dies bei den Untersuchungen nach 30 Minuten dauernder Adsorption. Während sich beim Silberrhodanid im Falle des 4-(2'-Äthyl-phenylazo)-1-naphthylamin-hydrochlorids bei 30 Minuten dauernder Adsorption kein chemischer Prozeß abspielte, konnte beim p-Äthoxy-α-naphthylrot in neutralem Medium eine geringe Änderung der Farbe beobachtet werden. Beim letztgenannten Indikator ist auch der Ablauf des chemischen Prozesses deutlicher ausgeprägt als beim 4-(2'-Äthyl-phenylazo)-1-naphthylamin-hydrochlorid und dies kann gleichfalls auf die Wirkung der beiden Substituenten mit positiver mesomerer Wirkung in para-Stellung zurückgeführt werden.

Die Adsorptionsmessungen gestatten bezüglich der Adsorptionsindikation des p-Äthoxy-α-naphthylrots folgende Schlußfolgerungen:

1. Im Falle des Bromids, Jodids und Rhodanids spielt sich zwischen dem Indikator und dem Adsorbens auch ein chemischer Prozeß ab.

2. Die Anfangsadsorption ist beim Silberchlorid geringfügig.

3. Beim Silberchlorid und Silbercyanid wird der Indikator in Gegenwart von überschüssigen Silberionen in saurem Medium mit saurer Farbe adsorbiert, daraus folgt, daß die positive Ladung des Niederschlags auf den adsorbierten Farbstoff keine Wirkung ausübt.

ZUSAMMENFASSUNG

Durch Diazotierung von p-Phenetidin und Kupplung mit α-Naphthylamin wurde ein neuer Säure-Basen- und Adsorptionsindikator hergestellt. Das p-Äthoxy-α-naphthylrot kann bei argentometrischen Titrationen zur Bestimmung von Bromid, Jodid, Rhodanid und Cyanid verwendet werden. Bei der Verbindung wurde eine Oberflächen-Säure-Basen-Indikation nachgewiesen. Die Änderung des p_H während der Titration und die Änderung der Dissoziationskonstante des Farbstoffadsorbats auf Wirkung von Eigenionüberschuß wurde bestimmt. Die Bestimmung der Adsorption zu Beginn und nach 30 Minuten zeigte, daß der Indikator auch an einem chemischen Prozeß teilnimmt. Die Adsorptionswerte sind größer als im Falle des 4-(2'-Äthyl-phenylazo)-1-naphthylamin-hydrochlorids, woraus folgt, daß sowohl bei der Adsorption als auch beim chemischen Prozeß die positive mesomere Wirkung der Substituenten in para-Stellung (Amino, Äthoxy) eine wesentliche Rolle spielt.

LITERATUR

1. TANDON, K. N., MEHROTRA, R. C.: Anal. chim. Acta **27,** 97 (1962).
2. LÉGRÁDI, L., Magyar Kém. Foly. **70,** 27 (1964); Acta Chim. Hung. **42,** 107 (1964).
3. LÉGRÁDI, L., Magyar Kém. Folyóirat **70,** 333 (1964).
4. PUNGOR, E., SCHULEK, E.: Z. anal. Chem. **150,** 166 (1956).
5. SCHULEK, E., PUNGOR, E.: Anal. Chim. Acta **4,** 213 (1950).
6. LÉGRÁDI, L.: Magyar Kém. Foly. **70,** 271 (1964)

p-Ethoxy-α-naphthylred, a New Adsorption Indicator

L. LÉGRÁDI

Summary. A new acid-base and adsorption indicator was prepared by the diazotation of p-phenetidine and coupling the product with α-naphthylamine. The indicator obtained in this way: p-ethoxy-α-naphthylred proved suitable for use in argentometric titrations, in the determination of bromide, iodide, thiocyanate and cyanide. On applying p-ethoxy-α-naphthylred, an acid-base surface indication takes place. The changes in p_H value during titration and the changes in the dissociation constant on the effect of excess own ions of the dye adsorbate were measured. In addition to these, also the adsorption was measured in the initial stage and after 30 minutes. The results showed that the indicator also participates in the chemical process. The adsorption values were higher than those observed with 4-(2'-ethylphenylazo)-1-naphthylamine hydrochloride. From that it follows that both in the adsorption and in the chemical process, the p-positioned substituents of positive mesomeric effect (such as amino or ethoxy groups) play an essential role.

Новый адсорбционный индикатор — п-этокси-α-нафтил-красный

Л. ЛЕГРАДИ

Резюме. Был получен новый кислотно-основной и адсорбционный индикатор путем диазотирования п-фенетидина с последующим присоединением α-нафтиламина. п-Этокси-α-нафтил-красный может быть использован для определения бромидов, иодидов, роданидов и цианидов методом аргентометрии. Была обнаружена кислотно-основная индикация на поверхности п-этокси-α-нафтил-красного. Измерялись изменение pH при титровании, а также изменение константы диссоциации адсорбируемого красителя при использовании избытка собственного иона. Кроме того, измерялось значение адсорбции вначале опыта и по истечении 30 минут. На основании результатов этих измерений можно заключить, что индикатор также принимает участие и в химических процессах. Найденное значение величины адсорбции оказалось выше, чем в случае солянокислого 4-(2'-этилфенилазо)-1-нафтиламина, откуда следует, что как при адсорбции, так и в химическом процессе существенную роль играют заместители с положительным мезомерным влиянием, находящиеся в пара-положении (амино, этокси).

László LÉGRÁDI; Fűzfőgyártelep, Hungary

OXIDATION METHODS IN ORGANIC ANALYSIS, I.

DETERMINATION OF PHENYLHYDRAZINE IN THE PRESENCE OF ANILINE

L. LÉGRÁDI and J. HUSZÁR

(Nitrokémia Industrial Plants, Füzfőgyártelep, Hungary)

Received July 24, 1964

In the oxidation methods used for the determination of phenylhydrazine [1], the calculations are based on the following oxidation reaction of hydrazine:

$$H_2N-NH_2 - 4\,e^- = N_2 + 4\,H^+ \quad (1)$$

The oxidation of phenylhydrazine may lead, depending on the oxidizing agent and conditions, to benzene

$$C_6H_5-NH-NH_2 - 2\,e^- = C_6H_6 + N_2 + 2\,H^+ \quad (2)$$

or to aniline and phenyl azide [1, 2], or to phenol [3]:

$$C_6H_5-NH-NH_2 + O - 2\,e^- = C_6H_5-OH + N_2 + 2\,H^+ \quad (3)$$

Several methods are known for the bromatometric determination of hydrazine and phenylhydrazine. According to one of them, hydrazine is titrated with potassium bromate in the presence of hydrochloric acid until the titrant is in excess, then the excess bromate is measured by iodometric back titration [4]. In another procedure, phenylhydrazine is titrated with potassium bromate in the presence of hydrochloric acid and potassium bromide, and potentiometric end point detection is used [5]. However, neither of these methods can be applied when the phenylhydrazine sample contains aniline as an impurity.

Experimental

Reagents

0.2 *N* potassium bromate
0.1 *N* iodine solution
Starch solution as indicator
Concentrated hydrochloric acid, analytical grade.

The method proposed for the determination of phenylhydrazine is based on the following reaction:

$$C_6H_5-NH-NH_2 + HCl - 4\,e^- = C_6H_5-\overset{+}{N}\equiv N\,Cl^- + 4\,H^+ \quad (4)$$

Phenylhydrazine is titrated with potassium bromate in hydrochloric acid solution, in the presence of iodine-starch indicator. In this way, phenylhydrazine can be determined in the presence of aniline. The reliability of the suggested method is demonstrated by measurements shown in Table I.

Table I

Bromatometric determination of phenylhydrazine

Phenylhydrazine weighed, g	Aniline weighed, g	Phenylhydrazine found, g	Deviation	
			g	%
0.1364	0.0204	0.1365	+0.0001	0.07
0.1412	0.0227	0.1410	−0.0002	0.14
0.1560	0.0221	0.1555	−0.0005	0.32
0.1637	0.0225	0.1643	+0.0006	0.37
0.1172	0.0252	0.1168	−0.0004	0.34
0.1149	0.0252	0.1147	−0.0002	0.17
0.1520	0.0252	0.1525	+0.0005	0.33

Proof of the course of the reaction

It is general practice to apply Equation (1) to describe the oxidation of phenylhydrazine by potassium bromate [1], but the product has not been characterized. One of the aims of the present investigation was the elucidation of the oxidation process by identification of the formed product. According to Equations (2) and (3) the oxidation of phenylhydrazine yields benzene or phenol, and gaseous nitrogen, respectively. When phenylhydrazine was oxidized by potassium bromate, none of these products could be detected. The actual product reacted with bromine only on prolonged standing or heating. It may be concluded that the oxidation by potassium bromate yields a non-brominable product which is converted by heating into a brominable compound (presumably into phenol). Our investigations proved that the primary product is a diazonium salt (which cannot be brominated); heating with hydrochloric acid converts this compound into phenol. Final evidence was obtained by pouring the titrated mixture into an alkaline solution of β-naphthol; an orange-coloured azocompound was obtained in quantitative yield.

Indicators

Fig. 1 shows the potentiometric titration of phenylhydrazine with potassium bromate in acid solution. Such experiments were carried out in the presence of aniline impurity, with various indicators; electrodes of smooth platinum and saturated calomel were used. It can be seen that in the presence of iodine indicator, the potential jump is markedly greater than with the other indicators examined. Iodine as an indicator has previously been applied in bromatometric measurements [6]. The explanation of the indicator action is as follows. When the equivalent point is reached, potassium bromate reacts with the potassium bromide formed in the oxidation of phenylhydrazine to

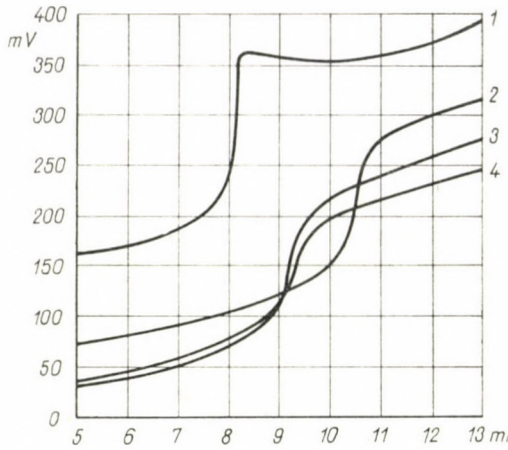

Fig. 1. 1: Iodine starch; 2: methyl orange; 3: formaldehyde; 4: sodium thiosulphate

give bromine, which converts iodine into bromine iodide. In the presence of starch, the blue colouration disappears, permitting the visual observation of the end point.

When a hydrochloric acid solution of phenylhydrazine is allowed to stand with iodine starch, the colour of the solution disappears, because phenylhydrazine is oxidized by iodine, while it becomes reduced to iodide. However, on the addition of potassium bromate, iodide is reconverted into iodine, the blue colour reappears and persists during the titration. The quantity of iodine to be used as indicator depends on the amount of the sample. One drop of a 0.1 N iodine solution is satisfactory for not more than 0.2 g of phenylhydrazine.

Experimental conditions

The rate of oxidation of phenylhydrazine by potassium bromate increases at higher temperatures. At room temperature, the reaction rate is satisfactory to allow direct titration, however, the procedure is to be carried out with vigorous shaking, and when the equivalent point is approached, the titrant must be added dropwise. Below room temperatures the reaction becomes so slow that the results are incorrect.

The role of acid concentration in the process has also been studied. This may affect not only the oxidation of phenylhydrazine, but also the indication process. Namely, phenylhydrazine is oxidized by the iodine indicator even before potassium bromate is added; this reaction depends on the acid concentration. Meanwhile, iodine is reduced to iodide. Later, similarly depending on the acid concentration, iodide is reoxidized by potassium bromate to iodine, and the latter is converted into bromine iodide in the end point. The oxidation of phenylhydrazine by iodine takes place according to the following reaction [7]:

$$C_6H_5-NH-NH_2 + 2\,I_2 = C_6H_5-I + N_2 + 3\,HI \qquad (5)$$

and the formed iodide is oxidized by bromate:

$$2\,I^- + 6\,H^+ + KBrO_3 = I_2 + KBr + 3\,H_2O \qquad (6)$$

The oxidation of phenylhydrazine by bromate is characterized by Equation (4). The effect of the acid concentration on reactions (4), (5) and (6) is shown by the data in Table II.

It appears from Table II that the oxidation of phenylhydrazine by iodine [reaction (5)] takes place at low acid concentrations, and is suspended at high acid concentrations, while just the opposite is true for the oxidation of iodide by bromate [reaction (6)]. The oxidation of phenylhydrazine by bromate [reaction (4)]does not occur if the hydrochloric acid concentration is below 1.75%, and it is not completely quantitative in the presence of iodine indicator at HCl concentrations higher than 5.9%. A quantitative reaction may be attained at hydrochloric acid concentrations of 1.75 to 5.9%. However, within this range, between 1.75 and 3.00%, iodine also reacts with phenylhydrazine;

Table II

Role of acid concentration in the determination of phenylhydrazine

Acid concentration % HCl	Reaction (4)	Reaction (5)	Reaction (6)	Amount of indicator required, drops of 0.1 N I_2	Observation
0.3	does not take place	takes place	does not take place	10	Colour of I_2 does not appear during titration
0.6	does not take place	takes place	slow	6	Colour of I_2 does not disappear in the end point
1.75	quantitative	takes place	fairly quick	1	Colour of I_2 appears after one third has been titrated
3.00	quantitative	slow	quick	1	Prior to titration the colour of iodine does not disappear completely, and reappears at the beginning of titration
4.10	quantitative	does not occur	quick	1	Prior to titration, the colour of iodine does not disappear; greenish-grey tint
5.90	quantitative	does not occur	quick	1	Prior to titration, the colour of iodine does not disappear; greenish-grey tint
8.9	slow	does not occur	quick	2	Colour of iodine starch; greenish yellow does not disappear before titration
11.80	slow	does not occur	quick	6	Colour of iodine starch; greenish yellow does not disappear before titration, but disappears before the end point

therefore, a correction for the indicator should be applied that is equal to an increase of the titration results by 0.1%. At hydrochloric acid concentrations between 4.10 and 5.90% iodine does not react with phenylhydrazine, thus no indicator correction is necessary.

Procedure

0.1 to 0.15 g of phenylhydrazine is weighed in a weighing bottle and transferred into a titration beaker containing 50 ml of water. 7 to 10 ml of concentrated hydrochloric acid is added, and any precipitated phenylhydrazine is redissolved by shaking. After the addition of 1 ml of 1% starch solution and two drops of 0.1 *N* iodine solution, the sample is immediately titrated with 0.2 *N* potassium bromate. The titrant is added dropwise, first rapidly, then in the vicinity of the end point slowly, and the solution is shaken for a few seconds after the addition of each drop of titrant. On adding the last drop of titrant, the greenish colour (which may be blue at lower acid concentrations) turns violet-orange and later yellow.

1 ml of 0.2 *N* potassium bromate is equal to 0.0054072 g of phenylhydrazine.

Hydrazine, hydroxylamine or other reducing agents interfere with the determination, but aniline does not.

SUMMARY

The oxidation of phenylhydrazine by potassium bromate in hydrochloric acid solution gives a diazonium salt in quantitative yield. This process has been utilized for the determination of phenylhydrazine. The indicator is starch iodine which is converted into bromine iodide in the equivalence point, and so becomes colourless. At hydrochloric acid concentrations between 4.10 and 5.90%, no indicator correction is required. The presence of aniline does not interfere with the determination. The error of the method is about 0.3%, the standard deviation being ± 0.04 ml.

REFERENCES

1. Browne, A. W., Shetterly, F. F.: J. Am. Chem. Soc. **29,** 1274 (1907); **31,** 221, 783 (1909).
2. Fischer, E.: Ber. **10,** 1331 (1877).
3. Budesinsky, B.: Collection Czechoslov. Chem. Communs. **26,** 781 (1961).
4. Kurtenacker, A., Wagner, J.: Z. anorg. allgem. Chem. **120,** 261 (1922).
5. Jancik, F., Cinkova, O., Körbl, I.: Collection Czechoslov. Chem. Communs. **24,** 2695 (1959).
6. Szekeres, L.: Magyar Kém. Foly. **64,** 249 (1958).
7. Meyer, E.: J. prakt. Chem. **2/36,** 115 (1887);
Stollé, R.: J. prakt. Chem. **2/66,** 332 (1902).

Über Oxydationsverfahren in der organischen Analyse, I.

Bestimmung von Phenylhydrazin in Gegenwart von Anilin

L. LÉGRÁDI und J. HUSZÁR

Zusammenfassung. Bei der in salzsaurem Medium durchgeführten Oxydation des Phenylhydrazins mittels Kaliumbromates ergab sich quantitativ ein Diazoniumsalz. Dieser Vorgang wurde zur Bestimmung des Phenylhydrazins verwertet. Es wurde dabei Jodstärke als Indikator angewendet, die im Äquivalenzpunkt zu Bromjod umgesetzt und entfärbt wurde. Bei Salzsäurekonzentrationen von 4,10 bis 5,90% ist keine Indikatorkorrektion nötig. Die Anwesenheit von Anilin übt keine Störwirkung aus. Der Fehler der Methode beträgt ungefähr 0,3%, während die Standardabweichung $\pm 0{,}04$ ml.

Окислительные методы в органическом анализе, I.

Определение фенилгидразина в присутствии анилина

Л. ЛЕГРАДИ и Й. ГУСАР

Резюме. При окислении броматом калия фенилгидразина в солянокислой среде количественно образуется его диазониевая соль. Этот процесс применялся для определения фенилгидразина. В качестве индикатора использовали иодный крахмал, который в точке эквивалентности обесцвечивается в результате образования IBr. При использовании соляной кислоты с концентрацией 4,10—5,90% не нужно вводить поправку на индикатор. Присутствие анилина не влияет на точность определений. Погрешность метода приблизительно 0,3%, стандартное отклонение $\pm$ 0,04 ml.

László LÉGRÁDI
József HUSZÁR
Füzfőgyártelep, Hungary

ANALYSIS OF STEROIDS, III*

DETERMINATION OF STEROIDS CONTAINING ISOLATED CARBONYL GROUPS

S. GÖRÖG and L. TOMCSÁNYI

(Gedeon Richter Chemical Works, Budapest)

Received December 4, 1964

The majority of a great number of papers dealing with the analysis of ketosteroids deals with the determination of steroids containing a carbonyl group in conjugation with the double bond, or vicinal to a $-CH_2-OH$ groupf For this purpose, excellent spectrophotometric [1], colorimetric [1, 2] and polarographic [3] methods are available. A much more difficult problem is presented in the analysis of steroids containing isolated carbonyl groups. In contrast to α,β-unsaturated ketosteroids, the former compounds do not disclose a light absorption useful for analytical measurements; the number and efficiency of the available colorimetric methods are also less satisfactory [1, 2], and polarographic analysis can only be carried out in an indirect way [3]. Most methods recommended for the determination of steroids containing an isolated carbonyl group deal with substances of biological origin. In the analysis of such materials, the requirements of accuracy are, in general, not very high. Thus, methods evolved for this purpose are in most cases unsatisfactory for the accurate determination of the pure basic compounds.

In order to evolve a method of sufficient accuracy, we selected, from among the possible methods of determining the carbonyl group, the procedure based on the formation of oxime with hydroxylamine. There are only a few references about the application of this method to the determination of ketosteroids. OPPENAUER [4] checked the progress of oxidation of cholesterol to cholestenone by measuring the formed carbonyl groups. LIGHT [5], in turn, determined triketocholanic acid in this way, while TROZZOLO and LIEBER described the determination of two ketosteroids [6], and PESEZ that of four ketosteroids [7]. However, these methods have been evolved for the determination of individual compounds and cannot be applied to the determination of ketosteroids in general. In order to generalize the method, a solvent, a reagent and a titrant suitable for general use had to be found.

A 2 : 1 mixture of chloroform and methanol proved to be the best solvent for this purpose. Though chloroform as a component of the reaction mixture

* Part II: Acta Chim. Hung. **47**, 7 (1966).

retards the reaction leading to oxime formation, and in certain cases affects the equilibrium adversely [8], the mixture containing chloroform was found to be the sole solvent which dissolved satisfactorily all steroids examined, and ensured the stability of the reagent solution.

In order to find the adequate reagent, the main types described in literature were tried. As a result, hydroxylammonium formate suggested first by PESEZ [7] and applied also by RUCH, JOHNSON and CRITCHFIELD [9] was found to be the most suitable reagent for the analysis of steroids. When the oxime is made with hydroxylammonium formate and an appropriate solvent and indicator are used, the excess reagent can be titrated back by alkalimetry, since formic acid does not interfere with the titration. However, our experiments showed that in the case of ketosteroids of lower reactivity, not examined by PESEZ, long periods at elevated temperatures were necessary to complete the reaction, but at higher temperatures the stability of hydroxylammonium formate is unsatisfactory [7, 10]. A reagent of adequate stability could be prepared at last on the basis of the following considerations. The free hydroxylamine base is very unstable in solution. Its acetate ($pK_{ACOH} = 4.76$) has somewhat better stability, though it is not very stable [11]; the formate ($pK_{HCOOH} = 3.75$) is markedly more stable than the acetate [7], and the hydrochloride is practically stable for any length of time. Thus, there is an unambiguous correlation between the stability of hydroxylamine and the strength of the acid linked to it. Consequently, the task was to find an acid which is stronger than formic acid, but not so strong as to interfere with the titration of hydroxylamine in the mixture of chloroform and methanol. These requirements are met by salicylic acid ($pK = 2.98$). Hydroxylammonium salicylate is a stable, non-hygroscopic, crystalline substance which can be conveniently handled. The reagent solution may be prepared by direct weighing of the solid compound. Boiling for three hours of a 0.1 *N* solution prepared in a 2 : 1 mixture of chloroform and methanol, caused only a 0.7% decrease of the normality. When the standard solution was stored at about 20° in a tightly stoppered ground-glass flask for a month, the normality diminished by 15%. Standard solutions stored for longer periods were not used in our experiments. Within a month, the reagent can be used with unchanged accuracy, because the decomposition products (H_2O, N_2) are indifferent from the aspect of oxime formation [12].

Hydroxylammonium salicylate was applied in an excess of three equivalents, and the reaction was carried out at the boiling point of the solution. The necessary reaction period varied from a few minutes to 90 minutes, depending on the nature of the steroid. In our detailed investigations, invariably a boiling period of two hours was used. The results obtained with a number of substances showed that boiling for two hours is equivalent to standing for

about 24 hours at room temperature. This latter alternative may also be applied when the analysis is not urgent.

In choosing the standard solution for the back-titration of the unreacted hydroxylamine, our aim was that it should allow the determination of minute amounts of the substance, permitting visual end point detection, in order to accelerate the procedure. For this purpose, a 0.05 *N* solution of hydrochloric acid in a mixture of propylene glycol and chloroform was found the most suitable, in the presence of an indicator mixture of dimethyl yellow and methylene blue.

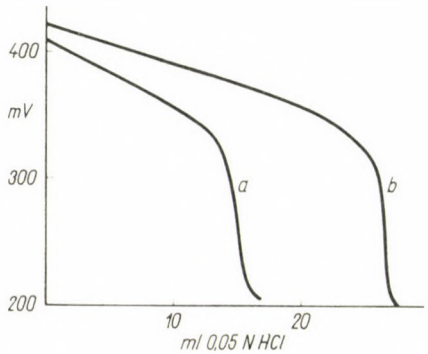

Fig. 1. Titration curves; curve (a): titration of excess hydroxylammonium salicylate after reaction with estrone; curve (b): titration of blank

As it is seen from the titration curve in Fig. 1, when the above-described reagents are used, a sufficiently large potential jump is observed in the end point, and under such conditions the basicity of the formed oxime does not interfere with the determination. The equivalent point of the indicator precisely coincides with the place of the potential jump.

Experimental

Reagents

1. Hydroxylammonium salicylate was prepared by dissolving 40 g of sodium salicylate in 75 ml of water, separately dissolving 17.4 g of hydroxylamine hydrochloride in another 75 ml portion of water, and mixing in ice, the precipitated hydroxylammonium salicylate was filtered off, washed with 20 ml of ice water, and dried three hours under reduced pressure at 80°. Yield: about 15 g, m. p. 141°, precisely in accordance with the value in literature [13]. The substance prepared in this way contains about 2% of sodium chloride which does not affect its suitability for use.

In order to prepare a 0.1 *N* solution, 8.55 g of the substance is dissolved in a mixture of 167 ml of methanol and 333 ml of chloroform.

2. 0.05 *N* hydrochloric acid in propylene glycol and chloroform was prepared by dissolving 4.5 ml of concentrated hydrochloric acid in a mixture of 500 ml of propane-1,2-diol and 500 ml of chloroform. The solution was standardized against diphenyl guanidine, using dimethyl yellow and methylene blue mixed indicator.

3. This indicator mixture was prepared by dissolving 1 g of diethylaminoazobenzene and 0.1 g of methylene blue in methanol to give exactly 100 ml of solution.

The potentiometric titrations were carried out with a p_H-titrimeter of type Radelkisz OP 401/1, with the aid of calomel electrodes in methanol saturated with potassium chloride.

Description of the procedure

A sample of 0.3, 0.15 or 0.1 millimole of the steroid containing 1, 2 or 3 carbonyl groups, respectively, is weighed in a 50-ml. flask with ground glass stopper. The substance is dissolved in 10 ml of 0.1 *N* hydroxylamine salicylate, and the solution refluxed two hours (or allowed to stand 24 hours at room temperature in the tightly stoppered flask). After cooling, the solution is titrated in the presence of one drop of indicator mixture by means of 0.05 *N* hydrochloric acid dissolved in a mixture of propylene glycol and chloroform, while the green colour of the liquid turns red. In the end point the solution is brown.

A blank containing no steroid is titrated in the same way. The difference between the titration value of the blank and the sample is characteristic of the ketosteroid content.

The equivalent weight is the quotient of the molecular weight of the steroid and the number of carbonyl groups in the molecule.

Results and discussion

The analysis of about 25 compounds proved that the suggested method allows the unequivocal and accurate determination of steroids which contain isolated carbonyl groups, not conjugated with a double bond. Under the given conditions, the reaction leading to oxime formation occurs, even when the reaction period is prolonged, to about 90—95% with the Δ^4-3-carbonyl system and only to about 50% with the $\Delta^{1,4}$-3-carbonyl system. (In case of the 1—1 Δ^4-3-ketosteroid examined by PESEZ, and by TROZZOLO and LIEBER, no quantitative reactions were attained, either.) Interestingly, quantitative oxime formation was experienced with two compounds of the examined α,β-unsaturated ketosteroids, namely with 16-methylene-androst-5-ene-3β-ol-17-one, and with pregna-5,16-diene-3β-ol-20-one-3-acetate. It is likely that conjugation is prevented by steric hindrance in these compounds.

The reaction leading to oxime formation may be adversely influenced not only by the conjugation effect of the double bonds, but also by steric hindrance. This latter effect can be particularly well studied in case of pregnane derivatives carrying the carbonyl groups in position 20. If there is no substituent present in positions 17 or 21 in the vicinity of such a carbonyl group, oxime formation takes place quickly and quantitatively. In the presence of a C_{17} or C_{21} hydroxy or acetoxy group, the reaction is slower, but the results are still

quantitative. When, however, both mentioned carbon atoms are substituted, a quantitative reaction can no longer be attained.

With 16,17-epoxy compounds, too high values were obtained, probably owing to an interfering side reaction of the epoxy ring with hydroxylamine. Consequently, these compounds cannot be determined with the desired accuracy.

Some results obtained by the present method in the investigation of various ketosteroids are summarized in Table I.

It can be seen from the data of Table I that the probable error of the individual measurements is less than $\pm$ 1.5%.

Table I

Compound	Number of measurements	Assay (mean value), %	Probable error, %
Estra-1,3,5(10)-triene-3-ol-17-one	5	99.5	±1.6
Estra-1,3,5(10)-triene-3-methoxy-17-one	3	100.2	—
Estra-2,5(10)-diene-3-methoxy-17-one	2	101.5	—
Estra-4-ene-17-one	2	98.8	—
Androst-5-ene-3β-ol-17-one	8	100.4	±0.7
Androst-5-ene-3β-ol-17-one-3-acetate	10	98.7	±1.3
16-Methylene-androst-5-ene-3β-ol-17-one	2	98.6	—
5α-Chloro-6β,19-oxidoandrostane-3β-ol-17-one	3	98.1	—
Pregn-5-ene-3β-ol-20-one	7	100.4	±1.1
Pregn-5-ene-3β,17α-diol-20-one	3	98.0	—
Pregn-5-ene-3β,17α-diol-20-one-3-acetate	2	98.4	—
Pregn-5-ene-3β,21-diol-20-one-21-acetate	3	98.0	—
Pregna-5,16-diene-3β-ol-20-one-3-acetate	15	99.0	±0.9
19-nor-α-Pregn-5(10)-ene-20-ine-17β-ol-3-one	3	98.4	—
Estra-5(10)-ene-3,17-dione	2	97.7	—
5α-Chloro-6β,19-oxidoandrostane-3,17-dione	3	98.4	—
3,7,12-Triketocholanic acid	4	98.9	±1.0

It was found that acids of pK $>$ 3 do not interfere with the determination.

The presence of ketals and enol ethers is also indifferent. Consequently, the free carbonyl group can be determined in the presence of these latter systems frequently applied as protecting groups.

The method suggested by us was utilized, in addition to the assay of ketosteroids, for solving some practical problems, such as the determination of estrone as an impurity in estradiol, checking the progress of oxidation of

3- and 17-hydroxy compounds to the corresponding ketone, following the ketalization of carbonyl groups, etc.

The authors' thanks are expressed to Dr. I. GYENES for his valuable discussions, and to Miss M. KAPÁS for her useful assistance in the experiments.

SUMMARY

An analytical method has been evolved for the determination of ketosteroids, based on oxime formation with hydroxylamine, and back titration of the excess hydroxylamine by alkalimetry.

The reagent to produce the oxime is 0.1 *N* hydroxylammonium salicylate dissolved in a mixture of chloroform and methanol; 0.05 *N* hydrochloric acid in a mixture of propylene glycol and chloroform is used as the titrant, and a mixture of dimethyl yellow and methylene blue as indicator.

The method allows, in general, the determination of steroids containing an isolated carbonyl group, in which steric hindrance is not too strong; the accuracy is $\pm 1.5\%$.

REFERENCES

1. ZIMMERMANN, W.: Chemische Bestimmungsmethoden von Steroidhormonen in Körperflüssigkeiten. (Springer Verlag, Berlin—Göttingen—Heidelberg) 1955. pp. 38—86.
2. KAKÁC, B., VEJDELEK, J.: Handbuch der Kolorimetrie, II. (VEB Gustav Fischer Verlag, Jena) 1963. pp. 894—979.
3. ZUMAN, P., KOLTHOFF, I. M.: Progress in Polarography, II. (Interscience Publishers, New York—London). 1962. pp. 677—678.
4. OPPENAUER, R. V.: Rec. trav. chim. Pay-Bas **56,** 142 (1937).
5. LIGHT, A. E.: Ind. Eng. Chem. Anal. Ed. **14,** 42 (1942).
6. TROZZOLO, A. M., LIEBER, E.: Anal. Chem. **22,** 764 (1950).
7. PESEZ, M.: Bull. soc. chim. France **1957,** 417.
8. FRITZ, J. S., HAMMOND, G. S.: Quantitative Organic Analysis. (John Wiley and Sons, Inc. New York) 1957. pp. 6—22.
9. RUCH, J. E., JOHNSON, J. B., CRITCHFIELD, F. E.: Anal. Chem. **33,** 1566 (1961).
10. CRITCHFIELD, F. E.: Organic Functional Group Analysis. (Pergamon Press) 1963. p. 74.
11. HIGUCHI, T., BARNSTEIN, H. C.: Anal. Chem. **28,** 1022 (1956).
12. PERRETT, J. J.: Helv. Chim. Acta **34,** 1531 (1951).
13. OESPER, R. E., BALLARD, M. P.: J. Am. Chem. Soc. **47,** 2426 (1925).

Zur Analytik von Steroiden, III.

Bestimmung solcher Steroide, die eine isolierte Ketongruppe enthalten

S. GÖRÖG und L. TOMCSÁNYI

Zusammenfassung. Auf Grund von Oximbildung mittels Hydroxylamins und einer alkalimetrischen Rücktitration des überschüssigen Hydroxylamins wurde ein analytisches Verfahren zur Bestimmung von Ketosteroiden entwickelt.

Eine 0.1 n Hydroxylammoniumsalicylat-Lösung in einem Gemisch von Chloroform und Methanol diente dabei als oximbildendes Reagens, eine 0,05 n Salzsäurelösung in einem Gemisch von Propylenglykol und Chloroform als Meßlösung, schließlich ein Gemisch von Dimethylgelb und Methylenblau als Indikator.

Mittels der vorgeschlagenen Methode können allgemein nur jene Steroide mit einem Fehler von $\pm 1{,}5\%$ bestimmt werden, die eine sterisch nicht zu stark behinderte, isolierte Ketongruppe tragen.

Анализ стероидов, III.

Определение стероидов, содержащих изолированную кетоновую группу

Ш.ГЁРЁГ и Л. ТОМЧАНИ

Резюме. Был разработан аналитический метод для определения кетостероидов, основанный на образовании оксимов при их реакции с гидроксиламином и на последующем алкалиметрическом обратным титровани избыточного гидроксиламина.

В качестве реагента, образующего оксим, применялся 0,1 н раствор салицилата гидроксиламмония в смеси хлороформа с метанолом, а в качестве титрующего раствора — 0,05 н раствор соляной кислоты в смеси хлороформа с пропиленгликолем. Индикатором служила смесь диметилового желтого с метиленовым синим.

С помощью данного метода можно определять лишь стероиды, содержащие стерически не слишком экранированные изолированные кето-группы, с точностью ± 1,5%.

Dr. Sándor GÖRÖG
László TOMCSÁNYI
Budapest X. Cserkesz u. 63

REACTION OF DISULFUR DICHLORIDE AND SULFUR DICHLORIDE WITH CYANIDE; THEIR DETERMINATION THROUGH THIOCYANATE

E. SCHULEK, L. BARCZA, M. GÁBOR-FEHÉR and L. LADÁNYI

(Department of Inorganic and Analytical Chemistry, L. Eötvös University, Budapest)

Received December 8, 1964

Disulfur dichloride is a compound of interest from many aspects. On the basis of its chemical properties (primarily the way of its hydrolysis) one may conclude that the two sulfur atoms present in the molecule are not equivalent. Therefore, the compound had been considered earlier as thio-thionyl chloride. STAMM and GOEHRING [1] who thoroughly investigated the hydrolysis of disulfur-dichloride, presumed that the initial reaction product was the otherwise unknown thiosulfurous acid:

$$S_2Cl_2 + H_2O \longrightarrow S_2(OH)_2 + 2\,HCl \qquad (1)$$

Further decomposition of thiosulfurous acid would lead to the end product consisting of sulfide, elementary sulfur, sulfite, thiosulfate and polythionates.

However, detailed investigations proved later, mainly by the evaluation of the Raman spectra, that the two sulfur atoms in the molecule of disulfur dichloride are equivalent, and the molecule has a chain-like structure [2, 3]. This statement has been confirmed by some chemical reactions; namely, under appropriate conditions disulfur dichloride reacts with sulfite to yield unambiguously tetrathionate, while with thiosulfate hexathionate is obtained [4].

Thus, the hydrolysis reaction had to be interpreted in some other way. The theory of BÖHME and SCHNEIDER is of interest; they assume in the first step of hydrolysis the formation of hydrogen disulfide and hypochlorous acid:

$$S_2Cl_2 + 2\,H_2O \longrightarrow H_2S_2 + 2\,HOCl \qquad (2)$$

All other products derive from the actions of these compounds [5]. At first sight, the hypothesis appears to be highly improbable, however, evidence is presented in support of this view: in the presence of iodide, iodine is liberated in a stoichiometric reaction:

$$2\,I^- + S_2Cl_2 \longrightarrow 2\,S + I_2 + 2\,Cl^- \qquad (3)$$

As a further piece of evidence, BÖHME and SCHNEIDER showed that in a mixture of hydrogen sulfide and iodide hypochlorite behaves as an oxidizing agent, producing indeed the end products found above.

Sulfur dichloride reacts similarly to disulfur dichloride.

Though the above interpretation cannot be accepted in spite of the presented evidence, the described reaction is of great interest. Namely, on the basis of former experience with disulfur dichloride and sulfur dichloride it was unexpected that compounds liberating iodine in the presence of iodide may be formed in the hydrolysis.

It should be mentioned here that this reaction may be used to determine these compounds [5]. This is one of the few specific analytical methods known. Disulfur dichloride (or sulfur dichloride) is generally analyzed by subjecting the sample to hydrolysis, and measuring the produced chloride ; the total sulfur content may also be established.

Direct determinations are rarely described in literature. Two photometric procedures may be mentioned here. One of them is based on the fact that in an alkaline medium disulfur dichloride gives with *p*-aminophenol, or even better with *p*-dimethylaminoaniline, a product of intensive red colour which can be extracted with carbon tetrachloride [6]. The value of the other method is questionable: the sulfite formed during the alkaline hydrolysis of disulfur dichloride is measured by the fuchsin-formaldehyde method [6]; however, this reaction is far from quantitative.

These introductory comments explain why our present investigations had the purpose of finding a reaction of disulfur dichloride which lends itself to serving as basis of a new reliable analytical method.

In the present investigations, disulfur dichloride prepared by us and purified by distillation was used. The substance was prepared in the known way, by reacting elementary sulfur with a slight excess of chlorine. On distilling the product, a forerun boiling at 58—60° was separated and redistilled. The analysis of this product showed that it was pure sulfur dichloride, as expected.

A number of reactions of disulfur dichloride have been examined. Most interesting of these was the reaction of disulfur dichloride in an organic solvent with an aqueous solution of potassium cyanide of adequate concentration. The yellow tint of the organic phase momentaneously disappeared during the reaction, indicating the transfer of disulfur dichloride into the aqueous phase, while the aqueous solution became coloured, and within a few minutes a brown precipitate was deposited. Further investigations proved that thiocyanate was formed in the aqueous phase in stoichiometric amounts, according to the equation

$$S_2Cl_2 \xrightarrow{CN^-} 2\,SCN^- \qquad (4)$$

In this reaction no other sulfur-containing compound is formed in detectable amounts. Thus, the presumption that disulfur dichloride first undergoes hydrolysis according to equation (1), then the produced $S_2(OH)_2$ (which cannot properly be denoted as thiosulfuric acid) suffers disproportionation:

$$2\,S_2(OH)_2 \longrightarrow 3\,S + SO_3^{2-} + H_2O + 2\,H^+ \tag{5}$$

and thiocyanate is formed in the reaction of elementary sulfur with cyanide, can fully be excluded. (In this process, which appears very likely at first sight, the ratio of S_2Cl_2 to SCN^- would be 2 : 3 instead of 1 : 2.)

It was found that in the first step of the reaction (in the interval between the decolouration of the organic phase and the appearance of precipitate in the aqueous phase) the presence of a substance of oxidizing nature could be detected in the reaction mixture. The primary reaction, leading to the formation of the oxidizing substance, is apparently very quick, while the formation of the dark precipitate is a time reaction. To interpret these facts we presumed that the reduction of the primarily formed oxidizing agent gives rise to the formation of dicyanogen which is then polymerized in time to paracyanogen:

$$x\,CN^- - x\,e \longrightarrow \frac{x}{2}(CN)_2 \longrightarrow (CN)_x \tag{6}$$

This presumption is supported by the analysis of the brown precipitate. (The presence of paracyanogen does not interfere with the subsequent analytical procedures.)

It was still necessary to elucidate the course of the oxidation—reduction reaction, and the nature of the oxidizing substance formed as primary product.

In order to investigate the first problem, disulfur dichloride dissolved in an organic solvent was shaken with a cyanide solution containing a known amount of sulfite. In notable contrast to the process described previously, the aqueous solution remained colourless. Determination of the excess of sulfite and the quantity of formed sulfate unambiguously indicated the following overall reaction:

$$S_2Cl_2 + 2\,CN^- + 2\,e = 2\,SCN^- + 2\,Cl^- \tag{7}$$

The parallelism between the reaction examined by us and that studied by BÖHME and SCHNEIDER [5] is apparent. However, while the primary reaction presumed in Eq. (2) may perhaps be possible in the latter case, it is entirely improbable in our experiments, since the aqueous solution, owing to the hydrolysis of potassium cyanide, is alkaline.

A new hypothesis was evolved to interpret the first step of reaction; we assume that under the effect of the relatively large excess of cyanide ions, the chloride atoms of disulfur dichloride are exchanged against cyanide ions:

$$S_2Cl_2 + 2\ CN^- = (SCN)_2 + 2\ Cl^- \tag{8}$$

The formed thiocyanogen, as a strong oxidizing agent, is responsible for the oxidation—reduction reaction

$$(SCN)_2 + 2\ e = 2\ SCN^- \tag{9}$$

in which thiocyanogen is quantitatively converted into thiocyanate.

Similar reactions are known in other cases, too. *E.g.*, FEHÉR and RISTIC [7] prepared polysulfuro-dibromide from polysulfuro-dichloride by exchange reaction with HBr. A similar exchange may also be possible in the case of CN^- ions.

In support of the possibility of such an analogy, direct evidence was obtained for the formation of dithiocyanate. In a distilling apparatus, disulfur dichloride was reacted with a concentrated solution of potassium cyanide under nitrogen. In the trap applied as receiver the presence of an oxidizing substance, and after reduction, of thiocyanate was detected. On the basis of carefully conducted blank experiments, this phenomenon can only be explained by the formation of dithiocyanate.

As a further proof of thiocyanogen formation, dithiocyanate was prepared and allowed to react with a number of substances. It was found that dithiocyanate behaved identically with the substance formed in the reaction of disulfur dichloride and CN^- ions, *e.g.* it oxidized cyanide ions to paracyanogen.

The above-described investigations proved that the process represented by Eq. (7) consists really of the reactions shown in Eqs. (8) and (9). It is highly probable that the reaction of disulfur dichloride with iodine ions takes place in a similar way; instead of hypochlorous acid the unstable sulfur iodide is formed by means of exchange of Cl^- against I^-, and this compound spontaneously decomposes to give elementary sulfur and iodine. This presumption (also considering, of course, the interaction of disulfur dichloride and cyanide ions as proved above) is in accordance with the chemistry of sulfur halides much better than the suggestion of BÖHME and SCHNEIDER. However, we restrict ourselves here solely to mentioning this presumption, and no attempt has been made to prove its correctness.

With sulfur dichloride the process is completely similar to that observed with disulfur dichloride:

$$SCl \xrightarrow{+\,2\,CN^-} S(CN)_2 \xrightarrow{+\,2\,e} SCN^- + CN^- \tag{10}$$

The actual course of this reaction can be confirmed in the same way as above.

These interesting reactions quantitatively afford thiocyanate as the final product. After the excess cyanide has been removed by boiling with boric

acid, thiocyanate may be measured conveniently and very accurately through cyanogen bromide [8]. Thus, elucidation of this reaction offered a way for a novel specific determination of thiocyanate.

Description of the method

Reagents

Gasoline (fraction of b. p. 70—90°, carefully refined)
Potassium cyanide
Boric acid
20% phosphoric acid
Saturated bromine water, freshly prepared
5% phenol solution
Potassium iodide
1% starch solution, treated and preserved with 0.1% of salicylic acid
0.01 *N* sodium thiosulfate.

A sample of 20—60 mg of disulfur dichloride or 40—80 mg of sulfur dichloride was weighed in a tightly sealable 1 ml weighing flask with analytical accuracy. Then the substance was dissolved in 2 ml of gasoline in a similarly airtight glass-stoppered 100 ml Erlenmeyer flask. A solution of 0.20 g of potassium cyanide in 5 ml water was added, and the mixture was shaken for a few minutes. The mixture was allowed to stand for ten minutes, diluted with 70—80 ml of water, 1 g of boric acid and some coarse pumice stone, as anti-bumping agent, were added and the system was vigorously boiled for 10 to 15 minutes over an electric hot plate in a hood. After cooling, the solution was rinsed into a 100.0 ml volumetric flask, and completed to volume with water.

An aliquot of 5.00 to 10.00 ml of the stock solution was transferred into a 100 ml glass-stoppered Erlenmeyer flask, diluted to 20 to 25 ml, and acidified with 2 ml of phosphoric acid solution. Bromine water was added dropwise until a permanent brownish-yellow coloration of the solution was attained. After one or two minutes, 5 ml of the phenol solution was rapidly added to the mixture, thoroughly shaken several times, and after a few minutes about 0.2 g of potassium iodide was dissolved in the solution. The amount of iodine liberated was measured after 20 minutes by titration with thiosulfate solution, in the presence of starch solution as indicator.

1 ml of 0.01 *N* titrant is equivalent to 0.3376 mg of S_2Cl_2 or to 0.5149 mg of SCl_2.

The results of the determination of disulfur dichloride are presented in Table I, those of sulfur dichloride in Table II.

The products were also analysed for chlorine content. For this purpose, the following procedure was found best suitable.

A sample of 40—80 mg, weighed with analytical accuracy, was added to a mixture of 4 ml of water, 1 ml of 20% sodium hydroxide and 1 ml of

concentrated hydrogen peroxide, previously prepared in a 100 ml glass-stoppered Erlenmeyer flask. The carefully stirred mixture was allowed to stand 10 minutes, diluted with 20 to 25 ml of water, then vigorously boiled for 4—5 minutes.

Table I

S_2Cl_2 weighed for the preparation of stock solution, mg	Calculated S_2Cl_2-content of aliquot, mg	0.01 *N* $Na_2S_2O_3$ consumed, ml	S_2Cl_2 found		%
			data, mg	mean value, mg	
		6.10	2.059		
21.0	2.106	6.11	2.063	2.055	97.58
		6.05	2.043		
		4.41	1.489		
30.1	1.520	4.42	1.492	1.491	98.09
		4.42	1.492		
		5.71	1.928		
39.2	1.980	5.71	1.928	1.928	97.37
		5.71	1.928		
		5.92	1.999		
40.6	2.050	5.94	2.005	2.003	97.71
		5.94	2.005		
		8.34	2.816		
57.0	2.878	8.35	2.819	2.821	98.02
		8.38	2.829		
				Mean value	97.75

Table II

SCl_2 weighed for the preparation of stock solution, mg	Calculated SCl_2 content of aliquot mg	0.01 *N* $Na_2S_2O_3$ consumed, ml	SCl_2 found		%
			data, mg	mean value, mg	
		8.26	4.253		
42.2	4.233	8.26	4.253	4.253	100.5
		8.26	4.253		
		5.13	2.641		
52.5	2.651	5.16	2.657	2.653	100.1
		5.17	2.661		
		10.67	5.494		
54.1	5.432	10.73	5.525	5.513	101.5
		10.72	5.520		
		6.06	3.120		
60.6	3.060	6.04	3.110	3.115	101.7
		6.05	3.115		
		6.74	3.470		
68.6	3.464	6.71	3.455	3.462	99.94
		6.72	3.460		
				Mean value	100.7

The system was acidified with 10—12 ml of 10% nitric acid, boiled again for 1—2 minutes, cooled and filtered. A known volume of 0.1 *N* potassium permanganate was added dropwise to the clear filtrate, the excess permanganate decolorized with one drop of 3% hydrogen peroxide solution, and mixed with 20.00 ml of 0.1 *N* silver nitrate solution. The mixture containing a precipitate was boiled a few minutes, allowed to cool, and excess silver was titrated with 0.1 *N* thiocyanate solution in the presence of 1 ml of a 10% solution of iron (II)nitrate containing some nitric acid as indicator.

According to the the results of our experiments the analysis of the chloride gave 100.2% S_2Cl_2 for disulfur dichloride, and an assay of 98.82% for sulfur dichloride. By comparing these values with those obtained in the determination of the thiocyanate content, we may state that despite of the extremely careful purification of the substances, minute contamination of SCl_2 remained in disulfur dichloride and a minute impurity of S_2Cl_2 was present in sulfur dichloride.

It is seen that comparison of the analysis of chloride with the determination of sulphur (as thiocyanate) permits some conclusions to estimate the impurities in SCl_2 and S_2Cl_2.

SUMMARY

Investigation of the interaction of disulfur dichloride with cyanide revealed that the first product formed in this reaction is actually thiocyanogen. In the absence of another reducing agent, thiocyanogen oxidizes the excess of cyanide to paracyanogen it becomes reduced to thiocyanate, in a stoichiometric reaction.

Similarly thiocyanate is formed in a stoichiometric ratio in the reaction of sulfur dichloride with cyanide ions.

Elucidation of these reactions has led to a new method of determining disulfur dichloride or sulfur dichloride through thiocyanate. The formed thiocyanate is measured by iodimetry through cyanogen bromide.

REFERENCES

1. Stamm, H., Goehring, M.: Z. anorg. allg. Chem. **250,** 56 (1942).
2. Stammreich, H., Forneris, R.: Spektrochim. Acta **8,** 46 (1956).
3. Eiri Hirota: Bull. Chem. Soc. Japan **31,** 130 (1958).
4. Schmidt, M., Wirwoll, B.: Z. anorg. allg. Chem. **303,** 177, 184 (1960).
5. Böhme, H., Schneider, E.: Ber. **76,** 483 (1943).
6. Tubina, A. Ya.: Trudy Kom. Anal. Khim. Akad. Nauk SSSR **11,** 447 (1960).
7. Fehér, F., Ristic, S.: Z. anorg. allg. Chem. **293,** 311 (1957).
8. Schulek, E.: Z. anal. Chem. **62,** 337 (1923).

Über die Reaktion von Dischwefeldichlorid mit Cyanid; ihre Bestimmung mittels Rhodanids

E. SCHULEK, L. BARCZA, M. GÁBOR-FEHÉR und L. LADÁNYI

Zusammenfassung. Bei der Untersuchung der Reaktion von Dischwefeldichlorid mit Cyanid wurde festgestellt, daß sich im Laufe dieses Vorganges zuerst Dirhodan bildet. Wenn kein anderes Reduziermittel anwesend ist, wird das überschüssige Cyanid durch Dirhodan zu Paracyan oxydiert, während das Dirhodan selbst stöchiometrisch zu Rhodanid reduziert wird.

Ähnlicherweise bildet sich Rhodan stöchiometrisch auch bei der Reaktion $SCl_2 - CN^-$.

Die Aufklärung dieser Reaktionen ermöglicht die Bestimmung des Dischwefeldichlorids bzw. des Schwefeldichlorids mittels Rhodanids. Das entwickelte Rhodanid wird mittels Bromcyans jodometrisch gemessen.

Реакции S_2Cl_2 и SCl_2 с цианидом, определение их через роданид

Э. ШУЛЕК, Л. БАРЦА, М. ГАБОР-ФЕХЕР и Л. ЛАДАНИ

Резюме. При изучении реакции S_2Cl_2 с цианидом было установлено, что в процессе сперва образуется дироданд, который в свою очередь — в отсутствии прочих восстановителей — окисляет избыток цианида в парацианан, и сам восстанавливается стехиометрически в роданид.

Подобным образом, стехиометрически образуется роданид и в реакции SCl_2 с цианидом.

Выяснением указанных реакций дается возможность для определения S_2Cl_2 или SCl_2 через роданид. Образовавшийся при этом роданид определяется иодометрически через бромциан.

Dr. Lajos BARCZA
Mrs. Magda GÁBOR-FEHÉR
László LADÁNYI

Budapest VIII. Múzeum körút 4/b

CONTRIBUTIONS TO THE CHEMISTRY OF SELENIUM AND SELENIUM COMPOUNDS, XIV*

DETERMINATION OF SELENIUM IN ORGANIC SELENIUM COMPOUNDS

L. BARCZA

(Institute of Inorganic and Analytical Chemistry, L. Eötvös University, Budapest)

Received December 8, 1964

A number of methods are known for the determination of selenium in organic compounds. Some excellent reviews of the field can be found in literature [1, 2]. Though also some other data could be mentioned, reference is made in the first line to these reviews.

It is necessary to divide the problem of analysis into two parts: decomposition of the sample and determination of the components. These problems have been discussed thoroughly in an earlier paper [3], though from a different point of view.

Methods of rendering the sample soluble may be classified in three groups [1]: (a) wet processing; (b) fusion in a sealed tube; (c) combustion methods. The so-called Schöniger combustion [4], a procedure offering many advantages and becoming recently rather wide-spread, has been found suitable for use also in the analysis of organic selenium compounds [5, 6, 7, 8].

It must be emphasized that the adequate choice of the ways of sample preparation is of decisive importance in the analysis of selenium compounds [3]. In this connection we refer to an earlier, very detailed paper [9] where decomposition with concentrated sulfuric acid was found best suitable as pretreatment. According to our own experience, when minute amounts of selenium are to be determined in organic substances *(e.g.*, in natural products), destruction with a mixture of sulfuric acid, nitric acid and hydrogen peroxide is the best method. Indeed, it should be carried out in a so-called "reversed" way [10], if a large quantity of organic substance is to be decomposed.

In the case of organic compounds containing much selenium, the Schöniger method of combustion [14] is to be preferred, because it does not require the use of reagents which would later interfere with the analysis or which would be difficult to remove. Another advantage of this method is that organic selenium compounds can be decomposed in this way much easier than other organic substances.

Several methods have been suggested [1] for the determination of selenium after the sample has been brought into solution. Of these, however, only

* Part XIII: Acta Chim. Hung. **45**, 23 (1965).

the gravimetric and iodimetric procedures have been actually adopted in analytical practice. The photometric method using diaminobenzidine [8, 3] may be recommended solely, if a very minute amount of selenium is present in the sample to be tested. This is usually not the case in the analysis of organic selenium compounds. The photometric determination of selenium as elementary selenium [11] is unjustified, and cannot be recommended for theoretical reasons either [3].

In the course of the decomposition or combustion processes, the minimum possible amounts of substance are to be applied; therefore, volumetric methods evolved on a 0.01 *N* scale, which are essentially quicker, have an advantage over the otherwise accurate but cumbersome gravimetric procedures where elementary selenium is measured.

Of the volumetric methods, iodimetric titration is most frequently recommended [5, 6, 7]. However, it must be noted that it is not quite easy to determine elementary iodine, particularly on 0.01 *N* scale, which is liberated in the reaction of selenium(IV) with iodide, because at the same time also elementary selenium of intensive red colour is formed and it is suspended in the solution in colloidal form. Though a number of modifications of this process are known [3], their accuracy is not satisfactory.

The method suggested by KAINZ and RESCH [11] should be mentioned separately. The wide-spread use of this method is due, in addition to its several advantages, to the fact that the procedure is recommended by the well-known textbook of PREGL and ROTH [12]. The determination is based on the oxidation of selenium to selenate during the decomposition achieved with sodium peroxide. After elimination of other oxidizing agents, selenate may be determined by iodimetry: the iodine formed during the reduction of selenate is distilled, and titrated in the distillate. The crucial point of the method is that other oxidizing agents should be reduced in weakly acid medium by iodide before the reaction of selenium(VI) and iodide is accomplished; the latter process occurs quantitatively in a strongly acidic solution. However, loss of selenate during the former process can only be avoided under very strictly controlled conditions.

This state of the problem gave the background of our present investigations which dealt with a detailed study of determining selenium in organic selenium compounds. First, it was confirmed that in the course of the Schöniger combustion any selenium contained in the organic substance is quantitatively converted into selenium dioxide which can be simply collected in distilled water.

The combustion is to be conducted in a way that selenium should be present in the sample between 1 and 3 mg, that is in the range which was found optimum in the procedure evolved by us earlier [14] for the determination of selenium(IV), based on the Schulek and Kőrös method [13] of determining selenocyanide. The procedure consists essentially in the reduction by

ascorbic acid of selenium dioxide absorbed in water (more precisely, selenous acid); the elementary selenium is converted with cyanide into selenocyanide; excess cyanide is removed and the selenocyanide is measured by iodimetry through cyanogen bromide.

The method is accurate, quick and simple; the whole process from combustion to the final titration can be carried out in the same flask. The method was checked first with selenium of analytical grade, then with selenium diluted with glucose. Finally, selenium was determined in some carefully prepared and purified organic selenium compounds. Some of the experimental results are listed in the Table and the description of the method is given below.

Description of the method

Reagents

5% solution of ascorbic acid
5% solution of potassium cyanide
Boric acid
Sodium tungstate
0.1% ethanolic solution of methyl red
10% solution of perchloric acid
Freshly prepared saturated bromine water
5% solution of phenol
Potassium iodide
1% starch solution treated and preserved with 0.1% salicylic acid
0.01 *N* sodium thiosulfate preserved with 1% of isobutanol.

An aliquot of the substance to be analysed, containing 0.4 to 4.0 mg of selenium, is weighed accurately, and wrapped in a strip of filter paper of the size and shape normally used in the Schöniger combustion. The sample is placed in a platinum spoon fastened to the stopper. 5 ml of water is poured into a heavy wall 200 ml iodine flask, and the flask is filled with oxygen. The edge of the filter paper containing the sample is ignited, it is quickly transferred into the flask, and the stopper is held down tightly until the combustion is complete. The flask is shaken from time to time to achieve complete dissolution of the selenium dioxide smoke, which requires about ten minutes, 1 ml of ascorbic acid solution is poured into the rim around the stopper. Cautiously loosening the stopper, the liquid is allowed to be sucked into the flask, the rim is rinsed with 5 ml of water in a similar manner (possibly so as to leave some residual vacuum in the flask). The mixture is allowed to stand ten minutes with occasional shaking, then 1 ml of cyanide solution is added to the solution. If the selenium content is relatively high, a minute amount of selenium may sublime to the part above the platinum spoon; in this case the cyanide solution is allowed to flow along this surface in order to dissolve the sublimate. Selenium is dissolved in a few seconds. The platinum spoon and the stopper are thoroughly rinsed with a total of 25 ml of water, some coarse pumice powder is added into the flask, and the liquid is vigorously boiled for 15 minutes in a fume cupboard,

Table

Investigated substance and its selenium content (%)	Weight of sample mg	0.01 *N* $Na_2S_2O_3$ required ml	Selenium found		
			mg	%	
				single analyses	mean
Elementary selenium (100.0%)	0.566	1.44	0.569	100.5	
	1.101	2.79	1.102	100.1	
	1.807	4.58	1.808	100.1	100.0
	2.590	6.55	2.586	99.8	
	2.906	7.35	2.902	99.9	
	3.680	9.28	3.664	99.6	
Elementary selenium diluted with glucose (32.26%)	3.190	2.64	1.042	32.66	
	4.706	3.82	1.508	32.04	
	5.484	4.52	1.785	32.55	32.32
	6.323	5.15	2.033	32.15	
	7.800	6.30	2.487	31.89	
	8.577	7.09	2.799	32.63	
Anilinium hydrogen selenite ($C_6H_5NH_3.HSeO_3$) (35.58%)	5.616	5.06	1.998	35.58	
	6.096	5.55	2.191	35.94	
	6.134	5.45	2.152	35.08	35.56
	6.243	5.57	2.199	35.22	
	6.480	5.92	2.337	36.06	
	7.878	7.08	2.795	35.48	
Piazselenol (2,1,3-benzoselenadiazole) ($C_6H_4N_2Se$) (43.17%)	3.155	3.48	1.374	43.55	
	3.251	3.55	1.402	43.13	
	3.482	3.81	1.504	43.19	43.20
	3.575	3.92	1.548	43.30	
	4.342	4.72	1.863	42.91	
	5.660	6.18	2.440	43.11	
Dipiazselenol $(SeN_2C_6H_3)_2$ (43.41%)	3.838	4.20	1.658	43.20	
	4.172	4.67	1.844	44.20	
	4.686	5.08	2.006	42.81	43.32
	4.851	5.31	2.096	43.21	
	4.915	5.40	2.132	43.38	
	5.584	6.10	2.408	43.12	
5-(3,4-Diaminophenyl)-2,1,3-benzoselenadiazole) $(C_6H_3(NH_2)_2-C_6H_3N_2Se)$ (27.33%)	4.383	3.02	1.192	27.20	
	4.481	3.10	1.224	27.32	
	4.771	3.26	1.258	26.37	27.08
	5.143	3.61	1.426	27.71	
	5.572	3.81	1.504	26.99	
	6.023	4.10	1.619	26.88	

periodically replacing evaporated water. After cooling, 0.2 g of sodium tungstate is dissolved in the mixture, neutralized with perchloric acid in the presence of 1 drop of methyl red indicator solution, and bromine water is added until the liquid turns brownish yellow. The flask is closed with an ordinary ground-glass stopper. After allowing the system to stand for 2 minutes, 2 to 4 ml of phenol solution is quickly poured into the flask, the mixture is thoroughly shaken, allowed to stand for a few minutes, acidified with 2 ml of perchloric acid, and 0.1—0.2 g of potassium iodide is dissolved in the solution. The liberated iodine is measured after 20 minutes by titration with standard thiosulfate solution using starch solution as indicator.

1 ml of 0.01 *N* $Na_2S_2O_3$ is equivalent to 0.3948 mg of selenium.

SUMMARY

A method has been evolved for the determination of selenium in organic selenium compounds. Selenium dioxide formed in the course of the Schöniger combustion is absorbed in water, the dissolved selenium(IV) is converted into selenocyanide and measured by iodimetry as cyanogen bromide. The method is rapid, simple and accurate.

REFERENCES

1. Belcher, R., Gibbon, D., Sykes, A.: Mikrochemie **40,** 76 (1952).
2. Schöniger, W.: Mikrochim. Acta **1963,** 52.
3. Barcza, L.: Magyar Tud. Akad. Kémiai Oszt. Közl. (in press)
4. Schöniger, W.: Mikrochim. Acta **1955,** 123; **1956,** 867.
5. Meier, E., Shaltiel, N.: Mikrochim. Acta **1960,** 580.
6. Musto, O., Dittrich, S.: An. Fac. Quin. **6,** 115 (1960).
7. Ihn, W., Hesse, G., Neuland, P.: Mikrochim. **1962,** 628.
8. Dye, W. B., Bretthauer, E., Seim, H. J., Blincoe, C.: Anal. Chem. **35,** 1687 (1963).
9. Konek, F., Schleifer, O.: Ber. **51,** 842 (1918).
10. Schulek, E., Laszlovszky, J.: Mikrochim. Acta **1960,** 485.
11. Kainz, G., Resch, A.: Mikrochemie **40,** 332 (1952).
12. Roth, H.: Pregl-Roth: Quantitative organische Mikroanalyse. 7th ed. (Springer-Verlag, Wien) 1958, 167.
13. Schulek, E., Kőrös, E.: Z. anal. Chem. **139,** 20 (1953).
14. Schulek, E., Barcza, L.: Talanta **3,** 27 (1959).

Angaben zur Chemie des Selens und der Selenverbindungen, XIV.

Bestimmung des Selengehaltes organischer Selenverbindungen

L. BARCZA

Zusammenfassung. Es wurde ein Verfahren zur Bestimmung des Selengehaltes organischer Selenverbindungen entwickelt. Dabei wird das bei der Schönigerschen Verbrennung gebildete Selendioxid in Wasser aufgefangen, sodann das Selen(IV) — nach Umsetzung zu Selenocyanid — durch Bromcyan jodometrisch gemessen. Das Verfahren ist rasch, einfach und genau.

Данные к химии селена и его соединений, XIV.

Определение содержания селена в селенорганических соединениях

Л. БАРЦА

Резюме. Разработан способ определения содержания селена в селенорганических соединениях. Образующаяся, в ходе сжигания по Шёнигеру, двуокись селена улавливалась водой, затем переводили Se(IV) в селенцианид и измеряли иодометрически через бромциан. Способ является быстрым простым и точным.

Dr. Lajos Barcza; Budapest VIII. Múzeum körút 4/b

SOME THEORETICAL AND PRACTICAL PROBLEMS IN THE USE OF ORGANIC REAGENTS IN CHEMICAL ANALYSIS, VIII*

INFLUENCE OF THE CHELATE EFFECT AND RING SIZE ON THE STABILITY OF THE DIOXIME COMPLEXES OF TRANSITION METALS

I. RUFF and K. BURGER

(Institute of Inorganic and Analytical Chemistry, L. Eötvös University, Budapest)

Received March 30, 1965

1. Introduction

In our earlier communications [1, 2] we showed the importance of two effects among the other factors stabilizing the dioxime complexes of transition metals; these are 1. the stabilizing action of hydrogen bridges formed in the complexes, and 2. the effect of metal → ligand donor π bonds. The former factor is significant mainly in the complexes of metals of small ionic radius. Owing to this effect, in solutions of such complexes the constant of formation of a complex having the composition $Me(dmg)^+$ (where dmg = dimethylglyoxime) deviates from the statistical case, and it is even lower than that of the complex of composition $Me(dmg)_2$ [1]. The effect of the donor π bond is shown in the infrared spectra of the complexes by a decrease of the C=N vibration frequency of the ligand in the order Cu(II), Ni(II), Co(II), Fe(II) [2] indicating that on passing from Cu(II) to Fe(II), the conjugation increases in the chelate ring which contains the C=N double bond. The participation of the d-electrons of the central metal ion in the π electron system of the conjugated ring is the greater, the lower the bond energy of the d-electrons of the metal ion which do not participate in a σ bond. This can be measured, in first approximation, by the ionization work Me(II)—Me(III). That explains the reason why maximum stabilizing effect of the donor π bond is found in case of the Fe(II) complex of the mentioned series where the work of ionization is the smallest.

On basis of the frequencies of the O—H valence vibrations we succeeded in proving the presence of more or less strong hydrogen bridges in the dioxime complexes of all divalent transition metals [2]. Thus, it is likely that these dioxime complexes have an approximately square-planar arrangement. Their formula may be written as follows on page 144.

It can be seen in this structural formula that the molecule actually consists of four condensed rings. The stabilizing effect of the hydrogen bridges is due to the formation of the two rings denoted by 1, while in the two five-

* Part VII: BURGER, K., EGYED, I., RUFF, I.: J. Inorg. Nucl. Chem. **28**, 139 (1966).

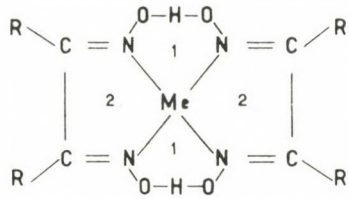

membered rings, denoted by 2, conjugation is extended through the metal ion (quasi-aromatization). Consequently, the stabilizing effect of the donor π bond manifests itself primarily through these rings.

In dioxime complexes both stabilizing effects appear parallel to each other, contributing to the stabilization of the ligand field. Thus, it appeared promising to carry out investigations by which these two effects may separately be studied. Such an investigation can be conducted in two different ways:

1. Investigating the complexes of a ligand where the formation of hydrogen bridges is somehow inhibited. A comparison of the stability of these complexes with those of the corresponding dioxime chelates affords information as regards the extent of stabilization by the hydrogen bridge. In order to prevent the formation of the hydrogen bridge, *e.g.*, one oxime group may be converted into an $=N-O-CH_3$ group. Investigations of this type have been carried out by CHARLES and FREISER [3] with dimethylglyoxime monomethyl ether. However, this substitution may lead, in addition to inhibiting the formation of the hydrogen bridge, to changes in the electron distribution of the molecule, and may even cause steric hindrance. Consequently, this method gives only an approximative information about the stabilizing effect of the hydrogen bridge.

2. The second possibility involves the use of a ligand where the formation of the "aromatic" ring (denoted by 2) is inhibited or at least hindered. In this way information may be obtained concerning the extent of the stabilizing effect of the donor π bond. The formation of the "aromatic" ring can be inhibited by applying in place of dimethylglyoxime (dmg) ligand, *e.g.*, the unidentate ligand acetaldoxime (aao). Using the latter, the decrease of stability compared with the corresponding dimethylglyoxime complex is due to two factors: (a) to chelate effect and (b) to the absence of the stabilizing action of an aromatic ring.

In order to study these two effects separately, a ligand is to be selected in which only one of the effects is possible. In the case of acetylacetonedioxime (aado) as the ligand, the ring is six-membered, in contrast to dimethylglyoxime complexes. A continuous conjugation in this ring is impossible, and stabilization due to aromatization cannot take place. However, the chelate effect is not suspended, because acetylacetone dioxime is a bidentate ligand.*

* It must be noted that any changes in the number of carbon atoms of the ring also affect the strength of chelate effect. Still, according to literature [12], this factor is negligible compared with the effect examined in our present study.

On the basis of the above considerations, the scope of our present investigations was the determination of the stabilities of the acetaldoxime and acetylacetonedioxime complexes of transition metals. Thus far, of these complexes only the acetylacetonedioxime complexes of copper(II) [4, 5] and nickel(II) [6] have been investigated by preparative studies and by measurements by ultraviolet and infrared spectrophotometry. BEN BASSAT and BINENBOYM [5, 6] reported that these complexes have the composition $Me(aado)_2$, and that binuclear hydroxo mixed complexes are precipitated from an aqueous copper(II) solution in which the ratio metal: aado is 1 : 1. In respect to the cobalt(II) complex of acetylacetonedioxime, the mentioned authors referred merely to their observation that it may be utilized as a sensitive reagent for the detection of cobalt(II) ions in the presence of nickel(II). On the basis of the Job curve of the nickel(II) complex of acetylacetonedioxime, the apparent stability constant of the complex was established, but the acidic dissociation constant of the ligand was not taken into account in the calculations.

The acetaldoxime complexes have been studied so far only in non-aqueous media, mainly from preparative aspects [7].

2. Experimental

2.1. Reagents and instruments

The potentiometric measurements were carried out with an instrument "Radiometer Type p_H meter 28", the ultraviolet spectrophotometric investigations with a Unicam SP 700 spectrophotometer, while the infrared spectra were established in potassium bromide discs with a Zeiss UR 10 spectrometer. The magnetic measurements were made with the magnetic proton resonance measuring instrument of the Department for Nuclear Physics of the L. Eötvös University, Budapest.

Acetaldoxime was prepared according to the prescriptions of PETRACZEK [8] (b. p. 114—115°).

The acetylacetonedioxime (Eastman Organic Chemicals) was of analytical grade.

The metal salts and perchloric acid were Merck reagents of analytical grade.

Sodium perchlorate used for adjusting a constant ionic strength was prepared from concentrated perchloric acid with sodium carbonate of analytical grade.

2.2. Determination of the acidic dissociation constant of the ligands

The acidic dissociation constant of acetaldoxime was measured owing to its low value, by spectrophotometry in carbonate-free solutions of sodium hydroxide of various concentrations prepared by accurate weighing, at an aao concentration of $5 \cdot 10^{-4}$ mole ($I = 0.3$). The extinction was determined at the point of maximum absorption of the dissociated ligand, *i.e.*, at 37 000 cm^{-1}.

The acidic dissociation constant of acetylacetonedioxime was determined at $2 \cdot 10^{-4}$ *M* concentration in aqueous solution and in a 50% aqueous dioxane solution, at an ionic strength of 0.3 *M*, by spectrophotometry at 34 000 cm^{-1}.

2.3. Determination of the stability constants of the complexes

The stability constants of the acetylacetone dioxime complexes were determined by the potentiometric method of BJERRUM [10] modified by CALVIN and MELCHIOR [9]. In the aqueous and 50% aqueous dioxane solutions, the following concentrations were used: in case of the nickel(II) and cobalt(II) complexes $C_{Me(II)} = 10^{-3}$ *M* and $C_{aado} = 5 \cdot 10^{-3}$ *M*; 100.0 ml

of this solution was titrated with 0.2 N sodium hydroxide; in case of copper(II): $C_{Cu(II)} = 10^{-4}$ M and $C_{aado} = 10^{-2}$ M; 100.0 ml of this solution was titrated with 0.01 N sodium hydroxide.

The stability constant of the copper(II) complex of acetaldoxime was determined by potentiometry, by titration with 0.01 N sodium hydroxide at a copper(II) concentration of 10^{-4} M and an acetaldoxime concetration of 10^{-2} M. Stability measurements by spectrophotometry were carried out at a copper(II) concentration of 10^{-4} M and a ligand concentration of 10^{-2} M, in the p_H range between 3 and 10; measurements were also made at ligand concentrations varying between 10^{-4} and 10^{-1} M.

The magnetic proton resonance spectra were determined in complex solutions of 10^{-2} M.

All measurements were made at an ionic strength of $I = 0.3$ M. The potentiometric titrations were carried out at $25 \pm 0.01°$.

3. Evaluation methods

The following equilibria of acetylacetonedioxime complexes must be taken into account in the solutions:

$$Me^{2+} + aado^- \overset{K_1}{\rightleftharpoons} Me(aado)^+ \tag{1}$$

and

$$Me(aado)^+ + aado^- \overset{K_2}{\rightleftharpoons} Me(aado)_2 \tag{2}$$

Thus, the formation function of Bjerrum reads

$$\bar{n} = \frac{[Me(aado)^+] + 2\,[Me(aado)_2]}{[Me^{2+}] + [Me(aado)^+] + [Me(aado_2)]} \tag{3}$$

or, applying the conventional expressions for K_1 and K_2:

$$\bar{n} = \frac{K_1\,[aado^-] + 2\,K_1 K_2\,[aado^-]^2}{1 + K_1\,[aado^-] + K_1 K_2\,[aado^-]^2} \tag{4}$$

If

$$v = K_1\,[aado^-] \tag{5}$$

and

$$p = \frac{K_2}{K_1} \tag{6}$$

then it follows from Equation (4):

$$\bar{n} = \frac{v + 2pv^2}{1 + v + pv^2} \tag{7}$$

On comparing, according to the usual Sillén method of normalization (11), the functions $\bar{n} = f(\lg v; p)$ and $\bar{n} = f(-\lg [\text{aado}^-])$ (the latter being obtainable experimentally), the values of K_1 and K_2 can be determined (Fig. 1).

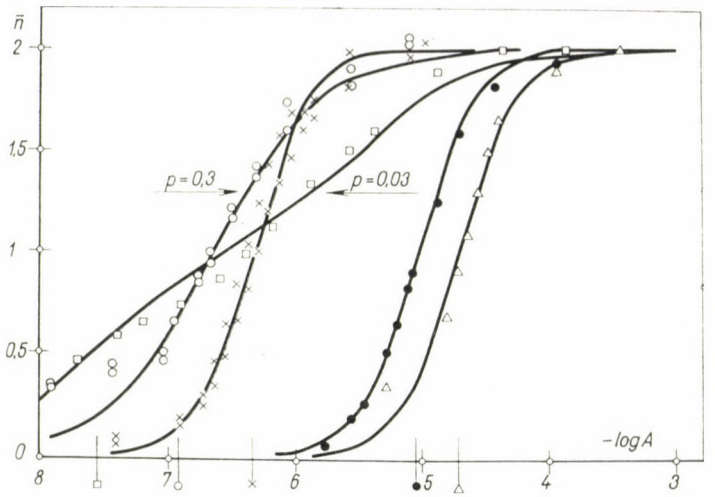

Fig. 1. Curves of formation of the transition metal complexes of acetylacetonedioxime. △ △ △ $Co(aado)_2$ in water; ● ● ● $Ni(aado)_2$ in water; □ □ □ $Cu(aado)_2$ in water; × × × $Ni(aado)_2$ in 50% dioxan; ○ ○ ○ $Co(aado)_2$ in 50% dioxan. Curves drawn in full lines are the best fitting normalized curves (the corresponding site $\lg v = 0$ is denoted in the curve by a vertical line)

In the case of the acetaldoxime complex, the equilibria prevailing in the solution can be expressed by the following equations (on the basis of evidence to be discussed later):

$$Cu^{2+} + aao^- \overset{K_1}{\rightleftharpoons} Cu(aao)^+ \tag{8}$$

$$Cu(aao)^+ + Haao \overset{K_2}{\rightleftharpoons} Cu(aao)\,(Haao)^+ \tag{9}$$

$$Cu(aao)\,(Haao)^+ + aao^- \overset{K_3}{\rightleftharpoons} Cu(aao)_2\,(Haao) \tag{10}$$

$$Cu(aao)_2\,(Haao) + Haao \overset{K_4}{\rightleftharpoons} Cu(aao)_2\,(Haao)_2 \tag{11}$$

From the above equilibria, for the function of formation we have:

$$\bar{n} = \frac{\beta_1[aao^-] + 2\beta_2[aao^-][Haao] + 3\beta_3[aao^-]^2[Haao] + 4\beta_4[aao^-]^2[Haao]^2}{1 + \beta_1[aao^-] + \beta_2[aao^-][Haao] + \beta_3[aao^-]^2[Haao] + \beta_4[aao^-]^2[Haao]^2} \tag{12}$$

where

$$\beta_n = K_1 K_2 \ldots K_n \tag{13}$$

When the analytical concentration of acetaldoxime in the solution (c_{Haao}) is sufficiently high, its portion consumed by dissociation and complex formation can be neglected, therefore:

$$[\mathrm{Haao}] \approx c_{\mathrm{Haao}} \tag{14}$$

On introducing the symbols

$$\beta'_2 = \beta_2\,[\mathrm{Haao}] \tag{15}$$

$$\beta'_3 = \beta_3\,[\mathrm{Haao}] \tag{16}$$

$$\beta'_4 = \beta_4\,[\mathrm{Haao}]^2 \tag{17}$$

Equation (12) can be simplified as follows:

$$\bar{n} = \frac{(\beta_1 + 2\,\beta'_2)\,[\mathrm{aao}^-] + (3\,\beta'_3 + 4\,\beta'_4)\,[\mathrm{aao}^-]^2}{1 + (\beta_1 + \beta'_2)\,[\mathrm{aao}^-) + (\beta'_3 + \beta'_4)\,[\mathrm{aao}^-]^2} \tag{18}$$

Now let us introduce the term

$$v = \sqrt{(3\,\beta'_3 + 4\,\beta_4)\,[\mathrm{aao}^-]} \tag{19}$$

as a new variable. Then, we have

$$\bar{n} = \frac{p_1\,v + v^2}{1 + p_2\,v + p_3\,v^2} \tag{20}$$

where

$$p_1 = \frac{\beta_1 + 2\,\beta'_2}{\sqrt{3\,\beta'_3 + 4\,\beta'_4}} \tag{21}$$

$$p_2 = \frac{\beta_1 + \beta'_2}{\sqrt{3\,\beta'_3 + 4\,\beta'_4}} \tag{22}$$

and

$$p_3 = \frac{\beta'_3 + \beta'_4}{3\,\beta'_3 + 4\,\beta'_4} \tag{23}$$

The experimental points were found to fit the curve $n = f(\lg v)$ corresponding to the equation

$$\bar{n} = \frac{v^2}{1 + \frac{1}{4} v^2} \tag{24}$$

with the parameters $p_1 = p_2 = 0$ and $p_3 = \frac{1}{4}$ (Fig. 4). According to Equations (21)—(23), this means that $\beta'_4 \gg \beta'_3$.

In the spectrophotometric measurements, the degree of formation

$$\alpha = \frac{[\mathrm{Cu(aao)_2\,(Haao)_2}]}{c_{\mathrm{Cu}}} \tag{25}$$

referred to the complex $\mathrm{Cu(aao)_2\,(Haao)_2}$ was determined as the function of the $\mathrm{p_H}$ of the solution. Allowing for the presence of complexes of various composition, and considering the corresponding stability constants, α can be written in the form:

$$\alpha = \frac{\beta_4 [\mathrm{aao^-}]^2 [\mathrm{Haao}]^2}{1 + \beta_1 [\mathrm{aao^-}] + \beta_2 [\mathrm{aao^-}][\mathrm{Haao}] + \beta_3 [\mathrm{aao^-}]^2 [\mathrm{Haao}] + \beta_4 [\mathrm{aao^-}]^2 [\mathrm{Haao}]^2} \tag{26}$$

When the conditions (14) to (17) hold, this simplifies to

$$\alpha = \frac{\beta'_4 [\mathrm{aao^-}]^2}{1 + (\beta_1 + \beta'_2)[\mathrm{aao^-}] + (\beta'_3 + \beta'_4)[\mathrm{aao^-}]^2} \tag{27}$$

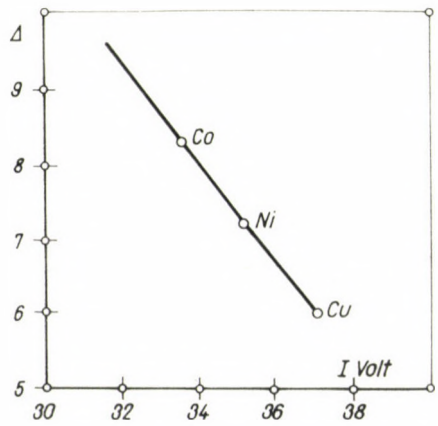

Fig. 2. π bond stabilization of the transition metal complexes of dioxime plotted against the third ionization potential of the metal ion

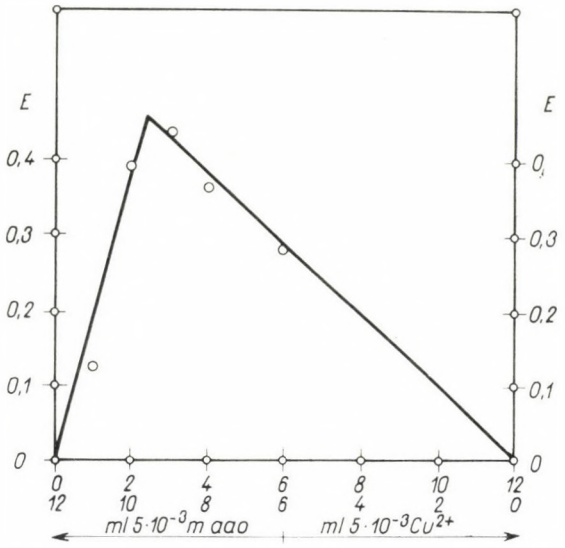

Fig. 3. Job curve of the copper(II) complex of acetaldoxime, measured at 3300 cm^{-1}

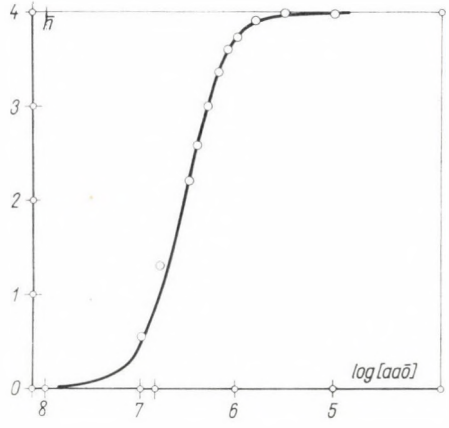

Fig. 4. Potentiometric curve of formation of the complex $Cu(aao)_2(Haao)_2$
(The curve represents the best fitting normalized curve)

Introducing the new variable

$$v = \sqrt{\beta'_4}\,[\mathrm{aao}^-] \tag{28}$$

formula (27) will read:

$$a = \frac{v^2}{1 + p_1 v + p_2 v^2} \tag{29}$$

where

$$p_1 = \frac{\beta_1 + \beta_2'}{\sqrt{\beta_4'}} \tag{30}$$

and

$$p_2 = \frac{\beta_3' + \beta_4'}{\sqrt{\beta_4'}} \tag{31}$$

When the usual normalizations are carried out, the stability constants are obtained. (The experimental points fit the curve $p_1 = 0$, $p_2 = 1$; see Fig. 5.)

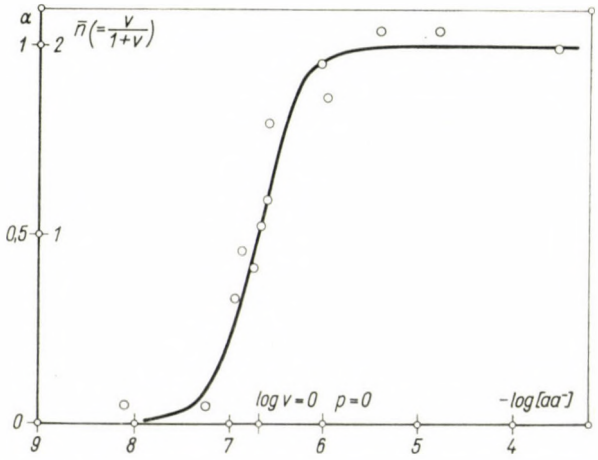

Fig. 5. Spectrophotometrically determined formation function of the complex $Cu(aao)_2(Haao)_2$ (The curve represents the best fitting normalized curve)

4. Results and discussion

4.1. *Acidic dissociation constants*

The acidic dissociation constants of the investigated ligands determined at an ionic strength of 0.3 *M* are summarized in Table I. For the sake of comparison also the corresponding data of dimethylglyoxime are given.

Table I

Acidic dissociation constants of the investigated ligands in 0.3 M sodium perchlorate

Ligand	Solvent	pK_a
Acetaldoxime	water	11.5 ± 0.2
Acetylacetonedioxime ..	water	9.9 ± 0.2
	50% dioxan	11.6 ± 0.2
Dimethylglyoxime	water	10.6
	50% dioxan	11.8

4.2. *Effect of ring size*

As it has been mentioned in the introduction, the stabilizing effect of ring size and through this that of the π conjugation were studied on the copper(II), nickel(II) and cobalt(II) complexes of acetylacetone dioxime. The determined stability constants are presented in Table II, while the function of formation is shown in Fig. 1.

Table II

Stability constants of acetylacetone dioxime complexes at 25°

(I = 0.3)

Complex	Solvent	$\lg \beta_1$	$\lg \beta_2$	Δ	Reference
$Cu(aado)_2$	water	7.6	13.2	6.0	13
$Ni(aado)_2$	water	—	10.1	7.2	14
$Co(aado)_2$	water	—	9.4	8.3	15
$Ni(aado)_2$	50% dioxan	—	12.7	9.8	1
$Co(aado)_2$	50% dioxan	6.9	13.3	7.7	1

The determination of the data shown in Table II was not difficult in case of the nickel(II) and cobalt(II) complexes because these metals, at the concentrations used in the measurements, begin to hydrolyze only at rather high p_H values (7.5 to 8.5). Thus, the p_H range of complex formation (from 6 to 7) is satisfactorily distinct. Accordingly, one need not consider the possibility that hydroxo mixed complexes are formed along with the "regular" complexes which were desired to be studied.

The situation is not so favourable with the complexes of copper(II) and iron(II). Namely, in the first case, as already experienced by BEN BASSAT and BINENBOYM, binuclear or polynuclear copper-hydroxo compounds precipitate from the solution because complex formation occurs (at the same concentrations as used in case of the nickel(II) and cobalt(II) complexes) nearly in the same p_H range where hydrolysis does. Though iron(II) ions begin to hydrolyze only at p_H 7—8, the stability of the corresponding complex is so low that hydroxo mixed complexes are formed in this case as well.

In these instances we attempted to separate the p_H range of hydrolysis from that of complex formation by using a relatively great (hundredfold) excess of the ligand, and the metal ion concentration was decreased by one order of magnitude. Under such circumstances it was possible to determine the stability of the copper(II) complex, but that of the iron(II) complex proved to be so small that its determination by this method was impossible.

Table II also shows the decrease of stability (Δ) in respect to the corresponding dimethylglyoxime complexes:

$$\Delta = \lg \beta_{2,\mathrm{dmg}} - \lg \beta_{2,\mathrm{aado}}$$

This difference in stability, according to what has been said in the introduction, is due mainly to the fact that ring conjugation is no longer possible thus in the aado complex there is no possibility for metal-to-ligand electron transfer (formation of a donor π-bond). This appears in a convincing way in Fig. 2 where the values of Δ have been plotted against the ionization potentials, $Me^{2+} \rightarrow Me^{3+}$, of the metal ions. If the work of ionization is higher, this stabilizing effect is decreased, in accordance with the consideration that the probability of the presence on the ligand of electrons belonging to metal orbitals and not involved in σ bonds is greater, if they are bound with less energy to the metal.

In the case of bidentate ligands where there are no incomplete orbitals, and thus the formation of donor π bonds is excluded, the complexes of various central metal ions show, in general, a nearly identical decrease of stability when the number of atoms of the ring is altered. By way of example, the stability of ethylene- and 1,3-propylenediamine complexes can be mentioned [12].

The problem may arise that "ligand exchange" may lead to essential alterations also in the electronic structure of the metal ions. In contrast to the dimethylglyoxime complexes of low spin, the complexes of acetylacetonedioxime may have high spin. Magnetic proton resonance investigations with the $Ni(aado)_2$ complex proved the presence of diamagnetic complex particles. This result confirms that acetylacetonedioxime is a strong-field ligand in this complex, similarly to dimethylglyoxime. However, this method falls short of permitting an exact determination of the magnetic moments, and other methods could not be applied, owing to the poor solubility of the complex.

4.3. *Chelate effect*

The extent of chelate effect observed in dioxime complexes can be studied, *e.g.*, by comparing the stabilities of the dimethylglyoxime and acetaldoxime complexes. For this purpose, complex formation has been investigated by potentiometric titrations in aqueous solutions containing iron(II), cobalt(II), nickel(II) or copper(II) ions and acetaldoxime. Of the examined metals, only copper(II) formed a "regular" complex with acetaldoxime, while with the other metals precipitates having colours similar to that of the corresponding metal hydroxides precipitated in the course of titration. The examination of these products by infrared spectrometry showed, indeed, that they consisted of the metal hydroxides containing some, possible only adsorptively bound, acetaldoxime. In solutions of concentrations higher than $5 \cdot 10^{-4}$ M, also copper(II) ions gave the blue hydroxo mixed complexes. However, these mixed complexes have not been studied in greater detail in the present work.

The composition of the "regular" copper(II) complex of acetaldoxime has been established by the Job method (Fig. 3). According to our measurements, this complex has the composition $Cu(aao)_4$.*

Potentiometric titrations carried out as described in the experimental part indicated, however, a complex formation process involving the liberation of two protons only, proving that the complex has really the composition $Cu(aao)_2\ (Haao)_2$. By the same potentiometric measurements, the overall stability constant was found to be $\lg \beta_4 = 17.0$ (Fig. 4).

The stability constants were determined by spectrophotometric measurements as well (Fig. 5). These measurements were carried out at the wave number where, according to the Job curve, light is absorbed only by the complex having the composition 1 : 4. This arrangement similarly indicated that in the presence of a hundred-fold excess of acetaldoxime binding of all the four ligands takes place in one step, and the stability constant is $\lg \beta_4 = 17.4$. The stability constant of the copper(II) complex of dimethylglyoxime is $\lg \beta_2 = 19.24$.

The above results show that the decrease of stability of the complex $Cu(aao)_2\ (Haao)_2$ in comparison with $Cu(dmg)_2$ is less significant than that of the complex $Cu(aado)_2$. This can be explained by premising that the absence of the stabilizing effect of a donor π bond and of a chelate effect has been partially compensated by the increase of stabilization due to the hydrogen bridge. Namely, on ring cleavage, the oxygen atoms bound rigidly in the dimethylglyoxime complex may freely move up to an optimum distance required for hydrogen bonding, and thus the stabilizing effect by hydrogen bridge formation may markedly increase.

The authors express their thanks to Mr. E. ANTAL for his assistance in the experiments.

SUMMARY

The stability conditions of the acetylacetonedioxime complexes of cobalt(II), nickel(II) and copper(II), and of the acetaldoxime complex of copper(II) have been investigated. In the case of acetylacetonedioxime, the decrease of stability compared with the corresponding dimethylglyoxime complexes is ascribed to the fact that any conjugation of the ring, and consequently a stabilizing effect by donor π bonds are impossible. The stability decrease of the acetaldoxime complex is attributed to two reasons, (a) chelate effect, and (b) lack of a conjugated ring. This stability decrease is compensated in part by the formation of stronger hydrogen bridges.

Magnetic measurements indicate an electronic arrangement of low spin in acetylacetonedioxime complexes.

REFERENCES

1. BURGER, K., RUFF, I.: Talanta **10,** 329 (1963).
2. BURGER, K., RUFF, I., RUFF, F.: J. Inorg. Nucl. Chem. **27,** 179 (1965).
3. CHARLES, R. G., FREISER, H.: Anal. Chim. Acta **11,** 101 (1954).

* Obviously, the Job curve is not sufficiently accurate to decide whether the complex has 1 : 4, 1 : 5 or 1 : 6 composition. However, in the present case a coordination number higher than 4 can be excluded on the basis of ligand-field theoretical considerations, and other measurements alike.

4. SUTOK, T., NAKAHARA, A.: Sci. Reps. **9,** 67 (1960).
5. BEN BASSAT, A. H. I., BINENBOYM, I.: Bull. soc. chim. France **1963,** 2769.
6. BEN BASSAT, A. H. I., BINENBOYM, I.: Bull. soc. chim. France **1963,** 2774.
7. HIEBER, W., LEUTERT, F.: Ber. **60B,** 2296 (1927).
8. PETRACZEK, J.: Ber. **15,** 2784 (1882).
9. CALVIN, M., MELCHIOR, C. N.: J. Am. Chem. Soc. **70,** 3270 (1948).
10. BJERRUM, J.: Metal Ammine Formation in Aqueous Solution. (P. Haase and Son, Copenhagen) 1941.
11. SILLÉN, L. G.: Acta Chem. Scand. **10,** 186 (1956).
12. Stability Constants. (Chemical Society, London) 1957. Part I.
13. DYRSSEN, D., HENNICHS, M.: Acta Chem. Scand. **15,** 47 (1961).
14. DYRSSEN, D., KRAŠOVEC, F., SILLÉN, L. G.: Acta Chem. Scand. **13,** 50 (1959).
15. BURGER, K., RUFF, I.: Acta Chim. Hung. **41,** 75 (1965).

Über einige theoretische und praktische Probleme der analytischen Anwendung organischer Reagenzien, VIII.

Wirkung des Chelateffektes und der Ringgröße auf die Stabilität der Dioximkomplexe von Übergangsmetallen

I. RUFF und K. BURGER

Zusammenfassung. Die Stabilitätsverhältnisse der Acetylacetondioximkomplexe des Kobalt(II) Nickel(II) und Kupfer(II), ferner des Acetaldoximkomplexes von Kupfer(II) wurden untersucht Die im Verhältnis zur Stabilität der entsprechenden Dimethylglyoximkomplexe beobachtete Stabilitätsverminderung wird im Falle des Acetylacetondioxims dem Aufhören der Konjugation des Ringes, und dadurch der Einstellung der Stabilisierwirkung der Donor-π-Bindung zugeschrieben. Die Stabilitätsverminderung des Acetaldoximkomplexes wird durch den Chelateffekt und durch das Verschwinden des konjugierten Ringes erklärt. Diese Stabilitätsverminderung wird teils durch Entwicklung stärkerer Wasserstoffbrücken kompensiert.

Die magnetischen Messungen wiesen auf eine Elektronenverteilung mit kleine Spinzahl bei den Acetylacetondioximkomplexen hin.

О некоторых теоретических и практических вопросах аналитического применения органических реагентов, VIII

Влияние хелатного эффекта и размеров кольца на стабильность комплексов диоксимов с переходными металлами

И. РУФФ и К. БУРГЕР

Резюме. Были изучены стабильности комплексов ацетилацетон-диоксима с двухвалентными кобальтом, никелем и медью, а также ацетальдоксима с медью(II). Уменьшение стабильности ацетилацетон-диоксимных комплексов по отношению к соответствующим диметил-глиоксимным комплексам приписывается прекращению конюгации в кольце и, в результате этого, ослаблению стабилизирующего влияния донорной π-связи. Уменьшение стабильности ацетальдоксимных комплексов может быть объяснено, с одной стороны, хелатным эффектом, а с другой стороны, исчезновением конюгации кольца. Это уменьшение стабильности частично компенсируется образованием более сильных водородных связей.

Согласно измерениям магнитной восприимчивости было обнаружено, что ацетилацетон-диоксимные комплексы представляют собой электронные упорядочения с низким значением результирующего спина.

Dr. Imre RUFF
Dr. Kálmán BURGER
Budapest VIII. Múzeum körút 4/b

THERMAL STABILITY OF THE EUTECTIC MIXTURE OF DIPHENYL AND DIPHENYLMETHANE

M. RÓDER, I. OPAUSZKY and I. KISS

(Department of Chemistry, Central Research Institute for Physics, Hungarian Academy of Sciences, Budapest)

Received December 15, 1964

Previous investigations have shown [1, 2] that, among the organic compounds, aromatic hydrocarbons have to be considered in the first place as potential neutron moderators and coolants in nuclear reactors. For this reason, the eutectic mixture of diphenyl and diphenylmethane (D—DM) was subjected to detailed investigations. The experimental data thus obtained are summarized in Table I.

The chosen mixture was expected to be more suitable than other compounds suggested so far, since it has a melting point lower than ro om temperatur contrary to the more radiation-resistant higher melting terphenyl isomers or their mixtures, and is more stable under radiation [3] than the low melting-point isopropyldiphenyl suggested for this purpose in U.S.A. patents [4].

For evaluating the suitability of a substance to be used as moderator or coolant also its thermal stability must be accurately known. Furthermore, a comparison of pyrolytic and radiolytic products may yield valuable information about the differences in the mechanisms of the chemical reactions involved in these two different ways of energy transfer.

Table I

Physical properties of the eutectic mixture of diphenyl and diphenylmethane (D—DM)

Composition, % by weight		M. p., °C	B. p., °C	Vapour pressure, atm.
Diphenyl	28	12.2	261.3 (760 Torr)	360°C 6.50
Diphenylmethane ..	72			400°C 10.88
				450°C 20.32

The pyrolysis of diphenyl has been studied by several authors [5, 6, 7] in the temperature range between 425 and 526°C. The formation of liquids with higher boiling points as compared with the initial substance, and of gases was observed, and the rates of formation determined; and attempts were made to establish the mechanism of the pyrolytic reaction on the basis

of these rates. The values obtained by various authors for the mean activation energy in the pyrolysis of diphenyl vary from 66 to 93 kcal/moles.

As regards the thermal decomposition of diphenylmethane, thus far only the main gaseous (hydrogen, methane and carbon monoxide) and liquid (triphenylmethane, tetraphenylethylene) products from one-hour pyrolysis at 476°C have been known [8].

Experimental

In the experiments diphenyl and diphenylmethane (Fluka), refined by repeated vacuum distillation and sublimation, were used. From the eutectic mixture (D—DM) samples of 0.5 to 2.0 g were weighed in ampoules of 10 mm diameter made of pyrex glass. The samples were degassed by repeated freezing out, the vacuum-sealed ampoules were then placed in a stainless steel container and kept in an electrical furnace for 50 to 330 hours at temperatures of 350, 370, 400, 425, 450 and 470°C. The temperature was kept constant in each case to an accuracy of ±3°C.

After heating, the quantity and composition of the gas evolved, and the amount of products ("polymers") having higher boiling points than the initial mixture were determined.

In order to measure the quantity of the gas evolved, the ampoules were opened in an evacuated system of known volume equipped with a manometer, and the increase in pressure was measured. The composition of the pyrolysis gas, and the nature of liquid products boiling below the b. p. of the initial mixture were established with the aid of a mass spectrometer of type MI—1305.

In order to establish the amount of the polymeric products, they were isolated by vacuum distillation. An aliquot of the heated mixture was distilled under conditions which ensured that only higher boiler products than the initial mixture were left behind as a residue. Since the molecular weight of a polymeric product is usually at least twice as high as that of the initial component, distillation resulted in a satisfactory separation. In several cases it was checked by chromatography (by a gas chromatograph of the Pye type) that no traces of the initial mixture were present in the distillation residue. On completing the distillation, the weight of the residue was measured. The mean molecular weight of the polymeric products was determined by cryoscopic method in Freon-112 as solvent.

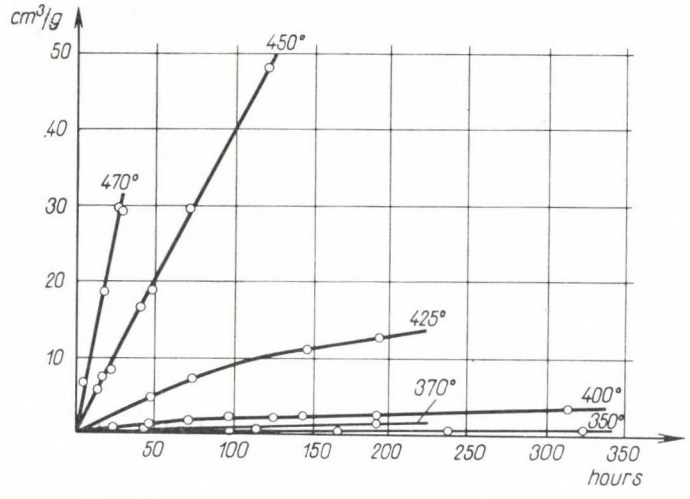

Fig. 1. Pyrolytic gas formation at various temperatures

Experimental results

On heating, the D—DM mixture began to turn yellow already at 360°. This colouration became more intensive with increasing temperature and pyrolysis. At 450 and 470°, carbon was precipitated even after relatively short periods (15—50 hours) of heating. 120 hours at 450° led to the coking of the starting material.

Fig. 1 shows the total volume of gases evolved from mixtures pyrolyzed at various temperatures, plotted against the time of pyrolysis. It can be seen that in the first stage of pyrolysis, gas evolution changes linearly with the duration of the heating. The rate of gas evolution was calculated from the linear sections of the curves (*cf.* Table II).

Table II

Rates of gas and polymer formation in the pyrolyzed mixture

Temperature °C	Quantity of gas formed ml/g per hour	Quantity of polymers formed % by wt. per hour
350	0.004	0.008
370	0.007	0.015
400	0.026	0.048
425	0.092	0.20
450	0.40	0.90
470	1.06	2.6

The analysis of the gaseous products showed that at 400 and 425° mainly hydrogen and methane, and only 2 to 4% of C_2—C_4 hydrocarbons were formed. In the initial stage of pyrolysis round 90% of the gaseous products was hydrogen, however, the relative hydrogen content decreased to 50% on heating for 200 hours. Accordingly, the ratio of hydrocarbons rose from 10 to 50%. When on pyrolysis at 450 or 470°, the hydrogen content of 80% observed after 5 hours of heating, decreased to 20% in a relatively short time. About 50 to 55% of the hydrocarbons consisted of methane. The changes in the composition of the gaseous product during pyrolysis at 450° are shown in Fig. 2.

Other detected decomposition products, having molecular weights lower than those of the initial products, were benzene and toluene. The amount of these hydrocarbons rose with increasing pyrolysis temperatures.

The polymer content of samples pyrolyzed at various temperatures showed in the initial section an approximately linear change with the period of heating (*cf.* Fig. 3). The data in Fig. 3 indicate that the error of determination is greater if the polymer content is low; as to be expected for the experimental method

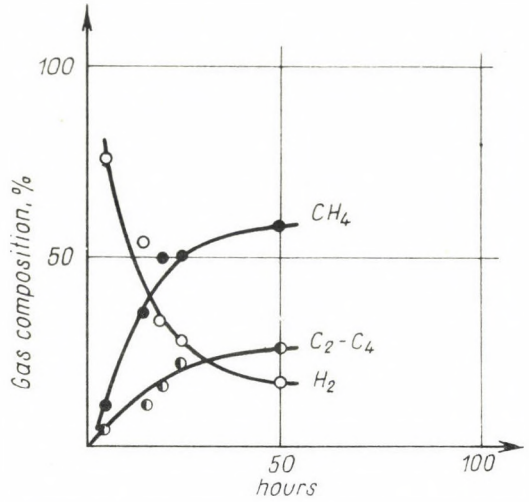

Fig. 2. Composition of the gaseous product of pyrolysis at 450°C

applied. The rates of polymer formation listed in Table II were obtained by graphical calculation from the diagrams given in Fig. 3.

The values of the mean molecular weights of the polymers (Table III) show that up to 425° the mean molecular weights increase with the time of heating. The molecular weights of samples heated to 450 and 470° could be

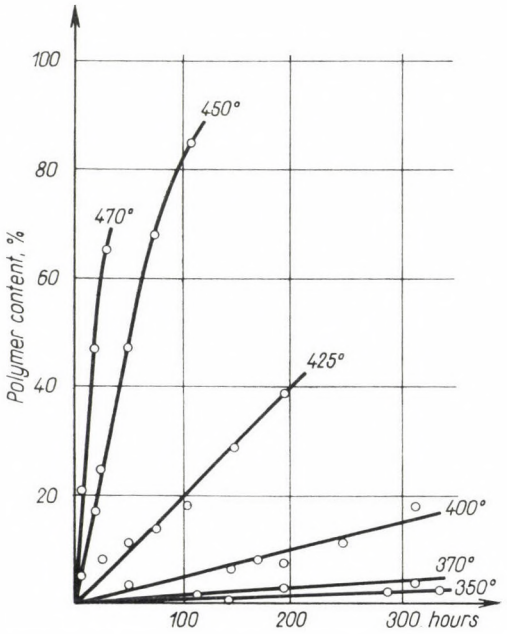

Fig. 3. Polymer formation at various temperatures

determined for very short periods of pyrolysis only owing to considerable charring.

Table III

Mean molecular weights of polymers

Time of pyrolysis hrs	Polymer content %	Mean molecular weight of polymers at various pyrolysis temperatures				
		350	400	425	450	470°C
285	2.06	282				
144	6.05		317			
313	18.0		326			
49	11.3			316		
146	28.8			392		
19	17.5				341	
5	20.9					367

Discussion

In Fig. 4 the logarithmic values of the rates of formation of the gaseous and polymeric products plotted versus the reciprocal values of absolute temperature are shown. It is seen that the dependence of the rate of pyrolytic decomposition on temperature can be described in fair approximation by the Arrhenius equation.

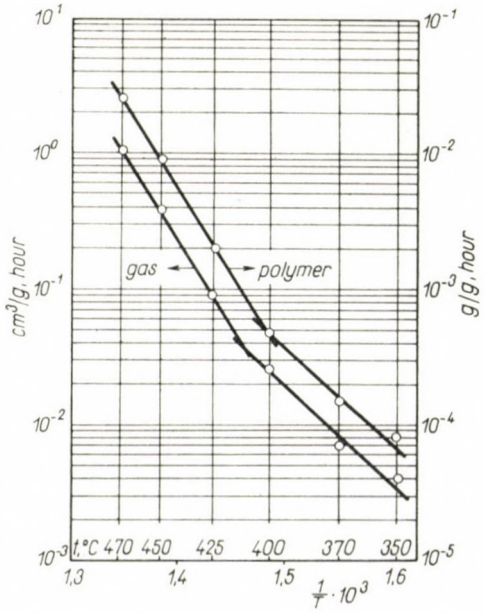

Fig. 4. The rates of gas and polymer formation plotted against the temperature of pyrolysis

The overall activation energy of both gas evolution and polymer formation processes shows a sudden change above $\sim 400°$. The activation energies of the process below and above this temperature, as calculated on the basis of the data in Fig. 4 are given in Table IV.

Table IV

Activation energies of the processes of gas and polymer formation

Temperature °C	Activation energy, kcal/mole	
	Gas formation	Polymer formation
below about 400°	35 ± 2	33 ± 2
above about 400°	56 ± 2	59 ± 2

This sudden increase in the activation energy indicates the thermal cracking of the mixture to begin presumably at the temperature of this change of energy.

A chain reaction below 400° is improbable because, according to Semionov's theory [9], one of the prerequisites of a chain reaction is:

$$E = \varepsilon + \frac{Q}{2}$$

where E is the overall activation energy of the process determined experimentally, Q the energy of chain initiation, and ε the activation energy of the slowest step of the chain reaction.

In the components of the D—DM mixture, the bond between the phenyl and benzyl radicals [$C_6H_5 - CH_2C_6H_5$] has the lowest binding energy: ~ 76.5 kcal/mole [10]. Even if chain initiation takes place with the rupture of this weakest bond, *i.e.* $\frac{Q}{2} = 38.2$ kcal/mole and $\varepsilon = 0$, the overall activation energy should be markedly greater than the value found in the experiments.

Comparing the activation energies of the gaseous and polymeric products formed in the thermal cracking of the D—DM mixture with data reported for other compounds, we find that the energy of activation is lower than that of diphenyl, and it approximately agrees with that of monoisopropyl- and monomethyl-diphenyl. A comparison, in turn, of the rates of polymer formation with data of literature (Table V) shows that the thermal stability of the eutectic mixture is lower by about one order of magnitude than that of diphenyl, and is of the same order of magnitude as that of monoisopropyldiphenyl and of Santowax R.

On comparing the results of pyrolysis with the data obtained from the radiolysis of the mixture, an essential difference is observed in the composition

Table V

Rates of polymer formation

Substance	g/g, hrs				References
	400	425	450	470	
Diphenyl		0.000018	0.00015	0.0006	[11]
Santowax R	0.00029	0.00067	0.0027	0.012	[12]
Mono-isopropyl diphenyl ..		0.001	0.004	0.015	[1]
D—DM	0.00048	0.002	0.009	0.026	

of the gaseous products. The radiation resistance of the mixture D—DM was examined by irradiation tests in a nuclear reactor [3]. The composition of the gases formed on irradiation at 115° plotted against the absorbed radiation doses is shown is Fig. 5. These data show that the gaseous products of radiolysis consist of $\sim 91\%$ hydrogen, $\sim 1-2\%$ methane and $\sim 7-8\%$ C_2H_n, and the ratio of the components remains practically unchanged when the doses are increased (up to about 30% polymer content). On pyrolysis, in turn, the prolonged heat treatment gives rise to marked changes in the composition of the formed gaseous products: the hydrogen content is considerably decreased (from $\sim 90\%$ to $\sim 50\%$) with

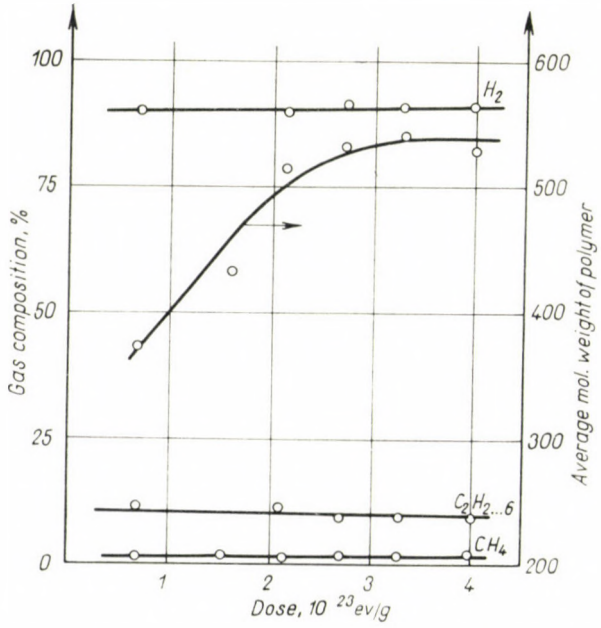

Fig. 5. Composition of the gaseous product formed during the radiolysis of the mixture D—DM and the influence of the dose on the mean molecular weight of the polymeric products

a corresponding increase of the ratio of hydrocarbons. The hydrocarbons formed at 400—425° consist almost exclusively of methane, and appreciable amounts of C_2H_n—C_4H_n appear only at higher temperatures.

Since the gaseous product of a pyrolysis performed at lower temperature consists mainly of hydrogen and methane, it may be presumed that at 400—425° the gas products are formed mainly by the rupture of C—H and C_6H_5—CH_2—C_6H_5 bonds, and the rupture of the strong C—C bonds in the aromatic ring takes place at higher temperatures only. It is known from literature [13] that probability of the rupture of an aromatic ring is higher on irradiation than in the case of low-temperature pyrolysis.

The pyrolysis of the mixture D—DM leads to polymeric products of molecular weights lower than those afforded by radiolysis (Fig. 5). This fact indicates that the probability of formation of longer polymers on pyrolysis is much lower. This is readily understood, since radiolysis offers much more favourable conditions for polymerization, furthermore higher temperatures may cause the decomposition of polymer molecules formed previously.

The authors' thanks are expressed to Mr. K. Ujszászi for carrying out the mass spectrometric measurements.

SUMMARY

The thermal stability of the eutectic mixture of diphenyl and diphenylmethane has been investigated by determining the amount and composition of the gaseous product formed and the degree of polymerization of the initial compounds in pyrolysis reactions of 5 to 300 hours, in the temperature range between 350 and 470°C.

Thermal cracking of the mixture takes place above 400°. Consequently, the mixture may be used as a reactor coolant only below that temperature.

Comparison of the gaseous, liquid and polymeric products of pyrolysis with those obtained on irradiation clearly shows the different mechanisms of pyrolytic and radiolytic processes.

REFERENCES

1. de Halas, D. R.: Second United Nations International Conference on the Peaceful Uses of Atomic Energy P/611.
2. Boyd, A. W.: J. Nucl. Materials **9,** No. 1, 1 (1963).
3. Kiss, I., Kósa Somogyi, I., Kules, I., Schiller, R., Gróh, R., Vizesy, M.: Proc. Tihany Symposium (Akadémiai Kiadó, Budapest) 1964. p. 67;
   Kiss, I., Szabó, F.: Third United Nations International Conference on the Peaceful Uses of Atomic Energy, Genf, 1964. A/Conf. 28/P/449.
4. Kosmin, M., McEwen, M.: U. S. Pat. 2 902 425 (1959).
5. Gäumann, T., Rayoux, J. M.: Helv. Chim. Acta **45,** 1563 (1962).
6. Rainey, W. T., Yeatts, L. B.: The Third Conference on Nuclear Reactor Chemistry, Gatlinburg, Oct. 1962. TID—7641.
7. Barrera Pinero, R.: Junta de Energia Nuclear Report, 123—DQA 37 Madrid, 1963.
8. Madison, J. J., Roberts, R. M.: Ind. Eng. Chem. **50,** 237 (1928).
9. Semionov, N. N.: O nekatorykh problemakh khimicheskoi kinetiki i reaktsionnoi sposobnosti (Izdat. Akad. Nauk. SSSR, Moskva) 1958.
10. Szwarc, M.: Chem. Rev. **47,** 75 (1950).
11. De Halas, D. R.: Report HW—56 769 Hanford (USA) (1958).
12. Singer, K. A. J.: EAES Symposium on the Use of Organic Liquids as Moderators and Coolants, Rome, March 1961.
13. Swallow, A. J.: Radiation Chemistry of Organic Compounds. (Pergamon Press, London) 1960.

Über die Wärmestabilität des eutektischen Gemisches von Diphenyl und Diphenylmethan

M. RÓDER, I. OPAUSZKY und I. KISS

Zusammenfassung. Die Wärmestabilität des eutektischen Gemisches von Diphenyl und Diphenylmethan wurde durch Messung der Menge und Zusammensetzung jener Gasprodukte die auf Einwirkung einer 5—300stündigen Wärmebehandlung im Temperaturintervall 350—470°C gebildet wurden, ferner durch Ermittlung des Polymerisationsgrades der Ausgangsverbindungen untersucht.

Es wurde dabei festgestellt, daß der Wärmeabbau des Gemisches über 400°C stattfindet. So kann das Gemisch nur unter dieser Temperatur als Reaktorkühlstoff verwendet werden.

Ein Vergleich der pyrolytischen gasförmigen, flüssigen und Polymerprodukte mit den auf Einwirkung von Bestrahlung gebildeten Produkten wies auf die voneinander abweichenden Mechanismen der pyrolytischen und radiolytischen Vorgänge hin.

Термическая стабильность эвтектической смеси дифенила с дифенилметаном

М. РОДЕР, И. ОПАУСКИ и И. КИШ

Резюме. На основе количества и состава газовых продуктов, образованных при 5—300-часовой термической обработке в интервале температур: 350—470° С, а также на основе степени полимеризации исходных соединений была исследована термическая стабильность эвтектической смеси дифенил-дифенилметан.

Было установлено, что термический крекинг смеси наступает выше 400° С; поэтому ее можно использовать в качестве теплоносителя реактора лишь ниже этой температуры.

На основе сравнения газообразных, жидких и полимерных продуктов пиролиза с продуктами, образующимися под влиянием облучения, можно показать различие между механизмами процессов пиролиза и радиолиза.

Miss Magda Róder
István Opauszky
Dr. István Kiss
} Budapest XII. Konkoly Thege út

SURFACE TENSION STUDIES OF SOME BINARY SYSTEMS

PYRIDINE AND ACETIC ACID

(SHORT COMMUNICATION)

K. M. S. SUNDARAM

(Department of Chemistry, University of Ghana, Legon, Ghana)

Received June 10, 1965

Introduction

Various physico-chemical studies of the system pyridine—acetic acid have been reported, such as electrical conductance [1—5], viscosity [6—9], density [10], boiling point determinations [11—13], freezing point depression [14, 15], heat of mixing [16], vapour pressure [17], compressibility [18], Raman effect [19—22], light scattering [23], electric polarization [24, 25], magnetic susceptibility [23, 26], NMR [27—29], infrared spectra [30], and X-ray diffraction [31] measurements. The overall conclusions presented to explain the singularities observed in the property—concentration relationship have been either compound formation or the maximum ionization of the acid at a particular composition of the mixture. During the course of a study of various physical and thermodynamical properties of nonaqueous organic acid—base systems, it has been considered desirable to measure the surface tension of acetic acid—pyridine mixtures of varying mole fractions not only due to the paucity of such data but also to critically examine and draw suitable conclusions to substantiate either of the two explanations offered so far.

Experimental

Materials

B. D. H. "AnalaR" samples of pyridine (b. p. $_{760\ \mathrm{Torr}}$ 115.6°, n_D^{25} 1.5067 and d_4^{25} 0.9782) and glacial acetic acid (b. p. $_{760\ \mathrm{Torr}}$ 118.5°, n_D^{25} 1.3698 and d_4^{25} 1.0436) were purified by fractional distillation in an all-glass apparatus. The physical constants of the reagents used conformed to those found in the literature [32, 33].

Measurements and results

Mixtures of different compositions (of about 25 ml volume) were prepared by weighing and transferring the required amounts of pyridine and acetic acid in glass stoppered pyrex flasks, and the mole % composition was calculated from the weights of the individual components and their respective molecular weights.

Surface tension measurements were carried out in a thermostat at 25° ± 0.05°C using capillary height apparatus similar to that of HARKINS and JORDAN [34], and the values were calculated using the equation given in the literature [35] after applying the necessary correction for variation in the diameter of the capillary tube. The measurements were repeated several times with each mixture to get concordant values. In all cases the maximum error in the surface tension values of the system reported herein was within ±0.03%.

Density determinations were carried out at 25° ± 0.05°C using a pyknometer with stoppers on either side of the arms to minimize the error due to evaporation. In calculating the density of the mixtures, correction for the buoyancy of the air was taken into consideration. Results are recorded in Table I and in Fig. 1.

Discussion

Most of the physico-chemical studies of the system pyridine—acetic acid have shown that a singularity is observed at 84 mole % of acid, although some workers [19, 23] expressed disagreement with this conclusion, and suggested that particular behaviour is found at 60 and 40 mole % acid concentration,

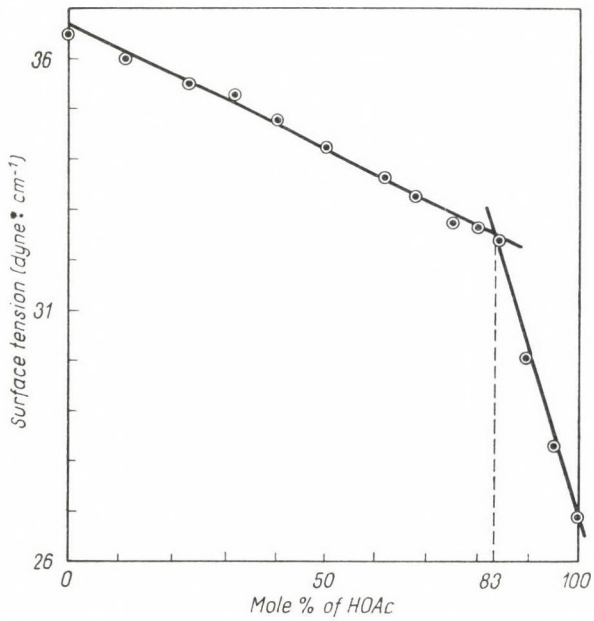

Fig. 1

respectively. The present surface tension measurements of this system do not reveal any notable change at 40 or 60 mole % acid. Many earlier workers interpreted the singularity noted at 83 mole % of acid as being due to complex formation between the organic acid and the weak base, though the mechanism of such complex formation and the intermolecular bonds involved have remained obscure. VENKATESAN and SURYANARAYANA [5], though they observed a maximum in the property—concentration curve at 83 mole % of acid, ascribed this to the maximum ionization of acetic acid. This concept is rather pertinent for our present discussion.

From conductivity studies of organic acids in pyridine, HANTZSCH and CALDWELL [36] concluded that in pyridine these substances form pyridinium

salts of the formula $C_5H_5NH^+$, X^-; this view is corroborated by the Raman spectra [37] of various heterocyclic bases in aliphatic acids.

The electron density of the nitrogen atom in the pyridine ring calculated by the M. O. method is found to be 1.633, therefore LONGUET-HIGGINS and COULSON [38] argue that the nitrogen atom will show strong affinity towards cations, especially protons. Similar views are expressed by IWAIZUMI [39]. FREYMANN *et al.* [28] explained the low field shift of the NMR spectra of pyridine — acetic acid mixtures at high acid concentrations as due to the dissociation of the complex formed with the two components. The two extra p electrons of the nitrogen atom in pyridine readily coordinate with a proton to form pyridinium ion, thus stabilizing the heteropolar resonance structures of the acceptor molecule. Following the reasoning of VENKATESAN and SURYANARAYANA [5], addition of pyridine to acetic acid causes the latter to ionize more and at low concentrations of the base, giving rise to acetic ions, pyridinium ions and some free hydrogen ions, the concentration of which diminishes with increasing concentration of pyridine; it is understandable that beyond 50 mole % pyridine, no free hydrogen ions can possibly exist. At least 17 mole % of pyridine has been shown to be necessary for complete ionization of acetic acid in pyridine. It is pointed out [5] that owing to this maximum ionization, various physical properties such as conductance, viscosity, density, refractive index, volume concentration, etc. exhibit a maximum at a composition of 83 mole % of acetic acid.

Table I

% by weight of acetic acid	Mole % of acetic acid	Density	Surface tension, dynes · cm^{-1}
	0	0.9782	36.50
8.45	0.184	0.9858	36.02
18.39	22.89	0.9963	35.49
24.68	30.15	1.0031	35.27
33.05	39.40	1.0129	34.80
42.62	49.45	1.0250	34.25
55.56	62.22	1.0440	33.63
61.94	68.19	1.0541	33.25
69.54	75.05	1.0653	32.73
75.18	80.00	1.0721	32.64
79.31	83.47	1.0750	32.46
86.62	89.51	1.0742	30.06
93.45	94.94	1.0631	28.29
	100	1.0436	26.88

In Table I the density and surface tension data of the system pyridine—acetic acid are recorded. A plot of the surface tension against the mole % composition (not reproduced here) shows that the linearly decreasing values have an abrupt break at the percentage composition of 83 mole % of acetic acid. This is presumably due to stronger attraction between solvent molecules and ionic species present in the system at that composition. The force of attraction between an ion and a dipole having the most favourable orientation is very strong, especially in systems of low dielectric constant. GURNEY [40] has stated that in any ionic co-sphere molecular dipoles which have a favourable orientation will be attracted, while those that have the opposite orientation will be repelled. Since the former are more numerous, the solvent in the co-sphere is attracted strongly toward the ion which may perhaps be responsible for the deviation from linearity at 83 mole % of acid in the surface tension-composition curve. Beyond this point, co-sphere-ion attraction diminishes due to the scarceness of ions; consequently, the surface tension depends here on the mole fraction and hence the curve is perfectly linear.

SUMMARY

Surface tension measurements of mixtures of pyridine and acetic acid at different compositions have shown that this property has a maximum at a composition of 83 mole % of acetic acid. The observed singularity is attributed to maximum ionization of acetic acid, and not to complex formation as suggested by many earlier workers.

REFERENCES

1. SACKHANOV, A. N.: J. Russ. Phys. Chem. Soc. **43,** 526 (1912).
2. TRIFONOV, N. A., CHERBOV, S. I.: Bull. inst. recherches biol. univ. Perm (Russia) **6,** 313 (1929).
3. SWEARINGEN, L., ROSS, R. F.: J. Phys. Chem. **38,** 395 (1934).
4. NAUMOVA, A. S.: Zhur. Obshchei Khim. **2,** 1222 (1949).
5. VENKATESAN, V. K., SURYANARAYANA, C. V.: J. Phys. Chem. **60,** 777 (1956).
6. TSAKALOTOS, D. E.: Bull. Soc. Chim. **3,** 235 (1908).
7. DUNSTAN, A. E., THOLE, F. B.: J. Chem. Soc. **95,** 1556 (1909).
8. SWEARINGEN, L., HECK, N.: J. Phys. Chem. **38,** 395 (1934).
9. FAUST, O.: Z. physik. Chem. **79,** 97 (1911).
10. TSAKALOTOS, D. E.: Bull. soc. chim. France **3,** 134 (1908).
11. ANDRÉ, M. G.: Compt. rend. **125,** 1187 (1897).
12. ANDRÉ, M. G.: Compt. rend. **126,** 1105 (1898).
13. GARDNER, J. A.: Ber. **23,** 1587 (1890).
14. SWEARINGEN, L., ROSS, R. F.: J. Phys. Chem. **38,** 1141 (1934).
15. PUSHIN, N. A., RIKOVSKII, I. I.: Z. physik. Chem. **161,** 336 (1932).
16. PUSHIN, N. A., FEDJUSHKIN, A. V., KROGVIE, B.: Bull. soc. chim. Belg. **11,** (No. 1—2) 12 (1940—46).
17. ZAWIDZKI, N.: Z. physik. Chem. **35,** 129 (1900).
18. BALACHANDRAN, N.: J. Indian Inst. Sci. **36,** 10 (1954).
19. MIERZECKI, R.: Acta Phys. Polon. **11,** 329 (1953); **19,** 41 (1960).
20. MIERZECKI, R.: Byull. Pol'sk. Akad. Nauk Otdel. **3,** 255 (1955); Current Sci. (India) **25,** 200 (1956).
21. LAKSHMANAN, B. R.: J. Indian Inst. Sci. **36,** 97 (1954).
22. SCHWAB, G. M., GLATZER, N.: Z. Elektrochem. **61,** 1028 (1957).
23. VENKATARAMAN, R.: J. Indian Chem. Soc. **17,** 297 (1940).

24. Hurwic, Michalezik, Pogorzeska: Roczniki Chem. **31,** 265 (1957).
25. Abgrall, Barre: Compt. rend. **253,** 439 (1961).
26. Deshpande, V. T., Pathki, K. G.: Trans. Faraday Soc. **58,** 2134 (1962).
27. Shimizu, N.: Nippon Kagaku Zasshi **81,** 1025 (1960).
28. Freymann, R., Freymann, M., Koechlin, M., Martin, M., Marvel, M. G.: Arch. Sci. (Geneva) **12,** 207 (1959).
29. Shimizu, H., Fujiwara, S.: Chem. Pharm. Bull. (Tokyo) **8,** 272 (1960).
30. Hadzi, D.: Vestnik Sloven. Kemi. drustva **5,** 21 (1958).
31. Lakshmanan, B. R.: Proc. Indian Acad. Soc. **43A,** 152 (1956).
32. Timmermans: Physico-Chemical Constants (Elsevier Book Co. Inc., New York) 1950.
33. Weissberger, Proskauer (editors): Organic Solvents (Interscience Publisher, Inc., New York) 1955.
34. Harkins, Jordan: J. Am. Chem. Soc. **52,** 1751 (1930).
35. Weissberger (editor): Physical Methods of Organic Chemistry, 2nd ed., Vol. I., Part I (Interscience Publishers, Inc., New York) 1949.
36. Hantzsch, Caldwell: Z. physik. Chem. **61,** 227 (1908).
37. Chiorboli, Bertoluzza: Ann. Chim. (Rome) **49,** 245 (1958).
38. Longuet-Higgins, Coulson: Trans. Faraday Soc. **43,** 87 (1947).
39. Iwaizumi, M.: Nippon Kagaku Zasshi **82,** 306 (1961).
40. Gurney, R. W.: Ionic Processes in Solution (McGraw-Hill Book Co., New York, N. Y.) 1935, p. 186.

Dr. K. M. S. Sundaram: University of Ghana, Legon, Accra, Ghana, Africa.

CALCULATION OF FORCE FIELD ON ETHYLENE MODEL

S. Szőke and T. Faragó

(Central Research Institute for Chemistry of the Hungarian Academy of Sciences, Budapest)

Received July 22, 1965

As the potential energy equation for polyatomic molecules cannot be given exactly and directly, we have to apply the indirect method of constructing convenient expressions derived from vibrational frequencies, *i.e.* from experimental data. The potential energy depends on the atomic and electronic arrangements, therefore it is advisable to make a coordinate analysis so as to find the existing analogies between force fields of molecules having similar electronic and atomic structures.

Because of the widely adopted calculation techniques, a great number of force-field parameter sets can satisfy the basic equations used for proper value determination. Among this great number of parameter sets a judicious choice can be made only by correlating them to a general physical picture.

In working out methods for coordinate analysis, an important part is played by the use of molecular models, such as ethylene, methane, or benzene. For quantum chemists, ethylene is one of the most thoroughly studied molecules. It was chosen as the model of the present study by reason of its following features:

(a) it has a simple geometry consisting of relatively few atoms, and its molecular properties are known with sufficient accuracy;

(b) the available assignments of the vibration and rotation frequencies of the basic as well as of the partly and totally deuterated molecules can be accepted as competent, offering thus a great variety of experimental data for constructing force-field equations. From the point of view of both the General Valence (GVFF) and the Urey-Brandley Force Field (UBFF) methods, it is of outstanding importance that simple interaction equations can be set up, owing to the fact that the molecule possesses almost exceedingly CH stretching coordinates;

(c) the regular arrangement of the basic compounds has a high degree of symmetry, thus allowing the set-up of its potential equation by means of relatively few force constants. Nearly all of the 15 in-plane vibration force constants of the basic molecule belonging to the V_h point group can be computed by methods which may be considered exact, using data of the basic and perdeuterated ethylene molecules only.

Several authors have treated the problem of assignment [1—9]. Their results agree well except the case of one of the CH stretching vibrations. To the B_{1g} CH stretching, a frequency of 3272 cm^{-1} has been assigned by WU [10] as well as by CRAWFORD and co-workers [7], while PLYLER [4] suggested 3075 cm^{-1} as the most probable value for this vibration. Recently CYVIN and CYVIN [9] found 3102.5 cm^{-1}.

The assignment is considerably advanced by additional information afforded by isotope rules and polarized Raman spectra.

Dealing with the potential functions of these molecules, the GVFF and SVFF (Single Valence Force Field) methods have been applied by the majority of authors. The main feature of these methods consists in the use of a coordinate system based on bond parameters and principles of group theory.

The Urey-Bradley (UBFF) method [11] has been used by SCHERER and OVEREND [12]. They take into account also the repulsion forces acting between nonneighbouring atoms. Since there is no difficulty in finding correlation between the two theories, we based our calculations on the simpler SVFF method.

Problem of anharmonicity

The question whether frequency data have to be transformed as a consequence of their anharmonicity or not, is open to discussion even today. Extreme views are represented in this respect by CRAWFORD and co-workers [3, 7]. They use anharmonicity coefficients arising from data for CH and CD stretching vibrations for computing harmonic frequencies. The greatest drawback of their method is that force constants obtained in this way deviate very strongly from the conventional ones.

Soviet authors have attempted to approach the influence of anharmonicity by introducing the concept of "spectroscopic mass". This solution was suggested by HEMPTINNE and MANNEBACK [12a], and employed in works of STEPANOV [13], KOVNER [14], SVERDLOV and PAKHOMOVA [5], and RYTEL [15].

Although in extreme cases harmonic frequencies may differ by 10% from anharmonic (experimental) ones [16], the corresponding eigenvalues do not deviate by more than 5%; this may be the reason why the great majority of authors do not use any corrections [17]. This reasoning has been accepted in our present paper, too.

Physical interpretation of the force constants

The physical interpretation of the force constants has not been solved in the coordinate analysis so far; in the case of the stretching force constants, the empirically obtained potential functions of diatomic molecules can be used as approximations [18], and attempts have also been made to interpret

the deformation force constants of simple polyatomic molecules [19]. However, no significant methods are available for interpreting the interaction terms.

As a physical interpretation we mean that the basis of the calculation should be some empirical value, *i.e.* measured data of physico-chemical parameters, such as bond distance, dissociation energy, ionization potential, electronegativity, etc.

Our method allows the calculations of force constants owing to the fact that the equations of motion are connected with the valence theory through the internal coordinates.

While kinetic energy depends on the velocity of a moving mass, the potential energy is determined by the position occupied by the atoms and electrons. The potential energy constants may be expressed in coordinates of bond distance changes and bond angle deformations.

Potential energy equation of the ethylene molecule

The general form of a quadratic potential energy equation is:

$$U = \frac{1}{2} \sum_{i,j} k_{ij} \Delta r_i \Delta r_j + \frac{1}{2} \sum_{i,j} h_{ij} \Delta \alpha_i \Delta \alpha_j + \sum_{i,j} l_{ij} \Delta r_i \Delta \alpha_j$$

where Δr_i is the increase of interatomic distances, $\Delta \alpha_i$ denotes angle deformations, while the coefficients k_{ij}, h_{ij} and l_{ij} are the corresponding force constants. The value for the inner coordinates [20] can be given as follows:

r(CH) = 1.086 Å
r(CC) = 1.339 Å
HCH$\sphericalangle$ = 115°
HCC$\sphericalangle$ = 122.5°

In our calculations we assumed that the values of r(CH) and r(CD) are equal; 120° was used as the value of the valence angles. These neglections cause only insignificant alterations in the force field parameters.

In the potential energy equation there are four C—H and one C—C stretching vibrations, thus we have four deformation constants in addition to six interaction factors. The same basic constants were used with slight modifications in our calculations. We have dealt with in-plane vibrations only, for in the out-of-plane representations of the ethylene molecule the number of normal coordinates is zero or one.

To simplify the construction of the secular equation, the change of the bisectrices of the angles HCC are used as internal coordinates based on the well-known equation [21]:

$$\beta = \frac{1}{2}(\varphi_1 - \varphi_2) \tag{2}$$

Constants of the potential—energy equation

Ethylene and deuteroethylene belong to the pointgroup V_h, while dideuterated molecules to the groups C_{2v} and C_{2h}, respectively. In the symmetry group V_h, the nine in-plane vibrations can be reduced to one three-dimensional and three two-dimensional representations.

The independent force constant matrix components are:

(a) diagonal elements:

$$F_s^1,\ F_s^2,\ F_s^3,\ F_s^4,\ F_t,\quad F_a^1,\ F_a^2,\ F_\beta^1,\ F_\beta^2$$

(b) out-of-diagonal elements:

$$F_{st},\ F_{s\alpha}^1,\ F_{s\alpha}^2,\ F_{s\beta}^1,\ F_{s\beta}^2,\ F_{t\alpha}$$

In the first approximation, F_s^2, F_s^3 and $F_{s\alpha}^2$ can be taken as zero. (It is more convenient to obtain the exact values of the components of F_s not directly from the secular equations, but rather by the Jacobi approximation, in the course of a further force-constant refinement.) Thus, the force-constant components combine in their different representations in the following manner:

$$A_{1g}: F_s^1,\ F_t,\ (F_a^1 + F_a^2),\ F_{st},\ F_{s\alpha}^1,\ F_{t\alpha}$$
$$B_{1g}: F_s^1,\ (F_\beta^1 - F_\beta^2),\ (F_{s\beta}^1 - F_{s\beta}^2)$$
$$B_{2u}: F_s^1,\ (F_\beta^1 + F_\beta^2),\ (F_{s\beta}^1 + F_{s\beta}^2)$$
$$B_{3u}: F_s^1,\ (F_a^1,\ - F_a^2,\ F_{s\alpha}^1)$$

On the basis of the characteristic equation, the eleven force constant components can be found by starting from the following type of equation:

for species A_{1g} : 2 trace, 2 secondary minor, 1 tertiary minor equation
,, ,, B_{1g} : 2 ,, 1 determinant equation
,, ,, B_{2u} : 2 ,, 1 ,, ,,
,, ,, B_{3u} : 2 ,, 1 ,, ,,

Now let us write the secular equation in the following form:

$$\begin{vmatrix} H_{11}-\lambda & H_{12} & \dots & H_{1n} \\ H_{21} & H_{22}-\lambda & \dots & H_{2n} \\ \vdots & & & \\ H_{n1} & H_{n2} & \dots & H_{nn}-\lambda \end{vmatrix} = 0 \tag{3}$$

On the basis of the approximate equations set up from minors

$$\begin{vmatrix} H_{ii} & H_{ij} \\ H_{ji} & H_{jj} \end{vmatrix} = \lambda_i \lambda_j \tag{4}$$

and

$$\begin{vmatrix} H_{ii} & H_{ij} & H_{ik} \\ H_{ji} & H_{jj} & H_{jk} \\ H_{ki} & H_{kj} & H_{kk} \end{vmatrix} = \lambda_i \lambda_j \lambda_k \tag{5}$$

respectively, in addition to the equations derived from the basic molecule, the missing number of approximate equations might be obtained from the data of the deuterated derivatives. (It is convenient to construct approximate equations, in which the eigenvalues differ significantly from each other.) The resulting equations may be solved by one of the known approximate methods. We applied the method of least squares [22]. In favour of the existence of an analogy prevailing between the bonds of the ethylene molecule and of the corresponding C_2 and CH diatomic molecules, the following arguments might be advanced:

1. The bond distances in diatomic C_2 and CH molecules are 1.312 and 1.20 Å, respectively [9], whereas in ethylene the accepted bond distance values, C=C and C—H, are 1.339 Å and 1.086 Å, respectively.

2. The dissociation energy of the C_2 molecule is taken as 137 kcal [23], and the CH bond dissociation energy as 83.6 kcal (in the diatomic molecule). The analogous values in ethylene are 125 kcal and 102 kcal, respectively.

3. According to COTTRELL [16], the anharmonic force constant of the C_2 molecule is $9.25 \cdot 10^5$ dyn $\cdot$ cm^{-1}. This corresponds to $4.090 \cdot 10^5$ dyn $\cdot$ cm^{-1} in the CH molecule.

The near equality of parameters to those of the C=C bond suggests a C=C stretching force constant nearly equal in C_2 and in ethylene. The circumstance that the C—H distance is smaller in ethylene suggests a higher CH stretching force constant, the difference being approximately 15%. The greater difference in the dissociation energies of the CH bonds supports this supposition.

Assumptions for the potential terms

In order to obtain the sufficient number of equations for our approximate method, the secular equations of the deuterated molecules must be set up, too. Representations A_1 and B_1 of the point groups C_{2v} and C_{2h} are five and four-dimensional, respectively, each containing two representations of the point group V_h. In general, it is not necessary to determine all the 15 force constants in the five-dimensional, or the 10 in the four-dimensional F matrix. It is suf-

ficient to link the subgroups of point group V_h with one or two interaction constants [24]. Thus the forms of the G and F matrices will not differ essentially from those of the diagonal supermatrices of ethylene.

The kind of potential energy coefficients which will appear in the secular equation cannot be automatically deduced for every molecule. In each case it is a matter of careful consideration which of the constants may be taken as zero, and to what extent neglections seem justifiable. In a zero order approximation it is more convenient to construct the potential equations with regard to the deviations of the eigenvalues from the value of the leading diagonal matrix elements.

For the determination of the perturbation terms, the representations of both point groups, C_{2v} and C_{2h}, are taken in a zero order approximation, with no interaction between the two diagonal supermatrices:

$$\begin{vmatrix} H_{11} & H_{12} & & 0 \\ H_{21} & H_{22} & & \\ & & H_{33} & H_{34} \\ 0 & & H_{43} & H_{44} \end{vmatrix}$$

Then we may look for any divergence existing between the experimental eigenvalues and the eigenvalues of the diagonal supermatrix of the above form.

It is a postulate resulting from the invariance of the trace sum that if one of the diagonal members is diminished, another one ought to be correspondingly increased. If correction is taken on the H_{ii} and H_{jj} values, the corresponding values of the interaction terms H_{ij} and H_{ji} may be estimated according to the relation:

$$\pm \Delta = \frac{H_{ij}\, H_{ji}}{H_{ii} - H_{jj}} \tag{6}$$

The modifying equation is reminiscent of the diagonal approximation process of matrices [13]. The subsequent approximation can also be used:

$$\pm \Delta = \frac{H_{ij} - H_{ji}}{H_{ii} - \lambda_j} \tag{7}$$

Table I lists the force constants calculated by us. Tables II and IIa contain the experimental frequency values obtained on the basis of Plyler's assignments, and those resulting from our own calculations.

Table I

F. 10^5 dyn/cm	
$F_s = 5.1$	$F_{st} = -0.112$
$F_t = 8.84$	$F_{s\alpha} = 0.34$
$F_\alpha^1 = 0.595$	$F_{t\alpha} = -0.3$
$F_\alpha^2 = 0.025$	$F_{s\beta}^1 = 0.9$
$F_\beta^1 = 1.15$	$F_{s\beta}^2 = 0.5$
$F_\beta^2 = 0.025$	

Table IIa

Frequencies of ethylene-d_2 (1,1)

$\omega_{calc.}(cm^{-1})$	$\omega_{obs}(cm^{-1})$
3000	3019
1599	1579
1016	1032
2180	2228
1391	1384
2327	2326
1129	1150
3102	3095
673	700

Table II

Frequencies of ethylene

$\omega_{calc.}(cm^{-1})$	$\omega_{obs}(cm^{-1})$
3007	3019
1653	1623
1308	1342
3077	3075
1230	1236
3127	3105
839	810
2987	2990
1439	1444

Calculation of the vibrational modes

If the force constants are known, it is relatively easy to calculate the vibrational modes. The eigenvectors are obtained by the equation

$$| GF - E\lambda | X = 0 \tag{8}$$

in symmetry coordinates. The knowledge of the eigenvectors in Cartesian coordinates might often be of interest. The relationship between symmetry and Cartesian coordinate systems is usually described by the following equations [17]:

$$R = B\,x \tag{9}$$

where R denotes the inner coordinate, x = Cartesian coordinate, and B = a transformation matrix; further,

$$S = U\,R \tag{10}$$

where S = symmetry coordinate, and U = transformation matrix;

$$S = L\,Q \tag{11}$$

where Q = normal coordinate, and L = the transformation matrix;

$$G = L'\,L'^{T} \tag{12}$$

where G = the matrix constructed of inverse constants from the expression for the kinetic energy, while

$$L' = U^{T}\,L \tag{13}$$

where the superscription T denotes the transpose of the original matrix [17].

Let us take by definition

$$A\,B = 1 \tag{14}$$

then the following expression is readily derived:

$$A^{T}\,M\,A = G^{-1} \tag{15}$$

where M is the diagonal matrix formed from the atomic masses. As it follows from correlations (9), (10), (11), (12), (13), (14), and (15):

$$x = M^{-1} B^T U^T (L^T)^{-1} Q \tag{16}$$

The $(L^T)^{-1}$ matrix obtained for ethylene in symmetry coordinates as the result of our calculations is given in Table III. The corresponding Cartesian coordinates are shown in Table IV. The vector model of the vibrational modes may be seen in Fig. 1.

Table III

$(L^T)^{-1}$

1.0	0.089	−0.360	0	0	0	0	0	0
−0.187	1.0	−3.524	0	0	0	0	0	0
0.075	0.235	1.0	0	0	0	0	0	0
0	0	0	1,0	0.156	0	0	0	0
0	0	0	0,045	1.0	0	0	0	0
0	0	0	0	0	1.0	−0.089	0	0
0	0	0	0	0	0.288	1.0	0	0
0	0	0	0	0	0	0	1.0	−0.059
0	0	0	0	0	0	0	0.075	1.0

Table IV

−0.290	−0.154	−0.474	−0.261	−0.320	−0.167	0.303	−0.290	−0.548
0.406	−0.038	−0.480	0.422	−0.096	0.477	0.125	0.406	−0.350
0	0	0	0	0	0	0	0	0
−0.290	−0.154	−0.474	0.261	0.320	0.167	−0.303	−0.290	−0.548
−0.406	0.038	0.480	0.422	−0.096	0.477	0.125	−0.406	0.350
0	0	0	0	0	0	0	0	0
0.290	0.154	0.474	−0.261	−0.320	0.167	−0.303	−0.290	−0.548
0.406	−0.038	−0.480	−0.422	0.096	0.477	0.125	−0.406	0.350
0	0	0	0	0	0	0	0	0
0.290	0.154	0.474	0.261	0.320	−0 167	0.303	−0.290	−0.548
−0.406	0.038	0.480	−0.422	0.096	0.477	0.125	0.406	−0.350
0	0	0	0	0	0	0	0	0
0.065	−0.057	0.371	0	0	0	0	0.049	0.092
0	0	0	−0.067	0.104	−0.080	−0.021	0	0
0	0	0	0	0	0	0	0	0
−0.065	0.057	−0.371	0	0	0	0	0.049	0.092
0	0	0	0.067	−0.104	−0.080	−0.021	0	0
0	0	0	0	0	0	0	0	0

Table V

0.9861	−0.0672	−0.0152	−0.0013	0.0593
−0.0296	0.7225	0.8300	−0.0907	1.7677
−0.0096	−0.0872	1.3398	−0.0750	0.0301
0.0061	0.0331	−0.0251	0.9996	0.0141
−0.1575	−0.1791	−0.5091	0.0402	1.7301

0.9668	0.2782	0.0239	−0.1692
−0.1416	0.9594	−0.0038	0.0435
−0.0156	−0.0015	0.9898	0.1032
−0.0427	−0.0052	−0.0978	0.9978

0

Matrix L indicates the displacements in symmetry coordinates referred to the unit change in normal coordinates. The normal coordinates may be calculated by the relation:

$$S_t = L_{tk}\, Q_k$$

For the sake of better understanding the values of the Cartesian coordinates of the vibrational modes are also given. In Tables V and VI the matrices L and X (Cartesian coordinate matrices) of dideuteroethylenes are shown; Fig. 2 represents the corresponding vibrational modes.

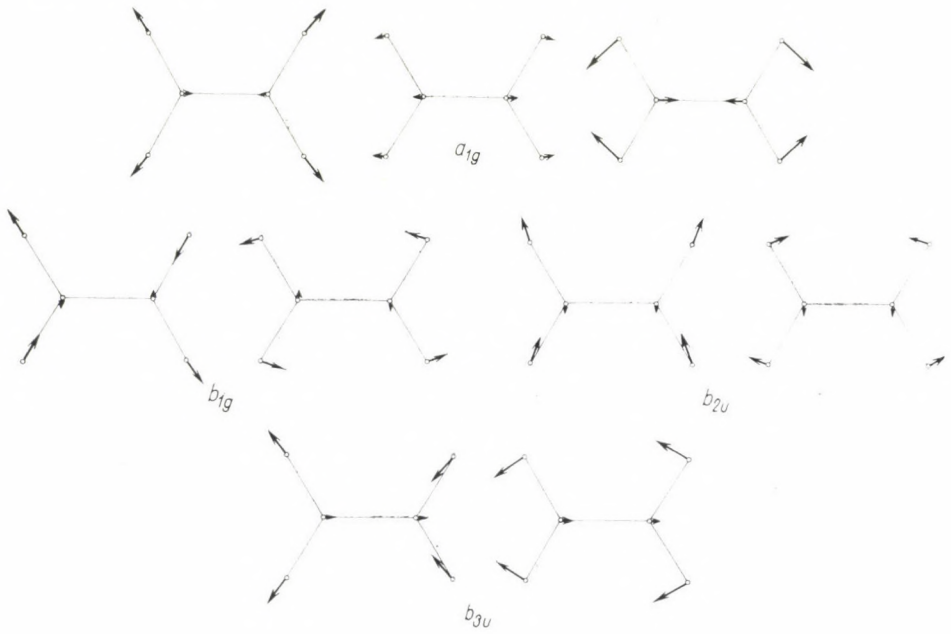

Fig. 1

Table VI

—0.354	0.027	0.564	0.046	—0.025	—0.410	—0.297	0.004	—0.057
0.605	0.064	0.276	0.031	—0.092	0.573	—0.406	—0.004	0.115
0	0	0	0	0	0	0	0	0
—0.354	0.027	0.564	0.046	—0.025	0.410	0.297	—0.004	0.057
—0.605	—0.064	—0.276	—0.031	0.092	0.573	—0.406	—0,004	0.115
0	0	0	0	0	0	0	0	0
0.031	0.057	0.027	—0.175	0.172	—0.007	0.001	0.156	—0.217
—0.016	—0.019	—0.036	—0.304	—0.110	0.008	—0.002	0.315	0.084
0	0	0	0	0	0	0	0	0
0.031	0.057	0.027	—0.175	0.172	0.007	—0.001	—0.156	0.217
0.016	0.019	0.036	0.304	0.110	0.008	—0.002	0.315	0.084
0	0	0	0	0	0	0	0	0
0.071	—0.087	—0.011	—0.012	0.087	0	0	0	0
0	0	0	0	0	—0.084	0.129	0.007	—0.041
0	0	0	0	0	0	0	0	0
—0.022	0.066	—0.092	0.063	—0.141	0	0	0	0
0	0	0	0	0	—0.015	—0.061	—0.111	—0.091
0	0	0	0	0	0	0	0	0

By substitution in the ethylene molecule, the symmetry is gradually decreased; thus the doubly deuterated molecules belong to the point groups C_{2v} and C_{2h}, respectively. Apart from the deuterated inner coordinates, there is hardly any difference between the frequencies of the basic and of the derived molecules, therefore the corresponding force constant components are transferable. But the vibrational modes of the different molecules differ considerably, giving a true picture of the symmetry conditions.

It is easily discernible from these figures that the assignment of certain normal vibrations to particular inner coordinates may be sometimes incorrect.

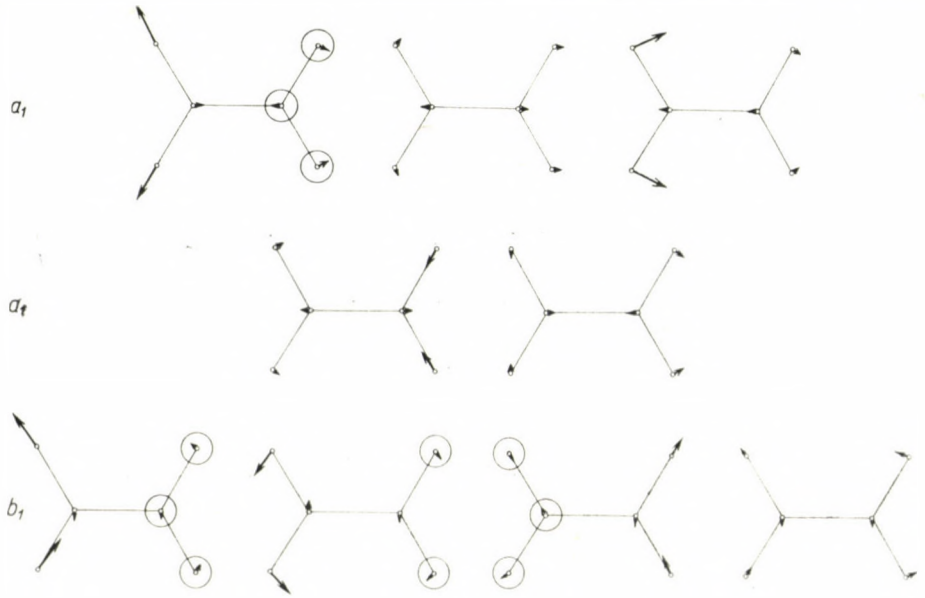

Fig. 2

Vectors designated by circles are fivefold magnified with regard to the others

It is clearly shown by the resulting vibrational modes that the use of linear combinations would be more correct in constructing the symmetrycoordinates. The correct proportions could be determined with relative ease by the method of iterative calculations.

The determination of the vibrational modes is strongly dependent on the potential assumptions, and essentially on the chosen set of force constants Thus the data reported and the assumptions are in strict correlation.

SUMMARY

The force constants of the ethylene molecule have been calculated. Fourteen equations were used to calculate 11 force constant components applying the method of least squares. In the calculation of the constants of the stretching vibrations, the force constants of diatomic molecules were used as approximative values. By this procedure the relationship of the force constants with the applied empirical data has been established.

REFERENCES

1. HERZBERG, G.: Infrared and Raman Spectra of Polyatomic Molecules (Van Nostrand, New York) 1950.
2. RANK, D. H., SHULL, E. R., AXFORD, D. W.: J. Chem. Phys. **18,** 116 (1950).
3. ARNETT, R. L., CRAWFORD, B. L.: J. Chem. Phys. **18,** 118 (1950).
4. PLYLER, E. K.: J. Chem. Phys. **19,** 658 (1954).
5. SVERDLOV, L. M., PAKHOMOVA, N. L.: Doklady Akademii Nauk SSSR **91,** 51 (1953).
6. TORKINGTON, P.: Proc. Phys. Soc. (London) A**64,** 32 (1951).
7. CRAWFORD, B. L., LANCASTER, J. E., INSKEEP, R. G.: J. Chem. Phys. **21,** 678 (1953).
8. STOICHEFF, B. P.: J. Chem. Phys. **2,** 755 (1953).
9. CYVIN, B. N., CYVIN, S. J.: Acta Chem. Scand. **17,** 1831 (1963).
10. WU, T. J.: Phys. Rev. **16,** 465 (1934).
11. SIMANOUTI, T.: J. Chem. Phys. **17,** 848 (1949).
12. SCHERER, J. R., OVEREND, J.: J. Chem. Phys. **33,** 1861 (1960).

12a. HEMPTINNE, M., MANNEBACK, G.: Proc. Ind. Acad. Sci. **9,** 286 (1939).

13. VOLKENSTEIN, M. V., JELJASHEVICH, M. A., STYEPANOV, B. I.: Kolebaniya Molekul (G. I. T. T. L., Moskva) 1949.
14. KOVNER, M. A.: Doklady Akad. Nauk SSSR **97,** 65 (1954).
15. RYTEL, M.: Acta Physica Polonica **21,** 537 (1962).
16. COTTRELL, T. L.: The strengths of chemical bonds (Butterworths Scientific Publications, London) 1954.
17. DUINKER, J. C.: Normal Coordinate Analysis of Molecules. Dissertation, Amsterdam 1964.
18. SZŐKE, S.: Acta Chim. Hung. **41,** 325 (1964).
19. PLIVA, J.: Collection Czechoslov. Chem. Communs. **23,** 777 (1958).
20. Tables of interatomic distances and configuration in molecules and ions. (The Chemical Society) 1958.
21. WILSON, E. B. JR., DECIUS, J. C., CROSS, P. C.: Molecular Vibrations. (McGraw-Hill, New York) 1955.
22. MAJANTS, L. S.: Teoriya i raschot kolebanij molekul. (I. A. N. SSSR Moskva) 1960.
23. MORTIMER, C. T.: Reaction heats and bond strengths. (Pergamon Press London) 1962.
24. MILLER, F. A., CRAWFORD, B. L.: J. Chem. Phys. **14,** 282 (1946).

Über die Berechnung des Kraftfeldes beim Äthylen als Modellverbindung

S. SZŐKE und T. FARAGÓ

Zusammenfassung. Die Kraftfeldkonstanten des Äthylenmoleküls wurden berechnet. Zur Berechnung der elf Kraftkonstantkomponenten wurden vierzehn Gleichungen herangezogen, und die Methode der kleinsten Quadrate angewendet. Bei der Berechnung der Konstanten der Valenzschwingungen wurden dagegen die Kraftkonstanten der zweiatomischen Moleküle als annähernde Werte verwendet. Durch Anwendung dieser Methode konnte der Zusammenhang der Kraftkonstanten mit den angewandten empirischen Daten festgestellt werden.

Расчет силового поля на модели этилена

Ш. СЁКЕ и Т. ФАРАГО

Резюме. Рассчитали силовые постоянные молекулы этилена. Для расчета одиннадцати компонентов силовой постоянной использовали четырнадцать уравнений и применяли метод наименьших квадратов.

С другой стороны, при расчете постоянных растянутых колебаний использовали, в качестве приближенных величин, силовые постоянные двухатомных молекул. С помощью этого способа авторам удалось установить зависимость между силовыми постоянными и прикладными эмпирическими данными.

Dr. Sándor SZŐKE
Mrs. Teréz FARAGÓ
Budapest II. Pusztaszeri út 57/69

BERECHNUNG DER KORROSIONSWIRKUNG DES KRIECHWECHSELSTROMES AUF EIN IN EINEM ELEKTROLYTEN ANGEBRACHTES METALL

(KURZMITTEILUNG)

J. DÉVAY und L. MÉSZÁROS

(Lehrstuhl für physikalische Chemie der Universität für die chemische Schwerindustrie, Veszprém)

Eingegangen am 5. August 1965

In unseren früheren Mitteilungen [1—3] wurden Berechnungen durchgeführt, um die Frage zu klären, wie die Korrosion von homogenen Metalloberflächen durch den Wechselstrom beeinflußt wird. Für den Fall, in dem die Geschwindigkeiten der auf der Oberfläche gleichzeitig stattfindenden Anoden- und Kathodenvorgänge gleicherweise durch Tafelsche Gleichungen beschrieben werden können, wird die Korrosion durch den Wechselstrom erhöht, und zwar in einem um so höheren Maße, je größer die Intensität und je geringer die Frequenz des Wechselstromes ist. Wenn dagegen der eine von den Kathoden- und Anodenvorgängen durch die Tafelsche Gleichung beschrieben werden kann, während die Geschwindigkeit des anderen Vorganges von dem Elektrodenpotential unabhängig ist, so wird die Geschwindigkeit der Korrosion durch den Wechselstrom nicht beeinflußt. Ausgehend vom obigen Ergebnis, wurde die Korrosionswirkung des Wechselstromes für den Fall berechnet, in welchem der Strom durch eine in einen Elektrolyten verlegte, unisolierte Metalleitung fließt, wobei ein Teil des Stromes aus dem Metall in den Elektrolyten austritt [4]. Die korrodierende Wirkung des Wechselstromes auf Zink- und Stahloberflächen wurde auch experimentell nachgewiesen [5—10].

Im vorliegenden Aufsatz wollen wir unsere Berechnungen mitteilen, die wir bezüglich der Korrosion durchgeführt haben, die durch einen Kriechwechselstrom auf einem, in einen Elektrolyten (Boden, Elektrolytlösung) verlegten Metallleiter hervorgerufen wird.

Die aufgeworfene Frage wurde auf eine aus Abb. 1 ersichtliche Weise modelliert. Die bezüglich der Korrosion zu untersuchende Metallplatte, deren Dicke vernachlässigt werden kann, befinde sich in der Ebene xz, bei $y = 0$. Die Metallplatte möge sich in der Richtung x ins Unendliche erstrecken, während ihre Breite in der Richtung z d betragen möge. Die Elektrolytschicht möge sich in den Richtungen x und y ins Unendliche erstrecken, während ihre Dicke in der Richtung z gleicherweise d beträgt.

Es seien in einem Abstand von der Metallplatte $+a$ bzw. $-a$ in der Richtung y zwei Elektroden angebracht, deren Längen in der Richtung z d beträgt, und deren Querschnitt ebenfalls vernachlässigt werden kann. Auf

die Elektroden soll ein Wechselstrom von der effektiven Intensität $I\sim$ geschaltet werden. Der Wechselstrom muß auch die Metallplatte durchströmen, seine Verteilung auf der Oberfläche wird jedoch nicht gleichmäßig sein (siehe die gestrichelten Kurven, die die Stromlinien versinnbildlichen). Es muß somit die Verteilung des Wechselstromes auf der Metallplatte untersucht werden, und auf Grund dieser Verteilung kann anschließend — unseren bisherigen Kenntnissen nach — die Wechselstromkorrosion der Metalloberfläche von Punkt zu Punkt bestimmt werden.

Die Aufgabe läßt sich als ein ebenes Problem behandeln. Unter Ver-

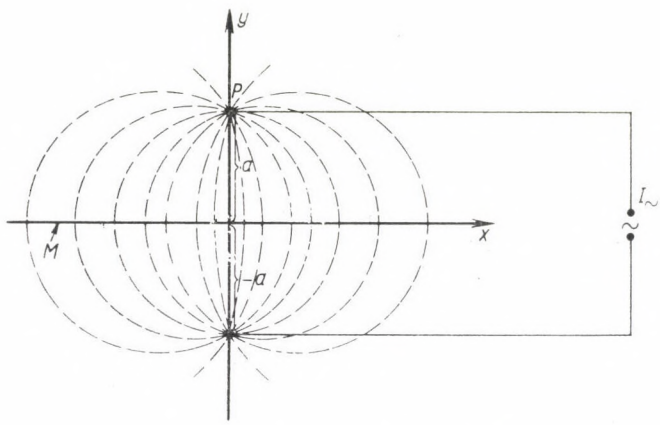

Abb. 1. Modellierung der Aufgabe

wendung der bekannten Analogie, die zwischen dem elektrostatischen Feld und dem Feld eines stationären Stroms besteht, wird die Potentialfunktion und als deren Gradient die Stromdichte bestimmt. Das entsprechende elektrostatische Problem besteht darin, das elektrische Feld einer Ladung zu bestimmen, die auf zwei parallelen geraden Leitern gleichmäßig verteilt ist [10]. Nach der wohlbekannten Lösung [10] lautet die Potentialfunktion:

$$U = \frac{1}{2} \ln \frac{x^2 + (y - a)^2}{x^2 + (y + a)^2} \tag{1}$$

Die elektrische Feldstärke E bzw. die der Feldstärke proportionale Stromdichte $i_\sim$ kann in aus der Potentialtheorie wohlbekannter Weise als Gradient der Potentialfunktion dargestellt werden:

$$i_\sim = K \operatorname{grad} U = \frac{K}{x^2 + (y - a)^2} \left[\frac{4axy}{x^2 + (y + a)^2} i - \frac{2a(x^2 - y^2 + a^2)}{x^2 + (y + a)^2} j \right], \tag{2}$$

wo i und j die in die Richtung der Achsen x bzw. y weisenden Einheitsvektoren sind, während K eine noch zu bestimmende Konstante darstellt.

Die Verteilung der Stromdichte auf der Metalloberfläche, d. h. an der Stelle $y = 0$ (da es sich um Wechselstrom handelt, wird das Vorzeichen außer Acht gelassen) ergibt sich zu

$$i_{\sim} = K \frac{2a}{x^2 + a^2} \tag{3}$$

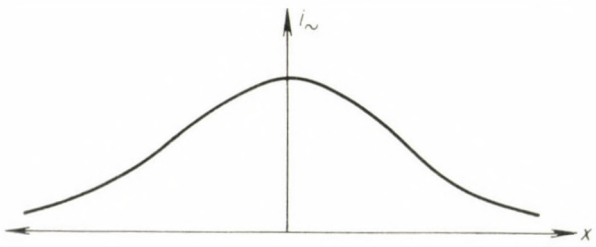

Abb. 2. Schematische Verteilung des Wechselstromes auf der Oberfläche der Metallplatte

Offenbar ergibt das Integral von $i_{\sim}$ über die ganze Oberfläche den eingespeisten Strom $I_{\sim}$, fließt doch der ganze Strom durch das Metall:

$$I_{\sim} = K\, d \int_{-\infty}^{+\infty} \frac{2a}{x^2 + a^2}\, dx = 2\, K\, d\pi\,, \tag{4}$$

somit ist

$$K = \frac{I_{\sim}}{2\, d}\,. \tag{5}$$

Setzt man diesen Ausdruck in Gl. (3) ein, so wird die Verteilung der Stromdichte auf der Metalloberfläche als eine Funktion von x erhalten:

$$i_{\sim} = \frac{I_{\sim}}{d\pi} \frac{a}{x^2 + a^2} \tag{6}$$

Diese Funktion wird schematisch in Abb. 2 dargestellt.

Wenn — im Sinne unserer früheren Mitteilung [1] — die auf der Metalloberfläche stattfindenden Kathoden- und Anodenvorgänge nach Tafelschen Gleichungen des gleichen Typs beschrieben werden können, so ergibt sich der zeitliche Mittelwert der Stromdichte, die jener auf der Metallfläche stattfindenden Korrosion entspricht, zu

$$\bar{i}_a = i_0\, I_0 \frac{\sqrt{2}\, i_{\sim}}{\sqrt{(\omega\, Cb)^2 + (2\, i_0)^2}} \tag{7}$$

wo i_0 die Korrosionsstromdichte ohne Durchfluß des Wechselstromes, I_0 eine modifizierte Bessel-Funktion erster Art, mit dem Index = 0, $i_\sim$ den effektiven Wert der Stromdichte des Wechselstromes auf der Metalloberfläche, ω die Kreisfrequenz des Wechselstromes, C die Kapazität der Flächeneinheit des Metalls und b die Konstante der Tafelschen Gleichung darstellen. Setzt man den Ausdruck (6) in Gl. (7) ein, so wird die Korrosionsstromdichte, die an unserem Modell beobachtet werden kann, als eine Funktion von x erhalten:

$$i_a = i_0 I_0 \left(\frac{\sqrt{2}\, I_\sim a}{d\pi(x^2 + a^2)\sqrt{(\omega Cb)^2 + (2i_0)^2}} \right). \tag{8}$$

Wie aus der letzteren Gleichung ersichtlich ist — unter sonst gleichen Bedingungen — ist die Korrosion bei gegebenem Wert von a um so geringer, je höher der Wert von x liegt. Es ist ferner zu ersehen, daß die Verteilung der Korrosion auf der Metalloberfläche um so gleichmäßiger ist, je größer der Wert von a ist.

Auch auf Grund der Ergebnisse, die in unseren beiden anderen Mitteilungen [2, 3] beschrieben wurden, können die gleichen Folgerungen gezogen werden.

ZUSAMMENFASSUNG

An dem von den Verfassern entwickelten Modell wurde die Korrosion der in einen Elektrolyten verlegten Metallplatte berechnet, die unter der Wirkung eines Kriechwechselstromes auftritt. Nach den erhaltenen Ergebnissen wird die Korrosion durch den Wechselstrom in einem, sich von Stelle zu Stelle änderndem Maße erhöht. Die Verteilung der Korrosion auf der Metalloberfläche ist um so gleichmäßiger, je gleichmäßiger die Verteilung des Wechselstromes ist.

LITERATUR

1. DÉVAY, J., MÉSZÁROS, L.: Magyar Kém. Foly. **71,** 68 (1965); Acta Chim. Hung. **43,** 25 (1965).
2. DÉVAY, J., MÉSZÁROS, L.: Magyar Kém. Foly. **71,** 238 (1965); Acta Chim. Hung. **44,** 397 (1965).
3. DÉVAY, J., MÉSZÁROS, L.: Magyar Kém. Foly. **71,** 240 (1965); Acta Chim. Hung. **45,** 119 (1965).
4. DÉVAY, J., MÉSZÁROS, L.: Magyar Kém. Foly. **71,** 277 (1965); Acta Chim. Hung. **45,** 37 (1965).
5. DÉVAY, J., SZEGEDY, R., LÁBODY, I.: Magyar Kém. Foly. **70,** 281 (1964); Acta Chim. Hung. **42,** 192 (1965).
6. DÉVAY, J., SZEGEDY, R., LÁBODY, I.: Magyar Kém. Foly. **70,** 288 (1964); Acta Chim. Hung. **42,** 207 (1965).
7. DÉVAY, J., MOSONI, F.: Magyar Kém. Foly. **79,** 492 (1964); Acta Chim. Hung. **42,** 243 (1965).
8. DÉVAY, J.: Magyar Kém. Foly. **70,** 497 (1964); Acta Chim. Hung., **42,** 255 (1965).
9. ERDEY-GRÚZ, T., DÉVAY, J., SZEGEDY, R., GÁLDI, A.: Magyar Kém. Foly. **69,** 296 (1963), Acta Chim. Hung. **38,** 325 (1963).
10. DÉVAY, J.: Magyar Kém. Foly. **70,** 497 (1964); Acta Chim. Hung. **42,** 255 (1965).

Prof. Dr. József DÉVAY
Lajos MÉSZÁROS
Universität, Veszprém, Ungarn

СТРУКТУРА СВЯЗИ АЛКЕНИЛ-КРЕМНИЙ-ОРГАНИЧЕСКИХ СОЕДИНЕНИЙ

Й. НАДЬ, Ш. ФЕРЕНЦИ-ГРЕС и В. Ф. МИРОНОВ

(Будапештский Политехнический Университет, Кафедра Неорганической Химии)

Поступило 9 февраля 1965 г.

Многие авторы [1] занимались изучением структуры и реакционной способности алкенил-силанов, однако определенного решения относительно природы связей и их взаимодействия в этих соединениях так и не было предложено. Наше внимание привлекли интересные закономерности реакций присоединения галогенов, галоидоводородов, диродана и пр. к алкенил-силанам с α, β, γ-положениями кратных связей относительно атома кремния, а также симбатно изменяющиеся физические свойства этих же соединений (Рамановские, ИК, УФ спектры и т. д.). Можно было полагать, что изучение диэлектрических свойств этих алкенил-силанов поможет выяснить природу связей и объяснить их химические и физические свойства.

На основании работ *Х. Хуанга* и *К. Х. Хуи* [2] известно, что связи фенил-кремний и фенил-олово подобно алкенил-силанам обладают частичным двойным характером, что объясняется наличием $d\pi-p\pi$ дативной π связи (табл. I).

Табл. I

M	$C_6H_5M(CH_3)_3$	$C_6H_5CH_2M(CH_3)_3$
C	μ = 0,53 D	—
Si	μ = 0,44 D	μ = 0,55 D
Sn	μ = 0,51 D	μ = 0,91 D

Кремний и олово электроположительнее, чем углерод, поэтому если бы налицо был бы лишь индуктивный эффект, то дипольный момент аналогичных фенил-соединений был бы больше, чем дипольный момент (0,53 D) третичного бутил-бензола. Вопреки этому было найдено, что дип. момент триметил-фенил-силана меньше (0,44 D), а триметил-фенил-олова почти таков же (0,51 D). Отсюда следует, что сопряжение распространяется на этом кремния и олова, т. е. обе группы обладают +I и —M эффектом. Двойной характер связи Si—C подтверждается также и тем, что дипольный момент бензильных производных групп $(CH_3)_3$ Si и $(CH_3)_3$ Sn больше (0,71 D и 0,69 D), чем аналогичных соединений углерода.

Очевидно, что в случае алкенил-силанов должен наблюдаться подобный эффект, что в дальнейшем нами и будет подтверждено.

В качестве образцов для наших исследований мы выбрали триметил-винил-силан, триметил-аллил-силан и триметил-бутенил-силан. Эти соединения были получены известным в литературе [3] методом, их чистота была проверена газовой хроматографией.

Газохроматографический анализ проводился на приборе **W. G. PYE & Co LTD PYE**-аргон, снабженном стеклянной колонкой длиной 2 м и диаметром 4 м. В качестве неподвижной фазы использовался силанизированный целит **BDH** 80—120 меш. с 3% силикона **SE**—30. Температура колонки в случае триметил-винильного триметил-аллил-силана равнялась комнатной температуре, а в случае триметил-бутенил-силана составляла 50° С. Напряжение на детекторе 1250 в, скорость газа 45 и 50 мл аргона/мин. Результаты анализа показали, что во всех трех случаях соединения содержали лишь один компонент и, таким образом, была достигнута чистота соединений, необходимая для проведения диэлектрических измерений.

Для определения дипольного момента соединений нами был выбран метод *Онзагера* [4]. Измерения проводились при температуре 25,00 $\pm$ 0,05° С, которая поддерживалась ультратермостатом.

Определение диэлектрической постоянной проводилось на приборе собственной конструкции [5] при частоте 10 000 гц, коэффициенты преломления n_D^2, а также разность $n_F - n_C$ (дисперсия), определялись на рефрактометре Аббэ. Плотность определялась дилатометром.

Дипольный момент был рассчитан по методу Онзагера при помощи следующего известного уравнения:

$$\mu = 0{,}22\sqrt{P^*}$$

$$P^* = V(\varepsilon_0 - \varepsilon_{эфф}) \cdot \frac{2\varepsilon_0 + \varepsilon_{эфф}}{\varepsilon_0 (\varepsilon_{эфф} + 2)^2}$$

где ε_0 — диэл. постоянная при частоте 10 000 гц и 25° С

V — мольный объем

$$\varepsilon_{эфф} = \frac{2R + V}{V - R}$$

Значение R равно сумме атомной (P_A) и электронной (P_e) поляризации, а также приблизительно может быть рассчитано из мольной поляризации, отнесенной к **D** линии:

$$R = P_A + P_e \qquad \text{или} \qquad R = MR_D \cdot 1{,}05$$

Сумма атомной и электронной поляризации была рассчитана обеими методами. Значение электронной поляризации, необходимое для более точных расчетов, было определено при помощи интерполяционной формулы, относящейся к аномальной дисперсии. Значение атомной поляризации было

рассчитано по методу *А. П. Альпшюлер* и *Л. Розенблюм* [6] аддитивно из инкрементов связей, учитывая поправку на анизотропию дипольного поля.

На основании сумм атомных и электронных поляризаций, рассчитанных обеими методами, при помощи уравнения Онзагера нами рассчитаны дипольные моменты перечисленных соединений. Значения дипольных моментов, рассчитанные двумя методами, практически совпадают.

Результаты измерений и расчетов сведены в следующую таблицу, в которой показаны коэффициенты преломления (n_D^{25}) плотность (d_4^{25}), диэлектрические постоянные (ε^{25}) мольный объем (V_4^{25}), молярная рефракция, отнесенная к **D**-линии (MR_D^{25}), коэффициенты преломления, относящиеся к электронной поляризации (n_∞), атомная (P_A) и электронная (P_e) поляризация, а также их сумма ($P_A + P_e$), сумма приблизительно определенной атомной и электронной поляризации (1,05 MR_D) и рассчитанный при помощи двух последних значений дипольный момент (μ) винил-, аллил- и бутенил-триметил-силанов.

Табл. II

	$CH_2{=}CH{-}SiR_3$	$CH_2{=}CH{-}CH_2{-}SiR_3$	$CH_2{=}CH{-}CH_2{-}CH_2{-}SiR_3$
n_D^{25}	1,3880	1,4047	1,4112
d_4^{25}	0,6864	0,7112	0,7313
ε^{25}	2,07	2,28	2,20
V_4^{25}	145,94	160,53	175,43
MR_D	34,43	39,32	43,56
n_∞	1,3736	1,3895	1,3969
P_A	2,965	3,03	3,19
Pe	33,29	38,01	42,24
$P_A + Pe$	36,25	41,04	45,43
MR_D 1,05	36,16	41,29	45,74
μ_1	0,331	0,59	0,477
μ_2	0,338	0,58	0,46

По данным таблицы видно, что максимальное значение дипольного момента наблюдается у аллильного соединения, а минимальное у винилпроизводного.

Методом *Дебая* [7] дипольный момент триметил-аллил-силана был определен также в среде циклогексана. Дипольный момент, рассчитанный известным путем на основании суммарной поляризации, отнесенной к бесконечно разбавленному раствору, меньше (—0,45 **D**), чем рассчитанный по методу *Онзагера* (0,58 **D**). Известно, что метод Дебая из-за эффекта растворителя приводит к искаженным результатам, что подтверждается эмпирической

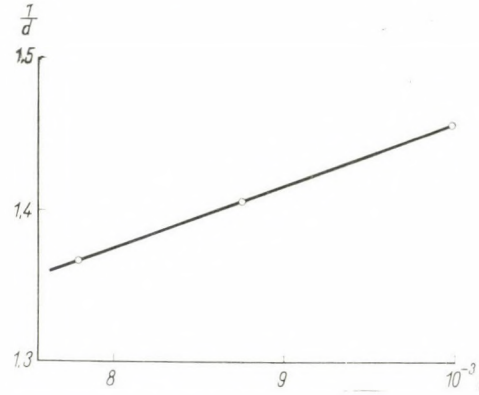

Рис. 1. Зависимость удельного объема от обратной величины молекулярного веса членов гомологического ряда $(CH_3)_3\ Si\ (CH_2)_n\ CH = CH_2$

зависимостью *Мюллера* [8]. Опыт показывает, что значения дипольных моментов, рассчитанные по методу Онзагера, лучше совпадают с истинными значениями, измеренными в парах, чем рассчитанные по Дебаю. Поэтому за основу дальнейших расчетов нами приняты значения дипольных моментов, рассчитанные по Онзагеру.

На основании перечисленных данных интересно было проверить по работам *К. Х. Мейера, ван дер Вайка* [9] и *Геци Иштвана* [10], выполняются ли эмпирические зависимости, установленные ими для гомологических рядов.

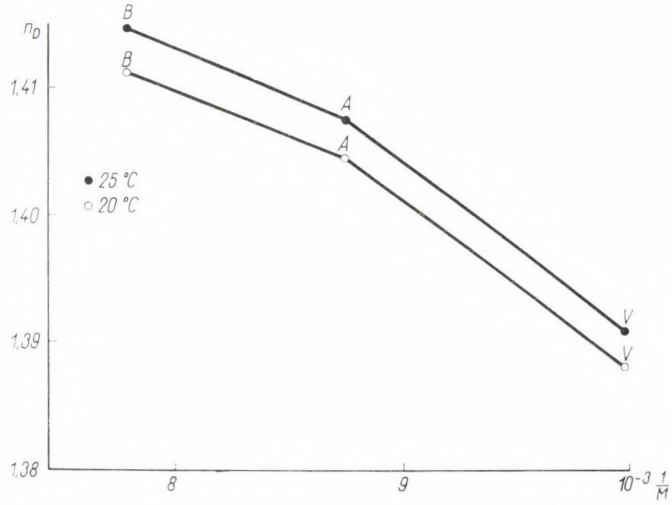

Рис. 2. Зависимость показателей преломления, измеренных при разных температурах, от обратной величины молекулярного веса членов гомологического ряда $(CH_3)_3\ Si\ (CH_2)_n\ CH = CH_2$

Удельные объемы $\left(\frac{1}{d}\right)$, измеренные при 25° С, в зависимости от обратного значения молекулярного веса $\left(\frac{1}{M}\right)$ дают прямую (рис 1). Таким образом в этом отношении правило гомологических рядов выполняется, что одновременно служит доказательством достаточной точности наших измерений плотности и чистоты веществ.

При изображении коэффициентов преломления, измеренных при 20° С и 25° С в зависимости от обратной величины молекулярного веса, в отличии от экспериментальной зависимости, не получается прямая линия, что означает, что поляризуемость аллильного соединения больше ожидаемой (рис. 2.).

Выбрав за основу триметил-бутенил-силан, двойная связь в котором может считаться изолированной, мы провели сравнение свойств отдельных членов гомологического ряда триметил-алкенил-силанов (рис. 3). Графически изобразили:

1. способность к диродановому присоединению,
2. характер кривой валентных колебаний связи C = C в спектре комбинационного рассеяния света (1630—1649 $см^{-1}$),
3. характер кривой валентных колебаний (1630—1649 $см^{-1}$),
4. изменение дипольного момента,
5. изменение диэлектрической постоянной в зависимости, от числа метиленовых групп. Максимум в каждом случае — подобно зависимости n_D от 1/M — наблюдается у аллильногосое динения.

Отличие аллильного соединения от винилпроизводного подчеркивается и тем экспериментальным наблюдением, что присоединение галоидоводорода в случае винил-производного идет против правила Марковникова, а в случае аллильного соединения согласно правилу Марковникова.

Эти изменения обусловлены очевидно природой связи данных соединений, которая — на основе экспериментальных данных — должна быть следующей:

$\overrightarrow{CH_2—CH}\leftarrow Si\,R_3$ $\qquad \mu = 0{,}33D\ (+I;\ -M)$

$\overleftarrow{CH_2—CH—CH_2}\leftarrow Si\,R_3$ $\qquad \mu = 0{,}58D\ (+I)$

$\overleftarrow{CH_2—CH}—CH_2—CH_2\leftarrow Si\,R_3$ $\qquad \mu = 0{,}46D\ (+I)$

В винил-производном дипольный вектор связи кремний—углерод направлен к углероду, т. е. атом кремния заряжен относительно положительно, а атом углерода относительно отрицательно. Это очевидно простой индуктивный эффект (+I). Перпендикулярная к оси σ связей $p\pi$ орбита α и β углеродных атомов, а также пустая $3d$ орбита кремния перекрывают друг друга, что приводит к образованию трицентричной связывающей молекулярной

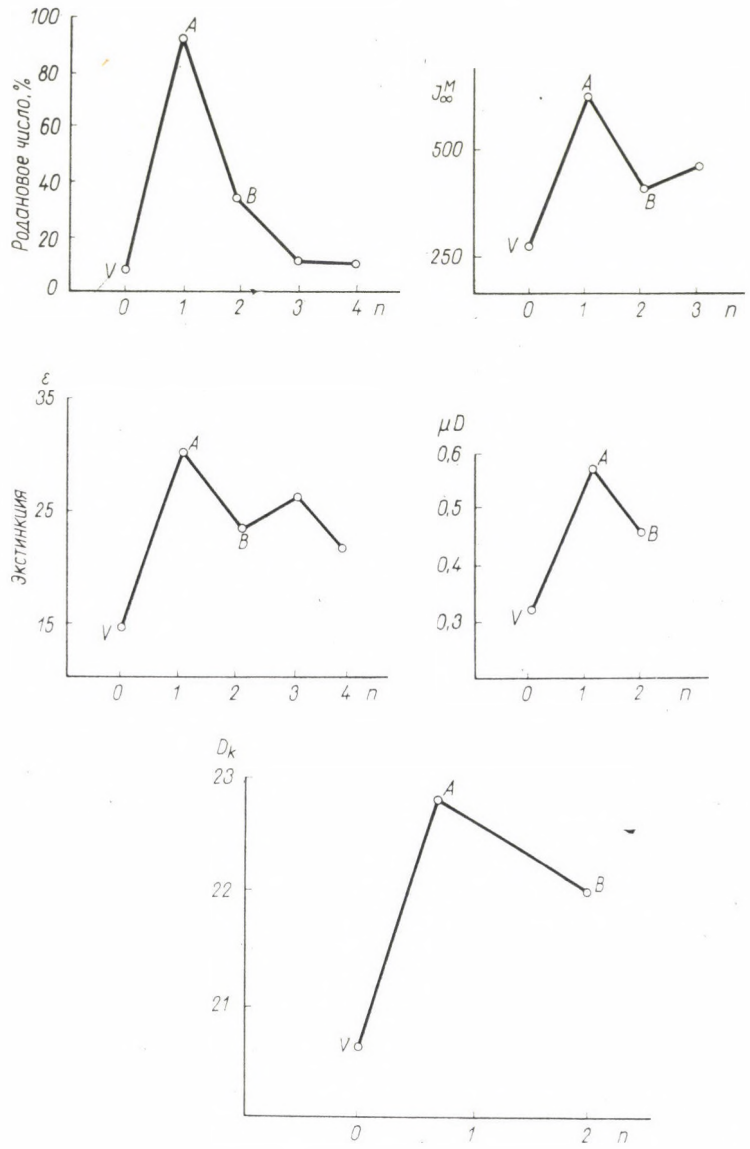

Рис. 3. Зависимость изменения

1. способности к дироданового присоединению (родановое число, %),
2. кривых интенсивности в спектрах комбинационного рассеяния света связи C = C,
3. кривых инфракрасной интенсивности связи C = C (экстинкция)
4. дипольного момента
5. диэлектрической постоянной

от числа метиленовых групп в гомологическом ряду $(CH_3)_3\,Si\,(CH_2)_n\,CH = CH_2$.

орбите, заполненной двумя электронами, а это означает, что в силу-М—эффекта кремния π-электронная пара сдвигается в сторону кремния и понижает дипольный момент первоначальной σ-связи кремния. Это явление так называемого сопряжения. В силу —М эффекта кремния β-углеродный атом по отношению к атому кремния становится относительно положительно, а α-углеродный атом относительно отрицательно заряженным. Этим объясняется, что наименьшее значение дипольного момента наблюдается у винилпроизводного. Электромерный эффект, благодаря эффекту сопряжения, также мал, что понижает, например, способность к диродановому присоединению. С этим утверждением хорошо согласуется понижающаяся тенденция значений интенсивности поглощения в инфракрасной области и в спектре комбинационного рассеяния света, а также реакция присоединения галоидоводорода, идущая против правила Марковникова.

В аллильном соединении двусторонний эффект сверхсопряжения засчет кремния и метиленовой группы, а также +I эффект кремния приводит к явлению, подобному в пропилене, но обратному по сравнению с винилпроизводным.

Электронное облако аллильной группы смещается в сторону γ-углеродного атома, что в некоторой степени усиливается непосредственным пространственным эффектом кремния. Таким образом, γ-углеродный атом приобретает относительно отрицательный заряд. М и Е эффекты связи C = C сильно возрастают и поэтому дипольный момент, поляризуемость и связанные с этими двумя свойствами интенсивности поглощения в инфракрасной области и в спектрах комбинационного рассеяния света также сильно возрастают. Таким образом становится ясно, почему присоединение галоидоводорода идет по правилу Марковникова, а также понятна высокая реакционная способность в реакциях электрофильного и нуклеофильного характера. Известно также, что в кислой и щелочной среде при действии воды происходит отщепление аллильной группы с образованием пропилена. В случае OH^- иона это явление объясняется тем, что данный ион по механизму S_{N_2} вступает во взаимодействие с одной из 3d орбит кремния, а образующийся переходный комплексный анион под действием воды превращается в силанол, а затем в силоксан.

Бутенильное соединение может считаться за олефинпроизводное и двойная связь в нем рассматриваться почти полностью изолированной, а $\beta - \gamma$- и δ-углеродные атомы обладают химическими свойствами, подобными пропилену. Этим объясняется, что данные, приведенные для бутенильного соединения, занимают промежуточное положение между значениями для винил-производного с одной стороны и аллильного соединения с другой. Используя приведенные данные, нами был проделан приблизительный расчет отдельных дипольных моментов связей в винил-триметилсилане.

Известно, что дипольный момент связи C—H 0,4 D, а связи $C_{алиф.}$ — Si 0,6 D [6]. При помощи этих значений, дипольного момента винильного соединения, правильного расставления векторов, значений длины связей, а также относительного распределения зарядов в зависимости от индуктивного и мезомерного эффектов, векторным анализом можно рассчитать дипольный момент связи Si — C и C = C в винильной группе.

Из тетраэдрической симметрии следует, что результирующий вектор группы $'CH_3'$ ← Si 0,2D. На основании sp^2 гибридных уровней углеродных атомов винильной группы валентные углы вокруг углеродных атомов винильной группы ~ 120°.

Учитывая I и M эффекты, можно написать следующую структрную формулу, обладающую парциальными зарядами из-за сдвига электронов:

$$\overset{\delta(+)}{(CH_3)_3}\overset{\delta(+)}{Si}\rightarrow\overset{\delta(-)}{CH}\leftarrow\overset{\delta(+)}{CH_2}$$

$2\varepsilon_i$	$-\varepsilon_i$	$-\varepsilon_i$	I эффект
$-{}^1/_2\varepsilon_t$	$-{}^1/_2\varepsilon_t$	$+\varepsilon_t$	M эффет

где ε_i — относительная заряженность, вызываемая I эффектом

ε_t — относительная заряженность, вызываемая M эффектом

δ — первоначальная относительная заряженность

Дипольный момент винил-силана $\mu = 0{,}34$ D, длины связей $R_{SiC} = 1{,}89$Å и $R_{CC} = 1{,}337$Å (винил).

На основании этого неизвестные дипольные векторы связи m_1 и m_2 могут быть выражены ($2\varepsilon_i R_{SiC} = 0{,}6$ D)

$$m_1 = (2\,\varepsilon_i - {}^1/_2\varepsilon_t)\,R_{SiC} = 0{,}6 - 0{,}945\,\varepsilon_t \tag{1}$$

$$m_2 = (\varepsilon_t - \varepsilon_i)\,R_{CC} = 1{,}337\,\varepsilon_t - 0{,}214 \tag{2}$$

а также

$$m_A = 0{,}6 - m\,; \quad m_B = m_2 \tag{3}$$

На основании этого для дипольного момента винил-триметил-силана и дипольных моментов указанных групп можно применить теорему косинусов

$$\mu^2 = m_A^2 + m_B^2 + 2\,m_A \cdot m_B \cos\Theta$$

где $\Theta = 120°$ (4)

Подставляя уравнения (1), (2) и (3) в (4) для ε_t получается следующее выражение:

$$3{,}935\;\varepsilon_t^2 - 0{,}369\,\varepsilon_t - 0{,}063 = 0 \tag{5}$$

после решения которого

$$\varepsilon_t = 0{,}176 \quad \text{и} \quad \varepsilon_i = 0{,}16$$

Таким образом характер связи кремний-винил, распределение зарядов и дипольный момент связи триметил-винил-силана можно изобразить следующим символом:

$$(CH_3)_3\,Si \xrightarrow{0{,}438D} CH \xrightarrow{0{,}021D} CH_2$$
$$+\,0{,}048e \qquad -\,0{,}051e \qquad +\,0{,}003e$$

Дипольный момент связи Si — C с 0,6 D понижается до 0,438 D по сравнению с дипольным моментом связи $H_3C \leftarrow Si$

$$(CH_3)_3Si \xleftarrow[0{,}6D]{} CH_3 \quad (+\,I) \quad m_{SiC} = 0{,}6\,D$$

Дипольный момент связи C = C, направленный в сторону α-углеродного атома, равен 0,021 — т. е. не равен нулю, как в этилене — таким образом данная связь является в некоторой степени полярной, ковалентной связью. Приведенные значения дипольных векторов связи могут рассматриваться как результирующая связей и векторов сопряженных связей.

Мы намерены продолжить наши исследования и результаты, полученные опытным путем, подтвердить квантомеханическими расчетами.

Наконец, выражаем благодарность д-р *Габриэлле Гарзо* за проведение газохроматографического анализа, а также *Ренате Фаркаш* и *Тамашу Габор* за синтез исследуемых соединений.

РЕЗЮМЕ

Проведены диэлектрические измерения триметил-винил-, аллил- и бутенил-силанов. Установлено, что триметил-винил-силан обладает строением, подобным триметил-фенил-силану, с той разницей, что в винильном соединении два π-электрона находятся на трицентричной, а в фенильном соединении же 6 π-электронов находятся на гептацентричной молекулярной орбите. В обоих случаях атом кремния обладает индуктивным (+I) и мезомерным (—M) эффектом. Реакционная способность аллильных соединений связана с сильно повышенными M и E эффектами, которые в свою очередь объясняются +I эффектом кремния и эффектом сверхсопряжения группы CH_2.

ЛИТЕРАТУРА

1. *Петров, А. Д., Миронов, В. Ф., Пономаренко, В. А.* и *Чернышев, Е. А.:* Синтез кремнийорганических мономеров. (Изд. АН СССР, Москва), 1961.
2. Huang, H. H., Hui, K. H.: J. Org. Metallic Chem. **2**, 288 (1964).
3. а) *Петров, А. Д., Миронов, В. Ф., Глуховцев, В. Г.:* Журн. Общей Химии **27**, 1535 (1957).
   б) *Петров, А. Д., Миронов, В. Ф.:* Изв. АН СССР, ОХН **1952**, 635.
   в) *Миронов, В. Ф., Погонкина, Н. А.:* Изв. АН СССР, ОХН **1959**, 81.
4. Onsager, L.: J. Am. Chem. Soc. **58**, 1486 (1963).
5. Nagy, J., Gresz, I., Gresz, S.: Periodica Polytechnica (В печати).

6. ALTSHULLER, A. P., ROSENBLUM, L.: J. Am. Chem. Soc. **77,** 272 (1955).
7. DEBYE, P.: Physik. Z. **13,** 97 (1912).
8. MÜLLER, H.: Physik. Z. **34,** 689 (1933).
9. MEYER, K. H., VAN DER WYK: Helv. Chim. Acta **20,** 1313 (1937).
10. *Геци, И.:* Пластмассы **1964,** 312.

Über die Bindungsstruktur der alkenylsiliciumorganischen Verbindungen

J. NAGY, S. FERENCZI-GRESZ und V. F. MIRONOV

Zusammenfassung. Die Ergebnisse der mit Trimethylvinyl-, Allyl- und Butenylsilan durchgeführten dielektrischen Messungen bestätigen, daß das Vinyltrimethylsilan eine dem Phenyltrimethylsilan ähnliche Struktur besitzt, jedoch mit dem Unterschied, daß sich bei der Vinylverbindung die beiden π-Elektronen auf einem trizentrischen, während bei der Phenylverbindung die sechs π-Elektronen auf einem heptazentrischen Molekülniveau befinden. In beiden Fällen weist das Silicium eine +induktive (+I) und mesomere (−M) Wirkung auf. Die Reaktionsfähigkeit der Allylverbindungen steht mit den stark vergrößerten M und E Effekten im Zusammenhang. Dies kann mit dem +I-Effekt des Siliciums und mit dem Hyperkonjugationseffekt der CH_2-Gruppe erklärt werden.

Bond Structure of Alkenyl Siliconorganic Compounds

J. NAGY, S. FERENCZI-GRESZ and V. F. MIRONOV

Summary. Dielectric measurements were carried out with trimethyl vinyl, allyl and butenyl silane. It was found that vinyl trimethyl silane has a structure similar to that of the phenyl trimethyl silane, with the difference, however, that in the vinyl compound the two π electrons are on a tricentric molecule level while in the phenyl compound the six π electrons are present on a heptacentric molecule level. Silicium possesses in both cases +inductive (+I) and mesomeric (−M) effects. The reactivity of allyl compounds is correlated with the appreciably increased M and E effect which can be interpreted by the +I effect of silicon and by the hyperconjugation effect of the CH_2 group.

Dr. József NAGY
Mrs. Sarolta FERENCZI-GRESZ } Budapest XI. Gellért tér 4
V. F. MIRONOV; Institut Kremniyorganicheskikh Soedinenii, Moskva E 275, SSSR

ALLYLPHENOL AND PROPENYLPHENOL DERIVATIVES

O. H.-HANKOVSZKY, K. HIDEG and GY. MÉHES

(Institute of Pharmacology, University Medical School, Pécs, Hungary)

Received March 8, 1965

The main components of the ethereal oil obtained from *Asarum Europeaum L.* have been described by GATTERMAN and EGGERS [1], and by BRUCKNER and SZÉKI [2].

These compounds are: asarone (2,4,5-trimethoxy-1-propenylbenzene), eugenol (2-methoxy-4-allylphenol), methyleugenol (3,4-dimethoxy-1-allylbenzene), isoeugenol (2-methoxy-4-propenylphenol) and methylisoeugenol (3,4-dimethoxy-1-propenylbenzene).

Recently, a derivative of eugenol (Estil, G-29505), (2-methoxy-4-allylphenoxyacetic acid N,N-diethylamine) has been marketed by Geigy A. G. as a short-period narcotic agent [3] possessing also a stimulating effect on the respiratory organs. However, this compound is insoluble in water, and has some undesirable secondary effects. Thus, in clinical tests it proved unsatisfactory [4].

The scope of our experiments was the preparation of various amino-substituted derivatives of eugenol and isoeugenol, in order to study the possible correlations between the pharmacological effects (such as coronary dilatatory, hypotensive, spasmolytic activity) and the structure. The present report comprises a description of the synthetic work, while the pharmaceutical tests will be published in detail elsewhere.

Methods of synthesis

Method A

(a) Preparation of 2-methoxy-4-alkenyl-2'-aminoethoxybenzene derivatives

The phenolates of isoeugenol (**I**) and eugenol (**II**) formed in alkaline solution (sodium hydroxide) are reacted with N(2'-chloroethyl)-amino compounds to afford 4-(2'-aminoethyl) ethers; the latter products are converted in polar solvents (such as acetone or ethanol) into quaternary salts, by treatment with methyl iodide.

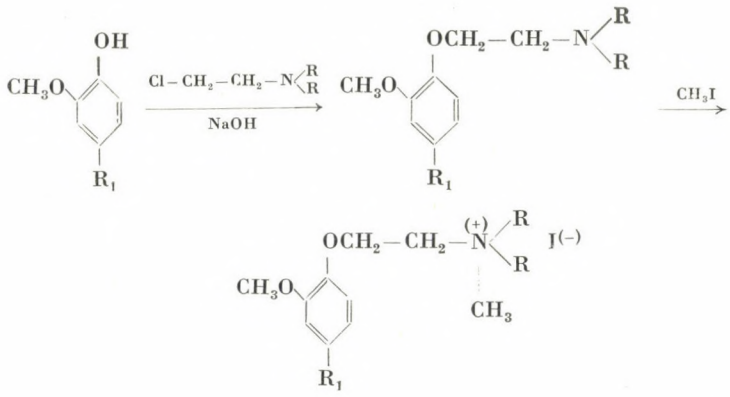

(b) Preparation of 2-methoxy-4-alkenylphenoxyacetamides

The reaction of chloroacetic amides with **I** or **II** in alkaline solution yields the corresponding glycolamides.

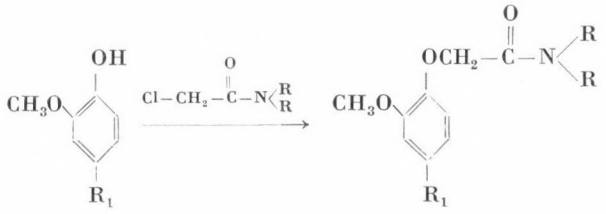

When 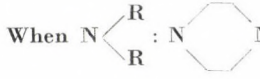 also the quaternary salt of the amide can be prepared.

(c) Selective reduction of 2-methoxy-4-alkenylacetamides with lithium aluminium hydride

Lithium aluminium hydride selectively reduces the amide group to amine. However, the unsaturated bond is not saturated, also its position remains unchanged.

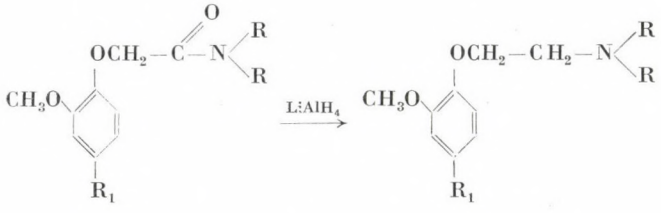

$R_1 = -CH=CH-CH_3$ or $-CH_2-CH=CH_2$

Method B

Preparation of 2'-(3-methoxy-4-hydroxyphenyl)-isopropylamines

On reacting 2'-(3-methoxy-4-hydroxyphenyl)-isopropyl bromide [5] with an excess of a primary or secondary amine, 2'-(3-methoxy-4-hydroxyphenyl)-isopropylamines are obtained in fair yields. When a secondary amine is used, the formed tertiary amine can be converted into the corresponding quaternary amine in good yield, by treatment with methyl iodide.

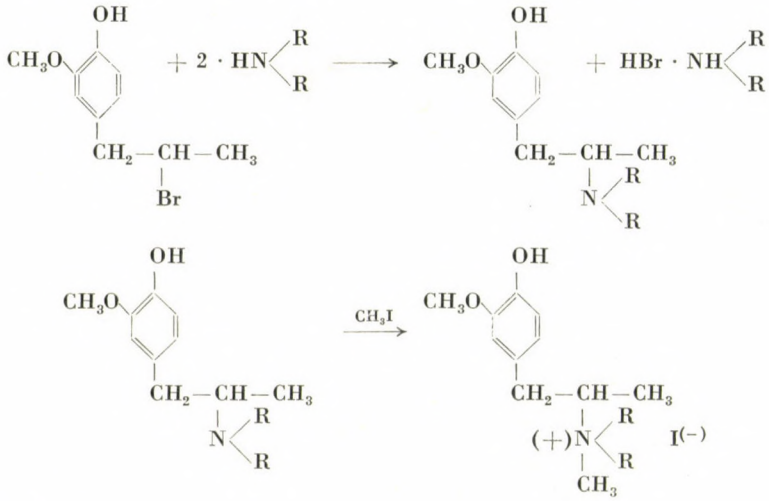

Method C

The Mannich reaction of isoeugenol and eugenol

The reaction of isoeugenol or eugenol with formaldehyde and with a secondary or primary amine affords derivatives containing an aminomethyl group in ortho position; the yields are satisfactory. The side chain is left unchanged. The products cannot be distilled without decomposition even at 0.05 Torr. However, they could be isolated from the reaction mixture in fair yields in the form of various salts (such as hydrochloride, tartrate).

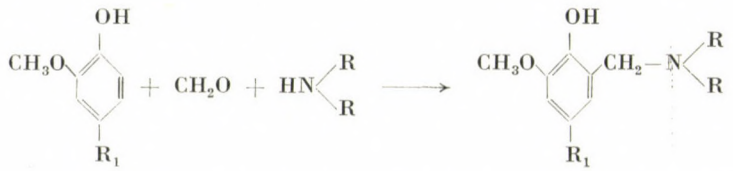

The compounds prepared by the above-described methods are summarized in Tables I, II and III.

Acta Chimica Academiae Scientiarum Hungaricae 47, 1966.

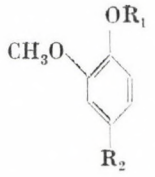

Table I

Compd. No.	R_1	R	M. p., °C	Formula (Molecular weight)	N% Calcd. Found	Hal. % Calcd. Found
1	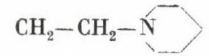	$-CH=CH-CH_3$	172—73	$C_{17}H_{25}NO_2.HCl$ (311.86)	4.49 4.98	11.37 11.05
2	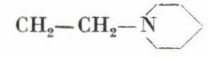	$-CH_2-CH=CH_2$	129—30	$C_{17}H_{25}NO_2.HCl$ (311.86)	4.49 4.59	11.37 11.18
3	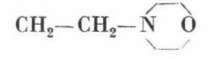	$-CH=CH-CH_3$	167—69	$C_{16}H_{23}NO_3.HCl$ (313.81)	4.46 4.35	11.30 11.65
4	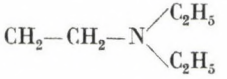	$-CH_2-CH=CH_2$	109—12	$C_{16}H_{25}NO_2.HCl$ (299.85)	4.67 4.62	11.83 11.75
5	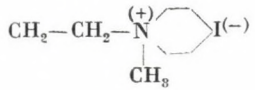	$-CH=CH-CH_3$	148—49	$C_{18}H_{28}INO_2$ (417.34)	3.36 3.12	30.41 30.08
6	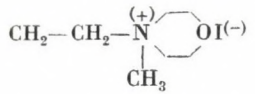	$-CH=CH-CH_3$	173—76	$C_{17}H_{26}INO_3$ (419,29)	3.34 3.57	30.27 30.25
7	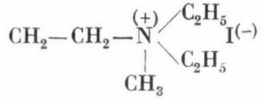	$-CH_2-CH=CH_2$	177—79	$C_{17}H_{28}INO_2$ (405.33)	3.46 4.05	31.31 31.12

Compd. No.	R_1	R_2	M. p. °C	Formula (Molecular weight)	N% Calcd. Found	Halogen % Calcd. Found
8	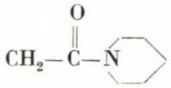	$-CH=CH-CH_3$	220/0.9*	$C_{17}H_{23}NO_3$ (289.38)	4.84 4.76	— —
9	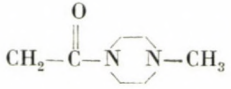	$-CH=CH-CH_3$	178—80	$C_{17}H_{24}N_2O_3.HCl$ (340.86)	8.22 8.11	10.41 10.28
10	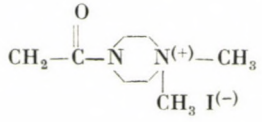	$-CH=CH-CH_3$	258—60	$C_{18}H_{27}IN_2O_3$ (446.34)	6.28 6.25	28.43 27.96

* B. p./Torr

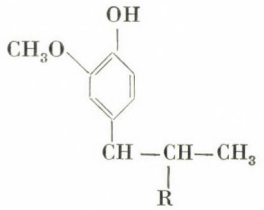

Table II

Compd. No.	R	M. p., °C	Formula (Molecular weight)	N% Calcd. Found	Halogen % Calcd. Found
11		220—23	$C_{15}H_{23}NO_2.HCl$ (285.82)	4.90 4.57	12.32 12.50
12		186—87	$C_{14}H_{21}NO_3.HCl$ (287.80)	4.87 5.19	12.33 12.50
13	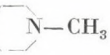	214—16	$C_{15}H_{24}N_2O_2.2HCl$ (337.31)	8.31 8.44	21.03 20.76
14	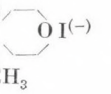	146—48	$C_{15}H_{24}INO_3$ (393.27)	3.56 3.95	32.27 32.40
15	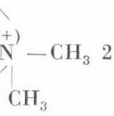	204—05	$C_{17}H_{30}I_2N_2O_2$ (548.26)	5.11 5.41	46.30 46.70

Relationships between structure and pharmacological effect

The pharmacological effects of the synthesized compounds can briefly be characterized as follows.

1. The O-alkylamine ethers (No. 1 to 4), and particularly their quaternary salts (No. 5 to 7), were found to possess hypotensive action.

2. The O-glycolamide compounds (No. 8 and 9) are narcotics and relaxants, similarly to Estil; the action is of short duration.

3. When the amide group is reduced, the narcotic and relaxant effects of the molecule are lost.

4. All compounds had some stronger or weaker papaverinlike spasmolytic effect.

5. The O-alkylamine ethers stimulated respiration (e.g., No 1 to 3).

6. Compound No. 13 disclosed a qualitative coronary dilatatory activity.

Experimental

Method A

(a) 2-Methoxy-4-propenyl-2'-morpholinoethoxybenzene (No. 3)*

A solution containing 16.4 g (0.1 mole) of isoeugenol in 200 ml of ethanol was mixed with 5.0 g (0.125 mole) of sodium hydroxide dissolved in some water, and with 14.9 g (0.1 mole) of β-chloroethylmorpholine base. After boiling the mixture for three hours, the precipitated sodium chloride (4.5 g) was removed by filtration, and the filtrate distilled; yield, 15 g (54%), b.p.$_{0.4\text{Torr}}$: 192°. On acidifying the ethanolic solution of the product, white crystals of the monohydrochloride of the base were obtained, m.p. 167—169°.

(b) 2-Methoxy-4-propenyl-2'-morpholinoethoxybenzene monoethiodide (No. 6)

On treating the solution of 13.0 g (0.05 mole) of the base in acetone with excess methyl iodide, and allowing the mixture to stand an hour, the quaternary salt precipitated, yield 18.95 g (47%), m.p. 173—176°.

(b) 2-Methoxy-4-propenylphenoxyacetyl-piperidine (No. 8)

A solution containing 16.4 g (0.1 mole) of isoeugenol in 150 ml of ethanol was reacted with 5.0 g (0.125 mole) of sodium hydroxide dissolved in 10 ml of water and with 20 g (0.12 mole) of chloroacetylpiperidine. After refluxing the reaction mixture for five hours, the precipitated sodium chloride was removed by filtration, and the filtrate distilled. Yield 16 g (55%), b.p.$_{0.9\text{Torr}}$ 220°.

2-Methoxy-4-propenylphenoxyacetyl N-(N'methyl)-piperazine (No. 9)

This compound was prepared from isoeugenol and N-(chloroacetyl)N'-methylpiperazine by the method described in the preceding experiment. Yield 13 g (43%), b.p.$_{04\text{Torr}}$ 165°. On acidifying the ethanolic solution of the base with ethanolic hydrochloric acid, the corresponding hydrochloride was obtained, m.p. 178—180°. When a solution of the base in acetone is treated with excess methyl iodide, and the mixture allowed to stand an hour, the monoethiodide of the base (No. 10) is precipitated, m. p. 258—260°.

(c) Reduction of 2-methoxy-4-propenylphenoxyacetyl N-piperidine (No. 8) with lithium aluminium hydride to 2-methoxy-4-propenyl-ß-piperidinoethoxybenzene (No. 1)

The solution of 10 g (0.4 mole) of lithium aluminium hydride in anhydrous ether (100 ml) was added dropwise to 28.9 g (0.1 mole) of the glycolamide base dissolved in 150 ml of ether. After refluxing the mixture for an hour, excess lithium aluminium hydride and the formed complex were decomposed, the ethereal phase was dried over sodium sulfate, and the formed phenol ether was distilled. Yield 20 g (72%), b.p.$_{1\text{Torr}}$ 182—184°.

Method B

2'-(3-Methoxy-4-hydroxylphenyl)-isopropylmorpholine (No. 12)

The solution of 12.2 g (0.05 mole) of β-(3-methoxy-4-hydroxyphenyl)-isopropyl bromide in 100 ml of benzene was treated with 20 g of potassium carbonate and 13.0 g (0.15 mole) of morpholine. The mixture was refluxed for two hours, filtered, the filtrate evaporated, and the base distilled at 0.1 Torr at 166° to yield 7 g (55%) of the product.

Acidifying the acetone solution of the compound with hydrochloric acid gave the monochloride, m.p. 186—187°.

The quaternary salt was prepared by refluxing for an hour 12.6 g (0.05 mole) of 2'-(3-methoxy-4-hydroxyphenyl)-isopropylmorpholine base in 100 ml of acetone with 14 g (0.1mole) of methyl iodide. Yield: 5 g (25%), m.p. 146—148°.

* The numbers behind the names of the compounds refer to the Tables.

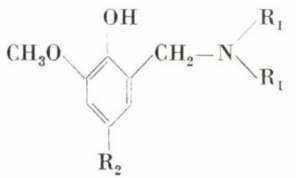

Table III

Compd. No.	$N\langle^{R_1}_{R_1}$	R_2	M. p., °C	Formula (Molecular weight)	N% Calcd. Found	Cl% Calcd. Found
16		$-CH_2-CH=CH_2$	151—52	$C_{15}H_{21}NO_2.HCl$ (283.81)	4.94 5.07	12.50 12.38
17		$-CH_2-CH=CH_2$	172—73	$C_{16}H_{23}NO_2.HCl$ (297.83)	4.70 4.66	11.91 12.20
18		$-CH_2-CH=CH_2$	178—79	$C_{15}H_{21}NO_3.HCl$ (299.81)	4.67 4.57	11.83 12.18
19		$-CH=CH-CH_3$	190—91	$C_{15}H_{21}NO_3.HCl$ (299.81)	4.67 4.60	11.83 11.70
20	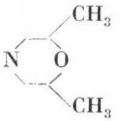	$-CH_2-CH=CH_2$	89—91	$C_{17}H_{25}NO_3.HCl$ (327.86)	4.27 4.35	10.82 10.36
21	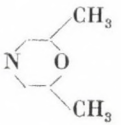	$-CH=CH-CH_3$	104—106	$[C_{17}H_{25}NO_3]_2.C_4H_6O_6$* (732.79)	3.82 3.58	
22	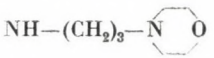	$-CH=CH-CH_3$	115—17	$C_{18}H_{28}N_2O_3.C_4H_6O_6$* (469.52)	5.96 5.98	

Compd. No.	$N\langle^{R_1}_{R_1}$	R_2	M. p., °C	Formula (Molecular weight)	N% Calcd. Found	Cl% Calcd Found
23	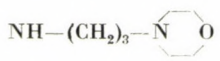	$-CH_2-CH=CH_2$	175—80	$C_{18}H_{28}N_2O_3 . 2HCl$ (392.36)	7.14 7.29	18.07 18.34
24	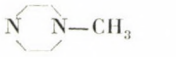	$-CH=CH-CH_3$	176—78	$C_{16}H_{24}N_2O_2 . 2HCl$ (349.32)	8.02 8.28	20.30 19.80
25		$-CH_2-CH=CH_2$	181—83	$C_{16}H_{24}N_2O_2 . 2HCl$ (349.32)	8.02 7.84	20.30 19.90
26	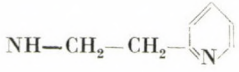	$-CH_2-CH=CH_2$	233—35	$C_{13}H_{22}N_2O_2 . 2HCl$ (371.32)	7.54 7.51	19.09 19.30
27		$-CH_2-CH=CH_2$	165—66	$C_{21}H_{26}N_2O_2 . 2HCl$ (411.38)	6.81 6.53	17.23 16.87
28	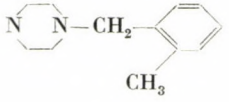	$-CH_2-CH=CH_2$	192—94	$C_{23}H_{30}N_2O_2 . 2HCl$ (439.44)	6.37 6.37	16.14 15.94
29	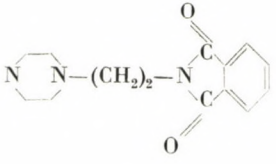	$-CH_2-CH=CH_2$	140—44	$C_{25}H_{29}N_3O_4 . 2HCl$ (508.47)	8.26 8.43	13.95 13.45

* tartrate

Method C

2-Methoxy-4-allyl-6-pyrrolidinomethylphenol (No. 16)

The solution of 16.4 g (0.1 mole) of 2-methoxy-4-allylphenol in 200 ml of ethanol was refluxed for two hours with 15 ml of 35% formaldehyde and 8.1 ml (0.1 mole) of the pyrrolidine base. After evaporating the solution, the residual thick viscous oil (16 g, 64%) was dissolved in acetone. Hydrogen chloride was introduced in the solution to adjust the pH to 3. On the addition of ether, the salt precipitated in almost quantitative yield, m.p. 151—152°.

2-Methoxy-4-allyl-6-(-N-)2'-phthalimidoethyl(-piperazinomethyl)-phenol (No. 29)

The solution of 16.4 g (0.1 mole) of 2-methoxy-4-allylphenol in 200 ml of ethanol was boiled two hours with 15 ml of 35% formaldehyde and 25.9 g (0.1 mole) of N-(2'-phthalimidoethyl)-piperazine base. On evaporating the mixture, dissolving the residue in ethanol, and acidifying the solution, the dihydrochloride of 2-methoxy-4-allyl-6-(N-)2'-phthalimidoethyl-(-piperazinomethyl)-phenol was precipitated, yield 39.7 g (78%), m p. 140—144°.

The authors' thanks are expressed to Miss T. HUSZÁR and Mrs. M. OTT for the microanalyses and for the technical assistance.

SUMMARY

Isoeugenol (**I**) and eugenol (**II**) react with haloethylamides in alkaline solution to give 2-methoxy-4-alkenyl-2'-aminoethoxybenzenes.

In alkaline medium, the reactions of eugenol and isoeugenol with chloroacetamides yield 2-methoxy-4-alkenylphenoxyacetamides whose amide group may be selectively reduced with lithium aluminium hydride:

$$-CON(R)_2 \xrightarrow{LiAlH_4} -CH_2-N(R)_2$$

By reacting 2'-(3-methoxy-4-hydroxyphenyl)-isopropyl bromide with amines 2'-(3-methoxy-4-hydroxyphenyl)-isopropylamines have been prepared.

Eugenol and isoeugenol have been aminomethylated with formaldehyde and primary or secondary amines in ortho position to the phenolic hydroxyl, to give 2-methoxy-4-alkenyl-6-aminomethylphenols.

REFERENCES

1. GATTERMANN, EGGERS; Ber. **32,** 290 (1899).
2. BRUCKNER, V., SZÉKI, T.: J. pract. Chem. N. F. **134,** 107 (1932).
3. THUILLIER, M. J., DOMENJOZ, R.: Anesthesist **6,** 163 (1964).
4. ZENKER, R., BEER, R.: Dtsch. med. Wschr. **87,** 468 (1962).
5. RIEGEL, B., WITTHOFF, H.: J. Am. Chem. Soc. **68,** 1913 (1946).

Allyl- und Propenylphenolderivate

O. H.-HANKOVSZKY, K. HIDEG und GY. MÉHES

Zusammenfassung. Isoeugenol (**I**) und Eugenol (**II**) reagieren in alkalischem Medium mit Halogenäthylaminen unter Bildung von 2-Methoxy-4-alkenyl-2'-aminoäthoxybenzolen.

Die Reaktion von Eugenol und Isoeugenol mit Chloracetamiden in einem alkalischen Medium liefert 2-Methoxy-4-alkenylphenoxyacetamide, deren Amidgruppe mit Lithiumaluminiumhydrid selektiv reduziert werden kann:

$$-CON(R)_2 \xrightarrow{LiAlH_4} -CH_2-N(R)_2$$

Durch die Reaktion von 2'-(3-Methoxy-4-hydroxyphenyl)-isopropylbromid mit Aminen erhielt man 2'-(3-Methoxy-4-hydroxyphenyl)-isopropylamine.

Bei der Aminomethylierung mit Formaldehyd und primären bzw. sekundären Aminen wurden Eugenol und Isoeugenol in Orthostellung zum phenolischen Hydroxyl aminomethyliert, und 2-Methoxy-4-alkenyl-6-aminomethylphenole ergaben sich als Reaktionsprodukte.

Аллил- и пропенилпроизводные фенола

О. Х.-ХАНКОВСКИ, К. ХИДЕГ и ДЬ. МЕХЕШ

Резюме. Описывается синтез 2-метокси-4-алкенил-2'-аминоэтоксибензенов — производных, образующихся при взаимодействии эвгенола и изоэвгенола с галогенэтиламинами в щелочной среде.

В щелочной среде эвгенол и изоэвгенол с хлорацетамидами образует 2-метокси-4-алкенил-феноксиацетамиды, амидо группа которых может быть селективно восстановлена алюмогидридом лития:

$$-\mathrm{CON(R)_2} \xrightarrow{\mathrm{LiAlH_4}} -\mathrm{CH_2}-\mathrm{N(R)_2}$$

2'-(3-метокси-4-гидроксифенил)-изопропиламины были получены на основе реакции бромистого 2'-(3-метокси-4-гидроксифенил)-изопропила с аминами.

При взаимодействии эвгенола и изоэвгенола с формальдегидом и (первичными или вторичными) аминами, находящаяся в орто-положении по отношению к гидроксильной группе, амино группа фенола метилируется и образуется 2-метокси-4-алкенил-6-аминометилфенол.

Dr. Olga H. Hankovszky
Dr. Kálmán Hideg
Prof. Dr. Gyula Méhes
Pécs, Rákóczi út 2, Hungary

INVESTIGATIONS IN THE FIELD OF RADIATION-INDUCED SOLID STATE POLYMERIZATION, XIV*

THE γ-RADIATION-INITIATED POLYMERIZATION OF ALLYL PALMITATE

GY. HARDY, L. NAGY and F. CSER

(Research Institute for the Plastics Industry, Budapest)

Received August 13, 1965

The solid state polymerization of vinyl monomers containing long-chain aliphatic substituents has been studied on the example of cetyl methacrylate [1] and vinyl laurate [2]. It was found that these monomers polymerize in the solid phase according to linear kinetics, and the rate of polymerization reaches a maximum near the melting point. Contrary to the solid state polymerization of other monomers, radical inhibitors markedly slow down the solid state polymerization of vinyl laurate and cetyl methacrylate. Several papers have been published [3, 4, 5] on the solid state polymerization of vinyl stearate; X-ray diffraction studies have led to the conclusion that in vinyl monomers containing long-chain aliphatic substituents, the vinyl groups are situated in one plane and the monomeric crystal has laminar structure.

Some time ago we tried unsuccessfully to polymerize allyl alcohol and some of its esters by γ-radiation in both the liquid and solid states. We wished to extend now the formerly recognized polymerization promoting effect of long chain aliphatic substituents to allylic compounds which are known to have low tendency for polymerization; for this purpose the radiation-induced polymerization of allyl palmatite was investigated in the liquid and in the solid states.

Experimental

Allyl palmitate monomer was synthesized by direct esterification. After vacuum distillation repeated three times, the melting point was 18—20°C, $n_D^{27} = 1.4440$. The methods used for the study of the polymerization process had been described in an earlier communication [1]. p-Benzoquinone (BQ) and diphenylpicrylhydrazile (DPPH) were recrystallized from benzene. After irradiation, the monomer was extracted with acetone containing 0.1% of BQ. The molecular weights of the polymers were determined cryoscopically in benzene solution. The phase diagram of the solid system BQ-allyl palmitate was determined by polarization microscopy. X-ray diffraction patterns were recorded with pure allyl palmitate and with allyl palmitates containing 3 and 5% of BQ, respectively. The substances were filled into 3 mm diameter Lindemann capillaries, sealed and cooled to −10°. The patterns were recorded by means of a Debye-Scherrer camera with a TUR X-ray test apparatus, for a study of the fine structure; Cu K_α radiation was applied through a Ni filter, using 49 kV exciting voltage and 20 mA exciting current. Exposition time was 3 hours.

* Part XIII*: Magyar Kémiai Folyóirat, in the press.

Results and discussion

Fig. 1 shows the kinetic curves of the gamma-radiation induced solid phase polymerization of allyl palmitate at different temperatures. Fig. 2 represents the same at 0°, up to a high degree of conversion. It can be seen that the kinetic curves of the solid phase polymerization of allyl palmitate have

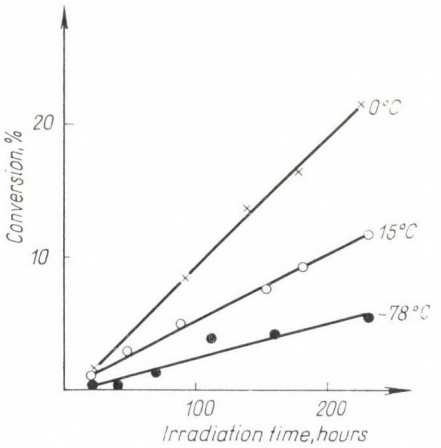

Fig. 1. Kinetic curves of the solid state polymerization of allyl palmitate at different temperatures. Irradiation with a dose rate of 22 500 r/hr.

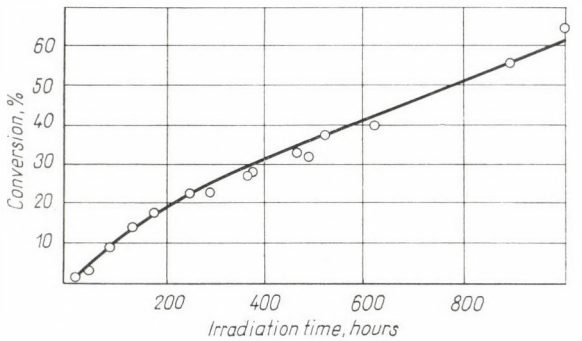

Fig. 2. Kinetic curve of the solid state polymerization of allyl palmitate at 0° up to a high conversion. Irradiation with 22 500 r/hr.

linear character up to 20% conversion. Fig. 3 shows kinetic curves obtained with different dose rates at 0°. These curves indicate that the rate of solid phase polymerization is the function of the 1.0—1.2th power of the dose rate.

The curves in Fig. 4 are the kinetic curves of liquid phase polymerizations at different temperatures. Here, too, the curves indicate a linear relationship. Fig. 5 shows the temperature dependence of the polymerization rates measured

at different temperatures. Also in the case of allyl palmitate, the rate of polymerization in the solid state becomes higher near the melting point. The maximum was observed by about 20° below the melting point, at 0°. Differential thermoanalytical measurements did not indicate a second order transition

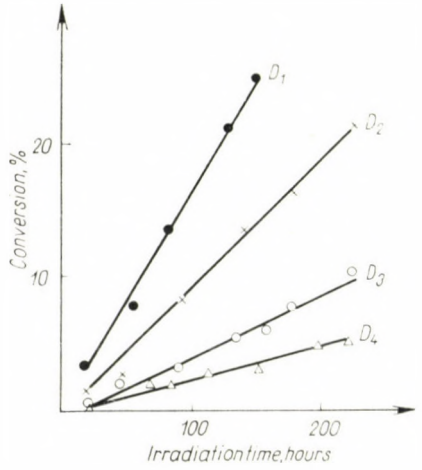

Fig. 3. Kinetic curves of the solid state polymerization of allyl palmitate at 0° when irradiated with various dose rates. $D_1 = 48\,000$ r/hr, $D_2 = 22\,500$ r/hr., $D_3 = 14\,500$ r/hr., $D_4 = 9\,300$ r/hr.

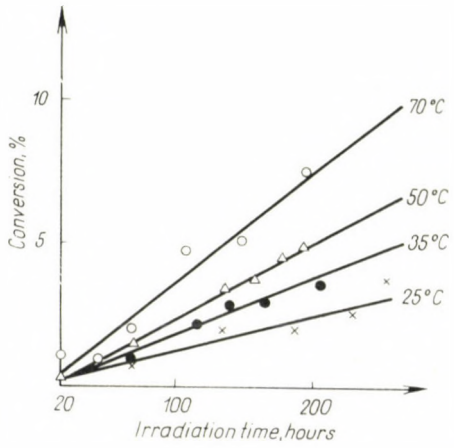

Fig. 4. Kinetic curves of the polymerization of allyl palmitate in the liquid phase at various temperatures. Irradiation with 22 500 r/hr.

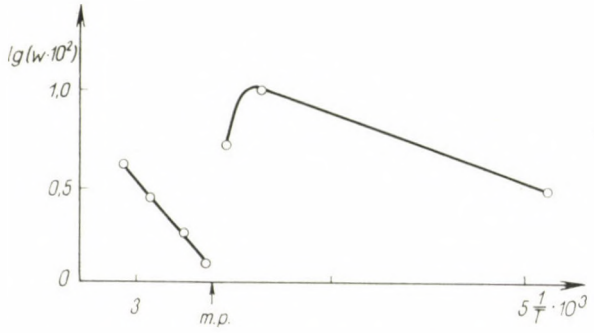

Fig. 5. Temperature dependence of the rate of polymerization of allyl palmitate. Irradiation with 22 500 r/hr.

point at this temperature. The overall activation energy of the liquid phase polymerization was 5.16 kcal/mole, the overall activation energy 1.67 kcal/mole, respectively, calculated from the data obtained at 0° and −78°.

The average molecular weights of the polymers obtained in the solid state at different temperatures are shown in Fig. 6 as the functions of the conversion, and of the integral dose of irradiation. The effect of the dose rate on

the average molecular weight of the polymers was also studied at 0°, when, however, no deviation could be detected. Fig. 7 shows the changes in the average molecular weights of the polymers formed by liquid phase polymerization at different temperatures as functions of the conversion, and of the integral dose of irradiation. Both series of measurements indicate a rise in the molecular weights of the polymers, whether formed in the solid or in the liquid state, with higher conversions, and with the increase of the integral dose. In the solid state, the temperature dependence of the molecular weight corresponds to

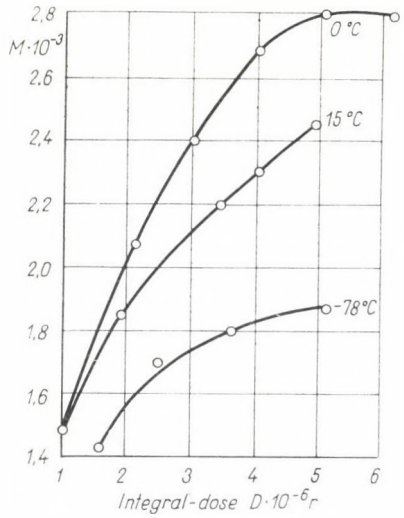

Fig. 6. Molecular weights of polymers formed in the solid state polymerization of allyl palmitate as the functions of temperature and of the integral dose of irradiation. Irradiation with 22 500 r/hr.

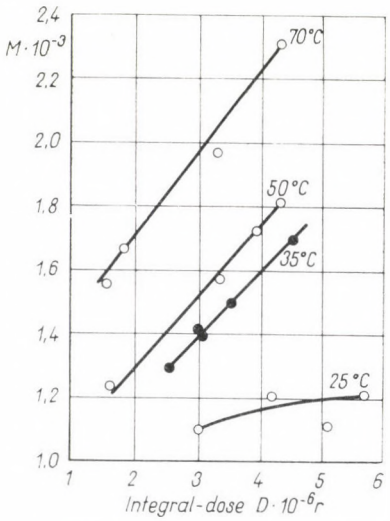

Fig. 7. Molecular weights of polymers formed in the liquid phase polymerization of allyl palmitate as the functions of temperature and the integral dose of irradiation. Irradiation with 22 500 r/hr.

the temperature dependence of the polymerization rate, that is to say, at 0° the molecular weight of the polymers reaches a maximum, just as there is a maximum in the rate of the solid state polymerization at this temperature. In the liquid phase, the molecular weights of the polymers increase parallel to the increase of the temperature of polymerization. The molecular weight of the polymers formed in the solid state is higher than of those formed in the liquid phase, and the dependence in the solid state approaches a limit value which, when expressed as the degree of polymerization, corresponds to approximately $P = 10$. This fact indicates that the degradative chain transfer known from the free radical liquid phase polymerization of allyl compounds, is in operation in the solid state polymerization, too.

Owing to this circumstance, it was possible to determine G_{init} indirectly. If we assume that degradative chain transfer is the principal reaction terminating the polymer chain, then it is probable that each radical which initiates polymerization gives rise to one polymer molecule. Thus, if $G_{polymer}$ and the average degree of polymerization are known, the value of G_{init} can be calculated. The G_{init} values calculated from the molecular weights pertaining to 5% conversions are presented in Table I as the functions of the dose rate and reaction temperature. The data clearly show the changes of the G_{init} values with temperature in both the liquid and solid states; in the solid state the highest value was obtained at 0°, while in the liquid phase G_{init} increases monotonously with the rise of the temperature.

Table I

Changes in the G_{init} values in the gamma-radiation induced solid state polymerization of allyl palmitate as the functions of temperature and the dose rate

Temperature °C	Dose rate r/hr,	$G_{init.}$ radical/100 eV
0	48 000	19.5
0	22 500	22.9
0	14 500	16.1
0	9 330	15.7
15	22 500	12.3
—78	22 500	5.9
70	22 500	8.8
50	22 500	6.1
35	22 500	5.9
25	22 500	4.8

Fig. 8 shows the kinetic curves of the solid state polymerization of allyl palmitate in vacuum (curve A) and in the presence of oxygen (air, curve B). It can be seen that in the presence of oxygen the first stage of the polymerization proceeds more slowly than in oxygen-free system, but after about 3—4% conversion the two kinetic curves run parallel to each other. No difference was observed between the infrared spectra and average molecular weights of the polymers obtained in the two series of experiments.

The radiation-induced solid state polymerization of allyl palmitate — similarly to the polymerization of other monomers containing long-chain aliphatic substituents — can be easily retarded by the addition of a relatively small quantity of some inhibiting agent.

Fig. 9 shows the decrease of the rate of solid state polymerization as a function of the concentration of BQ (curve A) and DPPH (curve B). After the addition of not more than 0.1% of inhibitor, the rate of solid state polymerization is reduced to about one-fourth of the initial value with BQ, and to about one half with DPPH; additional quantities of the inhibitors effect practically no further changes. The kinetic curves in Fig. 10 represent the solid state polymerization of allyl palmitate without inhibitor (curve A), in the presence of 0.1 (0.27 mole) of BQ (curve B), and 3.0% (7.6 mole) of BQ (curve C). In the presence of the inhibitor, hardly any polymer is formed in the initial stage of the polymerization, and polymer formation begins only

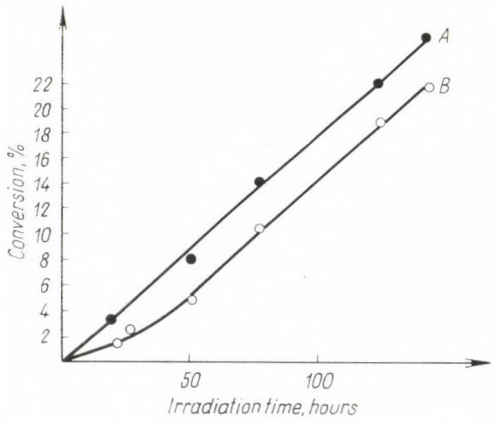

Fig. 8. Kinetic curves of the solid state polymerization of allyl palmitate at 0°. Irradiation with 48 100 r/hr. Curve *A*: in the absence of air. Curve *B*: in the presence of air

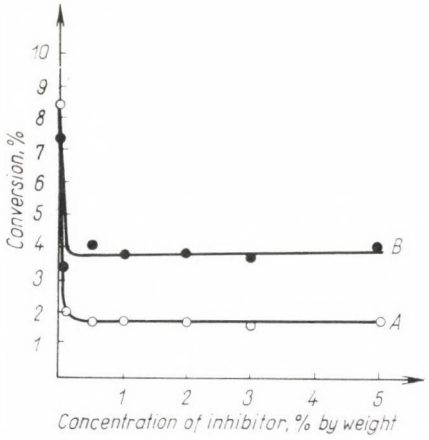

Fig. 9. Changes in the conversion of the solid phase polymerization of allyl palmitate at 0° as the function of inhibitor concentration. Irradiation with 48 100 r/hr. Curve *A*: p-benzoquinone; irradiation for 50 hrs. Curve *B*: diphenylpicrylhydrazile; irradiation for 45 hrs.

after relatively long irradiation, but even then the quantity formed is much smaller than in the system which contains no inhibitor. We have pointed out in our earlier communication [6] that the effect of inhibiting agents on solid state polymerizations cannot be evaluated without a knowledge of the phase diagram of the monomer-inhibitor system. We have therefore determined the phase diagram of the system allyl palmitate-p-benzoquinone (Fig. 11) which clearly shows the formation of an extreme eutectic containing 7.6 mole% of BQ and melting at 14°. In the case of vinyl laurate, we have suggested the hypothesis [2] that the action of inhibitors might be explained here and in similar cases with the bundle-like structural arrangement of the monomer molecules, and with the fact that the inhibitor is practically concentrated near the polar groups (*i.e.*, around the vinyl groups) of the monomer which are

capable of polymerization. This hypothesis may be regarded as experimentally confirmed by our X-ray diffraction studies of the structure of pure allyl palmitate and of the monomer-BQ solid system. The three strongest lines on the X-ray diffraction pattern were: $d_1 = 4.13$ Å (intensity 100%), $d_2 = 3.68$ Å (intensity 40%) and $d_3 = 12.2$ Å (intensity 10%). The other lines were hardly discernible from the basic blackness. The X-ray diffraction patterns of the pure material and of an allyl palmitate containing 7.6% of BQ (eutectic mixture) were practically identical, only one new line appeared at $d \sim 5.5$ Å which agrees with the second strongest line of BQ. On the X-ray diffraction pattern

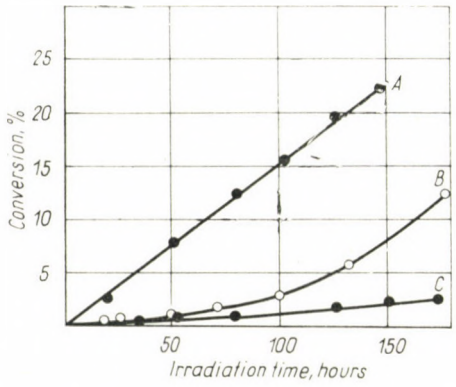

Fig. 10. Kinetic curves of the solid state polymerization of allyl palmitate at 0°. Irradiation with 44 000 r/hr. Curve *A*: pure monomer. Curve *B*: 0.1% of BQ. Curve *C*: 3.0% of BQ

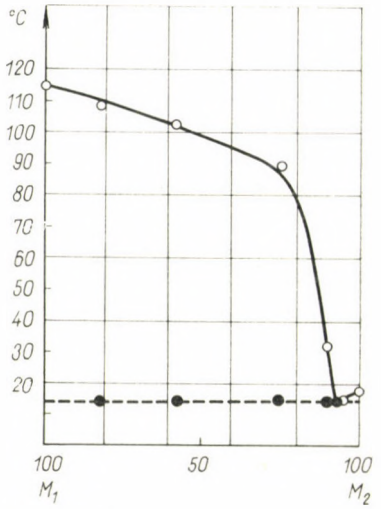

Fig. 11. Phase diagram of the system allyl palmitate (M_2) and p-benzoquinone (M_1)

of the mixture containing 5% BQ, the lines of pure allyl palmitate are visible with unchanged Bragg angles, in addition to five new lines which agree with the five strongest lines of BQ. The two strongest lines agree with the two strongest lines of vinyl stearate, consequently allyl palmitate has also a crystal structure which does not differ from that of vinyl stearate.

Comparison of the phase diagram (Fig. 11) with the results of X-ray diffraction studies allows the assumption that the BQ crystals are present in the eutectic in a very fine distribution, in contact with the plane of the allyl groups of the allyl palmitate layers. Such an arrangement might be highly advantageous for displaying an inhibiting action, and it might explain the extraordinarily great effect of inhibitors on the course of the solid state poly-

merization; in fact, this effect is unparalleled in the solid state polymerization of monomers of other character.

These results may also provide evidence for a very high mobility of the inhibitor molecules which are in contact with the plane of the allyl groups, *e.g.*, in the case of 0.1 of BQ, when there are about 370 allyl palmitate molecules present for each inhibitor molecule, and nevertheless a significant inhibiting effect is displayed.

The above experimental facts (allylic degradative chain transfer in the solid state process, and the inhibiting action of radical inhibitors) provide also unequivocal evidence for the radical mechanism of the solid phase process. Since radical inhibitors display an inhibiting effect on the liquid phase process, thus the latter must proceed also according to radical mechanism.

The X-ray diffraction pattern of the polymers has a maximum at 4.18 Å. Similar results were obtained for polyvinyl stearate [5] and for the polymers of acrylate and methacrylate derivatives containing long hydrocarbon side chains [7, 8]. This is a structure similar to that of pure paraffins, and corresponds to the identicity period of aliphatic side chains. The scale model of the poly (allyl palmitate) molecule shows that the polymer has very probably a syndiotactic structure.

SUMMARY

The kinetic character of the radiation polymerization of allyl palmitate is linear in both the solid and the liquid states. The rates of polymerization in the solid state represented as functions of the temperature, show a maximum near the melting point. Degradative chain transfer which is characteristic of allylic compounds, plays a part in both the liquid and solid state polymerizations. Polymerization proceeds in both phases according to radical mechanism, as it is proved unequivocally by the effectiveness of radical inhibitors. The system p-benzoquinone-allyl palmitate has an extreme eutectic when containing 7.6 mole % of p-benzoquinone. On basis of the results of X-ray diffraction studies, an interpretation is presented to account for the particular activity of radical inhibitors in the solid state polymerization of monomers containing long-chain aliphatic substituents.

REFERENCES

1. Hardy, Gy., Nyitrai, K., Kovács, G., Fedorova, N.: Magyar Kém. Foly. **69,** 437 (1963); Acta Chim. Hung. **43,** 121 (1965).
2. Hardy, Gy., Nyitrai, K., Varga, J., Patkó, M.: Magyar Kém. Foly. **71,** 175 (1965).
3. Mesrobian, R., Morawetz, H., Ballantine, D., Dienes, J., Metz, D.: J. Am. Chem. Soc. **78,** 2939 (1956).
4. Burlant, W., Adicoff, A.: J. Polymer. Sci. **28,** 269 (1958).
5. Morawetz, H.: Am. Chem. Soc. Polymer Preprints **5,** 975 (1964).
6. Hardy, Gy., Varga, J., Cser, F., Detrekőy, E.: Magyar Kém. Foly., in the press.
7. Kaufman, H. S., Sacher, A., Alfrey, T., Faukuchen, I.: J. Am. Chem. Soc. **70,** 3147 (1948).
8. Greenberg, S. A., Alfrey, T.: J. Am. Chem. Soc. **76,** 6280 (1954).

Untersuchungen über strahlenchemische Polymerisation in fester Phase, XIV

Die mit Gammastrahlen initiierte Polymerisation von Allylpalmitat

G. HARDY, L. NAGY und F. CSER

Zusammenfassung. Die Kinetik der strahlenchemischen Polymerisation von Allylpalmitat weist in flüssiger und fester Phase einen linearen Charakter auf. Die Polymerisationsgeschwindigkeiten zeigen ein Maximum in Abhängigkeit von der Temperatur in fester Phase beim Schmelzpunktgebiet. Eine charakteristische, für die Allylverbindungen degradative Kettenübertragung, kommt ebenso in flüssiger, wie in fester Phase zur Geltung. Der Mechanismus der Polymerisation läuft in beiden Phasen radikalisch ab, was durch die Wirksamkeit der Inhibitoren von radikalartigen Prozessen eindeutig bewiesen wurde. Das feste System von p-Benzochinon und Allylpalmitat zeigt ein Eutektikum bei einem Gehalt von 7,6 mol% p-Benzochinon. Die Resultate der Untersuchungen mit Röntgenstrahlen-Diffraktion ermöglichen die Erklärung der Wirkung der Inhibitoren von radikalartigen Prozessen in fester Phase auf die Polymerisation der Monomeren mit einem langkettigen aliphatischen Substituenten.

Исследования в области радиационной твердофазной полимеризации, XIV

Полимеризация аллилпальмитата, инициированная гамма-лучами

ДЬ. ХАРДИ, Л. НАДЬ и Ф. ЧЕР

Резюме. Кинетика радиационной полимеризации аллилпальмитата в жидком и в твердом состояниях имеет линейный характер. Скорость полимеризации в зависимости от температуры достигает максимальной величины в твердой фазе в области точки плавления. В жидком и в твердом состояниях одинаково наблюдается деградативный перенос цепи, характерный для аллиловых соединений. Механизм полимеризации в обоих состояниях является радикальным, что однозначно доказывается эффективностью действия ингибиторов радикальных процессов. Твердая смесь парабензохинона и аллилпальмитата образует эвтектическую смесь при концентрации пара-бензохинона 7,6 молярных %-ов. Результаты рентгено-диффракционных исследований позволяют объяснить эффективность ингибирующего действия ингибиторов радикальных процессов в случае твердофазной полимеризации мономеров, имеющих длинный алифатический заместитель в молекуле.

Dr. Gyula HARDY
Lajos NAGY
Ferenc CSER

Budapest XIV. Hungária körút 114

ÜBER DIE STRUKTUR UND RINGSTABILITÄT EINIGER O-ACETYLMONOSE-2,4-DINITRO-PHENYLHYDRAZONE

A. Fóti, Á. Gerecs und F. Ruff

(Lehrstuhl für Chemische Technologie der L. Eötvös Universität, Budapest)

Eingegangen am 7. September 1965

In einer unserer früheren Mitteilungen wurde schon beschrieben, daß die Struktur der Monose-arylhydrazone durch die am aromatischen Teil befindlichen Substituenten beeinflußt wird [1, 2]. Es wird nämlich durch die Anwesenheit von elektronenanziehenden Substituenten die Bildung einer Pyranosestruktur begünstigt, während der Gegenfall für die Bildung der offenkettigen, echten Hydrazonstruktur als vorteilhaft gefunden wurde.

In der vorliegenden Mitteilung wurden jene Untersuchungen beschrieben, in welchen der Einfluß einiger Änderungen in dem Pyranoseteil des »Hydrazons« über die Struktur und Stabilität des Pyranoseringes in den Vordergrund gerückt wurde.

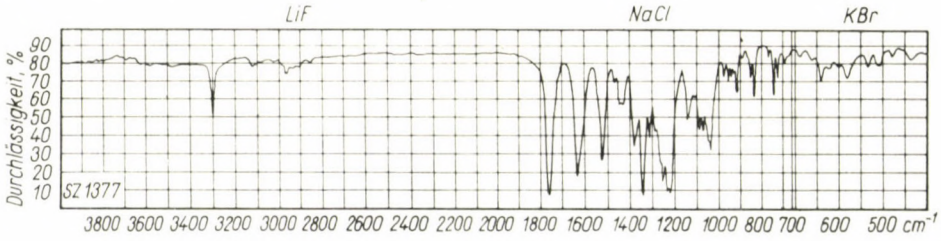

Abb. 1

Zunächst wurde das 2-Desoxy-D-glucose-2,4-dinitro-phenylhydrazon (**I**) dargestellt und dasselbe bei 0° mit Essigsäureanhydrid-Pyridin acetyliert. Es entstand ein O-Tetraacetat des offenkettigen Hydrazons (**II**), dessen Struktur außer Stickstoff- und Acetylbestimmung auch durch ultraviolette (Tab. I) und infrarote Absorptionsmessungen (Abb. 1 und Tab. II) bestätigt wurde. Aus der entsprechenden D-Glucoseverbindung bildete sich demgegenüber unter denselben Umständen das O-Tetraacetat des Glucopyranose »Hydrazons« [3]. Dieser Unterschied zwischen dem Verhalten der D-Glucose- und 2-Desoxy-D-glucoseverbindung kann durch die Pyranosestruktur nicht erklärt werden. Nach Reeves befindet sich in der β-Glucopyranose kein Instabilitätsfaktor, da sämtliche Hydroxylgruppen des Pyranoseringes äquatoriale

Tabelle I

	λ max log ε			λ infl log ε	Lösungsmittel
O-Pentaac.-D-glucose-H*	225 4,14	254 4,05	351 4,35		96%iges Äthanol
O-Tetraac.-D-glucose-H		254 4,01	344 4,23	390 3,85	,,
O-Tetraac.-2-desoxy-D-glucose-H (**II**)	255 4,13	252 4,03	354 4,32		,,
O-Tetraac.-6-desoxy-D-glucose-H (**V**)	222 4,13	256 4,02	352 4,29		,,
O-Triac.-6-desoxy-D-glucose-H (**IV**)		260 3,98	344 4,20	390 3,81	,,
O-Tetraac.-6-desoxy-6-nitro-D-glucose-H (**VIII**)	217 4,20	253 4,01	353 4,28		,,
		259 4,07	351 4,32	400 3,90	Chloroform
O-Triac.-6-desoxy-6-nitro-D-glucose-H (**VII**)		263 4,01	339 4,20	385 3,78	,,
O-Tetraac.-6-O-methyl-D-glucose-H (**XI**)		257 4,06	351 4,35	400 3,86	,,
O-Triac.-6-O-methyl-D-glucose-H (X)		262 4,01	340 4,22	384 3,90	,,

H* = 2,4-dinitro-phenylhydrazon

Stellung besitzen und auch die β-Konfiguration die Ringstruktur begünstigt [4]. In derselben Weise befindet sich natürlich auch in der 2-Desoxy-D-glucopyranose kein Instabilitätsfaktor. Die Ursache des verschiedenen Verhaltens der betreffenden Monosehydrazone kann also nur in der mit der Pyranoseform im Gleichgewicht befindlichen offenkettigen Form gefunden werden. In der Grenzform der offenkettigen Struktur, in der das Glucosemolekül in gestreckter Form besteht, befinden sich die Sauerstoffe der Kohlenstoffatome 2, 3 und 4 so sehr eng beieinander (Abb. 2), daß durch die zwischen denselben wirkende abstoßende Kraft eine gekrümmte bzw. eine Pyranoseform begünstigt wird. Mit dieser Erklärung wird auch der Unterschied zwischen dem Verhalten des D-Glucose- und 2-Desoxy-D-glucose-2,4-dinitro-phenylhydrazons verständlich. In der letzteren Verbindung besteht durch Ersatz der Hydroxylgruppe des Kohlenstoffatomes 2 durch Wasserstoff schon eine bedeutend schwächere abstoßende Kraft im Raum der Kohlenstoffatome 2, 3 und 4, demzufolge

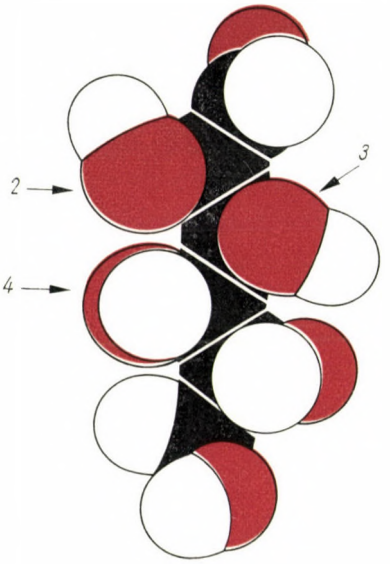

Abb. 2

Tabelle II

	NH-Bänder, cm^{-1}
O-Pentaac.-D-glucose-H*	3290
O-Tetraac.-D-glucose-H	3250, 3360
O-Tetraac.-2-desoxy-D-glucose-H (**II**)	3300
O-Tetraac.-6-desoxy-D-glucose-H (**V**)	3300
O-Triac.-6-desoxy-D-glucose-H (**IV**)	3278, 3310, 3340, 3355
O-Tetraac.-6-desoxy-6-nitro-D-glucose-H (**VIII**)	3300
O-Triac.-6-desoxy-6-nitro-D-glucose-H (**VII**)	3290, 3322, 3355, 3372
O-Tetraac.-6-O-methyl-D-glucose-H (**XI**)	3300
O-Triac.-6-O-methyl-D-glucose-H (**X**)	3300**, 3362

* H = 2,4-dinitro-phenylhydrazon
** Breite, undeutliche Bänder

die Existenzfähigkeit einer offenkettigen Form schon gegeben ist. Dieser Fall bildet einen direkten Beweis für jene fast selbstverständliche Annahme, wonach die hohe Ringstabilität der Glucopyranose nicht nur durch die Abwesenheit von Instabilitätsfaktoren in der Pyranoseform, sondern auch durch die Anwesenheit solcher Faktoren in der offenkettigen Grenzform zu erklären ist. Können letztere teilweise beseitigt werden, wie dies bei 2-Desoxy-D-glucose der Fall ist, so besitzt die offenkettige Form die höhere Stabilität.

Es wurde in einer unserer früheren Untersuchungen bewiesen, daß der Pyranosering im D-Glucose-2,4-dinitro-phenylhydrazon höhere Stabilität besitzt als in demselben Hydrazon der D-Xylose [5]. Infolge der Ähnlichkeit der Konformation von D-Glucose und D-Xylose ist die Ursache der höheren Ringstabilität nur beim Kohlenstoffatom 6 zu suchen. Zwecks Sammeln von diesbezüglichen Angaben wurden folgende Untersuchungen durchgeführt.

Es wurden von uns 6-Desoxy-(**III**), 6-Desoxy-6-nitro-(**VI**) und 6-O-Methyl-D-glucose-2,4-dinitro-phenylhydrazon (**IX**) dargestellt. Diese Hydrazone wurden bei 0° mit Essigsäureanhydrid-Pyridin acetyliert und festgestellt, daß alle drei O-Acetate eine Ringstruktur besitzen (**IV**, **VII**, **X**). Bei der 6-Desoxy-6-nitro-D-glucoseverbindung wurde festgestellt, daß ein O-Acetat von einer Ringstruktur (**VII**) sich nur aus dem Kristalläthanol enthaltenden Hydrazon bildete, wogegen aus dem äthanolfreien Hydrazon ein offenkettiges O-Acetat (**VIII**) anfiel. Die Struktur ließ sich außer Stickstoffbestimmung durch ultraviolette (Tab. I) und infrarote Absorption beweisen. Die Daten der NH-Frequenzen sind in Tab. II angegeben. Gleichzeitig wurden in dieser Tabelle die Daten der NH-Frequenzen der offenkettigen O-Acetylhydrazone und der beiden O-Acetylhydrazone der D-Glucose angeführt. Als

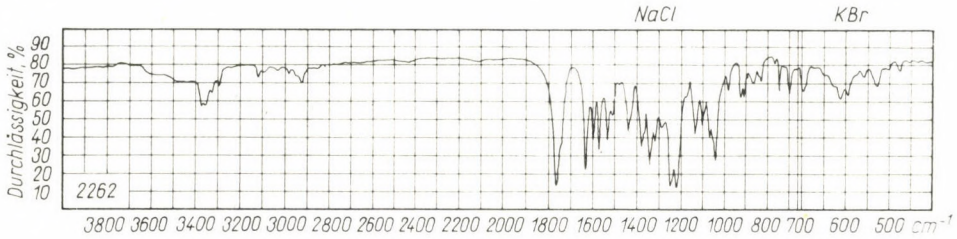

Abb. 3

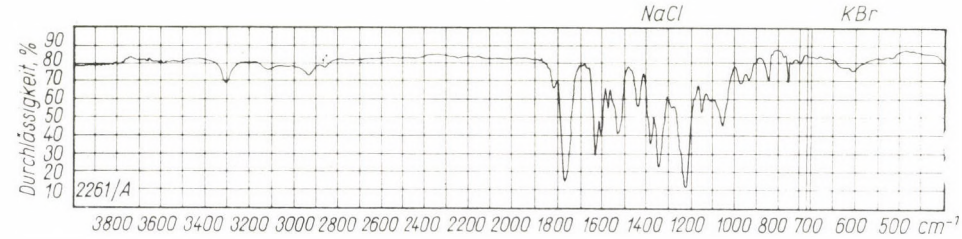

Abb. 4

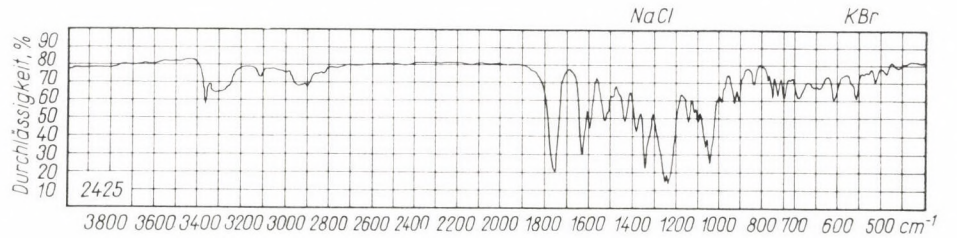

Abb. 5

Beispiele für die infrarote Absorption wurden die Aufnahmen folgender 2,4-Dinitro-phenylhydrazone angegeben:

O-Triacetyl-6-desoxy-6-nitro-D-glucose-	(Abb. 3)
O-Tetraacetyl-6-desoxy-6-nitro-D-glucose-	(Abb. 4)
O-Triacetyl-6-O-methyl-D-glucose-	(Abb. 5)
O-Tetraacetyl-6-O-methyl-D-glucose-	(Abb. 6)

Es wurde von uns schon früher beschrieben, daß die O-Acetyl-monose-hydrazone mit einer Pyranosestruktur durch Acetylieren bei etwa 100° in die O-Acetate der offenkettigen, echten Hydrazone umgewandelt werden können und weiters, daß die Geschwindigkeit dieser Umwandlung verfolgt und dadurch die relative Ringstabilität des betreffenden Pyranoseringes bestimmt werden kann. Aus den oben genannten O-Acetylhydrazonen mit

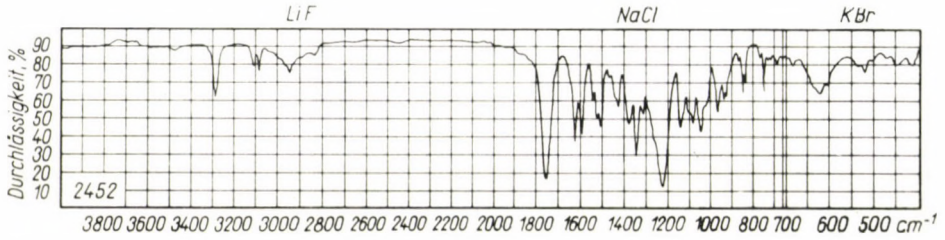

Abb. 6

Pyranosestruktur ließ sich nur die Geschwindigkeit der Ringspaltung des O-Triacetyl-6-desoxy-D-glucopyranose-2,4-dinitro-phenylhydrazons mit den entsprechenden Verbindungen von D-Glucose und D-Xylose vergleichen, da das Reaktionsgemisch des 6-Desoxy-6-nitroderivates sich während der Acetylierung bei 70—100° so intensiv färbt, daß die Reaktion durch das Drehvermögen nicht verfolgt werden konnte, während sich aus dem 6-O-Methylderivat eine Verbindung von unbekannter Struktur neben dem offenkettigen O-Acetylhydrazon bildete und so auch diese Ringspaltung für die betreffenden kinetischen Messungen ungeeignet war.

Entgegen unserer früheren Methode [5] wurde die Geschwindigkeit der Ringspaltung in einem Gemisch von Essigsäureanhydrid und Eisessig in Gegenwart von Natriumacetat bei 100° gemessen. Wir beobachteten nähmlich, daß bei der Ringspaltung mit Essigsäureanhydrid schon durch geringe Mengen Essigsäure die Reaktionsgeschwindigkeit beträchtlich erhöht wird, wodurch die Reproduzierbarkeit gefährdet wurde. Bei der Anwendung eines Gemisches von 75 Vol.% Essigsäureanhydrid und 25 Vol.% Eisessig ist eine kleine Schwankung des Essigsäuregehaltes auf die Reaktionsgeschwindigkeit ohne Einfluß. Andererseits wurden mit diesem Reaktionsgemisch die sekundären Reaktionen soweit beseitigt, daß die durch das spezifische Drehvermögen direkt erhaltene Halbierungszeit als Maß der relativen Ringstabilitäten betrachtet werden konnte.

Die Resultate dieser Untersuchungen sind in den folgende Tabellen III—V zusammengefaßt.

Tabelle III

0,2003 g O-Triac.-D-xylopyranose-2,4-dinitro-phenylhydrazon, 0,1002 g wasserfreies Natriumacetat, 15 ml Essigsäureanhydrid, 5 ml Eisessig, 100°. Reaktionsprodukt: O-Tetraac.-D-xylose-2,4-dinitro-phenylhydrazon.

Zeit, Min.	0	30	60	120	240	360
$[\alpha]_D^{20}$	−18°	+42°	+58°	+66°	+68°	+68°

Graphisch bestimmte Halbierungszeit 21 Min.

Tabelle IV

0,2000 g O-Tetraac.-D-glucopyranose-2,4-dinitro-phenylhydrazon, 0,0999 g wasserfreies Natriumacetat, 15 ml Essigsäureanhydrid, 5 ml Eisessig, 100°. Reaktionsprodukt: O-Pentaac.-D-glucose-2,4-dinitro-phenylhydrazon.

Zeit, Min.	0	60	120	240	360	480
$[\alpha]_D^{20}$	+4°	+40°	+53°	+69°	+76°	+77°

Graphisch bestimmte Halbierungszeit 63 Min.

Tabelle V

0,1002 g O-Triac.-6-desoxy-D-glucopyranose-2,4-dinitro-phenylhydrazon, 0,502 g wasserfreies Natriumacetat, 7,5 ml Essigsäureanhydrid, 2,5 ml Eisessig, 100°. Reaktionsprodukt: O-Tetraac.-6-desoxy-D-glucose-2,4-dinitro-phenylhydrazon.

Zeit, Min.	0	60	120	180	240	480	720	840
$[\alpha]_D^{20}$	+2°	+27°	+39°	+46°	+52,5°	+69°	+76°	+77°

Graphisch bestimmte Halbierungszeit 120 Min.

Betrachtet man beim Vergleich der Halbierungszeiten die Xyloseverbindung als Grundsubstanz, so erhöhen die betreffenden Substituenten am Kohlenstoffatom 5 die Stabilität des Pyranoseringes in folgender Reihenfolge: $H < CH_2OOCCH_3 < CH_3$. Die einfachste Erklärung dieser Reihenfolge kann derart formuliert werden, daß durch die elektronenabstoßenden Substituenten des Kohlenstoffatomes 5 die Stabilität des betreffenden Pyranoseringes erhöht wird.

Im vorstehenden wurde darauf hingewiesen, daß bei der Acetylierung von O-Triacetyl-6-O-methyl-D-glucose-2,4-dinitrophenylhydrazon bei etwa 100° neben dem O-Tetraacetat des offenkettigen Hydrazons auch ein Nebenprodukt (**XII**) von unbekannter Struktur erhalten wurde. Die bisherigen infraroten Absorptionsuntersuchungen weisen dahin, daß dieses Nebenprodukt strukturell mit jenen Verbindungen von unbekannter Struktur identisch ist, welche aus O-Acetyl-D-glucopyranose-, -D-xylopyranose- und -D-mannopyranose-2,4-dinitro-phenylhydrazon mit Pyridin enthaltendem Essigsäureanhydrid von uns erhalten wurden [6].

Beschreibung der Versuche

2-Desoxy-D-glucose-2,4-dinitro-phenylhydrazon (I).

Das Reaktionsgemisch von 1,64 g 2-Desoxy-D-glucose, 1,98 g 2,4-Dinitro-phenylhydrazin und 100 ml abs. Äthanol wurde 14½ Stunden unter Rückfluß gekocht, abgekühlt und danach sofort filtriert: 2,30 g hell-orangegelbe nadelförmige Kristalle, Schmp. 171—172°. Die Substanz wurde ½ Stunde mit 26 ml siedendem Äthanol behandelt und nach dem Abkühlen filtriert: 2,04 g, Schmp. 172—173°.

$C_{12}H_{16}O_8N_4$ (344,290). Ber. N 16,27%. Gef. N 16,24; 16,37%.

O-Tetraacetyl-2-desoxy-D-glucose-2,4-dinitro-phenylhydrazon (II).

a) 0,50g Hydrazon **I** wurden bei 0° mit 2,8 ml Pyridin und 2,4 ml Essigsäureanhydrid acetyliert: 0,72 g. Schmp. 140—143°. Aus Methanol zweimal (30 bzw. 27 ml) umkristallisiert; 0,574 g, Schmp. 146—148°, $[\alpha]_D^{20} = +26{,}8°$ (Chloroform, c = 0,670).

$C_{20}H_{24}O_{12}N_4$ (512,444). Ber. N 10,93%; Acetyl 33,60%. Gef. N 10,87; 10,88% Acetyl: 33,74; 33,56%.

b) Es wurde durch Acetylieren von 0,50 g Hydrazon **I** mit 3 ml Essigsäureanhydrid, 0,50 g wasserfr. Natriumacetat bei 100° (3 Stdn.) dieselbe Verbindung erhalten: 0,488 g zweimal umkristallisierte Substanz, Schmp. 146—147°, $[\alpha]_D^{20} = +27{,}7°$ (Chloroform, c = 492).

6-Desoxy-D-glucose-2,4-dinitro-phenylhydrazon (III).

Das Reaktionsgemisch von 0,1 g 6-Desoxy-D-glucose, 0,12 g 2,4-Dinitro-phenylhydrazin und 5 ml abs. Äthanol wurde 14 Stunden unter Rückfluß gekocht. In der 10. Stunde entstand eine klare Lösung, in der 11. Stunde begann die Ausscheidung des Produktes: 0,19 g Rohprodukt, aus Äthanol umkristallisiert: Schmp. 178°, $[\alpha]_D^{20} = -5{,}02°$ (Pyridin—Methanol = 1 : 1, c = 0,99).

$C_{12}H_{16}O_8N_4$ (344,292). Ber. N 16,27%. Gef. N 16,33; 16,30%.

O-Triacetyl-6-desoxy-D-glucose-2,4-dinitro-phenylhydrazon (IV).

3,00 g entsprechendes Hydrazon wurden mit Essigsäureanhydrid-Pyridin (30—30 ml) bei 0° (16 Stunden) acetyliert. 4,09 g, Schmp. 198°, aus 490 ml abs. Äthanol umkristallisiert (aktive Kohle): 3,62 g, Schmp. 200°, $[\alpha]_D^{20} = +2{,}90$ (Chloroform, c = 1,04). Nach der zweiten Kristallisation blieben Schmp. und $[\alpha]_D$ unverändert.

$C_{18}H_{22}O_{11}N_4$ (470,406). Ber. N 11,91%. Gef. N 11,67; 11,71%.

O-Tetraacetyl-6-desoxy-D-glucose-2,4-dinitro-phenylhydrazon (V).

a) 0,3 g entsprechendes Hydrazon wurden mit 1,5 ml Essigsäureanhydrid und 0,3 g wasserfreiem Natriumacetat auf dem siedenden Wasserbad acetyliert (3 Stunden). Auf Eiswasser gegossen wurde amorphes Tetraacetat erhalten, welches nach 24stündigem Stehen bei 0° titriert wurde: 0,4 g, sintert bei 60—75°, $[\alpha]_D^{20} = +83{,}0°$ ($CHCl_3$, c = 1,00). Das Rohprodukt wurde in 4 ml Eisessig gelöst, die Lösung mit aktiver Kohle behandelt, in Eiswasser gegossen und der amorphe Niederschlag filtriert: 0,32 g, sintert bei 68—79°, $[\alpha]_D^{20} = +93{,}1°$ ($CHCl_3$ c = 1,02).

$C_{20}H_{24}O_{12}N_4$ (512,444). Ber. N 10,93%. Gef. N 10,99; 11,04%.

b) 0,2 g O-Triacetyl-6-desoxy-D-glucose-2,4-dinitro-phenylhydrazon in 1 ml Essigsäureanhydrid wurden 5 Stunden auf dem siedenden Wasserbad erwärmt. Aufgearbeitet wie unter *a)* wurden 0,18 g amorphes Tetraacetat erhalten. Gef. N 10,82; 10,86%. 0,047 g des Rohproduktes wurden in 4 ml Eisessig gelöst und die Lösung in Eiswasser gegossen: 0,032 g amorphes Tetraacetat, sintert bei 65—77°, $[\alpha]_D^{20} = +95{,}9°$ ($CHCl_3$, c = 0,49). Gef. N 10,95%.

6-Nitro-6-desoxy-D-glucose-2,4-dinitro-phenylhydrazon (VI).

Das Reaktionsgemisch von 4,0 g 6-Nitro-6-desoxy-D-glucose, 3,8 g 2,4-Dinitro-phenylhydrazin und 100 ml abs. Äthanol wurde 11 Stunden unter Rückfluß gekocht und am nächsten Tag das Reaktionsprodukt filtriert: 3,65 g, Schmp. 174°, $[\alpha]_D^{20} = +1{,}03°$ (Pyridin, c = 0,97). Aus der auf 30 ml eingeengten Mutterlauge wurden noch 1,15 g (Schmp. 140—155°) und nach 24 Stdn 1,1 g (Schmp. 140—165°) erhalten. Die erste Fraktion (3,65 g) wurde aus 190 ml abs. Äthanol (mit akt. Kohle) umkristallisiert: 2,4 g, Schmp. 172—174°; aus der auf 40 ml eingeengten Mutterlauge 0,5 g, Schmp. 170—172°. Nach der zweiten Kristallisierung: Schmp. 173—175°.

$C_{12}H_{15}O_{10}N_5$ (389,292). Ber. N 17,99%. Gef. N 17,85; 17,95%.

Die zweite Fraktion des Hydrazons (1,15 g) wurde in 20 ml abs. Äthanol (mit akt. Kohle) umkristallisiert: 0,83 g, Schmp. 162°. Nach dem dritten Umkristallisieren Schmp. 164°.

Ber. N, mit 1 Mol Kristalläthanol: 16,08%. Gef. N 16,28; 16,24%. Nach Trocknen bei 100° und 10 Torr (10 Stunden): Gewichtsverlust: 10,6%; Gef. N 17,87; 17,97%.

O-Triacetyl-6-nitro-6-desoxy-D-glucose-2,4-dinitro-phenylhydrazon (VII).

0,3 g ein Kristalläthanol enthaltendes 6-Nitro-6-desoxy-D-glucose-2,4-dinitro-phenylhydrazon (Schmp. 164°) wurden mit 3 ml Essigsäureanhydrid und 0,18 ml Pyridin bei 0° acetyliert (16 Stunden): 0,36 g, Schmp. 202°. Aus 16 ml Dichloräthan umkristallisiert: 0,27 g, Schmp. 223°, $[\alpha]_D^{20} = -33{,}5°$ (Pyridin, c = 0,655). Beim zweiten Umkristallisieren blieb Schmp. und $[\alpha]_D$ unverändert.

$C_{18}H_{21}O_{13}N_5$ (515,406). Ber. N 13,58%. Gef. N 13,57; 13,60%.

O-Tetraacetyl-6-nitro-6-desoxy-D-glucose-2,4-dinitro-phenylhydrazon (VIII).

0,3 g kein Kristalläthanol enthaltendes 6-Nitro-6-desoxy-D-glucose-2,4-dinitro-phenylhydrazon (Schmp. 175°) wurden mit 3 ml Essigsäureanhydrid und 0,18 ml Pyridin bei etwa 0° (16 Stunden) acetyliert: 0,45 g amorphes O-Tetraacetat, $[\alpha]_D^{20} = +52{,}4°$ (c = 1,01, Chloroform). Das Rohprodukt wurde in 10 ml Eisessig mit aktiver Kohle behandelt, die Lösung in Eiswasser gegossen, der Niederschlag zentrifugiert, gewaschen und getrocknet: 0,13 g amorphe Substanz, $[\alpha]_D^{20} = +51{,}9°$ (c = 0,77, Chloroform).

$C_{20}H_{23}O_{14}N_5$ (557,444). Ber. N 12,56%. Gef. N 12,21; 12,30%.

6-O-Methyl-D-glucose-2,4-dinitro-phenylhydrazon (IX).

Ein Reaktionsgemisch von 0,68 g 6-O-Methyl-D-glucose, 0,6 g 2,4-Dinitro-phenylhydrazin und 12 ml abs. Äthanol wurde 12 Stunden gekocht und dann bis zur Hälfte eingedampft: 0,95 g, Schmp. 52—56°. Aus abs. Äthanol umkristallisiert: 0,65 g, Schmp. 56—59° $[\alpha]_D^{20} = +12{,}2°$ (c = 0,98; Pyridin : Methanol = 1 : 1). Nach weiterem, zweimaligem Umkristallisieren blieb der Schmp. unverändert.

$C_{13}H_{18}O_9N_4$ (374,319). Ber. N 14,96%. Gef. N 14,74; 14,62%.

Aus der Luft nimmt die Substanz Kristallwasser auf. 0,12 g wasserfreie Substanz aus 4 ml Wasser umkristallisiert: 0,092 g, Schmp. 119—121°.

$C_{13}H_{18}O_9N_4.H_2O$ (392,335). Ber. N 14,28%. Gef. N 14,41; 14,44%. Ber. CH_3O 7,91%. Gef. CH_3O 7,87%.

6-O-Methyl-O-triacetyl-D-glucose-2,4-dinitro-phenylhydrazon (X).

1,65 g 6-O-Methyl-D-glucose-2,4-dinitro-phenylhydrazon wurden mit Essigsäureanhydrid-Pyridin (16,5—16,5 ml) bei 0° acetyliert: 2,07 g O-Triacetat, Schmp. 202°; aus 550 ml abs. Äthanol umkristallisiert (akt. Kohle) 1,45 g, Schmp. 204°, $[\alpha]_D^{20} = +10{,}4°$ (c = 1,05, Chloroform). Nach dem zweiten Kristallisieren blieben Schmp. und $[\alpha]_D$ unverändert.

$C_{19}H_{24}O_{12}N_4$ (500,433). Ber. N 11,19%. Gef. N 11,21; 11,20%. Ber. CH_3O 6,20%. Gef. CH_3O 6,19; 6,24%.

6-O-Methyl-O-tetraacetyl-D-glucose-2,4-dinitro-phenylhydrazon (XI).

0,5 g des Triacetates **X** wurden mit 10 ml Essigsäureanhydrid und 0,5 g wasserfreien Natriumacetat bei etwa 100° acetyliert (3 Stunden): 0,5 g Substanz, Schmp. 80—100°, $[\alpha]_D^{20} = +73{,}1°$ (c = 0,505, Chloroform). Aus 4 ml abs. Äthanol umkristallisiert wurden 0,35 g eines aus Nadeln und Blättchen bestehenden Gemisches erhalten, Schmp. 121°. $[\alpha]_D^{20} = +89{,}1°$ (c = 0,505, Chloroform). Nach der zweiten Kristallisation fiel ebenfalls ein Gemisch an, welches dann bei Zimmertemperatur mit 10×3 ml Äther behandelt wurde. Die zurückgebliebenen Blättchen wurden aus 2 ml abs. Äthanol umkristallisiert: 0,104 g, Schmp. 133° (Koffler-Block).

$C_{21}H_{26}O_{13}N$ (542,471). Ber. N 10,32%. Gef. N 10,31; 10,37%.

Der Rückstand der ätherischen Lösung wurde mit 12 ml Äther bei Zimmertemperatur behandelt, die Lösung eingedampft und der Rückstand aus 1 ml abs. Äthanol umkristallisiert: 0,007 g nadelförmige Kristalle (**XII**), Schmp. 175° (Koffler Block).

Wir danken Frau M. BARTA für die wertvolle Hilfe bei der präparativen Arbeit, Frau M. BALOGH für die Mikroanalysen und Frl. I. MÉRŐ für die technische Hilfe.

ZUSAMMENFASSUNG

Es wurde festgestellt, daß sich aus 2-Desoxy-D-glucose-2,4-dinitro-phenylhydrazon durch Acetylieren bei 0° ein offenkettiges O-Acetylhydrazon bildet, während das entsprechende D-Glucosederivat eine Ringstruktur besitzt. Die Ursache dieses Unterschiedes kann nicht mit dem Aufbau des Pyranoseringes, sondern mit der verschiedenen Stabilität der mit den Pyranoseformen im Gleichgewicht befindlichen offenkettigen Formen erklärt werden. Es wurden auch Untersuchungen über die Struktur und relative Ringstabilität von einigen solchen Monosehydrazonen durchgeführt, welche als am Kohlenstoffatom 5 substituierte D-Xylosederivate betrachtet werden können. Es ergab sich, daß diese Substituenten in folgender Reihenfolge die Stabilität des Pyranoseringes im betreffenden Hydrazon erhöhen: $H < CH_2OCOCH_3 < CH_3$.

LITERATUR

1. GERECS, Á., SOMOGYI, F., FÓTI, A.: Acta Chim. Hung. **34,** 113 (1962); Magyar Kém. Foly. **68,** 179 (1962).
2. FÓTI, A., RUFF, F., GERECS, Á.: Magyar Kém. Foly. **70,** 314 (1964).
3. GERECS, A., SOMOGYI, L., KÓNYA, A., BUKOVECZ, M.: Acta Chim. Hung. **30,** 95 (1962); Magyar Kém. Foly. **68,** 492 (1962).
4. REEVES, R. E.: J. Am. Chem. Soc. **72,** 1499 (1950).
5. GERECS, Á., FÓTI, A.: Acta Chim. Hung. **35,** 217 (1963); Magyar Kém. Foly. **69,** 82 (1963).
6. GERECS, Á., FÓTI, A., RUFF, F.: Acta Chim. Hung. **42,** 145 (1964).

Structure and Ring Stability of Some O-Acetyl-monose-2,4-dinitrophenylhydrazones

A. FÓTI, Á. GERECS and F. RUFF

Summary. It was found that on subjecting 2-deoxy-D-glucose-2,4-dinitrophenylhydrazone to acetylation at 0° an O-acetylhydrazone of open-chainstructure is formed, while the corresponding D-glucose derivative has a cyclic structure. This difference cannot be ascribed to the structure of the pyranose ring but rather to differences in the stabilities of aliphatic forms being in equilibrium with the pyranose forms. Experiments were carried out to study the structure and relative ring stability of some monose hydrazones which may be taken into account as C(5)-substituted D-xylose derivatives. The results proved that the mentioned substituents increase the stability of the pyranose ring in the corresponding hydrazone in the order $H < CH_2OCOCH_3 < CH_3$.

Структура и стабильность колец нескольких О-ацетил-моноз-2,4-динитрофенилгидразонов

А. ФОТИ, А. ГЕРЕЧ и Ф. РУФФ

Резюме. Установили, что ацетилированием при 0° из 2-дезокси-D-глюкоз-2,4-динитрофенилгидразона образуется О-ацетилгидразон с открытой цепью, а соответствующие производные D-глюкозы имеют кольцевую структуру. Причина различия не может быть объяснена структурой пиранозового кольца, а объясняется различной стабильностью форм с открытой цепью, находящихся в равновесии с формами пиранозы. Далее, были проведены исследования структуры и относительной стабильности колец таких моноз-гидразонов, которые могут рассматриваться, как производные D-ксилозы, замещенные в C_5. Из результатов вытекает, что указанные выше заместители увеличивают стабильность пиранозового кольца в соответствующем гидразоне в следующем порядке:

$$H < CH_2OCOCH_3 < CH_3.$$

András FÓTI
Prof. Dr. Árpád GERECS
Ferenc RUFF
Budapest VIII. Múzeum körút 6—8.

SYNTHESE CYCLISCHER N-LOSTDERIVATE AUS β-SUBSTITUIERTEN SERINEN, CYSTEIN UND LYSIN

M. SZEKERKE, M. T. KAJTÁR und V. BRUCKNER

(Organisch-Chemisches Institut der L. Eötvös Universität, Budapest)

Eingegangen am 19. Oktober 1965

Unlängst haben wir über die Synthese cytotoxische Gruppen enthaltender Serinderivate berichtet [1]. Die biologische Prüfung dieser Produkte ergab, daß cyclische N.N-Bis-(β-chloräthyl)-phosphorsäureamidester, d. h. N-Lostderivate, die aus stereoisomeren Serinen, Serylserinen und Polyserinen erhältlich waren (z. B. aus Serin **I**), eine erhebliche tumorwachstumshemmende Wirkung aufweisen.

Um den Einfluß des Trägermoleküls auf die biologische Wirkung ein und derselben cytotoxischen Gruppe weiter zu untersuchen, haben wir vor allem die Derivate **III**, **IV** und **V** des früher hergestellten [1] N.O-[(Bis-2-chloräthyl)-amido]-phosphoryl-DL-serins (**I**), bzw. seines Äthylesters (**II**) aufgebaut. Andererseits wurde statt des Sauerstoffatoms ein Schwefel- bzw. Stickstoffatom in den Heteroring eingebaut (**VII** bzw. **VIII**). Verbindung **VII** stellt ein cyclisches Thiophosphorsäurediamid-, Verbindung **VIII** ein cyclisches Phosphorsäuretriamidderivat dar; die letztgenannte Abänderung des Trägermoleküls war zugleich mit der Vergrößerung des Heteroringes verbunden. Die Synthese der letztgenannten beiden Verbindungen (**VII**, **VIII**) wurde auch deshalb angestrebt, weil sie — **VII** als Cysteinderivat, **VIII** als Lysinderivat — eine Kombination der cytotoxischen Gruppe mit nicht-zellfremden Trägermolekülen darstellen.

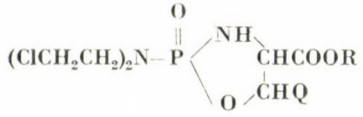

I R = Q = H **II** R = C_2H_5; Q = H
III R = C_2H_5; Q = C_6H_5
IV R = H; Q = C_6H_5
V R = C_2H_5; Q = $CH_2COOC_2H_5$
VI R = $CH_2C_6H_5$; Q = C_6H_5

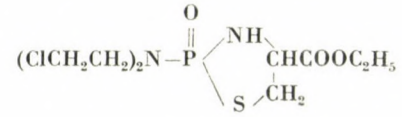

VII

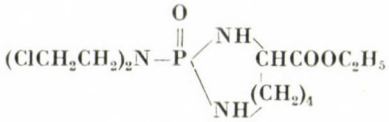

VIII

Die Verbindungen **III**, **V** und **VI** ließen sich aus β-substituierten Serinestern (**X**) mit N.N-Bis-(2-chlor-äthyl)-phosphorsäureamid-dichlorid (**IX**) in Chloroform in Gegenwart von Triäthylamin herstellen:

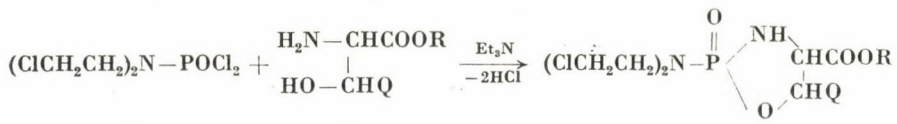

IX **X**

Auf diese Weise wurde zuerst *threo*-, dann auch *erythro*-DL-β-Phenylserinäthylester (**X**: $R=C_2H_5$; $Q=C_6H_5$) umgesetzt, wobei zwei stereoisomere Racemate des Typs **III**, d. h. N.O-[(Bis-2-chlor—äthyl)-amido]-phosphoryl-DL-*threo*-β-phenylserinäthylester (**IIIa**: Carbäthoxy- und Phenylgruppe in *trans*-Stellung) und N.O-[(Bis-2-chlor-äthyl)-amido]-phosphoryl-DL-*erythro*-β-phenylserinäthylester (**IIIb**: Carbäthoxy- und Phenylgruppe in *cis*-Stellung) als gut kristallisierende Produkte (Schmp. 100—102°, bzw. 124—126°)anfielen. In beiden Fällen betrug die Ausbeute rund 52% d. Th. — Durch analogen Umsatz des *threo*- und *erythro*-DL-β-Phenylserinbenzylesters (**X**: $R=C_6H_5CH_2$; $Q=C_6H_5$) konnten zwei stereoisomere Racemate des Benzylesters **VI** (aus *threo*-**X VIa** vom Schmp. 110—111°, aus *erythro*-**X VIb** vom Schmp. 90—91°) gewonnen werden. Hier erreichte die Ausbeute in beiden Fällen rund 80% d. Th. Die Hydrogenolyse von **VIa** lieferte als sehr hygroskopisches Produkt N.O-[(Bis-2-chlor-äthyl)-amido]-phosphoryl-DL-*threo*-β-phenylserin (**IV**).

Obzwar das in den Ring eingebaute Phosphoratom ein zusätzliches Asymmetriezentrum darstellt, konnte bei jedem der oben angeführten Umsätze nur je ein kristallines Racemat gefaßt werden. Diese Produkte erwiesen sich laut chromatographischer Kontrolle als einheitlich. Es bleibt noch zu entscheiden, ob der Ringschluß in bezug auf die Konfiguration des neuen Asymmetriezentrums stereospezifisch verlief, oder ob das zu erwartende zweite Racemat der Beobachtung entfiel.

Von den als Ausgangssubstanzen dienenden *threo*- und *erythro*-DL-β-Phenylserinestern stellten die Äthylester (**X**: $R=C_2H_5$; $Q=C_6H_5$) bereits bekannte Verbindungen dar [2, 3]. Die bisher unbekannten Benzylester (**X**: $R=C_6H_5CH_2$; $Q=C_6H_5$) ließen sich auf folgendem Umweg herstellen: *threo*- bzw. *erythro*-DL-β-Phenylserin (**Xa** bzw. **Xb**; $R=H$; $Q=C_6H_5$) wurde auf übliche Weise N-carbobenzoxyliert, dieses Produkt (*threo*, **XIa**, bzw. *erythro*, **XIb**) in Gegenwart von Triäthylamin in den entsprechenden Benzylester (*threo*, **XIIa**: Schmp. 103—104°; *erythro*, **XIIb**: Schmp. 111—112°) überführt und schließlich die N-Schutzgruppe bei Raumtemperatur mit 35%igem Bromwasserstoff-Dioxan abgespalten. Man erhielt die gut kristallisierenden Hydrobromide **XIII** (*threo*, **XIIIa**: Schmp. 164—165°; *erythro*, **XIIIb**: Schmp. 167°; Misch-Schmp. 159—161°).

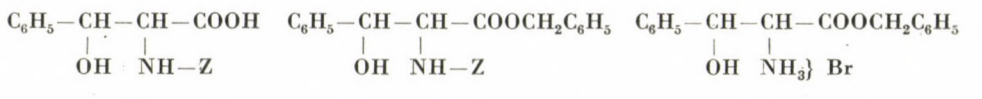

XI **XII** **XIII**

Z = $C_6H_5CH_2OOC$

Als β-substituiertes Serinderivat wurde schließlich DL-*threo*-β-Hydroxyglutaminsäure-diäthylester (**X**: R = C_2H_5; Q = $CH_2COOC_2H_5$) mit N.N-Bis-(2-chlor-äthyl)-phosphorsäureamid-dichlorid (**IX**) umgesetzt, wobei das eine Racemat des Verbindungstyps **V** (R und Q in *cis*-Stellung) anfiel (Schmp. 80—81°).

Durch den üblichen Umsatz von N.N-Bis-(2-chlor-äthyl)-phosphorsäureamid-dichlorid (**IX**) mit L-Cysteinäthylester bzw. DL-Lysinäthylester ließ sich N.S-[(Bis-2-chloräthyl)-amido]-phosphoryl-L-cysteinäthylester (**VII**), bzw. $N^{\alpha}N^{\varepsilon}$-[(Bis-2-chlor-äthyl)-amido]-phosphoryl-DL-lysinäthylester (**VIII**) herstellen. Verbindung **VII** ist ölig, Verbindung **VIII** konnte nur als amorphes Pulver gefaßt werden, doch ließen sich beide Produkte durch Umfällen in analysenreinen Zustand bringen.

Im IR-Spektrum der Verbindung **VIII** (Frequenzen im Versuchsteil angegeben) erscheinen zwei NH-Banden; die eine (3225 cm^{-1}) kann einer intermolekularen Wasserstoffbindung (=N—H...O=) zugeordnet werden, während die andere (in Chloroformlösung 3400 cm^{-1}, in KBr-Preßlingen 3390 cm^{-1}) von einer freien NH-Gruppe herrühren dürfte. Es läßt sich am *Stuart—Briegleb* Modell zeigen, daß aus sterischen Gründen gleichzeitig nur eine NH-Gruppe mit dem Sauerstoffatom des Estercarbonyls oder der PO-Gruppe eines zweiten Moleküls eine Wasserstoffbindung eingehen kann. Derartige Wasserstoffbrücken können erfahrungsgemäß auch in verhältnismäßig verdünnten Lösungen recht stabil sein. Diese Deutung des IR-Spektrums wird auch von den Daten der Molekulargewichtbestimmung unterstützt. Aus der in Chloroformlösung gemessenen Siedepunkterhöhung ließ sich nämlich ein Molekulargewicht von 950 berechnen, das mehr als das Doppelte des auf Formel **VIII** berechneten Wertes (360) beträgt. Hingegen ergab die Bestimmung in Eisessig den Wert 378, ein Zeichen dessen, daß wegen der intensiven Wechselwirkung der Essigsäure- und der Substanzmoleküle in dieser Lösung intermolekulare Wasserstoffbindungen zwischen den Molekülen der Verbindung **VIII** nicht mehr bestehen.

Es ist des öfteren darauf hingewiesen worden, das zwischen der biologischen Aktivität der Stickstoff-Lostderivate und der anionischen Abspaltungstendenz ihrer Chloratome ein gewisser Zusammenhang besteht. Untersuchungen von Ross [4] und PREUSSMANN [5] haben jedoch ergeben, daß eine derartige Parallelität eher nur bei Verbindungen mit weitgehend analoger Struktur zu beobachten ist. Um diesbezügliche weitere Anhaltspunkte zu gewinnen,

haben wir die jetzt und auch früher [1] aufgebauten Stickstoff-Lostderivate der Aminosäuren unter den zuerst von Ross [4] und später auch von Bergel und Stock [6] angewandten standarden Versuchsbedingungen auf die Hydrolysebereitschaft der Cl—C-Bindung untersucht. Die Ergebnisse sind im Versuchsteil verzeichnet.

Die Testung auf ihre biologische Aktivität der in dieser Arbeit beschriebenen neuen Verbindungen ist in der unter der Leitung von Prof. A. Haddow stehenden pathologischen Abteilung des Chester Beatty Research Institute, Institute of Cancer Research: Royal Cancer Hospital (London) im Gange. Die Ergebnisse dieser Untersuchungen werden an anderer Stelle veröffentlicht, hier soll bloß erwähnt werden, daß die meisten Verbindungen bei geringer Toxicität eine bedeutende tumorwachstumshemmende Wirkung zeigen.

Bei der Ausführung unserer experimentellen Arbeit hat uns Frau G. Németh technische Hilfe geleistet. Die IR-Spektren wurden in unserem Institut von Herrn F. Ruff aufgenommen und gedeutet. Die Mikroanalysen haben in unserem mikroanalytischen Laboratorium Frau H. M.-Schweiger, Frau S. Kutassy und Frau J. Kajtár ausgeführt. Allen unseren Mitarbeitern sei auch an dieser Stelle bestens gedankt.

Beschreibung der Versuche*

N.O-[(Bis-2-chlor-äthyl)-amido]-phosphoryl-DL-threo-β-phenylserinäthylester (IIIa)

Eine Suspension von 2,46 g (0,01 Mol) DL-*threo*-β-Phenyl-serinäthylester-hydrochlorid [2] in 40 ml wasserfreiem Chloroform wurde zuerst mit 4,18 ml (0,03 Mol) Triäthylamin, dann mit einer Lösung von 2,59 g (0,01 Mol) N.N-Bis-(2-Chloräthyl)-phosphorsäureamid-dichlorid [7] in 10 ml wasserfreiem Chloroform versetzt. Nach 4stündigem Stehen wurde das Gemisch mit 150 ml trockenem Benzol vermischt und über Nacht sich selbst überlassen. Man filtrierte das ausgeschiedene Triäthylammoniumchlorid ab, wusch die Lösung zweimal mit je 30 ml 0,5N Salzsäure, nachher zweimal mit je 30 ml Wasser und trocknete sie schließlich mit Magnesiumsulfat. Nach Abtreiben des Lösungsmittels wurde der Rückstand aus Benzol-Petroläther kristallisiert. Schmp. 100—102°. Ausbeute 2,06 g (52% d. Th.). — $R_F = 0{,}9$.

$C_{15}H_{21}O_4N_2Cl_2P$ (395,24). Ber.: C 45,6, H 5,4, N 7,1, Cl 17,9, P 7,8, C_2H_5O 11,4%. Gef.: C 46,0, H 6,0, N 7,2, Cl 17,9, P 7,2, C_2H_5O 11,6%.

IR-Spektrum: ν_{NH} 3160 cm^{-1}; $\nu_{C=O}$ 1758 cm^{-1} (Ester); ν_{C-O-C} 1220 cm^{-1} (Ester); $\nu_{P=O}$ 1245 cm^{-1}; ν_{P-N} 990 cm^{-1}.

N.O-[(Bis-2-chlor-äthyl)-amido]-phosphoryl-DL-erythro-β-phenylserinäthylester (IIIb)

Die Verbindung wurde aus 2,46 g (0,01 Mol) DL-*erythro*-β-Phenyl-serinäthylesterhydrochlorid [3] auf oben angegebene Weise hergestellt. Die aus Benzol-Petroläther umkristallisierte Substanz schmolz bei 124—126°. Ausbeute 2,09 g (53% d. Th.). — $R_F = 0{,}91$.

$C_{15}H_{21}O_4N_2Cl_2P$ (395,24). Ber.: C 45,6, H 5,4, N 7,1, Cl 17,9, P 7,8, C_2H_5O 11,4%. Gef.: C 45,45, H 5,4, N 6,6, Cl 18,4, P 7,2, C_2H_5O 11,2%.

IR-Spektrum: ν_{NH} 3370 cm^{-1}; $\nu_{C=O}$ 1745 cm^{-1} (Ester); $\nu_{P=O}$ 1205 cm^{-1}; ν_{P-N} 990 cm^{-1}

* Die Schmelzpunkte sind unkorrigiert. — Die R_F-Werte sind für aufsteigende Chromatographie an Whatman No. 1. Papier durch Anwendung des Lösungsmittels Butanol : Pyridin : Wasser = 1 : 1 : 1 angegeben.

N-Carbobenzoxy-DL-threo-β-phenylserin (XIa)

Die N-Carbobenzoxylierung des DL-*threo*-β-Phenylserins (**Xa**) wurde der Herstellung des N-Carbobenzoxy-L-serins [8] nachgebildet. Eine mit Eis gekühlte Lösung von 18,12 g (0,1 Mol) DL-*threo*-β-Phenylserin [2] in 400 ml N Natriumhydrogencarbonatlösung (0,4 Mol) wurde mit 100 ml Äther überschichtet, dann unter Rühren mit 24 g (0,14 Mol) Chlorameisensäurebenzylester binnen 20 Minuten tropfenweise versetzt. Man rührte nachher das Gemisch unter Eiskühlung noch weitere 4 Stunden. Die abgetrennte wäßrige Lösung wurde zuerst zweimal mit je 100 ml Äther ausgeschüttelt, nachher unter Eiskühlung mit konz. Salzsäure angesäuert und das ausgeschiedene Öl dreimal mit je 100 ml Essigester extrahiert. Die mit Magnesiumsulfat getrocknete Essigesterlösung lieferte nach dem Eindampfen bei Unterdurck ein gelbes Öl, das allmählich zu einem weißen Kristallgut erstarrte. Nach einmaligen Umkristallisieren aus wasserfreiem Essigester-Petroläther war die Substanz analysenrein. Schmp. 78—80°. Ausbeute 25 g (79% d. Th.).

$C_{17}H_{17}O_5N$ (315, 33). Ber.: C 64,75, H 5,4, N 4,4%. Gef.: C 64,9, H 5,7, N 4,6%.

N-Carbobenzoxy-DL-erythro-β-phenylserin (XIb)

Nach BERGMANN und Mitarbeitern [3] hergestelltes DL-*erythro*-β-Phenylserinäthylesterhydrochlorid wurde nach der Angabe dieser Forscher mit 2 N Salzsäure hydrolysiert und die Lösung bei Unterdruck bis zur Hälfte eingeengt. Das in dieser Lösung befindliche DL-*erythro*-β-Phenylserin-hydrochlorid wurde ohne Isolierung nach Zusatz der entsprechenden Menge Natriumhydrogencarbonats — wie oben angegeben — carbobenzoxyliert. Die aus wasserfreiem Essigester-Petroläther umkristallisierte, analysenreine Substanz schmolz bei 134—135°. Ausbeute 30% d. Th.

$C_{17}H_{17}O_5N$ (315.33). Ber.: C 64,75, H 5,4, N 4,4%. Gef.: C 64,55, H 5,9, N 4,2%.

N-Carbobenzoxy-DL-threo-β-phenylserinbenzylester (XIIa)

Die Veresterung des N-Carbobenzoxy-β-phenylserins wurde der Herstellung des N-Carbobenzoxy-L-threoninbenzylesters [9] nachgebildet. — Ein Gemisch von 6,3 g (0,02 Mol) N-Carbobenzoxy-DL-*threo*-β-phenylserin, 7,6 g (0,06 Mol) Benzylchlorid und 4,2 ml (0,03 Mol) Triäthylamin wurde am Wasserbad 15 Minuten auf 75° erwärmt (beginnende Erstarrung), weitere 2,28 ml (0,02 Mol) Benzylchlorid und 1,4 ml (0,01 Mol) Triäthylamin hinzugefügt und noch eine Stunde bei dieser Temperatur gehalten. Nach Abtreiben des unreagierten Benzylchlorids und Triäthylamins bei Unterdruck (Badtemperatur 70—75°) blieb ein gelbliches, viskoses Öl zurück, das man in 120 ml heißem Essigester löste. Diese Lösung wurde zuerst mit 60 ml, nachher dreimal mit je 20 ml 2 N Salzsäure, zweimal mit je 20 ml Wasser, dreimal mit je 20 ml 5-prozentiger Natriumhydrogencarbonatlösung, dann abermals zweimal mit je 20 ml Wasser durchgeschüttelt, mit Magnesiumsulfat getrocknet und schließlich bei Unterdruck eingedampft. Der weiße, kristalline Rückstand ließ sich aus wasserfreiem Essigester-Petroläther umkristallisieren. Schmp. 111—112°. Ausbeute 5,66 g (70% d. Th.).

$C_{24}H_{23}O_5N$ (405,46). Ber.: C 71,1, H 5,7, N 3,5%. Gef.: C 71,4, H 6,0, N 3,3%.

N-Carbobenzoxy-DL-erythro-β-phenylserinbenzylester (XIIb)

Die Verbindung wurde aus 6,3 g (0,02 Mol) N-Carbobenzoxy-DL-*erythro*-β-phenylserin ebenso hergestellt wie das isomere *threo*-Derivat (s. oben). Die aus wasserfreiem Essigester-Petroläther umkristallierte Substanz schmolz bei 103—104°. Ausbeute 70% d. Th.

$C_{24}H_{23}O_5N$ (405,46). Ber.: C 71,1, H 5,7, N 3,5%. Gef.: C 71,3, H 5,9, N 3,5%.

DL-threo-β-Phenylserinbenzylester-hydrobromid (XIIIa)

Eine eiskalt bereitete Suspension von 4,05 g (0,01 Mol) N-Carbobenzoxy-DL-*threo*-β-phenylserinbenzylester (**XIIa**) in 40 ml Bromwasserstoff-Dioxan (35% HBr) wurde unter Feuchtigkeitsausschluß bei Raumtemperatur bis zum Aufhören der CO_2-Entwicklung gerührt (ungefähr 30 Minuten). Das Hydrobromid ließ sich mit wasserfreiem Äther in Form feiner Kristalle ausfällen. Nach 2 stündigem Stehen im Eisschrank wurde abgesaugt und das Kristallgut mit wasserfreiem Äther gründlich gewaschen. Ausbeute 2,67 g (76% d. Th.). Die Substanz war nach einmaligem Umkristallisieren aus wasserfreiem Äthanol-Äther analysenrein. Schmp. 164—165°. — $R_F = 0.90$.

$C_{16}H_{18}O_3NBr$ (352,24). Ber.: C 54,6, H 5,15, N 4,0, Br 22,7%. Gef.: C 54,6, H 5,0, N 4,1, Br 22,55%.

DL-erythro-β-Phenylserinbenzylester-hydrobromid (XIIIb)

Die Verbindung wurde aus 4,05 g (0,01 Mol) N-Carbobenzoxy-DL-*erythro*-β-phenylserinbenzylester (**XIIb**) ebenso hergestellt wie das isomere *threo*-Derivat (s. oben). Ausbeute an Rohprodukt 58% d. Th. Durch einmaliges Umlösen aus wasserfreiem Äthanol-Äther ließ sich ein analysenreines Produkt gewinnen. Schmp. 167°. — $R_F = 0{,}95$.

$C_{16}H_{18}O_3NBr$ (352,24). Ber.: C 54,6, H 5,15, N 4,0, Br 22,7%. Gef.: C 54,4, H 5,0, N 3,7, Br 23,2%.

N.O-[(Bis-2-chlor-äthyl)-amido]-phosphoryl-DL-threo-β-phenylserinbenzylester (VIa)

Die Verbindung wurde auf übliche Weise (s. *threo*-**III**) hergestellt. Ansatz: 1,76 g (0,005 Mol) DL-*threo*-β-Phenylserinbenzylester-hydrobromid, 2,09 ml (0,015 Mol) Triäthylamin, 1,3 g (0,005 Mol) N.N-Bis-(2-chlor-äthyl)-phosphorsäureamid-dichlorid, 20 ml Chloroform. Das kristalline Rohprodukt wurde einmal aus wasserfreiem Benzol-Petroläther umgelöst. Schmp. 110—111°. Ausbeute 79% d. Th. — $R_F = 0{,}91$.

$C_{20}H_{23}O_4N_2Cl_2P$ (457,31). Ber.: C 52,5, H 5,1, N 6,1, Cl 15,5, P 6,8%. Gef.: C 52,65, H 5,7, N 6,0, Cl 15,25, P 6,7%.

IR-Spektrum: ν_{NH} 3200 cm^{-1}; $\nu_{C=O}$ 1761 cm^{-1} (Ester); $\nu_{P=O}$ 1230 cm^{-1}; ν_{C-O-C} 1205 cm^{-1} (Ester); ν_{P-N} 985 cm^{-1}.

N.O-[(Bis-2-chlor-äthyl)-amido]-phosphoryl-DL-erythro-β-phenylserinbenzylester (VIb)

Die Herstellung der Verbindung erfolgte aus DL-*erythro*-β-Phenylserinbenzylesterhydrobromid auf die für das *threo*-Derivat angegebene Art (s. oben). Das ölig anfallende Rohprodukt wurde zweimal aus Benzol mit Petroläther ausgefällt, nachher mit Petroläther verrieben, wobei es zu Mikrokristallen zerfiel. Schmp. 90—91°. Ausbeute 80% d. Th. — $R_F = 0{,}94$.

$C_{20}H_{23}O_4N_2Cl_2P$ (457,31). Ber.: C 52,5, H 5,1, N 6,1, Cl 15,5, P 6,8%. Gef.: C 52,15, H 5,0, N 5,8, Cl 15,8, P 6,5%.

IR-Spektrum: ν_{NH} 3375 cm^{-1}; $\nu_{C=O}$ 1754 cm^{-1} (Ester); ν_{C-O-C} 1205 cm^{-1} (Ester); $\nu_{P=O}$ 1230 cm^{-1}; ν_{P-N} 985 cm^{-1}.

N.O-[(Bis-2-chlor-äthyl)-amido]-phosphoryl-DL-threo-β-phenylserin (IV)

Eine Lösung von 2,29 g (0,05 Mol) des Benzylesters **VIa** in 200 ml absol. Äthanol wurde in Anwesenheit von 0,3 g Pd-Tierkohle (10%) hydrogenolysiert. Die berechnete Wasserstoffaufnahme war binnen 30 Minuten beendet. Nach Eindampfen (Unterdruck) der vom Katalysator befreiten Lösung blieb ein öliger Rückstand zurück, der nach dem Anreiben mit absol. Äther zu einem Pulver zerfiel. Die sehr hygroskopische Substanz ließ sich durch Ausfällen mit absol. Äther aus ihrer absol. alkoholischen Lösung reinigen.

Ausbeute 65%. — $R_F = 0{,}58$.

$C_{13}H_{17}O_4N_2Cl_2P$ (367,19). Ber.: C 42,5, H 4,7, N 7,6, Cl 15,3, P 8,4%. Gef.: C 42,9, H 4,4, N 7,4, Cl 15,1, P 8,1%.

N.O-[(Bis-2-chlor-äthyl)-amido]-phosphoryl-DL-threo-β-hydroxyglutaminsäure-diäthylester (V)

Die Verbindung wurde aus 2,56 g (0,01 Mol) DL-*threo*-β-Hydroxyglutaminsäure-diäthylester-hydrochlorid [10] und 2,59 g (0,01 Mol) N.N-Bis-(2-chlor-äthyl)-phosphorsäureamiddichlorid (**IX**) auf übliche Weise (s. die Herstellung von **IIIa**) hergestellt. Das Rohprodukt ließ sich aus absol. Benzol-Petroläther umkristallisieren. Schmp. 80—81°. Ausbeute 1,75 g (46% d. Th.). — $R_F = 0{,}89$.

$C_{13}H_{23}O_6N_2Cl_2P$ (405.24). Ber.: C 38,5, H 5,7, N 6,9, Cl 17,5, P 7,65, C_2H_5O 20,75%. Gef.: C 38,5, H 6,0, N 7,2, Cl 17,95, P 7,35, C_2H_5O 21,0%.

IR-Spektrum, aufgenommen nach der KBr-Preßtechnik: ν_{NH} 3220 cm^{-1}; $\nu_{C=O}$ (Ester) 1757 und 1731 cm^{-1} (diese Aufspaltung der Ester C=O Bande dürfte auf eine intermolekulare Wasserstoffbindung, die sich zwischen der NH und C=O Gruppe bilden kann, zurückzuführen sein, da Lösungen der Substanz keine Aufspaltung der Ester C=O Bande zeigen); $\nu_{P=O}$ 1235 cm^{-1}; ν_{P-N} 990 cm^{-1}.

N.S-[(Bis-2-chlor-äthyl)-amido]-phosphoryl-L-cysteinäthylester (VII)

Die Verbindung wurde aus 1,85 g (0,01 Mol) L-Cysteinäthylester-hydrobromid [11] und 2,59 g (0,01 Mol) N.N-Bis-(β-chloräthyl)-phosphorsäureamid-dichlorid (**IX**) auf übliche Weise hergestellt. Das Produkt stellt ein Öl dar, das nicht kristallisiert werden konnte, es ließ sich jedoch durch Umfällen aus absol. Benzol mit abs. Petroläther reinigen. Die im Vakuumexsiccator vom Lösungsmittel befreite Substanz erwies sich als analysenrein. Ausbeute 65% d. Th. — R_F = 0,88.

$C_9H_{17}O_3N_2Cl_2SP$ (335,21). Ber.: C 32,25, H 5,1, N 8,4, Cl 21,15, S 9,6, P 9,2%. Gef.: C 32,2, H 5,6, N 8,2, Cl 21,3, S 9,4, P 8,9.

IR-Spektrum: ν_{NH} 3200 cm^{-1}; ν_{CO} 1751 cm^{-1} (Ester); $\nu_{P=O}$ 1230 cm^{-1}; ν_{P-N} 985 cm^{-1}.

DL-Lysinäthylester-dihydrochlorid

Die Veresterung des DL-Lysins war der des L-Lysins [12] nachgebildet. Kristallisierung aus absol. Alkohol. Schmp. 162—163°. Ausbeute 84% d. Th.

$C_8H_{20}O_2N_2Cl_2$ (247,18). Ber.: C 38,9, H 8,2, N 11,3, Cl 28,7, C_2H_5O 18,2%. Gef.: C 38,5, H 8,2, N 11,5, Cl 28,4, C_2H_5O 18,3%.

N^{α}.N^{ε}-[(Bis-2-chlor-äthyl)-amido]-phosphoryl-DL-lysinäthylester (VIII)

Die Verbindung wurde aus 2,47 g (0,01 Mol) DL-Lysinäthylester-dihydrochlorid und 2,59 g (0,01 Mol) N.N-Bis-(2-chlor-äthyl)-phosphorsäureamid-dichlorid (**IX**) auf übliche Weise hergestellt. Das ölig anfallende Rohprodukt ließ sich durch Umfällen aus absol. Chloroform mit absol. Petroläther reinigen. Nach Vertreiben des Lösungsmittels war nur ein hygroskopischer fester Schaum erhältlich, der sich nicht kristallisieren ließ. Ausbeute 51%. Molgewicht (in Eisessig) 378. — R_F = 0,97.

$C_{12}H_{24}O_3N_3Cl_2P$ (360,24). Ber.: C 40,0, H 6,7, N 11,7, Cl 19,7, P 8,6, C_2H_5O 12,5%. Gef.: C 40,1, H 7,0, N 11,5, Cl 19,5, P 8,9, C_2H_5O 12,4%.

IR-Spektrum: ν_{NH} *a)* in KBr-Pressling 3390 und 3225 cm^{-1}, *b)* in $CHCl_3$-Lösung 3400 und 3225 cm^{-1}; $\nu_{C=O}$ 1740 cm^{-1} (Ester); ν_{C-O-C} (Ester) und $\nu_{P=O}$ (zusammengeschmolzen) 1200 cm^{-1}, ν_{P-N} 900—1000 cm^{-1}.

Vergleich der Hydrolysebereitschaft der C—Cl Bindung der N.N-Bis(β-chloräthyl)-aminophosphoryl Gruppe in einigen Derivaten

Die Untersuchungen wurden nach der Standardmethode von ROSS [4] durchgeführt. Eine Lösung von 0,25 Mol der Substanz in einem Gemisch von je 12,5 ml Aceton und Wasser wurden 30 Minuten rückfließend gekocht, danach rasch abgekühlt und der Gehalt der Lösung an Chlorid Ionen nach Volhard titrimetrisch bestimmt. Zu diesem Zweck wurde die kalte Lösung mit 5 ml 0,1 N Silbernitratlösung, hierauf mit 2 ml 2 N Salpetersäure versetzt, geschüttelt, filtriert, der Niederschlag mit Wasser gewaschen und das Filtrat — unter Anwendung von Ammonsulfat als Indikator — mit 0,1 N Ammoniumrhodanidlösung titriert. Die Menge der unter den oben angegebenen Bedingungen entstandenen Cl-Ionen sind in Prozenten des gesamten Chlorgehaltes der Substanz angegeben; es wurden folgende Werte gefunden: **I** 8%, **IIIa** 9%, **IIIb** 8%, **V** 9%, **VIa** 13%, **VIb** 15%, **VII** 12% und **VIII** 24%.

ZUSAMMENFASSUNG

Um den Einfluß des Trägermoleküls auf die biologische Wirkung ein und derselben cytotoxischen Gruppe untersuchen zu können, wurden DL-β-Phenylserinester der *threo-* und *erythro-*Konfiguration, weiterhin DL-*threo*-β-Hydroxyglutaminsäure-diäthylester, L-Cysteinäthylester und DL-Lysinäthylester mit N.N-Bis-(2-chlor-äthyl)-phosphorsäureamid-dichlorid **(IX)** zu cyclischen N-Lostderivaten **(III, V, VI, VII** und **VIII)** umgesetzt. Über die biologische Testung dieser Verbindungen wird an anderer Stelle berichtet.

LITERATUR

1. SZEKERKE, M., CSÁSZÁR, J., BRUCKNER, V.: Acta Chim. Hung. **46,** 379 (1965).
2. FONES, W. S.: J. Org. Chem. **17,** 1534 (1952).
3. BERGMANN, E. D., GENAS, M., BENDAS, H.: Compt. rend. **231,** 361 (1950); BERGMANN, E. D., BENDAS, H., RESNICK, C.: J. Chem. Soc. **1953,** 2564.
4. ROSS, W. C. J.: J. Chem. Soc. **1949,** 183.
5. PREUSSMANN, R.: Arzneimittelforsch. **8,** 638 (1958).
6. BERGEL, F., STOCK, J. A.: J. Chem. Soc. **1954,** 2409.
7. FRIEDMAN, O. M., SELIGMAN, A. M.: J. Am. Soc. **76,** 655 (1954).
8. GUTTMANN, ST., BOISSONNAS, R. A.: Helv. Chim. Acta **41,** 1852 (1958).
9. BAER, E., ECKSTEIN, F.: J. Biol. Chem. **237,** 1450 (1962).
10. HARINGTON, C. R., RANDALL, S. S.: Biochem. J. **25,** 1917 (1931).
11. CHERBULIEZ, E., PLATTNER, PL.: Helv. Chim. Acta **12,** 315 (1929).
12. WERBIN, H., PALM, A.: J. Am. Chem. Soc. **73,** 1382 (1951).

Synthesis of Cyclic N-Lost Derivatives from β-Substituted Serines, Cysteine and Lysine

M. SZEKERKE, M. T. KAJTÁR and V. BRUCKNER

Summary. In order to study the effect of the carrier molecule on the biological activity of the same cytotoxic group, DL-β-phenylserinesters of threo and erythro configuration, further DL-threo-β-hydroxy-glutamine acid diethylester, L-cysteine ethylester and DL-lysine ethylester were converted into cyclic N-lost derivatives **(III, V, VI, VII** and **VIII)** with the aid of N.N-bis-(β-chloroethyl)-phosphoric acid amide dichloride **(IX).** The results of biological test of the prepared compounds will be reported elsewhere.

Синтез циклических производных N-иприта из β-замещенных серинов цистеина и лизина

М. СЕКЕРКЕ, М. Т. КАЙТАР и В. БРУКНЕР

Резюме. С целью исследования влияния несущей молекулы на биологическое воздействие той же самой цитотоксической группы авторы, с помощью амид-дихлорида N,N-бис-(β-хлорэтил)-фосфорной кислоты, перевели DL-β-фенилсериновые эфиры, трео и эритро конфигурации, далее этиловые эфиры DL-трео-β-гидроксиглутаминовой кислоты, L-цистеина и DL-лизина в циклические производные N-иприта (III, V, VI, VII и VIII).

О биологическом испытании полученных соединений авторы отчитываются в другом месте.

Dr. Mária SZEKERKE; Budapest VIII. Múzeum körút 4/b
Mária T. KAJTÁR; Budapest II. Pusztaszeri út 57/69
Prof. Dr. Viktor BRUCKNER; Budapest VIII. Múzeum körút 4/b

INDEX

SÁNDOR (ALEXANDER) MÜLLER, 1903—1966 101

ANORGANISCHE UND ANALYTISCHE CHEMIE — INORGANIC AND ANALYTICAL CHEMISTRY — — НЕОРГАНИЧЕСКАЯ И АНАЛИТИЧЕСКАЯ ХИМИЯ

LÉGRÁDI, L.: p-Äthoxy-α-naphthylrot, ein neuer Adsorptionsindikator 103
LÉGRÁDI, L. and HUSZÁR, J.: Oxidation Methods in Organic Analysis, I. Determination of Phenylhydrazine in the Presence of Aniline 115
GÖRÖG, S. and TOMCSÁNYI, L.: Analysis of Steroids, III. Determination of Steroids Containing Isolated Carbonyl Groups 121
SCHULEK, E., BARCZA, L., GÁBOR-FEHÉR, M. and LADÁNYI, L.: Reaction of Disulfur Dichloride and Sulfur Dichloride with Cyanide; their Determination through Thiocyanate 129
BARCZA, L.: Contributions to the Chemistry of Selenium and Selenium Compounds, XIV. Determination of Selenium in Organic Selenium Compounds 137
RUFF, I. and BURGER, K.: Some Theoretical and Practical Problems in the Use of Organic Reagents in Chemical Analysis, VIII. Influence of the Chelate Effect and Ring Size on the Stability of the Dioxime Complexes of Transition Metals 143

PHYSIKALISCHE CHEMIE — PHYSICAL CHEMISTRY — ФИЗИЧЕСКАЯ ХИМИЯ

RÓDER, M., OPAUSZKY, I. and KISS, I.: Thermal Stability of the Eutectic Mixture of Diphenyl and Diphenylmethane 157
SUNDARAM, K. M. S.: Surface Tension Studies of Some Binary Systems. Pyridine and Acetic Acid. (Short Communication) 167
SZŐKE, S. and FARAGÓ, T.: Calculation of Force Field on Ethylene Model 173
DÉVAY, J. und MÉSZÁROS, L.: Berechnung der Korrosionswirkung des Kriechwechselstromes auf ein in einem Elektrolyten angebrachtes Metall. (Kurzmitteilung) 185

ORGANISCHE CHEMIE — ORGANIC CHEMISTRY — ОРГАНИЧЕСКАЯ ХИМИЯ

Надь, Й., Ференци-Грес, Ш. и *Миронов, В. Ф.:* Структура связи в алкенил-кремнийорганических соединений (NAGY, J., FERENCZI-GRESZ, S. and MIRONOV, V. F.: Bond Structure of Alkenyl Siliconorganic Compounds) 189
H.-HANKOVSZKY, O., HIDEG, K. and MÉHES, GY.: Allylphenol and Propenylphenol Derivatives 199
HARDY, GY., NAGY, L. and CSER, F.: Investigations in the Field of Radiation-Induced Solid State Polymerization, XIV. The γ-Radiation-initiated Polymerization of Allyl Palmitate 211
FÓTI, A., GERECS, Á. und RUFF, F.: Über die Struktur und Ringstabilität einiger O-Acetylmonose-2,4-dinitro-phenylhydrazone 221
SZEKERKE, M., KAJTÁR, M. T. und BRUCKNER, V.: Synthese cyclischer N-Lostderivate aus β-substituierten Serinen, Cystein und Lysin 231

Printed in Hungary

A kiadásért felel az Akadémiai Kiadó igazgatója — Műszaki szerkesztő: Farkas Sándor

A kézirat nyomdába érkezett: 1965. XII. 15. — Terjedelem: 12,50 (A/5) ív. 40 ábra (1 színes), 1 melléklet

66.61712 Akadémiai Nyomda, Budapest — Felelős vezető: Bernát György

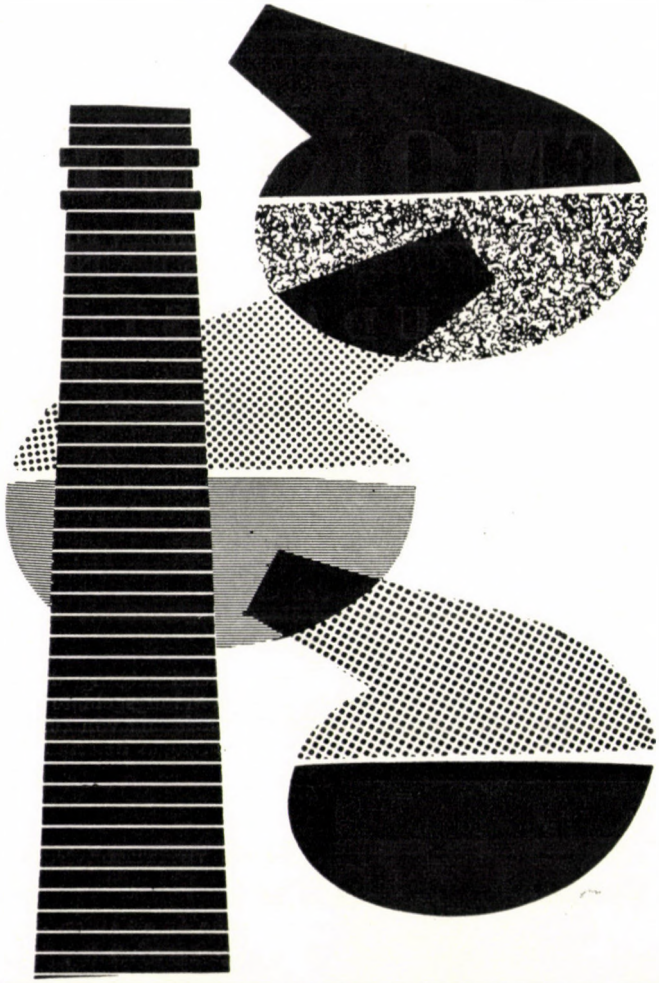

CHEMOKOMPLEX

WE EXPORT

Corrosion resistant glass-enamelled LAMPART equipments:

a) Reaction vessels, 30—3000 lit. ✳ b) Distilling plants ✳ c) Pressure and vacuum filters ✳ d) Evaporating pans ✳ e) Single- and multi-bottle type heat exchangers and Shell condensers ✳ f) Super- and Pendulum-centrifuges ✳ g) Corrosion resistant steel reaction vessels ✳ Furthermore, we export chemical equipment processed on the basis of individual designs as well as serial machines for the chemical and pharmaceutical industry and complete plants

HUNGARIAN TRADING COMPANY OF MACHINES AND EQUIPMENT FOR THE CHEMICAL INDUSTRY
VI., NÉPKÖZTÁRSASÁG ÚTJA 64. BUDAPEST—HUNGARY

TELEPHONE: 316—720 P. O. B. 141. BUDAPEST 62.
TELEGRAM: CHEMOKOMPLEX

CHEMOKOMPLEX

UNGARISCHES AUSSENHANDELSUNTERNEHMEN FÜR MASCHINEN
UND EINRICHTUNGEN DER CHEMISCHEN INDUSTRIE

BUDAPEST

P. O. B. 141, BUDAPEST 62 Telex: BUDAPEST 264

EXPORTIERT MIT AUSSCHLIESSLICHEM RECHT

mit Ionenaustausch-Filterharzen funktionierende Wasserenthärtungs- und Vollentsalzungsanlagen

zur Wasserreinigung und
für verschiedene chemische Prozesse
(in der pharmazeutischen und chemischen Industrie
sowie Spirituosenfabrikation usw.)

Unsere Ionenaustauschanlagen werden — unter Berücksichtigung der quantitativen und qualitativen Anforderungen der verschiedenen Verwendungsgebiete — auf Grund Einzelprojektierung hergestellt. Die Anlagen sind mit einer Leistung von 100 l/Stunde bis 400 000 l/Stunde in beliebigen Größenordnungen lieferbar.

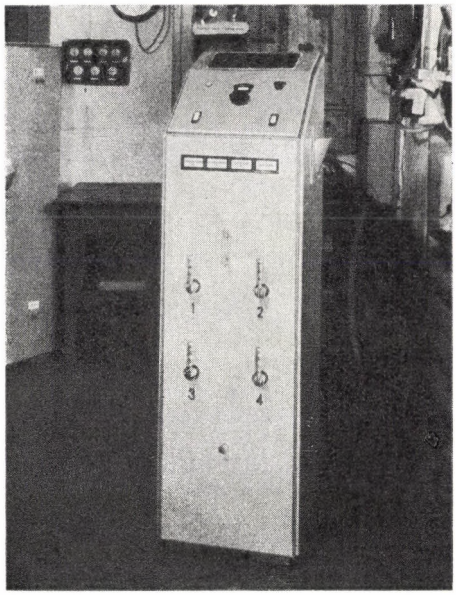

DIE VORTEILE DER ANLAGEN SIND:

rasche Amortisation der Investitionskosten
lange Lebensdauer,

✳

minimale Betriebskosten,

✳

einfache Betätigung,

✳

sichere Inbetriebhaltung,

✳

automatische Kontrollmöglichkeit während des Betriebes

Unsere Einrichtungen sind mit »VARION« Ionenaustausch-Kunstharzen ungarischer Produktion gefüllt. Die angewendeten Harze sind hinsichtlich Qualität und Lebensdauer im Vergleich zu den auf dem Weltmarkt erhältlichen Kunstharzqualitäten, konkurrenzfähig.

Bei der Auswahl der gewünschten Typen sind wir stets gerne bereit den Interessenten mit Fachberatung — und falls gewünscht — mit Vorschlägen oder ausführlichen Angeboten zu dienen.

REANAL CHEMICALS

Reagents

Fine Chemicals

Amino Acids

and

Derivatives

Peptides

Indicators

Enzymes

Nucleoproteides

Carbohydrates

Biochemicals

Radiochemicals

Photochemicals

"REANAL" Factory of Laboratory Chemicals.

BUDAPEST 70. HUNGARY
P.O.B. 54.

Exported by MEDIMPEX, Budapest 502 P. O. B. 34.

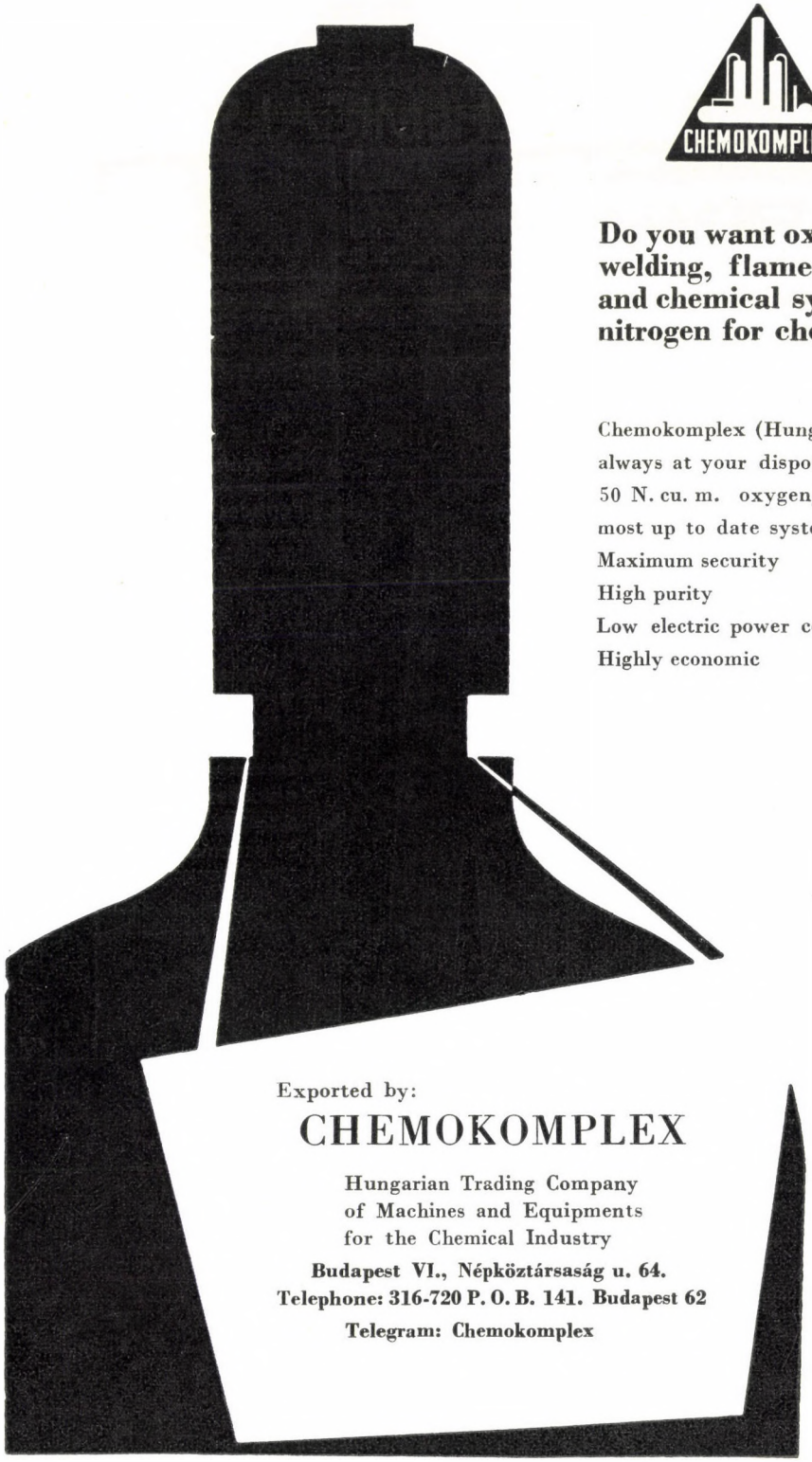

CHEMOKOMPLEX

Do you want oxygen for welding, flame cutting and chemical synthesis, nitrogen for chemicals?

Chemokomplex (Hungary) is
always at your disposal with its
50 N. cu. m. oxygen/hour units
most up to date system
Maximum security
High purity
Low electric power consumption
Highly economic

Exported by:

CHEMOKOMPLEX

Hungarian Trading Company
of Machines and Equipments
for the Chemical Industry

Budapest VI., Népköztársaság u. 64.
Telephone: 316-720 P. O. B. 141. Budapest 62
Telegram: Chemokomplex

The Acta Chimica publish papers on chemistry, in English, German, French and Russian.

The Acta Chimica appearsin volumes consisting of four parts of varying size, 4 volumes being published a year.

Manuscripts should be addressed to

Acta Chimica
Budapest 502, Postafiók 32

Correspondence with the editors should be sent to the same address.

The rate of subscription is 110 forints a volume. Orders may be placed with "*Kultúra*" Foreign Trade Company for Books and Newspapers (Budapest I., Fő utca 32. Account No. 43-790-057-181) or with representatives abroad.

Les Acta Chimica paraissent en français, allemand, anglais et russe et publient des mémoires du domaine des sciences chimiques.

Les Acta Chimica sont publiés sous forme de fascicules. Quatre fascicules seront réunis en un volume (4 volumes par an).

On est prié d'envoyer les manuscrits destinés à la rédaction à l'adresse suivante:

Acta Chimica
Budapest 502, Postafiók 32

Toute correspondance doit être envoyée à cette même adresse.

Le prix de l'abonnement est de 110 forints par volume.

On peut s'abonner à l'Entreprise pour le Commerce Extérieur de Livres et Journaux «*Kultúra*» (Budapest I., Fő utca 32. Compte-courant No. 43-790-057-181) ou à l'étranger chez tous les représentants ou dépositaires.

«*Acta Chimica*» издают трактаты из области химической науки на русском, французском, английском и немецком языках.

«*Acta Chimica*» выходят отдельными выпусками разного объема. 4 выпуска составляют один том. 4 тома публикуются в год.

Предназначенные для публикации рукописи следует направлять по адресу:

Acta Chimica
Budapest 502, Postafiók 32

По этому же адресу направлять всякую корреспонденцию для редакции.

Подписная цена «*Acta Chimica*» — 110 форинтов за том. Заказы принимает предприятие по внешней торговле книг и газет «*Kultúra*» (Budapest I., Fő utca 32. Текущий счет № 43-790-057-181) или его заграничные представительства и уполномоченные.

36,— Ft

All the reviews of the Hungarian Academy of Sciences may be obtained among others from the following bookshops:

ALBANIA

Ndermarja Shtetnore e Botimeve
Tirana

AUSTRALIA

A. Keesing
Box 4886, GPO
Sidney

AUSTRIA

Globus Buchvertrieb
Salzgries 16
Wien I.

BELGIUM

Office International de Librairie
30, Avenue Marnix
Bruxelles 5
Du Monde Entier
5, Place St. Jean
Bruxelles

BULGARIA

Raznoiznos
1Tzar Assen
Sofia

CANADA

Pannonia Books
2 Spadina Road
Toronto 4, Ont.

CHINA

Waiwen Shudian
Peking
P. O. B. Nr. 88.

CZECHOSLOVAKIA

Artia A. G.
Ve Smeckách 30
Praha II.
Postova Novinova Sluzba
Dovoz tisku
Vinohradska 46
Praha 2
Postova Novinova Sluzba
Dovoz tlace
Leningradska 14
Bratislava

DENMARK

Ejnar Munksgaard
Nörregade 6
Kopenhagen

FINLAND

Akateeminen Kirjakauppa
Keskuskatu 2
Helsinki

FRANCE

Office International de Documentation et Librairie
48, rue Gay Lussac
Paris 5

GERMAN DEMOCRATIC REPUBLIC

Deutscher Buch-Export und Import
Leninstraße 16.
Leipzig C. 1.
Zeitungsvertriebsamt
Clara Zetkin Straße 62.
Berlin N. W.

GERMAN FEDERAL REPUBLIC

Kunst und Wissen
Erich Bieber
Postfach 46
7 Stuttgart S.

GREAT BRITAIN

Collet's' Subscription Dept.
44—45 Museum Street
London W. C. 1.
Robert Maxwell and Co. Ltd.
Waynflete Bldg. The Plain
Oxford

HOLLAND

Swetz and Zeitlinger
Keizersgracht 471—487
Amsterdam C.
Martinus Nijhof
Lange Voorhout 9
The Hague

INDIA

Current Technical Literature
Co. Private Ltd.
Head Office:
India House OPP.
GPO Post Box 1374
Bombay 1.

ITALY

Santo Vanasia
71 Via M. Macchi
Milano
Libreria Commissionaria Sansoni
Via La Marmora 45
Firenze

JAPAN

Nauka Ltd.
2 Kanada-Zimbocho 2-chome
Chiyoda-ku
Tokyo
Maruzen and Co. Ltd.
P. O. Box 605
Tokyo
Far Eastern Booksellers
Kanada P. O. Box 72
Tokyo

KOREA

Chulpanmul
Korejskoje Obshchestvo po Exportu i Importu Proizvedenij Pechati
Phenjan

NORWAY

Johan Grundt Tanum
Karl Johansgatan 43
Oslo

POLAND

Export und Import Unternehmen RUCH
ul. Wilcza 46.
Warszawa

ROUMANIA

Cartimex
Str. Aristide Briand 14—18.
Bucuresti

SOVIET UNION

Mezhdunarodnaja Kniga
Moscow
G—200

SWEDEN

Almquist and Wiksell
Gamla Brogatan 26
Stockholm

USA

Stechert Hafner Inc.
31 East 10th Street
New York 3 N. Y.
Walter J. Johnson
111 Fifth Avenue
New York 3. N. Y.

VIETNAM

Xunhasaba
Service d'Export et d'Import des Livres et Périodiques
19, Tran Quoc Toan
Hanoi

YUGOSLAVIA

Forum
Vojvode Misica broj 1.
Novi Sad
Jugoslovenska Kniga
Terazije 27.
Beograd

11. III. 1966

Index: 26.007

ACTA CHIMICA

ACADEMIAE SCIENTIARUM HUNGARICAE

ADIUVANTIBUS

L. ERDEY, K. POLINSZKY, G. SCHAY

AC

R. BOGNÁR, GY. BRUCKNER, L. CHOLNOKY, Z. CSŰRÖS, T. ERDEY-GRŰZ, Z. FÖLDI, M. FREUND, Á. GERECS, GY. HARDY, Á. KISS, M. KORACH, P. MÁRTA, J. PROSZT, Z. SZABÓ, P. SZŐR, L. VARGHA, K. VAS

REDIGIT

B. LENGYEL

TOMUS 47. FASCICULUS 3.

AKADÉMIAI KIADÓ, BUDAPEST

1966

ACTA CHIM. HUNG.

ACTA CHIMICA

A MAGYAR TUDOMÁNYOS AKADÉMIA KÉMIAI TUDOMÁNYOK OSZTÁLYÁNAK IDEGEN NYELVŰ KÖZLEMÉNYEI

SZERKESZTI

LENGYEL BÉLA

TECHNIKAI SZERKESZTŐK

DEÁK GYULA és TAKÁCS VILMOS

Az Acta Chimica német, angol, francia és orosz nyelven közöl értekezéseket a kémiai tudományok köréből.

Az Acta Chimica változó terjedelmű füzetekben jelenik meg, egy-egy kötet négy füzetből áll. Évente átlag négy kötet jelenik meg.

A közlésre szánt kéziratok a szerkesztőség címére (Budapest 502, postafiók 32) küldendők.

Ugyanerre a címre küldendő minden szerkesztőségi levelezés. A szerkesztőség kéziratokat nem ad vissza.

Az Acta Chimica előfizetési ára kötetenként belföldre 80 Ft, külföldre 110 Ft. Megrendelhető a belföld számára az „Akadémiai Kiadó"-nál (Budapest V., Alkotmány utca 21. Bankszámla 05-915-111-46), a külföld számára pedig a „Kultúra" Könyv- és Hírlap Külkereskedelmi Vállalatnál (Budapest I., Fő utca 32. Bankszámla: 43-790-057-181) vagy annak külföldi képviseleteinél és bizományosainál.

Die Acta Chimica veröffentlichen Abhandlungen aus dem Bereiche der chemischen Wissenschaften in deutscher, englischer, französischer und russischer Sprache.

Die Acta Chimica erscheinen in Heften wechselnden Umfanges. Vier Hefte bilden einen Band. Jährlich erscheinen 4 Bände.

Die zur Veröffentlichung bestimmten Manuskripte sind an folgende Adresse zu senden:

Acta Chimica
Budapest 502, Postafiók 32.

An die gleiche Anschrift ist auch jede für die Redaktion bestimmte Korrespondenz zu richten.

Abonnementspreis pro Band: 110 Forint. Bestellbar bei dem Buch- und Zeitungs-Außenhandels-Unternehmen »*Kultúra*« (Budapest I., Fő utca 32. Bankkonto No. 43-790-057-181) oder bei seinen Auslandsvertretungen und Kommissionären.

ON THE ROLE OF WATER IN ELECTRON TRANSFER REACTIONS, II.*

I. RUFF

(Department of Inorganic and Analytical Chemistry, L. Eötvös University, Budapest)

Received July 8, 1965

In a previous paper [1] a new model was used to calculate the rate of isotopic electron exchange reactions. According to this hypothesis, the electron transfer reaction is regarded as the transfer of an electron through a potential barrier defined by the normal redox potentials prevailing in the solvent. Namely, in aqueous solution, only those ions are stable, which possess redox potentials between the values defined by the chemical decomposition of water:

$$H \rightleftharpoons H^+ + e \qquad \varepsilon^\circ = 2.10 \text{ volt [2]} \tag{1}$$

$$H_2O \rightleftharpoons OH + H^+ + e \qquad \varepsilon^\circ = -2.4 \text{ volt [1]} \tag{2}$$

In Fig. 1 these potential values are represented by the upper and lower horizontal lines. The electron-donor and electron-acceptor levels characterizing the reactants are between these potential limits. Their heigt is defined by their normal oxidation-reduction potential values. In the case of an isotopic electron-exchange reaction, the acceptor and donor levels have the same energy values, since the initial and final states of the reaction are identical.

The electron may reach the acceptor level in two ways: (*i*) if the activation energy is enough to pass the potential barrier (dotted lines in Fig. 1), the activation entropy change will be positive:

$$\frac{\Delta S^*}{R} \geqslant 0 \tag{3}$$

(*ii*) if the activation energy is smaller than the height of the barrier, the electron can reach the acceptor ion by tunnel effect only, thus

$$\frac{\Delta S^*}{R} = -\frac{4\pi}{h} d \sqrt{2m(U - E^*)} + \ln D' . \tag{4}$$

* Part I: J. Phys. Chem., **69**, 3183 (1965).

This expression can be written on the basis of the *Gamow* equation obtained for a rectangular potential barrier, where h is the *Planck* constant, d = optimal distance of ions (about 9.4 Å),* m = mass of the electron, U = height of the barrier, E^* = activation energy, and D' is a function of U and E^*, and does not considerably differ from unity.

In both cases, there are again two possibilities how the electron may reach the acceptor level: (*a*) by "electron transfer" with respect to the upper

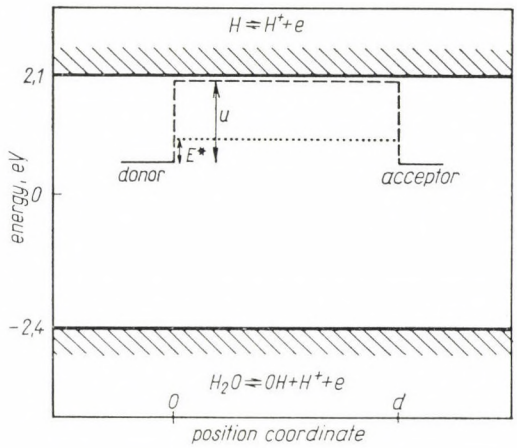

Fig. 1

limit of the potential; and (*b*) by "hole-transfer", when the lower limit is considered.

Good agreements have been found for the calculated and experimental values of ΔS^*, or the equivalent action constants.

In the present paper the applicability of this theory to non-isotopic electron exchange reactions is discussed. Furthermore, the nature of activation energy in, and the pH-dependence of electron transfer reactions are studied.

I. Calculation of the action constans of non-isotopic electron transfer reactions

In electron transfer reactions proceeding by isotopic exchange, the corresponding normal redox potentials of the reactants are identical. Thus the

* The reaction may occur at an arbitrary d, but on account of the exponential dependence of the rate on d, the rate for the smallest possible interionic distance is the highest and thus it is rate determining. The probability of very small distances is, however, negligible since the activation energy is markedly increased by the immersion of coordination spheres. It seems reasonable to take the smallest possible ionic distance to be such where the second coordination sphere of the ions is already immersed. This represents thus a distance corresponding to three water molecules.

energy of the donor and acceptor levels is the same. The enthalpy change of conventional redox reactions is usually finite, i.e. the bond energy of the electron to be transferred is greater on one of the ions (in most cases on the acceptor) than on the other. So the potential conditions of Fig. 1 become modified as shown in Fig. 2, the potential barrier is now asymmetric. The calculation of ΔS^* for such electron transfer reactions can be made similarly to the case of an isotopic electron exchange reaction, but this asymmetry

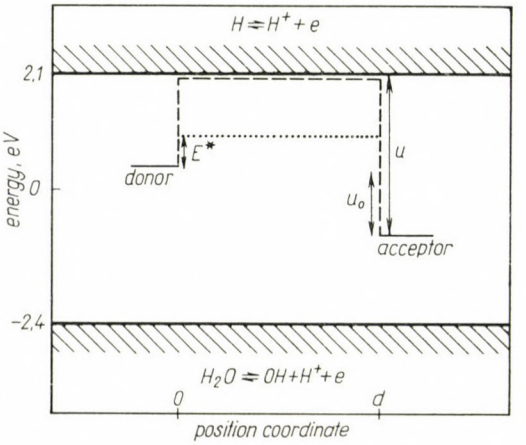

Fig. 2

must be taken into account:

$$\frac{\Delta S^*}{R} = -\frac{4\pi}{h} d \sqrt{2 m (U - U_0 - E^*)} + \ln D' . \tag{5}$$

It can be shown (see Appendix) that Eq. (5) is applicable to the case of tunnel effect at such an asymmetric potential barrier. D' is now a function of U, U_0 and E^*, but this slight effect is in most cases negligible. The corrections due to D', at different asymmetries, are shown in Fig. 3.

MARCUS [3] obtained results, based on his electrostatic non-equilibrium polarization theory, that are entirely different from those mentioned above. According to him, the rate constant (k) of an oxidation-reduction reaction is in the following correlation with the equilibrium constant (K) of the process:

$$k = \sqrt{k_1 k_2 K f} \tag{6}$$

where k_1 and k_2 are the rate constants of the corresponding isotopic electron exchange reactions of the reactants, and f may be obtained from the

expression:

$$\ln f = \frac{(\ln K)^2}{4 \ln \frac{k_1 k_2}{Z^2}} . \tag{7}$$

where Z is the collision frequency of two uncharged species in solution (about 10^{11} lit. mole^{-1} · sec^{-1}).

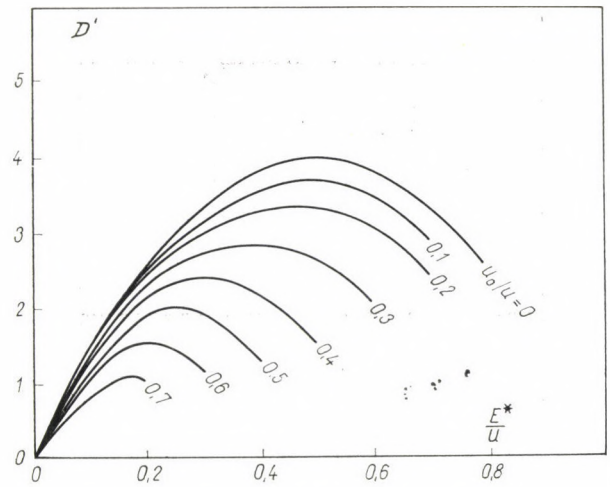

Fig. 3

This result is more or less in agreement with some experimental data [4, 5], namely, in the investigated cases, the function $\ln k = f(\ln K)$ was obtained as a linear plot with a slope of 1/2; however, the intercepts did not give the theoretically expected values. Thus, these investigations do not seem to prove the applicability of MARCUS' theory unambiguously.

II. Activation energy of electron transfer reactions

The activation energy requirements of electron transfer reactions have been explained on the basis of the *Franck—Condon* principle [1]. This activation mechanism is essentially based on photon-electron interaction: to make it possible for the electron (or hole) to leave the ion, the valence vibrations of the ligands in the first coordination sphere of the ion must be sufficiently excited.

That the *Franck—Condon* restriction really has a role in the process can be proved by this model as follows. Let us suppose that the ions can

absorb any kind of different E_i^* activation energies, and the electron is able to leave the ion in any of these activated states. Then the reaction paths due to different E_i^* activation energies can be considered parallel, among which the fastest one is the rate determining factor. The probability of tunneling increases and the number of activated ions decreases with increasing E_i^*. The rate constant, given by the following equation:

$$k = \frac{\mathbf{k}T}{h} \exp\left(-\frac{4\pi}{h} d \sqrt{2m(U - U_0 - E_i^*)} - \frac{E_i^*}{RT} + \ln 10 \frac{E_i^*}{U}\right)^*, \quad (8)$$

is expected to be obtainable by using the optimal E_i^*, i.e. the measurable activation energy should be calculated by the following equation:

$$\left(\frac{\partial \mathbf{k}}{\partial E_i^*}\right) = 0. \quad (9)$$

However, it can be proved that Eq. (9) leads to $E_i^* = RT$, with which the experimental results, are not in accord.

As the energy uptake of continuous spectrum is excluded as explained above, the possibility and conditions of energy uptake quantized by the *Franck—Condon* restriction should be investigated.

For electron transfer, for instance, the activation mechanism consists of removing the ligands in the first coordination sphere of reduced state from their equilibrium position to a distance that equals to the ion-ligand distance (r) of the ion of oxidized state. In this case the electron transfer can occur at a constant r, there is no need for simultaneous nuclear movements.

The imparting of this energy causes a decrease in the potential energy of complex ion, e.g. for aquo ions the hydration energy is decreased. The chemical potential (redox-potential) of the complex ion consists of the following terms:

$$\Delta\mu = \Delta F_{\text{subl.}} + \Delta F_{\text{ioniz.}} + \Delta F_{\text{hydr.}} \quad (10$$

where $\Delta F_{subl.}$, $\Delta F_{ioxiz.}$ and $\Delta F_{hydr.}$ are the free enthalpy changes needed for the formation of the gas phase metal atom, the gas phase ion and for the dissolved ion, respectively; the decrease in the last term in Eq. 10 results an increase of redox-potential in the activated state. It is thus justified to use the total activation energy in the *Gamow* equation as the energy of electron.

* Here the term containing ln D' was roughly approximated by ln $10 \frac{E_i}{U}$, for the exact expression would lead to an equation of high order in Eq. 9.

For the calculation of activation energy the difference of hydration energies of the ground and activated state is necessary. (For non-aquo ligands, instead of hydration energy the *total* formation free enthalpy of the complex is to be taken.) Generally this calculation calls for a full quantum mechanical knowledge of the complex ion, i.e. a knowledge of the ψ-functions, or that of the experimentally determined values of hydration energies. Unfortunately none of the two alternatives is possible due to obvious difficulties.

In first approximation, for transition metal ions some information can be obtained on activation energy by the model of crystal field theory. For the changing of hydration energy requires the same work as that performed on the repulsion potential of the ligand-electron and ligand-ligand interaction by decreasing the ion-ligand distance. In first approximation, however, this work passes into the increase of $10Dq$ splitting of the d orbits, for according to the crystal field theory, in case of ion ligand

$$10\,Dq = \frac{5}{3} z^- e \frac{\overline{\varrho^4}}{r^5} \tag{11.a}$$

and in case of dipol ligand

$$10\,Dq = 5\,(\mu_0 + \mu_i)\, e \frac{\overline{\varrho^4}}{r^6} \tag{11.b}$$

where z^- is the charge of the ion ligand, $\overline{\varrho^4}$ is the average of the nuclei-electron distance on the 4th power of the central ion, r is the distance of the nuclei of the central metal ion and ligand centre, while μ_0 and μ_i are respectively the permanent and induced dipol moments of the ligand.

The activation energy put in can be thus measured by the difference in the two splittings:

$$E^* = (10\,Dq)_{0x} - (10\,Dq)_{red}. \tag{12}$$

(Since for hole the energy scale is the reverse, in case of a reaction occurring with hole transfer the same relation is valid.)

III. pH-dependence of the rate of electron transfer reactions

On basis of the considerations described above it is readily understood that all changes occurring in the coordination sphere of the ion produce a change of the activation energy. Since these processes governed by the laws of coordination chemistry, depend in general on the pH, the reaction rate will also be a function of the pH, corresponding to the individual coordination chemical properties of the reactants.

In addition, in all electron transfer reactions a slight pH-dependence of another type is also to be expected. Namely, the potential limits (Eqs. 1 and 2) also change with the pH, from which, on the basis of Eq. (5), the following pH-dependence can be derived:

$$\ln k = -a\sqrt{U - U_0 - E^* \pm \mathbf{k}T\mathrm{p\,H}} + b \tag{13}$$

where

$$a = \frac{4\pi}{h} d\sqrt{2m} = 7.6 \cdot 10^6, g^{-1/2}\,\mathrm{cm}^{-1}\,\mathrm{sec}^{-3} \tag{14}$$

$$b = \ln\frac{\mathbf{k}T}{h} - \frac{E^*}{RT'} \tag{15}$$

and $\mathbf{k}T$ is the potential change due to unit pH-change. The sign of $\mathbf{k}T$ is positive or negative if the reaction proceeds prevalently by "electron transfer" or "hole-transfer", respectively.

The dependence of this type is usually accompanied by some other pH-dependences due to coordination chemical changes, thus the slight effect to be attributed to the change of the limit potentials cannot be identified separately. Namely, in general, the reaction order of the hydrogen ion concentration does not give directly an integer, and this slight pH-dependence gets lost during the usual procedure of expansion in a power series.

If the change of the activation entropy is positive, this slight pH-dependence turns into a dependence of $[H^+]$ order or $1/[H^+]$ order, respectively, depending on wheather the process is "electron transfer" or "hole-transfer". Namely, a positive entropy change corresponds to an activation energy greater than the height of the barrier, and so tunneling is unnecessary. The "free" electron or hole, produced in such cases is essentially identical with the formation of a hydrogen atom or OH radical, which can very rapidly "transport" the electron or hole to the acceptor ("fluctuating cluster model") [6].

IV. Comparison of the consequences of the theory with the experimental results

In Table I the results of kinetic measurements, found in the literature, have been compared with the theoretical values, in cases when all parameters necessary for the calculation were available. The normal redox potentials compiled by LATIMER [2] have been used. In the column of $\lg A_{obs}$, the errors of measurements are also given if they have been reported. In the column of $\lg A_{calc}$, the action constant values calculated from Eq. (5) are shown. In case of a great oxidation-reduction potential difference, corrections due to $\lg D'$ were used.

Table I

System	ε° Volt	E* kcal/mole	lg A_{obs}	Ref.	lg $A_{calc.}$	[H*]-order
Hole transfer reactions						
Co(III) — Fe(II)	−1.82	17.2	15.2	7	>12.8	−1
Co(III) — Ce(III)	−1.82	19.0	15.9 ± 1.5	8	>12.8	−1
Mn(III) — Fe(II)	−1.51	12.1	12.3	9	10.3	0
Pu(V) — Pu(V)**	−1.15	18.8	11.4 ± 2.0	10	10.5	+1
V(V) — Fe(II)	−1.00	8.0	8.5	11	8.0	(*) ?
Pu(IV) — Fe(II)	−0.97	19.1	9.9 ± 0.3	12	9.5	0
Pu(VI) — Ti(III)	−0.93	10.3	9.6 ± 0.3	13	8.5	−1
Pu(VI) — Fe(II)	−0.93	7.6	8.8	14	8.3	(*)
Fe(III) — V(III)	−0.77	17.3	11.8 ± 2.9	15	8.8	0
Np(V) — V(III)	−0.75	14.6	10.1 ± 0.6	16	8.5	0
Np(V) — Np(V)**	−0.75	17.6	8.0 ± 0.1	17	8.4	+1
U(V) — U(V)**	−0.62	9.2	9.3 ± 0.5	18	8.4	+1
Electron transfer reactions						
Fe(II) — H_2O_2	−0.77	9.4	8.6	19	7.2	(*)
Fe(II) — Pu(IV)	−0.77	5.8	5.7 ± 0.3	12	6.0	−1

* Slight pH-dependence due to the change of the potential limits
** Disproportionation

As it is seen in Table I, the calculated and observed action constants generally agree within the order of magnitude.

The systems contain widely different ions, and so this relatively good agreement seems to substantiate, the correctness of the assumptions. Thus, in contradiction to MARCUS' theory [3], it is seen that the enthalpy change of the reaction affects the reaction rate only slightly.

The pH-dependence of the reaction rates also agrees in several cases with the theoretically expected behaviour. E.g., the observed $[H^+]^{-1}$ order is a direct consequence of the theoretically deduced positive activation entropy of the Co(III)—Fe(II) and Co(III)—Ce(III) reactions.

The slight pH-dependence of the Pu(VI)—Fe(II) and the Fe(II)—H_2O_2 reactions can be described by Eq. (13) (see Figs. 4 and 5). The slope of the line, defined by the experimental points, gives, in good approximation, the same value as Eq. (14). Probably the same phenomenon takes place in the V(V)—Fe(II) and in the Fe(II)—Fe(III) exchange [20] proceeding in ice medium, but in the first case proof cannot be obtained because of the other reaction

which depends linearly on the hydrogen ion concentration. Fe(II)—Fe(III) exchange has been measured only at two different acidities in ice. The slope of the line determined by these two points gives a value of $5.1 \cdot 10^6$.

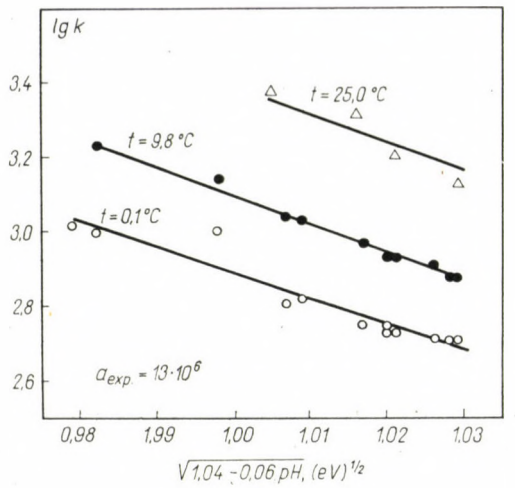

Fig. 4

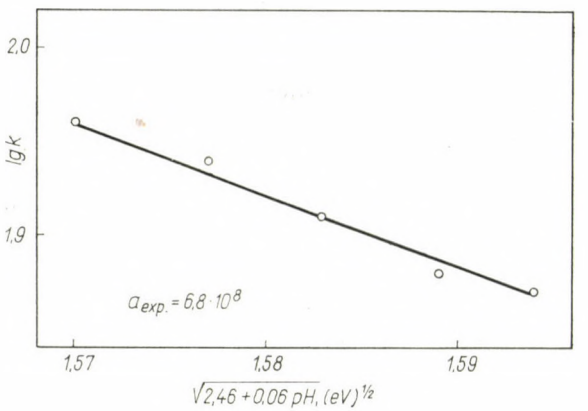

Fig. 5

The $[H^+]$-order of the other reactions listed in Table I cannot be explained similarly to the above cases. It is probable here that the observed pH-dependence is due to coordination chemical processes, such as hydrolysis, formation of oxo-complexes, etc.

In Table II the activation energies calculated on the basis of spectral data have been compared with the experimental values. The crystal field splitting values have been obtained from JØRGENSEN's data [21]. It can be seen that a good agreement is obtained only in that case when the electron

Table II

Activation process	Δ (10 Dq) kK	E* kcal/mole	E* kcal/mole	Ref.
V(IV) ←→ V(III)	3.9	10.7	11.2	22
V(III) ←→ V(II)	4.6	13.2	13.2	23
Mn(III) ←→ Mn(II)	2.1	12.1	6.0	9
Fe(III) ←→ Fe(II)	3.3	9.9	9.5	24
		9.4		19
		5.8		12
Co(II) ←→ Co(II)	8.4	21.6	24.0	25
		17.2		7
		19.0		8
$Co(en)_3^{3+}$ ←→ $Co(en)_3^{2+}$.....	12.0	14.3	64.0	26

transfer does not involve the change of the character of the crystal field: e.g., the activation process of the $Co(en)_3^{2+}-Co(en)_3^{3+}$ reaction results in the transformation of the weak ligand field into a strong one. This can probably be explained by the fact that changes of this magnitude may render important such factors (e.g. alterations in ϱ^4) wich have been neglected in our deductions.

Appendix

Electron tunneling through an asymmetric rectangular potential barrier

The *Schrödinger* equations of the three intervals shown in Fig. 2 (I: $x < 0$; II: $0 \leq x \leq d$; III: $d < x$), are the following:

$$\text{I:}\ \frac{d^2\psi}{dx^2} + \frac{8\pi^2 m}{h^2} E^* \psi = 0 \tag{A.1}$$

$$\text{II:}\ \frac{d^2\psi}{dx^2} + \frac{8\pi^2 m}{h^2} (U_0 + E^* - U)\psi = 0 \tag{A.2}$$

$$\text{III:}\ \frac{d^2\psi}{dx^2} + \frac{8\pi^2 m}{h^2} (U_0 + E^*)\psi = 0 \tag{A.3}$$

The special solutions of these equations are:

$$\psi_{\text{I}} = \exp(\pm ik_1 x)\,, \tag{A.4}$$

$$\psi_{\text{II}} = \exp(\pm ik_2 x)\,, \tag{A.5}$$

and

$$\psi_{III} = \exp(\pm ik_3 x) \tag{A.6}$$

where

$$k_1 = \frac{2\pi}{h}\sqrt{2mE^*}, \tag{A.7}$$

$$k_2 = \frac{2\pi}{h}\sqrt{2m(U_0 + E^* - U)}, \tag{A.8}$$

and

$$k_3 = \frac{2\pi}{h}\sqrt{2m(U_0 + E^*)}. \tag{A.9}$$

Since the electron wave is reflected both at the I—II and II—III interfaces, the general solutions are:

$$\psi_1 = a_1 \exp ik_1 x + b_1 \exp(-ik_1 x), \tag{A.10}$$

$$\psi_2 = a_2 \exp ik_2 x + b_2 \exp(-ik_2 x), \tag{A.11}$$

$$\psi_3 = a_3 \exp ik_3 x + b_3 \exp(-ik_3 x). \tag{A.12}$$

When the electron arrives from interval I, a_1 can be chosen as unity. Let us now take into account that the wave function and its first derivative have to be continuous at $x = 0$ and $x = d$, therefore:

$$\psi_1(0) = \psi_2(0) \tag{A.13}$$

$$\psi_2(d) = \psi_3(d) \tag{A.14}$$

$$\left(\frac{d\psi_1}{dx}\right)_{x=0} = \left(\frac{d\psi_2}{dx}\right)_{x=0} \tag{A.15}$$

$$\left(\frac{d\psi_2}{dx}\right)_{x=d} = \left(\frac{d\psi_3}{dx}\right)_{x=d}. \tag{A.16}$$

Combining the set of equations (A.13)—(A.16) with Eqs. (A.10)—(A.12), a_3 can be expressed as follows:

$$a_3 = \frac{4k_1 k_2 \exp(-ik_3 d)}{(k_1 + k_2)(k_2 + k_3)\exp(-ik_2 d) + [2k_2(k_1 - k_2) - (k_2 + k_3)(k_1 - k_3)]\exp(ik_2 d)}. \tag{A.17}$$

(The arrival of the electron from the right hand side is impossible, therefore, $b_3 = 0$). Since, if $E^* + U_0 < U$, k_2 is a pure imaginary quantity, we may introduce the denotation

$$k_2 = ik\,. \tag{A.18}$$

Forming the possibility expression of D

$$D = a_3 a_3^*, \tag{A.19}$$

where a_3^* is the conjugate of a_3, we may write:

$$D = \frac{4\,k_1^2\,k^2}{\mathrm{sh}^2\,kd\,[(k_1\,k_3 - k^2)^2 + k^2\,(k_1 + k_3)^2] + k^2\,(k_1 + k_3)^2}\,. \tag{A.20}$$

In deducing this correlation the following equation has been used:

$$\mathrm{ch}^2 kd - \mathrm{sh}^2 kd = 1. \tag{A.21}$$

When $kd > 0$, we have

$$\mathrm{sh}^2\,kd \cong \frac{1}{4}\exp 2\,kd\,, \tag{A.22}$$

and the second member of the denominator in (A.20) can be neglected compared with the exponential member. Therefore, the final form of (A.20) will be:

$$D = \frac{16\,k_1^2\,k^2}{(k_1\,k_3 - k^2)^2 + k^2\,(k_1 - k_3)^2}\,\exp(-2\,kd) \tag{A.23}$$

where the pre-exponential factor is denoted as D' in Eq. (4) and (5).

SUMMARY

The theoretical model, suggested in a previous paper of the author for calculating the rate of isotopic electron exchange reactions, has been applied to non-isotopic oxidation-reductions reactions. A correlation is shown to exist between the crystal field splitting values of transition metal ions and the activation energies of the corresponding electron transfer reactions. The types of the pH-dependence of these reactions have been studied.

The theoretical conclusions and the calculated results are compared with the experimental values.

REFERENCES

1. RUFF, I.: J. Phys. Chem. **69**, 3183 (1965).
2. LATIMER, W. M.: Oxidation Potentials. Prentice Hall, New York, 1953.
3. MARCUS, R. A.: Discs. Faraday Soc. **29**, 21 (1960).
4. DULZ, S., SUTIN, N.: Inorg. Chem. **2**, 917 (1963).
5. CAMPION, R. J., PURDIE, N., SUTIN, N.: Inorg. Chem. **3**, 1091 (1964).
6. HORNE, R. A., AXELROD, E. H.: J. Chem. Phys. **40**, 1518 (1964).
7. BENNETT, L. E., SHEPPARD, J. C.: J. Chem. Phys. **66**, 1275 (1962).
8. SUTCLIFFE, L. H., WEBER, J. R.: Trans. Faraday Soc. **52**, 1225 (1956).
9. NICOL, M. J., ROSSIENSKY, D. R.: Chem. Ind. 1166, 1963.
10. RABIDEAU, S. W.: J. Am. Chem. Soc. **79**, 6350 (1957).
11. DAUGHERTY, N. A., NEWTON, T. W.: J. Phys. Chem. **67**, 1090 (1963).
12. NEWTON, T. W., COWAN, H. D.: J. Phys. Chem. **64**, 244 (1960).
13. RABIDEAU, S. W., KLINE, R. J.: J. Phys. Chem. **63**, 1502 (1959).
14. NEWTON, T. W., BAKER, F. B.: J. Phys. Chem. **67**, 1425 (1963).
15. HIGGINSON, W. C. E., SYKES, A. G.: J. Chem. Soc. 2841, 1962.
16. APPELMAN, E. H., SULLIVAN, J. C.: J. Phys. Chem. **66**, 442 (1962).
17. SULLIVAN, J. C. et al.: J. Am. Chem. Soc. **76**, 4275 (1954).
18. IMAI, H.: Bull. Chem. Soc. Japan **30**, 873 (1957).
19. SOBLOWSKI, J.: Roczniki Chemii **36**, 1503 (1962).
20. HORNE, R. A.: J. Inorg. Nucl. Chem. **25**, 1139 (1963).
21. JØRGENSEN, C. K.: Absorption Spectra and Chemical Bonding in Complexes. Pergamon Press, 1962.
22. FURMAN, S. C., GARNER, C. S.: J. Am. Chem. Soc. **74**, 2333 (1952).
23. KRISHNAMURTY, K. V., WAHL, A. C.: J. Am. Chem. Soc. **80**, 5921 (1958).
24. SILVERMAN, J., DODSON, R. W.: J. Phys. Chem. **56**, 846 (1952).
25. SHANKAR, J., DE SOUZA, B. C.: J. Inorg. Nucl. Chem. **24**, 693 (1963).
26. LEWIS, W. B., CORYELL, C. D., IRVINE, J. W.: J. Chem. Soc. Suppl. Issue, No. 2., 5386 (1949).

Über die Rolle des Wassers in Elektronenübergangsreaktionen, II

I. RUFF

Zusammenfassung. Zur Erklärung der Geschwindigkeiten von Elektronenübergangsreaktionen wird das vom Verfasser in der ersten Mitteilung dieser Reihe vorgeschlagene Modell zur Berechnung der Aktionskonstant der Nichtisotopaustausch—Redoxreaktionen angewandt. Zwischen den Kristallraumaufspaltungswerten von Übergangsmetallionen und den Aktivierungsenergien der entsprechenden Elektronenübergangsreaktionen wurde ein Zusammenhang nachgewiesen. Die aus der Theorie folgenden Typen der pH-Abhängigkeit der Elektronenübergangreaktionen werden besprochen.

Die theoretischen Folgerungen und Berechnungsergebnissen werden mit der Erfahrungen verglichen.

Роль воды в реакциях с переходом электрона, II

И. РУФФ

Резюме. Автор применил, предложенную в предыдущей работе для объяснения скоростей реакций с переходом заряда, модель для расчета констант действия окислительно-восстановительных реакций неизотопного обмена. Автор показывает зависимость между величинами кристаллического распада ионов металлов и энергией активации соответствующих реакций с переходом электрона. Обсуждает, далее, зависимости pH, вытекающие из теории, реакций с переходом электрона.

Автор сравнивает теоретические выводы и результаты расчетов с опытными наблюдениями.

Dr. Imre RUFF; Budapest VIII. Múzeum krt. 4/b

ON THE ROLE OF WATER IN ELECTRON TRANSFER REACTIONS, III.

ELECTRODE REACTIONS

I. RUFF

(Department of Inorganic and Analytical Chemistry, L. Eötvös University, Budapest)

Received July 8, 1965

In the previous parts of this series [1, 2] the kinetics of electron transfer reactions were studied by a new theoretical model. In the expression of the rate constant,

$$k = \frac{\mathbf{k}T}{h} \exp\left(\frac{\Delta S^*}{R} - \frac{E^*}{RT}\right), \tag{1}$$

the factors were interpreted as follows:

$$\frac{\Delta S^*}{R} = -\frac{4\pi}{h} d \sqrt{2m(U - U_0 - E^*)} + \lg D' \tag{2}$$

if the electron transfer proceeds by tunnel effect. (In Eq. 2 h is the *Planck*-constant, d = the optimal distance between the reactants in solution, m = mass of the electron, U = energy difference between the potential limit and the energy level of the species, U_0 = difference between the redox potentials of the reacting ion pairs, and D' = constant which does not considerably differ from unity (see Fig. 2 of Part II in this number). If the electron transfer proceeds by hydrogen atom or OH-radical transfer, we have:

$$\frac{\Delta S^*}{R} \geq 0. \tag{3}$$

On the basis of the *Franck—Condon*-principle, the activation energy (E^*) was interpreted as the energy difference between the oxicized and reduced states of the ion:

$$E^* \geq E_{ox} - E_{red} \tag{4}$$

For transition metal ions may be written in the first approximation:

$$E^* = (10\,Dq)_{ox} - (10\,Dq)_{red} \tag{5}$$

where 10 Dq is the crystal field splitting of the ions.

An interesting correlation between the rates of chemical and electrochemical electron transfer reaction was pointed out first by MARCUS [3],

on the basis of his electrostatic polarization theory. However, according to this theory, electrochemical reaction rates cannot be calculated independently from the chemical ones.

In this paper the applicability of the model, introduced by us for chemical electron transfer reactions, is discussed in electron transfer reactions occurring on the surface of an electrode.

I. The redox potential

The electron transfer reactions taking place at an indifferent electrode surface differ from the processes which occur in the bulk of the solution, in two respects: (*i*) the electrode plays the part of one of the reactants, and (*ii*) it can behave both as an electron acceptor (for reduced ions) or an electron donor (for oxidized ones).

In order to give the energy conditions affecting the reaction similarly as shown in Fig. 1, the energy level due to the electrode, i.e., its *Fermi* level must be determined. To do this, the potential of the electrode must be defined taking into consideration all relevant factors of the model used.

It is known that the value of contact potential difference between two bodies is determined by the difference in their *Fermi* levels. On contact of the bodies, the *Fermi* levels become equalized. If the number of electrons in one of the bodies is much larger than in the other, the change in the *Fermi* level of the first body, produced by contacting, will be negligible, thus their equalized *Fermi* level can be considered identical with the original one of the first body.

In our concrete case this means that the electrode immersed in solution assumes the potential of the solution without changing it essentially. The *Fermi* evel of the solution is given by the following expression:

$$N = \sum_i \frac{1}{1 + \exp \frac{E_i - E_F}{kT}} \tag{6}$$

where E_F is the *Fermi* level, E_i = energy of the possible levels, N = number of all electrons of the system, and

$$i = 1, 2, 3, \ldots, n \tag{7}$$

where n is the number of all levels.*

* It is seen that the cases when $E_i \ll E_F$, thus e. g., the electrons of completed shells, need not be considered.

Let us consider a solution in which the number of M^{n+} ions in the oxidized state is N_{ox}, and the number of $M^{(n-1)+}$ ions in the reduced state is N_{red}, and let us accept the usual redox potential scale for energy scale. Furthermore, let the number of H_3O^+ ions be N_p and that of OH^- ions N_h. Thus, on the basis of the investigated model, the number of filled levels of E_0 energy is N_{red}, and that of E_h energy is N_h, whereas the number of unfilled levels

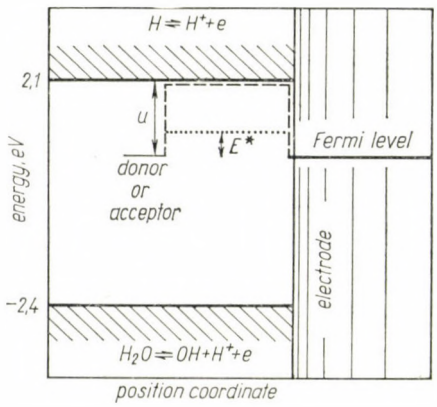

Fig. 1

of E_0 energy is N_{0x}, and that of E_p energy is N_p. Thus, according to Eq. (6) we have:

$$N_{red} + N_h = \frac{N_{red} + N_{ox}}{1 + \exp \frac{E_0 - E_F}{kT}} + \frac{N_h}{1 + \exp \frac{E_h - E_F}{kT}} + \frac{N_p}{1 + \exp \frac{E_p - E_F}{kT}} . \tag{8}$$

The E_F potential of the electrode is described by Eq. (8). Unfortunately, Eq. (8) contains implicitly E_F. To show the analogy with the *Nernst—Peters* equation, let us simplify Eq. (8) as follows: usually it is true that

$$E_p - E_F \gg kT \tag{9}$$

and

$$E_h \ll E_F . \tag{10}$$

(This means that the *Fermi* level is not too near to either of the potential limits.) In this case

$$\frac{N_h}{1 + \exp \frac{E_h - E_F}{kT}} \approx N_h \tag{11}$$

and

$$\frac{N_p}{1 + \exp \frac{E_p - E_F}{kT}} \approx 0\,, \tag{12}$$

therefore

$$E_F = E_0 - kT \ln \frac{N_{0x}^*}{N_{red}}\,. \tag{13}$$

Thus the electrode should be taken into account as a level having always the actual value of the redox potential of the solution. When $N_{ox} = N_{red}$, this potential is E_0, as it follows from Eq. (13). In this way the tunneling electron has to penetrate a symmetric rectangular potential barrier which is schematically shown (dotted lines) in Fig. 1.

II. Calculation of the exchange current

On an equilibrium electrode, the rate of electrochemical reaction is characterized by the exchange current density i_0. It seems useful therefore, to define the rate expression as follows:

$$i_0 = A' \frac{kT}{h} \exp\left(\frac{\Delta S^*}{R} - \frac{E^*}{RT}\right),\ \text{amp} \cdot \text{cm} \cdot \text{mmole}^{-1} \tag{14}$$

where the meaning of A' is understood from the following consideration: If the number of effective activations is $(kT/h) \exp(-E^*/RT)$ per unit time in one litre of a solution which is one molar for both reactants, only those activations will be useful for the electrode process (if $\Delta S^* = 0$) which affect the particles that are at a suitable distance from the electrode; thus, in case of the present model, only those which are nearer to the electrode surface than the next nearest species of acceptor character. Namely, in the opposite case the process is direct electron exchange without any participation of the electrode. In the bulk of the solution, the optimal distance of the particles has been assumed to be about 9.4 Å [1]. Therefore, the number of effective acti-

* It is interesting to note that Eq. (8) has a physical meaning and a finite E_F even if N_{ox} or N_{red} is equal to zero while the *Nernst-Peters*' formula, similarly to Eq. (13), affords $E_F = +\infty$ or $E_F = -\infty$, respectively.

vations is:

$$9.4 \cdot 10^{-8} \frac{kT}{h} \exp\left(-\frac{E^*}{RT}\right), \text{ cm} \cdot \text{mmole}^{-1} \cdot \text{sec}^{-1}.$$

If the *Faraday* number is also taken into account, Eq. (14) can be written (at 25 °C)

$$i_0 = 5.8 \cdot 10^6 \exp\left(\frac{\Delta S^*}{R} - \frac{E^*}{RT}\right). \tag{15}$$

The meaning of ΔS^* and E^* in Eq. (15) is the same as in Eqs (2)—(4) with the difference that in Eq. (2) d is 9.4 Å while in Eq. (15) this denotes only the upper limit of the width of the potential barrier existing before the tunneling electron. Now since the probability of the activated state can be considered identical in first approximation at any value of d between 0 and 9.4 Å, one can calculate with $d = 3.3$ Å in the electrode reaction which is the lowest possible ion-electrode distance without perturbing the hydration sphere of the ion.

In Tables I and II some experimentally observed i_0 values are compared with calculated ones.

Table I

System	ε°, Volt	E*, kcal/mole	lg $i_{0,\,obs}$	lg A_{obs}	lg A_{calc}
Electron transfer reactions					
Eu(II) — Eu(III)	0.43	9.0	—1.7	4.9	5.1
V(II) — V(III)	0.25	6.5	—0.4	4.4	5.1
Ti(III) — Ti(IV)	—0.1	7.0	0.0	5.1	4.8
Hole transfer reactions					
$Fe(CN)_6^{4-}$ — $Fe(CN)_6^{3-}$	—0.36	4	1.0	4.0	4.8
Fe(II) — Fe(III)	—0.77	9	—0.3	6.3	5.2

For the systems shown in Table I RANDLES and SOMERTON [4] made measurements at different temperatures and they determined the activation energies, too. So it was possible for us to compare the action constants which are interesting from the point of view of this hypothesis. In the case of systems shown in Table II the experimental activation energies have not been determined. Therefore the observed and calculated values of lg i_0 could be com-

Table II

System	ε°, Volt	E*, kcal/mole	lg $i_{e,\,obs}$	lg $i_{e,\,calc}$	Ref.
Electron transfer reactions					
Cr(II) — Cr(III)	0.41	9.5	−3.0	−1.8	4
$Co(NH_3)_6^{2+}$ — $Co(NH_3)_6^{3+}$ ...	−0.1	14.3**	−5.3	−5.7	4
$PtCl_4^{2-}$ — $PtCl_6^{2-}$	−0.68	11.2	−5.5	−3.7	6
Ce(III) — Ce(IV)	−1.44	7.7*	−1.7	−1.5	5
Hole transfer reactions					
Tl(I) — Tl(III)	−1.25	12.1*	0.4	−4.5	4
MnO_4^{2-} — MnO_4^-	−0.56	10.5*	1.3	−2.0	4

* These activation energies could not be calculated on basis of Eq. (5), thus the activation energy of the corresponding isotopic exchange reaction has been used (see references in [1]).

** In this system, the activation energy of the $Co(en)_3^{2+}$ — $Co(en)_3^{3+}$ system has been applied, since it is probable that these are approximately identical, and the crystal field approximation is no longer reliable for such low-spin complexes.

pared only. The activation energies have been calculated by Eq. (5) on basis of the spectrophotometric data compiled by JØRGENSEN [7]. This is the reason why the compared data do not show as good agreement as those listed in Table I, since the errors due to the approximations may be added up during the calculation of the two factors.

For the oxidation-reduction potentials required in the calculations, we refer to the book of LATIMER [8].

SUMMARY

The applicability of the model used previously in the theoretical interpretation of the rate of chemical electron transfer reactions, has been discussed for electrochemical reactions. Fair agreements were found between the observed and calculated exchange current values.

REFERENCES

1. RUFF, I.: J. Phys. Chem. **69**, 3183 (1965).
2. RUFF, I.: Acta Chim. Hung. **47**, 241 (1966)
3. MARCUS, R. A.: Can. J. Chem. **37**, 155 (1959). J. Phys. Chem. **67**, 853 (1963).
4. RANDLES, J. E. B., SOMERTON, K. W.: Trans. Faraday Soc. **48**, 937 (1952).
5. VETTER. K, J: Z. phys. Chem. **196**, 360 (1951).
6. KRAVTSOV, V. I., SIMAKOV, B. V.: Vestnik Leningr. Univ. **10**, 96 (1964).
7. JØRGENSEN, C. K.: Absorption Spectra and Chemical Bonding in Complexes. Pergamon Press, 1962.
8. LATIMER, W. M.: Oxidation Potentials. Prentice Hall, New York, 1953.

Über die Rolle des Wassers in Elektronenübergangsreaktionen, III

Reaktionen auf Elektroden

I. RUFF

Zusammenfassung. Die Anwendbarkeit des durch den Verfasser zur theoretischen Besprechung der Geschwindigkeit von Elektronenübergangsreaktionen eingeführten Modells in elektrochemischen Reaktionen wird untersucht. Zwischen den theoretisch berechneten und experimentell gefundenen Tauschstromwerten ergab sich eine genügende Übereinstimmung.

Роль воды в реакциях с переходом электрона, III

И. РУФФ

Резюме. Автор исследовал применимость модели, введенной для теоретического обсуждения скоростей химических реакций, идущих с переходом электрона, к электрохимическим реакциям. Автор нашел удовлетворительную согласованность между, рассчитанными теоретически и определенными экспериментально, величинами обменного тока.

Dr. Imre RUFF; Budapest VIII. Múzeum krt 4/b

INVESTIGATION OF THE ELECTRONIC STRUCTURE OF CATALYTICALLY ACTIVE SOLIDS

I. THE CHANGE OF THE ENERGY BAND STRUCTURE OF INFINITE Ni CRYSTALS WITH THE TEMPERATURE

J. LADIK and G. BICZÓ

(Central Research Institute for Chemistry of the Hungarian Academy of Sciences, Budapest)

Received May 31, 1965

Introduction

In order to establish a quantum mechanical theory of catalysis, such investigations have to deal first of all with the electronic structures of the catalytically active solids. This can be done in several steps only. In the first step the electronic structure of an infinite perfect crystal is investigated, followed by calculation of the surface states of the corresponding finite crystals. Later the effects of lattice imperfections and impurities must also be taken into account. Only the development of a theory of catalytically active solids will make possible to investigate the interaction of the catalyst and the substrate more quantitatively on the basis of quantum mechanics.

In recent years some work has been done to calculate the surface states of semiconductors [1], and the role of this factor in the process of catalysis has been investigated in a semiempirical way [2].

On the other hand, no calculation has dealt with the surface states of metals, thus it has not been possible to try to find correlations between the electronic structure of catalytically active metals and their activity. Therefore, the primary object of our work was to calculate the electronic structure of catalytically active metals. As the first step, we calculate the energy band structures of infinite metal crystals at different temperatures, and on the basis of these data we shall try to proceed to the calculation of the surface states.

In this paper which is intended to be the first of a series, we report the calculation of the energy band structure of an infinite Ni crystal at 0 °K and at 1373 °K. The band structure of this metal was calculated first by FLETCHER and WOHLFARTH [3] for absolute zero temperature. Assuming spherical potential, they used two-center approximation to determine the most important interaction integrals which occur in the tight binding method. From the results they calculated the energy bands of the face-centered cubic Ni lattice for a part of the first BRILLOUIN zone. A few years later KOSTER [4], using the interpolation method developed by SLATER and himself [5], extended the tight binding approximation to the whole first BRILLOUIN zone of Ni.

In his paper he gave the curve of the density of states, but unfortunately he did not report the detailed band structure at 0 °K. BELDING [6] repeated the calculation of KOSTER using the tight binding approximation in the form developed by SLATER and KOSTER [5], but he applied an analytical potential function, taking into account also interactions with second neighbours. His results show that the effect of the second neighbours is only ten per cent of that of the first neighbours.

Recently more sophisticated calculations have been made concerning the band structure of Ni. YAMASHITA et al. [7] used a modified tight binding approximation and a GREEN function method to determine the band structure in the whole first BRILLOUIN zone at 0 °K. They found 0.304 Ry for the total width of the 3d bands by the first method, and 0.314 Ry by the second. Further MATTHEISS [8] applied the *augmented plane wave* method to calculate the high symmetry parts of the first BRILLOUIN zone.

It should be emphasized, however, that all these calculations refer to the band structure of Ni at 0 °K (with the exception of MATTHEISS' work [8], in which the room temperature value of the lattice constant was considered), and no attempt has been made for the determination of the variation of the band structure with temperature. Therefore, the main purpose of this work has been to study the effect of the increase of temperature on the band structure of Ni.* Since catalytic reactions take place mostly at rather high temperatures, the results may contribute to the understanding of the catalytic activity of Ni.

Method

For the calculation of the energy band structures, we have used the tight binding approximation, taking into account the 4s and the five 3d states of Ni. In a face-centered cubic lattice each atom has twelve nearest neighbours, whose positions may be characterized by the lattice vectors $pa\mathbf{i} + qa\mathbf{j} + ra\mathbf{l}$, where a is the lattice constant and $\mathbf{i}$, $\mathbf{j}$ and $\mathbf{l}$ are unit vectors in the x, y, z directions, respectively. Of the integers, p, q and r, two are always equal to unity, and the third is zero [for instance $(p\ q\ r) = (1\ 1\ 0)$]. The elements of the matrix $\mathbf{H}(\mathbf{k})$ of order 6, whose

$$\mathbf{H}(\mathbf{k})\,\mathbf{c}_i(\mathbf{k}) = \varepsilon_i(\mathbf{k})\,\mathbf{c}_i(\mathbf{k}) \tag{1}$$

* The increase of temperature has a two-fold effect on the band structure of solids: first by the increase of the lattice constant (expansion of the crystal); secondly, the temperature-dependent interaction of electrons with phonons also influences the band structure. According to FAN'S calculations [9] the two phenomena have a comparable effect on the energy gap of Ge. In the present paper we deal only with the first effect.

eigenvalue problem provides the possible energy levels in the case of a given wave number vector,

$$\mathbf{k} = \frac{\xi}{a}\mathbf{i} + \frac{\eta}{a}\mathbf{j} + \frac{\zeta}{a}\mathbf{l}, \tag{2}$$

can be constructed with the aid of the formulas given by SLATER nad KOSTER [5] in their Table II, if we consider the terms (0 0 0), (1 1 0) and (0 1 1) only.

Numbering the s, xy, xz, yz, $x^2 - y^2$, $3z^2 - r^2$ functions in this order by 1, 2, 3, 4, 5, 6, and assuming that the interactions of the 4s orbital with the 3d orbitals is small, we have neglected the $H(\mathbf{k})_{1,\,j}$ ($j = 2, \ldots, 6$) elements in the symmetrical $\mathbf{H}(\mathbf{k})$ matrix. In this way, the original eigenvalue problem is split to a first order problem and to a fifth order one. Furthermore, from the symmetry of the 3d functions it follows, that $H(\mathbf{k})_{2,2} = H(\mathbf{k})_{3,3} = H(\mathbf{k})_{4,4}$, $H(\mathbf{k})_{2,3} = H(\mathbf{k})_{2,4} = H(\mathbf{k})_{3,4}$, $H(\mathbf{k})_{3,5} = H(\mathbf{k})_{4,5}$, and finally $H(\mathbf{k})_{3,6} = H(\mathbf{k})_{4,6}$. So we are left only with nine different elements of the matrix $\mathbf{H}(\mathbf{k})$, namely: $H(\mathbf{k})_{1\,1}$, $H(\mathbf{k})_{2,2}$, $H(\mathbf{k})_{5,5}$, $H(\mathbf{k})_{6,6}$, $H(\mathbf{k})_{2,3}$, $H(\mathbf{k})_{2,6}$, $H(\mathbf{k})_{3,5}$, $H(\mathbf{k})_{3,6}$ and $H(\mathbf{k})_{5,6}$. These nine quantities, as it is easy to show on the basis of the formulas of Table II of [5], can be expressed with the aid of ten energy integrals. These are the following: $E_{1,1}$ (0 0 0), $E_{1,1}$ (1 1 0), $E_{2,2}$ (0 0 0), $E_{6,6}$ (0 0 0), $E_{2,2}$ (1 1 0), $E_{2,2}$ (0 1 1), $E_{6,6}$ (1 1 0), $E_{5,5}$ (1 1 0), $E_{2,3}$ (0 1 1), $E_{2,6}$ (1 1 0). For the last six integrals we used at 0 °K the values obtainable from the results of FLETCHER and WOHLFARTH [3] (see Table IV of [5]). Since the values of the energy integrals $E_{2,2}$ (1 1 0) and $E_{2,2}$ (0 1 1) obtained by FLETCHER and WOHLFARTH for Ni and by HOWARTH [10] for copper (with the aid of the cellular method) agree quite well, we used for $E_{2,2}$ (0 0 0) the value of HOWARTH calculated for Cu. Further, since in a two-center approximation, which was applied FLETCHER and WOHLFARTH, $E_{2,2}$ (0 0 0) = $E_{6,6}$ (0 0 0), we used for both energy integrals the arithmetic mean of the two integrals given by HOWARTH for Cu. Finally, in the absence of satisfactory data for Ni (FLETCHER and WOHLFARTH did not take into account the 4s state of Ni), we used for these last two quantities the values obtained by HOWARTH [10] for Cu. Table I lists the used integral values in rydberg units.

Substituing the values of the integrals in the appropriate expression of the nine remaining different elements of the matrix $\mathbf{H}(\mathbf{k})$, listed above, we solved the eigenvalue problem for the whole $\mathbf{k}$ space. Since, however, the energy band structure shows a symmetry in respect of the reciprocal lattice of a face-centred cubic lattice, actually we had to perform the calculations only in one forty-eighth of the first BRILLOUIN-zone. Further, since we were interested mainly in the qualitative behaviour of the band structure with respect to the change of temperature, and since KOSTER [4] had already more

precisely determined the band structure at 0 °K taking into account 680 points, we used only a mesh of $\frac{\pi}{4}$ in the three directions of the reciprocal space.

To calculate the band structure at 1373 °K, we had to determine the integrals listed in Table I for this case. Assuming in the first approximation the validity of the relation

$$\frac{E_{i,j}^{(T)}}{E_{i,j}^{(0)}} = \frac{S_{i,j}^{(T)}}{S_{i,j}^{(0)}} \tag{3}$$

Table I

The used energy integrals of Ni (in rydbergs) at 0 °K

$E_{1,1}$ (0 0 0)	0.0366
$E_{1,1}^{(0)}$ (1 1 0)	−0.0683
$E_{2,2}$ (0 0 0) = $E_{6,6}$ (0 0 0) ...	−0.6156
$E_{2,2}^{(0)}$ (1 1 0)	−0.01928
$E_{2,2}^{(0)}$ (0 1 1)	0.00574
$E_{6,6}^{(0)}$ (1 1 0)	−0.00786
$E_{5,5}^{(0)}$ (1 1 0)	0.01353
$E_{2,3}^{(0)}$ (0 1 1)	−0.03116
$E_{2,6}^{(0)}$ (1 1 0)	−0.03917

where index (0) refers to 0 °K and index (T) to T °K, we calculated the appropriate $S_{i,j}$ overlap integrals for 0 °K and 1373 °K. In doing so, we had to take into account the change of the lattice constant with temperature. The lattice constant of Ni at 0 °K is $a = 3.517$ Å [11] and the largest known value of a, at 1373 °K, is $a' = 3.591$ Å [12].

Since the values of $E_{1,1}$ (0 0 0) and of $E_{2,2}$ (0 0 0) do not depend on the lattice constant, these integrals do not change with the temperature. The other seven integrals shown in Table I, however, depend on the lattice constant and therefore on the temperature. In order to be able to determine their values on the basis of equation (3), we calculated first the ratio of the overlap integrals of the 3d functions and of the 4s functions at $\sqrt{2}a$ (0° K) and at $\sqrt{2}a'$(1373 °K).

The overlap integrals of the 3d functions corresponding to the 6 last data of Table I may be expressed in the following way:

$$
\begin{aligned}
S_{2,2}\,(110) &= \frac{3}{4}\,S_{3\zeta,3\zeta} + \frac{1}{4}\,S_{3\xi,3\xi}\,,\\
S_{2,2}\,(011) &= \frac{1}{2}\,S_{3\eta,3\eta} + \frac{1}{2}\,S_{3\xi,3\xi}\,,\\
S_{6,6}\,(110) &= \frac{3}{4}\,S_{3\xi,3\xi} + \frac{1}{4}\,S_{3\zeta,3\zeta}\,,\\
S_{5,5}\,(110) &= S_{3\eta,3\eta}\,,\\
S_{2,3}\,(011) &= \frac{1}{2}\,S_{3\eta,3\eta} - \frac{1}{2}\,S_{3\xi,3\xi}\,,\\
S_{2,6}\,(110) &= \frac{\sqrt{3}}{4}\,S_{3\xi,3\xi} - \frac{\sqrt{3}}{4}\,S_{3\zeta,3\zeta}\,,
\end{aligned}
\tag{4}
$$

where we used the notation of KOTANI et al. [13] in the right hand side of the equations. The different overlap integrals occurring in Equations (4) are expressed with the aid of the auxiliary functions $A_n(\alpha)$ [12]. The tabulated values of the latter were taken from the Tables of MILLER et al. [14]. Calculating, in this way the overlap integrals at the distances $\sqrt{2}\,a$ and $\sqrt{2}\,a'$, we obtained the ratios of the corresponding overlap integrals (values between 0.67 and 0.69). Substitution of the latter, together with the $E_{i,j}^{(0)}$ values given in Table I, into Equation (3) gave the values of $E_{i,j}^{(T)}$.

In the case of the overlap integrals of the 4s functions there is a difficulty; according to SLATER's rules, in the wave function

$$\psi_{4s} = Ne^{-ar}\,r^{n'-1} \tag{5}$$

we have $n' = 3.7$. Therefore, it was necessary to perform the following procedure. After transforming to elliptical coordinate system and integrating according to the azimuths, we obtained for the overlap integral the expression

$$S_{4s,4s}\,(1\ 1\ 0) \sim a^{2\cdot 3.7+1} \int_{-1}^{1}\int_{1}^{\infty} e^{-a a\sqrt{2}\mu}\,(\mu^2 - \nu^2)^{3.7}\,d\mu\,d\nu\,. \tag{6}$$

Fortunately, it can be shown that the ratio

$$R_{n'} = \frac{I_{n'}(a')}{I_{n'}(a)}\,, \tag{7}$$

where

$$I_{n'}(a) = \int_{-1}^{1}\int_{1}^{\infty} e^{-a a\sqrt{2}\mu}\,(\mu^2 - \nu^2)^{n'}\,d\mu d\nu\,, \tag{8}$$

is a slowly varying function of n'. Therefore, we could determine $R_{3.7}$ by means of linear interpolation between R_3 and R_4. So we obtained the ratio

$$\frac{S^{(T)}_{4s,4s}(1\ 1\ 0)}{S^{(0)}_{4s,4s}(1\ 1\ 0)} = \left(\frac{a'}{a}\right)^{2\cdot 3.7+1} R_{3.7}. \tag{9}$$

Substituting the latter into Equation (3), we have got also $E^{T}_{4s,4s}(1\ 1\ 0)$.

In Table II we give the energy integrals obtained as described above for $T = 1373$ °K.

Table II

The used integrals of Ni (in rydbergs) at 1373° *K*

$E_{1,1}$ (0 0 0)	0.0366
$E^{(T)}_{1,1}$ (1 1 0)	−0.0478
$E_{2,2}$ (0 0 0) = $E_{6,6}$ (0 0 0) ...	−0.6156
$E^{(T)}_{2,2}$ (1 1 0)	−0.01328
$E^{(T)}_{2,2}$ (0 1 1)	0.00386
$E^{(T)}_{6,6}$ (1 1 0)	−0.00541
$E^{(T)}_{5,5}$ (1 1 0)	0.00906
$E^{(T)}_{2,3}$ (0 1 1)	−0.02085
$E^{(T)}_{2,6}$ (1 1 0)	−0.02701

Results

Table III summarizes the results of the calculations for 0 °K, and Table IV for 1373 °K. In both Tables the limits of the bands ($\lambda_{i_{\min}}$ and $\lambda_{i_{\max}}$) are given in 10^5 cm^{-1} units. The Tables also contain the widths of the bands ($\Delta\lambda_i$). Since in the matrix eigenvalue equation (1) all the elements corresponding to the interaction of the 4s orbitals with the 3d orbitals were chosen to be 0, the λ_1 values correspond to pure 4s bands. On the other hand, the five 3d band obtained correspond to a mixture of the original five 3d functions. Therefore, in the last rows of the Tables, the data of the common 3d band are also given.

In connection with λ_i values of the 3d bands, given in Tables III and IV, it should be mentioned that we always arranged the eigenvalues of the matrix **H** by a given vector **k** according to their magnitude. In order to be able to decide which eigenvalues belong to the individual bands, it would be necessary to calculate the band structure at much more points of space **k**, than we have done. Since, however, all 3d bands overlap to form a common 3d band,

the determination of the limits of the individual 3d bands has not been very interesting from the point of view of the present work.

Table III

The energy band structure of Ni at $T = 0°$ K, in 10^5 cm^{-1} units

	i	$\lambda_{i_{min}}$	$\lambda_{i_{max}}$	$\Delta\lambda_i$
4s band	1	−0.859	+0.340	1.199
3d bands	2	−0.651	−0.310	0.341
	3	−0.724	−0.510	0.214
	4	−0.810	−0.591	0.219
	5	−0.833	−0.594	0.239
	6	−1.001	−0.700	0.301
Common 3d band		−1.001	−0.310	0.691

Table IV

The energy band structure of Ni at $T = 1373°$ K, in 10^5 cm^{-1} units

	i	$\lambda_{i_{min}}$	$\lambda_{i_{max}}$	$\Delta\lambda_i$
4s band	1	−0.590	+0.250	0.840
3d bands	2	−0.652	−0.428	0.224
	3	−0.747	−0.561	0.186
	4	−0.767	−0.617	0.150
	5	−0.783	−0.619	0.164
	6	−0.898	−0.688	0.210
Common 3d band		−0.898	−0.428	0.470

Discussion

It is seen from Tables III and IV, that we have a rather broad 4s band and a somewhat narrower common 3d band at both temperatures. In both cases, the 4s band and the common 3d band overlap each other considerably. These deductions are in agreement with the results of the more detailed calculations of KOSTER [4] for the energy band structure of Ni at 0 °K.

Comparing our value obtained for the width of the total 3d band at 0 °K ($\Delta\lambda_{3d} = 0.69 \cdot 10^5$ cm^{-1}) with the corresponding values of YAMASHITA et al. [7] ($\Delta\lambda_{3d} = 0.33 \cdot 10^5$ cm^{-1} in the modified tight binding approximation, and $\Delta\lambda_{3d} = 0.35 \cdot 10^5$ cm^{-1} by the GREEN function method), it is seen that our value is nearly twice as great, as his results. On the other hand, MATTHEISS [8] using the room temperature lattice constant of Ni and calculating by the method of augmented plane wave approximation only for the high symmetry

part of the first BRILLOUIN zone, obtained the value $0.94 \cdot 10^5$ cm^{-1} for $\Delta\lambda_{3d}$. This is considerably larger, than our value. It is evident that the calculated width of the 3d band of Ni strongly depends on the method of approximation applied.

Comparing the results obtained for 0 °K and 1373 °K (cf. Tables III and IV), it is apparent that the band structure of Ni depends strongly on the temperature, i.e., on the lattice constant. The width of the 4s band decreases from $1.20 \cdot 10^5$ cm^{-1} to $0.84 \cdot 10^5$ cm^{-1}, and that of the common 3d band from $0.69 \cdot 10^5$ cm^{-1} to $0.47 \cdot 10^5$ cm^{-1}. It should be emphasized that the correspondig change of the lattice constant is only $\Delta a = a' - a = 3.59 - 3.52 = 0.07$ Å. So we conclude that the energy band structures of transition metals depend (at least, if we take into account only the expansion of the lattice with the increase of the temperature, neglecting the temperature-dependence of the interaction of electrons with phonons) so strongly on the temperatnre that for an interpretation of catalytic effects we have to use the band structures determined for the temperature of the catalytic reaction, and the energy band structures obtained for 0 °K cannot be applied. We intend to return to the problem of the effect on the band structure of the interaction of electrons and phonons in a subsequent paper.

We wish to express our gratitude to Academician Dr. G. SCHAY and to Dr. F. NAGY, Corresponding Member of the Hungarian Academy of Sciences, for calling our attention to the problem, and for their inspiring interest during this work. We are indebted to Mr. F. BELEZNAY for many stimulating discussions and for calling our attention to important data in the literature, to Miss J. RÉDLY for solving the matrix eigenvalue problems on the Ural II computer of the State Institute of Statistics, and finally to Miss A. JESZENÁK for performing the tedious desk calculations.

SUMMARY

The energy bands of Ni have been calculated in the whole first BRILLOUIN zone for 0° K and 1373° K, using the tight binding approximation in its interpolation form suggested by SLATER and KOSTER. The effect of the expansion of the crystal by the increase of the temperature has been considered, neglecting, however, the interaction of electrons with phonons. The energy integrals at 1373° K were estimated from the corresponding energy integrals at 0° K, and from the overlap integrals at 0° K and 1373° K.

According to the results, the widths of the 4s band and of the common 3d band are decreased considerably with the increase of the temperature. Therefore, any theoretical interpretation of the catalytic properties of transition metals has to consider the band structures computed for the temperature of the catalytic reaction.

REFERENCES

1. See, e. g., KOUTECKÝ, J.: Phys. Rev. **108,** 13 (1957); KOUTECKÝ, J., TOMÁŠEK, M.: Phys. Rev. **120,** 1212 (1960).
2. WOLKENSTEIN, T.: Elektronentheorie der Katalyse an Halbleitern. (VEB. Deutscher Verlag der Wissenschaften, Berlin) 1964.
3. FLETCHER, G. C., WOHLFARTH, E. P.: Phil. Mag. **42,** 106 (1951); FLETCHER, G. C.: Proc. Phys. Soc. (London) **A65,** 192 (1952).
4. KOSTER, G. F.: Phys. Rev. **98,** 901 (1955).

5. SLATER, J. C., KOSTER, G. F.: Phys. Rev. **94,** 1498 (1954).
6. BELDING, E. F.: Phil. Mag. **4,** 1145 (1959).
7. YAMASHITA, J., FUKUCHI, M., WAKOH, S.: J. Phys. Soc. Japan **18,** 999 (1963).
8. MATTHEISS, L. F.: Phys. Rev. **134,** A971 (1964).
9. FAN, H. Y.: Phys. Rev. **82,** 900 (1951).
10. HOWARTH, D. J.: Proc. Roy. Soc. (London) **A220,** 513 (1953).
11. HEUMANN, T.: Naturwiss. **32,** 296 (1944).
12. ESSER, H., EILENDER, W., BURGHARDT, K.: Arch. Eisenhüttenwesen **12,** 157 (1938).
13. KOTANI, M., AMEMIYA, A., ISHIGURO, E., KIMURA, T.: Tables of Molecular Integrals. (Maruzen Co. Ltd., Tokyo) 1955.
14. MILLER, J., GERHAUSER, J. M., MATSEN, F. A.: Quantum Chemistry Integrals and Tables. (University of Texas Press, Austin) 1959.

Untersuchung der Elektronenstruktur katalytisch aktiver Feststoffe, I

Durch Temperaturänderung hervorgerufene Modifizierung der Energiebandenstruktur infinitesimaler Nickelkristalle

J, LADIK und G, BICZÓ

Zusammenfassung. Mittels der durch SLATER and KOSTER eingeführten Interpolationsform der LCAO-Annäherung wurden die Energiebanden des Nickels in der ersten ganzen BRILLOUIN-Zone bei den Temperaturen 0° K und 1373° K berechnet. Im letzteren Fall wurde die durch Temperaturzunahme hervorgerufene Ausdehnung des Kristalles in Betracht genommen, jedoch die Wechselwirkung der Elektronen mit den Phononen vernachlässigt. Die auf 1373° K beziehenden Energie-Integrale wurden mittels der auf 0° K beziehenden Energie-Integrale und der zu den Temperaturen 0° K bzw. 1373° K gehörenden Überlappungsintegrale geschätzt.

Nach den Ergebnissen nimmt die Bandenbreite der Bande 4s und der gemeinsamen Bande 3d mit Temperaturzunahme wesentlich ab. Daher muss man bei der theoretischen Erklärung der katalytischen Eigenschaften von Übergangsmetallen aus der zur Temperatur der katalytischen Reaktion gehörenden Bandenstruktur ausgehen.

Исследование электронной структуры каталитически активных твердых тел, I

Видоизменение структуры полосы энергии бесконечных кристаллов Ni, наступающее с изменением температуры.

Я. ЛАДИК и Г. БИЦО

Резюме. Используя введенную Слатером и Костерем интерполяционную форму приближения ЛКАО, авторы рассчитали полосы энергии Ni в первой Brillouin зоне при температурах 0° К и 1373° К. В последнем случае принимали во внимание расширение кристалла, наступающее вследствие увеличения температуры, но пренебрегли взаимодействием электронов и фононов. Энергетические интегралы, относящиеся к 0° К и 1373° К, оценивали с помощью интегралов перекрывания, относящихся к температурам 0° К и 1373° К.

Согласно полученным результатам, ширина полосы 4s и общей 3d значительно уменьшается с возрастанием температуры. Поэтому, при теоретическом объяснении каталитических свойств переходных металлов необходимо исходить из структуры полосы, относящейся к температуре каталитической реакции.

Dr. János LADIK
Géza BICZÓ
Budapest II., Pusztaszeri út 57/69

ON THE PARAMETER FORM OF MATRIX F, II*

INVESTIGATION OF THE ASSIGNMENT WITH THE AID OF THE PARAMETER FORM

(SHORT COMMUNICATION)

P. PULAY and F. TÖRÖK

(Institute of General and Inorganic Chemistry, L. Eötvös University, Budapest)

Received July 14, 1965

1.

In our previous work [1] we dealt with the real symmetric force constant matrices F, reproducing the proper normal frequencies of the molecule. These matrices can be formed on the basis of the following relation:

$$F = g^{-1} U \Lambda U' g^{-1} \tag{1}$$

where $g = G^{1/2}$; G is the familiar matrix [2], Λ is the diagonal matrix consisting of the elements $\lambda_i = 4\pi^2 \nu_i^2$ ($i = 1,2, \ldots, n$), where ν_i denotes the normal frequencies of the molecule. U is an orthogonal matrix with a determinant $+1$, and can be given as a function of $\binom{n}{2}$ parameters.

On the basis of expression (1), one can obtain the matrices F corresponding to all the possible $n!$ assignments, containing, however, a lot of improbable values, too. If we deal with a given assignment only, the force constants fluctuate within a much narrower interval. In order to utilize the information got from the assignment, it is reasonable to define which of the F matrices gives the closest correspondence between the internal and normal coordinates. In this work we are studying the possibilities by which one can define the closest assignment, the possibility for defining the assignment by the matrix U, and we shall give F matrices being close to the best assignment, and compare them with the most reliable force fields, as determined from additional data (zeta constants, centrifugal stretching constants, etc).

2.

Between the two sets of coordinates $S_1, \ldots, S_n$ (the sequence being defined by the matrix G) and the normal coordinates $Q_1, \ldots, Q_n$ (the sequence

* Part I: Acta Chim. Hung. **44**, 287 (1965).

is given by the matrix Λ), the following relation holds:

$$S = LQ, \quad Q = L^{-1}S \tag{2}$$

where S and Q are column matrices consisting of the internal and normal coordinates, respectively, and L is the matrix which consists of the eigenvectors of GF and is normed by $LL' = G$.

From Equation (2) it follows that the coefficients showing the weight of the internal coordinates $S_1, \ldots . S_n$ in the normal coordinate Q_i can be found in the i-th row of the matrix L^{-1}, and the elements of the i-th column of L are characteristic of the distribution of Q_i among the internal coordinates. The strength of the connection between the i-th normal and j-th internal coordinates may be concluded from the value of L_{ji} and L_{ij}^{-1}, respectively. From the matrices L and L^{-1}, being general ones, an easily interpretable information for the connection between the internal and normal coordinates cannot be obtained. For this reason YONEZO MORINO and KOZO KUCHITSU [3] proposed the potential energy as basis for assigning the normal coordinates. Thus the connection of the i-th normal and j-th internal coordinates is characterized by the value of $L_{ji}^2 F_{jj}$.

J. W. TAYLOR emphasized that in judging the assignment one must take into account not only the potential, but also the kinetic energy distribution [4]. Thus, if the j-th internal coordinate is favoured in the i-th normal one, then not only $L_{ji}^2 F_{jj}$ but also $L_{ji}^2 G_{jj}^{-1}$ must be relatively great.

When we are investigating the F matrices quite generally, it seems more reasonable to take into account not only the diagonal terms, but also the total kinetic and potential energy proportions belonging to the internal coordinate S_j from the i-th normal vibration. Denoting these quantities by T_j^i and V_i^j, we have

$$T_j^i = \sum_i L_{ji} L_{ki} G_{jk}^{-1}; \quad V_j^i = \sum_i L_{ji} L_{ki} F_{jk}/\lambda_i . \tag{3}$$

The trends of the diagonal terms $L_{ji}^2 G_{jj}^{-1}$ and $L_{ji}^2 F_{jj}/\lambda_i$ differ from each other, and the absolute value of the off-diagonal terms may be greater than that of the corresponding diagonal ones. This may cause serious inconsistencies in interpreting the results. On the other hand, the following equation is valid for T_j^i and V_j^i

$$T_j^i = V_j^i = L_{ij}^{-1} L_{ji} = M_{ij} \tag{4}$$

i.e., the distribution of the kinetic and potential energy is given by the same expression, which contains those elements of L and L^{-1} which are characteristic of the connection between the normal and internal coordinates. The matrix M consisting of the elements M_{ij} seems to be suitable for the description of the

assignment. Nevertheless, the application of M is hindered because the best assignment does not correspond to the unit matrix. M will be unit matrix if L is either a lower or an upper triangular matrix. Moreover, the diagonal elements of M may be negative, and the application would be more comfortable, if the quadrate sum (in place of the sum) of the elements in a row or in a column gave unity.

The matrix U in (1) enables us to express not only F, but also L and L^{-1} in a simple manner:

$$L = gU \qquad L^{-1} = U'g^{-1}. \tag{5}$$

Therefore, it is obvious to consider U as the basis for judging the assignment. The orthogonality and the independence from the concrete problem are great advantages of U. Thus one regard the assignment characterized by $U = I$ (unit matrix) as the best assignment. Then, of course:

$$F = F_0 = g^{-1} \Lambda g^{-1}. \tag{6}$$

A difficulty arises, however, in connection with the matrix U. If we transform from the internal coordinates S to $S_1 = \mu S$, where the elements of the diagonal matrix μ are the scale factors (i.e., we alter the unit of measurement in S), then each row and colum of G will be multiplied with the corresponding scale factor. The new G matrix will be $G_1 = \mu G \mu$. The alteration of g is, however, not so simple: $g_1 = G_1^{1/2} \neq g \mu$. We can express g_1 in the form: $g_1 = Vg \mu$, where V is an orthogonal matrix. On substituting the above expression into (6), we obtain

$$F_1 = \mu^{-1} g^{-1} V' \Lambda V \quad g^{-1} \quad \mu^{-1}.$$

Returning to the original coordinates S, we get

$$F = g^{-1} V' \Lambda V g^{-1}.$$

Therefore, the best assignment depends on the units of measure for the internal coordinates. Nevertheless, the results obtained in the 2 by 2 case indicate that this dependence cannot be so strong that F may turn into a matrix F which belongs to another assignment.

If we define a criterion for the best assignment, scale factors can be determined in such a manner, that the matrix F_0 from the transformed matrix G should be the best one, according to this criterion. For example, one can define the best assignment in such a manner that the sum of the squares of the off-diagonal elements of U divided by the sum of the squares of the elements in

the corresponding row, should be minimal. Making use of the parameter form of U, we obtain, that it is necessary to choose the scale factors in such a manner that $g_{ii} = G_{ii}$ $(i = 1,2, \ldots, n)$. Another closely related weighing of G_1 is considerably simpler, where we demand that $G_{ii} = 1$ $(i = 1, \ldots, n)$. So far we have not succeeded in obtaining a condition ideal from every point of view.

3.

In the preceding paragraph the view-points for defining the best assignment have been summarized. On investigating concrete cases, it is seen that the "best assignment" F matrices corresponding to the various definitions, do not differ considerably from one another.

The determination of the F_0 matrix, proposed by us, is very simple contrary to the methods using Jacobian matrices, because we have a rapidly converging simple iteration method for computing the square root of a positive definite matrix [5].

We remark that a relation like (1) was given first by J. W. TAYLOR [6]. We prefer (1) for two reasons: it requires less computation, and when $U = I$ (unit matrix) is substituted into Taylor's formula, the resulting F matrix may be far from the force constant matrix corresponding to the best assignment.

The force constants of some methyl and silyl halides are presented in Tables I and II. Elements of F_0 are given in the first and second columns, while the last column contains the Hybrid Orbital Force Field (HOFF) constants as given by MILLS and ALDOUS [7] and by DUNCAN [8]. All force constants refer to the usual scaled valence symmetry coordinates, as defined by ALDOUS and MILLS [9]. Computations were performed on a NE 803 B and an Ural-2 digital computer.

In most cases, as in our examples, the real force field of the molecule does not differ considerably from the F_0 matrix, and generally lies between F_0 and the diagonal F matrix. It is remarkable that the signs of all off-diagonal elements are the same in F_0 and in the most reliable H. O.F. F. This statement may be probably generalized for the significant off-diagonal force constants in molecules, where a definite assignment can be given. It may be hoped that the easily determinable F_0 matrix will provide considerable help in the assignment of molecular vibrations.

Table I

Force constants of methyl halides (mdyne/A)

A spec.	CH_3F	CD_3F	HOFF	E spec.	CH_3F	CD_3F	HOFF
F_{11}	5.273	5.514	5.36	F_{44}	5.464	5.703	5.39
F_{12}	0.122	0.210	0*	F_{45}	−0.266	−0.455	−0.124
F_{13}	0.607	0.781	0*	F_{46}	0.406	0.676	0.124
F_{22}	0.595	0.669	0.618	F_{55}	0.524	0.523	0.492
F_{23}	−0.506	−0.747	−0.58	F_{56}	−0.125	−0.092	−0.055
F_{33}	5.682	5.567	5.79	F_{66}	0.778	0.798	0.759
A spec.	CH_3Cl	CD_3Cl	HOFF	E spec.	CH_3Cl	CD_3Cl	HOFF
F_{11}	5.478	5.633	5.45	F_{44}	5.601	5.812	5.53
F_{12}	0.122	0.203	0*	F_{45}	−0.271	−0.472	−0.115
F_{13}	0.629	0.801	0*	F_{46}	0.372	0.640	0.115
F_{22}	0.514	0.550	0.547	F_{55}	0.527	0.525	0.485
F_{23}	−0.362	−0.536	−0.45	F_{56}	−0.126	−0.105	−0.038
F_{33}	3.412	3.531	3.42	F_{66}	0.632	0.670	0.618
A spec.	CH_3Br	CD_3Br	HOFF	E spec.	CH_3Br	CD_3Br	HOFF
F_{11}	5.479	5.587	5.44	F_{44}	5.611	5.806	5.53
F_{12}	0.116	0.188	0*	F_{45}	−0.271	−0.473	−0.117
F_{13}	0.679	0.868	0*	F_{46}	0.359	0.621	0.117
F_{22}	0.469	0.503	0.504	F_{55}	0.525	0.518	0.476
F_{23}	−0.333	−0.495	−0.394	F_{56}	−0.123	−0.106	−0.031
F_{33}	2.916	3.072	2.90	F_{66}	0.560	0.599	0.546
A spec.	CH_3J	CD_3J	HOFF	E spec.	CH_3J	CD_3J	HOFF
F_{11}	5.476	5.661	5.48	F_{44}	5.662	5.847	5.61
F_{12}	0.114	0.187	0*	F_{45}	−0.272	−0.478	−0.157
F_{13}	0.685	0.885	0*	F_{46}	0.345	0.601	0.157
F_{22}	0.438	0.474	0.480	F_{55}	0.524	0.518	0.472
F_{23}	−0.292	−0.434	−0.351	F_{56}	−0.121	−0.107	−0.026
F_{33}	2.364	2.521	2.337	F_{66}	0.494	0.531	0.480

* Constrained to be zero.

Table II

Force constants of silyl halides (mdyne/A)

A spec.	SiH_3F	SiD_3F	HOFF	E spec.	SiH_3F	SiD_3F	HOFF
F_{11}	2.863	2.905	2.865	F_{44}	2.747	2.874	2.781
F_{12}	0.034	0.059	0.022	F_{45}	−0.064	−0.119	−0.032
F_{13}	0.220	0.316	0*	F_{46}	0.104	0.186	0.032
F_{22}	0.274	0.271	0.276	F_{55}	0.221	0.222	0.216
F_{23}	−0.206	−0.354	−0.156	F_{56}	−0.061	−0.050	−0.056
F_{33}	5.289	5.668	5.321	F_{66}	0.295	0.295	0.291
A spec.	SiH_3Cl	SiD_3Cl	HOFF	E spec.	SiH_3Cl	SiD_3Cl	HOFF
F_{11}	2.851	2.921	2.870	F_{44}	2.742	2.871	2.786
F_{12}	0.033	0.060	0.033	F_{45}	−0.063	−0.119	−0.047
F_{13}	0.218	0.296	0*	F_{46}	0.093	0.173	0.047
F_{22}	0.251	0.264	0.259	F_{55}	0.221	0.220	0.212
F_{23}	−0.140	−0.223	−0.159	F_{56}	−0.062	−0.053	−0.043
F_{33}	2.959	2.965	2.978	F_{66}	0.265	0.265	0.258
A spec.	SiH_3Br	SiD_3Br	HOFF	E spec.	SiH_3Br	SiD_3Br	HOFF
F_{11}	2.850		2.870	F_{44}	2.744		2.780
F_{12}	0.032		0.031	F_{45}	−0.063		−0.044
F_{13}	0.246		0*	F_{46}	0.090		0.044
F_{22}	0.241		0.249	F_{55}	0.220		0.211
F_{23}	−0.132		−0.150	F_{56}	−0.061		−0.040
F_{33}	2.461		2.450	F_{66}	0.246		0.240
A spec.	SiH_3J	SID_3J	HOFF	E spec.	SiH_3J	SID_3J	HOFF
F_{11}	2.829	2.903	2.850	F_{44}	2.768	2.836	2.780
F_{12}	0.031	0.054	0.020	F_{45}	−0.063	−0.117	−0.028
F_{13}	0.251	0.340	0*	F_{46}	0.086	0.160	0.028
F_{22}	0.227	0.237	0.235	F_{55}	0.216	0.213	0.209
F_{23}	−0.115	−0.182	−0.138	F_{56}	−0.058	−0.052	−0.047
F_{33}	1.955	2.006	1.953	F_{66}	0.219	0.225	0.216

* Constrained to be zero.

REFERENCES

1. PULAY, P., TÖRÖK, F.: Acta Chim. Hung. **44**, 287 (1965).
2. WILSON, E. B., DECIUS, J. C. JR., CROSS, P. C.: Molecular Vibrations. (McGraw-Hill, New York) 1955.
3. MORINO, Y., KUCHITSU, K.: J. Chem. Phys. **20**, 1809 (1952).
4. TAYLOR, J. W.: J. Chem. Phys. **22**, 1780 (1954).
5. PULAY, P.: Z. Angew. Math. Mech., To be published.
6. TAYLOR, J. W.: J. Chem. Phys. **18**, 1301 (1950).
7. ALDOUS, J., MILLS, I. M.: Spectrochim. Acta **19**, 1567 (1963).
8. DUNCAN, J. L.: Spectrochim. Acta **20**, 1807 (1964).
9. ALDOUS, J., MILLS, I. M.: Spectrochim. Acta **18**, 1073 (1962).

SUMMARY

The possibilities for defining the matrix F giving the closest assignment between the internal and normal coordinates were investigated. In our previous work an orthogonal parameter matrix U was defined, by means of which all the matrices F reproducing the normal frequencies properly can be constructed. By means of matrix U equal to the unit matrix, one gets matrix F_0 assuring a close, unambiguous connection between the internal and normal coordinates. Where a definite assignment can be given, the elements of F_0 are almost equal to the force constants of the most reliable "Hybrid Orbital Force Field".

Péter PULAY
Ferenc TÖRÖK
Budapest VIII., Múzeum krt. 6—8.

POLYMERISATION DES METHYLMETHAKRYLATS BEI HOHEN UMSÄTZEN, I.

UNTERSUCHUNG DER INITIALWIRKUNG VON BENZOYLPEROXID

I. MONDVAI

(Lehrstuhl für die Plast- und Gummiindustrie der Technischen Universität, Budapest)

Eingegangen am 30. Juli 1965

Es ist bekannt, daß bei der Blockpolymerisation mehrerer Monomeren, besonders des Methylmethakrylats, die Reaktionsgeschwindigkeit nach Erreichen eines gewissen Umsatzgrades plötzlich ansteigt. Diese Erscheinung erklärte man zuerst mit der infolge ungenügender Abführung der Polymerisationswärme auftretenden spontanen Erwärmung. Später bewiesen jedoch SCHULZ [1] und NORRISH [2], daß die Polymerisationsgeschwindigkeit auch unter streng isothermen Bedingungen anwächst, und nach Erreichen der maximalen Geschwindigkeit schnell zum Nullwert abfällt.

Wegen der Viskositätserhöhung des Mediums infolge des Anwachsens der Polymermenge wird eine Geschwindigkeitserhöhung im System verursacht. In diesem Fall sinkt die Abbruchsgeschwindigkeit, die hauptsächlich von der Geschwindigkeit der Diffusion der Polymerradikale zueinander abhängt. Mit dem Sinken der Abbruchsgeschwingidkeit wächst die Konzentration der Polymerradikale, also auch die Polymerisationsgeschwindigkeit. Diese Erklärung durch den Geleffekt, die heute schon allgemein anerkannt ist, haben in erster Linie SCHULZ [3], MELVILLE [4], FUJII [5] und MIYAMA [6] ausgearbeitet.

Neuerdings, nach Versuchsdaten bei der Untersuchung der Photopolymerisation des Methylmethakrylats, haben BURNETT und DUNCAN [7] für die Reaktionsgeschwindigkeit bis zu hohen Umsätzen Gleichungen aufgestellt. Auf Grund ihrer Untersuchungen kann die Geschwindigkeitserhöhung nach einer für einen großen Teil der Polymerisation — der vom Erscheinen des Geleffekts bis zum Erreichen der maximalen Geschwindigkeit reicht — gültigen Gleichung mit der Konstante K_1 gut charakterisiert werden. Die zweite Gleichung ist für den großen Abschnitt der Reaktion vom Erreichen der maximalen Geschwindigkeit bis zum Sinken der Reaktionsgeschwindigkeit auf Null gültig, und die Konstante K_2 ist für die Geschwindigkeitsabnahme charakteristisch.

SAWADA [8] leitete, ausgehend von der Geschwindigkeitsgleichung der Polymerisation, einen vom Auftreten des Geleffekts bis nahezu zum Erreichen des Grenzumsatzes geltenden Zusammenhang ab. Bei Benutzung seiner Gleichung, kann man das durch den Geleffekt verursachte Anwachsen der Geschwindigkeit mit einer einzigen Konstante charakterisieren.

Experimenteller Teil

Als Initiator gebrauchten wir Benzoylperoxyd, das wir im Interesse der Reinheit in Chloroform (Kp 61,4—61,6 °C; $n_D^{20} = 1{,}4459$) lösten und die Lösung sofort in Methanol (Kp 64,5 °C; $n_D^{20} = 1{,}3286$) filtrierten. Die ausgefallenen Kristalle sammelten wir auf eine Fritte G 1 und trockneten durch Durchsaugen von Luft. Nach zweimaligem Umkristallisieren veränderte sich der Schmelzpunkt des Benzoylperoxyds nicht mehr und betrug, nach der Mikromethode von KOFLER bestimmt, 108,5 °C.

Das handelsübliche Methylmethakrylat fraktionierten wir im Vakuum über eine Kolonne mit zwanzig Böden unter einem Rückflußverhältnis von eins zu eins. Das Vakuum hielten wir mittels eines Quecksilbermanostaten konstant. Der Siedepunkt der Mittelfraktion betrug bei 200 Torr 62,8 °C. Diese Fraktion füllten wir in Spezialampullen, die zwei Räume enthielten, und

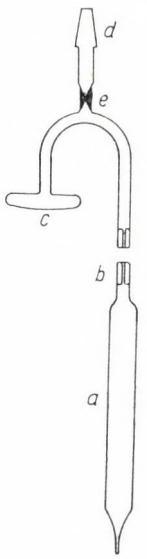

Abb. 1. Dilatometer (a: Quecksilberbehälter, b: Kapillare, c: Monomerbehälter, d: Anschlußschliff, e: Abschmelzstelle)

frohren sie mittels einer Aceton-Kohlendioxydschnee-Kältemischung ein. Dann entfernten wir unter Anlegen von Vakuum die in den Ampullen enthaltene Luft und ließen das Monomere in einer sauerstoffreien Stickstoffatmosphäre schmelzen. Dieses Verfahren wiederholten wir zweimal, um den Sauerstoff restlos zu entfernen. Dann, nach dem letzten Einfrieren, schmolzen wir die Ampullen im Vakuum (etwa 10^{-3} Torr) ab. Den mit Monomeren gefüllten Teil der Ampullen gaben wir in eine Kältemischung und lagerten sie derart. Vor Gebrauch hielten wir die Ampullen so, daß sich der leere Teil in der Kältemischung befand. So destillierte das Monomere nach Aufschmelzen in den zweiten Raum der Ampulle und ließ sich nach Öffnen der Ampulle für die Experimente verwenden. Das gereinigte Monomer besaß einen Brechnungsindex von $n_D^{20} = 1{,}41447—1{,}41449$.

Unsere Experimente führten wir in einem aus Abb. 1. ersichtlichen Spezialdilatometer aus, bei welchem der zur Lagerung des Monomers dienende Teil (*c*) so ausgebildet ist, daß seine Wand bei senkrechter Stellung des Dilatometers dem Quecksilbermeniskus genau folgt. Dadurch bleibt das eingefüllte Monomer in einer gleichmäßigen, ungefähr 1 mm dicken Schicht über der Quecksilberoberfläche. Dieser Umstand ist im Interesse eines guten Wärmeüberganges wichtig. Das Dilatometer ist mit Hilfe eines Schliffes (*d*) an die Hochvakuumeinrichtung und die Stickstoffreinigung anschließbar.

Das in das Dilatometer eingefüllte, im Vakuum destillierte Quecksilber erwärmten wir zwecks Luftentfernung gelinde bei einem Druck von ungefähr 10^{-3} Torr. Das Erwärmen setzten wir bis zum sichtbaren Beginn der Verdampfung des Quecksilbers fort, und ließen dann das Dilatometer im Vakuum abkühlen.

Nach Einwägen von Initiator und Monomeren entfernten wir die Luft durch wiederholtes Durchspülen mit Stickstoff und schmolzen dann das Dilatometer bei einem Druck von 10^{-6} Torr ab. Darauf drehten wir das Dilatometer um und schnitten es am oberen Ende des Quecksilberbehälters ab. Damit erreichten wir, daß das Quecksilber das Dilatometer vollständig ausfüllte. Das überflüssige Quecksilber entfernten wir mit Hilfe einer Kapillare unter Verwendung von Vakuum und brachten das Dilatometer in einem Thermostaten unter. Der für unsere Messungen benutzte Ultrathermostat war mit Glasfenstern versehen, um das Ablesen zu ermöglichen; die Schwankung der Temperatur war geringer als 0,05 °C.

Den Umsatz berechnen wir aus der abgelesenen Volumenverminderung, unter Verwendung der Daten von SCHULZ [9].

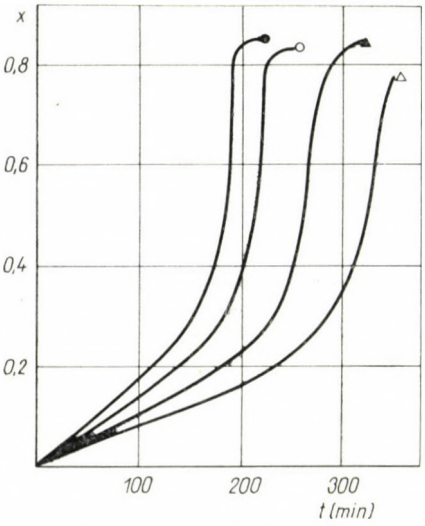

Abb. 2. Zeit-Umsatz Kurven für die Polymerisation bei 50°C. Initiatorkonzentration: (●): 11,24 · 10^{-2} mol/l; (○): 7,48 · 10^{-2} mol/l (▲): 4,13 · 10^{-2} mol/l; (△): 2,30 · 10^{-2} mol/l

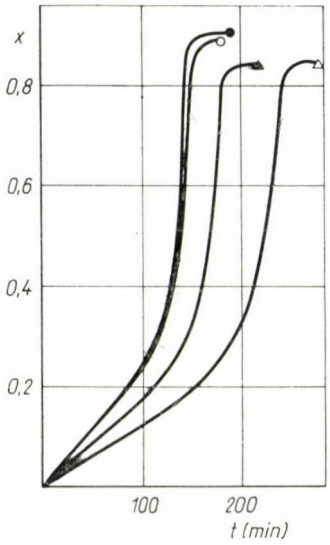

Abb. 3. Zeit-Umsatz Kurven für die Polymerisation bei 60°C. Initiatorkonzentration: (●): 4,13 · 10^{-2} mol/l; (○): 3,31 · 10^{-2} mol/l; (▲): 1,86 · 10^{-2} mol/l; (△): 9,28 · 10^{-3} mol/l

Ergebnisse

Unsere Versuche führten wir bei 50, 60 und 70 °C durch, die Zeit-Umsatz Zusammenhänge veranschaulichten wir auf Abbildung 2, 3 und 4.

Im Anfangsabschnitt der Polymerisation ist die gebildete Polymermenge der Zeit direkt proportional, und es gilt der folgende Zusammenhang:

$$W_{st} = -\frac{dm}{dt} = K i^{\frac{1}{2}} m. \tag{1}$$

wobei W_{st} die Anfangsgeschwindigkeit der Polymerisation, m die Monomerkonzentration, t die Zeit, K die Bruttogeschwindigkeitskonstante der Polymerisation, und i die Initiatorkonzentration bedeuten.

Auf Grund von Gleichung (1) geben wir die aus unseren eigenen Messungen, sowie die aus den Literaturangaben errechneten Geschwindigkeitskonstanten in Tab. I an. Wie man aus derselben ersieht, stimmen die errechneten Geschwindigkeitskonstanten K mit jenen der Literatur gut überein. Dementsprechend deckt sich auch die Bruttoaktivierungsenergie der Polymerisation $E = 19{,}7$ kcal/mol gut mit dem Literaturwert [10] von $E = 19{,}5$ kcal/mol.

Ordnen wir Gleichung (1) um, integrieren wir und setzen den Umsatzgrad der Monomerkonzentration ein, so erhalten wir:

$$\lg \frac{1}{1-x} = \frac{K i^{\frac{1}{2}} t}{2{,}303} \tag{2}$$

worin x den Umsatzgrad bedeutet.

Tabelle I

Geschwindigkeitskonstanten der Polymerisation von Methylmethakrylat

Temperatur °C	K $\text{mol}^{-1/2}\, l^{1/2}\, \text{sec}^{-}$	Lit. Zit.
50	$8{,}07 \cdot 10^{-5}$	[11]
50	$8{,}98 \cdot 10^{-5}$	[3]
50	$8{,}67 \cdot 10^{-5}$	eigene Messung
60	$2{,}23 \cdot 10^{-4}$	[12]
60	$2{,}14 \cdot 10^{-4}$	eigene Messung
70	$5{,}07 \cdot 10^{-4}$	[11]
70	$4{,}95 \cdot 10^{-4}$	[3]
70	$5{,}16 \cdot 10^{-4}$	eigene Messung

Wenn wir die linke Seite der Gleichung (2) in Abhängigkeit von der Zeit auftragen, wie aus den Abb. 5, 6 und 7 ersichtlich, dann erhalten wir Geraden. Der Anstieg dieser Geraden ist der Anfangsgeschwindigkeit der Polymerisation proportional, und aus dem Abweichen der Meßpunkte von den Geraden kann man auf den Beginn des Auftretens des Geleffekts folgern.

Im Abschnitt der Polymerisation, der sich an das Auftreten des Geleffekts anschließt, verwendeten wir die Formel von SAWADA [8] in der folgenden Form:

$$\frac{1}{x_2 - x_1} \lg \frac{x - x_1}{x_2 - x} = K_1 t \tag{3}$$

wobei x_1 den »kritischen« Umsatzgrad bei Auftreten des Geleffekts, x_2 den Grenzumsatz, bei welchem die Polymerisationsgeschwindigkeit auf Null sinkt

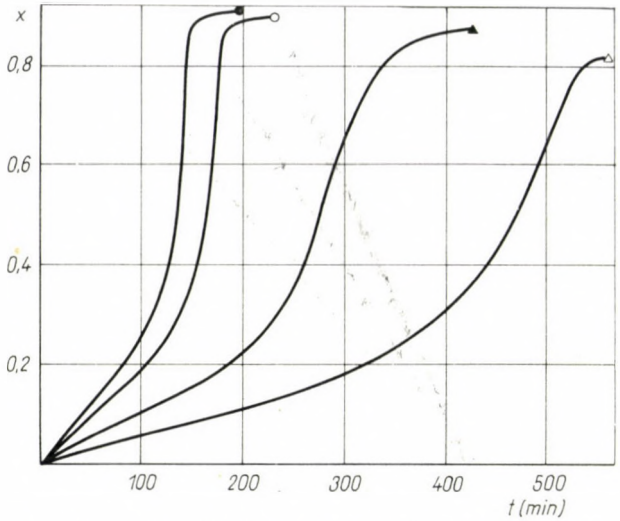

Abb. 4. Zeit-Umsatz Kurven für die Polymerisation bei 70 °C. Initiatorkonzentration: (●): $6{,}61 \cdot 10^{-3}$ mol/l; (○): $3{,}69 \cdot 10^{-3}$ mol/l; (▲); $1{,}16 \cdot 10^{-3}$ mol/l; (△): $4{,}16 \cdot 10^{-4}$ mol/l

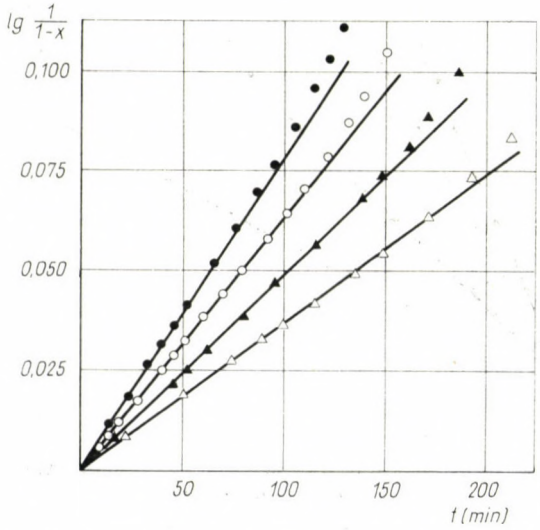

Abb 5. Einfluß der Veränderung der Initiatorkonzentration auf die Anfangsgeschwindigkeit der Polymerisation bei 50 °C

und K_1 die durch den Geleffekt verursachte Geschwindigkeitszunahme charakterisierende Konstante bedeuten.

Wenn wir auf Grund der Gleichung (3) die Werte $\lg \dfrac{x - x_1}{x_2 - x}$ in Abhängigkeit von der Zeit auftragen, so erhalten wir Geraden, welche die Abbildungen

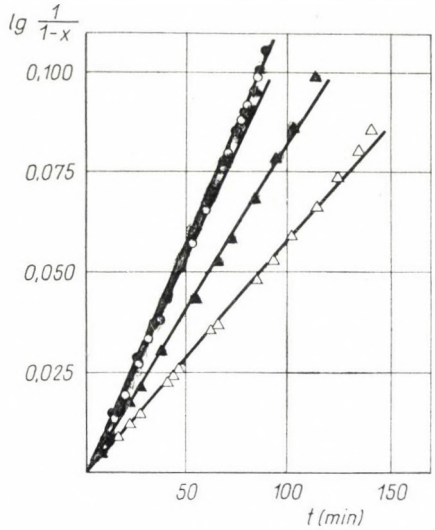

Abb. 6. Einfluß der Veränderung der Initiatorkonzentration auf die Anfangsgeschwindigkeit der Polymerisation bei 60 °C

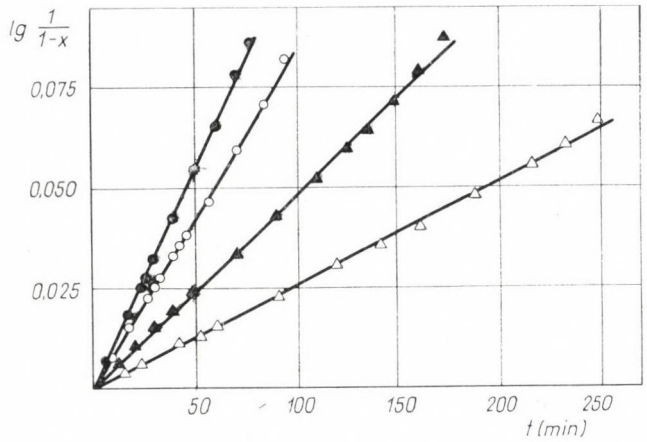

Abb. 7. Einfluß der Veränderung der Initiatorkonzentration auf die Anfangsgeschwindigkeit der Polymerisation bei 70 °C

8, 9 und 10 zeigen. Der Anstieg der Geraden gibt die K_1 Werte an. Den Wert für den Grenzumsatz kann man aus den Zeit-Umsatz Kurven (Abb. 2, 3 und 4) abschätzen, während sich das Auftreten des Geleffekts aus den auf Abb. 5, 6 und 7 gezeigten Zusammenhängen ergibt. Die genaue Bestimmung beider Werte kann dann erfolgen, wenn sich die errechneten Meßpunkte bestmöglichst der Geraden annähern.

Sowohl die Werte für x_1, wie für x_2 hängen von der Initiatorkonzentration und der Temperatur ab. Aus den angegebenen Daten ist ersichtlich, daß mit

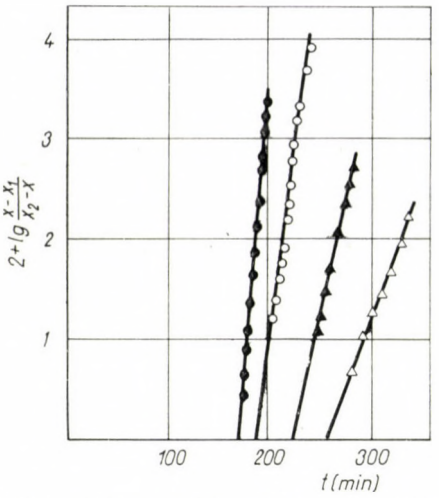

Abb. 8. Einfluß der Veränderung der Initiatorkonzentration auf die Polymerisation bei hohen Umsätzen. Temperatur 50 °C. (●): $K_1 = 10{,}85 \cdot 10^{-2}$ $x_1 = 0{,}390$ $x_2 = 0{,}855$ (○): $K_1 = 7{,}70 \cdot 10^{-2}$ $x_1 = 0{,}339$ $x_2 = 0{,}837$ (▲): $K_1 = 4{,}66 \cdot 10^{-2}$ $x_1 = 0{,}306$ $x_2 = 0{,}864$ (△): $K_1 = 2.76 \cdot 10^{-2}$ $x_1 = 0{,}255$ $x_2 = 0{,}900$

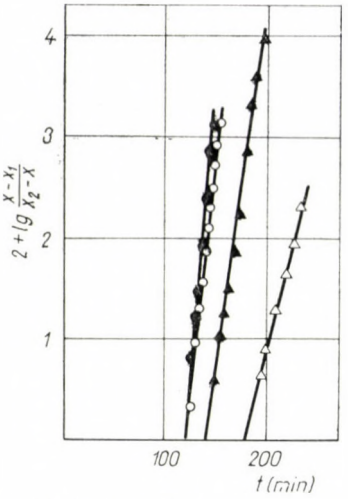

Abb. 9. Einfluß der Veränderung der Initiatorkonzentration auf die Polymerisation bei hohen Umsätzen. Temperatur 60 °C. (●): $K_1 = 11{,}90 \cdot 10^{-2}$ $x_1 = 0{,}367$ $x_2 = 0{,}916$ (○): $K_1 = 10{,}50 \cdot 10^{-2}$ $x_1 = 0{,}360$ $x_2 = 0{,}900$ (▲): $K_1 = 7{,}10 \cdot 10^{-2}$ $x_1 = 0{,}296$ $x_2 = 0{,}846$ (△): $K_1 = 4{,}25 \cdot 10^{-2}$ $x_1 = 0{,}290$ $x_2 = 0{,}855$

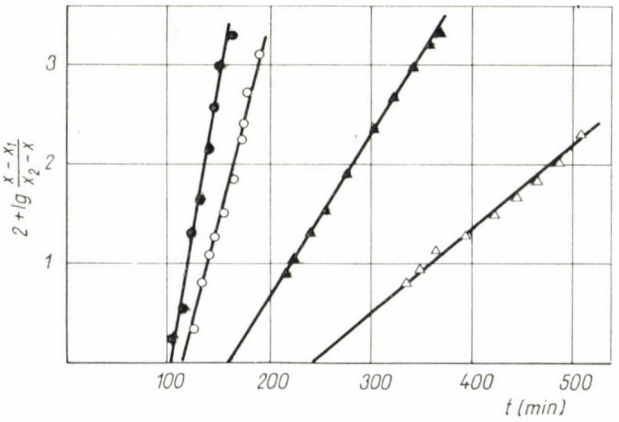

Abb. 10. Einfluß der Veränderung der Initiatorkonzentration auf die Polymerisation bei hohen Umsätzen. Temperatur 70 °C. (●): $K_1 = 6{,}08 \cdot 10^{-2}$ $x_1 = 0{,}250$ $x_2 = 0{,}930$ (○): $K_1 = 4{,}08 \cdot 10^{-2}$ $x_1 = 0{,}240$ $x_2 = 0{,}927$ (▲): $K_1 = 1{,}64 \cdot 10^{-2}$ $x_1 = 0{,}200$ $x_2 = 0{,}876$ (△): $K_1 = 0{,}85 \cdot 10^{-2}$ $x_1 = 0{,}170$ $x_2 = 0{,}930$

Absinken der Initiatorkonzentration auch der Umsatzgrad x_1 fällt, bei welchen der Geleffekt auftritt. Diese Abhängigkeit von der Initiatorkonzentration nimmt bei Absinken der Temperatur immer höhere Werte an. Bei gleicher Initiatorkonzentration ist für die niedrigere Temperatur x_1 geringer. Der Grenzumsatz

hängt nicht eindeutig von der Initiatorkonzentration ab, da sich bei allen drei Temperaturen bei einer bestimmten Konzentration ein Minimum zeigt. Man kann jedoch beobachten, daß bei niedrigerer Temperatur auch der Grenzumsatz geringer ist. Die Gültigkeitsbereiche der Gleichungen (2) und (3) liegen zueinander näher, wenn die Abläufe der Zeit-Umsatz Kurven weniger steil sind.

Die Anfangsgeschwindigkeit der Polymerisation und den Wert $K_1(x_2-x_1)$ in Abhängigkeit von Initiatorkonzentration zeigt Abb. 11. Auf Grund der Mes-

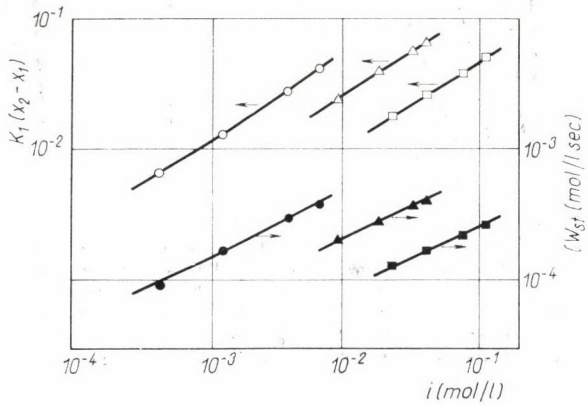

Abb. 11. Abhängigkeit der Anfangsgeschwindigkeit der Polymerisation und der $K_1(x_2 - x_1)$ Werte von der Initiatorkonzentration. Temperatur (□): 50 °C, (△): 60 °C, (○): 70 °C

sungen ist die Anfangsgeschwindigkeit der Polymerisation der Quadratwurzel der Initiatorkonzentration proportional, während der Anstieg der zweiten Geraden der Initiatorkonzentration einem Exponenten von 2/3 entspricht. Dies kann man formal als einen Kettenabbruch betrachten, der zwischen erster und zweiter Ordnung liegt [13]. Bei hohen Umsätzen verursacht der physikalische Zustand des Monomer—Polymer-Gels einen Kettenabbruch erster Ordnung [14].

Für die Hilfe bei der experimentellen Arbeit möchte der Verfasser Herrn Dipl. Ing. J. NAGY auf diesem Wege Dank sagen.

ZUSAMMENFASSUNG

Wir untersuchten die mit Benzoylperoxyd initierte Blockpolymerisation von Methylmethakrylat bei verschiedenen Temperaturen. Dabei stellten wir fest, daß der Beginn des Geleffekts und der erreichbare Grenzumsatz Funktionen der Initiatorkonzentration und der Temperatur darstellen. Den Abschnitt der Polymerisation nach Auftreten des Geleffekts werteten wir auf Grund der Gleichung von SAWADA aus. Die in der Gleichung auftretende Konstante stellt bei mit hohen Umstätzen durchgeführten Reaktionen eine ähnlich charakteristische Größe dar, wie im Bereich niedriger Umsatzgrade die Anfangsgeschwindigkeit der Polymerisation.

LITERATUR

1. Schulz, G. V., Blaschke, F.: Z. Elektrochem. **47,** 749 (1941).
2. Norrish, R. G. W., Smith, R. R.: Nature (London) **150,** 336 (1942).
3. Schulz, G. V., Harborth, G.: Makromol. Chem. **1,** 106 (1947).
   Schulz, G. V.: Z. Physik. Chem. (Frankfurt) **8,** 290 (1956).
4. Melville, H. W.: Z. Elektrochem. **60,** 276 (1956).
5. Fujii, S.: Bull. Chem. Soc. Japan **27,** 216; 238 (1954).
6. Miyama, H.: Bull. Chem. Soc. Japan **30,** 459 (1957).
7. Burnett, G. M., Duncan, G. L.: Makromol. Chem. **51,** 154 (1962).
8. Sawada, H.: J. Polymer Sci. B **1,** 305 (1963).
9. Schulz, G. V.: Angew. Chem. A **59,** 90 (1947).
10. Bagdaszarjan, H. Sz.: Die Theorie der Radikalpolymerisation. Akademie Verlag. Budapest, 1961. Seite 112.
11. Schulz, G. V., Blaschke, F.: Z. Physik. Chem. B **51,** 75 (1942).
12. Baysal, B., Tobolsky, A. V.: J. Polymer Sci. **8,** 529 (1952).
13. Allen, P. E. M., Patrick, C. R.: Trans. Faraday Soc. **59,** 1819 (1963).
14. Burnett, G. M., Loan, L. D.: Coll. Czech. Chem. Comm. **22,** 113 (1957).

Polymerization of Methyl Methacrylate at High Conversion Degrees, I

Investigation of the Initiation Effect of Benzoyl Peroxide

I. MONDVAI

Summary. The bulk polymerization of methyl methacrylate was investigated at various temperatures. It was found that the beginning of gel effect and the attainable limit of conversion depend on the concentration of the initiator and on temperature. The stage of polymerization following the gel effect was interpreted on the basis of the Sawada equation. The constant present in this equation is a kinetic parameter of the reaction occurring at high degrees of conversion, just as the initial rate of polymerization is a similar parameter in the domain of low conversion degrees.

Полимеризация метилметакрилата при больших степенях превращений, I

Исследование инициирующего влияния перекиси бензоила

И. МОНДВАИ

Резюме. Исследовали инициированную, блочную полимеризацию метилметакрилата при различных температурах. Установили, что начало гель-эффекта и возможно достигаемый предел превращений являются функциями концентрации инициатора и температуры. Участок полимеризации, наступающий после появления гель-эффекта оценивали с помощью уравнения Шавада. Фигурирующая в уравнении постоянная является аналогичной кинетической характеристикой степени полимеризации, как начальная скорость полимеризации в области малых степеней превращений.

dr. Imre Mondvai; Budapest, XI., Műegyetem rkp. 3—9.

METALLKOMPLEXE DER PEPTIDE, V.

UNTERSUCHUNG DER HYDROLYSE UND OXYDATION VON DIPEPTID-METALLKOMPLEXEN

J. Nyilasi, M. Bihari-Varga und P. Orsós

(Institut für Allgemeine und Anorganische Chemie der L. Eötvös Universität, Budapest)

Eingegangen am 28. Juni 1965

Nach der Untersuchung der Metallkomplexe von monotonen Glycylpeptiden verschiedener Kettenlänge [1] wurde die Komplexbildung mit Kupfer-, Nickel- und Kobaltionen der untenfolgenden Dipeptide bzw. der Einfluß dieser Komplexbildung auf die Hydrolyse- und Oxidationsgeschwindigkeit studiert: Glycylglycin, DL-α-Alanylglycin, L-Leucylglycin, Glycyl-DL-α-Alanin, Glycyl-L-Leucin, DL-α-Alanyl-DL-α-Alanin, DL-Leucil-DL-Leucin. Glycyl-β-Alanin, DL-α-Alanyl-β-Alanin, β-Alanyl-β-Alanin, β-Alanyl-L-Histidin, Glycyl-L-Tyrosin, L-Tyrosylglycin, L-α-Alanyl-L-Tyrosin, L-Tyrosyl-L-α-Alanin, L-Leucyl-L-Tyrosin, Glycyl-L-Triptophan.

Die Reinheit der Peptide, Präparate von Hoffmann-La-Roche, Light bzw. Reanal, wurde mit Papierchromatographie [2] kontrolliert.

Vor allem wurde mittels Extinktionsmessungen untersucht, welche der obigen Dipeptide in 0,5 n NaOH-Medium bei 20 °C mit Cu-, Ni- und Co-Ionen Komplexe bilden. Die Dipeptidkonzentration der Gemische betrug 0,02 Mol, ihr Metallgehalt 0,01 Grammatomgewicht je Liter. Bei der Herstellung der Gemische wurden die Peptide zuerst mit der $CuSO_4$-, $NiSO_4$- bzw. $CoSO_4$-Lösung vermischt, und erst dann die Natriumhydroxidlösung zugesetzt. Da die Bildung der Kobaltkomplexe längere Zeit beansprucht, wurden diese Lösungen in Gegenwart von Sauerstoff 100 Stunden bei 20 °C aufbewahrt. (Die in den Tabellen für Co-Komplexe unter 0 Stunde angeführten Werte beziehen sich auf diesen Zeitpunkt.)

Die mit einem Pulfrich-Photometer in einer Küvette von 1 cm und unter Verwendung eines Farbfilters J61,8 für Cu-Komplexe bzw. S53E für Co-Komplexe gemessenen Extinktionswerte ergaben (Tab. I, 0 Stunde), daß unter den untersuchten Dipeptiden bloß β-Alanyl-β-Alanin keinen Komplex mit dem Kupferion bildet, während mit Cobaltionen außer β-Alanyl-β-Alanin auch Glycylleucin und Leucylleucin keine Komplexe ergeben. Der Grund dafür ist im Falle des β-Alanyl-β-Alanins der Länge der die die Stickstoffatome trennenden Kohlenstoffkette, im Falle des Glycylleucins und des Leucylleucins der sterischen Hemmung der großen Alkylgruppe zuzuschreiben. Es ist interessant zu erwähnen, daß beim Leucylglycin, bei dem sich dieselbe Alkylgruppe zwischen

Tabelle I

Änderung der Extinktionswerte von Dipeptid-Metallkomplexe während der Hydrolyse bzw. Oxydation

Peptid	Cu			Co		
Stunde	0	4 Hydr.	4 Oxyd.	0	4 Hydr.	4 Oxyd.
Gly-Gly	0,480	—	—	0,675	0,190	0,030
α-Ala-Gly	0,620	0,410	0,150	0,670	0,110	0,030
Leu-Gly	0,670	0,515	0,240	0,580	0,080	0,020
Gly-α-Ala	0,660	0,550	0,390	0,385	0,060	—
Gly-Leu	0,670	0,590	0,580	—	—	—
α-Ala-α-Ala ...	0,720	0,660	0,710	0,190	0,110	0,020
Leu-Leu	0,730	0,715	0,220	—	—	—
Gly-β-Ala	0,400	0,080	—	0,230	0,090	—
α-Ala-β-Ala ...	0,590	0,180	0,060	0,245	0,100	0,050
β-Ala-β-Ala ..	—	—	—	—	—	—
β-Ala-Hist ...	0,710	0,700	0,320	0,780	0,430	0,210
Gly-Tyr	0,630	0,620	0,635	0,550	0,535	0,574
Tyr-Gly	0,635	0,630	0,230	0,525	0,270	0,320
α-Ala-Tyr	0,690	0,695	0,680	0,470	0,425	0,510
Tyr-α-Ala	0,700	0,708	0,740	0,575	0,350	0,315
Leu-Tyr	0,740	0,730	0,630	0,325	0,320	0,130
Gly-Tript	0,524	0,540	0,590	0,810	0,080	0,040

dem Aminostickstoff und der Peptidbindung befindet, die Komplexbildung nicht gehemmt wird.

Mit dem Nickelion gaben die untersuchten Dipeptide keine Komplexe, so daß diese Systeme weiter nicht untersucht wurden. Es soll erwähnt werden, daß laut unseren früheren Untersuchungen Tri- und Tetrapeptide unter identischen Umständen mit dem Nickelion bereits Komplexe von Biurettyp bilden, wobei die Stabilität dieser Komplexe mit der Länge der Peptidkette bedeutend ansteigt.

Zur Bestimmung der Zusammensetzung der bei 20 °C in einem Medium von 0,5 n Alkalität sich bildenden Dipeptid-Kupfer-Komplexe wurde die Methode der Molverhältnisse [3] verwendet. Die Entstehung der Kobaltkomplexe ist unter den gegebenen Umständen wesentlich verwickelter, so daß in diesem Fall Messungen dieser Art unterlassen wurden. Mit Ausnahme des

Tabelle II

Das perzentuelle Maß der alkalischen Hydrolyse von Dipeptiden und ihrer Metallkomplexe

Peptid	metallionfrei			Cu			Co			
Stunde	1	2	4	1	2	4	0	1	2	4
Gly-Gly	96	100	100	75	90	98	47	60	80	90
α-Ala-Gly	52	73	91	46	61	77	5	34	63	78
Leu-Gly	13	49	78	5	19	48	+	17	22	33
Gly-α-Ala	19	51	65	4	15	31	18	57	75	98
Gly-Leu	13	32	58	6	12	24	4	16	30	59
α-Ala-α-Ala	10	24	51	5	11	20	5	30	42	60
Gly-β-Ala	73	86	99	72	87	97	30	81	96	99
α-Ala-β-Ala	40	78	91	38	76	89	18	56	85	94
β-Ala-Hist	+	5	15	+	+	+	+	+	+	+
Gly-Tyr	4	9	17	2	4	17	+	7	13	28
Tyr-Gly	+	3	6	+	3	4	+	7	14	25
α-Ala-Tyr	2	5	14	+	+	4	—	+	+	7
Tyr-α-Ala	+	+	+	—	+	+	—	+	+	5
Leu-Tyr	—	—	—	—	—	—	—	—	—	—
Gly-Tript	+	+	3	—	+	+	—	+	+	+

\+ die Anwesenheit von freier Aminosäure ist kaum nachweisbar
— die Anwesenheit von freier Aminosäure ist nicht nachweisbar

Glycyltriptophans und des β-Alanylhistidins — die Komplexe mit der Zusammensetzung 1 Grammiongewicht Cu: 1 Mol Dipeptid bilden — ergaben unsere Untersuchungen für alle übrige Fälle ein Verhältnis von 1 Grammiongewicht Cu: 2 Mol Dipeptid. Die Moleküle sämtlicher Peptide, welche Komplexe von letzterer Zusammensetzung bilden, enthalten zwei Stickstoffatome, während das zu den Ausnahmen gehörende Glycyltriptophan drei, β-Alanylhistidin hingegen vier Stickstoffatome enthält. Es ist anzunehmen, daß bei diesen Dipeptiden auch das Stickstoffatom im Ring an der Komplexbildung beteiligt ist, was übrigens auch durch das Beispiel des Hystidin-Kupferkomplexes [4] angezeigt wird.

Die Geschwindigkeit der bei 100 °C erfolgenden Hydrolyse der Dipeptide und ihrer Metallkomplexe wurde durch die papierchromatographische Analyse der gebildeten Aminosäuren, sowie durch die Messung der Extinktionswerte der Gemische verfolgt. Über die Einzelheiten dieser Methoden verweisen wir auf eine unserer früheren Arbeiten [1].

Die mit chromatographischer Analyse erhaltenen Daten sind aus Tab. II, die nach vierstündiger Hydrolyse gemessenen Extinktionswerte aus Tab. I ersichtlich. Auf Grund dieser Untersuchungen kann folgendes festgestellt werden:

Unter den aus aliphatischen α-Aminosäuren bestehenden Dipeptiden von der allgemeinen Formel $H_2N-CH(R)-CO-NH-CH(R)-COOH$ weist das Glycylglicin die größte Hydrolysegeschwindigkeit auf. Wenn sich zwischen der freien Aminogruppe und der Peptidbindung eine Methyl- oder Isobutylgruppe befindet (α-Ala-Gly, Leu-Gly), ist die Neigung zur Hydrolyse geringer. Eine weitere Verringerung dieser Geschwindigkeit ist dann zu beobachten, wenn sich diese Alkylgruppen zwischen der Peptidbindung und der Carboxylgruppe befinden (Gly-α-Ala, Gly-Leu). Schließlich weisen jene Peptide gegen alkalische Hydrolyse den größten Widerstand auf, die an beiden Seiten der Peptidbindung mehr oder weniger große Alkaligruppen enthalten (α-Ala-α-Ala, Leu-Leu).

Diese Beobachtungen stehen übrigens im allgemeinen mit den Befunden anderer Autoren im Einklang [5]. Cristol, Benezech und Crastes de Paulet [6], die unter anderem die Hydrolyse des Glycylglycins, Alanylglycins und Leucylglycins in 5 n NaOH-haltigem Medium bei 37 °C untersuchten, fanden eine Abnahme derselben in der angegebenen Reihenfolge. Unter den von den genannten Autoren angewendeten Umständen weichen die Hydrolysegeschwindigkeiten der inversen Peptide, wie Leucylglycin und Glycylleucin verhältnismäßig wenig von einander ab. Resultate eigener Versuche zeigen hingegen, daß die stabilisierende Wirkung der R-Gruppe bei inversen Peptiden (Ala-Gly, Gly-Ala, Leu-Gly, Gly-Leu) von deren Lage stark abhängig ist, u. zw. wird diese Wirkung stets größer sein, wenn die R-Gruppe an das asymmetrische Kohlenstoffatom der C-terminalen Aminosäure gebunden ist. Es soll erwähnt werden, daß nach den genannten und anderen Autoren [7] bei der sauren Hydrolyse von Dipeptiden die Verhältnisse eben umgekehrt liegen, wie die von uns im alkalischen Medium beobachteten. Das R-Radikal verleiht nämlich gegen saure Hydrolyse dann einen größeren Widerstand, wenn es sich an der Seite der Carbonylgruppe der Peptidbildung befindet.

Die eigenen Befunde werden teils darauf zurückgeleitet, daß die Alkylgruppen infolge ihres Donorcharakters, in Abhängigkeit von ihrer Natur und Lage, hemmend auf die Hydrolyse der Peptidbindung wirken. Da die elektronenabstossende Wirkung der Alklygruppen mit der Anzahl der Kettenverzweigungen zunimmt, wird es verständlich, daß Leucin ($R = -CH_2-CH(CH_3)_2$) enthaltende Peptide weniger stark hydrolysieren, als die Alanin($R = -CH_3$)-Peptide mit analoger Struktur. Außer der verschiedenen elektronen-abstossenden Wirkung muß aber auch die hemmende sterische Wirkung der Alkylgruppen beachtet werden. Der ansteigende Raumbedarf der R-Gruppe hemmt

nämlich das Herankommen des OH^--Ions an die Peptidbindung und demzufolge die Hydrolyse

Die auch cyclische Aminosäuren enthaltenden Dipeptide sind im allgemeinen widerstandfähiger gegen eine alkalische Hydrolyse, als die nur aus aliphatischen Aminosäuren bestehenden. Unter den tyrosinhaltigen Peptiden neigen jene stärker zur Hydrolyse, in welchen Tyrosin die C-terminale Aminosäure ist.

Die auch β-Alanin enthaltenden Dipeptide werden, mit Ausnahme des β-Alanylhistidins, leicht hydrolysiert. Die Hydrolyse des β-Alanyl-β-Alanins wurde mit Papierchromatographie nicht untersucht, da die Ninhydrinreaktion in diesem Fall nicht verwendet werden kann. Die Hydrolyse wird bei Peptiden, die sich in kupferionenfreien Medium wesentlich zersetzen, durch die Bildung der Kupferkomplexe gehemmt. Eine Ausnahme bilden bloß jene Peptide, die β-Alanin als C-terminale Aminosäure enthalten.

Während die Komplexbildung mit Kupferionen — von den erwähnten Ausnahmen abgesehen — die Spaltung der Peptidbindung hemmt, findet man beim Kobaltion auch eine Wirkung in entgegengesetzter Richtung. Unter den aus aliphatischen α-Aminosäuren bestehenden Dipeptiden bilden — wie bereits erwähnt — Glycylleucin und Leucylleucin unter den gegebenen Umständen keine Komplexe mit Kobaltionen. Dies wird auch aus den Daten über ihre alkalische Hydrolyse ersichtlich. Die Hydrolysengeschwindigkeit des Glycylglycins, α-Alanylglycins und Leucylglycins wird durch die Komplexbildung mit Kobaltionen gehemmt. In diesen Peptiden ist Glykokoll die C-terminale Aminosäure. Hingegen zeigen die Kobaltkomplexe des Glycyl-α-Alanins und des α-Alanyl-α-Alanins eine stärkere Neigung zur Hydrolyse, als die metallionenfreien Peptide. Demgemäß wird in den untersuchten Fällen die alkalische Hydrolyse durch die Komplexbildung mit Kobaltionen gefördert, falls α-Alanin die C-terminale Aminosäure ist. Diese Wirkung kann auch im Falle des Glycyltyrosins und des Tyrosylglycins beobachtet werden.

In Verbindung mit diesen Befunden soll darauf hingewiesen werden, daß die in Komplexbindung vorliegenden Kobaltionen in der Betätigung der Dipeptidasen oft eine Schlüsselrolle spielen [8]. Anderseits verweisen wir auf die Untersuchungen von COLLEMAN und BUCKINGHAM [9]. Durch Verwendung von Kobaltkomplexen konnten diese Autoren einfachere Peptide selektiv hydrolysieren.

Schließlich wurde die Desaminierung der Cu- und Co-Komplexe von Dipeptiden untersucht, wenn Luft bei 100 °C durch ihre 0,5 n alkalischen Lösungen geleitet wurde. Außer der Bestimmung der freiwerdenden Ammoniakmenge (Tab. III) wurden auch die Extinktionswerte der Filtrate der 4 Stunden oxydierten Gemische gemessen (Tab. I).

Im allgemeinen kann festgestellt werden, daß die Kupferkomplexe viel mehr zur oxydativen Desamination neigen, als die Kobaltkomplexe. Zur

Deutung der gefundenen Abweichungen in der Freisetzungsgeschwindigkeit des Ammoniaks kann die Hydrolysierbarkeit der Peptide, die verschiedene Desaminationsbereitwilligkeit der enthaltenen Aminosäuren (Tab. III) sowie

Tabelle III

Perzentuelle Menge des aus Dipeptid-Metallkomplexen freigesetzten NH_3-Stickstoffes

Peptid: Stunde:	1	2	4	1	2	4
	Cu			Co		
Gly-Gly	15,3	39,0	75,9	19,9	23,5	25,8
α-Ala-Gly	9,7	22,6	51,4	18,6	22,9	25,0
Leu-Gly	3,8	19,4	39,7	9,4	12,7	14,6
Gly-α-Ala	7,0	18,3	37,2	12,2	12,9	13,8
Gly-Leu	1,6	3,4	8,0	—	—	—
α-Ala-α-Ala ...	1,3	3,2	7,1	—	0,5	0,8
Leu-Leu	—	—	—	—	—	—
Gly-β-Ala	9,8	19,5	42,6	1,9	3,2	4,7
α-Ala-β-Ala ...	7,9	18,5	42,7	7,0	7,4	7,9
β-Ala-β-Ala ..	—	—	—	—	—	—
β-Ala-Hist ...	14,6	31,4	50,3	5,0	8,4	13,9
Gly-Tyr	3,6	5,9	10,2	2,4	3,1	4,2
Tyr-Gly	7,4	17,2	44,1	16,9	26,3	30,2
α-Ala-Tyr	3,0	4,2	8,4	0,1	0,3	0,7
Tyr-α-Ala	3,7	6,3	9,3	1,4	3,1	5,6
Leu-Tyr	1,9	3,0	5,3	0,3	0,5	0,8
Gly-Tript	3,9	8,1	13,0	0,8	1,7	3,0

Perzentuelle Menge des aus Aminosäure-Metallkomplexen (0,04 Mol Aminosäure — 0,01 Grammatom Metall) freigesetzten NH_3-Stickstoffes

Glykokoll	4,4	9,6	19,5	—	—	—
α-Alanin	0,7	1,3	3,6	—	—	—
Leucin	0,3	0,8	1,1	—	—	—
Tyrosin	3,6	6,8	13,2	0,3	0,6	1,1
Triptophan ...	9,0	21,7	46,0	0,3	0,7	1,9
Histidin	50,1	62,6	74,5	19,1	27,0	40,3
β-Alanin	—	—	—	—	—	—

die Bildungsmöglichkeit von gemischten Übergangskomplexen herangezogen werden.

Das Maß der Desamination der aus aliphatischen α-Aminosäuren bestehenden Dipeptide ändert sich in derselben Weise mit der Natur und der Reihenfolge der Kopplung der Aminosäuren, wie ihre Neigung zur Hydrolyse. Wie dies bereits für die früher untersuchten monotonen Glycylpeptide gezeigt wurde, werden bei einer Oxydation in alkalischem Medium vor allem die kettendigen Aminogruppen desaminiert. Der Freisetzung der die Peptidbindungen bildenden Stickstoffatome in Form von Ammoniak muß jedoch die

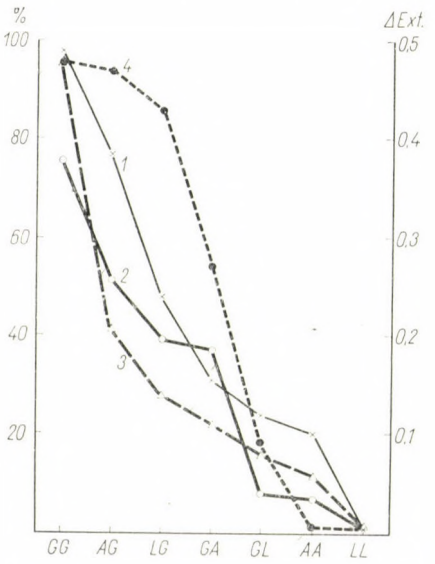

Abb. 1. Vierstündige Hydrolyse bzw. Desamination verschiedener Dipeptid- Kupferkomplexe: 1. Hydrolyse, %; 2. oxydative Desamination, %; 3. auf die Ausgangsmischungen bezogene Änderung des Extinktionswertes nach vierstündiger Hydrolyse; 4. Änderung des Extinktionswertes nach vierstündiger Oxydation (G = Glykokoll; A = α-Alanin; L = Leucin

Hydrolyse der Peptidbindungen vorangehen. Im gegenwärtigen Fall kommt man zu demselben Schluß, wenn man die Daten über die Hydrolyse und die Desamination der Dipeptide verschiedenen Types vergleicht (Abb. 1).

In Verbindung mit der Oxydierbarkeit der anderen Dipeptide sollen noch die Komplexe des Glycyltyrosins und des Tyrosylglycins hervorgehoben werden. Tyrosylglycin wird nämlich in Gegenwart beider Metallionen auffallend stärker desaminiert, als das Glycyltyrosin.

ZUSAMMENFASSUNG

Es wurde die Komplexbildung verschiedener Dipeptide mit Kupfer-, Nickel- und Kobaltionen in alkalischem Medium untersucht, weiterhin die Zusammensetzung der Komplexe, sowie der Einfluß der Komplexbildung auf die alkalische Hydrolyse bzw. auf die oxydative Desamination der Peptide. Es konnte ein Zusammenhang zwischen der Zusammensetzung der Peptide und ihrer Neigung zur Hydrolyse bzw. zur Oxydation gefunden werden.

LITERATUR

1. NYILASI, J., BIHARI-VARGA, M.: Magyar Kém. Folyóirat **63**, 500. (1963); Acta Chim. Hung. **39**, 235 (1963).
NYILASI J., BIHARI-VARGA, M., ORSÓS P.: Magyar Kém. Folyóirat **71**, 49. (1965); Acta Chim. Hung. **42**, 365 (1964).
NYILASI J., POMOGÁTS E.: Magyar Kém. Folyóirat; Acta Chim. Hung. **43**, 33 (1965).
NYILASI J., ORSÓS P.: Magyar Kém. Folyóirat; Acta Chim. Hung. **43**, 45 (1965).
2. PARTRIDGE, M.: Biochem. J. **42**, 238 (1948).
3. HARVEY, A. E., MANNING, D. L.: J. Am. Chem. Soc. **72**, 3217, 4488 (1950).
SCHLÄFER, H. L.: Komplexbildung in Lösung. S. V. Berlin—Göttingen—Heidelberg, 1961, p. 253.
4. BURK, D., HEARON, C. I., SHADE, A. L.: J. Biol. Chem. **165**, 723 (1946).
MALEY, L. E., MELLOR, D. P.: Nature **165**, 453. (1950).
5. ABDERHALDEN, E., SICKEL, H.: Z. Physiol. Chem. **170**, 134 (1927).
ABDERHALDEN, E., BROCKMANN, H.: Z. Physiol. Chem. **170**, 146 (1927).
LEVENE, P. A., STEIGER, R. S., ROCKEN, A.: J. Biol. Chem. **97**, 717 (1932).
GORDON, A. H., MARTIN, A. J. P., SYGE, R. L. M.: Biochem. J. **35**, 1369 (1941).
SYNGE, R. L. M.: Biochem. J. **38**, 285 (1944); **39**, 351 (1945); **44**, 542 (1949).
SANGER, F.: Advances Protein Chemistry VII., Acad. Press New York, 1952, p. 1.
MARTIN, R. J. L.: Nature **175**, 771 (1955).
6. CRISTOL, P., BENEZECH, CH., CRASTES DE PAULET, A.: Bull. de la Soc. Chim. de France 684. (1954).
7. HARRIS, J. I., COLE, R. D., PON, N. G.: Biochem. J. **62**, 164 (1965).
8. BERGER, I., JOHNSON, M. J.: J. Biol. Chem. **130**, 641, 655 (1939); **133**, 639. (1940).
SMITH, E. L., BERGMANN, M.: J. Biol. Chem. **138**, 789. (1941).
SMITH, E. L.: J. Biol. Chem. **173**, 571.(1948); **176**, 921.(1948); Federation Proc. **8**, 581 (1949); Proc. Nat. Acad. Sci. **35**, 80. (1949).
MERIWETHER, L., WESTHEIMER, F. H.: J. Am. Chem. Soc. **78**, 5119 (1956).
9. COLLEMAN, J. P., BUCKINGHAM, D. A.: J. Am. Chem. Soc. **85**, 3039 (1963).

Metal Complexes of Peptides, V

Investigation of the Hydrolysis and Oxidation of the Metal Complexes of Dipeptides

J, NYILASI, M, BIHARI-VARGA and P, ORSÓS

Summary. The formation of the copper, nickel and cobalt complexes of various dipeptides was studied in alkaline medium. The composition of the complexes were determined, and the effect of complex formation on the alkaline hydrolysis and oxidative deamination of peptides was investigated. A correlation has been found between the composition of complexes and the tendency of the peptides to undergo hydrolysis and oxidation.

О комплексах пептидов с металлами, V

Исследование гидролиза и окисления комплексов дипептид — металл

Я. НИЛАШИ, М. БИХАРИ-ВАРГА и П. ОРШОШ

Резюме. Исследовали образование комплексов различных дипептидов с ионами меди, никкеля и кобальта в щелочной среде. Изучали состав комплексов и влияние комплексообразования на щелочной гидролиз пептидов и их окислительное дезамидирование. Установили зависимость между составом пептидов и их склонностью к гидролизу и окислению.

Dr. János NYILASI
Frau Dr. Magdolna BIHARI-VARGA
Piroska ORSÓS

Budapest VIII., Múzeum krt. 6—8.

THE STEPWISE TOTAL HYDROLYSIS OF ALGINIC ACID

J. SZEJTLI

(Norwegian Institute of Seaweed Research, The Technical University of Norway, Trondheim, Norway)

Received April 5, 1965

In a previous paper [1] experiments have been published concerning the hydrolysis limit of alginic acid. In the present work the hydrolysis limit has been investigated with freshly precipitated alginic acid. In freshly precipitated state, the specific surface of alginic acid is much higher than that of a material which has been dried.

The solutions used in the experiments were prepared from *L. digitata alginate*, *L. hyperborea alginate* and from a residue of *L. digitata* alginic acid, that had been hydrolyzed until the limit was reached (see Exp. 1). An appropriate amount of hydrochloric acid was added to the hot homogeneous solutions to adjust 0.4 N concentration. The hydrolysis curves are shown in Fig. 1. Two conculsions may be drawn from these curves: (a) the hydrolysis limit of *L. digitata* alginic acid is higher than that of *L. hyperborea stipes* alginic acid (the limits are 45.4 and 30.9%, resp.); (b) the residue resistant to hydrolysis was now hydrolyzed to a considerable extent. From this fact it may be concluded that one part of the alginic acid, as a consequence of the precipitation by strong acid, takes up a structure which is not hydrolyzable. When dissolved in alkali, the water-soluble alginate structure is re-established and after re-acidifying a part of it remains hydrolizable, while the other part becomes again resistant to hydrolysis.

Therefore, each of the three solutions in which the hydrolysis had reached the hydrolysis limit (see Fig. 1) was neutralized until all the precipitate was dissolved, then it was again acidified to adjust an acid concentration of 0.4 N, and the mixture was hydrolyzed on a boiling water bath.

As it is seen in Fig. 1, the hydrolysis continued to approach now a new hydrolysis limit. From this experiment it was concluded that the total hydrolysis of alginic acid might be achieved by a stepwise technique. As it is shown in Fig. 2 (Experiment 2) this attempt was succesful. At its maximum, the curve representing the reducing power reached 86%, while the curve characterizing the reaction with phenol-sulphuric acid attained 80% of the theoretical value. In the course of this experiment, the uronic acids formed were for the most part converted into their alkali salts 1, 2, 3 or 4 times (which involved the

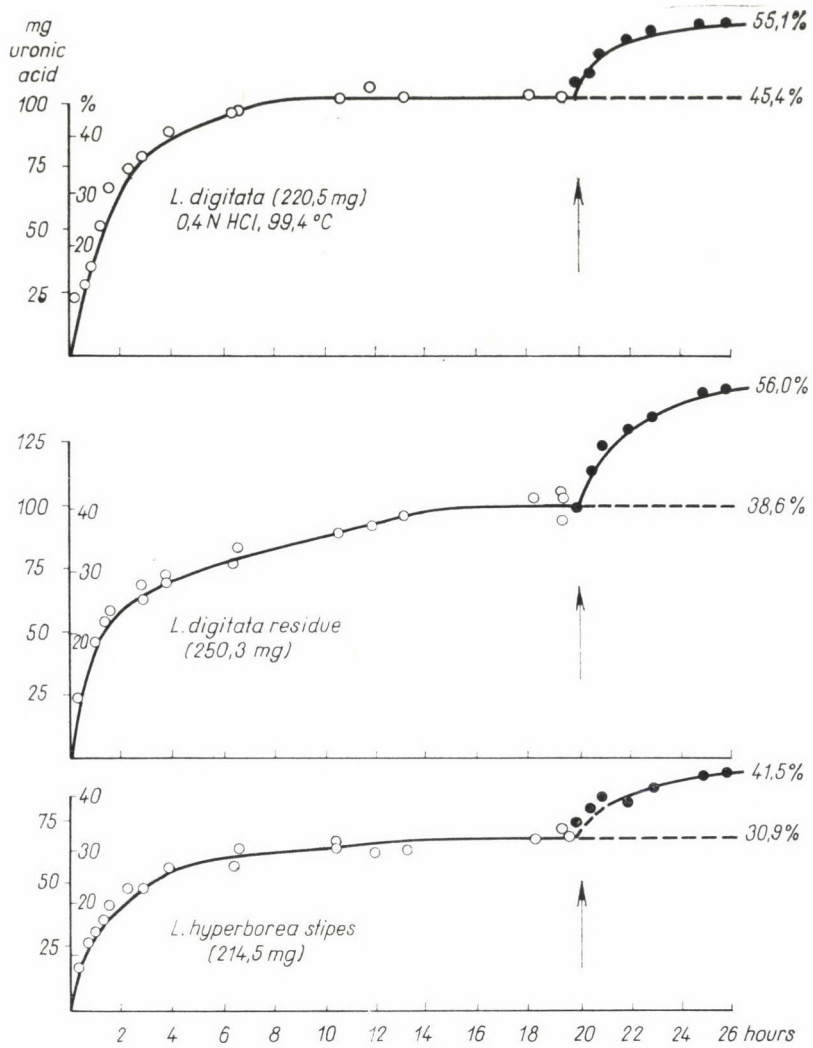

Fig. 1. Repeated hydrolysis of three different samples of alginic acid. At the marked point (20 hr.) the hydrolysis-resistant residues were dissolved in alkali, then re-acidified and hydrolyzed further. (Uronic acid content calculated from reducing power data: 41% of guluronic acid and 59% of mannuronic acid.)

possibility for isomerization of mannuronic acid to guluronic acid) and they were heated with the mineral acid for a long time (the total time of hydrolysis was 43.5 hours). This may have caused considerable destruction. Actually, after 43.5 hours, 14% of a brown, insoluble, powderlike furfural polymer was found. Since a part of the decomposition products has reducing properties but gives weaker colours than the intact uronic acids with phenol sulphuric acid

reagent, the presence of such products may be the explanation for the difference between the two maxima. The solution after 43.5 hours was dark brown.

This stepwise degradation was repeated combined with the stepwise separation of the monomers (see Experiment 3). After the hydrolysis limit had been reached, the solution, which contained the produced monomers, was separated from the residual precipitate, and only this residue was dissolved in alkali, re-acidified and subjected to further hydrolysis. This process was

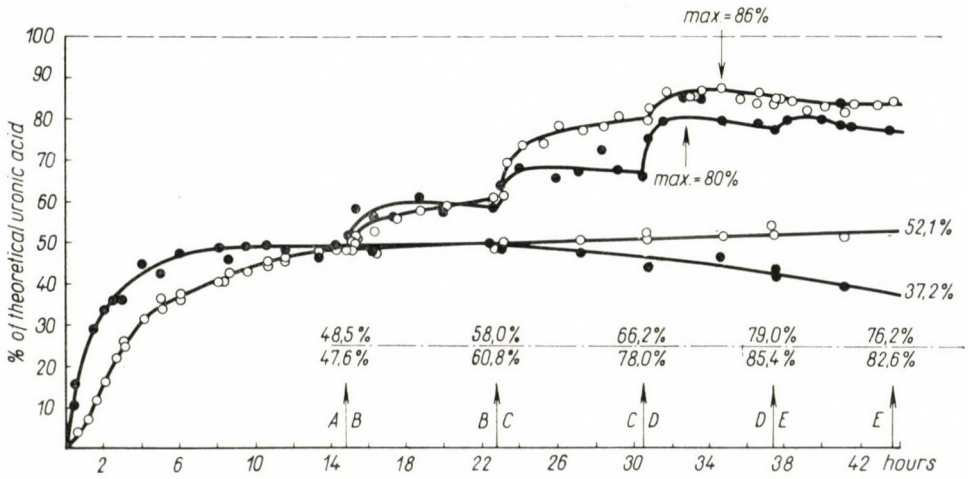

Fig. 2. Stepwise acidic degradation of alginic acid. *(L. digitata* alginic acid; 100 °C; 0.4 N HCl) x = phenol-sulphuric acid reaction; 0 = reducing power

repeated until no undissolved material remained in the acidic solution. The amount of uronic acids formed was determined in each step. In the first and second step the M/G ratio (mannuronic/guluronic acid ratio) was also determined by ion exchange chromatography. The results are listed in Table I. None of the solutions were brown or contained any furfural polymers. In this experiment the formed uronic acids were not neutralized, so the possibility of isomerization was excluded.

Investigation of the glycosidic bonds hydrolyzed in the different stages of the stepwise hydrolysis.

The question, whether the bonds hydrolyzed were of the same type in the three different materials shown in Fig. 1, was investigated on basis of kinetical data.

If the different alginic acids are hydrolyzed under strictly identical conditions (as it was the case with the materials shown in Fig. 1), and the reaction rate constants calculated from the hydrolysis data coincide, then it is very probable that the cleaved bonds were identical.

As it was mentioned in a previous paper [1], 100% hydrolysis in presence of strong acids in one step is practically impossible. Consequently, the limit value was used for calculating the first order reaction rate constants according to the formula log [limit/(limit $-$ x)]. These values are plotted against the reaction time in Fig. 3. The points lie along a single straight line, and this fact demonstrates that the bonds split during the hydrolysis were identical in the three different materials. Since the "limit residue" was prepared from the same *L. digitata* alginic acid which was hydrolyzed in this

Table I

Stepwise hydrolysis of alginic acid from L. digitata (0.4 N HCl, 100 °C)

Step No.	Reducing power, % Σ	Phenolsulphuric acid reaction, % Σ	Orcinol reaction, % Σ	M/G	Time hr.
I	40.8	41.8	35.1	2.15	13
II	55.7	57.5	49.5	2.70	10
III	61.8	64.2	56.2		10
IV	67.9	70.3	61.7		10
V	75.4	77.6	68.9		10
VI	77.3	80.5	71.4		8
	+ residue	97.1			

experiment, it means that the bonds cleaved in the second step had to be nearly identical with those split in the first step. Additional evidence is afforded by the second part of Fig. 3. These curves are calculated from the first and second steps of the curve of the reducing power shown in Fig. 2. As the reaction rate is the same during the different stages of the stepwise hydrolysis, it is very probable that the same types of glycosidic bonds are hydrolyzed in the different steps. However, within one step, different types of bonds may be split simultaneously.

Characterization of the hydrolysis-resistant fraction

The earlier assumption that alginic acid consists of two components, a hydrolyzable and a non-hydrolyzable part, is obviously refuted by Fig. 2. As it is seen from Table I and Fig. 3, there is no such striking difference in chemical composition and in the rate of hydrolysis which could be accepted as the reason for the existence of a hydrolysis limit. It means that the non-hydrolyzed fraction is chemically not very different from the hydrolyzable

substance, but under the conditions of acid hydrolysis the former is somehow protected against hydrolysis.

This protected form may be a 3,6-lactone or, according to JEVTUSHENKO [2], an acid anhydride. According to JEVTUSHENKO the lacton ring is unstable under the conditions of acid hydrolysis, but the neighbouring carboxyl groups of the same chain may form anhydrides with each other. However, it is not very probable that such bonds would be really stable in hot water in the presence of strong acids, and it is not clear why the cleavage of glycosidic linkages should be hindered by the presence of acid anhydrides.

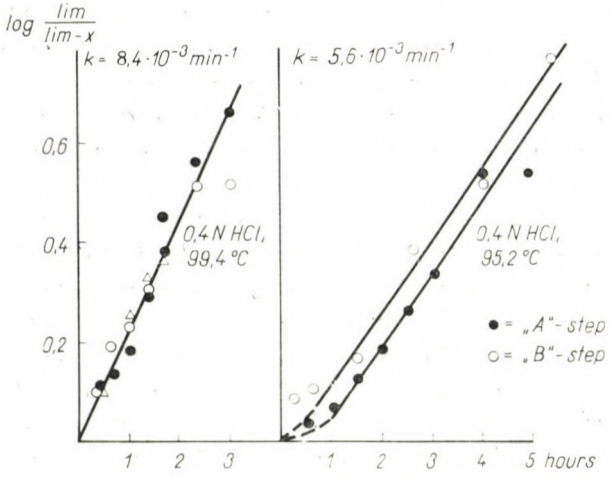

Fig. 3. The logarithmic curves for the first stage of the reaction. x = *L. digitata*, ○ = *L. hyperborea*, △ = *L. digitata* residue

DRUMMOND, HIRST and PERCIVAL [3] suggested that the presence of alternating 1,3 and 1,4 bonds and ester linkages between the neighbouring chains may be responsible for the incomplete periodate oxidation of alginic acid. The ester linkages probably would not be stable against acid hydrolysis; the existence of 1,3 bonds — though possible — gives no direct explanation for the hydrolysis limit, either.

It seems probable from our experiments of stepwise degradation that the hydrolysis-resistant structure is formed reversibly as a result of treating the material with strong acid. The change of the structure may consist in the following.

Sodium alginate is soluble in water. As a salt of a strong base and a weak acid, it dissociates to a large extent. Many of the units of the polymer chains are charged on account of the dissociated carboxyl groups. The molecules do not associate, since repelling forces between the hydrated molecules are considerable. When a strong acid is added to this solution, the carboxyl

groups are liberated, the chains loose their charge and hydrate hull. The neighbouring chains approach each other and the formation of hydrogen bonds begins between the carboxyl groups. The ultimate result of the addition of a strong acid to the aqueous solution of alginate is the precipitation of alginic acid. Actually a semicrystalline structure is formed. A smaller or larger part of the molecule, depending on the dissociation of carboxyls, forms a compact, crystalline region, impermeable for hydroxonium ions, while the remaining part of the same molecule remains amorphous and accessible to the acid catalyst. This process is analogous to the retrogradation of amylose [5].

Evidence for the presence of hydrogen bonding is presented by the behaviour of alginic acid in 50% chloral hydrate solution. Chloral hydrate is a good hydrogen bond forming agent. From a neutral solution of 50% chloral hydrate and 0.3% alginate, on the addition of hydrochloric acid only a part of the formed alginic acid is precipitated. After filtration, the dissolved alginic acid may be precipitated from the clear solution either with alcohol or with water by diluting to about 5 volumes.

It is possible that at least a part of the uronic acid units has different conformations in precipitated and in the dissolved state. HIRST, PERCIVAL and WOLD [4] recently reported the preparation of oligosaccharides from reduced alginic acid. Neither mannosyl-gulose nor the mannosyl-guliitol showed any mobility in molybdate buffer in ionophoretic experiments. It means that the gulose could not form a complex with the molybdate. A possible explanation is that the gulose exists in C1 or in some B conformation. The difference of the instability factors in the C1 and 1C conformations of guluronic acid is less than 1.0; lactone formation is impossible in both conformations, since the carboxyl and C_2 and C_3 hydroxyls are on different sides of the ring.

Mannuronic acid of 1C conformation may form a 3,6-lactone. In this case a new ring is formed. A five-membered ring is superposed on the six-membered one. As a consequence, the unstable 1C conformation becomes stabilized. This lactone formation may also occur when the substance is acted upon by strong acids, but the part played by this reaction in hindering acid hydrolysis is not clear.

In the course of the heterogeneous hydrolysis of alginic acid, water-soluble oligomers (ultimately converted into monomers and destruction products) and a water-insoluble, nearly crystalline residue are obtained. This residue is split only very slowly.

When this crystalline, hydrolysis-resistant residue is treated with alkali, dissociation of the carboxyl groups results in the cleavage of the hydrogen bonds, and eventually the lactone ring is opened; as a consequence the material becomes soluble. On re-acidifying the solution, the process is repeated: the shortened molecules form a new, but less-extended crystalline region, and a part of the molecules remains again accessible to the hydroxonium ion.

Fig. 2 shows that after the third hydrolysis the molecules are so much shortened that in the fourth step they suffer complete hydrolysis.

After these experiments were completed, LARSEN [6] in this laboratory achieved the total hydrolysis of alginic acid in homogeneous phase at pH 3.5. At this pH, alginic acid is not precipitated yet, and the greatest part of the carboxyl groups are free. At 100° after 60 hours no unhydrolyzed material is left — only a considerable amount of destruction products of the formed monomers — so the hydrolysis is complete in one step.

Difference between the rates of hydrolysis of guluronic and mannuronic linkages

The acid hydrolysis of alginic acid consists of two different processes; either of them is a hydrolysis reaction, but they are characterized by different reaction rate constants. Fig. 4 shows two curves; one of them is the curve of the reducing power (proportional to the —CHO groups liberated), the other represents the colour reaction with phenol-sulphuric acid (proportional to the amount of solubilized alginic acid). As it is seen from the figure, the solubilization is a faster reaction than the hydrolysis. Fig. 5 demonstrates the same data expressed as log [limit/(limit — x)] values plotted against the time of hydrolysis, used for determination of the rate constants. A break point can be observed on the curve of the reducing power.

The G→ linkages are split faster than the M→ bonds. In the first stage of the hydrolysis the cleavage of the G→ bonds that is, of the G→ G→ (or G→ M→) linkages prevails, but at the same time the M→ bonds (M→ M→

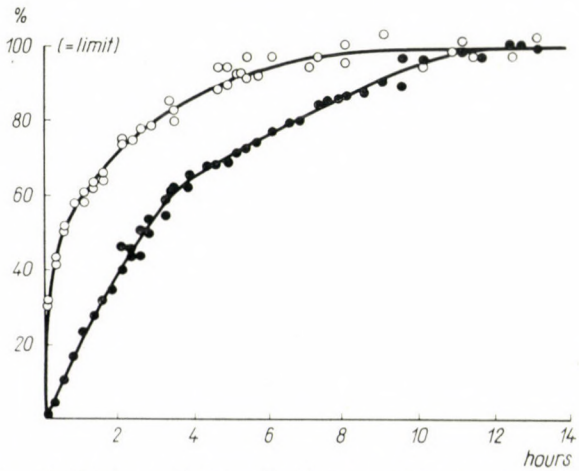

Fig. 4. Hydrolysis of alginic acid from *L. digitata*. 95.2 °C; 0.36 N HCl; ○ = phenol-sulphuric acid reaction; ● = reducing power

or M→ G→) are also split. When the majority of the G→ bonds are hydrolyzed, the process decelerates and continues at a rate characteristic of the splitting of the M→ bonds. The intersection of these two different rate lines produces the break point on the curve of the reducing power in Fig. 5. As it is seen from this figure, extrapolating to zero time gave the intersection point log [limit/(limit − x)] = 0.17, corresponding to 32% hydrolysis. Thus, the proportion of the faster splitting linkages is 32%. The assumption of a greater stability of M→ bonds is supported by the work of VINCENT [7]: he prepared oligouronides after partial hydrolysis, and in each of them the reducing end group was

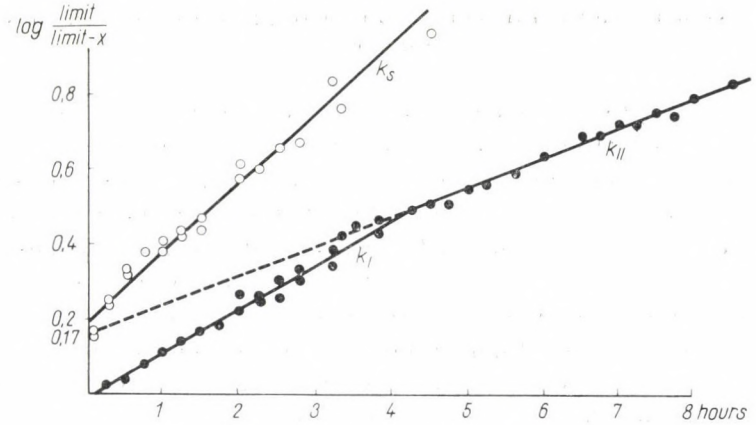

Fig. 5. Determination of the rate constants

guluronic acid. The same result was found by HIRST and his co-workers [4, 8]. Methyl gulosides are split faster in acid than methyl mannosides [9, 10].

It is seen from Fig. 5 that the first stage of the hydrolysis is faster than the second. During this first stage, the reducing groups are formed partly as a consequence of solubilization, partly by further hydrolysis of the dissolved molecule fragments. If only a single type of bond existed in the molecule, the first stage ought to be the slower, since hydrolysis occurs here in heterogeneous phase. In practice the situation is just reversed: the stage of hydrolysis taking place in homogeneous phase is slower. Thus, the first stage must be the result of the simultaneous splitting of two different types of linkages. At the end of this period, the type of bonds splitting faster is practically completely hydrolyzed. Therefore, only the linkages splitting slower are hydrolyzed during the second period. The rate constant of this second stage is characteristic probably for the mannuronic linkages.

The exact values of $k_{\text{guluronic}}$ and $k_{\text{mannuronic}}$ cannot be calculated from these experiments, because the hydrolysis occurs partly in heterogeneous phase.

Substituting k_{II} and k_s into the KUHN [11] equation, — for simultaneous splitting of two different types of linkages — the curve of the reducing power was calculated. The deviations between the calculated and measured values within the first 9 hours of hydrolysis (0—90% hydrolysis) were less than $\pm 3\%$.

Experimental

Exp. 1. (a) 271.7 mg of *L. digitata Na-alginata (Svellingen*, 1960, M/G = 1.54) (corresponding to 220.5 mg of water- and ash-free material) was dissolved in 39.3 g of water. 10.7 ml of 2 N HCL was added. After reaction with the bound Na the HCl concentration was 0.4 N.

(b) 273.0 mg (= 214.5 mg, as above) of *L. hyperborea stipes (Hustad* 4/5) Na-alginate was dissolved and precipitated as above.

(c) 250.3 mg of the water- and ash-free residue from a 20-hr. treatment of *L. digitata* alginic acid at 100° in 0.2 N HCl was used. The residue was centrifuged, washed and dried. It was dissolved in the calculated amount of alkali, then treated further as under (a) and (b).

Each solution was heated in a water-bath (99.4°). Samples were withdrawn periodically, and the reducing power was determined. After reaching the hydrolysis limit, the solutions were weighed on an analytical balance, then neutralized. The precipitate was dissolved. The solutions were weighed again and the calculated amount of HCl was added to make each solutions 0.4 N with respect to HCl, and the hydrolysis was continued (see Fig. 1).

Exp. 2. Successive degradation of alginic acid. 2510 mg of Na-alginate (= 2050 mg of alginic acid), the same as in Exp. 1(a), was dissolved in 225 ml of water, and 63 ml of 2 N HCl was added. The mixture was hydrolyzed in a boiling water-bath. Samples were withdrawn and analyzed by the ferricyanide method and by the phenol-sulphuric acid reaction. After reaching the hydrolysis limit, the solution containing the precipitate was cooled, weighed and divided into two flasks. One of them was neutralized with $NaHCO_3$ until the precipitate dissolved, and then again acidified to adjust 0.4 N concentration of the hydrochloric acid, and the hydrolysis was continued. This was repeated still 3 times. The other part of the solution was heated in the same water-bath without neutralization. From time to time samples were taken for determination of the uronic acid content. After 43.5 hrs., the contents of both flasks were filtered, the precipitate washed and dried. After step "E" (see Fig. 2) there remained 14% of a dark brown, powderlike material; after the prolonged step "A", 29% of a brown fluffy precipitate was obtained. The temperature of the hydrolsis was 95.2°.

Exp. 3. (a) 2527 mg of sodium alginate (= 2060 mg of alginic acid), the same as in Exp. 1 (a), was dissolved and hydrolyzed in 250 ml of 0.4 N HCl at 95.2°. Samples were taken for analysis.

(b) In another flask the same amount of alginic acid was hydrolyzed under identical conditions without taking samples. When (a) reached the limit, the hydrolysis in both flasks was stopped. The mixture from experiment (b) was centrifuged, the precipitate washed, and the supernatant analyzed (see Table I). The precipitate was dissolved in $NaHCO_3$, the re-acidified and subjected to further hydrolysis. This was repeated four times. The chromatographic separation of uronic acids was achieved by the LARSEN—HAUG method [12], the orcinol reaction according to BROWN [13].

The author is very much indebted to the ROYAL NORWEGIAN COUNCIL FOR SCIENTIFIC AND INDUSTRIAL RESEARCH for an award of Postdoctorate Fellowship that made this work possible, to Mr. B. LARSEN for revision of the English text, and to Mr. A. HAUG for column chromatographic separation of the uronic acids.

SUMMARY

It is known that alginic acid is hydrolyzable only up to a certain extent, and a residue resistant to hydrolysis is generally obtained. The present experiments showed that the hydrolysis-resistant structure is formed as a consequence of precipitation by strong acids. When the precipitate left behind after reaching the hydrolysis limit is dissolved in alkali and the solution is acidified again, alginic acid may be further hydrolyzed to a higher limit of hydrolysis. Repeating such hydrolysis steps about four times, the alginic acid may be completely hydrolyzed by relatively dilute strong acids. If the formed monomers are separated from the residual precipitate in every step after reaching the hydrolysis limit, and if the residue is dissolved and further hydrolyzed, the yield of uronic acids is higher than obtainable by former procedures.

The nature of the hydrolysis-resistant residue is discussed. It has beeen found that guluronic linkages are split more rapidly than mannuronic bonds.

REFERENCES

1. Szejtli, J.: Acta Chim. Hung. **45,** 369 (1965).
2. Jevtushenko, U. A.: Koll. Zhurnal **16,** 255, 340 (1954).
3. Drummond, D. W., Hirst, E. L., Percival, E.: J. Chem. Soc. 1208 (1962).
4. Hirst, E. L., Percival, E., Wold, J. K.: J. Chem. Soc. 1493 (1964).
5. Holló, J., Szejtli, J., Gantner, G. S.: Periodica Polytechnica (Chem.) **3,** 95, 163 (1959).
6. Larsen, B.: Private communication, Trondheim, 1964.
7. Vincent, D. L.: Chem. Ind. 1109 (1960).
8. Hirst, E. L., Percival, E., Wold, J. K.: Chem. Ind. 257 (1963).
9. Pigman, W.: The Carbohydrates (Academic Press, New York) 1957.
10. Shafizadeh, F.: Tappi **46,** 381 (1963).
11. Kuhn, W.: Ber. 63, 1503 (1930).
12. Larsen, B., Haug, A.: Acta Chem. Scand. **15,** 1397 (1961).
13. Brown, H. H.: Arch. Biochem. **11,** 269 (1946).

Über die stufenweisen Totalhydrolyse der Alginsäure

J, SZEJTLI

Zusammenfassung. Bekanntlich ist die Alginsäure nur bis zu einem bestimmten Grade hydrolysierbar, wobei ein hydrolysenresistenter Restanteil verbleibt. Weitere Experimente zeigten, daß sich die hydrolysenresistente Struktur infolge Ausfällung durch starke Säure ausgebildet nat. Wird das restliche Präzipitat nach Erreichen der Hydrolysengrenze in Alkali gelöst und erneut angesäuert, so läßt sich die Alginsäure bis zu einer höheren Hydrolysengrenze abbauen. Führt man diese stufenförmige Hydrolyse in etwa 4 Schritten durch, so kann die Alginsäure durch relativ verdünnte starke Säuren vollständig hydrolysiert werden. Wenn man die entstandenen Monomeren bei jeder einzelnen Stufe nach Erreichen der Hydrolysengrenze von dem restlichen Präzipitat abtrennt und lediglich das letztere auflöst und weiterhydrolysiert, so ist eine höhere Ausbeute an Uronsäuren erzielbar als vorher.

Die Beschaffenheit des hydrolysenresistenten Restes wird diskutiert. Beobachtungen zeigen, daß die Guluronsäurebindungen rascher gespalten werden als die Mannuronsäurebindungen.

Ступенчатый, полный гидролиз альгиновой кислоты

Я. СЕЙТЛИ

Резюме. Известно, что альгиновая кислота может быть гидролизована только до определенного предела. Последующие опыты позволили прийти к тому заключению, что гидролизнорезистентная структура образуется вследствие осаждения, проведенного сильной кислотой. Растворяя, оставшийся после достижения предела гидролиза, осадок в щелочи и затем подкислив его снова, можно гидролизовать альгиновую кислоту дальше, до более высокого предела. Повторяя эти ступени гидролиза (приблизительно 4 раза), альгиновую кислоту можно полностью гидролизовать относительно разбавленными сильными кислотами. Если мономеры, образовавшиеся в каждой ступени, отделять от осадка, оставшегося после достижения предела гидролиза, и только гидролизнорезистентный остаток растворять в щелочи и гидролизовать дальше, тогда может быть достигнут более высокий выход уроновой кислоты, чем в случае применяемых до настоящего времени способов гидролиза альгиновой кислоты.

В сообщении обсуждается характер гидролизнорезистентного остатка. Наблюдения показали, что связь гулуроновой кислоты разрывается быстрее, чем маннуроновой.

József Szejtli, Deutsche Akademie der Wissenschaften zu Berlin, Institut für Ernährung, 1505 Potsdam-Rehbrücke.

UNTERSUCHUNG DER OXYDATIONS-(LAGERUNGS-)VORGÄNGE DER KOHLEN MIT DERIVATOGRAPHISCHER METHODE

M. WELTNER

(Forschungsinstitut für Elektrische Energie, Budapest)

Eingegangen am 23. August 1965

Der Betrieb der Kohlengruben erfordert einen gleichmäßigen Produktionsgang, denn nur dieser bürgt für eine gleichmäßige Betätigung der zur Verfügung stehenden Arbeitskräfte und für eine gute Ausnützung der Maschinen. Anderseits werden die Kohlenverbraucher durch die Unregelmässigkeiten der Verwendung, wie auch durch unerwartete Störungen der Anlieferung zu einer Lagerung der Kohle gezwungen.

Die Lagerung der Kohle ist also unvermeidlich.

Während der Lagerung der Kohle treten infolge einer Oxydation derselben schwere Verluste auf, deren Verringerung eine wichtige volkswirtschaftliche Aufgabe bedeutet [1].

Während der Lagerung verschlechtert sich die Qualität der Kohle. Diese Verschlechterung betrifft gleichermaßen den Heizwert, den Gasgehalt, die Verkokbarkeit usw., und kann unter ungünstigen Umständen sogar zur Selbstentzündung führen [2]. Wegen der Unzulänglichkeit unserer Kenntnisse über die physikalisch-chemische Beschaffenheit der Kohle stoßen die experimentellen Untersuchungen über die Struktur und den Oxydationsvorgang der Kohle auf große Schwierigkeiten [3, 4].

Die in der Literatur vorliegenden und oft einander widersprechenden Daten können teils damit erklärt werden, daß Kohlen von verschiedenem Inkohlungsgrad, d. h. von verschiedenen Eigenschaften, während der Lagerung, also auf oxydative Einwirkung, verschieden reagieren.

Es gibt auch Fälle, in denen die widersprechenden Daten und Ansichten einer Unzulänglichkeit oder einer ungenügenden Empfindlichkeit der Untersuchungsmethoden zuzuschreiben sind.

Die Oxydation ändert vor allem, besonders am Anfang, die Oberflächeneigenschaften der Kohle, und beeinflußt dadurch beträchtlich das Verhalten derselben in Vorgängen die von seinen Oberflächeneigenschaften abhängig sind (so z. B. bei der Verkokung oder in Verbrennungsvorgängen). Dies trifft selbst dann zu, wenn aus den konventionellen Kohlenanalysedaten noch bei weitem nicht auf eine derart wesentliche Änderung der Kohleneigenschaften zu folgern ist [5, 6, 7].

Das moderne und vielseitige Verfahren, die derivatographische Methode, bietet mehr Hilfe und Möglichkeiten in dieser Forschungsarbeit, als die bisher verwendeten Methoden, so daß zu hoffen ist, daß auch in diesem volkswirtschaftlich sehr wichtigen Gebiet durch die Verwendung der Derivatographie neue und verläßlichere Resultate erzielbar sein werden [8].

Wenn mineralische Kohlen in größeren Mengen gelagert werden (in Wärmekraftwerken, Kokereien, Gaswerken, Berggrubenbetrieben), kann in den meisten Fällen eine Erwärmung der Kohlenhalden, und falls rechtzeitig keine Vorbäugungsmaßnahmen getroffen werden, auch eine Selbstentzündung der Kohle beobachtet werden.

Die aus der Verschlechterung der Kohle während der Lagerung, aber noch mehr die aus der Selbstentzündung der Kohle stammenden materiellen Verluste sind, ähnlich wie die Korrosionsschäden, sehr beträchtlich.

Bereits 1866 bat eine Schiffahrtsgesellschaft Liebig um Rat bezüglich einer Verhinderung der Selbstentzündung der transportierten Kohlen. Das Problem der Lagerung und der Selbsentzündung der Kohlen beschäftigt noch heute die Forscher dieses Gebietes auf der ganzen Welt, und man ist bestrebt mit einer Reihe von Theorien die Fragen in Verbindung mit der Lagerung und Selbstentzündung der Kohlen zu beantworten und die Erscheinungen zu erklären.

Anfangs wurde der Grund einer Selbstentzündung der Kohle der sulfatisierenden Verwitterung ihres Pyritgehaltes zugeschrieben. Später dachte man an die Oxydation der organischen Bestandteile der Kohle, der Huminoide, und man sprach auch von der Oxydation der in der Kohle enthalteten ungesättigten Verbindungen.

In gewissen Fällen fand man, daß die Erwärmung der Kohle auch infolge Betätigung der an der Kohle lebenden Bakterien verursacht werden kann.

Heute stimmen die meisten Ansichten darin überein, daß der Grund der Erwärmung und der Selbstentzündung der Kohle in der Oxydation der organischen Kohlensubstanz, die auf Einwirkung des Luftsauerstoffes erfolgt, zu suchen ist [9].

Während der Oxydation verarmt die Kohle an C + H und der Sauerstoff wird angereichert. Die Destillation der oxydierten Kohlen gibt einen geringeren Gas- und Teerertrag, als die der nicht oxydierten Kohlen.

Es konnte festgestellt werden, daß die gut lagerbaren Eozänkohlen während ihrer vier Monate dauernden Lagerung bis zu 10% ihres Heizwertes einbüßen können, während bei jüngeren Kohlen mit einem viel größeren Verlust zu rechnen ist.

Eine Lösung der Probleme in Verbindung mit der Kohlenlagerung ist nur dann zu erhoffen, wenn die Oxydationsvorgänge unter Verwendung moderner Untersuchungsmethoden gründlich studiert werden.

Über den Oxydationsmechanismus der Kohle sind die Meinungen verschieden. Vom chemischen Gesichtspunkt am besten begründet erscheint die Phenol-Oxydationstheorie von TRONOW. Im Sinne dieser Theorie häufen sich in der organischen Substanz der Kohle im Laufe der Oxydation die Phenol-, Carbonyl- und Carboxylgruppen an [10].

Viele Autoren beschäftigten sich mit der experimentellen Untersuchung der Kohlenoxydation. Aus diesen Untersuchungen kann darauf gefolgert werden, daß sich die verschiedenen Kohlen im Laufe der Oxydation während der Lagerung ihrem Inkohlungsgrad und ihren Eigenschaften gemäß unterschiedlich verhalten, so daß die für eine gegebene Kohlenart oder für Kohlengruppen mit ähnlichen Eigenschaften gefundenen Gesätzmäßigkeiten nicht ohne weiteres auf irgendeine andere Kohlenart oder Kohlengruppe zu übertragen sind.

Oxydationsversuche müssen also stets mit der gleichen Kohle vorgenommen werden, deren Verhalten vom praktischen Gesichtspunkt Interesse besitzt.

Wie bekannt, werden in den Kraftwerken große Kohlenmengen für energetische Zwecke verwendet.

Vor ihrer Verwendung werden die Kohlen über kürzere oder längere Zeit gelagert, wodurch Kohlen verfeuert werden, deren Eigenschaften sich wärend der Lagerung mehr oder weniger veränderten.

Die Kohlenoxydationsversuche wurden mit Kohlenarten, die für Kraftwerke am wichtigsten sind und dort gelagert sowie verwendet werden, vorgenommen.

Für die Oxydationsversuche muß man auch die Eigenschaften der ursprünglichen, also nicht oxydierten frischen Kohlen kennen.

Es wurden die folgenden Braunkohlensorten untersucht:

a) Lignitgriess aus *Gyöngyös* für Kraftwerke,

b) Durchschnittliche energetische Kohle aus *Ajka (Zentrale Kohlenklassierung, Ajka)*,

c) Kohle aus *Borsod (Zentrale Kohlenklassierung, Berente)*,

d) Kohle aus *Nagybátony (Nógráder Kohlenbergbautrust)*.

Außerdem wurden noch zwei ungarische Steinkohlentypen: eine Kohle aus *Pécs* (0—8 mm) und eine Kohle aus *Komló* untersucht, die von den *Budapester Gaswerken* bzw. von den *Donau-Eisenwerken* eingesandt wurden.

Die frische, also nicht oxydierte Kohlenprobe wurde nach Analyse in einen mit Sauerstoff gefüllten Exsikkator gelegt und bei Zimmertemperatur aufbewahrt. Da zur Oxydation der Kohle auch Feuchtigkeit benötigt wird, wurde während der Kohlenoxydationsversuche der Trockenstoff aus dem Exsikkator entfernt und durch eine Wasserschicht ersetzt. Später fanden wir aber, daß die oxydierte Kohle, deren Hygroskopizität infolge von Oxydation ohnehin erhöht wird, aus diesem dunsterfüllten Raum zu viel Feuchtigkeit

aufnimmt. Deshalb wurde statt Wasser eine 50%-ige Schwefelsäurelösung (spez. Gew. 1,399) verwendet. Über eine Schwefelsäurelösung dieser Konzentration bildet sich ein Raum mit 35,2% relativer Feuchtigkeit; diese sorgt für die zur Oxydation benötigte Feuchtigkeit, ohne daß dabei die Kohle übertrieben viel Wasser aufnehmen würde.

Es wurden die Permanganatzahl und der pH-Wert der urpsrünglichen und der oxydierten Kohlen bestimmt.

Zur Bestimmung der Permanganatzahl der Kohlen wurde die von DREES—KOVALSKI abgeänderte Methode von FRANCIS WHEELER benützt.

Zur Bestimmung der Permanganatzahl werden 0,5 g der zu einer Feinheit von unterhalb 0,2 mm gemahlenen Kohle in einen 500 ml Erlenmeyerkolben eingewogen, mit 200 ml einer 0,1 n Kaliumpermanganatlösung und 50 ml einer 0,1 n Natriumhydroxidlösung versetzt, und für 2 Stunden in einem Trockenschrank bei 75 °C aufbewahrt. Nach dieser Oxydation wird der Inhalt des Kolbens durch einen Filtertrichter aus Glas in einen 500 ml Meßkolben gefiltert, mit destilliertem Wasser bis zur Marke aufgefüllt, und gut umgeschüttelt. 100 ml dieser Lösung werden in einen Jodzahlkolben pipettiert und mit 25 ml 10%iger Kaliumjodidlösung, sowie mit 15 ml n Schwefelsäure versetzt. Nach 5—10 Minuten Stehen wird das freigesetzte Jod mit 0,1 n Natriumthiosulfatlösung titriert.

Wenn zur Titrierung a ml 0,1 n Natriumthiosulfatlösung verbraucht wurde, ist die Permanganatzahl (p)

$$p = 200 - 5a.$$

Die Versuchsergebnisse zeigten, daß in dem untersuchten Oxydationsabschnitt die Permanganatzahl der oxydierten Kohlen unverändert blieb oder abnahm. So betrug z.B. für Lignit aus *Gyöngyös* die Permanganatzahl der ursprünglichen Kohle 125, die der oxydierten Kohle 106, für die ursprüngliche Kohle aus *Borsod* 128, für die oxydierte 119, für die ursprüngliche Kohle aus *Komló* 33, für die oxydierte 25, während sich sowohl für die ursprüngliche wie auch für die oxydierte Kohle aus *Pécs* eine Permanganatzahl von 13, für die urpsrüngliche und oxydierte Kohle aus *Ajka* eine von 44, für die ursprüngliche Kohle aus *Nagybátony* eine von 88, für die oxydierte hingegen eine von 89, also kaum eine Änderung, ergab.

Zur Bestimmung des pH-Wertes der Kohlen wurden 5 g der zur analytischen Feinheit gemahlenen Kohle in einen 100 ml Meßkolben eingewogen und der Kolben (unter periodischem Schütteln) mit destillertem Wasser bis zur Marke aufgefüllt. Die Suspension wurde im Laufe des Tages mehrmals geschüttelt, über Nacht stehen gelassen, und der pH-Wert am nächsten Tag bestimmt.

Zur pH-Bestimmt wurde ein Rohrvoltmeter Typ *Radelkisz* 2518/*S* verwendet, wobei als Bezugselektrode eine Kalomelelektrode in 0,1 n KCl und als Arbeitselektrode eine Glaselektrode diente.

Bekannterweise versauert im Laufe der Oxydation die organische Substanz der Kohle infolge des Anwachsens der Anzahl der Carboxylgruppen.

Dieses Sauerwerden ist bei einigen Kohlen gut feststellbar und spiegelt sich auch im pH-Wert, wie z.B. bei der Kohle aus *Borsod*, wo die ursprüngliche Kohle einen pH-Wert von 5,1, die oxydierte hingegen von 4,4 besitzt, ferner bei der Kohle aus *Nagybátony*, wo der pH-Wert von 6,5 auf 5,9 sowie bei der Kohle aus *Komló*, deren pH-Wert von 6,2 auf 4,2 verringert wird. Eine geringere Versauerung ist bei der Kohle aus *Pécs* zu beobachten, wo sich der pH-Wert von 4,9 auf 4,5 verringerte.

Beim Lignit aus *Gyöngyös* änderte sich hingegen der pH-Wert trotz starker Oxydation nicht, denn sowohl die ursprüngliche, wie auch die oxydierte Kohle hatten einen pH-Wert von 4,5, während sich bei der Kohle aus *Ajka* das pH vom ursprünglichen Wert von 6,4 auf 7,3 erhöhte.

Dieser experimentelle Befund kann damit erklärt werden, daß der für Kohlen gemessene pH-Wert nicht nur von der Struktur der organischen Kohlensubstanz, sondern auch von der Zusammensetzung der Asche bzw. des die Kohle begleitenden tauben Gesteines abhängig ist.

Wenn die bei der Oxydation der Kohle sich bildenden Carbonsäuren von irgendeinem Aschenbestandteil gebunden werden, wird deren saure Wirkung an der Ausbildung des pH-Wertes nicht mehr beteiligt sein.

Wie bekannt, enthält die Kohle aus *Ajka* beträchtliche Mengen von Calciumcarbonat (was auch an den Derivatogrammen in Form eines Maximums bei hoher Temperatur, zwischen 700 und 800 °C, zum Ausdruck kommt).

Dieses Calciumcarbonat bindet die im Laufe der Oxydation sich bildenden Carbonsäuren. Von diesen Ausnahmen abgesehen, zeigt eine Abnahme des pH-Wertes der ursprünglichen Kohle stets eine Oxydation der Kohle an.

Im Laufe der derivatographischen Untersuchungen wurde für jede Kohlenprobe die thermische Zersetzung der ursprünglichen und der oxydierten Kohle in einem Stickstoffstrom von 15 Lit./h Geschwindigkeit, ferner der Verbrennungsvorgang in Luft untersucht.

Die thermische Zersetzung wurde in tiefen, mit Deckel versehenen Platintiegeln, stets an genauen Einwaagen von 1 g beobachtet.

Zur Untersuchung des Verbrennungsvorganges wurde eine genau eingewogene Probe von 0,5 g in seichten Platintiegeln flach ausgebreitet. In den Verbrennungsversuchen wurde der Luftstrom durch das aus dem Tiegelofen ragende Kalitrohr eingesogen.

Die Aufheizungsgeschwindigkeit betrug stets 5 °C/min. Bei der Aufnahme der DTA-Kurven wurde als inerter Stoff Aluminiumoxid verwendet.

Tabelle I

Derivatographische Untersuchungen im Stickstoffstrom von 15 Lit./h Durchflußgeschwindigkeit

Ursprüngliche Kohlen

Derivatogramm No.	Kohlenprobe	Feuchtigkeitsgehalt %	DTG-Maxima		DTA-Maxima	
			°C	Höhe, %	°C	Charakter
694	Kohle aus *Pécs*, 0—8 mm *Budapester Gaswerke*	1,2	80	44		
			470	518	470	--
			700	151	690	+
695	Lignitgrus aus *Gyöngyös* für Kraftwerke	15,6	100	287	100	—
			360	139		
			500	142	500	—
			620	91		
			790	80	790	—
703	Energetische Durchschnittskohle aus *Ajka Zentrale Kohlenklassierung, Ajka*	12,4	85	154	85	—
			410	138	360	—
					410	—
			505	143	495	—
			710	167	700	—
			780	328	780	—
729	Kohle aus *Borsod Zentrale Kohlenklassierung, Berente*	23,2	85	463	90	—
			340	170		—
					400	—
			460	79	470	
717	Kohle aus *Nagybátony Nógráder Kohlenbergbautrust*	14,6	105	302	110	—
			410	135	400	—
			490	164		
					520	—
728	Kohle aus *Komló Donau-Eisenwerke*	2,4	50	51		
			400	656		
					495	—
			650	72	640	—

Oxydierte Kohlen

Derivatogramm No.	Kohlenprobe	Feuchtigkeitsgehalt %	DTG-Maxima		DTA-Maxima	
			°C	Höhe, %	°C	Charakter
714	Lignitgrus aus *Gyöngyös* für Kraftwerke Oxydiert (15 Tage)	20,4	110	344	110	—
			380	118	365	—
			510	91	520	—
			670	108		
715	Kohle aus *Pécs*, 0—8 mm Oxydiert (15 Tage)	2,4	60	115		
			450	493	460	—
			670	128	700	+
716	Energetische Durchschnittskohle aus *Ajka Zentrale Kohlenklassierung, Ajka* Oxydiert (15 Tage)	15,2	90	303	90	—
			400	118	410	—
			520	128	520	—
			790	368	790	—
757	Kohle aus *Borsod Zentrale Kohlenklassierung, Berente* Oxydiert (32 Tage)	25,2	110	551	120	—
			350	135		
					405	—
			490	71	500	—
759	Kohle aus *Nagybátony Nógráder Kohlenbergbautrust* Oxydiert (50 Tage)	17,0	110	622	110	—
			400	136	400	—
			500	110	500	—
			620	Inflexion	620	Inflexion
758	Kohle aus *Komló Donau-Eisenwerke* Oxydiert (39 Tage)	4,0	80	133	70	—
			440	740	455	—
			510	Inflexion	510	Inflexion
			660	,,		

Bei der Untersuchung des thermischen Zersetzungsvorganges wurde die Temperatur der zu untersuchenden Substanz gemessen, bei der Untersuchung des stark exothermen Verbrennungsvorganges hingegen die des inerten Stoffes.

Die Ergebnisse der derivatographischen Untersuchungen sind in Tab. I und II zusammengefaßt. In den Tabellen wird die Höhe der DTG-Maxima in

Tabelle II

Derivatographische Untersuchungen in Luft

Ursprüngliche Kohlen

Derivatogramm No.	Kohlenprobe	Feuchtigkeitsgehalt %	DTG-Maxima		DTA-Maxima	
			°C	Höhe, %	°C	Charakter
700	Kohle aus *Pécs*, 0—8 mm *Budapester Gaswerke*	1,6	30	10		
			220	—58	230	+
			255	62		
					350	+
			390	410	400	+
698	Lignitgrus aus *Gyöngyös* für Kraftwerke	15,6	60	197	50	—
					100	—
			245	612	230	+
			330	351	325	+
			370	356	355	+
			460	96	455	+
			560	27		
702	Energetische Durchschnittskohle aus *Ajka Zentrale Kohlenklassierung, Ajka*	12,0	65	188	50	—
					105	—
			240	256	230	+
			320	528	315	+
			695	188	670	—
731	Kohle aus *Borsod Zentrale Kohlenklassierung, Berente*	25,6	70	274	60	—
			250	314	260	+
			330	274	330	+
			410	292	400	—
719	Kohle aus *Nagybátony Nógráder Kohlenbergbautrust*	15,0	65	270	55	—
			260	330	260	+
			330	714	340	+
			440	65	430	—
726	Kohle aus *Komló Donau-Eisenwerke*	2,0	40	15	50	—
			220	—51		
			280	59	280	+
			410	459	400	+

Oxydierte Kohlen

Derivatogramm No.	Kohlenprobe	Feuchtigkeitsgehalt %	DTG-Maxima		DTA-Maxima	
			°C	Höhe, %	°C	Charakter
711	Kohle aus *Pécs* 0—8 mm *Budapester Gaswerke* Oxydiert (15 Tage)	2,5	30	17		
			230	—42		
			245	45	245	+
			410	427	400	+
710	Lignitgrus aus *Gyöngyös* für Kraftwerke Oxydiert (15 Tage)	19,6	65	243		
			105	113	100	—
			220	955	215	+
			320	311	310	+
			445	Inflexion	450	Inflexion
			570	62		
713	Energetische Durchschnittskohle aus *Ajka Zentrale Kohlenklassierung, Ajka* Oxydiert (15 Tage)	14,5	50	175		
			220	577	210	+
			330	577	315	+
			695	201	680	—
756	Kohle aus *Borsod Zentrale Kohlenklassierung, Berente* Oxydiert (32 Tage)	24,0	60	259		
			100	Inflexion	100	Inflexion
			260	857	270	+
			370	455	360	+
753	Kohle aus *Nagybátony Nógráder Kohlenbergbautrust* Oxydiert (50 Tage)	17,0	95	215	90	—
			325	238	320	+
			405	831	405	+
			480	46	490	—
755	Kohle aus *Komló Donau-Eisenwerke* Oxydiert (39 Tage)	3,0	50	35		
			240	—23		
					270	+
			430	470	470	+

Prozent angegeben, indem die zwischen Zimmertemperatur und 800 °C gefundene durchschnittliche Geschwindigkeit der thermischen Zersetzung bzw. des Verbrennungsvorganges zu 100% angenommen wird.*

Auf Grund des Vergleichs der derivatographischen Analyseergebnisse ursprünglicher und oxydierter Kohlen können die bisherigen experimentellen Befunde folgendermaßen zusammengefaßt werden:

Den Erwartungen entsprechend, ist bei Kohlen von niedrigerem Inkohlungsgrad, so vor allem beim Lignit aus *Gyöngyös* die stärkste Wirkung der Oxydation zu beobachten. Bei Kohlen von höherem Inkohlungsgrad, wie z.B. bei Steinkohlen, ist die Wirkung der Oxydation weniger auffallend. Bei in Stickstoffstrom vorgenommenen Untersuchungen der thermischen Zersetzung ist die Wirkung der Oxydation erst bei höheren Oxydationsgraden an den Derivatogrammen zu beobachten. Bei Verbrennungsversuchen hingegen macht sich die Wirkung der Oxydation schon viel früher bemerkbar.

Während der Verbrennungsversuche in Luft erscheint bei Steinkohlen, zum Unterschied von den Braunkohlen, nach dem Entweichen des Wassers sowohl an den TG- wie auch an den DTG-Kurven ein Abschnitt, der eine Gewichtszunahme anzeigt. Dieser Abschnitt kann damit erklärt werden, daß die Kohle unter Bildung sauerstoffreicher Gruppen, vermutlich mit Peroxidcharakter, Sauerstoff aus der Luft aufnimmt. Die Höhe dieser mit Gewichtszunahme verbundenen Maxima wird in Tab. II durch ein negatives Vorzeichen von den mit Gewichtsabnahme verbundenen Maxima unterschieden.

Sowohl im Falle der Kohle aus *Pécs* wie auch in dem aus *Komló* ist dieses mit Gewichtszunahme verbundene Maximum für die oxydierte Kohle kleiner, als für die ursprüngliche, nicht oxydierte Kohle. Dies kann offensichtlich der Tatsache zugeschrieben werden, daß die oxydierte Kohle bereits vor Beginn des Versuches Sauerstoff aufgenommen hat, welcher einen Teil der aktiven Gruppen besetzte, wodurch während des Versuches diese Stellen natürlich nicht mehr an einer Gewichtszunahme teilnehmen können.

In den Untersuchungen des thermischen Zersetzungsvorganges ist die Wirkung der Oxydation im Falle des Lignits aus *Gyöngyös* klar ersichtlich. An dem gegen höhere Temperaturen liegenden Ast des Wassermaximums der 15 Tage hindurch oxydierten Kohle aus *Gyöngyös* treten sowohl an der DTG- wie auch an der DTA-Kurve bei 140 und 170 °C charakteristische Inflexionen auf (Abb. 1 und 2). Diese zeigen die Abspaltung der im Laufe der Oxydation gebildeten sauerstoffreichen Gruppen an. Da diese Abspaltungstemperaturen niedrig sind, verschmelzen sie mehr oder weniger mit dem Wassermaximum.

* Ähnlich wie in früheren Arbeiten bereits berichtet, wurde zur Bestimmung des durchschnittlichen DTG-Galvanometerausschlages die Fläche unter der Kurve zwischen Zimmertemperatur und 800 °C planimetriert, sodann unter Berücksichtigung der Länge der Grundlinie jener durchschnittliche Galvanometerausschlag berechnet, der einer Fläche von derselben Größe wie die durch Planimetrieren erhaltene zugehört.

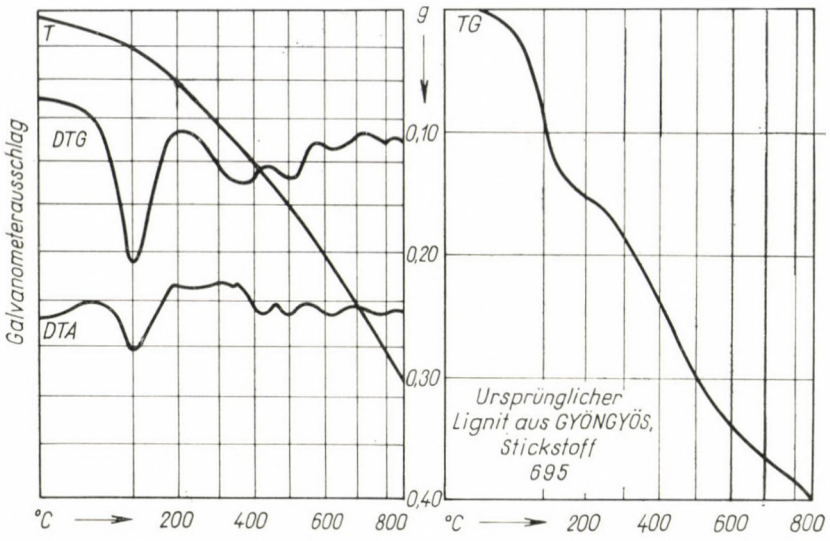

Abb. 1

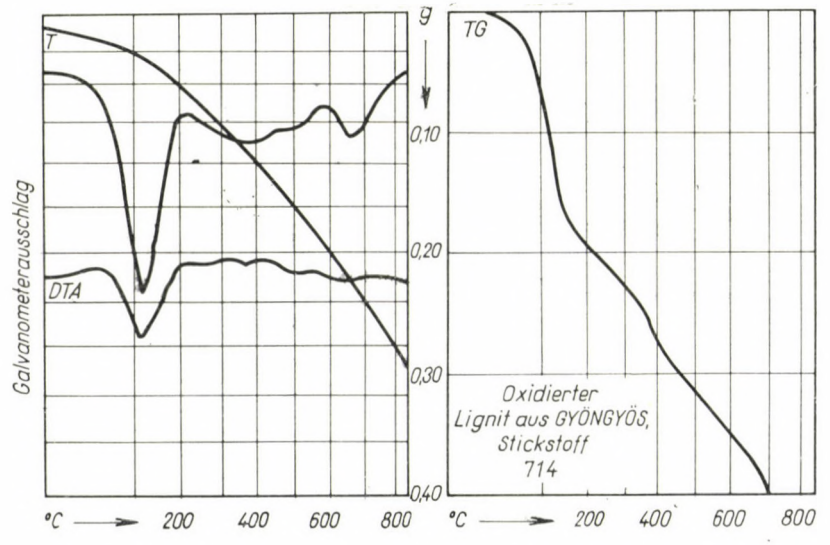

Abb. 2

Beim Untersuchen des Verbrennungsvorganges wird die Wirkung der Oxydation vor allem dadurch bemerkbar, daß ein größerer Teil der organischen Substanz der Kohle im Verbrennungsmaximum von niedriger Temperatur verbrennt, wie im Falle der ursprünglichen, nicht oxydierten Kohle.

Die Derivatogramme des ursprünglichen und des oxydierten Lignits aus *Gyöngyös* weisen bedeutende Unterschiede auf (Abb. 3 und 4).

An der DTG-Kurve des oxydierten Lignits erscheint bei 105 °C, unmittelbar nach dem Wassermaximum, ein kleines Zersetzungsmaximum, das der Abspaltung der im Laufe der Oxydation gebildeten sauerstoffreichen Gruppen entspricht. In diesem Fall handelt es sich nicht um ein Verbrennungsmaximum, was auch durch den endothermen Charakter des dem DTG-Maximum entsprechenden DTA-Maximums angezeigt wird.

Wenn die Endtemperaturen der DTG-Maxima auf die TG-Kurve projektiert werden, kann man quantitative Daten über die Menge der in den Maxima verbrennenden Substanzen erhalten.

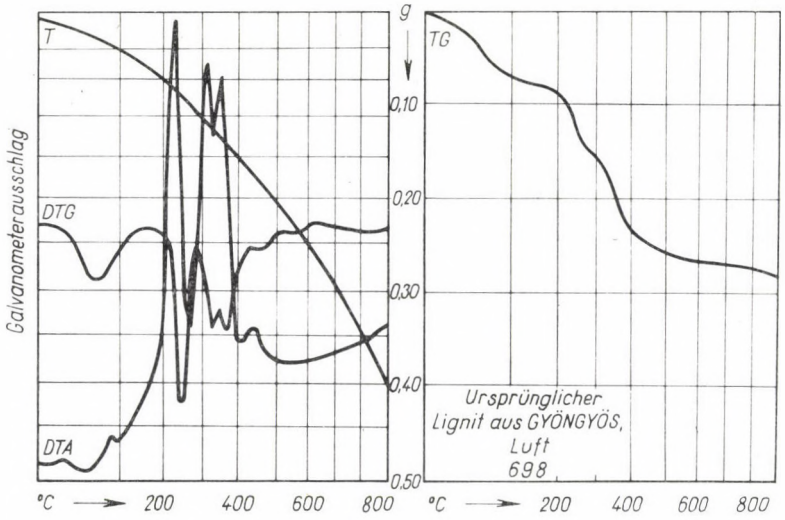

Abb. 3

Im Falle des ursprünglichen nicht oxydierten Lignits verbrennen im ersten Maximum bei 245 °C auf Trockensubstanz berechnet 15% der organischen Substanz. Beim oxydierten Lignit liegt dieses Maximum bei niedrigerer Temperatur, bei 220 °C, wobei 21% der organischen Substanz verbrennen, also mehr als im Falle der urpsrünglichen Kohle.

Die Derivatogramme des oxydierten und des frischen Lignits weisen noch andere interessante Unterschiede auf. Beim ursprünglichen Lignit bildet das zweite Verbrennungsmaximum sowohl an der DTG- wie auch an der DTA-Kurve ein Doppelmaximum (bei 330 und 370 °C), d.h. die Verbrennung verlauft in diesem Fall in zwei Stufen.

Auf Trockensubstanz berechnet verbrennen in der ersten Stufe 12%, in der zweiten hingegen 11% der Substanz.

Gegensätzlich erscheint im Falle des oxydierten Lignits das zweite Verbrennungsmaximum sowohl an der DTG- wie auch der DTA-Kurve als ein

einfaches Maximum, d.h. die Verbrennung verläuft hier in einer Stufe. In diesem einfachen Verbrennungsmaximum verbrennen auf die Trockensubstanz berechnet 17% der Substanz.

Die Verbrennungsderivatogramme der ursprünglichen und der oxydierten Kohle aus *Ajka* (Abb. 5 und 6) zeigen, daß im Falle der oxydierten Kohle ein größerer Teil im ersten Verbrennungsmaximum von niedriger Temperatur verbrennt, als im Falle der ursprünglichen Kohle.

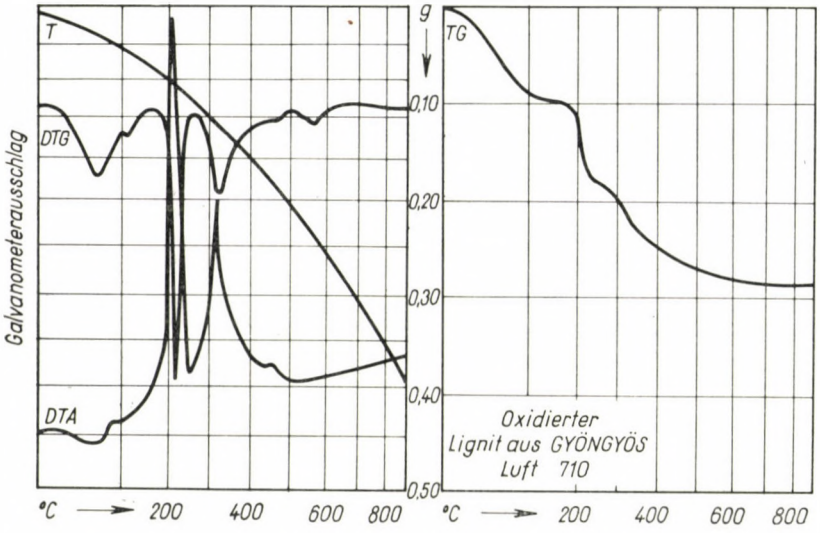

Abb. 4

Im Falle der ursprünglichen, nicht oxydierten Kohle verbrennen auf Trockensubstanz berechnet 6% im ersten Verbrennungsmaximum bei 240 °C, und 38% im zweiten Verbrennungsmaximum bei 320 °C.

Im Falle der oxydierten Kohle verbrennen auf die Trockensubstanz berechnet 13% im ersten Verbrennungsmaximum bei 220 °C, und 30% im zweiten Verbrennungsmaximum bei 330 °C.

Das bei etwa 700 °C erscheinende große Maximum kann mit dem hohen Calciumcarbonatgehalt der Kohle aus *Ajka* bzw. mit dessen thermischer Zersetzung erklärt werden.

Im Falle der Kohle aus *Borsod* verbrennt im ersten Verbrennungsmaximum — ähnlich wie beim Lignit aus *Gyöngyös* und bei der Kohle aus *Ajka* — von der oxydierten Kohle ebenfalls mehr, als von der ursprünglichen Kohle.

Auf Trockensubstanz berechnet verbrennen von der ursprünglichen Kohle 11% im ersten Maximum bei 250 °C und 55% im zweiten doppelten Maximum (bei 330 und 410 °C).

Von der oxydierten Kohle hingegen verbrennen 32% im ersten Maximum bei 260 °C und 35% im zweiten Maximum bei 370 °C, ebenfalls auf Trockensubstanz berechnet.

Die Kohle aus *Borsod* ergab, ähnlich wie der Lignit aus *Gyöngyös*, ein doppeltes zweites Verbrennungsmaximum für die ursprüngliche Kohle, während im Falle der oxydierten Kohle dieses Maximum einfach war.

Im zweiten Verbrennungsmaximum verbrennt also die ursprüngliche Kohle in zwei Stufen, die oxydierte hingegen in einer Stufe.

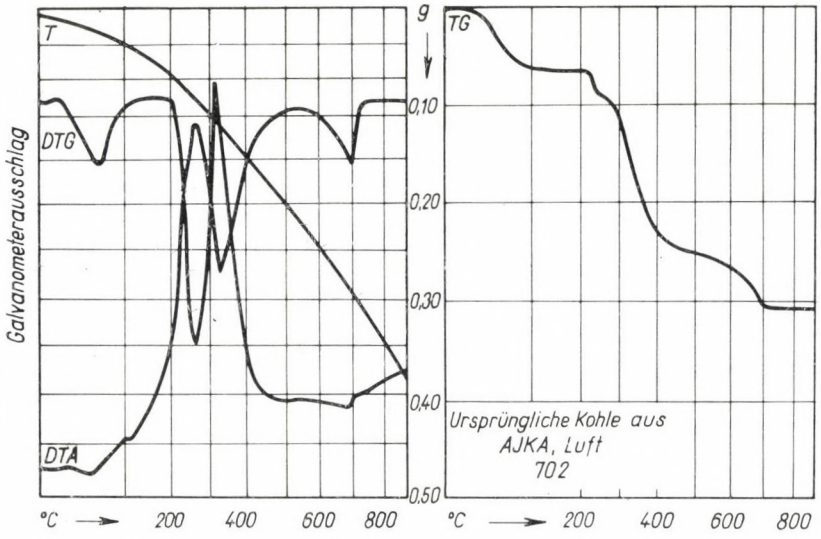

Abb. 5

Im Falle der Kohle aus *Nagybátony* wurden bei dem von uns untersuchten Oxydationsgrad nur geringere Änderungen der organischen Substanz durch die Oxydation hervorgerufen.

Unsere bisherigen Versuchsergebnisse zeigen, daß sich die derivatographische Methode auch in diesem Forschungsgebiet den Erwartungen gemäß bewehrte.

Die derivatographische Methode ermöglicht die Erfassung und Absonderung der einzelnen Abschnitte der thermischen Zersetzung und des Verbrennens, während die TG-Kurve auch die genaue quantitative Bestimmung der in den einzelnen Abschnittem sich zersetzenden bzw. verbrennenden Substanz möglich macht.

Die vergleichende Untersuchung der ursprünglichen und der oxydierten Kohle ermöglicht hingegen die Erkenntnis der im Laufe der Oxydation in der organischen Substanz der Kohle auftretenden Änderungen, u. zw. mit einer einfachen Versuchsmethodik.

Laut unserer Versuchsergebnisse zeigt sich die Wirkung der Oxydation vor allem bei der Untersuchung des Verbrennungsvorganges. Dies kann wahrscheinlich damit erklärt werden, daß der Verbrennungsvorgang an der Oberfläche der Kohle verläuft, und die Oxydation vor allem eben die Oberflächeneigenschaften der Kohle ändert.

Dadurch wird weiterhin verständlich, daß die Oxydation auch auf die Verkokbarkeit der Kohlen einen starken Einfluß ausübt, denn auch bei der

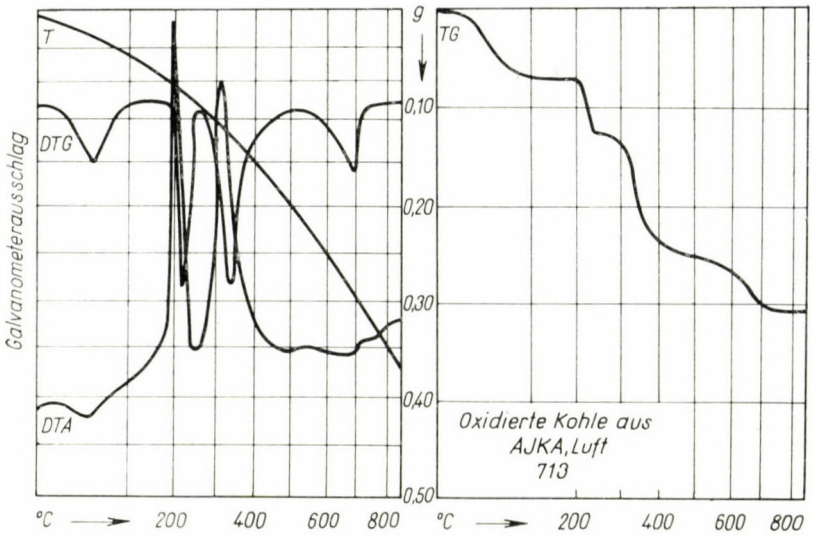

Abb. 6

Verkokung spielen besonders die Oberflächeneigenschaften der Kohle eine große Rolle.

Bei dem beobachteten Oxydationsgrad verbrannte im Falle der oxydierten Kohlen eine größere Menge von flüchtigen Bestandteilen im ersten Verbrennungsmaximum von niedriger Temperatur, als im Falle der frischen Kohlen.

Es ist offensichtlich, daß diese im Laufe der Oxydation auftretenden Änderungen auch in praktischen Feuerungen den Verbrennungsvorgang beeinflussen.

Die bei der Verfeuerung der Kohle in Kraftwerken auftretenden, oft unerklärlich erscheinenden Schwierigkeiten können in vielen Fallen sicherlich auf die veränderten Eigenschaften der im Laufe der Lagerung oxydierten Kohle zurückgeleitet werden.

ZUSAMMENFASSUNG

In unseren Kraftwerken werden große Mengen von Kohlen für energetische Zwecke verwendet, die auch dort lagern.

Die Eigenschaften der oxydierten Kohlen weichen von jenen der frischen Kohlen ab, was sich auch im Verbrennungsvorgang bemerkbar macht.

Es wurden die in ungarischen Kraftwerken verwendeten Kohlen, Lignit aus *Gyöngyös*, sowie Kohlen aus *Ajka*, *Borsod* und *Nagybátony* in frischem und in oxydiertem Zustand untersucht.

Die derivatographische Methode ist zur Verfolgung der während der Oxydation eintretenden Änderungen besonders geeignet.

Für oxydierte Kohlen sind die bei tiefen Temperaturen erscheinenden thermischen Zersetzungsmaxima sehr charakteristisch. Diese können auf die Abspaltung von, während der Oxydation gebildeten, sauerstoffreichen Gruppen zurückgeleitet werden.

Entsprechend der Erwartung werden Kohlen von geringerem Inkohlungsgrad (Lignite) rascher oxydiert, als stärker inkohlte Kohlen.

SCHRIFTTUM

1. Szikla, G.: Szeneink öngyulladási és tárolási kérdései (Über die Probleme der Selbstentzündung und der Lagerung unserer Kohlen) Vortrag gehalten am 25. März 1949. Mérnöki Továbbképző Intézet.
2. Michaelis, P.: Glückauf **71,** 413—423 (1935).
3. Oresko, V. F.: Dokladü Akademii Nauk USSR **70,** 445—448 (1950).
4. Zabawin, V. I., Surkowa, V. L.: Izv. Akad. Nauk USSR. Otdel. Tehn. Nauk **6,** 163—165 (1959).
5. Hrisanfowa, A. J., Sobolewa, G. N.: Himija i Tehnologia Topliva **1956,** Nr. 2. 45—53.
6. Jones, R. E., Townend, D. T. A.: Trans. Faraday Soc. **42,** 297—305 (1946).
7. Howard, H. C.: Bituminous Coal Reasearch **8,** 13 (1948).
8. Paulik, F., Paulik, J., Erdey, L.: Z. anal. Chem. **160,** 241—252 (1958).
9. Romwalter, A.: Magyar Technika **2,** Nr. 1. (1947).
10. Tronow, B. V.: Zhurnal prikladnoj him. **13,** 1053—1058 (1940).

Investigation of the oxidation (storage) of coals by derivatography

M. WELTNER

Summary. In power plants great quantities of coal are used, and thus also stored, for power generation.

The properties of oxidized coals differ from those of fresh coals, and this difference influences also the combustion process.

Coals used in Hungarian power plants, such as lignite from Gyöngyös and coals from Ajka, Borsod and Nagybátony have been studied in fresh and in oxidized state.

Derivatography was found to be a very suitable method for following of changes occurring during oxidation.

Very characteristic of oxidized coals are thermal decomposition maxima, occurring at low temperatures. These are to be ascribed to the splitting off of groups rich in oxygen, formed during oxidation.

As be expected, coals of lower carbonization grade (lignites) are oxidized at a higher rate, than coals in a higher state of carbonification.

Исследование процесса окисления (хранения) углей с помощью дериватографического метода

М. ВЕЛТНЕР

Резюме. На силовых станциях страны используются большие количества угля, которые там и хранятся, для энергетических целей.

Свойства оксидированных углей отличаются от свойств свежих углей, что оказывает влияние и на процесс горения углей.

Исследовали, используемые на отечественных силовых станциях, дьёньдёши лигнит, а также типы углей, добываемые в Айка, Боршоде и Надьбатоне в свежем и оксидированном состояниях.

Дериватографический метод является очень пригодным для наблюдения изменений, происходящих в ходе окисления.

Для окисленных углей очень характерными являются максимумы теплового распада, наступающие при низких температурах. Эти максимумы являются результатом отрыва, обогащенных кислородом групп, которые образуются в ходе окисления.

Как следовало ожидать, нашли, что быстрее окисляются угли с меньшей степенью обугливаемости, чем угли с большей степенью обугливаемости.

dr. Margit WELTNER; Budapest, IX., Ferenc krt. 10.

INDEX

ANORGANISCHE UND ANALYTISCHE CHEMIE — INORGANIC AND ANALYTICAL CHEMISTRY — НЕОРГАНИЧЕСКАЯ И АНАЛИТИЧЕСКАЯ ХИМИЯ

RUFF, I.: On the Role of Water in Electron Transfer Reactions, II. 241
RUFF, I.: On the Role of Water in Electron Transfer Reactions, III. 255

PHYSIKALISCHE CHEMIE — PHYSICAL CHEMISTRY — ФИЗИЧЕСКАЯ ХИМИЯ

LADIK, J. and BICZÓ, G.: Investigation of the Electronic Structure of Catalytically Active solids. I. The Change of the Energy Band Structure of Infinite Ni Crystals with the temperature 263
PULAY, P. and TÖRÖK, F.: On the Parameter Form of Matrix F, II. Investigation of the Assignment with the Aid of the Parameter Form (Short communication) 273

ORGANISCHE CHEMIE — ORGANIC CHEMISTRY — ОРГАНИЧЕСКАЯ ХИМИЯ

MONDVAI, I.: Polymerisation des Methylmethakrylats bei hohen Umsätzen I. Untersuchung der Initialwirkung von Benzoylperoxyd 281
NYILASI, J., BIHARI-VARGA, M. und ORSÓS, P.: Metallkomplexe der Peptide, V. Untersuchung der Hydrolyse und Oxydation von Dipeptid-Metallkomplexen 291
SZEJTLI, J.: The Stepwise Total Hydrolysis of Alginic Acid 301

CHEMISCHE TECHNOLOGIE — CHEMICAL TECHNOLOGY — ХИМИЧЕСКАЯ ТЕХНОЛОГИЯ

WELTNER, M.: Untersuchung der Oxydations- (Lagerungs-)vorgänge der Kohlen mit derivatographischer Methode 311

Printed in Hungary

A kiadásért felel az Akadémiai Kiadó igazgatója — Műszaki szerkesztő: Farkas Sándor

A kézirat a nyomdába érkezett: 1966 I. 3. — Terjedelem: 8 (A/5) ív. 29 ábra

66.61769 Akadémiai Nyomda, Budapest — Felelős vezető: Bernát György

The Acta Chimica publish papers on chemistry, in English, German, French and Russian.

The Acta Chimica appear in volumes consisting of four parts of varying size, 4 volumes being published a year.

Manuscripts should be addressed to

Acta Chimica
Budapest 502, Postafiók 24.

Correspondence with the editors should be sent to the same address.

The rate of subscription is 110 forints a volume. Orders may be placed with "*Kultúra*" Foreign Trade Company for Books and Newspapers (Budapest I., Fő utca 32. Account No. 43-790-057-181) or with representatives abroad.

Les Acta Chimica paraissent en français, allemand, anglais et russe et publient des mémoires du domaine des sciences chimiques.

Les Acta Chimica sont publiés sous forme de fascicules. Quatre fascicules seront réunis en un volume (4 volumes par an).

On est prié d'envoyer les manuscrits destinés à la rédaction à l'adresse suivante:

Acta Chimica
Budapest 502, Postafiók 24.

Toute correspondance doit être envoyée à cette même adresse.

Le prix de l'abonnement est de 110 forints par volume.

On peut s'abonner à l'Entreprise pour le Commerce Extérieur de Livres et Journaux «*Kultúra*» (Budapest I., Fő utca 32. Compte-courant No. 43-790-057-181) ou à l'étranger chez tous les représentants ou dépositaires.

«*Acta Chimica*» издают трактаты из области химической науки на русском, французском, английском и немецком языках.

«*Acta Chimica*» выходят отдельными выпусками разного объема. 4 выпуска составляют один том. 4 тома публикуются в год.

Предназначенные для публикации рукописи следует направлять по адресу:

Acta Chimica
Budapest 502, Postafiók 24.

По этому же адресу направлять всякую корреспонденцию для редакции.

Подписная цена «*Acta Chimica*» — 110 форинтов за том. Заказы принимает предприятие по внешней торговле книг и газет «*Kultúra*» (Budapest I., Fő utca 32. Текущий счет № 43-790-057-181) или его заграничные представительства и уполномоченные.

All the reviews of the Hungarian Academy of Sciences may be obtained among others from the following bookshops:

ALBANIA

Ndermarja Shtetnore e Botimeve
Tirana

AUSTRALIA

A. Keesing
Box 4886, GPO
Sidney

AUSTRIA

Globus Buchvertrieb
Salzgries 16
Wien I.

BELGIUM

Office International de Librairie
30, Avenue Marnix
Bruxelles 5
Du Monde Entier
5, Place St. Jean
Bruxelles

BULGARIA

Raznoiznos
1Tzar Assen
S fia

CANADA

Pannonia Books
2 Spadina Road
Toronto 4, Ont.

CHINA

Waiwen Shudian
Peking
P. O. B. Nr. 88.

CZECHOSLOVAKIA

Artia A. G.
Ve Smeckách 30
Praha II.
Postova Novinova Sluzba
Dovoz tisku
Vinohradska 46
Praha 2
Postova Novinova Sluzba
Dovoz tlace
Leningradska 14
Bratislava

DENMARK

Ejnar Munksgaard
Nörregade 6
Kopenhagen

FINLAND

Akateeminen Kirjakauppa
Keskuskatu 2
Helsinki

FRANCE

Office International de Documentation et Librairie
48, rue Gay Lussac
Paris 5

GERMAN DEMOCRATIC REPUBLIC

Deutscher Buch-Export und Import
Leninstraße 16.
Leipzig C. I.
Zeitungsvertriebsamt
Clara Zetkin Straße 62.
Berlin N. W.

GERMAN FEDERAL REPUBLIC

Kunst und Wissen
Erich Bieber
Postfach 46
7 Stuttgart S.

GREAT BRITAIN

Collet's' Subscription Dept.
44—45 Museum Street
London W. C. I.
Robert Maxwell and Co. Ltd.
Waynflete Bldg. The Plain
Oxford

HOLLAND

Swetz and Zeitlinger
Keizersgracht 471—487
Amsterdam C.
Martinus Nijhof
Lange Voorhout 9
The Hague

INDIA

Current Technical Literature
Co. Private Ltd.
Head Office:
India House OPP.
GPO Post Box 1374
Bombay I.

ITALY

Santo Vanasia
71 Via M. Macchi
Milano
Libreria Commissionaria Sansoni
Via La Marmora 45
Firenze

JAPAN

Nauka Ltd.
2 Kanada-Zimbocho 2-chome
Chiyoda-ku
Tokyo
Maruzen and Co. Ltd.
P. O. Box 605
Tokyo
Far Eastern Booksellers
Kanada P. O. Box 72
Tokyo

KOREA

Chulpanmul
Korejskoje Obshchestvo po Exportu i Importu Prozvedenij Pechati
Phenjan

NORWAY

Johan Grundt Tanum
Karl Johansgatan 43
Oslo

POLAND

Export und Import Unternehmen RUCH
ul. Wilcza 46.
Warszawa

ROUMANIA

Cartimex
Str. Aristide Briand 14—18.
Bucuresti

SOVIET UNION

Mezhdunarodnaja Kniga
Moscow
G—200

SWEDEN

Almquist and Wiksell
Gamla Brogatan 26
Stockholm

USA

Stechert Hafner Inc.
31 East 10th Street
New York 3 N. Y.
Walter J. Johnson
111 Fifth Avenue
New York 3. N. Y.

VIETNAM

Xunhasaba
Service d'Export et d'Import des Livres et Périodiques
19, Tran Quoc Toan
Hanoi

YUGOSLAVIA

Forum
Vojvode Misica broj 1.
Novi Sad
Jugoslovenska Kniga
Terazije 27.
Beograd

ACTA CHIMICA

ACADEMIAE SCIENTIARUM HUNGARICAE

ADIUVANTIBUS

L. ERDEY, K. POLINSZKY, G. SCHAY

AC

R. BOGNÁR, GY. BRUCKNER, L. CHOLNOKY, Z. CSŰRÖS,
T. ERDEY-GRÚZ, Z. FÖLDI, M. FREUND, Á. GERECS, GY. HARDY,
Á. KISS, M. KORACH, F. MÁRTA, J. PROSZT, Z. SZABÓ,
P. SZŐR, L. VARGHA, K. VAS

REDIGIT

B. LENGYEL

TOMUS 47. FASCICULUS 4.

AKADÉMIAI KIADÓ, BUDAPEST

1966

ACTA CHIMICA

A MAGYAR TUDOMÁNYOS AKADÉMIA KÉMIAI TUDOMÁNYOK OSZTÁLYÁNAK IDEGEN NYELVŰ KÖZLEMÉNYEI

SZERKESZTI

LENGYEL BÉLA

TECHNIKAI SZERKESZTŐK

DEÁK GYULA és TAKÁCS VILMOS

Az Acta Chimica német, angol, francia és orosz nyelven közöl értekezéseket a kémiai tudományok köréből.

Az Acta Chimica változó terjedelmű füzetekben jelenik meg, egy-egy kötet négy füzetből áll. Évente átlag négy kötet jelenik meg.

A közlésre szánt kéziratok a szerkesztőség címére (Budapest 112, postafiók 39) küldendők.

Ugyanerre a címre küldendő minden szerkesztőségi levelezés. A szerkesztőség kéziratokat nem ad vissza.

Az Acta Chimica előfizetési ára kötetenként belföldre 80 Ft, külföldre 110 Ft. Megrendelhető a belföld számára az „Akadémiai Kiadó"-nál (Budapest V., Alkotmány utca 21. Bankszámla 05-915-111-46), a külföld számára pedig a „Kultúra" Könyv- és Hírlap Külkereskedelmi Vállalatnál (Budapest I., Fő utca 32. Bankszámla: 43-790-057-181) vagy annak külföldi képviseleteinél és bizományosainál.

Die Acta Chimica veröffentlichen Abhandlungen aus dem Bereiche der chemischen Wissenschaften in deutscher, englischer, französischer und russischer Sprache.

Die Acta Chimica erscheinen in Heften wechselnden Umfanges. Vier Hefte bilden einen Band. Jährlich erscheinen 4 Bände.

Die zur Veröffentlichung bestimmten Manuskripte sind an folgende Adresse zu senden:

Acta Chimica
Budapest 502, Postafiók 24.

An die gleiche Anschrift ist auch jede für die Redaktion bestimmte Korrespondenz zu richten.

Abonnementspreis pro Band: 110 Forint. Bestellbar bei dem Buch- und Zeitungs-Außenhandels-Unternehmen »*Kultúra*« (Budapest I., Fő utca 32. Bankkonto No. 43-790-57-181) oder bei seinen Auslandsvertretungen und Kommissionären.

ON THE VIBRATIONAL SPECTRUM OF THE TRIMETHYLSILYL GROUP

F. TÖRÖK and GY. B. HUN

(Research Group for Inorganic Chemistry of the Hungarian Academy of Sciences, Budapest)

Received July 26, 1965

1.

The trimethylsilyl group may be readily connected to a variety of elements and compounds. Vibrational spectra revealing important data about the metal-oxygen-silicon bonds of such compounds have been published in previous papers (e.g. [1—10]). In the present work we wish to facilitate the quantitative evaluation of such spectra by applying the method of KING and CRAWFORD to the trimethylsilyl group.

2.

KING and CRAWFORD [11] discuss group vibrations on the basis of WILSON's GF matrix methods [12]. In the vibrational equation

$$GFL = L\Lambda \tag{1}$$

the matrices F and L are constructed from the force constants of the molecule and from the eigenvectors of matrix GF, respectively; Λ is a diagonal matrix with the elements $\lambda_i = 4\pi\nu_i^2$; $\nu_i (i = 1, 2, \ldots, n)$ denotes the normal frequencies;

$$G = BM^{-1}B'$$

where M is a diagonal matrix containing the masses of the corresponding atoms; B is a matrix of transformation defined by

$$S = BX$$

where X and S are column matrices constructed from the Cartesian and internal coordinates, respectively.

KING and CRAWFORD discuss the vibrations of groups the normal frequencies of which are only slightly affected by the molecular framework to which the group is bonded. The characteristic frequencies of the group may

thus be considered separately from other vibrations in the molecule whereby the treatment of the problem becomes considerably simpler.

If the molecule has g internal vibrations originating from the group to be considered and f framework vibrations, then $n = g + f$. In this case the matrix GF will be constructed in a way that the first g elements of the eigenvalue matrix Λ correspond to the internal group vibrations. According to the method of KING and CRAWFORD, in the knowledge of the first g rows of the matrix L^{-1}, one can construct an orthogonal matrix A, and with the aid of the latter the eigenvalues $\lambda_1, \ldots, \lambda_g$ are factored from the transformed secular equation. In the following discussion we shall apply matrix A divided into four submatrices:

$$A = \left(\begin{array}{c|c} A_{gg} & A_{gf} \\ \hline A_{fg} & A_{ff} \end{array}\right)$$

Let matrices G and F partitioned similarly.

Between the diagonal matrix Λ_{ff}, constructed from the framework eigenvalues $\lambda_{g+1}, \ldots, \lambda_n$, and the matrices G^+_{ff}, F^+_{ff}, which were obtained by a modification of the matrices G_{ff} and F_{ff} as described below, the following relation holds:

$$G^+_{ff} F^+_{ff} L^+ = L^+ \Lambda_{ff} \tag{2}$$

where matrix L^+ contains the eigenvectors of $G^+_{ff} F^+_{ff}$,

$$G^+_{ff} = B_f (M^{-1})^+ B'_f \tag{3}$$

B_f is a submatrix of B:

$$B = \left(\begin{array}{c} B_g \\ \hline B_f \end{array}\right)$$

$$(M^{-1})^+ = M^{-1} - M^{-1} B' W_{gg} B M^{-1}, \quad \text{where} \quad W_{gg} = A_g (A'_g G A_g)^{-1} A'_g .$$

The modified force constant matrix F^+_{ff} is also constructed with the aid of matrix A:

$$F^+_{ff} = F_{ff} + F_{fg} A_{gf} (A_{ff})^{-1} + (A'_{ff})^{-1} A'_{gf} F_{gf} + (A'_{ff})^{-1} A'_{gf} F_{gg} A_{gf} (A_{ff})^{-1} \tag{4}$$

3.

Let the trimethylsilyl group be connected to an atom X (Fig. 1). Having supposed that the silicon and carbon atoms have tetrahedral symmetry, the symmetry coordinates were constructed according to the point group C_{3v}. Neglecting torsional vibrations, the representation has the structure:

$$8\,a_1 + 3\,a_2 + 11\,e.$$

The symmetry coordinates are listed in Tables I—III. Assembling Tables I—III side by side, one gets matrix B'. In the Tables $a = x/y$, $b = z/y$, where x, y, z are lengths of the bonds SiX, SiC and CH, respectively. Considering the great importance of the trimethylsiloxy group, in our work X was chosen to be an oxygen atom, accordingly $a = 0.584$, $b = 1.147$. All the elements of Tables I—III are to be multiplied with a normalizing factor 1/36.

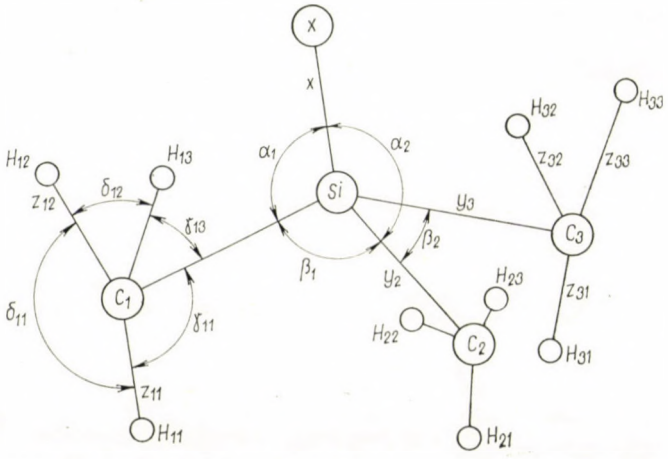

Configuration of the $XSi(CH_3)_3$ group of symmetry C_{3v}

As the published spectra show, the frequencies of the trimethylsiloxy group, with the exception of frequencies ν_7 (SiO stretching), ν_8 (OSiC sym. def.), ν_{21} (SiC_3 asym. def.) and ν_{22} (OSiC asym. def.), are almost constant in the different molecules.

In applying the method of KING and CRAWFORD, one has to know the first g rows of matrix L^{-1}; these were determined in this work with the aid of the UB force constants shown in Table IV.

In Table V, the computed internal group vibrations are compared with some experimental values. The first column of numbers contains the computed values; the second, third and fourth columns show the measured frequencies for $[Si(CH_3)_3]_2O$ [6], $Si[OSi(CH_3)_3]_4$ [2], and $B\,[OSi(CH_3)_3]_3$ [10], respectively. From the data of the third column it is evident that KRIEGSMANN [2], at variance with the present authors, considers the frequency at 760 cm^{-1} as a CH_3 rocking vibration, instead of a stretching vibration of the Si—C bond.

The frequencies ν_7, ν_8 and ν_{21}, ν_{22} of the trimethylsilyl group, which have different values depending on the nature of the framework, and the other vibrations of the molecule containing the trimethylsiloxy group may be deter-

Acta Chimica Academiae Scientiarum Hungaricae 47, 1966.

Table I

The symmetry coordinates for a_1 *and* a_2 *vibrations*

	R_1	R_2	R_3	R_4	R_5	R_6	R_7	R_8	R_9	R_{10}	R_{11}
x_1	0	0	0	0	0	0	0	0	0	0	0
y_1	0	0	0	0	0	0	0	0	0	0	0
z_1	0	0	0	0	0	0	36	0	0	0	0
x_2	0	0	0	0	0	0	0	0	0	0	0
y_2	0	0	0	0	0	0	0	0	0	0	0
z_2	0	0	0	0	72a	$12\sqrt{3}$	−36	$24\sqrt{12}$	0	0	0
x_3	8	$-8\sqrt{2}$	$8\sqrt{2}$	$-32\sqrt{2}$	$-6\sqrt{2}a-2\sqrt{2}$	$8\sqrt{6}$	0	$-4\sqrt{6}$	0	0	0
y_3	0	0	0	0	0	0	0	0	24	$-24\sqrt{2}$	$-6\sqrt{18}a-2\sqrt{18}$
z_3	$16\sqrt{2}$	4	32	16	−24a−8	$-4\sqrt{3}$	0	$-8\sqrt{12}$	0	0	0
x_4	−4	$4\sqrt{2}$	$-4\sqrt{2}$	$16\sqrt{2}$	$3\sqrt{2}a+\sqrt{2}$	$-4\sqrt{6}$	0	$2\sqrt{6}$	$-6\sqrt{12}$	$12\sqrt{6}$	$9\sqrt{6}a+3\sqrt{6}$
y_4	$4\sqrt{3}$	$-4\sqrt{6}$	$4\sqrt{6}$	$-16\sqrt{6}$	$-3\sqrt{6}a-\sqrt{6}$	$4\sqrt{18}$	0	$-2\sqrt{18}$	−12	$4\sqrt{18}$	$3\sqrt{18}a+\sqrt{18}$
z_4	$16\sqrt{2}$	4	32	16	−24a−8	$-4\sqrt{3}$	0	$-8\sqrt{12}$	0	0	0
x_5	−4	$4\sqrt{2}$	$-4\sqrt{2}$	$16\sqrt{2}$	$3\sqrt{2}a+\sqrt{2}$	$-4\sqrt{6}$	0	$2\sqrt{6}$	$6\sqrt{12}$	$-12\sqrt{6}$	$-9\sqrt{6}a-3\sqrt{6}$
y_5	$-4\sqrt{3}$	$4\sqrt{6}$	$-4\sqrt{6}$	$16\sqrt{6}$	$3\sqrt{6}a+\sqrt{6}$	$-4\sqrt{18}$	0	$2\sqrt{18}$	−12	$4\sqrt{18}$	$3\sqrt{18}a+\sqrt{18}$
z_5	$16\sqrt{2}$	4	32	16	−24a −8	$-4\sqrt{3}$	0	$-8\sqrt{12}$	0	0	0
x_6	0	0	$6\sqrt{2}$	$12\sqrt{2}$	$12\sqrt{2}$	0	0	0	0	0	0
y_6	0	0	0	0	0	0	0	0	0	$6\sqrt{18}$	0
z_6	$-12\sqrt{2}$	−12	0	0	0	0	0	0	0	0	0
x_7	−4	$4\sqrt{2}$	$-7\sqrt{2}$	$10\sqrt{2}$	$-5\sqrt{2}$	0	0	0	$2\sqrt{12}$	$-\sqrt{6}$	$5\sqrt{6}$
y_7	$4\sqrt{3}$	$-4\sqrt{6}$	$-5\sqrt{6}$	$2\sqrt{6}$	$-\sqrt{6}$	0	0	0	−12	$\sqrt{18}$	$\sqrt{18}$
z_7	$-2\sqrt{2}$	4	−16	−8	4	0	0	0	$2\sqrt{6}$	$4\sqrt{12}$	$-2\sqrt{12}$
x_8	−4	$4\sqrt{2}$	$-7\sqrt{2}$	$10\sqrt{2}$	$-5\sqrt{2}$	0	0	0	$-2\sqrt{12}$	$\sqrt{6}$	$-5\sqrt{6}$
y_8	$-4\sqrt{3}$	$4\sqrt{6}$	$5\sqrt{6}$	$-2\sqrt{6}$	$\sqrt{6}$	0	0	0	−12	$\sqrt{18}$	$\sqrt{18}$
z_8	$-2\sqrt{2}$	4	−16	−8	4	0	0	0	$-2\sqrt{6}$	$-4\sqrt{12}$	$2\sqrt{12}$
x_9	0	0	$-3\sqrt{2}$	$-6\sqrt{2}$	$-6\sqrt{2}$	0	0	0	0	$-9\sqrt{6}$	0

y_9	0	0	$3\sqrt{6}$	$6\sqrt{6}$	$6\sqrt{6}$	0	0	0	0	$-3\sqrt{18}$	0
z_9	$-12\sqrt{2}$	-12	0	0	0	0	0	0	0	0	0
x_{10}	-4	$4\sqrt{2}$	$11\sqrt{2}$	$-8\sqrt{2}$	$4\sqrt{2}$	0	0	0	$2\sqrt{12}$	$-\sqrt{6}$	$-4\sqrt{6}$
y_{10}	$-4\sqrt{3}$	$4\sqrt{6}$	$-\sqrt{6}$	$4\sqrt{6}$	$-2\sqrt{6}$	0	0	0	12	$-\sqrt{18}$	$2\sqrt{18}$
z_{10}	$-2\sqrt{2}$	4	-16	-8	4	0	0	0	$2\sqrt{6}$	$4\sqrt{12}$	$-2\sqrt{12}$
x_{11}	8	$-8\sqrt{2}$	$-4\sqrt{2}$	$-2\sqrt{2}$	$\sqrt{2}$	0	0	0	$4\sqrt{12}$	$-2\sqrt{6}$	$\sqrt{6}$
y_{11}	0	0	$-6\sqrt{6}$	$6\sqrt{6}$	$-3\sqrt{6}$	0	0	0	0	0	$-3\sqrt{18}$
z_{11}	$-2\sqrt{2}$	4	-16	-8	4	0	0	0	$-2\sqrt{6}$	$-4\sqrt{12}$	$2\sqrt{12}$
x_{12}	0	0	$-3\sqrt{2}$	$-6\sqrt{2}$	$-6\sqrt{2}$	0	0	0	0	$9\sqrt{6}$	0
y_{12}	0	0	$-3\sqrt{6}$	$-6\sqrt{6}$	$-6\sqrt{6}$	0	0	0	0	$-3\sqrt{18}$	0
z_{12}	$-12\sqrt{2}$	-12	0	0	0	0	0	0	0	0	0
x_{13}	8	$-8\sqrt{2}$	$-4\sqrt{2}$	$-2\sqrt{2}$	$\sqrt{2}$	0	0	0	$-4\sqrt{12}$	$2\sqrt{6}$	$-\sqrt{6}$
y_{13}	0	0	$6\sqrt{6}$	$-6\sqrt{6}$	$3\sqrt{6}$	0	0	0	0	0	$-3\sqrt{18}$
z_{13}	$-2\sqrt{2}$	4	-16	-8	4	0	0	0	$2\sqrt{6}$	$4\sqrt{12}$	$-2\sqrt{12}$
x_{14}	-4	$4\sqrt{2}$	$11\sqrt{2}$	$-8\sqrt{2}$	$4\sqrt{2}$	0	0	0	$-2\sqrt{12}$	$\sqrt{6}$	$4\sqrt{6}$
y_{14}	$4\sqrt{3}$	$-4\sqrt{6}$	6	$-4\sqrt{6}$	$2\sqrt{6}$	0	0	0	12	$-\sqrt{18}$	$2\sqrt{18}$
z_{14}	$-2\sqrt{2}$	4	-16	-8	4	0	0	0	$-2\sqrt{6}$	$-4\sqrt{12}$	$2\sqrt{12}$

Table II

The symmetry coordinates for e *vibrations (first part)*

	R_{12a}	R_{13a}	R_{14a}	R_{15a}	R_{16a}	R_{17a}	R_{18a}	R_{19a}	R_{20a}	R_{21a}	R_{22a}
x_1	0	0	0	0	0	0	0	0	0	0	$-18\sqrt{6}$b
y_1	0	0	0	0	0	0	0	0	0	0	0
z_1	0	0	0	0	0	0	0	0	0	0	0
x_2	0	0	0	0	0	0	18a	−54a	$-12\sqrt{12}$	$-24\sqrt{6}$	$18\sqrt{6}$b$+6\sqrt{6}$
y_2	0	0	0	0	0	0	0	0	0	0	0
z_2	0	0	0	0	0	0	0	0	0	0	0
x_3	$8\sqrt{2}$	0	−16	16	0	−64	−12a−4	0	$8\sqrt{12}$	$-2\sqrt{6}$	$-4\sqrt{6}$
y_3	0	0	0	0	0	0	0	0	0	0	0
z_3	32	0	$4\sqrt{2}$	$32\sqrt{2}$	0	$16\sqrt{2}$	$-24\sqrt{2}$ a$-8\sqrt{2}$	0	$-4\sqrt{6}$	$-4\sqrt{12}$	$-8\sqrt{12}$
x_4	$2\sqrt{2}$	$-18\sqrt{2}$	−4	4	36	−16	−3a−1	27a+9	$2\sqrt{12}$	$13\sqrt{6}$	$-\sqrt{6}$
y_4	$-2\sqrt{6}$	$-6\sqrt{6}$	$4\sqrt{3}$	$-4\sqrt{3}$	$12\sqrt{3}$	$16\sqrt{3}$	$3\sqrt{3}$a$+\sqrt{3}$	$9\sqrt{3}$a$+3\sqrt{3}$	−12	$5\sqrt{18}$	$\sqrt{18}$
z_4	−16	0	$-2\sqrt{2}$	$-16\sqrt{2}$	0	$-8\sqrt{2}$	$12\sqrt{2}$a$+4\sqrt{2}$	0	$2\sqrt{6}$	$2\sqrt{12}$	$4\sqrt{12}$
x_5	$2\sqrt{2}$	$-18\sqrt{2}$	−4	4	36	−16	−3a−1	27a+9	$2\sqrt{12}$	$13\sqrt{6}$	$-\sqrt{6}$
y_5	$2\sqrt{6}$	$6\sqrt{6}$	$-4\sqrt{3}$	$4\sqrt{3}$	$-12\sqrt{3}$	$-16\sqrt{3}$	$-3\sqrt{3}$a$-\sqrt{3}$	$-9\sqrt{3}$a$-3\sqrt{3}$	12	$-5\sqrt{18}$	$-\sqrt{18}$
z_5	−16	0	$-2\sqrt{2}$	$-16\sqrt{2}$	0	$-8\sqrt{2}$	$12\sqrt{2}$a$+4\sqrt{2}$	0	$2\sqrt{6}$	$2\sqrt{12}$	$4\sqrt{12}$
x_6	0	0	0	12	0	24	24	0	0	0	0
y_6	0	0	0	0	0	0	0	0	0	0	0
z_6	−24	0	$-12\sqrt{2}$	0	0	0	0	0	0	0	0
x_7	$-4\sqrt{2}$	0	8	−14	0	20	−10	0	0	0	0
y_7	$4\sqrt{6}$	0	$-8\sqrt{3}$	$-10\sqrt{3}$	0	$4\sqrt{3}$	$-2\sqrt{3}$	0	0	0	0
z_7	−4	0	$4\sqrt{2}$	$-16\sqrt{2}$	0	$-8\sqrt{2}$	$4\sqrt{2}$	0	0	0	0
x_8	$-4\sqrt{2}$	0	8	−14	0	20	−10	0	0	0	0
y_8	$-4\sqrt{6}$	0	$8\sqrt{3}$	$10\sqrt{3}$	0	$-4\sqrt{3}$	$2\sqrt{3}$	0	0	0	0
z_8	−4	0	$4\sqrt{2}$	$-16\sqrt{2}$	0	$-8\sqrt{2}$	$4\sqrt{2}$	0	0	0	0
x_9	0	0	0	3	−27	6	6	0	0	0	0

y_9	0	0	0	$-3\sqrt{3}$	$-9\sqrt{3}$	$-6\sqrt{3}$	$-6\sqrt{3}$	0	0	0	0
z_9	12	0	$6\sqrt{2}$	0	0	0	0	0	0	0	0
x_{10}	$2\sqrt{2}$	$6\sqrt{2}$	-4	-11	-3	8	-4	-12	0	0	0
y_{10}	$2\sqrt{6}$	$6\sqrt{6}$	$-4\sqrt{3}$	$\sqrt{3}$	$-3\sqrt{3}$	$-4\sqrt{3}$	$2\sqrt{3}$	$6\sqrt{3}$	0	0	0
z_{10}	2	6	$-2\sqrt{2}$	$8\sqrt{2}$	$12\sqrt{2}$	$4\sqrt{2}$	$-2\sqrt{2}$	$-6\sqrt{2}$	0	0	0
x_{11}	$-4\sqrt{2}$	$12\sqrt{2}$	8	4	-6	2	-1	3	0	0	0
y_{11}	0	0	0	$6\sqrt{3}$	0	$-6\sqrt{3}$	$3\sqrt{3}$	$-9\sqrt{3}$	0	0	0
z_{11}	2	-6	$-2\sqrt{2}$	$8\sqrt{2}$	$-12\sqrt{2}$	$4\sqrt{2}$	$-2\sqrt{2}$	$6\sqrt{2}$	0	0	0
x_{12}	0	0	0	3	-27	6	6	0	0	0	0
y_{12}	0	0	0	$3\sqrt{3}$	$9\sqrt{3}$	$6\sqrt{3}$	$6\sqrt{3}$	0	0	0	0
z_{12}	12	0	$6\sqrt{2}$	0	0	0	0	0	0	0	0
x_{13}	$-4\sqrt{2}$	$12\sqrt{2}$	8	4	-6	2	-1	3	0	0	0
y_{13}	0	0	0	$-6\sqrt{3}$	0	$6\sqrt{3}$	$-3\sqrt{3}$	$9\sqrt{3}$	0	0	0
z_{13}	2	-6	$-2\sqrt{2}$	$8\sqrt{2}$	$-12\sqrt{2}$	$4\sqrt{2}$	$-2\sqrt{2}$	$6\sqrt{2}$	0	0	0
x_{14}	$2\sqrt{2}$	$6\sqrt{2}$	-4	-11	-3	8	-4	-12	0	0	0
y_{14}	$-2\sqrt{6}$	$-6\sqrt{6}$	$4\sqrt{3}$	$-\sqrt{3}$	$3\sqrt{3}$	$4\sqrt{3}$	$-2\sqrt{3}$	$-6\sqrt{3}$	0	0	0
z_{14}	2	6	$-2\sqrt{2}$	$8\sqrt{2}$	$12\sqrt{2}$	$4\sqrt{2}$	$-2\sqrt{2}$	$-6\sqrt{2}$	0	0	0

Table III

The symmetry coordinates for e *vibrations (second part)*

	R_{12b}	R_{13b}	R_{14b}	R_{15b}	R_{16b}	R_{17b}	R_{18b}	R_{19b}	R_{20b}	R_{21b}	R_{22b}
x_1	0	0	0	0	0	0	0	0	0	0	0
y_1	0	0	0	0	0	0	0	0	0	0	$18\sqrt{6}$b
z_1	0	0	0	0	0	0	0	0	0	0	0
x_2	0	0	0	0	0	0	0	0	0	0	0
y_2	0	0	0	0	0	0	18a	−54a	$-12\sqrt{12}$	$-24\sqrt{6}$	$18\sqrt{6}$b+$\sqrt{6}$
z_2	0	0	0	0	0	0	0	0	0	0	0
x_3	0	0	0	0	0	0	0	0	0	0	0
y_3	0	$-8\sqrt{18}$	0	0	48	0	0	36a+12	0	$18\sqrt{6}$	0
z_3	0	0	0	0	0	0	0	0	0	0	0
x_4	$-2\sqrt{6}$	$-6\sqrt{6}$	$2\sqrt{12}$	$-4\sqrt{3}$	$12\sqrt{3}$	$16\sqrt{3}$	$3\sqrt{3}$a+$\sqrt{3}$	$9\sqrt{3}$a+$3\sqrt{3}$	−12	$15\sqrt{2}$	$3\sqrt{2}$
y_4	$2\sqrt{18}$	$-2\sqrt{18}$	−12	12	12	−48	−9a−3	9a+3	$6\sqrt{12}$	$3\sqrt{6}$	$-3\sqrt{6}$
z_4	$16\sqrt{3}$	0	$2\sqrt{6}$	$16\sqrt{6}$	0	$8\sqrt{6}$	$-12\sqrt{6}$a−$4\sqrt{6}$	0	$-6\sqrt{2}$	−12	−24
x_5	$2\sqrt{6}$	$6\sqrt{6}$	$-2\sqrt{12}$	$4\sqrt{3}$	$-12\sqrt{3}$	$-16\sqrt{3}$	$-3\sqrt{3}$a−$\sqrt{3}$	$-9\sqrt{3}$a−$3\sqrt{3}$	12	$-15\sqrt{2}$	$-3\sqrt{2}$
y_5	$2\sqrt{18}$	$-2\sqrt{18}$	−12	12	12	−48	−9a−3	9a+3	$6\sqrt{12}$	$3\sqrt{6}$	$-3\sqrt{6}$
z_5	$-16\sqrt{3}$	0	$-2\sqrt{6}$	$-16\sqrt{6}$	0	$-8\sqrt{6}$	$12\sqrt{6}$a+$4\sqrt{6}$	0	$6\sqrt{2}$	12	24
x_6	0	0	0	0	0	0	0	0	0	0	0
y_6	0	0	0	0	−36	0	0	0	0	0	0
z_6	0	0	0	0	0	0	0	0	0	0	0
x_7	0	$-4\sqrt{6}$	0	0	$2\sqrt{3}$	0	0	$-10\sqrt{3}$	0	0	0
y_7	0	$4\sqrt{18}$	0	0	−6	0	0	−6	0	0	0
z_7	0	$-4\sqrt{3}$	0	0	$-8\sqrt{6}$	0	0	$4\sqrt{6}$	0	0	0
x_8	0	$4\sqrt{6}$	0	0	$-2\sqrt{3}$	0	0	$10\sqrt{3}$	0	0	0
y_8	0	$4\sqrt{18}$	0	0	−6	0	0	−6	0	0	0
z_8	0	$4\sqrt{3}$	0	0	$8\sqrt{6}$	0	0	$-4\sqrt{6}$	0	0	0
x_9	0	0	0	$-3\sqrt{3}$	$-9\sqrt{3}$	$-6\sqrt{3}$	$-6\sqrt{3}$	0	0	0	0
y_9	0	0	0	9	−9	18	18	0	0	0	0

z_9	$-12\sqrt{3}$	0	$-6\sqrt{6}$	0	0	0	0	0	0	0	0
x_{10}	$-2\sqrt{6}$	$2\sqrt{6}$	$2\sqrt{12}$	$11\sqrt{3}$	$-\sqrt{3}$	$-8\sqrt{3}$	$4\sqrt{3}$	$-4\sqrt{3}$	0	0	0
y_{10}	$-2\sqrt{18}$	$2\sqrt{18}$	12	-3	-3	12	-6	6	0	0	0
z_{10}	$-2\sqrt{3}$	$2\sqrt{3}$	$2\sqrt{6}$	$-8\sqrt{6}$	$4\sqrt{6}$	$-4\sqrt{6}$	$2\sqrt{6}$	$-2\sqrt{6}$	0	0	0
x_{11}	$4\sqrt{6}$	$4\sqrt{6}$	$-4\sqrt{12}$	$-4\sqrt{3}$	$-2\sqrt{3}$	$-2\sqrt{3}$	$\sqrt{3}$	$\sqrt{3}$	0	0	0
y_{11}	0	0	0	-18	0	18	-9	-9	0	0	0
z_{11}	$-2\sqrt{3}$	$-2\sqrt{3}$	$2\sqrt{6}$	$-8\sqrt{6}$	$-4\sqrt{6}$	$-4\sqrt{6}$	$2\sqrt{6}$	$2\sqrt{6}$	0	0	0
x_{12}	0	0	0	$3\sqrt{3}$	$9\sqrt{3}$	$6\sqrt{3}$	$6\sqrt{3}$	0	0	0	0
y_{12}	0	0	0	9	-9	18	18	0	0	0	
z_{12}	$12\sqrt{3}$	0	$6\sqrt{6}$	0	0	0	0	0	0	0	0
x_{13}	$-4\sqrt{6}$	$-4\sqrt{6}$	$4\sqrt{12}$	$4\sqrt{3}$	$2\sqrt{3}$	$2\sqrt{3}$	$-\sqrt{3}$	$-\sqrt{3}$	0	0	0
y_{13}	0	0	0	-18	0	18	-9	-9	0	0	0
z_{13}	$2\sqrt{3}$	$2\sqrt{3}$	$-2\sqrt{6}$	$8\sqrt{6}$	$4\sqrt{6}$	$4\sqrt{6}$	$-2\sqrt{6}$	$-2\sqrt{6}$	0	0	0
x_{14}	$2\sqrt{6}$	$-2\sqrt{6}$	$-2\sqrt{12}$	$-11\sqrt{3}$	$\sqrt{3}$	$8\sqrt{3}$	$-4\sqrt{3}$	$4\sqrt{3}$	0	0	0
y_{14}	$-2\sqrt{18}$	$2\sqrt{18}$	12	-3	-3	12	-6	6	0	0	0
z_{14}	$2\sqrt{3}$	$-2\sqrt{3}$	$-2\sqrt{6}$	$8\sqrt{6}$	$-4\sqrt{6}$	$4\sqrt{6}$	$-2\sqrt{6}$	$2\sqrt{6}$	0	0	0

Table IV

Urey-Bradley force constants (md/A)

K_x	(Si—O)	2.59	F_α (X...C)	0.162
K_y	(Si—C)	2.71	F_β (C...C)	0.03
K_z	(C—H)	4.54	F_γ (Si...H)	0.13
H_α	(O—Si—C)	0.085	F_δ (H...H)	0.10
H_β	(C—Si—C)	0.11	$\varkappa$ ($OSiC_3$)	0.09
H_γ	(Si—C—H)	0.20	$\varkappa$ ($SiCH_3$)	—0.05
H_δ	(H—C—H)	0.40		

mined according to relation (2). The submatrix of $(M^{-1})^+$ which is necessary for computing G_{ff}^+ is shown in Table VI. To be able to construct matrix F_{ff}^+, one must know the matrices A shown in Tables VII—IX.

We should like to thank G. Koszó *(Computing Centre of the Hungarian Academy of Sciences)* for his assistance in resolving the numerical procedures on a NE 803 B digital computer.

Table V

Computed internal group frequencies compared with the experimental values

		Computed	$(Me_3Si)_2O$	$Si(OSiMe_3)_4$	$B(OSiMe_3)_3$
ν_1	CH_3 asym. str.	2949	2950	2958	2945
ν_2	CH_3 sym. str.	2899	—	2900	2885
ν_3	CH_3 asym. def.	1417	1420	1412	1410
ν_4	CH_3 sym. def.	1262	1255	1252	1261
ν_5	CH_3 sym. rock.	863	890,850	760	845
ν_6	SiC sym. str.	658	619,686	640	645
ν_7	CH_3 asym. str.	2948	2950	2964	2945
ν_{10}	CH_3 asym. def.	1415	1420	1412	1454
ν_{11}	CH_3 sym. rock.	822	834	822	845
ν_{12}	CH_3 asym. str.	2949	2950	2964	2945
ν_{13}	CH_3 asym. str.	2949	2950	2964	2945
ν_{14}	CH_3 asym. str.	2890	—	2899	2885
ν_{15}	CH_3 asym. def.	1416	1420	1458	1454
ν_{16}	CH_3 sym. def.	1415	1420	1442	1454
ν_{17}	CH_3 sym. def.	1264	1255	1268	1246
ν_{18}	CH_3 asym. rock.	863	850	846	845
ν_{19}	CH_3 asym. rock.	825	834	846	845
ν_{20}	SiC asym. str.	746	754	688,697	757

Table VI

The submatrix of $(M^{-1})^{+}$ for the calculation of G^{+}_{ff}

0.0625	0.0000	0.0000	0,0000	0.0000	0.0000	0.0000	0.0000
0.0000	0.0625	0.0000	0.0000	0.0000	0.0000	0.0000	0.0000
0.0000	0.0000	0.0625	0.0000	0.0000	0.0000	0.0000	0.0000
0.0000	0.0000	0.0000	0.0178	0.0000	0.0000	0.0186	0.0000
0.0000	0.0000	0.0000	0.0000	0.0178	0.0000	0.0000	0.0042
0.0000	0.0000	0.0000	0.0000	0.0000	0.0204	−0.0104	0.0000
0.0000	0.0000	0.0000	0.0186	0.0000	−0.0104	0.0281	0.0000
0.0000	0.0000	0.0000	0.0000	0.0042	0.0000	0.0000	0.0540
0.0000	0.0000	0.0000	−0.0056	0.0000	0.0088	0.0102	0.0000
0.0000	0.0000	0.0000	0.0078	−0.0062	0.0052	0.0017	−0.0012
0.0000	0.0000	0.0000	−0.0062	0.0150	−0.0090	−0.0022	−0.0002
0.0000	0.0000	0.0000	0.0028	−0.0049	0.0088	0.0007	0.0003
0.0000	0.0000	0.0000	0.0078	0.0062	0.0052	0.0017	0.0012
0.0000	0.0000	0.0000	0.0062	0.0150	0.0090	0.0022	−0.0002
0.0000	0.0000	0.0000	0.0028	0.0049	0.0088	0.0007	−0.0003

0.0000	0.0000	0.0000	0.0000	0.0000	0.0000	0.0000
0.0000	0.0000	0.0000	0.0000	0.0000	0.0000	0.0000
0.0000	0.0000	0.0000	0.0000	0.0000	0.0000	0.0000
−0.0056	0.0078	−0.0062	0.0028	0.0078	0.0062	0.0028
0.0000	−0.0062	0.0150	−0.0049	0.0062	0.0150	0.0049
0.0088	0.0052	−0.0090	0.0088	0.0052	0.0090	0.0088
0.0102	0.0017	−0.0022	0.0007	0.0017	0.0022	0.0007
0.0000	−0.0012	−0.0002	0.0003	0.0012	−0.0002	−0.0003
0.0501	−0.0001	0.0008	−0.0008	−0.0001	−0.0008	−0.0008
−0.0001	0.0475	0.0112	−0.0050	−0.0012	−0.0005	−0.0006
0.0008	0.0112	0.0346	0.0087	0.0005	0.0027	0.0005
−0.0008	−0.0050	0.0087	0.0502	−0.0007	−0.0006	−0.0008
−0.0001	−0.0012	0.0005	−0.0007	0.0475	−0.0112	−0.0051
−0.0008	−0.0005	0.0027	−0.0006	−0.0112	0.0346	−0.0088
−0.0008	−0.0006	0.0005	−0.0008	−0.0051	−0.0088	0.0501

Table VII

Matrix A belonging to a_1

0.99994	0.00103	−0.00562	0.00057	−0.00098	−0.00160	−0.00008	−0.00796
0.00102	−0.99998	−0.00010	0.00240	−0.00179	0.00285	0.00087	−0.00091
0.00440	0.00000	0.95187	−0.01240	−0.26719	−0.12673	−0.05086	−0.06114
0.00001	−0.00346	−0.00214	−0.89254	0.19368	−0.38522	0.13177	−0.00976
0.00396	−0.00001	0.30305	0.00668	0.79551	0.46059	0.23417	0.09096
−0.00084	−0.00161	0.01938	0.45022	0.36699	−0.77811	0.23725	0.02213
−0.00190	0.00196	−0.03376	0.01273	−0.31007	0.13363	0.91632	−0.21232
−0.00771	0.00051	−0.02365	0.01786	0.16563	0.00806	−0.17118	−0.97070

Table VIII

Matrix A belonging to a_2

1.00007	−0.00533	−0.00256
−0.00433	−0.95504	0.29644
0.00402	0.29642	0.95504

SUMMARY

The force field of the trimethylsilyl group affixed to oxygen was approached by Urey-Bradley force constants. The group frequencies which are almost constant in different molecules have been separated from the framework frequencies by the method of KING and CRAWFORD. Matrices are given for the calculation of the remaining framework frequencies.

REFERENCES

1. BARRACLOUGH, C. G., BRADLEY, D. C., LEWIS, J., THOMAS I. M.: J. Chem. Soc. 2601 (1961).
2. KRIEGSMANN, H., LICHT, K.: Electrochem. **62,** 1163 (1958).
3. LICHT, K., KRIEGSMANN, H.: Z. anorg. allg. Chem. **325,** 1 (1963).
4. SCHMIDBAUR, H.: Chem. Ber. **96,** 2696 (1963).
5. SCHMIDBAUR, H., PEREZ-GARCIA, J. A., ARNOLD, H. S.: Z. anorg. allg. Chem. **328,** 105 (1964).
6. SCOTT, D. W., MESSERLY, J. F., TODD, S. S., GUTHRIE, G. B., HOSSENLOPP, I. A., MOORE, R. T., OSBORN ANN, BERG, W. T., MCCULLOUGH, J. P.: J. Am. Chem. Soc. **65,** 1320 (1961).
7. SCHMIDBAUR, H.: Chem. Ber. **97,** 836 (1964).
8. GOUBEAU, J., SOMMER, H.: Z. anorg. allg. Chem. **289,** 1 (1957).
9. WANNAGAT, U., BRANDMAIR, F., LIEHR, W., NIEDERPRÜM, H.: Z. anorg. allg. Chem. **302,** 185 (1959).
10. PULAY, P., TÖRÖK, F.: Acta Chim. Hung. **45,** 123 (1965).
11. KING, W. T., CRAWFORD, B. Jr.: J. Mol. Spect. **5,** 421 (1960).
12. WILSON, E. B., DECIUS, J. C., CROSS, P. C.: "Molecular Vibrations" McGraw-Hill Book Company, New York 1955.

Table IX

Matrix A belonging to e

0.24191	0.97025	−0.00156	−0.00052	−0.00543	0.00064	−0.00105	0.00206	0.00006	0.00095	0.00488
0.97025	−0.24192	0.00044	0.00549	−0.00056	−0.00003	0.00090	0.00044	0.00143	−0.00548	0.00221
−0.00005	0.00162	0.99998	0.00007	0.00000	0.00184	0.00300	−0.00012	−0.00236	0.00062	0.00090
0.00106	0.00423	0.00001	0.09126	0.95015	0.01299	−0.06177	0.28278	−0.05792	0.00921	0.03897
−0.00426	0.00104	0.00001	0.94834	−0.09272	0.02673	−0.20421	−0.08012	−0.19821	0.05940	−0.02001
0.00000	0.00003	0.00345	0.00567	0.00267	−0.86811	−0.38459	0.00547	0.31139	0.03396	0.01638
0.00096	0.00386	−0.00001	0.03029	0.29542	0.00029	0.15774	−0.91463	0.21417	−0.02045	−0.06372
0.00385	−0.00097	0.00002	−0.29869	0.02726	0.00632	−0.57996	−0.26571	−0.69979	0.11262	−0.02546
−0.00002	−0.00122	0.00257	−0.04003	−0.01507	0.49511	−0.65520	0.01304	0.56684	0.04728	−0.00587
−0.00596	−0.00027	0.00027	0.02327	−0.01019	0.00561	−0.11122	−0.05048	−0.05460	−0.85333	0.50322
−0.00034	−0.00464	−0.00125	−0.00267	−0.01668	0.01687	0.06051	−0.06078	0.02301	0.50170	0.86013

Über das Schwingungsspektrum des Trimethylsilyl-Radikals, I.

F. TÖRÖK und GY. B. HUN

Zusammenfassung: Das Kraftfeld des zu Sauerstoff gebundenen Trimethylsilyl-Radikals wurde unter Zugrundelegung der UREY-BRADLEY-Annäherung charakterisiert. Die in verschiedenen Molekülen nahezu konstant sich erweisenden Frequenzen des Radikals wurden mit der Methode von KING und CRAWFORD von der Skelettschwingung abgesondert behandelt, und die zur Berechnung der Skelettschwingung benötigten Matrizen angegeben.

О колебательном спектре триметилсилильного радикала, I.

Ф. ТЁРЁК и ДЬ. Б. ХУН

Резюме. Силовое поле триметилсилильного радикала, соединенного с кислородом, характеризовалось с помощью приближения Юри—Брэдли. Частоты радикала, приблизительно постоянные в различных молекулах обсуждались с применением метода Кинга и Крауфорда отделив их от колебаний скелета. Кроме этого приведены матрицы, необходимые для расчета колебаний скелета.

Ferenc TÖRÖK
Gyöngyi B. HUN
Budapest VII. Múzeum krt. 6—8.

THE SIGNIFICANCE OF PHOSPHORESCENCE IN THE MEASUREMENT OF LOW ENERGY BETA ISOTOPES WITH LIQUID SCINTILLATOR AND SINGLE-CHANNEL COUNTER

P. FODOR-CSÁNYI and B. LÉVAY

(Electrochemistry Research Group of the Hungarian Academy of Sciences)

Received May 13, 1965

In connection with studies carried out in order to elucidate some questions related to the structure of electrolyte solutions and the migration mechanism of the hydrogen ion, it has been found necessary to determine the self-diffusion coefficient of ions and molecules in aqueous solutions and in mixtures of organic solvents with water.

It was decided that water should be labelled with tritium, and organic molecules with carbon isotope.

Both isotopes emit soft beta rays (the maximum energy of ^{14}C is 155 keV, that of tritium 18 keV), consequently they cannot be measured in the same way like high-energy isotopes, because absorption occurring in the measuring system and the self-absorption of the sample play an important role.

The liquid scintillation technique was chosen because it has the most advantages over other possible techniques, and a single-channel counter, type EKCO N 664 A, was used. The most serious problems presented by single-channel liquid scintillation counters are the dark current (noise) produced by the photomultiplier and phosphorescence. The latter is emitted by the bottle containing the liquid scintillator, the solvent in which the scintillator is dissolved, the bulb of the photomultiplier, and by other parts of the measuring device, in consequence of light falling on them. By painting all metal parts black and by the use of a light shutter it was possible to cancel the phosphorescence of these parts and of the photomultiplier bulb.

It is more difficult to eliminate the phosphorescence produced by the sample container and by the solvent. The latter are exposed to light until the beginning of the measurement, consequently the capacity and sensitivity of the measuring device is influenced by the rate of the decrease (in the following: decay) of phosphorescence and the value of residual phosphorescence. In certain cases, the time of decay may be as long as several days and this makes measurements impossible.

It is apparent from the aforesaid that in the course of the measurement of low energy beta radiation, the amount of noise and phosphorescence should be decreased to a possible minimum. The decreasing of noise can be regarded

as a problem practically solved by the use of selected low-noise tubes and of cooling; however, elimination of the phosphorescence in single-channel counters remains an important problem that has not been solved so far.

The level of signals brought about by phosphorescence is of the same order of magnitude as that of the signals generated by soft beta emitters, consequently it is either quite impossible to decrease by discrimination, or it can be done only with a certain loss in efficiency. Therefore, studies of this kind on phosphorescence have been carried on ever since single-channel counters became the subject of interest.

Experiments with the single-channel counter at our disposal showed that the instrument was in its original form practically useless under the circumstances prescribed by the manufacturers on account of the extraordinarily strong interference caused by phosphorescence. In the literature, relatively few and contradictory data [1—6] were found on the subject, thus it was decided that the problem should be studied thoroughly in order to decrease or eliminate interference brought about by phosphorescence.

This work included an investigation of the intensity and the intensity changes on time of the phosphorescence of bottles made of various sorts of glass, and of some solvents and scintillator solutions which are important in the liquid scintillation technique. Furthermore, experiments were made to study the interaction between sample container phosphorescence and scintillator solutions, and to reveal the possibilities of decreasing or eliminating phosphorescence by the use of discrimination, optical filter, or both.

The determinations were carried out with the EKCO instrument, under conditions corresponding to parameters expected in case of the isotopes ^{14}C and tritium, that is, an amplification factor of 1000 was used at 1300 V working voltage with a discriminator voltage of 5 and 20 V, or at 1600 V, with a discriminator voltage of 5 V, respectively. These parameters were determined in a way that the minimum detectable isotope quantity was calculated for every condition assuming that the measurement is feasible if the count is at least twice as high as the statistical error of the sum of the noise of the multiplier plus the background* plus the phosphorescence of the solvent and of the bottle [7].

For this case we have:

$$c_{\min} = \frac{5.49 \cdot 10^{-4}}{\eta \cdot V} \sqrt{\frac{n_b}{t}} \quad \mu C/ml \tag{1}$$

where the efficiency of the measurement (η) is expressed in per cent, the volume (V) in ml, the time of measurement (t) in seconds, and the value n_b

* It is only the pulses caused by the radioactivity of the surroundings and by cosmic rays that is meant here by "background".

(which is the sum of noise plus background plus residual phosphorescence) in counts/100 sec. units.

The measuring device

The measuring device contains a photomultiplier, type EMI 9514 S, of a light sensitivity of 2000 A/lumen and very low noise (7 to 15 m μA). During measurement, the sample containers are placed directly on the surface of the photomultiplier, good optical contact being provided by silicone oil. Protection of the photocathode against light is ensured by an automatic light shutter, which opens when the rubber cover has been closed; then the cover cannot be opened again. Accordingly, it is possible to change the samples without switching off the high voltage, moreover, any interference caused by the phosphorescence of the photomultiplier is eliminated. The bottle is placed on the photocathode by a lid plunger, when the lead lid is closed.

The measuring probe is surrounded by a lead shield of 5 cm wall thickness. The output signals from the multiplier are conducted to the amplifier; the amplification factor of the latter can be varied in 6 steps from 25 to 1000. The signals are counted by an automatic scaler type EKCO N 530 F. The latter is equipped with time- and pulse-preselection facilities. The discriminator voltage is adjustable in the range of 5 to 50 V.

The instrument has been modified to some extent by us, because the noise of the photomultiplier showed a steady increase in consequence of heating. To overcome this, a thermostating jacket was applied around the photomultiplier with tap-water cooling.

Instead of the TiO_2-coated containers supplied with the instrument, cylindrical medicine bottles, with plastic lid were used. These are cheaper and more convenient to handle. The containers were contained in an aluminium tube with polished inner surface; the tube served as a reflector. When optica glass filter was used, this was cemented to the lower end of the tube [8]

Phosphorescence of the glass containers

Glass containers, which had been kept in darkness for several days, were excited to phosphorescence by exposure to sunlight. The bottles were irradiated either for 1, or for 5 minutes, always in the same geometrical arrangement, and then the decrease in the intensity of phosphorescence was measured as a function of time (the time of placing the bottles into darkness was taken as zero time).

The measurements of the phosphorescence of the sample containers included test with sample containers made of different sorts of glass, coated

or not coated with a reflector. In the first test the phosphorescence was measured using the parameters which correspond to the carbon isotope (amplification factor 1000; working voltage 1300 V; discriminator voltage 5 V). At the parameters used for tritium, only bottles of the lowest phosphorescence were tested.

At first, the phosphorescence of the TiO_2-coated bottles made of Pyrex-glass and supplied with the EKCO instrument was determined at $+10$ and $-10°$ C (Fig. 1). The intensity of the phosphorescence started at 45,000 counts/

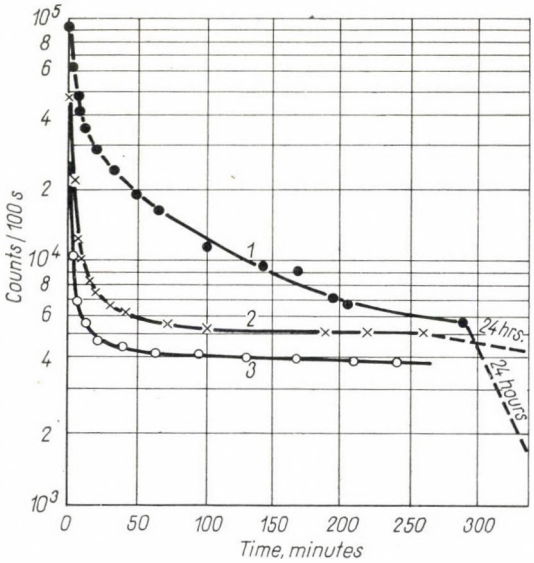

Fig. 1. The phosphorescence of the EKCO bottle plotted against time
Amplification: 1000; 1300 V; discriminator voltage 5 V. Time of irradiation: 1 min. (After subtraction of multiplier noise.)
Curve 1: bottle at $-10°$ C;
Curve 2: bottle at $+10°$ C;
Curve 3: bottle shielded against light at $+10°$ C

100 sec. but even after storage in darkness for 24 hours it was as high as 4000 counts/100 sec. (The number of counts corresponding to noise has been subtracted from the above values.) The decrease of intensity is slower at $-10°$ C, but after a longer period of time, the remaining degree of phosphorescence is lower than at a higher temperature. In order to decrease the phosphorescence, the outer surface of the sample container was coated with black paint. In this case, the initial level of phosphorescence was lower, however, the residual phosphorescence was as high as a few thousand counts/100 sec. Consequently, the original bottles could not be used on account of the reflecting TiO_2 layer, even if light had been kept away from the bottle for 24 hours before measurement, e.g., by changing the samples in darkness [9].

Bottles of shapes and sizes identical with those of the EKCO instrument were made of Pyrex, Rasotherm, soda glass and quartz. In some of the bottles the plane wall to be contacted with the photomultiplier was either welded by the glassblower, or cemented with Araldite to the body of the bottle. The rest of the bottles was made of one piece.

Bottles made of the same material and subjected to identical heat treatment had identical phosphorescence, and there was no difference between sample containers welded by the glassblower and those made of one piece [10]. These sample containers after having been kept for one hour in darkness, showed a value as low as 800—1000 counts/100 sec. There was no considerable difference with the use of pure quartz bottles either as opposed to results obtained by LLOYD and co-workers [6], who reported that sample containers made of pure quartz had practically no phosphorescence (Fig. 2).

The phosphorescence of bottles made of the same glass but subjected to different heat-treatments differed widely; here Araldite cannot be used for cementing the plane bottle walls. (Phosphorescence of a bottle cemented with Araldite started at about 45,000 counts/100 sec., and after 20 hours was still as high as 6000 counts/100 sec.)

A layer of aluminium was applied to the bottles showing the lowest amount of phosphorescence, by a vacuum evaporation process, in order to provide an optical reflector. A finish of lustreless black lacquer was applied for mechanical and optical protection. The phosphorescence of bottles prepared in this manner was considerably lower than that of the original bottles, since the bottle was exposed to light only through the bottom [9] (Fig. 2).

Further studies concerning phosphorescence were carried out using the medicine bottles, now applying not only the parameters corresponding to the measurement of the carbon isotope, but also those corresponding to tritium.

The decay curve of the phosphorescence of medicine bottles is shown [11] in Fig. 3. As opposed to the measurements discussed above in this case the bottles were exposed to light for a longer period of time (5 min.) in order to obtain less fluctuating initial phosphorescence. Even under such conditions, the initial phosphorescence of the individual bottles was different, but the time dependence of the decrease in intensity was well reproducible. The rate of decay was determined in such a manner that the intensity of phosphorescence measured at a given time was divided by the initial intensity. The factors obtained in this way and pertaining to identical times were in agreement within a few per cents. The half life on the decay curve is 2 to 3 min. in the initial stage, and about 20 hrs. in the final stage.

Using an amplification factor of 1000, and a discriminator voltage of 5 V at 1600 or 1300 V, the initial phosphorescence is very high (about 10^6 and $4 \cdot 10^5$ counts/100 sec., resp.) and remains at a considerable level even after one day. At 1300 V and 20 V discriminator voltage the shape of the curves

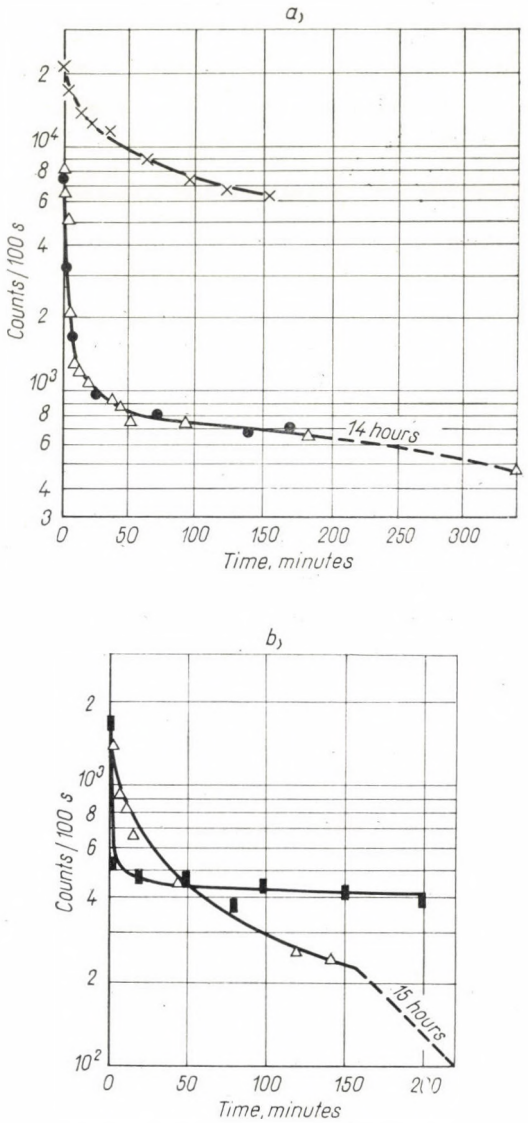

Fig. 2. Decay of the phosphorescence plotted against time
Amplification: 1000; 1300 V; discriminator voltage: 5 V. Irradiation time: 1 min.
(The value corresponding to noise has been subtracted.)

a) Bottles without reflector. b) Bottles coated with aluminium reflector

Rasotherm bottles:

▲ — uncemented
○ — welded by glassblower
× — uncemented, with different heat treatment

Quartz bottle:

▣ — with aluminium reflector

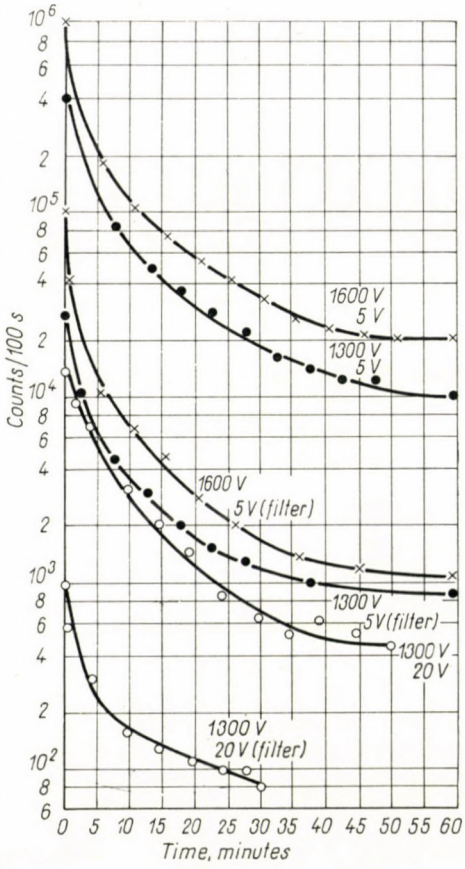

Fig. 3. Decay of the intensity of phosphorescence of glass bottles plotted against time, at different working and discriminator voltages at a 1000 times amplification and at 10° C. Irradiation time: 5 min. (After subtraction of the value corresponding to noise.)

is practically the same, however, the amount of phosphorescence is markedly decreased.

In addition to the decay rate of phosphorescence the amount of residual phosphorescence is also of great importance, because it is impossible to carry out the measurements if this value is high.

As it is seen from the data given in Table I, the residual phosphorescence corresponds at 1600 V, to 6000 counts/100 sec., even after a dark storage of 24 hours; it was only at 1300 V and at a discriminator voltage of 20 V that a phosphorescence sufficiently low to allow measurements (400 counts/100 sec.) was obtained; however, in serial determinations, if there is no sample changing device, even a waiting time of two hours is regarded as too long.

Table I

Phosphorescence of the glass bottle and of the solvent with and without optical filter at an amplification of 1000 and at 10° C

	Without optical filter									With optical filter Chance OX 7			In coincidence	
Working voltage, V	1600			1300			1300			1600	1300	1300	1900	1400
Discriminator voltage, V	5			5			20			5		20	7	
Time of dark storage, hrs.	0.08	12	24	0.08	2	8	0.08	0.5	2	2	1	0.5	0.16	0.08
Glass bottle, counts/100 sec.	800,000	10,000	6000	220,000	7000	4000	6000	700	400	1000	900	80	150	50
Toluene distilled from sodium metal, counts/100 sec.	1 400	200	0	1 200	400	200	900	250	200	0	0	0	30	0
Noise of photomultiplier counts/100 sec.	2000			600			50			2000	600	50	160	80
Total counts/100 sec.		12,200	8000		8000	4800	6950	1050	650	3000	1500	130	340	130

Accordingly, phosphorescence studies with glass sample containers have led to the conclusion that these sample containers are totally unsuitable for the measurement of tritium, and the carbon isotope can be measured with their use after rather long waiting only.

Phosphorescence of the solvents

In order to study the behaviour of the solvents, bottles that had been stored in darkness for several days were placed in the measuring instrument in red light, and the sum of the noise and the residual phosphorescence of the bottle was determined. (The photocathode of the multiplier is insensitive to red light.) After this, the solvent which had been exposed to light was poured into the sample container. The phosphorescence was measured similarly to the technique employed with the empty sample container, and the result was corrected with the value corresponding to the noise and the phosphorescence of the sample container.

Of the solvents and diluters used in the preparation of liquid scintillators, toluene, xylene, dioxane and ethyl alcohol were studied [9, 10].

Analytical grade toluene, xylene and ethyl alcohol were "Reanal" products, while the dioxane used was supplied by Nuclear Enterprises (NE). The toluene was fractionated three times, then refluxed with sodium metal for two hours, and distilled again. The phosphorescence of the solvents of different purity was compared with that of the scintillation grade toluene of Nuclear Enterprises.

According to the experimental results, toluene, xylene and dioxane behaved, as regards phosphorescence, in nearly identical manner (Fig. 4); however, ethyl alcohol showed considerably lower phosphorescence. The phosphorescence of the solvents, though markedly lower than that of the glass bottles was too high for practical use. In the course of purification, the phosphorescence of toluene decreased substantially, and the phosphorescence of toluene, when freshly distilled from sodium, was even lower than that of the NE scintillation grade toluene (Fig. 5).

The purity of the solvents is of importance not only on account of phosphorescence, but also in connection with light output, since among the impurities causing phosphorescence there are strong quenchers, too.

A number of experiments were carried out in order to study the effect of dissolved oxygen on phosphorescence. Oxygen was removed from the solvent by bubbling carefully purified nitrogen gas through it. The removal of oxygen caused in every case an increase of the phosphorescence (Fig. 5). An especially large increase was observed in toluene distilled from sodium metal. This observation is contradictory to results obtained by LLOYD and co-workers [6]

by the use of the same technique, who found that on removing oxygen the starting value of phosphorescence showed a considerable decrease. However, according to other data published in the literature, oxygen has a quenching action, and by its elimination the value of light output is increased by 20 to 30% [11].

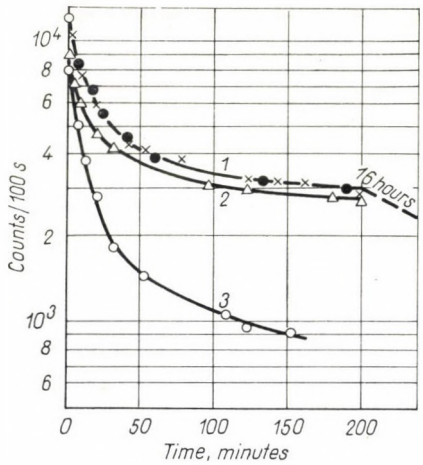

Fig. 4. The phosphorescence of solvents plotted against time
Amplification: 1000; 1300 V; discriminator voltage 5 V at 10° C. (Noise and bottle phosphorescence have been subtracted.)
Curve 1: × Doubly distilled toluene; ● Dioxane
Curve 2: Xylene
Curve 3: Abs. ethyl alcohol

Summing up, it may be stated that the phosphorescence of solvents can be decreased by rectification and boiling with sodium metal to such a degree that it will interfere neither with the measurement of tritium, nor with that of the ^{14}C isotope. However, in case of the determination of low activities, it would be advantageous to eliminate even this low residual phosphorescence, corresponding to a few hundred counts/100 sec.

Possibilites for decreasing the phosphorescence

Summarizing the results of phosphorescence measurements, it can be stated that with the use of a single-channel counter the phosphorescence of the glass bottles and of the solvent is so high that the instrument is not suitable for serial measurements (Table I), because dark storage for several hours is necessary before a measurement can be made. Accordingly, the utilization of the instrument is very much restricted.

In single-channel counters phosphorescence can be decreased by the use of a sample changer, which makes possible to keep a number of samples in darkness before measurement. However, the construction of a sample changer

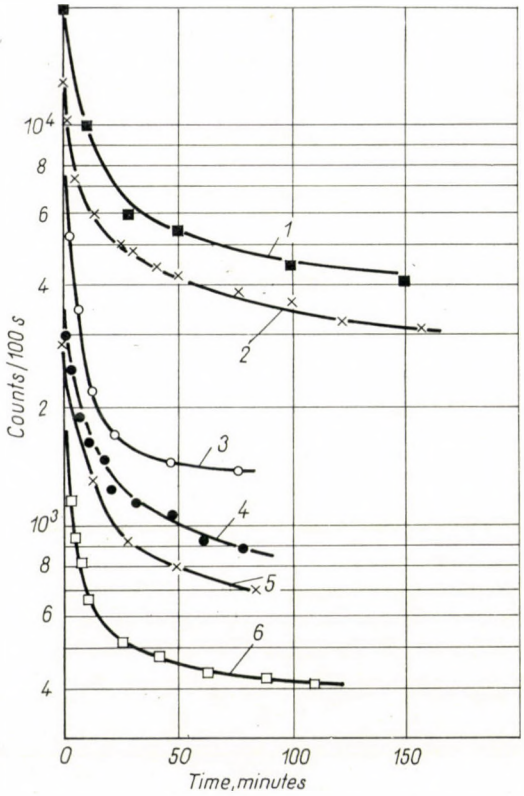

Fig. 5. The phosphorescence of toluene of various purity grades plotted against time Amplification: 1000; 1300 V; discriminator voltage 5 V, at 10° C. (Noise and bottle phosphorescence have been subtracted.)

Curve 1: Toluene distilled twice, bubbling with N_2
Curve 2: Toluene distilled twice
Curve 3: Toluene distilled three times
Curve 4: NE scintillation grade toluene
Curve 5: Toluene distilled from sodium metal, bubbling with N_2
Curve 6: Toluene distilled from sodium metal

would have involved, in our case, a highly expensive modification of the instrument, furthermore, the sample changer in itself would not have solved the problem, since the intensity of residual phosphorescence is, even after a dark storage of one day, very high. Accordingly, for the time being, the idea of the sample changer was abandoned and discrimination, further the use of optical glass filter, as proposed by LLOYD and co-workers, were tried to achieve the decrease of phosphorescence.

The applicability of discrimination and optical filter to decrease phosphorescence is restricted by the extent to which they decrease the efficiency of measurement.

A study on the absolute value of measuring efficiency will be given in a next paper, and only results of interest in connection with phosphorescence will be discussed here.

The variations of noise, phosphorescence and efficiency as the functions of discriminator voltage are shown in Fig. 6, for the sake of better compara-

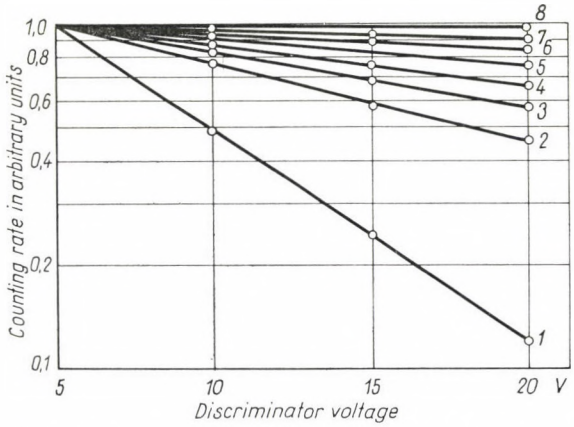

Fig. 6. The variations of noise, phosphorescence and efficiency of the determination of ^{14}C and tritium, plotted against the discriminator voltage
Amplification: 1000, with EMI 9514 S photomultiplier
Noise and phosphorescence at 1300 (1) and 1600 V (2).
Efficiency of the determination of ^{14}C, in toluene contaning *p*-terphenyl (4 g/l):
In a sample containing water, at 1300 V, with filter (3) and without filter (4). (Composition of sample: 68.25% by vol. of scintillator solution, 28.95% of ethyl alcohol, 2.8% of water.)
In a hydrocarbon, at 1300 V with filter (6) and without filter (7). At 1600 V, with filter and without filter (8).
Efficiency of the determination of tritium in toluene containing *p*-terphenyl (4 g/l):
In a sample containing water, at 1600 V, with filter (5). (Composition of the sample: 68.25% by vol. of scintillator solution, 28.95% of ethyl alcohol, 2.8% of water.)
In a hydrocarbon, at 1600 V, without filter (6)

bility, in arbitrary units. The value measured with a discriminator voltage of 5 V was taken as unity.

With increasing discriminator voltage, noise and phosphorescence decreased in equal proportion, the signals being produced in both cases by the emission or generation and multiplication of one electron. It is apparent from the Figure that noise and phosphorescence decrease in consequence of discrimination to a much smaller degree at 1600 V and 5 V discriminator voltage than at 1300 V.

According to the decay curves (Fig. 3) recorded at various voltages and discriminator voltages the length of the dark storage period decreases as it has been discussed above, to a considerable extent with the decrease of the absolute value of phosphorescence.

On the other hand, it is apparent from the efficiency curves that discrimination can not be used for decreasing the phosphorescence in case of tritium, because the efficiency of the determination is considerably decreased at higher discriminator voltages, and at the same time the intensity of residual phosphorescence is still high.

Discrimination can be used in case of carbon samples, if the measurement is carried out at 1300 V and with a discriminator voltage of 20 V. In this case, after a dark storage of 2 hours, 90% of the activity found at a discriminator voltage of 5 V is obtained. Such an efficiency is acceptable; however, dark storage for 2 hours is too long a period to be practicable in serial tests.

Since the experiments for reducing phosphorescence by discrimination did not afford satisfactory results, the use of the optical filter, types Chance OX 7, used by LLOYD for the measurement of tritium was tried [7, 12]. The fundamental theory of application of an optical filter is the following: if a filter is chosen which has a transmission range identical to the relatively narrow emission band of the scintillator, all parts of the continuous phosphorescence outside of this band are absorbed by the filter. Accordingly, the sensitivity of the photocathode is restricted by the filter essentially to the emission band of the scintillator.

For example, by the use of the optical filter type Chance OX 7, transmitting in the 2300 to 4300 Å range, the original sensitivity range of the photocathode which is 3000 to 6000 Å is restricted to the region 3000 to 4300 Å; the latter is practically the same as the emission band of *p*-terphenyl or PBD [2-phenyl-5-(4-biphenylyl)-1,3,4-oxadiazole] scintillators which is between 3200 and 4300 Å (Fig. 7). The price of *p*-terphenyl is about forty times lower than that of PBD, consequently the former was used. The phosphorescence of toluene distilled from sodium metal was totally cancelled by the optical filter; also scintillation grade toluene, which had been stored for a prolonged period of time, showed but a negligible phosphorescence.

In the presence of the filter, the phosphorescence of the glasses was decreased to one-twentieth of the original intensity. This is a very favourable result, since, e.g., in the measurement of the carbon isotope the combination of discrimination with the use of the optical filter results in a decrease of the intensity of phosphorescence by two orders of magnitude when 1300 V and a discriminator voltage of 20 V are used. Under such circumstances, dark storage of maximum half an hour or with tritium two hours is necessary, and the remaining phosphorescence corresponds to 80 and 1000 counts/100

sec., respectively. These phosphorescences intensities allow already also the use of a sample changer.

However, the applicability of an optical filter is influenced also by other factors. When measuring solutions of identical composition, the geometrical factor becomes somewhat less favourable, since the filter has a thickness of 2 mm; furthermore, the transmittancy of the filter is not 100%, either. This affects the efficiency of measurement the more, the fewer are the photons generated by a single radioactive disintegration, *i.e.*, the lower is the energy of the radioactive radiation and the light output in the scintillator.

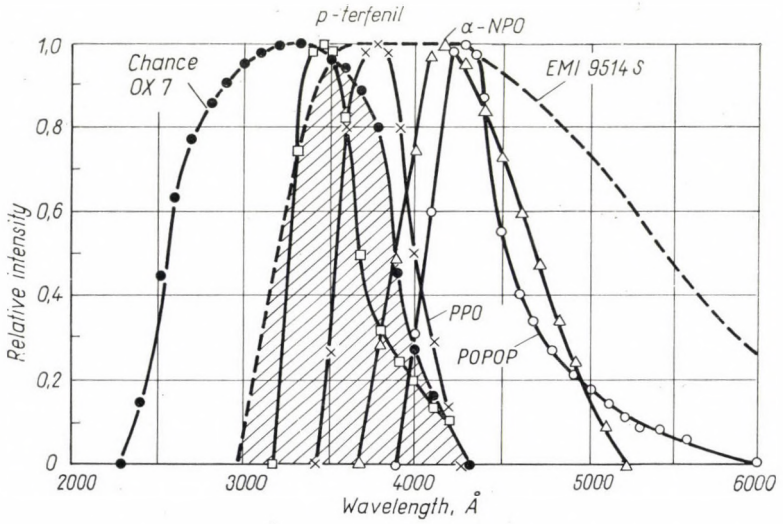

Fig. 7. Emission spectra of some scintillator solutions; sensitivity range of the photocathode and transmission range of the optical filter

Accordingly, in case of ^{14}C, the optical filter does not influence the efficiency of measurement substantially; an efficiency of 78% was obtained with filter, as opposed to the efficiency of 85% without filter [12]. However, in case of tritium, the efficiency was decreased by the filter Chance OX 7 by 20% and 25% when the isotope was incorporated in a hydrocarbon and in water, respectively [8]. This decrease is considerable, but the use of the optical filter is yet justified as it markedly increases the capacity of the instrument by eliminating a great deal of the idle periods.

A further disadvantage of the application of the optical filter in the determination of tritium is that it can be used only in connection with *p*-terphenyl scintillator; the solubility of this compound is poor at low temperatures, thus cooling cannot be used as a means of decreasing the noise.

Studies on the interaction between phosphorescence of sample container and scintillator solution

During our measurements with liquid scintillators and in the course of the study of phosphorescence two effects were observed which could be explained neither by data described in the literature, nor on the basis of our previous measurements. One of these was the remarkably high background level measured with liquid scintillators. The other phenomenon was that the phosphorescence of the bottle filled with scintillator solution (measured through an optical filter) was different from that of the empty bottle; this difference — negative or positive — is dependent on the nature of the scintillator [13].

The background value was, with the use of a lead shield of 5 cm thickness and a sample volume of 16 ml, in case of *p*-terphenyl approximately 1000, in case of POPOP* 2000 counts/100 sec., at a voltage of 1600 V and a discriminator voltage of 5 V. Under the same circumstances, a NaI crystal of 2 cm thickness and 4 cm diameter measured a background of 200 to 300 counts/100 sec. When comparing the two data, it must be taken into consideration that it is only radiations of higher energies which can pass the lead shield, and that these are detected by the NaI crystal with considerably higher efficiency than by liquid scintillators.

The background level, as measured by means of the liquid scintillator, showed a steep decrease with increasing discriminator voltage, and at 20 V discriminator voltage it was as low as 250 counts/100 sec. This shows that a considerable proportion of the background radiation is due to some low energy radiation, and the energy of the radiation is of the same order of magnitude as that of the tritium radiation. This phenomenon cannot be explained with the natural radioactivity of lead or the other materials of construction, since this is mostly absorbed by the glass bottle wall. The most significant is the beta radiation of 1.33 MeV, produced by the ^{40}K isotope present in the glass. However, according to numerous data published in the literature, its contribution to the background radiation is only 40 to 60 counts/100 sec., and its energy is higher than that corresponding to a discriminator voltage of 20 V [7, 14].

These facts necessitated a study of the phosphorescence of glass, solvent, and the scintillator solution, not only separately, but also in respect of their possible interactions. For this purpose, various scintillator solutions were examined concerning their influence on the variations of the phosphorescence of the bottles excited by sunlight and the light of a mercury vapour lamp; the measurements were made in the presence of an optical filter.

Bottles stored in darkness for several days were excited to phosphorescence partly by exposure to sunlight and partly by the light of the low-pres-

* 1,4-bis[2-(5-phenyloxazolyl)]-benzene.

sure mercury vapour lamp of the "UVIFOT" photometer, using a filter type UG 5. The excitation lasted for 5 minutes. (The transmission range of the filter is 2500 to 4000 Å.)

The interaction between the phosphorescence of the bottle and the scintillator solution was studied in the following manner. At first, the starting phosphorescence of the irradiated empty bottle was established and afterwards, in red light, scintillation grade solvent or scintillator solution that had been stored in darkness was poured in the bottle and the decay of phosphorescence was measured at every 100 sec. for about half an hour.

In order to be able to study the interaction with the scintillator solution it is necessary to know the phosphorescence of the empty bottle at any given time of the measurement. If the mean decay rate* of the bottles irradiated and measured under identical conditions and the initial phosphorescence of the bottle are known, the phosphorescence of the empty bottle can be calculated for every instant of the measurement; the phosphorescence measured with the scintillator solution was given as percentage of the former.

Results

The ratio of the phosphorescence of the bottle filled with a scintillator solution and that of the empty bottle was a constant value during the period of the measurement at any instant of time. The mean values for various scintillators are summarized in Table II.

In case of excitation with sunlight, the phosphorescence measured with *p*-terphenyl and PBD increased to 125% with the use of PPO (2,5-diphenyloxazole) to 113% while with *a*-NPO [2-(1-naphthyl)-5-phenyloxazole] and POPOP it was decreased, on the average, to 34%.

When excitation was effected with a mercury vapour lamp, the phosphorescence values obtained with *p*-terphenyl, PBD and toluene were practically identical with that of the empty cell. If the bottle contained a scintillator in which the wavelength corresponding to the maximum emission (column 2 in Table II) was shifted in the direction of the longer wavelengths as compared with *p*-terphenyl, the phosphorescence was smaller not only than that obtained with *p*-terphenyl (or PBD), but also than that of the empty bottle.

Let us consider the effects that may take place when a scintillator solution is placed into an excited glass bottle. In this case, part of the phosphorescence passes the solution and it may be absorbed by the solvent or directly by the scintillator; an other part will reach directly the photocathode.

* The mean decay rate was determined as described in connection with the study of the phosphorescence of glass bottles.

Table II

Variations in the phosphorescence of the bottle brought about by different scintillator solutions

	Wavelength of maximum emission, Å	Absorption band, Å	Emission band, Å	Excitation with sunlight			Excitation with mercury vapour lamp, through UG 5, %
				%	glass rod, %	through UG 5, %	
p-terphenyl in toluene	3450	2400—3200[15]	3200—4200[18]	125	206	102	97
PBD in toluene	3640			124			95
PPO in toluene	3800	2800—3300[15]	3400—4300[18]	113			79
α-NPO in toluene	4150		3700—5200[15]	37			57
PPO and POPOP in toluene	4250			35			55
p-terphenyl and POPOP in toluene	4250			35			52
POPOP in toluene	4250	3000—4000[16]	3900—5300[18]	30	15	52	58
NE 213 (POPOP*)	4250			31			55
NE 220 (POPOP*)	4250			37			58
toluene	2600	2300—2760[17]	2300—2760[19]			102	98

* Scintillator solutions produced by *Nuclear Enterprises* ; in No. 213 the solvent is toluene, in No. 220, dioxane.

If the phosphorescence is absorbed by the solvent, the excitation energy, in a manner similar to the scintillation mechanism, reaches the scintillator molecule with an efficiency that depends on the solvent used, and the scintillator will emit photons at its characteristic wavelength. If the phosphorescence is absorbed directly by the scintillator itself, the process is analogous to the energy transfer between primary and secondary scintillators, and also in this case light emission will result at the wavelength of the scintillator. Accordingly, in case of either mechanism one part of the phosphorescence will be absorbed and emitted by the scintillator at characteristic longer wavelength.

The optical filter, type Chance OX 7, transmits photons of the 2300 to 4300 Å wavelength range; at the same time, the sensitivity of the photocathode is restricted to the 3000 to 6000 Å range, and consequently it were photons corresponding to the 3000 to 4300 Å range which were measured in our experiments.

If follows from the aforesaid that if the absorption bands of the solvent and of the scintillator correspond to a range for which the photocathode is insensitive, and, at the same time, the emission of the scintillator is such that it coincides with the sensitive range of the photocathode, the scintillator will introduce such phosphorescence of the bottle into the sensitive region which

otherwise would not be detected by the photocathode. As the net result, an increase in phosphorescence is brought about by the scintillator. This has been named by us "introduction of phosphorescence".

The above effect is encountered in case of excitation with sunlight and the use *p*-terphenyl or PBD scintillator dissolved in toluene (Figs. 7 and 8). The exciting spectrum is, with sunlight, continuous; its end towards the shorted wavelengths is at 2000 Å. All of the absorption of toluene (2300 to 2760 Å), and most of the absorption of *p*-terphenyl and PBD fall between the wave-

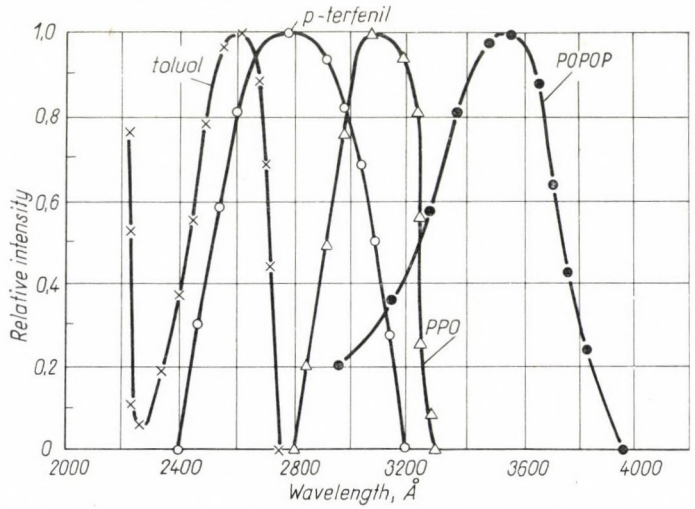

Fig. 8. Absorption spectra of some scintillator solutions and of toluene

length of the exciting light and the lower sensitivity limit of the photocathode. The measuring range includes the total emission spectrum of the scintillators. Accordingly, the measured phosphorescence is 125% in both cases.

If the absorption of the scintillator is between 3000 and 4300 Å, and its emission is outside of this range, the value of phosphorescence will decrease.

The absorption of POPOP is within the measuring range used by us, but its emission is not; this accounts for the considerable decrease in phosphorescence (34%). Photon emission is always characteristic of the scintillator which has the longest wavelength at maximum emission; this is the reason why every solution that contained POPOP showed about identical decrease in phosphorescence.

The absorption and emission of PPO are in intermediate position between that of *p*-terphenyl and POPOP. Part of the emission of PPO is outside of the measuring range (Fig. 7), but its absorption overlaps the insensitive range of the photocathode and the measuring range. This accounts for the fact

that it can introduce some phosphorescence; however, this is of smaller degree than that encountered in case *p*-terphenyl.

The situation is different when a mercury-vapour lamp is used for excitation. The light of the photometer lamp contains to 80% the 2537 Å line of mercury, and it is only this line which is transmitted by the filter type UG 5. Accordingly, the phosphorescence of the bottle consists of photons of the wavelength of 2537 Å or longer. It has been shown by the measurements that a substantial part of the phosphorescence is of a wavelength considerably higher than that of the exciting light. This is proved by the fact that in the 3000 to 6000 Å range, the phosphorescence of the bottle corresponded to $\sim 10^6$ counts/100 sec., while with the use of an optical filter (3000 to 4300 Å) a value of only $5 \cdot 10^4$ was obtained. Accordingly, the main portion of the phosphorescence of the bottle excited with a light of 2537 Å wavelength is in the 4300 to 6000 Å range. On this basis it may be inferred that in the 2537 to 3000 Å range only a small portion of the excitation energy is emitted in the form of phosphorescence. Consequently, *p*-terphenyl or PBD cannot give rise to an observable increase of the phosphorescence, in spite of the fact that part of the absorption both of toluene and of the scintillators is in the 2537 to 3000 Å range.

This is corroborated by the fact that in case of excitation with sunlight, PPO introduced additional phosphorescence (113%), while in case of excitation by mercury vapour lamp, the phosphorescence was decreased (79%).

The degree of the increase or decrease in phosphorescence is influenced also by the proportion of the phosphorescence of the bottle passing through the solution.

When POPOP scintillator is used, the explanation of the difference between excitation with mercury vapour lamp and sunlight is that in the latter case not only the bottom but the entire bottle was irradiated, thus a higher proportion of the radiation passed through the solution. On the other hand, the results were similar to those of mercury-vapour lamp excitation if the sunlight had passed through a filter of type UG 5, since, in this case, the geometry of irradiation was identical and the excitation range was similar.

In order to estimate the proportion of phosphorescence that was absorbed after passing the solution, a glass rod was irradiated instead of the bottles, and the former was immersed into the bottle containing the scintillator, in such a manner that it was fastened to the plastic lid. (The decay curve of the glass rods had been determined by a technique similar to that used for the bottles.) In this case, a phosphorescence corresponding to 206% was observed with *p*-terphenyl, while for POPOP a value of 15% was obtained. By comparison of the decreases in phosphorescence measured with the bottles and the glass rod, it is apparent that the phosphorescence observed with POPOP in case of the glass rod is one half (15%) of that measured with the bottle. (The opacity of the filter for the emission range of POPOP is well illus-

trated by the fact that, e.g., the ^{14}C isotope was measured in a solution containing POPOP with an efficiency of 83% while with the use of the filter and under otherwise similar conditions an efficiency as low as 0.7% was obtained.)

The question concerning the mechanism of the transfer of energy from the bottle to the scintillator has been only partly answered by the above-described experiments. The decrease of phosphorescence in the presence of POPOP can be explained only by assuming that POPOP absorbs directly, because it is only the absorption band of POPOP which is within the measuring range. Accordingly, it is not necessary to assume an intermediate action of the solvent.

Evaluation

On the basis of our results we have explained the fact that the phosphorescence of a sample container filled with a scintillator solution, when determined through an optical filter, is different as compared to that of the empty sample container, and that this positive or negative difference depends on the quality of the scintillator compound.

By assuming the introduction of phosphorescence it is also possible to supply an explanation for the extraordinarily high background radiation. By the use of *p*-terphenyl scintillator, the absorption band is — both with and without the use of an optical filter — outside of the measuring range or the sensitivity of the photocathode, consequently an increase in phosphorescence is possible. Actually it is not the background that has a high intensity, but the originally non-detectable part of shorter wavelengths in the phosphorescence of the bottle is introduced by the scintillator into the measuring range.

In order to explain the increase of the background radiation (*i.e.*, of phosphorescence) encountered in the presence of POPOP (without filter Chance OX 7), it must be assumed that toluene may play a role in the mechanism, too. Both the absorption and the emission bands of POPOP are within the sensitivity range of the photocathode, consequently an introduction of phosphorescence is possible only if the radiation is absorbed by toluene.

Therefore it is not sufficient to study the intensity of the phosphorescence of the bottle and that of the solvent separately, since the phosphorescence of a bottle filled with scintillator solution cannot be obtained as the sum of the individual phosphorescence values of the parts of the system.

On the basis of the above-mentioned results it must be pointed out that when considering the choice of the proper scintillator or optical filter, the possibility of the introduction of phosphorescence must also be examined as a new factor. Thus it is preferable to use *p*-terphenyl, which emits in the shorter wavelength range, together with the filter Chance OX 7, instead of employing

e.g., POPOP with a filter transparent as regards this substance. Namely, when a scintillator emitting at a longer wavelength and optical filter are used, the scintillator may introduce a higher amount of phosphorescence into the sensitive range of the photocathode. For instance in the case of a scintillator solution containing PPO and POPOP, this means that the phosphorescence corresponding to the absorption bands of toluene, PPO and POPOP (range 2300 to 3900 Å) will be measured in spite of the fact that the filter is transparent only for the emission band of POPOP (3900 to 5300 Å). On the other hand, with a scintillator solution containing *p*-terphenyl, it is only the phosphorescence corresponding to the range 2300—3000 Å which can be introduced; the absorption bands of toluene and *p*-terphenyl are largely overlapping, and the intensity of phosphorescence excited by sunlight is substantially lower in this range than in the region of longer wavelengths.

Similarly, any additive added to liquid scintillators must be studied as regards the possible introduction of phosphorescence.

Ultimately, an optical filter can completely eliminate only phosphorescence having longer wavelengths than the upper wavelength limit of the filter, while in the direction of shorter wavelengths there is no possibility for such elimination.

The authors express their gratitude to Academician TIBOR ERDEY-GRUZ and Professor SÁNDOR LENGYEL for their valuable advice, further to Mrs BÉLA JANKÓ and MÁRIA BARASITS for their help in the course of the experiments.

SUMMARY

The role of phosphorescence has been studied in the measurement of soft beta emitters (mainly tritium and ^{14}C isotope) by the liquid scintillation technique using a single-channel counter.

It has been found that the most serious problems encountered in the use of a single-channel counter — mainly in the determination of tritium — arise in consequence of the phosphorescence on the glass bottles and of the solvents. The lowest measurable activity and the number of measurements that can be carried out in one day are determined first of all by the decay rate of the phosphorescence and by the intensity of residual phosphorescence.

There is no significant difference between the phosphorescence of sample containers made of various glass sorts: the initial phosphorescence is, with any of these, in the order of magnitude of 10^6 counts/100 sec., and even after a day it remains as high as several thousand counts/100 sec.

No considerable differences have been found in the phosphorescence of various solvents (toluene, xylene, dioxane, ethyl alcohol); however, the purity of the solvents has a marked effect.

Techniques known from the literature as means for reducing phosphorescence (discrimination and the use of an optical filter), when applied separately, did not bring about satisfactory results. Discrimination involves even in the case of the ^{14}C isotope a decrease in efficiency, and requires several hours of storage in the dark; in the case of tritium, the use of this method is entirely impossible.

The phosphorescence of scintillation grade toluene can be totally cancelled by the use of an optical filter recommended by LLOYD and co-workers. In this manner, the intensity of the phosphorescence is decreased to such an extent that it becomes possible to measure tritium after a dark storage of 2 hours, and the capacity of the measuring device is increased ten times.

The lowest detectable activity level is decreased by 20%, in spite of the fact the measuring efficiency is — as opposed to the results obtained by LLOYD and co-workers — decreased by 20 to 25%.

By the simultaneous use of the optical filter and discrimination, ^{14}C isotope-containing samples can be measured after a dark storage of half an hour, and the intensity of the residual phosphorescence is 80 counts/100 sec.

With containing a scintillator it has been found that in the presence of the optical filter and a scintillator emitting at a suitable wavelength (*e. g.*, *p*-terphenyl), the intensity of observed phosphorescence has increased as compared to that of the empty bottle. A detailed study of this effect has revealed that the portion of the phosphorescence of glass outside of the sensitivity range of the photocathode is absorbed by the solvent and the scintillator, and it is emitted at a new wavelength characteristic of the scintillator, the latter wavelength being now within the measuring range. This phenomenon has been named "*introduction of phosphorescence*" by the authors.

In consequence of the introduction of phosphorescence, it is not reasonable to study the phosphorescence of the sample container and of the solvent independently from the scintillator solution, and when choosing the appropriate scintillator and optical filter, the possibility of the introduction of phosphorescence, as a novel factor, must be taken into consideration. In order to decrease this effect, it is preferable to use a scintillator which emits in the range of shorter wavelengths, together with a filter which is transparent with respect to the scintillator. Scintillators emitting in the range of longer wavelengths are apt to introduce a higher proportion of the phosphorescence of the bottle into the measuring range, and the intensity of phosphorescence is much higher at higher wavelengths.

An optical filter may completely cancel only phosphorescence of higher wavelengths than its own limit of transmission on the high wavelength side, in the direction of shorter wavelengths there is no possibility to eliminate phosphorescence.

REFERENCES

1. BERNSTEIN, W., BJERKNES, C. and STEELE, R.: Liquid Scintillation Counting, Pergamon Press, London, 1958, p. 74.
2. DAVIDSON, J. D.: Liquid Scintillation Counting, Pergamon Press, London, 1958, p. 88.
3. BROWN, W. O., and BADMAN, H. G.: Biochem. J., **78,** 571 (1961).
4. BUTLER, F. E.: Anal. Chem., **33,** 409 (1961).
5. RAPKIN, E. and PACKARD, L. E.: TID—7612, 216 (1960).
6. LLOYD, R. A., ELLIS, S. C. and HALLOWES, K. H.: Symposium on the Detection and Use of Tritium in the Physical and Biological Sciences, Vienna, 3—10 May 1961.
7. KAUFMAN, W. J., NIR, A., PARKS, G. and HOURS, R. M.: Symposium on the Detection and Use of Tritium in the Physical and Biological Sciences. Vienna, 3—10 May 1961.
8. FODOR-CSÁNYI, P., LÉVAY, B., and SALAMON, A.: Magy. Kém. Folyóirat **70,** 184 (1964).
9. ORMOS, Gy. and FODOR-CSÁNYI, P.: Magy. Kém. Folyóirat **69,** 198 (1963).
10. FODOR-CSÁNYI, P., LÉVAY, B. and KŐHEGYI, F.: Magy. Kém. Folyóirat **68,** 482 (1962).
11. OTT, D. G., HAYES, F. N., HAMMEL, J. E. and KEPHART, J. F.: Nucleonics **13,** No. 5, 62 (1955).
12. LÉVAY, B. and FODOR-CSÁNYI, P.: Magy. Kém. Folyóirat, **71,** 356 (1965).
13. FODOR-CSÁNYI, P., and LÉVAY, B.: Magy. Kém. Folyóirat, **71,** 360 (1965).
14. BOYCE, I. S. and CAMERON, J. F.: Symposium on the Detection and Use of Tritium in the Physical and Biological Sciences, Vienna, 3—10 May 1961.
15. HAYES, F. N.: LA—1639, 1953, Los Alamos Scientific Laboratory.
16. SWANK, R. K.: Liquid Scintillation Counting. Pergamon Press, London, 1958, p. 23.
17. LANDOLT-BÖRNSTEIN: Springer Verlag, Berlin, 1951, Vol. 1/3 p. 265.
18. OTT, D. G.: Liquid Scintillation Counting. Pergamon Press, London, 1958, p. 101.
19. BASS, A. M.: J. Chem. Phys., **18,** 1403 (1950).

Die Bedeutung der Phosphoreszenzstrahlung bei der Messung weiche β-Strahlen aussendender Isotopen mit Flüssigkeitsscintillator in einem Einkanal-Meßgerät

P. FODOR-CSÁNYI und B. LÉVAY

Zusammenfassung. Es wurde die Rolle der Phosphoreszenzstrahlung in einem Einkanal-Meßgerät bei der Messung mittels Flüssigkeitsscintillation von weiche β-Strahlung aussendenden Isotopen (vor allem Tritium und ^{14}C-Isotop) untersucht.

Es wurde festgestellt, daß in Einkanal-Meßeinrichtungen — besonders bei der Messung von Tritium — die größten Probleme durch die Phosphoreszenzstrahlung der Glasküvetten und der Lösungsmittel verursacht werden. Die geringste meßbare Aktivität und die Anzahl der täglich durchführbaren Messungen wird durch die Geschwindigkeit des Aufhörens der Phosphoreszenzstrahlung bzw. durch die Größe der Restphosphoreszenz am stärksten beeinflußt.

Zwischen der Phosphoreszenz der aus verschiedenen Glasarten verfertigten Küvetten wurde keine wesentliche Abweichung gefunden, die Ausgangsintensität einer jeden zeigte eine Größenordnung von 10^6 Impulse/100 s, und blieb selbst nach einigen Tagen mehrere tausend Impulse/100 s.

Die Phosphoreszenz der Lösungsmittel (Toluol, Xylol, Dioxan, Äthanol) wies nur einen geringen Unterschied auf, doch änderte sie sich beträchtlich mit der Reinheit.

Die in der Literatur beschriebenen Methoden (Diskrimination bzw. die Verwendung optischer Filter) gaben einzeln angewendet keine befriedigenden Resultate. So kann die Diskriminierung selbst im Falle des ^{14}C-Isotopen nur zu Lasten des Wirkungsgrades, mit Stehen im Dunklen während mehreren Stunden kombiniert, verwendet werden, und beim Tritium kommt diese Methode gar nicht in Frage.

Der von LLOYD und Mitarbeitern empfohlene optische Filter hob die Phosphoreszenz des Toluols von Scintillationsreinheit vollkommen auf. Dadurch wurde die Phosphoreszenzstrahlung derart verringert, daß die Messung des Tritiums nach 2 Stunden Stehen im Dunklen ermöglicht, und die Kapazität des Meßgerätes verzehnfacht wurde. Der Wert der geringsten nachweisbaren Aktivität nahm um 20% ab, obwohl der Filter im Gegensatz zu den Befunden von LLOYD und Mitarbeitern den Wirkungsgrad der Messung um 20—25% verringerte.

Durch gleichzeitige Verwendung des optischen Filters und der Diskriminierung konnte erreicht werden, daß das ^{14}C-Isotop nach halbstündigem Stehen der Proben meßbar wurde, und die Intensität der Restphosphoreszenz 80 Impulse/100 s betrug.

Im Falle von mit Scintillator gefüllten Küvetten fand man, daß die Intensität der beobachteten Phosphoreszenz in Gegenwart des optischen Filters und eines bei entsprechender Wellenlänge emittierenden Scintillators (z. B. des *p*-Terphenyls) im Vergeich zu der bei leerer Küvette gefundenen Intensität ansteigt. Eine eingehende Untersuchung dieser Erscheinung zeigte, daß der außerhalb des Empfindlichkeitsbereiches der Photokathode liegende Teil der Phosphoreszenz des Glases durch das Lösungsmittel bzw. den Scintillator absorbiert und bei einer für den Scintillator charakteristischen Wellenlänge, die in den Meßbereich fällt, emittiert wird. Diese Erscheinung wurde »Einbringen der Phosphoreszenzstrahlung« genannt.

Wegen des Einbringens der Phosphoreszenzstrahlung wäre es sinnlos, die Phosphoreszenz der Küvette und des Lösungsmittels unabhängig von der Scintillatorlösung zu untersuchen, vielmehr muß bei der Wahl des Scintillators und des optischen Filters als weiterer Einflußfaktor auch die Möglichkeit eines Einbringens der Phosphoreszenz beachtet werden. Um dies möglichst zu verhindern, wird man zweckmäßigerweise einen in dem kürzeren Wellenbereich emittierenden Scintillator und einen für denselben durchsichtigen Filter wählen. Der im längeren Wellenlängenbereich emittierende Scintillator kann nämlich einen größeren Teil der Phosphoreszenzstrahlung der Küvette in den Meßbereich einbringen, und im längeren Wellenbereich ist die Phosphoreszenz viel intensiver.

Letzten Endes wird nur die Phosphoreszenz oberhalb der Grenze gegen die größeren Wellenlängen vollständig durch den optischen Filter ausfiltriert, gegen kürzere Wellenlängen kann jedoch die Phosphoreszenz nicht beseitigt werden.

Важность фосфоресценции в жидкосцинтилляционных измерениях изотопов мягкой β-радиации, в одноканальном измерительном приборе

П. ФОДОР-ЧАНИ и Б. ЛЕВАИ

Резюме. Исследовали роль фосфоресценции в жидкосцинтилляционных измерениях изотопов мягкой β-радиации (в первую очередь изотопов трития и ^{14}C), в одноканальном измерительном приборе.

Установили, что в одноканальном измерительном приборе — в первую очередь при измерениях трития — самую большую проблему оказывают фосфоресценционные излучения стеклянных кюветт и растворителей. Скорость прекращения фосфоресценции или величина оставшейся фосфоресценции больше всего влияют на измеримую наименьшую активность и на число проводимых ежедневных измерений.

Между фосфоресценцией кюветт, изготовленных из различных сортов стекла, значительного расхождения не было найдено, начальная интенсивность каждой из кюветт была порядка 10^6 импульс/100 сек и оставалась даже по истечению одного дня порядка нескольких тысяч импульс/100 сек.

Фосфоресценция растворителей (толуол, ксилол, диоксан, этанол) не отличается значительно друг от друга, а изменяется в зависимости от чистоты растворителей.

Известные из литературы методы (применение дискриминирования или оптического фильтра) снижения фосфоресценции не привели к нужным результатам. Так, дискриминация еще применима в случае изотопа ^{14}C и то только за счёт снижения степени эффективности и при многочасовом нахождении изотопа в темноте; в случае же трития этот метод уже никаким образом не может быть использован.

Предложенный *Ллойдом* и сотрудниками оптический фильтр полностью устранил фосфоресценцию сцинтилляционно чистого толуола. Таким образом, величина фосфоресценции снизилась настолько, что стало возможным измерение трития, после двухчасового нахождения в темноте, и производительность измерительного прибора увеличилась в десять раз. Величина минимально детектируемой активности снизилась на 20%, хотя фильтр, в противоположность *Ллойду* и сотрудникам, на 20—25% снизил измерительную степень эффективности.

При совместном использовании оптического фильтра и дискриминации удалось, при измерении изотопа ^{14}C, достигнуть измеримости проб после получасового нахождения их в темноте и интенсивность оставшейся фосфоресценции была 80 импульс/100 сек.

В случае кюветт, заполненных сцинтиллятором, наблюдали, что в присутствии оптического фильтра и сцинтиллятора (напр., п-терфенил), эмиттирующего при соответствующей длине волны, имеет место возрастание, по сравнению с пустой кюветтой, интенсивности наблюдаемой фосфоресценции. Более обстоятельное изучение явления показало, что растворитель или сцинтиллятор абсорбирует часть фосфоресценции стекла, лежащую за пределами чувствительности фотокатода, и эмиттирует ее, при соответствующей сцинтиллятору длине волны; фосфоресценция попадает в пределы измерений. Это явление назвали вносом фосфоресценции.

Вследствие этого явления нет смысла в независимых от растворов сцинтиллятора измерениях фосфоресценции кюветты и растворителя, кроме этого, при выборе сцинтиллятора и оптического фильтра нужно принимать во внимание, как новую точку зрения, возможность вноса фосфоресценции. Для снижения такого вноса лучше всего использовать сцинтиллятор, эмиттирующий в области более коротких длин волн, с прозрачным, по отношению к сцинтиллятору, фильтром. Сцинтиллятор, эмиттирующий в более длинноволновой области, способен внести в область измерений большую часть фосфоресценции кюветты, кроме того, интенсивность фосфоресценции в более длинноволновой области, является более значительной.

В конечном итоге, оптический фильтр способен полностью фильтровать фосфоресценцию в области, лежащей у границы более длинных волн, при более же коротких длинах волн нет возможности устранения фосфоресценции.

Piroska Fodor-Csányi
Béla Lévay
Budapest VIII. Puskin u. 11-13.

RELATIONS BETWEEN THE INTEGRAL PRINCIPLE OF THERMODYNAMICS AND THE HAMILTON PRINCIPLE

I. GYARMATI

(Department for Physical Chemistry, Polytechnical University, Budapest)

Received October 26, 1965

Introduction

In several previous papers [1, 2, 3, 4] we have discussed the variational principles of non-equilibrium thermodynamics. The general local form of the principle of least dissipation of energy has been formulated in two different representations, further on the unified form and its equivalent, the Gaussian type principle have been given. Several examples for the application of the latter have been presented by J. VERHÁS [5, 6], and it seems, that the Gaussian type differential principle of thermodynamics is understood now in every respect. It is known that PRIGOGINE was the first who suggested the existence of the Gaussian type principle in a very intuitive work [7]. In the same paper he also made allusions to the existence of a thermodynamic integral principle, which may to a certain extent display a similarity to the Hamilton principle. Since in our above-mentioned papers (particularly in [2]) a general integral principle was formulated (the applicability of which has been proved beyond doubt by VERHÁS and BÖRÖCZ [8, 9]), thus a more detailed analysis of the relation between this integral principle and the Hamilton principle seems to be desirable.

1. The integral principle and its applications

We obtained the integral principle of thermodynamics by deduction of the differential equation of heat conduction and by generalization of the obtained results. The general Lagrange function of thermodynamics for the case of continuous system has been given in the following form [2, 4]:

$$\mathscr{L} = \varrho \dot{s} - \psi, \tag{1.1}$$

where ϱ is the density of medium, $\dot{s}$ is the substantial time derivative of the specific entropy, and ψ is the dissipation function given as the homogeneous quadratic function of the thermodynamic forces. The actual form of the Lagrange function for heat conduction in Fourier picture [1, 2, 4, 8] is:

$$\mathscr{L}_T = \varrho c_v T \frac{\partial T}{\partial t} + \frac{\lambda}{2} (\nabla T)^2 . \tag{1.2}$$

In the case of multicomponent isotherm diffusion [8]:

$$\mathscr{L}_{\mu k} = \varrho \sum_{k=1}^{K-1} (\mu_k - \mu_K) \frac{dc_k}{dt} + \frac{1}{2} \sum_{i,k=1}^{K-1} L_{ik} \nabla(\mu_i - \mu_K) \cdot \nabla(\mu_k - \mu_K). \quad (1.3)$$

The Lagrange function belonging to the Navier—Stokes equation of viscous fluids is the following [8]:

$$\mathscr{L}_{\mathbf{v}} = \mathbf{v}\left(\varrho \frac{d\mathbf{v}}{dt} + \operatorname{grad} p - \varrho \mathbf{F}\right) + \frac{1}{2}\left(\eta_v - \frac{2}{3}\eta\right)(\operatorname{div} \mathbf{v})^2 + \eta\left[(\operatorname{Grad} \mathbf{v})^s\right]^2. \quad (1.4)$$

Finally, the Lagrange function belonging to the generalized Navier—Stokes equation containing also the rotational viscosity is [9]:

$$\mathscr{L}_{\mathbf{v}\omega} = \mathscr{L}_v + \varrho \Theta \boldsymbol{\omega} \cdot \frac{d\boldsymbol{\omega}}{dt} + \frac{\xi r}{2} (\operatorname{rot} \mathbf{v} - 2\boldsymbol{\omega}). \quad (1.5)$$

The indices of the Lagrange functions are indicating the varied parameters in individual cases. Concerning the meaning of the other quantities, we refer to the original papers. Let us denote by Γ_j the scalar parameters whose negative gradients are the corresponding thermodynamic forces X_j, *i.e.*,

for heat conduction	$\Gamma \equiv T$	since $\mathbf{X}_q = -\nabla T$
for diffusion	$\Gamma_k \equiv \mu_k - \mu_K$	since $\mathbf{X}_k = -(\mu_k - \mu_K)$
for viscosity	$\Gamma_a \equiv v_a$	since $\mathbf{X}_v = -\operatorname{Grad} \mathbf{v}$

then in the case of f number of independent scalar parameters Γ_j, we obtain the corresponding Lagrange function $\mathscr{L}$ expressed as depending in general on these parameters Γ_j, on their gradients $\nabla\Gamma_j$, and their time derivatives $\dot{\Gamma}_j \equiv \frac{d\Gamma_j}{dt}$:

$$\mathscr{L} = \mathscr{L}(\Gamma_j, \nabla\Gamma_j, \dot{\Gamma}_j). \quad (1.6)$$

As it has been proved previously [1, 2, 4, 8, 9], the variational conditions valid for the volume integral of these Lagrange functions are:

$$\delta L = \delta \int_V \mathscr{L} dV = 0 \quad (1.7)$$

and the Euler—Lagrange equations of this variational problems

$$\frac{\partial \mathscr{L}}{\partial \Gamma_j} - \sum_{a=1}^{3} \frac{\partial}{\partial x_a} \frac{\partial \mathscr{L}}{\partial\left(\frac{\partial \Gamma_j}{\partial x_a}\right)} = 0, \qquad (j = 1, 2, \ldots f) \quad (1.8)$$

will be the Fourier, Fick, Navier—Stokes, etc. equations.

The conditions of the variational problem are the following:

(1) The thermodynamic fluxes J_j conjugated to the forces X_j, are considered fixed, while varying over Γ_j.

(2) The parameters Γ_j are not varied along the boundary surfaces.

(3) Quantities producing non-irreversible effects (such as hydrostatic pressure p and external forces $\mathbf{F}$) are not varied.

(4) The time derivatives $\frac{d\Gamma_j}{dt}$ $\left(\text{or } \frac{\partial \Gamma_j}{\partial t}\right)$ of the Γ_j parameters are not varied.

Under such conditions the foregoing statements are unambiguously valid. Of the given four conditions, the first three can easily be understood. The last condition, however, is fairly different from the variational methods familiar in other fields of physics. Therefore, when attempting to draw a parallelism between the integral principle (1.7) and the Hamilton principle, particular attention should be paid to condition (4).

2. Relation between the integral principle of thermodynamics and the Hamilton principle

First of all it must be pointed out that our Lagrange functions are actually Lagrangian densities, for which, in general, the integral principle (1.7) is valid. Furthermore, it can be easily seen, that the Euler—Lagrange equations (1.8) refer to a real, scalar, macroscopic parameter Γ_j which depends on space and time. Hence, in the most general sense all $\Gamma_j = \Gamma_j(\mathbf{r}, t)$ quantities represent real, scalar field quantities. In this respect we may speak of a temperature field of a material system, of its chemical potential field, and its field of velocity (which is, of course equivalent to three scalar fields). Based upon this fact, in the following discussion we shall examine the relation between the integral principle of thermodynamics (1.7) and the Hamilton principle with the aid of the mathematical apparatus of classical scalar field theories.

For such an examination of the relation between (1.7) and the field theoretical equivalent of the Hamilton principle it should be taken into consideration that the field quantities Γ_j (as generalized coordinates) are forming a continuum. Therefore, we define a Lagrangian density $\mathscr{L}$ of which we assume (just similarly to the case of the Hamilton principle) that it depends on the "field coordinates" Γ_j, on its gradients $\nabla\Gamma_j$, and on its time derivatives $\dot{\Gamma}_j$, moreover perhaps it explicitly depends also on time. Hence, the Lagrangian density (for the sake of simplicity expressed only for the j-th field quantity) will be:

$$\mathscr{L} = \mathscr{L}(\Gamma_j, \nabla\Gamma_j, \dot{\Gamma}_j, t) . \tag{2.1}$$

On integrating this over the volume for the (global) Lagrangian we have

$$L = \int_V \mathscr{L}(\Gamma_j, \nabla\Gamma_j, \dot{\Gamma}_j, t)\, dV. \tag{2.2}$$

Now the Hamilton principle is represented by the integral principle

$$\delta \int_{t_1}^{t_2} L\, dt = \delta \int_{t_1}^{t_2}\int_V \mathscr{L}\, dV dt = \int_{t_1}^{t_2}\int_V (\delta\mathscr{L})\, d\, V dt = 0\,, \tag{2.3}$$

if we agree that the field quantity Γ_j in the moments t_1 and t_2 is not varied, furthermore that time is not varied at all. Expressed in equation this condition of variation:

$$\delta\Gamma_j(\mathbf{r}, t_1) = \delta\Gamma_j(\mathbf{r}, t_2) = 0, \qquad \text{and} \qquad \delta t = 0\,. \tag{2.4}$$

Using now expression (2.1) of the Lagrangian density $\mathscr{L}$, we get:

$$\delta\mathscr{L} = \frac{\partial\mathscr{L}}{\partial\Gamma_j}\delta\Gamma_j + \sum_{\alpha=1}^{3} \frac{\partial\mathscr{L}}{\delta\left(\dfrac{\partial\Gamma_j}{\partial x_\alpha}\right)} \delta\left(\frac{\partial\Gamma_j}{\partial x_\alpha}\right) + \frac{\partial\mathscr{L}}{\partial\dot{\Gamma}_j}\delta\dot{\Gamma}_j \tag{2.5}$$

where in the two last terms the successive order of differentiation over the coordinates and over the time are commutable by the variation. Substituting expression (2.5) into (2.3), after partial integration with conditions (2.4), we get:

$$\int_{t_1}^{t_2}\int_V \left\{ \frac{\delta\mathscr{L}}{\partial\Gamma_j} - \sum_{\alpha=1}^{3} \frac{\partial}{\partial x_\alpha}\left[\frac{\partial\mathscr{L}}{\partial\left(\dfrac{\partial\Gamma_j}{\partial x_\alpha}\right)} \right] - \frac{d}{dt}\left(\frac{\partial\mathscr{L}}{\partial\dot{\Gamma}_j}\right) \right\} \delta\Gamma_j\, dV\, dt = 0\,. \tag{2.6}$$

Because this expression must be fullfilled for arbitrary volume and in case of arbitrary variations $\delta\Gamma_j$, thus we may write (see, *e.g.*, [10]):

$$\frac{\partial\mathscr{L}}{\partial\Gamma_j} - \sum_{\alpha=1}^{3} \frac{\partial}{\partial x_\alpha}\left[\frac{\partial\mathscr{L}}{\partial\left(\dfrac{\partial\Gamma_j}{\partial x_\alpha}\right)} \right] - \frac{d}{dt}\left(\frac{\partial\mathscr{L}}{\partial\dot{\Gamma}_j}\right) = 0\,. \tag{2.7}$$

This differential equation is the Euler—Lagrange equation of motion describing the variation of the field quantity $\Gamma_j = \Gamma_j(\mathbf{r}, t)$ in time and space, when the Lagrangian density is defined by (2.1). Comparing now the thermodynamic Lagrange function (1.6), the integral principle (1.7), and the Euler—Lagrange

equations (1.8), with (2.1), (2.3) and (2.7) existing in the case of the Hamilton principle, the similarities and differences of the two principles are conspicuous. The similarity consists in that, that the integral principle (1.7) is in the strictest sense of the word such a variational principle, which gives the basis of the field theoretical development of thermodynamics, just like the Hamilton principle (2.3) in other cases. The most essential difference between the two principles is that in case of (1.7) the integral L is a volume integral only, and during its variation the time derivatives of the field quantities are not varied, as required by condition (4). In other words, in the variational principle of thermodynamics the variation over the field quantities Γ_j must be made at a fixed time.

Now in order to analyse the difference between the integral principle of thermodynamics and the Hamilton principle by way of actual examples, let us write now the differential equations obtainable from (2.7) by means of the Lagrangian densities (1.2), (1.3) and (1.4).

(*a*) For the temperature field ($\Gamma \equiv T$), we get:

$$\varrho c_v \frac{\partial T}{\partial t} - \nabla \cdot (\lambda \nabla T) - \frac{d}{dt}(\varrho c_v T) = 0 . \tag{2.8}$$

If we apply now the same conditions which are necessary for heat conduction taking place in a solid body, *i.e.* ϱ, c_v are constants and $\frac{d}{dt} = \frac{\partial}{\partial t}$, the first and last terms of the above differential equation cancel each other. Hence, it can be said, that the existence of the Hamiltonian type principle in thermodynamics is incompatible with the validity of the Fourier equation. More exactly, the differential equation following from the Hamiltonian type integral principle refers to stationary state only. Indeed, (2.8) leads (if λ is independent of coordinates) to the Laplace equation:

$$\Delta T = 0 . \tag{2.9}$$

Therefore, in the light of PRIGOGINE's results [7] it seems, that the principle of the minimum production of entropy recognized by him (which applies to stationary states only [1, 2]) is in a more intrinsic relation with the Hamiltonian type principles than our integral principle.

(*b*) The fields $\Gamma_k = \mu_k - \mu_K$ of chemical potential of a diffusion system containing K components is obtained as the superposition of $K - 1$ independent scalar fields. Namely, the Gibbs—Duhem relation

$$\sum_{k=1}^{K-1} c_k \, d\mu_k + \left(1 - \sum_{k=1}^{K-1} c_k\right) d\mu_K = 0$$

can be written by using $\Gamma_k = \mu_k - \mu_K$ in the form

$$\sum_{k=1}^{K-1} c_k \, d\Gamma_k = - \, d\mu_K \, ,$$

boths sides of which are total differentials. Considering now the set of functions $c^k = c_k \, (\Gamma_1, \Gamma_2, \ldots, \Gamma_{K-1})$, we get:

$$dc_k = \sum_{j=1}^{K-1} \frac{\partial c_k}{\partial \Gamma_j} \, d\Gamma_j \, ,$$

where for the mixed derivatives it is valid that

$$\gamma_{ik} \equiv \frac{\partial c_k}{\partial \Gamma_i} = \frac{\partial^2 (-\mu_K)}{\partial \Gamma_k \, \partial \Gamma_i} = \frac{\partial^2 (-\mu_K)}{\partial \Gamma_i \, \partial \Gamma_k} = \frac{\partial c_i}{\partial \Gamma_k} \equiv \gamma_{ki} \, . \qquad (2.10)$$

$$(i, k = 1, 2, \ldots, K-1)$$

Herewith the diffusional Lagrangian density (1.3) may be written in the following general form:

$$\mathscr{L}_\Gamma = \varrho \sum_{i,k=1}^{K-1} \gamma_{ik} \Gamma_i \frac{d\Gamma_k}{dt} + \frac{1}{2} \sum_{i,k=1}^{K-1} L_{ik} \nabla \Gamma_i \nabla \Gamma_k \, . \qquad (2.11)$$

With this Lagrangian density and using the symmetry expressed by (2.10), (2.7) leads to the following differential equation:

$$\varrho \sum_{k=1}^{K-1} \gamma_{ik} \frac{d\Gamma_k}{dt} - \sum_{k=1}^{K-1} \nabla \cdot (L_{ik} \nabla \Gamma_k) - \frac{d}{dt} \left(\varrho \sum_{k=1}^{K-1} \gamma_{ik} \Gamma_k \right) = 0 \, . \qquad (2.12)$$

If the density of the medium and the γ_{ik} quantities are constant in time, then equation (2.12) is reduced to the middle term only, which refers again to stationary case. The set of differential equations obtained by omitting the last term may be considered as the most general set of equations of multicomponent isotherm diffusion. Its transformation to densities or to arbitrary concentrations is very simple.

(*c*) In the case of a velocity field ($\Gamma_a = v_a$), (2.7) yields with the Lagrangian density (1.4) by very simple computation:

$$\varrho \frac{d\mathbf{v}}{dt} + \operatorname{grad} p - \varrho \mathbf{F} - \eta \nabla \mathbf{v} - \left(\frac{\eta}{3} + \eta_v \right) \operatorname{grad} \operatorname{div} \mathbf{v} - \frac{d}{dt} (\varrho \mathbf{v}) = 0 \qquad (2.13)$$

which leads again, if $\varrho =$ constant to the time-independent form of the Navier—Stokes equation.

It is seen from each presented example, that the Hamilton principle (2.7) allows only the determination of those terms of the transport equations which are independent of time. The complete transport equations can only be deduced from the Euler—Lagrange equations (1.8) belonging to the true integral principle of thermodynamics.

3. Thermodynamics and canonical formalism

On the basis of what has been said so far it is reasonable — even as a problem of curiosity — to examine the existence of canonical formalism in thermodynamics. First let us define a canonical formalism valid for a real scalar field quantity Γ_j in the case, when the Lagrangian density $\mathscr{L}$ and the Lagrange function L are known as given by (2.1) and (2.2), respectively. We may start by changing the Lagrangian density $\mathscr{L}$ in (2.7) to the global Lagrange function L by means of the following functional (or variational) derivatives [10]:

$$\frac{\delta L}{\delta \Gamma_j} = \frac{\partial \mathscr{L}}{\partial \Gamma_j} - \sum_{\alpha=1}^{3} \frac{\partial}{\partial x_\alpha} \frac{\partial \mathscr{L}}{\partial \left(\frac{\partial \Gamma_j}{\partial x_\alpha} \right)}, \quad \text{and} \quad \frac{\delta L}{\delta \dot{\Gamma}_j} = \frac{\partial \mathscr{L}}{\partial \dot{\Gamma}_j}. \tag{3.1}$$

With these, (2.7) may be written in the form

$$\frac{d}{dt} \frac{\delta L}{\delta \dot{\Gamma}_j} - \frac{\delta L}{\delta \Gamma_j} = 0. \tag{3.2}$$

This Euler—Lagrange equation is formally similar to the corresponding equations of point mechanics. Let us now define the impulse conjugated to the field quantity $\Gamma_j = \Gamma_j(\mathbf{r}, t)$ by making use of this formal similarity, in the following manner:

$$\pi_j(\mathbf{r}, t) = \frac{\delta L}{\delta \dot{\Gamma}_j} = \frac{\partial \mathscr{L}}{\partial \dot{\Gamma}_j}, \tag{3.3}$$

then from (3.2) and (3.3) for the time derivative of these field quantities we get

$$\dot{\pi}_j(\mathbf{r}, t) = \frac{\delta L}{\delta \Gamma_j}. \tag{3.4}$$

Introducing the Hamilton density

$$\mathscr{H} = \pi_j \dot{\Gamma}_j - \mathscr{L} \tag{3.5}$$

the Hamilton function will be:

$$H = \int_V \mathscr{H}\, dV. \tag{3.6}$$

From these expressions the canonical equations valid for a Γ_j scalar field quantity is immediately obtained. Since, with the aid of (3.3), $\dot{\Gamma}_j$ can be eliminated from $\mathscr{H}$, the latter will be the functional of Γ_j and π_j only. Therefore,

$$\delta H = \int_V \left(\frac{\delta H}{\delta \Gamma_j}\, \delta \Gamma_j + \frac{\delta H}{\delta \pi_j}\, \delta \pi_j \right) dV \tag{3.7}$$

where the functional derivatives over the field quantities Γ_j and π_j are interpreted in a manner analogous to the first equation of (3.1):

$$\frac{\delta H}{\delta \Gamma_j} = \frac{\partial \mathscr{H}}{\partial \Gamma_j} - \sum_{\alpha=1}^{3} \frac{\partial}{\partial x_\alpha} \frac{\partial \mathscr{H}}{\partial \left(\frac{\partial \Gamma_j}{\partial x_\alpha} \right)}, \tag{3.8}$$

and

$$\frac{\delta H}{\delta \pi_j} = \frac{\partial \mathscr{H}}{\partial \pi_j} - \sum_{\alpha=1}^{3} \frac{\partial}{\partial x_\alpha} \frac{\partial \mathscr{H}}{\partial \left(\frac{\partial \pi_j}{\partial x_\alpha} \right)}. \tag{3.9}$$

On the other hand, the variation of L can be given with the variation of Γ_j and $\dot{\Gamma}_j$ as follows:

$$\delta L = \int_V \left(\frac{\delta L}{\delta \Gamma_j}\, \delta \Gamma_j + \frac{\delta L}{\delta \dot{\Gamma}_j}\, \delta \dot{\Gamma}_j \right) dV = \int_V (\dot{\pi}_j\, \delta \Gamma_j + \pi_j\, \delta \dot{\Gamma}_j)\, dV =$$

$$= \int_V \left[\delta(\pi_j \dot{\Gamma}_j) + \dot{\pi}_j\, \delta \Gamma_j - \dot{\Gamma}_j\, \delta \pi_j \right] dV = \delta H + \delta L + \int_V (\dot{\pi}_j\, \delta \Gamma_j - \dot{\Gamma}_j\, \delta \pi_j)\, dV, \tag{3.10}$$

meanwhile the expressions (3.3), (3.4), (3.5) and (3.6) have been used. From the last relation, however, it follows that

$$\delta H = - \int_V (\dot{\pi}_j\, \delta \Gamma_j - \dot{\Gamma}_j\, \delta \pi_j)\, dV \tag{3.11}$$

which on comparing with (3.7) yields the following canonical equations:

$$\dot{\Gamma}_j = \frac{\delta H}{\delta \pi_j}, \qquad \dot{\pi}_j = - \frac{\delta H}{\delta \Gamma_j}. \tag{3.12}$$

Let us apply now the given apparatus to write the canonical equations pertaining to the temperature field, the field of chemical potentials, and

the velocity field of a viscous fluid system. With the use of the Lagrangian densities (1.2), (2.11) and (1.4) we obtain the generalized impulse of the temperature field, chemical potential fields, and the velocity field from (3.3). These are:

$$\pi_T = \varrho\, c_v T\,, \qquad \pi_\Gamma = \varrho \sum_{k=1}^{K-1} \gamma_{ik}\, \Gamma_k\,, \quad \boldsymbol{\pi}_v = \varrho \mathbf{v}\,. \tag{3.13}$$

The last expression is, indeed, the impulse density of the streaming fluid. The Hamiltonian densities (3.5) with these expressions can be immediately given. Thus, the Hamiltonian density of the temperature field is

$$\mathscr{H}_T = -\frac{\lambda}{2} (\nabla T)^2\,, \tag{3.14}$$

i.e., it is just the negative of the second (spatial) term of Lagrangian density (1.2). Similarly, the Hamiltonian density of the chemical potential fields is:

$$\mathscr{H}_\Gamma = -\frac{1}{2} \sum_{i,k=1}^{K-1} L_{ik} \nabla \Gamma_i \nabla \Gamma_k\,. \tag{3.15}$$

Finally, the Hamiltonian density of a viscous fluid system from (3.5) is:

$$\mathscr{H}_v = \varrho \mathbf{v} \cdot \mathbf{F} - \mathbf{v} \cdot \operatorname{grad} p - \frac{1}{2}\left(\eta_v - \frac{2}{3}\eta\right) (\operatorname{div} \mathbf{v})^2 - \eta \left[(\operatorname{grad} \mathbf{v})^s\right]^2 \tag{3.16}$$

which is again the negative of the Lagrangian density (1.4), disregarding the term containing the time derivative. It might also be significant, that the Hamiltonian densities are identical with the negative expressions of the corresponding dissipation functions ψ. (In particular, in case of heat conduction, $\mathscr{H}_T = -T^2 \psi$, according to the Fourier picture [2.4].) Now since these local dissipation functions ψ are the unambiguous measures of the energy dissipated per unit volume and unit time of the continuum during heat conduction, diffusion or viscous flow, thus the same must be valid for the Hamiltonian densities. If the Hamiltonian densities are known, on the basis of (3.13) the first group of the canonical equations can be immediately given. Since $\mathscr{H}_T$ and $\mathscr{H}_\Gamma$ do not contain the impulse densities π_T and π_Γ, the first group of the canonical equations does not exist in case of a temperature field or a chemical potential field. For the velocity field of a viscous fluid from (3.12) and (3.16) we obtain that the acceleration is equal to the external force acting upon the unit mass, *i.e.*,

$$\frac{dv_\alpha}{dt} = F_\alpha \qquad (\alpha = x_1, x_2, x_3\,,) \tag{3.17}$$

which is really expected from the nature of canonical formalism. With the aid of (3.8) and (3.13), the second group of the canonical equations may be written in the form:

$$\varrho c_v \frac{dT}{dt} = - \nabla \cdot (\lambda \nabla T),$$

$$\varrho \sum_{k=1}^{K-1} \lambda_{ik} \frac{d\Gamma_k}{dt} = - \sum_{k=1}^{K-1} \nabla \cdot (L_{ik} \nabla \Gamma_k), \tag{3.18}$$

$$\varrho \frac{d\mathbf{v}}{dt} = - \left\{ \varrho \mathbf{F} - \operatorname{grad} p + \eta \Delta \mathbf{v} + \left(\frac{\eta}{3} + \eta_v \right) \operatorname{grad} \operatorname{div} \mathbf{v} \right\}$$

if ϱ, c_v and γ_{ik} are constants. Though these equations are differing only in sign from the equations of heat conduction and diffusion, and from the Navier—Stokes equations, it is evident that transport equations cannot be regarded as the second group of the canonical field equations. Namely, on the left hand side of the equations (3.18) stands the time derivative of the impulse densities (3.13), but this time derivative arises from the last term of (2.7), corresponding to the nature of the Hamilton principle and the canonical formalism. Owing to the fact that this term does not occur in the Euler—Lagrange equations (1.8) belonging to the thermodynamic integral principle (1.7), the similarity of equations (3.18) to the transport equations may be considered accidental. Thus, we have to state, in spite of several interesting conclusions, that only the integral principle (1.7) is equivalent with the total system of transport equations.

The author is indebted to his co-worker Mr. J. VERHÁS for having revised the manuscript. Thanks are also due to Prof. Dr. G. SCHAY for his stimulating interest in this work and for his constant help.

SUMMARY

The relationship between the thermodynamic integral principle, developed by us, and the Hamilton principle has been discussed. Several similarities and differences lead to the conclusion that the Hamiltonian type integral principle corresponds only to the time-independent parts of transport equations describing irreversible processes. This fact indicates that PRIGOGINE'S principle of minimum production of entropy is in a more intrinsic relation with the Hamiltonian type principles than our integral principle. Finally, the existence of canonical formalism was examined in thermodynamics. Though in this respect many interesting conclusions could be drawn, as a final conclusion it must be stated that alone the integral principle developed by us is equivalent to the total system of transport equations.

REFERENCES

1. GYARMATI, I.: Zhurn. Fiz. Khim. Moscow. **39,** 1489 (1965).
2. GYARMATI, I.: Acta Chim. Hung. **43,** 535 (1965).
3. GYARMATI, I.: Periodica Polytechnica **9,** 205 (1965).
4. GYARMATI, I.: Acta Chim. Hung. **47,** 63 (1965).
5. VERHÁS, J.: Periodica Polytechnica **9,** 209 (1965).
6. VERHÁS, J.: Zhurn. Fiz. Khim., in print.
7. PRIGOGINE, I.: Bull. Acad. roy. Belg. Cl. Sc. **40,** 471 (1954).
8. VERHÁS, J.: Z. phys. Chem. (under publication).
9. BÖRÖCZ, Sz.: Z. phys. Chem. (under publication).
10. YOURGRAU, W., MANDELSTAM, S.: Variational Principles in Dynamics and Quantum Theory, Second edition. (Pitman and Sons, Ltd., London), 1960.

Zusammenhänge zwischen dem Integralprinzip der Thermodynamik und dem Hamiltonschen Prinzip

I. GYARMATI

Zusammenfassung. Der Zusammenhang des vom Verfasser bereits früher dargelegten thermodynamischen Integralprinzips mit dem Hamiltonschen Prinzip wurde besprochen. Aus dieser Besprechung ging neben zahlreichen anderen Ähnlichkeiten und Unterschieden hervor, daß aus dem Hamiltonschen Integralprinzip nur die von der Zeit unabhängigen Teile der die irreversiblen Vorgänge beschreibenden Transportgleichungen folgen. Dies weist darauf hin, daß das Prigoginsche Prinzip der minimalen Entropieproduktion mit den Prinzipien vom Hamiltontyp in einem viel engerem Zusammenhang steht, als das vom Verfasser früher dargelegte Integralprinzip. Schließlich wurde die Existenzmöglichkeit des kanonischen Formalismus in der Thermodynamik untersucht. Obwohl man in dieser Beziehung auch zu zahlreichen interessanten Folgerungen gelang, wurde letzten Endes festgestellt, daß nur das vom Verfasser dargelegte Integralprinzip mit dem vollkommenen System der Transportgleichungen gleichwertig ist.

Зависимости между термодинамическим интегральным принципом и принципом Гамильтона

И. ДЬЯРМАТИ

Резюме. Обсуждается связь изложенного автором термодинамического интегрального принципа с принципом Гамильтона. Наряду с многочисленным сходством и разницей принципов, найдено, что из интегрального принципа типа Гамильтона вытекают только независимые от времени части транспортных уравнений, описывающих необратимые процессы. Этот факт указывает на то, что принцип минимальной продукции энтропии типа Пригогине более тесно связан с принципами типа Гамильтона, нежели с изложенным выше принципом. Наконец, исследовалась экзистенция канонического формализма в термодинамике. Несмотря на то, что автор и в этом отношении пришел к многочисленным интересным результатам, он старается зафиксировать в качестве окончательного результата тот факт, что только изложенный выше интегральный прицип является эквивалентным с полной системой транспортных уравнений.

Dr. István GYARMATI, Budapest XI. Gellért tér 4.

VAPOUR PRESSURE OF SOLID D_2O

I. KISS, G. JÁKLY and Mrs. H. ILLY

(Central Research Institute for Physics, Budapest)

Received January 12, 1965

Introduction

While the vapour pressure of liquid heavy water is known over a wide range of temperatures to high accuracy [1], that of solid D_2O has been measured with apparently discrepant results, as reported in the literature. BARTHOLOME and CLUSIUS [2], as well as NIWA and SHIMAZAKI [3] measured the vapour pressure of D_2O in the temperature range between the melting point temperatures of light and heavy water. The saturated vapour pressure of solid D_2O was investigated by direct manometry in the experiment performed by JOHANNIN-GILLES and JOHANNIN [4] and the values reported on the vapour pressure of D_2O and of ice with natural isotopic concentration at — 24°C are seen to be equal. This seems to be inconsistent with the observations reported on other compounds with different isotopic concentrations as well as with the theoretical predictions of increasing relative difference between the vapour pressures of isotopic varieties with decreasing temperatures.

Mixtures of light and heavy water are known to contain also HDO molecules. Water of exclusively this type, however, cannot be produced because of the current recombination of the molecules governed by the equilibrium formula

$$H_2O + D_2O \rightleftharpoons 2\ HDO. \qquad (1)$$

The HDO vapour pressure is taken to be the geometrical mean value of the vapour pressures measured on pure H_2O and pure D_2O (*e.g.* [1]). The validity of this approximation, known as the rule of the geometrical mean [5], has not yet been confirmed in the case of water by experimental evidence from direct measurements of vapour pressure. The data reported by MERLEVANT et al. [6] who measured the liquid—vapour equilibrium on natural water cannot be considered as conclusive evidence, they even seem to indicate some deviation from the predicted rule. In a recent paper of NARTEN [7] a comparison of the results reported by MERLEVANT et al. concerning the vapour pressure of HDO with WHALLEY's equation [8] obtained for the vapour pressure of D_2O, leads the author to question the validity of the rule of the geometrical mean in this case.

The growing extensiveness of investigations with the use of heavy water calls for the ever more accurate knowledge of the physico-chemical properties of this system which necessitates the elucidation of problems like those mentioned above.

In an earlier paper of one of the present authors [9] measurements have been reported in which the anomaly found by JOHANNIN-GILLES, JOHANNIN could not be observed. The experimental accuracy of the results then obtained was insufficient to permit more than the bare statement of this fact. Improve-

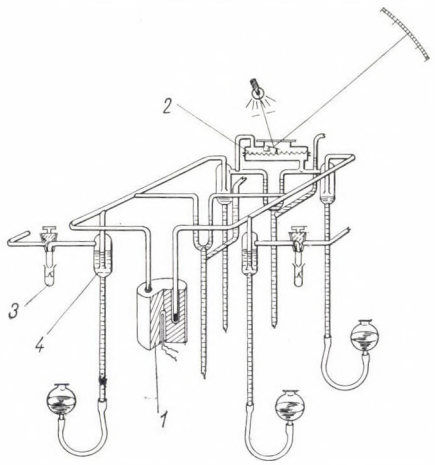

Fig. 1. Differential manometer with membrane; (1) equilibrium vessels, (2) sensin ε ccn cr t, (3 sample, (4) mercury seal

ment of the experimental setup made it possible now to perform measurements of higher accuracy on the vapour pressure of D_2O and HDO at temperatures below the freezing point.

Experimental method

The temperature behaviour of vapour pressure was evaluated for the different isotopic varieties involved from the differences between the vapour pressures measured on water of natural isotopic composition, D_2O and their mixture with 50 at. % D concentration. The experimental setup is shown in Fig. 1. In the measurement an extra-sensitive differential manometer, developed at our Laboratory was used. The membrane was a concentrically corrugated copper plate of 0.03 mm thickness and 10 cm in diameter. The pressure on the membrane was indicated by the displacement of a light beam reflected from the mirror mounted on the membrane, 1 m displacement of the light signal on the screen being equivalent to a pressure difference of 1 mmHg. Two holes of identical dimensions and positions drilled into a copper block, joined by metal to glass soldering to the glass components of the manometer, served to hold the samples (equilibrium vessels). The temperature of the equilibrium vessels was measured by iron-constantan thermocouple.

The manometer and the measuring assembly were calibrated for the vapour pressure of water, known to high accuracy [10], by filling one of the equilibrium vessels with water,

keeping the other at vacuum pressure of 10^{-6} mmHg. In the calibration measurement the sensitivity of the sensing element was found to be 5.10^{-3} mmHg for pressure differences up to 1.6 mmHg.

The thermocouple was calibrated at temperatures below $-35°C$ by measuring the vapour pressure of pure NH_3, while at higher temperatures with the use of calibrated thermometer of 0.1°C accuracy. The method proved to be inadequate for measuring differences in vapour pressure at temperatures close to the freezing points of both water and heavy water owing to the thermal effect of phase transformation and the simultaneous presence of two condensed phases.

The purification of the water samples was carried out by repeated distillation and repeated alternating boiling off and freezing out outgassing techniques. The samples were distilled from ampoule with break-seal, connected by ground joint to the feeder pipe, into the equilibrium vessel kept at vacuum pressure and at low temperature. 0.2 to 0.3 ml samples were used in the measurement.

Results and discussion

The results of the measurements covering the temperature range from $-40°$ to $+10°C$ are listed in Table I. The vapour pressure of the mixture with 50 at.% D concentration was evaluated also by measuring its difference from that of pure D_2O in order to check the reliability of the method. The values thus obtained agree within 1.5% with those listed in the table. Since the relative data include the error of the values obtained from the D_2O vapour pressure measurement, the results considered in the following will be only those obtained relative to H_2O vapour pressure.

The measurements are seen to confirm the earlier results which have shown that the vapour pressures of H_2O and D_2O at $-24°C$, contrary to the observations of JOHANNIN-GILLES and JOHANNIN, are not equal and the vapour pressure of D_2O below this temperature does not increase as compared with H_2O but the increase in the relative vapour pressure difference continues to be monotonical as the temperature decreases.

The values obtained in the vapour pressure measurement on the mixture of light and heavy water with 50 at.% D concentration confirm *the validity of the rule of the geometrical mean* in the temperature range covered by the measurement. The equilibrium distribution coefficient defined from (1) as

$$K = \frac{[HDO]^2}{[H_2O]\,[D_2O]}$$

is given in the literature as follows

K at 0°C		
3.94	UREY et al.	1947 [11]
3.76	KIRSHENBAUM	1951 [1]
4.15	NARTEN	1964 [7]
4.0 (25°C)	PYPER, LONG	1964 [12]

Table I

t C°	P_{H_2O} [10] mmHg	P_{D_2O} exp. mmHg	P_{HDO} calc. mmHg	$P_{50\%D_2O}$ exp. mmHg	$\left(\frac{\sqrt{P_{H_2O}}+\sqrt{P_{D_2O}}}{2}\right)^2$ mmHg	Δ %
−39.8	0.0988	0.0683				
−36.1	0.1490	0.1020				
−33.2	0.2040	0.1440				
−30.3	0.2775	0.1975				
−28.0	0.351	0.251	0.297	0.298	0.299	−0.33
−26.0	0.430	0.310	0.367	0.368	0.369	−0.27
−23.7	0.541	0.402	0.466	0.468	0.469	−0.21
−21.6	0.665	0.491	0.571	0.575	0.575	0.00
−18.7	0.879	0.657	0.759	0.761	0.764	−0.39
−16.7	1.060	0.794	0.917	0.920	0.922	−0.22
−14.6	1.288	0.969	1.117	1.124	1.123	+0.10
−12.5	1.559	1.185	1.359	1.366	1.365	+0.07
−10.5	1.866	1.425	1.631	1.639	1.638	+0.06
− 8.3	2.266	1.746	1.989	1.998	1.998	0.00
− 6.3	2.695	2.083	2.369	2.377	2.379	−0.08
− 4.2	3.225	2.512	2.846	2.847	2.858	−0.38
− 2.8	3.630	2.830	3.205	3.207	3.216	−0.28
− 1.5	4.045	3.174	3.583	3.597	3.596	+0.03
+ 5.0	6.543	5.443	5.968	5.971	5.980	−0.15
+ 5.8	6.917	5.767	6.316	6.322	6.329	−0.11
+ 6.5	7.259	6.062	6.634	6.644	6.647	−0.05
+ 7.2	7.617	6.363	6.962	6.979	6.976	+0.04
+ 7.9	7.990	6.685	7.308	7.326	7.323	+0.04
+ 8.6	8.380	7.028	7.674	7.695	7.689	+0.08
+ 9.3	8.786	7.398	8.062	8.072	8.077	−0.09

Taking the equilibrium coefficient to be approximately 4, it can be readily seen that the composition setting in on mixing equal mole quantities of H_2O and D_2O, will be 50% HDO, 25% H_2O and 25% D_2O. The vapour pressure of isotopic molecules for a mixture considered to be ideal, obeys Raoult's law, thus, in present case we have

$$P_{50\%D} = 1/4\, P_{H_2O} + 1/2\, P_{HDO} + 1/4\, P_{D_2O}.$$

Assuming the validity of the rule of the geometrical mean

$$P_{HDO} = (P_{H_2O} \cdot P_{D_2O})^{1/2} \qquad (2)$$

we obtain

$$P_{50\%D} = \left(\frac{P_{H_2O}^{1/2} + P_{D_2O}^{1/2}}{2} \right)^2 \tag{3}$$

Comparing now the experimental results with the predictions from (3), it is seen that the deviations do not exceed the value of the experimental error. Consequently the HDO vapour pressure can be calculated by Eq. (2).

The temperature dependence of the vapour pressure was calculated from the values listed in Table I for each of the combinations H_2O, HDO and D_2O by making use of the Clapeyron equation

$$\log P = -\frac{A}{T} + B .$$

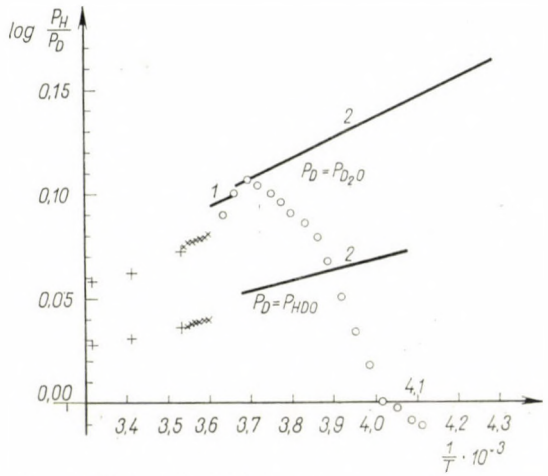

Fig. 2. Comparison of D_2O and HDO vapour pressure data reported in the literature NIWA and SHIMAZAKI (1); JOHANNIN-GILLES and JOHANNIN (○); KIRSHENBAUM (+); our measurements (2 and ×)

The coefficients computed by the method of least squares were found to be

	A	σ	B	σ
D_2O	2767.1	4.2	10.687	0.016
HDO	2718.2		10.559	

The results are compared with those reported in the literature in Fig. 2 by plotting, for convenience, the temperature dependences for log P_{H_2O}/P_{D_2O}.

The average value of the sublimation temperature of D_2O, as evaluated from the pressure equations for the temperature range from 0° to −40°C, was found to be

12,663.7 cal/mole

in good agreement with the data obtained by BARTHOLOME and CLUSIUS in direct measurement, namely, 12,631 ± 20 cal/mole at 3.8°C and 12,635 ± 20 cal/mole at 0°C.

Authors are indebted to Mr. L. MATUS and Mr. G. JANCSÓ for valuable discussions.

SUMMARY

The vapour pressure of solid D_2O has been measured in the temperature range from −40° to 0°C. The results show, contrary to the anomaly observed by JOHANNIN-GILLES and JOHANNIN, an increase in the relative vapour pressure difference between H_2O and D_2O with decreasing temperatures. The HDO vapour pressure at temperatures below 0°C determined from the vapour pressure measured on a H_2O and D_2O mixture with 50 at. % D concentration is found to obey the rule of the geometrical mean.

REFERENCES

1. KIRSHENBAUM, J.: Physical properties of heavy water, McGraw-Hill Book Co., New York, 1951.
2. BARTHOLOME, E., CLUSIUS, K.: Z. Phys. Chem. **B/28,** 175 (1935).
3. NIWA, K., SHIMAZAKI, E.: Faculty Sci. Hokkaido Imp. Univ. Ser. III. **3,** 35 (1940).
4. JOHANNIN-GILLES, A., JOHANNIN, P.: Compt. rend. **239,** 1470 (1954).
5. BIGELEISEN, J.: J. Chem. Phys. **23,** 2264 (1955).
6. MERLEVANT, L., BOTTER, R., NIEF, G.: J. Chim. Phys. **60,** 56 (1963).
7. NARTEN, A.: J. Chem. Phys. **41,** 1318 (1964).
8. WHALLEY, E.: Proceedings of the Joint Conference on Thermodynamic and Transport Properties of Fluids, Institute of Mechanical Engineering, London, 1957, p. 15.
9. KISS, I., MATUS, L.: MTA Központi Fizikai Kutató Intézetének Közleményei **10,** 61 (1962).
10. LANGE, N. A.: Handbook of Chemistry, 10th Ed., McGraw-Hill, New York, 1961, p. 1462.
11. UREY, H. C.: J. Chem. Soc. **1947,** 562.
12. PYPER, W. J., LONG, F. A.: J. Chem. Phys. **41,** 2213 (1964).

Über die Tension des festen Deuteriumoxids

I. KISS, GY. JÁKLI und H. ILLY

Zusammenfassung. Die Tension des festen Deuteriumoxids wurde im Temperaturintervall von −40° bis 0°C bestimmt. Auf Grund der Angaben wurde festgestellt, daß — in Gegensatz zur durch JOHANNIN-GILLES und JOHANNIN gefundenen Anomalie — der zwischen den Tensionen vom H_2O und D_2O bestehende relative Unterschied mit der Erniedrigung der Temperatur zunimmt. Auf Grund der Messung der Tension des 50 Atom % Deuterium enthaltenden H_2O-D_2O-Gemisches wurde nachgewiesen, daß bei Temperaturen unter 0°C die sogenannte Regel des geometrischen Mittels in Bezug auf die Tension des HDO gültig ist.

Давление пара твердой окиси дейтерия

И. КИШШ, ДЬ. ЯКЛИ и Х. ИЛЛИ

Резюме. Измерено давление паров твердой D_2O в интервале температур −40° — 0° С и установлено, что в противоположность аномалии, найденной Йоханнин-Гиллесом и Йоханнином, относительная разница в давлении паров H_2O и D_2O растет с уменьшением температуры. На основании измерений давления паров смеси H_2O — D_2O с 50 атом % D, установлено, что при температуре ниже 0° С для давления паров HDO действительно, так называемое, правило геометрического среднего.

István KISS
György JÁKLY
Mrs. H. ILLY
Budapest XII., Konkoly-Thege M. út

NEW METHOD FOR THE QUANTITATIVE ANALYSIS OF COMBUSTION PROCESSES WITH TOEPLER'S PARALLEL BEAM SCHLIEREN APPARATUS

A. NÉMETH and O. SZALAY

(Hungarian Oil and Gas Research Institute)

Received April 9, 1965

The intensive study of combustion processes calls pressingly for the development of measuring methods, which permit measuring of the quick changes taking place during combustion, without interfering with the process. Schlieren photography, meeting this requirement, has found use in qualitative analysis, and a few schlieren techniques suitable for quantitative analysis have also been developed.

Essentially, these methods involve the collecting of parallel beams that have passed through the flame on a slit placed in the focal plane of a lens. Photographs are taken at different positions of the slit, and the distance between two bands, appearing on the picture due to the light deflection, is measured [1].

To develop a method convenient for practical work, two approaches have been made. In both cases another slit is placed in the path of the light before the flame. According to one modification, this slit is arranged diagonally before the flame. In this case, the band obtained for the slit on light deflection shows a curvature. According to a further modification, several parallel slits are used, arranged diagonally, instead of a single slit. Actually, this arrangement gives directly, with the aid of one photograph, the distribution of the light deflection, with one point for each slit used.

According to the other modification, marking aperture is placed in the plane of the image of the slit [2, 3]. The displacement of the image of the slit, that is to say the deflection of light can be determined on the basis of the marking aperture constant. The momentary position of the image of the slit in uncovered state is easier to identify, if the apertures of the grate are covered with coloured glass. Thus, conclusions may be drawn from the colours of the object on the magnitude of the angular deflection.

In all these methods the angles of deviation have been actually determined by measurements of distance on the photograph. The method described below is based essentially on intensity measurements by densitometry. This method was first proposed by SCHARDIN [4], who found a correlation for the change in illumination intensity produced by undeflected light. Up to now,

this method involved the forming of a bubble — as a densitometric standard — with the aid of a film forming agent from a reference medium of known refractive index, *e.g.* from helium. This bubble is introduced into the medium to be tested. The testing light beam is passed through the system, and the change in illumination of the picture is measured. This method has been applied successfully, among others, for the evaluation of mixing processes [5]; however, this technique would be inconvenient under conditions existing in combustion processes and flames.

In developing our method, we started from the basic correlations characteristic of TOEPLER's schlieren apparatus. The working principle of the apparatus is shown in Fig. 1. Light rays emitted by the source F pass through the condenser K and are focussed on the slit R. Rays starting from slit R are collimated by the first objective O_1, so that a parallel light beam may be as-

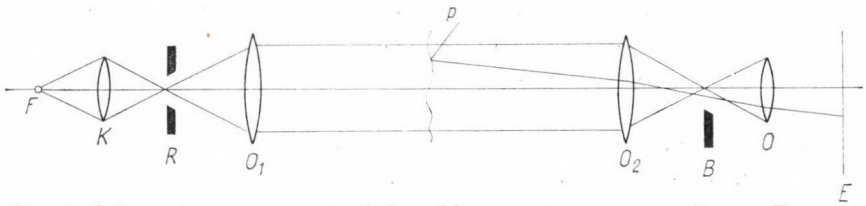

Fig. 1. Schematic arrangement of the schlieren apparatus according to TOEPLER

signed to each point of the slit. These elementary parallel light beams will have different directions corresponding to the different points of the slit. The second objective, O_2, produces the real image of slit R in its focal plane. Through point P, placed in between the two objectives, one light ray will pass from each of the elementary parallel light beams. In the plane of the image of the slit, this light cone is focussed to an elementary image of the slit. A marking aperture, B, is applied in the plane of the image of the slit. Essentially, this marking aperture is a knife terminating in a straight line, and is arranged parallel to the longitudinal edge of the slit. The objective O serves for the forming of the image of the object studied. When an object is placed between the lenses O_1 and O_2, which deflects the light ray at the point P, and if this deflection is perpendicular to the edge of the marking aperture, this latter will cover one part of the image of the slit corresponding to point P. Consequently, the intensity of the original illumination will change on the corresponding point of the image on screen E.

Next, let us examine the displacement of the image of the slit caused by an angular deflection θ of the light in point P of the object. According to Fig. 2, the displacement Δs of the image of the slit is:

$$\Delta s = f_2 \operatorname{tg} \theta \,, \tag{1}$$

where f_2 is the focal length of the objective O_2.

Since θ is generally small for gases, the following approximation is permissible:

$$\Delta s \simeq f_2 \, \theta \, , \tag{2}$$

where θ is expressed in radians, and Δs and f_2 are given in the same unit.

If the light ray is not deflected between O_1 and O_2, and the optical adjustment is correct, the illumination of the screen will be uniform. However, the intensity of the illumination will change, if a lesser or greater part of the

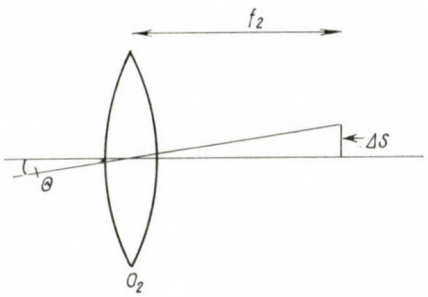

Fig. 2. Displacement of the image of the slit in the focal plane of O_2 $\Delta s = f_2$ tg θ

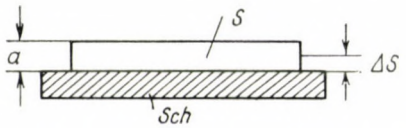

Fig. 3. Linear dependence of the intensity of illumination on the displacement Δs of the schlieren marking aperture

slit image is covered by the marking aperture. Since the intensity of the illumination depends only on the relative positions of the marking aperture and the slit image, an identical displacement of the marking aperture or of the slit image will cause the same change in the intensity of the illumination (if the marking aperture and the slit are suitably designed). When correct design is ensured, the illumination of the screen will change linearly, as the marking aperture is displaced by Δs (Fig. 3).

$$I = \alpha_1 + \alpha_2 \, \Delta s, \tag{3}$$

where I is the intensity of the illumination, α_1 and α_2 are constants characteristic of the apparatus and the basic adjustment.

To verify this relation, the intensity of the illumination of the image was determined at different positions of the marking aperture. It may be seen from Fig. 4 that the relation $I = f(\Delta s)$ is represented in good approximation by a straight line.

Thus, it has been shown on one hand that an unequivocal correlation exists between the angular deflection of the light rays and the displacement of the image of the slit; on the other hand, a correlation has been established between the intensity of the illumination and the displacement in the described optical system. It follows that when tg θ is substituted by θ, a linear correlation

exists also between the angular deflection produced by the object examined and the intensity of the illumination measured on the screen. From Equations (2) and (3)

$$\theta = \frac{1}{\alpha_2 f_2} \quad I - \frac{\alpha_1}{\alpha_2 f_2}. \tag{4}$$

Accordingly, for a fixed optical adjustment an unequivocal mutual relation exists between θ and I, and θ and Δs, respectively.

The determination involves therefore actually two steps. First, the con-

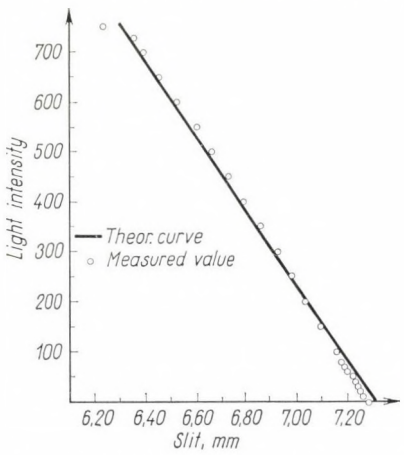

Fig. 4. The change of the intensity of light on the opaque plate of the schlieren apparatus in function of the position of the schlieren marking aperture

stants of Equation (3) are determined, that is to say, the exposure values are obtained for different marking aperture positions. From the intensity values of the illumination observed on the picture made of the object to be tested, the light deflections corresponding to the same points can be calculated from Equation (4).

In practice the determination can be further simplified by comparing the measured values of intensity with the same degree of intensity of a measured reference series, omitting thereby the determination of the absolute intensity. In this case, only the mutual unequivocal relation, given by Equation (3) is used. It follows that the method is applicable to any kind of slit and making aperture (thus, *e.g.*, in case of a point-type making aperture). The procedure of the determination consists of the following steps:

1. Corresponding to the purpose and the specific characteristics of the test, the marking aperture is adjusted to zero-setting.

2. Starting from this zero setting of the marking aperture, a series of pictures are taken at different values of Δs, in the absence of the substance to be tested.

3. On the basis of the equation $\Delta s \simeq \theta f_2$, a value of θ can be unequivocally assigned to each value of Δs.

4. The picture series mentioned in Paragraph 2 is photometered, assigning thus to each element of the series a definite value read on the scale of the photometer. (In principle, any kind of scale can be used.)

5. On the basis of Paragraphs 4 and 3, the function $\theta = \theta$ (scale reading) can be given.

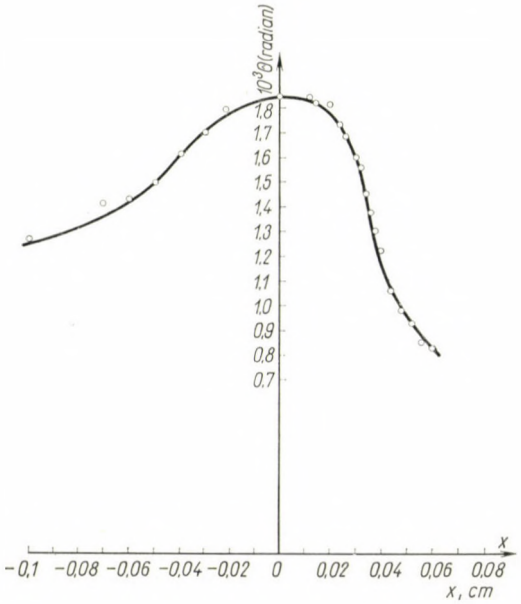

Fig. 5. Angular deflections measured in the elementary flame profile of a flat flame, perpendicularly to the profile of the flame. (Stoichiometric methane-air mixture. Axis x is perpendicular to the elementary flame profile, the origo is at the point where schlieren has its maximum. The path of the parallel light beam is parallel with the tangential plane of the elementary flame profile.)

6. A photograph is made of the object to be tested at a marking aperture setting according to Paragraph 1.

7. The schlieren picture — photographed on the same film as the above picture series — is photometered.

8. The angular deflection θ of the light rays at the individual points of the object can be given on the basis of the function $\theta = \theta$ (scale reading), mentioned in Paragraph 5.

To illustrate the applicability of the measuring method, Fig. 5 shows the angular deflections of light, measured perpendicularly to the generatrix of the cone in the flame of a methane-air mixture. According to experience, the shape of the curve shows that, starting from the side of fresh gas, the angle of deviation increases continuously to attain a maximum value corresponding

to the preheating zone, and decreases then continuously as product gases leave the reaction zone.

SUMMARY

A new method, based on the determination of blackening has been developed and applied in the schlieren records of combustion processes. It is shown theoretically that a mutual and unequivocal correlation exists in case of a fixed optical adjustment between the angular deflection of the light rays and the blackening, and between this angle and the displacement of the marking aperture. This makes the determination of the absolute blackening, that usually involves difficulties, unnecessary. It is sufficient to compare the measured blackening values with a measured reference series of blackenings. The applicability of the method is demonstrated by an example.

REFERENCES

1. Burgoyne, I., Weinberg, F.: Fourth Symposium on Combustion, Williams-Wilkins, Baltimore, 1953, p. 294.
2. Jeffree, H.: J. Sci. Instruments **33**, 29 (1926).
3. Thiele, W.: Jenaer Nachrichten **1958**, Nr. 2, 75.
4. Dery, J.: Third Symposium on Combustion, Williams-Wilkins, Baltimore, 1949, p. 235.
5. Keagy, W., Ellis, H.: Third Symposium on Combustion. Williams-Wilkins, Baltimore, 1949, p. 667.

Über eine neue Methode zur quantitativen Untersuchung von Verbrennungsvorgängen mittels Toeplerscher schlierenoptischer Einrichtung mit parallelem Strahlengang

A. NÉMETH und O. SZALAY

Zusammenfassung. Abweichend von den zur Untersuchung der Verbrennungsvorgängen bisher angewandten schlierenoptischen Methoden, wurde ein auf der Messung der Schwärzung fußendes Verfahren entwickelt. Es gelang nämlich zu beweisen, daß bei einer fixierten optischen Einstellung gegenseitig ein eindeutiger Zusammenhang zwischen dem Winkel der Richtungsänderung des Lichtstrahles und der Schwärzung, ferner zwischen dem genannten Winkel und der Blendenbewegung besteht. So kann man auf die bisher ziemlich schwer meßbaren Bestimmung des absoluten Schwärzungswertes verzichten. Statt dessen ist es genügend, die gemessenen Werte mit einer Vergleichsschwärzungsmeßreihe zu vergleichen. Die Brauchbarkeit des Verfahrens wurde durch Meßangaben veranschaulicht.

Новый метод количественного исследования процессов горения с помощью щелевой оптической установки Теплера, с параллельным ходом лучей

А. НЕМЕТ и О. САЛАИ

Резюме. Разработан метод для изучения явлений горения — отличающийся от используемых до настоящего времени щелевых оптических методов — основанный на измерении почернения. С помощью теоретических выводов доказали, что при фиксированной оптической наладке имеет место взаимооднозначная связь между углом изменения направления светового луча и почернением, а также между вышеуказанным углом и смещением диафрагмы. На основании этого, нет надобности в определении величины абсолютного почернения, представляющей до настоящего времени большие затруднения. Вместо этого достаточно сравнить измеренные величины с эталонами почернения. Используемость метода наглядно показана измерениями.

András Németh
Ottó Szalay } Veszprém, Wartha Vince u. 2—6.

HYDANTOINS, THIOHYDANTOINS AND GLYCOCYAMIDINES. XXIII*

QUATERNIZATION OF 2,5-BIS(METHYLTHIO)-4,4-DIPHENYL-4*H*-IMIDAZOLE AND THE REACTION OF THE QUATERNARY DERIVATIVE WITH NUCLEOPHILIC AGENTS

K. LEMPERT and K. ZAUER

(Department of Organic Chemistry, Technical University, and Research Group for Alkaloid Chemistry of the Hungarian Academy of Sciences, Budapest)

Received May 31, 1965

In order to carry out certain reactions which will be discussed in the following papers of this series, it was necessary to prepare a derivative of 2,5-bis(methylthio)-4,4-diphenyl-4*H*-imidazole (**I**) in which at least one of the ring carbon atoms linked to the methylthio groups possessed enhanced reactivity against nucleophilic agents as compared with that of the corresponding carbon atoms of the starting compound **I**. For this purpose derivatives of **I** carrying a positive charge on one of the ring nitrogen atoms as a consequence of quaternization were expected to be suitable.

In the present communication proof of the structure of the products (**II**) formed from **I** by methylating agents, and the reactions of **II** with some O-, N- and S-nucleophiles will be discussed.

On heeting in chlorobenzene with dimethyl sulfate, **I** yielded a poorly crystallizing compound which was found to be particularly sensitive to water and, on the basis of the analytical data and of its reactions, proved to be the methosulfate (**IIa**) of the quaternary methyl derivative of **I**. The position of the newly introduced methyl group was verified by the partial and total hydrolysis of the compound leading to the already known (see *e.g.* [3]) 1-methyl-4-methylthio-5,5-diphenyl-3-imidazolin-2-one (**III**) and to 1-methyl-5,5-diphenylhydantoin (**IV**), respectively.

Partial hydrolysis of **IIa** takes place when an aqueous or aqueous acetonic solution of **IIa** is simply allowed to stand for a few hours. The readiness to undergo hydrolysis confirms our presumption according to which, on introducing a positive charge to one of the nitrogen atoms of the imidazole ring, the reactivity of the product against nucleophilic agents will appreciably be raised. Similarly, partial hydrolysis takes place when **IIa** is boiled in aqueous ethanol *in the presence of pyridine or potassium hydroxide*. On carrying out the latter reaction in the *absence of bases*, total hydrolysis occurs, affording **IV**.

* Preliminary communication: LEMPERT, K. and ZAUER, K.: Tetrahedron Letters **1964**, 519.

Part XXII: LEMPERT, K. and NYITRAI, J.: Tetrahedron Letters **1965**, 2927.

The present paper was prepared partially on the basis of the B. Sc. thesis of K. ZAUER (Budapest, 1963).

Since compound **III**, on hydrolysis by mineral acids in aqueous ethanolic solution is also converted into **IV**, the direct total hydrolysis of **IIa** can be ascribed to the effect of the methylsulfuric acid formed in the first step. In the presence of bases, however, hydrolysis is stopped after the formation of **III** because the methylsulfuric acid is neutralized by the base.

The direction of the partial hydrolysis of **IIa** indicates that of the two methylthio groups activated by the positive charge, that linked to C-2 is

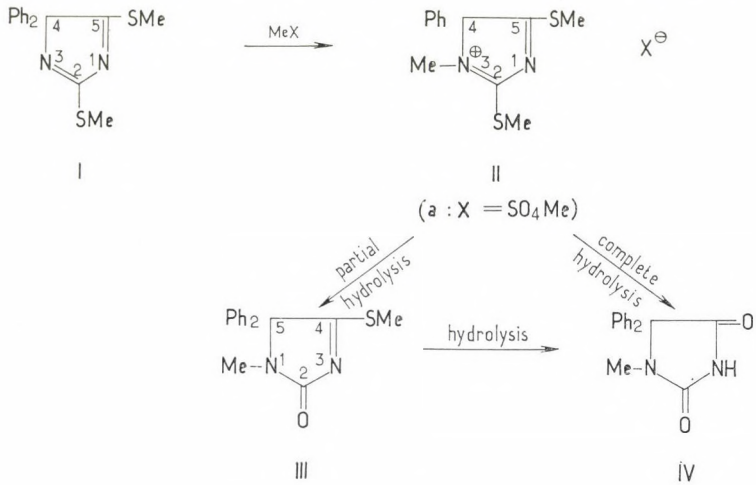

markedly more reactive (as observed already earlier also in the case of the non-quaternized compound **I** [4]).

Since compound **I** can be prepared by known procedures [3] from 5,5-diphenylhydantoin, *methylation at position* 1 of 5,5-diphenylhydantoin can be carried out by the reaction sequence described. So far, it was impossible to alkylate hydantoins selectively at position 1 because the first alkyl group is always introduced to N-3 [5].

Similarly to dimethyl sulfate, **I** can also be brought into reaction with methyl *p*-toluenesulfonate, methyl benzenesulfonate and methyl methanesulfonate, leading to the corresponding quaternary salts of **II**. However, these salts crystallize even poorer than **IIa**, and it was not possible to obtain them in an analytically pure crystalline state. The products obtained on hydrolysis of the crude oily substances proved nevertheless to be identical with those prepared from the methosulfate. This confirmed that quaternization took place also in these cases at N-1. From the quantity of **IV** formed on hydrolysis and from the observed sulfur content of crude **II** (X = *p*-Me-$C_6H_4SO_3$) the purity of this material could be estimated to be of the order of 90—95%, 5—10% of **III** being the contaminant.

*

In the followings, the reactions of **IIa** with N-nucleophiles will be described.

By treating **IIa** or **II** (X = *p*-Me-$C_6H_4SO_3$) in pyridine solution with 1 mole of benzylamine hydrochloride, it becomes converted into a monobenzylimide derivative. With respect to the higher electrophilic reactivity of C-2 proved above, structure **V** was assumed for this derivative.

It was impossible to verify the structure by way of direct hydrolytic degradation because **V** could be hydrolyzed neither by a mixture of acetic and hydrochloric acids, nor by ethanolic potassium hydroxide. Since, however,

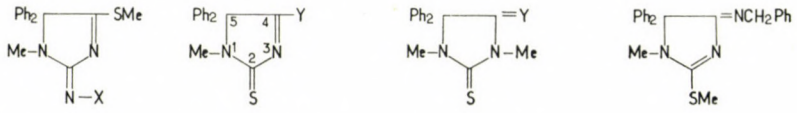

V : X = $PhCH_2-$
VI : X = OH
VII : X = PhNH

VIII : Y = SMe
IX : Y = $PhCH_2-NH-$*)

X : Y = S
XI : Y = $PhCH_2N=$

XII

* Although **IX** is potentially tautomeric, a "conjugated" C = N band appears at 1610 cm^{-1} in its infrared spectrum (KBr disc). This proves that the formula used above is correct, at least for the compound in crystalline state

according to our experiences [4], in compounds of structures similar to that of **V** the 4-methylthio group used to be relatively difficultly hydrolyzable, while in their isomers, where the double bond and the methylthio group are both linked to C-2 (*e.g.* in compound **XII** and in compounds of related structure), the methylthio group proved to be readily cleavable by aqueous acids, the observed stability against hydrolytic attacks of the examined compound is just an evidence in favour of structure **V**.

In order to prove the correctness of structure **V** exactly, the only possible structural alternative (**XII**) was prepared by the following way. First **VIII** [3] was allowed to react with benzylamine, and subsequently the 1-methyl-4-benzylamino-5,5-diphenyl-3-imidazoline-2-thione (**IX**) thereby obtained subjected to methylation. Although compound **IX** could react, in principle, at three centres (at N-3, at the exocyclic nitrogen or at the sulfur atom), under the applied experimental conditions only one product, the S-methyl derivative (**XII**) was formed.

The structure of this compound is proved by the fact that, on boiling with a mixture of glacial acetic and hydrochloric acids, it undergoes hydrolysis to 1-methyl-5,5-diphenyl-hydantoin-4-benzylimide (**XXI**; R = $C_6H_5CH_2$), which was also prepared by structure-proving synthesis (see below). For the rest, in accordance with these findings, the methylation product of **IX** was found to be different from compound **XI** obtained by a structure-proving synthesis,

viz. by reacting 1,3-dimethyl-5,5-diphenyl-dithiohydantoin (**X**) with benzylamine.*

Since compound **XII** proved to be different from the product obtained in the reaction of the quaternary compound **IIa** and benzylamine, this latter should necessarily possess structure **V**.**

*

Similarly, we succeeded in reacting **IIa** selectively with one mole of hydroxylamine in pyridine solution in a way that, under formation of compound **VI**, only one of the methylthio groups participated in the reaction. Structure **VI** for the product was verified, on the one hand, by the comparison of the ultraviolet spectra of the reaction product and the already known 2-hydroximino-4-methylthio-5,5-diphenyl-3-imidazoline (**XIII**) [4], and, on the other hand, by hydrolysis of **VI** by glacial acetic acid, affording the compound **III** already known [3].

*

Compounds **IIa** or **II** (X = *p*-Me-$C_6H_4SO_3$) yield in pyridine solution with one mole of phenylhydrazine hydrochloride or in ethanolic solution with one mole of phenylhydrazine base a monophenylhydrazone to which, on the basis of the above given analogies, formula **VII** may be assigned. In addition, this structure was also supported by the ultraviolet spectrum of the product which rather resembles that of compound **XIV** obtained from **I** with phenylhydrazine, the structure of **XIV** being already proved by hydrolysis [4]. Structure **VII** could, however, not be verified by hydrolysis as in the case of **VI**, because, on treatment with glacial acetic acid, **VII** did not react, while, on treatment with a mixture of acetic and hydrochloric acids, **VII** suffered "total" hydrolysis, affording **IV**; and the product of partial hydrolysis, viz. the 2-phenylhydrazone (**XV**) of 1-methyl-5,5-diphenylhydantoin could not be obtained either in pure state or by treatment with ethanolic alkali.

Structure **VII** was finally proved by quaternization of **VIII** with diethyl sulfate, leading to the quaternary salt **XVI**** (analogous to **IIa**) which, when

* It is known [3] that dithiohydantoins react with ammonia and with amines in a selective way at position 4.

** *Added in proof:*

By reacting crude **II** (X = *p*-Me-C_6H_4-SO_3), which has been exposed for some time to atmospheric moisture and, therefore, contained some free *p*-toluensulfonic acid, with 1 mole of benzylamine in the absence of any solvent, a compound melting at 249—250° was obtained which analysed for $C_{17}H_{16}N_2S$ and could be identified with 1,3-dimethyl-4,5-diphenyl-4-imi*p*azoline-2-thione [2]. The same substance was formed also by treatment of **II** (X = d-Me-C_6H_4-SO_3) pretreated as above, with 1 mole of potassium hydrogen sulfide in aqueous alcoholic solution. For the rearrangement involved in these reactions, which shall be investigated in the future, see also [2].

*** The structure of **XVI** is proved, besides the way of its formation, on the one hand, by the fact that, on treating **VIII** with dimethyl sulfate, it is converted analogously into **IIa**, and, on the other hand, that the reaction of **XVI** with phenylhydrazine affords the same product as the similar reaction of **IIa**.

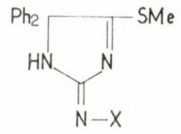

XIII : X = OH *)
XIV : X = PhNH—*)

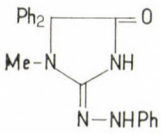

XV *)

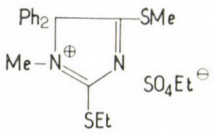

XVI

* A potentially tautomeric compound. Its existence in the above tautomeric form has not yet been verified.

allowed to react without isolation with phenylhydrazine, gave a product which was in every respect identical with **VII** obtained from **IIa**.

In addition, structure **VII** is verified by the fact that **VII** becomes converted by α-toluenethiol in the presence of the sodium salt of the latter into the analogous S-benzyl derivative (**XVII**) (cf. [6]) which latter compound can also be obtained by structure-proving syntheses either from **XVIII** [6] or from **XIX**.

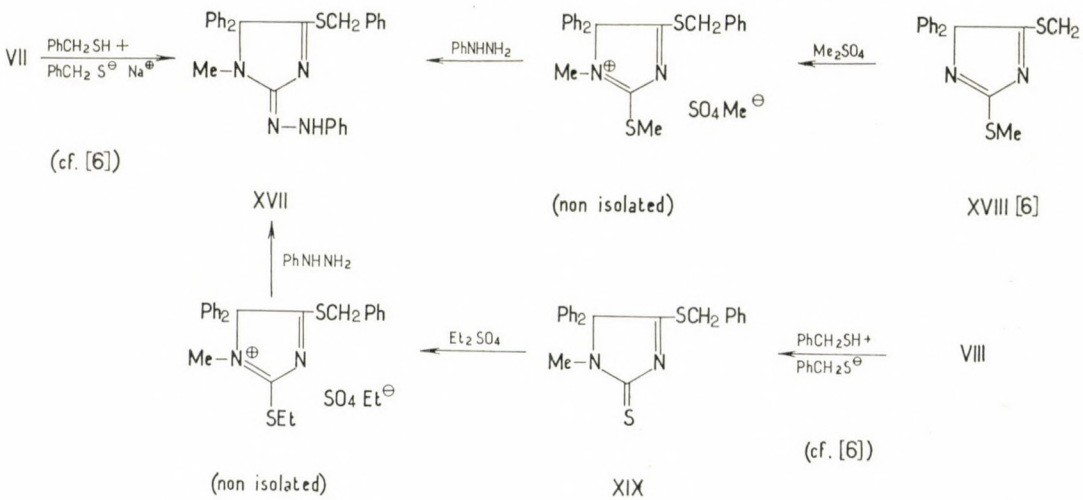

All these reactions with N-nucleophiles take place apparently according to the following scheme:*

* B means a base (in the present case pyridine). The electron shifts denoted in the first step do not necessarily take place in a synchronous way.

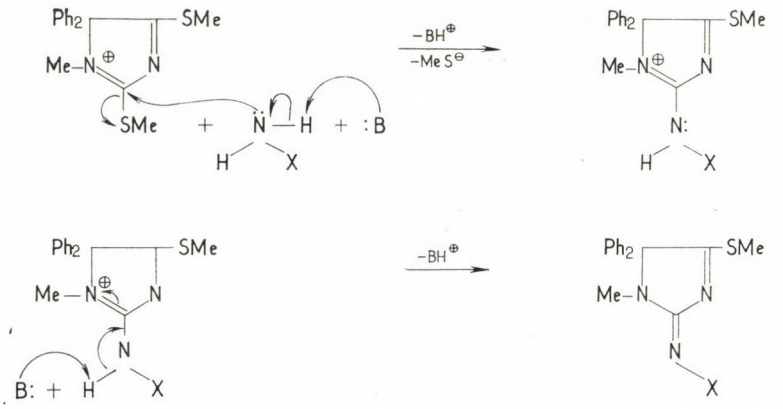

*

Accordingly, on the basis of the reactions outlined, the quaternary cation **II** proved to be more reactive in position C-2 than at C-5 also against N-nucleophiles. Thus the relative reactivity of both electrophilic centres is apparently the same against all types of nucleophiles.

On the other hand, it was also found that the quaternary compounds **II** react also with N-nucleophilic agents much easier than **I**, this obviously being as well due to the presence of the positive centre.

*

The reaction of compound **IIa** in ethanolic solution with potassium hydrogen sulfide applied in great excess, also proceeded according to expectations, both methylthio groups being exchanged to thioxo groups under formation of compound **XX**.**

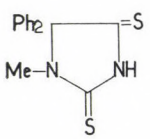

XX

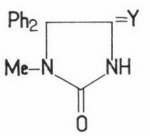

XXI : Y = RN=*)

XXII : Y = PhNHN=*)

XXXIII : Y = S

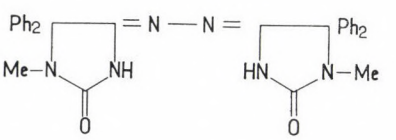

XXIV *)

* A potentially tautomeric compound. Its existence in the above tautomeric form has not yet been confirmed.

** c. f. Footnote ** on page 394.

Finally, the reaction of the partial hydrolysis product **III**, with some nucleophilic agents was also investigated. These reactions proceeded again according to our expectations. Thus with ammonia and amines **XXI**, while with hydrazine and potassium hydrogen sulfide **XXIV** and **XXIII** were formed, respectively.

Experimental*

2,5-Bis(methylthio)-3-methyl-4,4-diphenyl-4*H*-imidazolium methosulfate (IIa)

4.9 ml (6.62 g; 52.6 millimoles) of dimethyl sulfate were added at 70° to a solution of 15.2 g (48.6 mmoles) of **I** in 15 ml anhydrous chlorobenzene, the solution boiled 5 minutes and allowed to cool. After standing an hour, the product was brought to crystallization by seeding, and subsequently 15 ml of petroleum ether were added. After standing overnight the crystals were filtered off, and washed with petroleum ether and anhydrous acetone; yield 19.53 g (91.6%) of colourless stubby crystals, m. p. 180—181° (from a mixture of chloroform and petroleum ether).

$C_{19}H_{22}N_2O_4S_2$ (438.4). Calcd. C 52.05; H 5.06; N 6.39; S 21.90. Found C 52.44; 52.49; H 4.77; 5.00; N 6.87; 6.48; S 21.65; 21.78%.

Mesylate (II; X=$MeSO_3$)

A mixture of 1.0 g (3.2 mmoles) of **I**, 0.43 g (3.9 mmoles) of methyl methanesulfonate and 0.70 ml of anhydrous chlorobenzene was heated in a sealed tube 8 hours at 100°. On addition of 2.5 ml of anhydrous benzene and 1.5 ml of anhydrous *n*-hexane an oil separated which, on rubbing and seeding crystallized. The crystals were filtered off, and washed with a 1 : 1 mixture of benzene and n-hexane; yield 0.95 g (70.4%), m. p. 157—162° (crude product).

Benzene sulfonate (II; X=$PhSO_3$)

A mixture of 1.0 g (3.2 mmoles) of **I**, 0.60 g (3.5 mmoles) of methyl benzenesulfonate and 1.0 ml of anhydrous chlorobenzene was heated 4 hours at 110° in a sealed tube. On addition of 2 ml of anhydrous *n*-hexane, an oil separated which, on rubbing and stirring, solidified overnight. The precipitate was filtered off, and washed with a 1 : 1 mixture of benzene and *n*-hexane; yield 1.41 g (91%), m. p. 91—92° (decomp.) (crude product).

The *tosylate* (**II**; X = *p*-Me-$C_6H_4SO_3$) can be prepared similarly, but the same product is formed by fusing the components simply together without using any solvent (treatment for 1 to 3 hours at 100—150°).

Partial hydrolysis of 2,5-bis(methylthio)-3-methyl-4,4-diphenyl-4*H*-imidazolium salts (II)

a) A mixture of 0.44 g (1.0 mmole) of **IIa**, 0.2 ml (2.5 mmoles) of pyridine, 1 ml of methanol and 0.5 ml of water was brought to boiling. On cooling, the solidified crystalline mass was treated with 1 ml of water, the crystals filtered off, and washed with water; yield 0.22 g (73.4%) of **III**, m. p. 230—231°; lit. [3]: 229°.

b) The crude tosylate of **II** was dissolved in acetone under gentle heating. After cooling, 1 part (by volume) of water was added. Under evolution of methanthiol, a white crystalline substance (**III**) slowly separated; yield 77%, m. p. 229—230° (from a mixture of chloroform and ethanol).

$C_{17}H_{16}N_2OS$ (296.3). Calcd. C 68.90; H 5.44; N 9.45. Found C 68.63; H 5.26; N 9.44%.

"Total" hydrolysis of 2,5-bis(methylthio)-3-methyl-4,4-diphenyl-4*H*-imidazolium salts (II). Hydrolysis of 1-methyl-4-methylthio-5,5-diphenyl-3-imidazolin-2-one (III)

a) A mixture of 7.2 g (16.4 mmoles) of **IIa**, 30 ml of ethanol and 20 ml of concentrated hydrochloric acid was boiled 5 hours. The crystals which separated on the addition of 100 ml of

* The melting points given by us are uncorrected.

water were filtered off and washed with water; yield 3.8 g (87%) of 1-methyl-5,5-diphenylhydantoin (**IV**); m. p. 224°, lit. [7]: 224—226°.

b) On boiling for about an hour an aqueous ethanolic solution of the crude **II**-tosylate, similarly **IV** was obtained in 63% yield; m. p. 226—227° (from aqueous ethanol).

$C_{16}H_{14}N_2O_2$ (266.3). Calcd. C 72.16; H 5.30; N 10.52. Found C 72.39; 72.65; H 5.41; 5.38; N 10.80; 10.85%.

c) A mixture of 1.0 g (3.37 mmoles) of 1-methyl-4-methylmercapto-5,5-diphenyl-3-imidazolin-2-one (**III**), 8 ml of ethanol and 5 ml of concentrated hydrochloric acid was boiled 3 hours, evaporated to about 2/3 of its original volume, and diluted with 2 ml of water. The separated crystals were filtered off and washed with water; yield 0.88 g (98%) **IV**; m. p. 226—227° (from aqueous ethanol).

1-Methyl-2-benzylimino-4-methylthio-5,5-diphenyl-3-imidazoline (V)

a) A mixture of 0.88 g (2.0 mmoles) of **IIa**, 0.32 g (2.2 mmoles) of benzylamine hydrochloride and 3.5 ml of anhydrous pyridine was boiled 5 hours, and subsequently treated with 10 ml of water. After allowing the mixture to stand 30 minutes, the separated yellowish crystalline mass was filtered off, and washed with water; yield 0.38 g (49.3%) of **V**; m. p. 313° (from a mixture of pyridine and ethanol). Mixed m. p. with the product obtained according to *b)*: 313—314°.

b) To the crude **II**-tosylate, obtained by fusing 10 mmoles of **I** and 12 mmoles of methyl *p*-toluene-sulfonate (40 minutes at 135°) a mixture of 1.58 g (11 mmoles) of benzylamine hydrochloride and 14 ml of anhydrous pyridine was added. After boiling for 16 hours, 50 ml of water was added. A yellowish oil separated which partially solidified on standing. The aqueous phase was decanted, and the oil was boiled with 10 ml of methanol. The yellow crystalline mass thereby obtained was filtered off, and washed with methanol; yield 1.55 g (40.1%); m. p. 313—314° (from a mixture of pyridine and ethanol).

$C_{24}H_{23}N_3S$ (385.5). Calcd. C 74.78; H 6.01; N 10.90; S 8.30. Found C 74.63; 74.06; H 5.97; 6.06; N 11.39; 11.23; S 8.06; 8.59%.

λ_{max} (in ethanol): 254 nm (log $\varepsilon = 4.05$) and 323 nm (log $\varepsilon = 4.18$).

1-Methyl-4-benzylamino-5,5-diphenyl-3-imidazoline-2-thione (IX)

A mixture of 4.0 g (12.8 mmoles) of **VIII** [3], 3.0 g (20.9 mmoles) of benzylamine hydrochloride, 1.46 g (17.8 mmoles) of anhydrous sodium acetate and 30 ml of anhydrous pyridine was refluxed 18 hours. The substance which separated on the addition of 40 ml water was filtered off, and washed with water and with aqueous methanol; yield 3.96 g (83.4%) of **IX**; m. p. 258—259° (from aqueous ethanol).

$C_{23}H_{21}N_3S$ (371.4). Calcd. C 74.37; H 5.70; N 11.31; S 8.62. Found C 74.12; 74.23; H 5.23; 5.62; N 11.43; S 8.83; 8.81%.

The same product was obtained also by boiling **VIII** simply with benzylamine in the presence of some water.

1-Methyl-2-methylthio-4-benzylimino-5,5-diphenyl-2-imidazoline (XII)

A mixture of 1.0 g (2.7 mmoles) of **IX**, 0.4 g (2.8 mmoles) of ignited potassium carbonate, 15 ml of anhydrous ethanol and 0.40 ml (0.91 g; 6.44 mmoles) of methyl iodide was stirred 8 hours at room temperature. After standing overnight, the inorganic salts were filtered off, washed with ethanol, and the ethanolic solution evaporated to dryness in vacuum. The oily residue was dissolved in 70 ml of anhydrous ether, the solution filtered and again evaporated to dryness; yield 0.79 g (76.2%) of **XII**; m. p. 111—112° (from methanol and water).

$C_{24}H_{23}N_3S$ (385.5). Calcd. C 74.78; H 6.01; N 10.90; S 8.30. Found C 74.47; H 6.08; N 11.08; 11.17; S 8.32; 8.42%.

Hydrolysis:

a) 200 mg (0.52 mmoles) of **XII** were boiled 5 hours with a solution of 0.4 g (4.2 mmoles) of chloroacetic acid in 1.6 ml water. On adding 10 ml of 6% aqueous potassium hydroxide to the cooled solution, an oily substance separated. The aqueous phase was decanted, the oily phase dissolved in 2.5 ml of hot ethanol, clarified and treated with 5 ml of hot water. On cooling, 65.4 mg (35.4%) of **XXI** (R = $PhCH_2$) separated; m. p. and mixed m. p. with an authentic sample (see below): 222—223°. The identity of the two products was also confirmed by their infrared spectra.

b) 123 mg (0.32 mmoles) of **XII** were boiled 5 hours with a mixture of 2 ml of glacial acetic and 1 ml of concentrated hydrochloric acid; the solution was subsequently evaporated to dryness on the steam bath in vacuum. The residue was dissolved in 2 ml of methanol, and the solution mixed with 10 ml of hot water; yield 68 mg (60%) of **XXI** (R = $PhCH_2$); m. p. and mixed m. p. as under *a)*.

1,3-Dimethyl-4-benzylimino-5,5-diphenyl-2-imidazolidinethione (XI)

A mixture of 200 mg (0.64 mmoles) of 1,3-dimethyl-5,5-diphenyl-dithiohydantoin (**X**) [3] and 1.0 ml (0.98 g; 9.2 mmoles) of benzylamine was boiled 4 hours. On adding a mixture of 15 ml of water and 1 ml of glacial acetic acid an oily precipitate appeared which was separated and crystallized from 5 ml of ethanol after clarification with bone black; yield 160 mg (65%) of **XI**; m. p. 117—118° (from aqueous methanol).

$C_{24}H_{23}N_3S$ (385.5). Calcd. N 10.90; S 8.30. Found N 10.64; S 8.21%.

1-Methyl-2-hydroximino-4-methylthio-5,5-diphenyl-3-imidazoline (VI)

A solution of 340 mg (4.9 mmoles) of hydroxylamine hydrochloride in 8 ml of hot ethanol was treated with a solution of 230 mg (10 mg-atomes) of metallic sodium in 5 ml of anhydrous ethanol. The precipitated sodium chloride was filtered off and to the filtrate 2.0 g (4.6 mmoles) of **IIa** were added at room temperature. After standing overnight the solution was evaporated to dryness on the steam bath in vacuum, and the residue triturated with 25 ml of water. The carefully dried crude product (1.33 g) was dissolved in 5 ml of anhydrous methanol at room temperature, and the solution treated with 5 ml of petroleum ether whereupon a crystalline product slowly precipitated; yield 0.77 g (52%); m. p. 215—216° (decomp.).

$C_{17}H_{17}N_3OS$ (311.3). Calcd. C 65.68; H 5.50; N 13.50; S 10.30. Found C 65.58; 65.63, H 5.59; 5.81; N 13.22; S 10.55%.

Partial hydrolysis:

A mixture of 291 mg (0.93 mmoles) of **VI** and 12 ml of 40% aqueous acetic acid was boiled 5 hours. After cooling, the mixture was treated with 5 ml of water and the precipitate thereby formed was filtered off, washed with water and crystallized from aqueous methanol; yield 104 mg (37.7%); m. p. and mixed m. p. with authentic [3] **III**: 230—231°.

1-Methyl-4-methylthio-5,5-diphenyl-3-imidazoline-2-one-phenylhydrazone (VII)

a) A mixture of 1.75 g (4 mmoles) of **IIa**, 0.61 g (4.2 mmoles) of phenylhydrazine hydrochloride and 7 ml of anhydrous pyridine was boiled 2 hours. After cooling, the reaction mixture was treated with 21 ml of water. A dark brown oil appeared which slowly solidified on scrathing. The substance was pulverized, filtered off, and washed with water; yield 1.59 g (100%) of **VII**; m. p. 202—203° (decomp.; from a mixture of pyridine and ethanol).

b) To the crude **II**-tosylate, obtained by fusing (10 minutes at 150°) 5 mmoles each of **I** and methyl *p*-toluenesulfonate, a mixture of 0.73 g (5.05 mmoles) of phenylhydrazine hydrochloride and 5 ml of anhydrous pyridine was added. After boiling the mixture 4.5 hours, it was allowed to cool, and treated with 5 ml of ethanol and 25 ml of water. The separated orange-red oil gradually solidified. The aqueous phase was decanted, and the residue boiled with aqueous ethanol. After cooling, the solid substance was filtered off, and washed with aqueous acetone; yield 0.77 g (40%) of **VII**; m. p. 201—202° (decomp.; from a mixture of butanol and methanol).

$C_{23}H_{22}N_4S$ (386.4). Calcd. C 71.48; H 5.74; N 14.50; S 8.28. Found C 71.38; 71.08; H 5.99; 5.94; N 14.48; 14.64; S 8.01; 8.37%.

λ_{max} (in ethanol): 263 nm (log ε = 4.01); 360 nm (log ε = 3.64).

c) A solution of 2.3 ml (2.5 g = 23 mmoles) of phenylhydrazine base in 8 ml of ethanol was added to the solution of 5.0 g (11.4 mmoles) of **IIa** in 32 ml of anhydrous ethanol. Shortly orange-red crystals began to precipitate from the red liquid and methanethiol was evolved. After standing overnight, the crystals were filtered off, and washed with water and with some ethanol; yield 3.2 g (73%) of **VII**; m. p. 202—203° (decomp.; from acetone and water).

d) A mixture of 0.32 g (1.03 mmoles) of 1-methyl-4-methylthio-5,5-diphenyl-3-imidazoline-2-thione (**VIII**) [3] and 0.15 ml (0.28 g = 1.14 mmoles) of diethyl sulfate was heated in a sealed tube 30 minutes at 135°. After cooling, the obtained melt (**XVI**) was dissolved in 2 ml of anhydrous ethanol, and instantaneously treated with the solution of 0.25 ml (0.27 g =

= 2.5 mmoles) of phenylhydrazine base in 1 ml of anhydrous ethanol. The crystals of **VII** shortly began to precipitate from the red solution. The substance was separated as described under *c)*; yield 0.39 g (86.6%); m. p. 201—202° (decomp.).

The products obtained under *a)* to *d)* proved to be identical also on the basis of their infrared spectra.

Total hydrolysis:

A mixture of 0.54 g (1.44 mmoles) of **VII**, 3.5 ml of glacial acetic and 3 ml of concentratep hydrochloric acid was refluxed 8 hours. 20 ml of water and 5.0 g (89 mmoles) of potassium hydroxide were added (pH = 8), the reaction mixture filtered and the filtrate acidified with acetic acid (pH = 4.5). The orange-red amorphous precipitate was filtered off, and washed with water; yield 0.38 g (100%) of **IV**; m. p. and mixed m. p. with authentic **IV**; 223—224° (from methanol);

$C_{16}H_{14}N_2O_2$ (266.3) Calcd. C 72.16; H 5.30; N 10.52. Found C 72.18; H 5.23; N 10.52; 10.41%.

1-Methyl-4-benzylthio-5,5-diphenyl-3-imidazoline-2-one-phenylhydrazone (XVII)

a) 1.0 g (2.6 mmoles) of **VII** was refluxed 18 hours with a mixture obtained from 0.61 ml (0.65 g; 5.2 mmoles) of α-toluenethiol, 60 mg (2.6 mg-atom) of metallic sodium and 28 ml of anhydrous ethanol (ample development of methanethiol!). After cooling the orange-red crystals were filtered off and washed with ethanol; yield 1.1 g (93.5%) of **XVII**; m. p. 198—199° (from ethanol and acetone).

$C_{29}H_{26}N_4S$ (462.5). Calcd. C 75.30; H 5.67; N 12.11; S 6.82. Found C 75.03; 75.80; H 5.81; 5.83; N 12.25; 12.45; S 7.10; 7.05%.

b) 0.24 g (0.62 mmoles) of 2-methylthio-4,4-diphenyl-5-benzylthio-4*H*-imidazole **(XVIII)** [6] and 0.065 ml (88 mg; 0.7 mmoles) of dimethyl sulfate were heated 30 minutes in a sealed tube at 100°. After cooling, the melt was triturated with 7 ml of anhydrous ethanol, and immediately treated with the solution of 0.14 ml (0.15 g; 1.4 mmoles) of phenylhydrazine base in 1 ml of anhydrous ethanol. Crystals of **XVII** shortly began to separate from the orange coloured liquid. After standing overnight the mixture was processed as described under *a)*; yield 0.26 g (91%); m. p. 198—199° (from ethanol and acetone).

c) 2.0 g (6.4 mmoles) of 1-methyl-4-methylthio-5,5-diphenyl-3-imidazoline-2-thione **(VIII)** [3] were refluxed 5 hours with a mixture prepared from 0.79 ml (0.84 g; 6.7 mmoles) α-toluenethiol, 0.1 g (0.7 mmoles) of ignited potassium carbonate, 0.1 ml triethylamine and 30 ml anhydrous ethanol (ample development of methanethiol!). After cooling the formed **XIX** was precipitated by the addition of 20 ml of water, filtered off, and washed with aqueous ethanol; yield 2.2 g (87%); m. p. 167—168° (from methanol).

0.39 g (1.0 mmole) of crude **XIX** were heated an hour at 100° with 0.15 ml (0.28 g; 1.1 mmoles) of diethyl sulfate in a sealed tube. After cooling, the obtained melt of the quaternary salt was dissolved in 4 ml of anhydrous ethanol, and the solution treated immediately with the solution 0.25 ml (0.27 g; 2.5 mmoles) of phenylhydrazine base in 3 ml of anhydrous ethanol. The reaction product was isolated as described under *b* ; yield 0.30 g (65%) of a rather contaminated crude product. From this latter, on repeated recrystallization from ethanol and acetone, 0.10 g (22%) of pure **XVII** were obtained; m. p. 195—196°.

The products prepared according to *a)* to *c)* proved to be identical on the basis of their mixed melting points and of their infrared spectra.

1-Methyl-5,5-diphenyl-dithiohydantoin (XX)

1.31 g (3.0 mmoles) of **IIa** were heated 8 hours at 115° with a solution of sodium hydrogen sulfide (60 mmoles) in 20 ml methanol in a sealed tube. The mixture was treated with 30 ml of water, filtered, and the filtrate acidified with 4 ml (66 mmoles) of acetic acid. The precipitated yellow crystals were filtered off and washed with water and aqueous methanol; yield 0.68 g (76%); m. p. 214—215° (from aqueous ethanol); lit [3]: 217°.

$C_{16}H_{14}N_2S_2$ (298.3). Calcd. C 64.42; H 4.73; N 9.39. Found C 64.42; H 4.41; N 9.47%.

1-Methyl-4-imino-5,5-diphenyl-2-imidazolidinone (XXI; R = H)

The mixture of 0.94 g (3.2 mmoles) of 1-methyl-4-methylthio-5,5-diphenyl-3-imidazolin-2-one **(III)** and 15 ml of an anhydrous alcoholic ammonia solution (NH_3 content: 323 mg,

19 mmoles) was heated 25 hours at 110° in a sealed tube. After cooling the reaction mixture was evaporated (together with the precipitated crystals) to a volume of about 5 ml; 10 ml of water were subsequently added, the crystals filtered off, and washed with water; yield 0.72 g (85.6%); m. p. 334° (decomp.; from a 1 : 1 mixture of dimethylformamide and methanol).

$C_{16}H_{15}N_3O$ (265.3). Calcd. C 72.43; H 5.70; N 15.84. Found C 72.59; 72.41; H 5.50; 5.55; N 15.74; 15.58%.

1-Methyl-4-benzylimino-5,5-diphenyl-2-imidazolidinone (XXI; R = $PhCH_2$)

The mixture of 1.2 g (4 mmoles) of **III**, 2.14 g (20 mmoles) of benzylamine, 0.08 g (0.56 mmoles) of benzylamine hydrochloride and 15 ml of anhydrous ethanol was heated 23 hours at 120° in a sealed tube. After cooling the reaction mixture was filtered and the filtrate evaporated to a volume of about 5 ml, and subsequently treated with 30 ml of water. The white crystalline product was filtered off and washed with water; yield 1.40 g (98.5%); m. p. 224—225° (from aqueous methanol).

$C_{22}H_{21}N_3O$ (355.4). Calcd. C 77.72; H 5.96; N 11.82. Found C 77.98; H 6.05; N 11.43%.

λ_{max} (in ethanol); 207 nm (log ε = 4.20) and 252 nm (log ε = 3.88).*

1-Methyl-5,5-diphenylhydantoine-4-phenylhydrazone (XXII)

A mixture of 0.89 g (3 mmoles) of 1-methyl-4-methylthio-5,5-diphenyl-3-imidazolin-2-one (**III**), 0.87 g (6 mmoles) of phenylhydrazine hydrochloride, 0.45 g (5.5 mmoles) of anhydrous sodium acetate and 10 ml of anhydrous *n*-butanol was refluxed ten hours. After cooling 20 ml of water and 0.30 g (2.3 mmoles) of crystalline sodium acetate were added, and the butanol was distilled off in vacuum. The brown oil which separated on cooling was dissolved in 10 ml of hot ethanol, and the crop which precipitated on addition of 15 ml water was recrystallized from ethanol, affording 0.22 g (24.4%) of starting material. On adding water to the ethanolic mother liquor, **XXII** precipitated; yield 0.30 g (28%); m. p. 227—228° (from aqueous ethanol).

$C_{22}H_{20}N_4O$ (356.4). Calcd. C 74.04; H 5.66; N 15.72. Found C 74.00; H 5.49; N 15.55%.

λ_{max} (in ethanol): 283 nm (log ε = 3.14).

N,N'-Bis-(1-methyl-5,5-diphenyl-2-oxo-4-imidazolidinylidene)-hydrazine (XXIV)

A mixture of 1.48 g (5 mmoles) of 1-methyl-4-methylthio-5,5-diphenyl-3-imidazolin-2-one (**III**), 0.19 g (2.2 mmoles) of hydrazine hydrochloride, 0.21 g (2.5 mmoles) of anhydrous sodium acetate and 10 ml of anhydrous pyridine was boiled 18 hours, whereby some crystalline substance precipitated. The reaction mixture was concentrated to $^2/_3$ of its original volume, and subsequently 30 ml of water were added. The separated brown oil shortly solidified. It was filtered off, washed with water, and extracted by boiling with an about tenfold volume of pyridine whereby **XXIV** was left behind as an insoluble residue which proved to be insoluble in all common organic solvents. Thus, its purification was carried out by repeated reprecipitation from alkaline alcoholic solution by acetic acid; colourless crystals; yield 0.25 g (19%); m. p. above 420° (decomp.).

$C_{32}H_{28}N_6O_2$ (528.6). Calcd. 72.71; H 5.34; N 15.90. Found C 72.62; H 5.02; N 15.89%

1-Methyl-5,5-diphenyl-4-thiohydantoin (XXIII)

1.0 g (3.37 mmoles) of **III** was heated 44 hours at 120° in a sealed tube with a solution of 3.8 g (67 mmoles) of potassium hydroxide in 4 ml of water and 23 ml of ethanol, saturated

* *Added in proof.*

1-Methyl-4-(3-dimethylamino-propyl-imino)-5,5-diphenyl-2-imidazolidinone (**XXI**, R = = $Me_2N-CH_2-CH_2-CH_2$; mp. 142—3°, from benzene-petroleum ether; found C 72.17; 71.77. H 7.42; 7.18. N 15.97; calcd. for $C_{21}H_{26}N_4O$, Mwt: 350.4; C 71.97; H 7.48; N 15.97), and, starting from 4-methylthio-5,5-diphenyl-3-imidazolin-2-one, by the method described in [4] also the nonmethylated analogue 4-(3-dimethylamino-propyl-imino)-5,5-diphenyl-2-imidazolidinone (mp.: 203—4°, from aqueous methanol; found C 71.44; 71.11; H 7.23; 6.95; N 17.11, calcd. for $C_{20}H_{24}N_4O$, Mwt.: 336.4; C 71.40; H 7.19; N 16.66) were prepared similarly in 92 and 98% yield, respectively. Both compounds were tested for CNS and anticonvulsant activity by D. TEDESCHI of *Smtth Kline* and *French laboratories, Philadelphia*, but proved to be inactive.

previously with hydrogen sulfide. After cooling the solution was filtered, the filtrate acidified with 5 ml of glacial acetic acid, boiled up and treated while hot with 75 ml of water; the yellow crystalline product thereby precipitated was filtered off and washed with water; yield 0.84 g (88.5%); m. p. 266—268° (from aqueous ethanol).

$C_{16}H_{14}N_2OS$ (282.3). Calcd. C 68.07; H 5.00; N 9.92. Found C 68.14; 68.30; H 4.96; 5.13; N 10.00; 10.06%.

Acknowledgement: The authors are indebted to Dr. G. DOLESCHALL for establishing the ultraviolet spectra, and to Mrs. I. BALOGH-BATTA and her associates for carrying out the microanalyses.

SUMMARY

2,5-Bis(methylthio)-4,4-diphenyl-4*H*-imidazole (**I**) can be quaternized on N-3 by methylating agents, under formation of the corresponding salts of **II**. In the cation **II**, the reactivity of C-2 against O- and N-nucleophiles is on the one hand, markedly enhanced as compared with the starting compound **I**, and, on the other hand, as compared with C-5 of **II**. In this position selective hydrolysis and aminolyses can be, thus, easily attained. Under more vigorous hydrolytic conditions, respectively, also the residual methylthio group of the product **III**, obtained on partial hydrolysis can be split. By treating with potassium hydrogen sulfide, both methylthio groups of **II** can similarly be exchanged to thioxo groups under formation of compound **XX**.

REFERENCES

1. LEMPERT, K. and ZAUER, K.: Tetrahedron Letters **1964,** 519.
2. LEMPERT, K. and NYITRAI, J.: Tetrahedron Letters **1965,** 2927.
3. CARRINGTON, H. C. and WARING, W. S.: J. Chem. Soc. (London) **1950,** 354. (With references to earlier literature.)
4. LEMPERT, K., ZAUER, K. and BREUER, J.: Periodica Polytechn. (Budapest), Ser. Chem. Engng. **8,** 21 (1964).
5. WARE, E.: Chem. Reviews **46,** 427 (1950).
6. LEMPERT, K., NYITRAI, J. and SOHÁR, P.: Tetrahedron Letters **1965,** 1795.
7. LONG, L. M., MILLER, C. A. and TROUTMAN, H. D.: J. Amer. Chem. Soc. **70,** 900 (1948)

Hydantoine, Thiohydantoine, Glycocyamidine. XXIII

Quaternisierung des 2,5-Bis(methylmercapto)-4,4-dipheny-4*H*-imidazols und Reaktion des Methylquaternären mit nucleophilen Agenzien

K. LEMPERT und K. ZAUER

Zusammenfassung. Durch Einwirkung von Methylierungsmitteln läßt sich das 2,5-Bis (methylmercapto)-4,4-diphenyl-4*H*-imidazol (**I**) am N-3 quaternisieren, wobei die entsprechenden Salze von **II** gebildet werden. Im Kation **II** besitzt C-2 eine beträchtlich höhere Reaktivität gegen O- und N-Nucleophile als in der Grundverbindung **I** bzw. als C-5. So sind in dieser Stellung die selektive Hydrolyse und Aminolysen leicht durchführbar. Unter energischeren Bedingungen läßt sich auch die noch zurückgebliebene Methylmercaptogruppe des partiellen Hydrolyseproduktes (**III**) hydrolytisch oder aminolytisch abspalten. Mittels Kaliumhydrogensulfids lassen sich beide Methylmercaptogruppen von **II** — unter Bildung der Verbindung **XX** — auch gegen Thioxogruppen austauschen.

Гидантоины, тиогидантоины, гликоциамидины. XXIII

Кватернизация 2,5-бис(метилмеркапто)-4,4-дифенил-4*H*-имидазола и реакция метил-кватернера с нуклеофильными агентами

К. ЛЕМПЕРТ и К. ЗАУЭР

Резюме. 2,5-бис(метилмеркапто)-4,4-дифенил-4*H*-имидазол (**I**) может быть кватернизован метилирующими агентами по N-3, с образованием при этом соответствующих солей **II**. Реакционная способность C-2 в катионе **II**, по отношению к O- и N-нуклеофилам, значительно возрастает, по сравнению, с одной стороны, с исходным соединением (**I**) и, с другой стороны, по сравнению с C-5. Поэтому, в этом положении легко могут быть проведены избирательные гидролиз и аминолизы. При более энергичном гидролитическом или аминолитическом воздействии может быть отщеплена и метилмеркапто-группа, еще оставшаяся в частично гидролизованном продукте (**III**). Под влиянием кислого сернокислого калия, обе метил-меркапто-группы продукта **II**, могут быть заменены на тиоксо-группы, с образованием при этом **XX**.

Prof. Dr. Károly Lempert
Károly Zauer
Budapest XI. Gellért tér 4.

IMIDAZOQUINAZOLINEDIONES IV.*

STRUCTURE AND ULTRAVIOLET SPECTRA OF SOME POTENTIALLY TAUTOMERIC IMIDAZOQUINAZOLINEDIONES AND RELATED 4-QUINAZOLINONES

G. DOLESCHALL, L. LÁNG and K. LEMPERT

(Research Group for Alkaloid Chemistry of the Hungarian Academy of Sciences, Department of Physical Chemistry, and Department of Organic Chemistry, Technical University, Budapest)

Received March 17, 1965

In earlier papers of this series the synthesis of three isomeric imidazoquinazolinediones: that of 2,5(1*H*, 3*H*)-imidazo[2,1-b]quinazolinedione (**Ia**) [1a, 1b], of 2,5(1*H*, 3*H*)-imidazo[1,2-a]quinazolinedione (**IIa**) [2],** and of 1,5(2H, 3H)-imidazo[1,2-a]quinazolinedione (**IIIa**) [2]** has been reported.

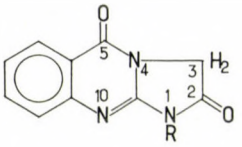

I

a : R = H

b : R = n−Bu

c : R = HO−CH_2−CH_2−

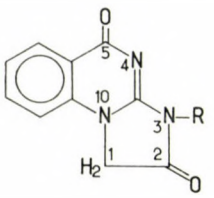

II

a : R = H

b : R = Et

c : R = HO−$(CH_2)_3$−

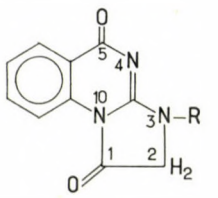

III

a : R = H

b : R = CH_3−C(=O)−

Although the structures of the *skeleton* of compounds **Ia** and **IIa** were unequivocally proved by the synthesis, it was not possible to confirm in all details the structures of these products. The occurrence of tautomerism, namely, cannot be excluded, at least in principle, and thus, the synthesis alone was insufficient for the exact proof of the position of the mobile hydrogen atoms, shown explicitely in the above formulas.

In the case of the third isomer an additional problem emerged because not even the mode of anellation followed unequivocally from the synthesis. Consequently, in addition to the angularly anellated structure **IIIa** and its tautomers, also the possibility of the structural alternative **IVa** with linear anellation and its tautomers had to be taken into consideration.

* Part III: Acta Chim. Hung. **45,** 357 (1965).

** Unfortunately, compounds **IIa** and **IIIa** were incorrectly numbered in the cited communication.

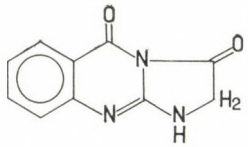

IVa

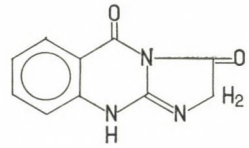

IVb

On slightly modifying the last step of the synthesis leading to **IIIa**, a new compound was obtained instead of **IIIa** [2]. This product was suspected, on the basis of the analytical data to be the acetyl derivative of **IIIa** (or of **IV**). On examining the infrared spectrum of this compound (showing *three* amide—I bands) it was possible to state that the compound is an N-acetyl derivative; however, the mode of anellation of its three rings, and the site of linkage of the N-acetyl group remained still unsolved problems.

The problems of tautomerism and anellation had been partly solved already earlier by physico-chemical methods. Thus, the correctness of the tautomeric structure **Ia** in *crystalline state* was unequivocally proved by the infrared spectrum, and a study of the ultraviolet spectrum of the ethanolic solution of **Ia** gave the same result [1]. It must be noted, however, that the ultraviolet

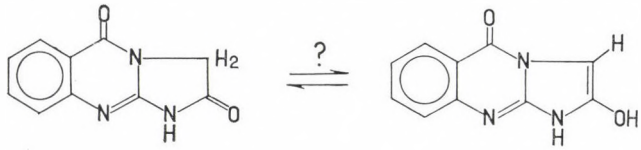

(Ia)

spectrum furnishes certainly less convincing evidence with respect to the oxo-enol tautomerism, which (at least principally) cannot be excluded for compounds **Ia**, than the infrared spectrum. The chromophoric group namely which undergoes changes in the course of this tautomeric conversion is of low intensity, and moreover, it is isolated from the main chromophoric system of the compound. Accordingly, the sensitivity of the ultraviolet spectroscopic method in our case is insufficient to make the evaluation of the position of the oxo-enol tautomeric equilibrium possible.*

* Actually, the carbonyl group linked to the imidazole ring has practically no influence on the ultraviolet spectrum of the compounds discussed. This follows convincingly from the observation that the ultraviolet spectra of the compounds **I** are identical with the spectrum of 1-ethyl-2,3-dihydro-5(1*H*)-imidazo [2,1-b]quinazolinone [8].

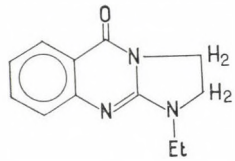

The same holds also for the analogous tautomerism of compounds **Ib**, **Ic**, **II** and **III**. For this reason, the study of the conditions of oxo-enol tautomerism (by methods of ultraviolet spectroscopy) was not included in our present work. Nevertheless, we believe to be right in considering these compounds to exist always as the oxo modifications since (*a*) the infrared spectra of the examined compounds in the crystalline state (KBr discs) in all cases contained the theoretically possible maximum number of carbonyl (amide-I) bands [3], and (*b*) according to general experience [4], heterocyclic compounds of the type investigated exist in solutions in most cases as the oxo instead of the hydroxy modification.

In case of the third isomer angular anellation, *i.e.* structure **IIIa** (or its tautomeric modifications) were made probable by comparison of its Debye—Scherrer diagram with those of compounds **Ia** and **IIa** whose structures (their mode of anellation) had already been clarified [2].

The aim of the present investigations was to find, with the aid of ultraviolet spectroscopy, further evidence for the tautomeric structure of **Ia**, as well as for the angular anellation of the third isomer and, finally, to elucidate the tautomeric structures of **IIa** and the third isomer and the structure of the N-acetyl derivative mentioned above.

For this purpose, a series of compounds, mainly N-alkylated derivatives of **Ia** and **IIa** (even theoretically incapable of tautomerism) have been prepared [5], and their ultraviolet spectra compared with those of the unsubstituted parent compounds (**Ia**—**IIIa**), and with those of some intermediates and analogues from the 4-quinazoline series [1, 2, 5].

Proof of the tautomeric structure of Ia and some 4(3*H*)-quinazolinone derivatives

If we presume, according to the above-mentioned considerations, that **Ia** exists also in solution as the dioxo modification, only one tautomeric structural alternative, *viz.* **Ia*** has to be considered. By studying the spectra of compounds **Ib**, **Ic** and **V**, whose structures are proved by their synthesis [5],

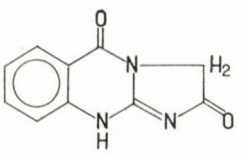

Ia *

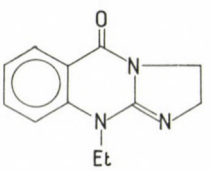

V

it becomes possible to decide between the alternatives **Ia** and **Ia***, *i.e.*, the position of the C=N double bond can be established. Namely, the chosen model compounds are partly incapable of tautomerism as far as the problem in question is concerned (**Ib**, **Ic**) and partly at all (**V**).

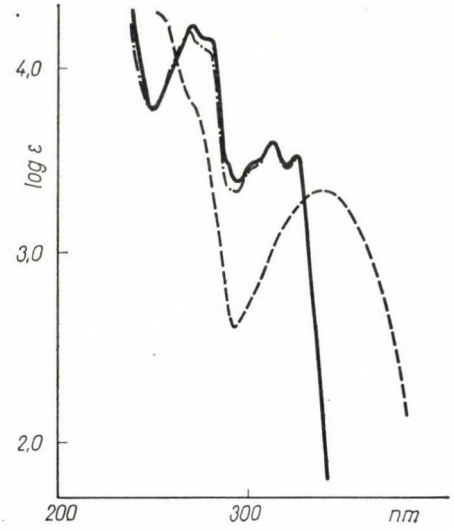

Fig. 1. **Ia** ·····; **Ib** ———; **V** - - - - (dioxane)

In Table I are listed the wavelengths and log ε values of the characteristic maxima, measured in dioxane, while Fig. 1 shows the spectra of compound **Ia** and of the two key models (**Ib** and **V**), recorded in dioxane. These data unequivocally prove the correctness of structure **Ia**, excluding at the same time alternative **Ia***. The spectra of the same compounds recorded in ethanol are shown in Fig. 2, the respective values being summarized in Table II.

Table I

*UV spectra in dioxane**

	Band system I			Band system II		Band system III
Ia	324 (3.50)	312 (3.59)	*300 (3.47)*	*274 (4.13)*	267 (4.18)	— — —
Ib	325 (3.53)	312 (3.61)	*300 (3.49)*	*276 (4.17)*	268 (4.23)	— — — —
V		339 (3.34)		*270 (3.78)*		250 (4.30)

* The wavelengths of the maxima are given (values of log ε in parentheses). Values in italics refer to inflexions

Table II

*UV spectra in ethanol**

	Band system I	Band system II	Band system III
Ia	322 (3.56)	278 (4.39)	237 (4.60)
Ib	*322 (3.50)* 312 (3.60) *300 (3.48)*	276 (4.16) 267 (4.22)	*233 (4.56)* 228 (4.60)
Ic	*322 (3.48)* 311 (3.57) *300 (3.46)*	275 (4.14) 267 (4.23)	*232 (4.61)* 228 (4.64)
V	337 (3.35)	*260 (3.94)*	*240 (4.46)* 232 (4.52)

* The wavelengths of the maxima are given (values of log ε in parentheses). Values in italics refer to inflexions

In addition to those of the imidazoquinazolinediones, the spectra of some derivatives (**VI—VIII**) of 4-quinazolinone have also been investigated in order to clarify the tautomeric nature of the intermediates **VI** and **VII** [2, 5]. For this purpose, besides the values obtained with the model compounds **Ib** and **V** already mentioned, the characteristic spectral data of the intermediate **VIII**

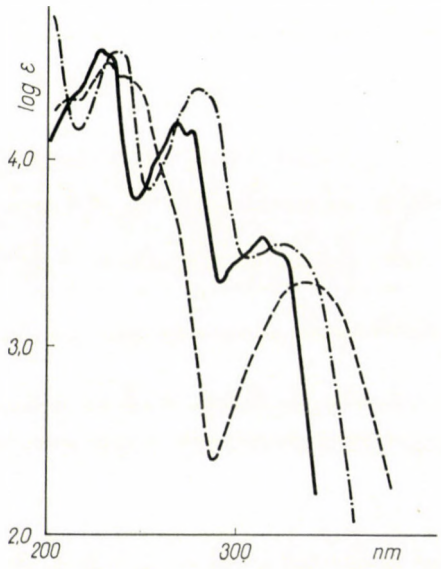

Fig. 2. **Ia** ·-·-·-; **Ib** ———; **V** - - - - (ethanol)

incapable of tautomerism [1], and of quinazoline (**IX**) available from literature [6] have also been utilized.

The study of the data of Table III reveals that the spectra of compounds **VI—VIII** are very similar to one another and to that of compound **Ib**, but they essentially differ from the spectra of either compound **IX** (cf., *e.g.*,

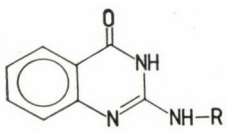

VI *

a : R = $-CH_2COOH$

b : R = $-CH_2COOEt$

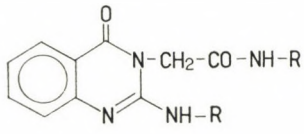

VII * *

R = n–Bu

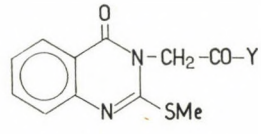

VIII

a : Y = OEt

b : Y = NH_2

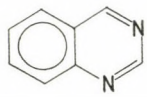

IX

* $\binom{4}{2} = 6$ potentially tautomeric modifications

** $\binom{2}{1} = 2$ potentially tautomeric modifications

the intensity values of the second band system) and of compound **V** (cf. Table II). Consequently, the structures suggested by us for compounds **VI** and **VII** are correct, and in the case of compound **VI** no fully aromatic tautomer, while

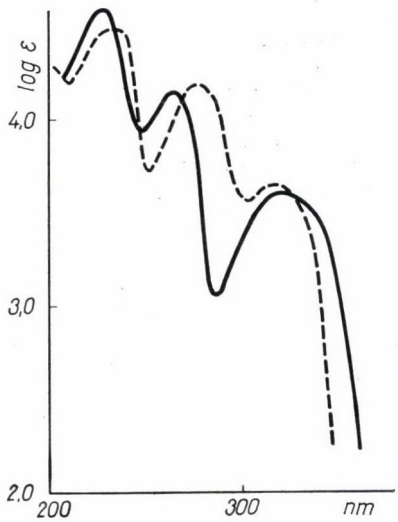

Fig. 3. **VIb** ——; **VIIIa** - - - - (ethanol)

in case of **VI** and **VII** no tautomer of the 1,2-dihydro-2-imino type containing an exocyclic C=N double bond is formed. The absorption spectra of compounds **VI**—**VIII** are similar; of these, only the spectra of **VIb** and **VIIIa**, recorded in ethanolic solution, are presented as examples in Fig. 3.

Table III

*UV spectra in ethanol**

	Band system I			Band system II		Band system III	
Ib	*322 (3.50)*	312 (3.60)	*300 (3.48)*	276 (4.16)	267 (4.22)	*233 (4.56)*	228 (4.60)
VIa		321 (3.49)		265 (4.08)		227 (4.52)	
VIb		321 (3.59)		265 (4.15)		*232 (4.57)*	228 (4.60)
VII		336 (3.56)		272 (4.18)		232 (4.52)	
VIIIa	*324 (3.57)*	315 (3.65)	305 (3.58)	278 (4.18)		235 (4.49)	228 (4.46)
VIIIb	*324 (3.48)*	316 (3.56)	— —	284 (4.07)	277 (4.11)	233 (4.39)	
IX	*320 (3.30)*	*310 (3.40)*	— —	275 (3.30)		225 (4.50)	

* The wavelengths of the maxima are given (values of log ε in parentheses). Values in italics refer to inflexions

Proof of the mode of anellation of IIIa and IIIb, and of the tautomeric structures of IIa, IIIa and some 4(1*H*)-quinazolinone derivatives

At first we examined whether "the third isomer" is really an angularly anellated derivative (**IIIa** or its tautomers) as it has been earlier suggested by our X-ray diffraction studies [2]. In case of a linear ring system (**IV**) the spectrum should be identical with that of **Ib** or **V**, respectively, depending on whether our compound exists as the tautomeric modification **IVa** or **IVb**. However, by comparison of the spectra recorded in dioxane (Fig. 4) it is seen

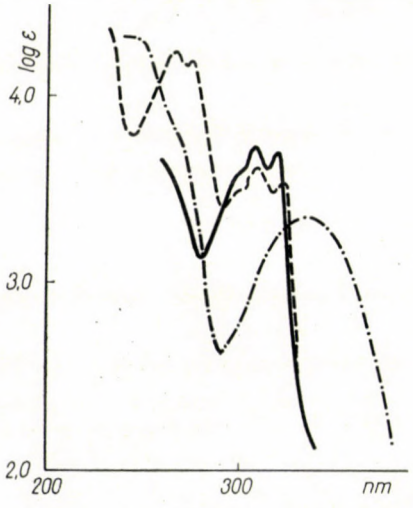

Fig. 4. **Ib** - - - - -; **IIIa** ———; **V** -·-·-· (dioxane)

that the spectrum of the third isomer does not resemble the spectra of either of the model compounds, nor can it be derived by superposing the spectra of the two model compounds. It follows that the third isomer is indeed an angularly anellated compound and furthermore, that in dioxane solution it exists in the tautomeric modification **IIIa**. If, in contrary, the mobile hydrogen were linked to N-4 instead of N-3, the compound should show a spectrum identical with that of **V**.

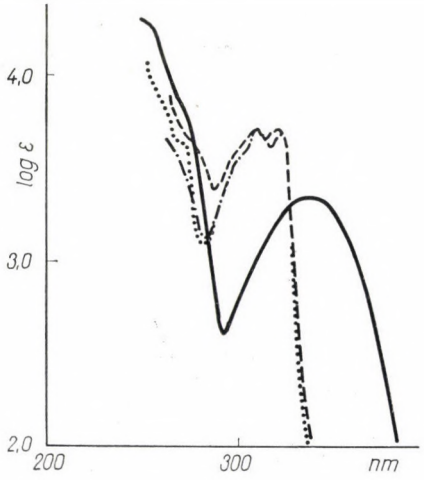

Fig. 5. **IIa** - - - -; **IIb** . . . .; **IIIa** ·-·-·-·; **V** ——— (dioxane)

Though at first sight the spectra of **Ib** and **IIIa** (Fig. 4) rather resemble each other, there actually exist essential differences which will be discussed later.

Since the spectra of the "second isomer" and **V** in dioxane markedly differ from each other (Fig. 5), the mobile hydrogen of this isomer must be linked again to N-3 instead of N-4; consequently structure **IIa** is correct. This is also confirmed by a comparison of the ultraviolet spectrum of **IIa**, with the spectra of **IIb** and **IIc** having "fixed" chromophoric systems, and, on the other hand, with that of **IIIa** whose structure has been proved above; the absorption curves recorded in dioxane have completely similar shapes, indicating that the mentioned compounds possess identical chromophoric systems.

The already mentioned N-acetyl derivative gave a completely similar ultraviolet spectrum in dioxane solution. Since that means the presence of the already known chromophoric system, the acetyl derivative must necessarily have structure **IIIb**.

The spectra of compounds **IIb** and **IIc** were examined in ethanolic solution as well,* in order to obtain also the part of the spectrum at shorter wavelengths. As the data of Table IV and Fig. 6 show, these spectra agree with those established in dioxane.

On comparing the data of the spectra established either in dioxane or in ethanol with those of the chromophoric system I, it is seen that the log ε values

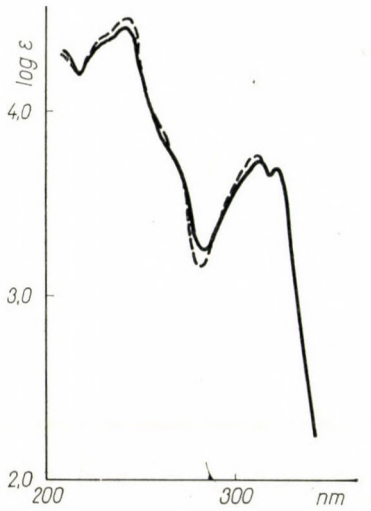

Fig. 6. **IIb** ———; **IIc** - - - - - (ethanol)

of band system I are consistently higher by about 0.20 unit, *i.e.*, these bands have 1.6 times higher intensity. This fact greatly facilitates the comparison of the chromophores and the spectra and the classification of the examined

Table IV**

	Band system I			Band system II	Band system III	Solvent
IIa	319 (3.70)	308 (3.70)	*300 (3.60)*	*274 (3.62)*	— — — —	dioxane
IIb	322 (3.73)	309 (3.77)	*300 (3.60)*	*270 (3.60)*	— — — —	dioxane
IIb	321 (3.67)	311 (3.74)	*300 (3.59)*	*268 (3.72)*	242 (4.45) *230 (4.73)*	ethanol
IIc	321 (3.76)	309 (3.80)	*299 (3.62)*	*270 (3.70)*	— — — —	dioxane
IIc	321 (3.69)	310 (3.76)	*300 (3.61)*	*270 (3.70)*	242 (4.50) *230 (4.40)*	ethanol
IIIa	322 (3.68)	310 (3.71)	*300 (3.55)*	*270 (3.54)*	— — — —	dioxane
IIIb	305 (3.73)	296 (3.74)	— —	*265 (3.55)*	— — — —	dioxane

* The spectrum of compound **IIIa** cannot be examined in ethanolic solution (see later).
** The wavelengths of the maxima are given (values of log ε in parentheses). Values in italics refer to inflexions

compounds, even if the structures of the band systems I are similar in both chromophoric systems. In case of compound **IIIb**, owing to the shift of the position of the maxima, just their intensity values and the shape of the minima were utilized for the identification of the chromophoric systems as secondary evidence.

In our further studies, the ultraviolet spectra of some related 4(1H)-quinazolinone derivatives (**X—XIII**) were investigated with the purpose to establish the tautomeric forms in which the compounds **X—XII** [5] exist under the given conditions.

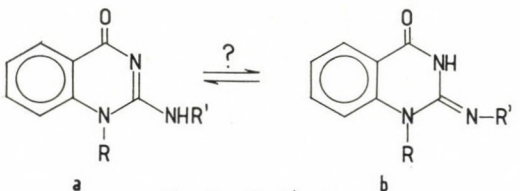

X : R = H, R' = Me
XI : R = R' = Me
XII : R = R' = Et

It was found that the spectra of compounds **X—XII** (Table V) are similar to one another, and also to the spectra of **IIb** and of **XIII**, the latter having a "fixed" chromophoric system (Fig. 7).

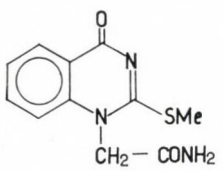

XIII

Table V

*UV spectra in ethanol**

	Band system I			Band system II	Band system III	
IIb	321 (3.67)	311 (3.74)	*300 (3.59)*	*268 (3.72)*	242 (4.45)	*230 (4.37)*
X	315 (3.60)	304 (3.68)	*292 (3.50)*	*255 (3.85)*	— —	226 (4.66)
XI	320 (3.62)	310 (3.71)	*298 (3.58)*	*258 (3.88)*	233 (4.56)	228 (4.55)
XII	320 (3.64)	308 (3.73)	*298 (3.58)*	*258 (3.93)*	233 (4.58)	*225 (4.57)*
XIII	319 (3.87)	308 (3.93)	*294 (3.77)*	— —	254 (4.47)	*230 (4.31)*

* The wavelengths of the maxima are given (values of log ε in parentheses). Values in italics refer to inflexions

On this basis, identical chromophoric systems must be presumed in all these compounds, and thus there is no trace of actual tautomerism in compounds **X**—**XII**; their structures correspond to those denoted by **a**.*

Finally, it is to be mentioned that compound **IIIa** is sparingly soluble in ethanol, the dissolved portion undergoing a transformation within a shorter or longer period, depending on the temperature of the solution. This conversion can be followed by observing the changes in the ultraviolet spectrum. When

Fig. 7. **XII** ——; **XIII** - - - - (ethanol)

the conversion process is completed, the spectrum of the solution becomes identical with those of compounds **I, VI, VII** and **VIII**. Consequently, the presumption is obvious that the ethanol effects cleavage of the imidazole ring of **IIIa** with the formation of **VIb**. Compound **IIIa** undergoes an identical but considerably more rapid conversion when dissolved in aqueous alkali. As soon as the solution is prepared, its spectrum becomes at once identical with that of **VIa** (Fig. 8). From this it may be concluded that the alkali effects the conversion **IIIa** → potassium salt of **VIa**. This latter process was verified in a preparative way: by acidification of an alkaline solution of **IIIa** compound **VIa** was precipitated.

The ultraviolet spectra were recorded with Unicam SP 500 and Spektromom 201 type *(Hungarian Optical Works*, Budapest) instruments. The results of the measurements are described in detail in another publication [7].

* The infrared spectra showing the presence of two bands corresponding to conjugated C=N and C=O groups similarly confirm structures **Xa**—**XIIa** in the crystalline state [3].

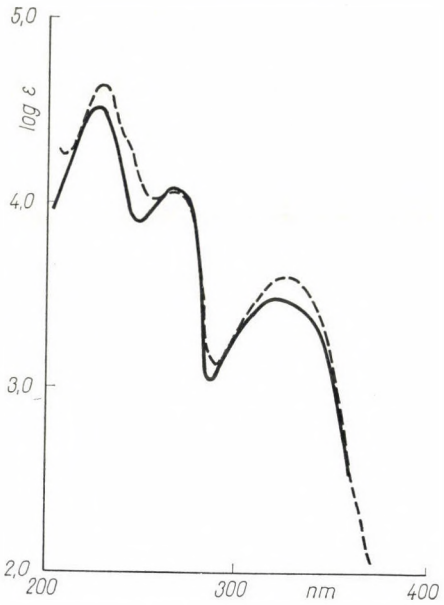

Fig. 8. **VIa** ——— (ethanol); **IIIa** - - - - (aqueous alkali)

Thanks are due to Mrs. E. BERECZKEY for her careful work in recording the absorption spectra.

SUMMARY

A series of potentially tautomeric 4-quinazolinone and imidazoquinazolinedione derivatives has been investigated. All compounds have been proved to exist, under the conditions of the present experiments, in a tautomeric modification which *does not* contain a C=N bond at C-2 exocyclic to the quinazoline ring, and in which the oxygen atom forms part of a carbonyl and not of a hydroxyl group.

In the case of our 4-quinazolinone derivatives this statement is in full agreement with the general experience [4] according to which in potentially tautomeric heterocyclic compounds the nitrogen atoms linked to the ring are inclined to form amino rather than imino groups, and the oxygen atoms affixed to the ring have a tendency to be present as carbonyl rather than hydroxyl groups.

In the case of the imidazoquinazolinediones, however, a C=N bond exocyclic to one of the hetero rings *must* be present. Here the problem is to decide which of the rings (the pyrimidine or the imidazole ring) has the stronger tendency to escape this type of bonding. It has been proved that the C=N double bond is always formed in the pyrimidine ring, thus it is exocyclic to the imidazole ring.

The investigation of the structure of the compounds by ultraviolet spectroscopy has been made possible by the fact that in dioxane solution, despite their extraordinary similarity, satisfactory differences exist in the band systems I of the spectra of the chromophoric systems of compounds **I** and **II** (**III**).

In general, it can be stated that the spectrum of the chromophoric system **I** consists of three separate band systems with intensity values (log ε) of about 3.50, 4.00 and 4.50. In the chromophoric system **II** (**III**), in turn, the band systems **II** and **III** are merged, thus the existence of band system **II** is indicated by an inflexion only.

Compound **V**, containing a C=N double bond exocyclic to the quinazoline ring, represents a new chromophoric system whose spectrum markedly differs from the spectra of compounds **I**—**III**.

REFERENCES

1. a) LEMPERT, K., DOLESCHALL, G.: Experientia [Basel] **18,** 401 (1962);
   b) LEMPERT, K., DOLESCHALL, G.: Acta Chim. Hung. **37,** 457 (1963).
2. LEMPERT, K., DOLESCHALL, G.: Chem. Ber. **96,** 1271 (1963); Magy. Kém. Folyóirat **69,** 387 (1963).
3. Unpublished investigations carried out with Dr. P. SOHÁR.
4. KATRITZKY, A. R., LAGOWSKI, J. M.: Advances in Heterocyclic Chemistry. (Ed. by KATRITZKY, A. R.) Vol. 1, pp. 341, 403, and 417; Vol. 2, pp. 5, 20, 36, and 66., Academic Press, New York and London, 1963.
5. DOLESCHALL, G., LEMPERT, K.: Acta Chim. Hung. **45,** 357 (1965).
6. MÜLLER, R., DÖRR, F.: Z. Elektrochem. **63,** 1150 (1959).
7. LÁNG, L. (editor): Absorption Spectra in the Ultraviolet and Visible Region. (Publishing House of the Hungarian Academy of Sciences, Budapest, and Academic Press, New York) Vol. IV, 1963; Vol. V, 1965; Vol. VI, in press.
8. GROUT, R. J., PARTRIDGE, M. W.: J. Chem. Soc. [London] **1960,** 3546.

Imidazochinazolindione, IV

UV Absorptionsspektren und Struktur einiger potentiell tautomerer Imidazochinazolindione und verwandter 4-Chinazolinone

G. DOLESCHALL, L. LÁNG und K. LEMPERT

Zusammenfassung. Unter den angewandten Versuchsbedingungen existieren alle Vertreter einer untersuchten Reihe potentiell tautomerer 4-Chinazolinon- und Imidazochinazolindionderivate in derjenigen tautomeren Modifikation, die keine, vom C-2 Atom des Chinazolinringes ausgehende, zu diesem Ring exocyclische C=N Bindung enthält, und in welcher der Sauerstoff nicht in Form einer Hydroxyl- sondern einer Carbonylgruppe vorliegt.

Im Falle der 4-Chinazolinonderivate steht dieser Befund in vollem Einklang mit der bei potentiell tautomeren heterocyclischen Verbindungen beobachteten allgemeinen Erfahrung [4], nach welcher die an den Ring gebundenen N-Atome eher Amino- als Iminogruppen, O-Atome dagegen eher Carbonyl- als Hydroxylgruppen zu bilden geneigt sind.

Im Falle der untersuchten Imidazochinazolindione muß dagegen eine, zu dem einem der Heteroringe exocyclische C=N Bindung unbedingt vorliegen. Hier besteht das Problem darin, zu entscheiden, welcher der Ringe (d. h. der Pyrimidin- oder der Imidazolring) eine stärkere Tendenz zur Vermeidung dieses Bindungstyps besitzt. Es wurde festgestellt, daß die C=N Doppelbindung hier immer im Pyridinring, d. h. exocyclisch zum Imidazolring ausgebildet wird.

Die Strukturermittlung der untersuchten Verbindungen mittels UV Spektroskopie wird dadurch ermöglicht, daß sich in Dioxanlösung zwischen den Spektren der Chromophorsysteme I und II (III) — trotz ihrer außerordentlichen Ähnlichkeit — bereits beim ersten Bandensystem doch genügend große Unterschiede finden lassen.

Im allgemeinen kann man feststellen, daß das Spektrum des Chromophorsystems I aus drei getrennten Bandensystemen besteht (mit Intensitätswerten log ε um 3,50, 4,00 bzw. 4,50), während beim Chromophorsystem II (III) das zweite und dritte Bandensystem verschmelzen und daher auf das zweite Bandensystem nur durch eine Inflexion hingewiesen wird.

Имидазохиназолиндионы IV

Ультрафиолетовые спектры и структура нескольких потенциально таутомерных имидазохиназолиндионов и родственных им 4-хиназолинонов

Г. ДОЛЕШАЛЛ, Л. ЛАНГ и К. ЛЕМПЕРТ

Резюме. Исследованные авторами все потенциально таутомерные производные 4-хиназолинона и имидазохиназолиндиона, в условиях опыта, существуют в той таутомерной форме, которая *не* содержит связь C = N, образующуюся с участием C-2 атома хиназолинового кольца и экзоциклическую к этому кольцу, и в которой кислород находится не в форме гидроксила, а в форме карбонила.

В случае производных 4-хиназолинона такой вывод находится в согласии с общими выводами, установленными для потенциально таутомерных гетероциклических соединений [4], согласно которым, находящиеся в связи с кольцом N-атомы, стремятся к образованию амино-, а не иминогрупп; находящиеся же в связи с кольцом O-атомы стремятся к образованию карбонильных групп, нежели гидроксильных.

Однако в случае имидазохиназолиндионов C = N связь, в эксоциклическом положении к *одному* гетерокольцу, всегда должна находиться. Следовательно, проблема здесь состоит в том, что которое из колец (пиримидиновое или имидазоловое) имеет более сильную тенденцию к обходу этого типа связи. Установлено, что двойная связь C = N всегда находится в пиримидиновом кольце, следовательно — экзоциклически к имидазоловому кольцу.

Определению структуры исследованных соединений, с помощью ультрафиолетового спектроскопического метода, способствует то обстоятельство, что в диоксановом растворе, в спектре I и II (III) хромофор-систем, несмотря на их чрезвычайное сходство, все же можно найти достаточную разницу уже у первой системы полос.

В качестве обобщения можно установить, что спектр I хромофор системы состоит из трех разностоящих систем полос, величины интенсивностей которых, приблизительно ($\log \varepsilon$): 3,50; 4,00; 4,50, в случае же II (III) хромофор-системы, однако, вторая и третья системы полос сливаются в одну систему, и только перегиб указывает на существование второй системы полос.

Соединение V, содержащее C = N двойную связь вне хиназолинового кольца, характеризуется новой хромофор-системой, спектр которой уже в значительной степени отличается от спектров соединений I—III.

Dr. Gábor Doleschall Budapest XI. Gellért tér 4
Dr. László Láng Budapest I. Batthyány u. 34
Prof. Dr. Károly Lempert Budapest XI. Gellért tér 4

CORRELATION BETWEEN THE PAPER CHROMATOGRAPHIC R_f AND R_m-VALUES AND THE STRUCTURE OF AZO DYES*

A. LŐRINC, F. PÉTER and O. DOBOZY

(Central Research Laboratory for Colouristics and Research Institute for Textile Industry, Budapest)

Received January 12, 1965

Introduction

A number of studies have been published on the chromatography of dyes [*e.g.*, 1, 2, 3, 4, 5], but only a few of them refer to azo dyes. A great part of azo dyes, examined chromatographically belong to the group of food dyes. Azo dyes applied in the dyeing of textile materials have been studied only by ZAHN [6] and ŠRÁMEK [7]. Some authors [8, 9, 10] examined a number of azo dyes, which have also been applied as acidic and substantive textile dyes, from the point of view of food dyes.

The aim of the chromatographic procedures reported in the literature has been generally the recognition and identification of dyes. The possibility of a correlation between structure and retention factor was mentioned for the first time by ZAHN [6]. ELLIOT and TELESZ [11] stated that the nature and position of the substituents attached to the aromatic ring have an influence on the R_f values. Hydroxylamine groups (in saturated methyl alcoholic petroleum ether developing solvent) slow down the migration, whereas alkyl and phenyl groups have accelerating effect. ŠRÁMEK [7] found that the R_f-values were the highest with mono-, lower with dis- and the lowest with trisazo disperse dyes. Within a single group, substitution has, in general, a decreasing effect on the R_f values, owing to the increase of the molecular weight.

In case of dyes of identical structures and molecular weights, generally those have higher R_f-values, whose dipole moments are lower, compared with the developing agent.

The technique of paper chromatography may be varied also in case of dyes. ELLIOT and TELESZ [11] used ascending, descending, circular and stripe chromatography, whereas TILDEN [12], ZAHN [6] and ŠRÁMEK [7] applied only the ascending technique.

Developing agents employed in the chromatography of azo dyes are of various character. TILDEN [12] tested 27 alternatives of solvent systems, among others different phenolic mixtures. VALENCIANO and IBARRA [14]

* Presented by the Central Research Laboratory for Colouristics, Budapest.
Read at the XIXth International Congress of Pure and Applied Chemistry (IUPAC,) 963, London.

experimented with solutions and mixtures of different alcohols, KOLSCHEK [13] with water-pyridine mixtures. RAO and SARMA [15] used mixtures of ethylenediamine hydrate and water, ZAHN [6] the mixture of isobutyric acid and water.

Generally, the conventional papers have been used for water-soluble azo dyes, and impregnated or acetylated chromatographic papers were only occasionally applied. (Impregnation was carried out, *e.g.*, by paraffin oil [10] or dimethyl phthalate [13].)

THALER [16] was the first to observe the salt sensibility of dyes in chromatography. He found that salts decreased the R_f-values in the following order: NH_4Cl, NaCl, $(NH_4)_2SO_4$, Na_2SO_4.

The dyes used in foodstuffs were purified according to the method of THALER and SOMMER [18] by dissolving them together with the food; clean wool was placed into the acidified solution, and it was boiled. The dye coloured the wool, which was rinsed afterwards with water and the dye recovered by a solvent. THALER [16, 18] mentioned the possibility of purifying the dyes by paper chromatography, but rejected this method as inconvenient.

The components of dyes were generally not separated, in fact, they were identified just on the basis of secondary spots. Only VENKATARAMAN [17] separated the additional components from the dyes. According to this method, the dye was adsorbed on a chromatographic column of cellulose, then dissolved, and recovered by recrystallization. The two methods described in the literature [16, 18] are suitable for the separation of dyes from impurities, such as foodstuffs, binders, etc., but not for the elimination of other dyes present as impurities.

Purpose of the experiments

Attempt was made to solve the following problems:

1. To find some mono-, dis- and trisazo dyes, the structures of which differ from each other by one, or by a few groups only (Table I).

2. To find optimum conditions of the paper chromatography of purified azo dyes.

3. To determine the R_f values of the selected substantive and acidic azo dyes and to examine whether a correlation between R_f values and the structures of the dyes on one hand, and between R_f values and some important dyeing properties on the other, can be found.

Purification of azo dyes

Among the 9 dyes listed in Table I, the first three are acidic-dyes (among monoazo dyes there are no direct [substantive] dyes) which are used for dyeing of fibres containing amino groups; the others are direct (substantive) dyes,

applied mostly for the dyeing of fibres capable of the formation of H-bonds. All the chosen dyes were mixtures consisting of several components. Consequently, they had to be purified before starting the experiments. The purification was carried out by removing the additional components from the main component by paper chromatography.

After trying several types of paper, Schleicher and Schüll 2043/b Gl paper was used. A line was drawn at a distance of 10 cm from the lower end of the paper with the solution of the technical dye in water, containing the by-components, then the paper was developed either by water-saturated phenol (Figs. 1—9) or by a mixture of pyridine (25%) and water (75%) (Figs. 10—18).

It was found in each case that on the chromatograms showed one spot (zone) of essentially higher colour intensity than the rest, which probably corresponded to the structure given by the Colour Index. The other coloured spots (zones) were due to by-products or coloured intermediates formed in the course of preparing the dye, or may have been attributed to the presence of shading dyes.

The strip containing the spot of the main component was cut out and extracted in a Soxhlet apparatus. After developing with phenol, firstly phenol was eluted with ether, then the ether evaporated, and the dye eluted with water. In case of developing with pyridine, first the pyridine had been evaporated (it has to be noted that complete removal of pyridine was not possible), then the dye could have been solved. The solution of a dye obtained by either purification method proved to be chromatographically homogeneous, thus verifying the adequacy of both purification methods.

An aliquot part of the extracts was evaporated to determine the quantity of dye, while the rest of the solution was adjusted to a concentration of 10 g/l either by evaporation or by dilution. The solutions of dyes purified by the pyridine method gave a precipitation on evaporation, therefore we used the dye solutions which were purified by the phenol method for our chromatographic experiments.

Determination of the optimal conditions for the chromatography of azo dyes

It is known that in the paper chromatography of azo dyes, especially substantive azo dyes, not only the partition of the stationary and moving liquid phases, but, due to the substantivity, secondary bonds between dye and paper play an important role [16, 19] and may influence the R_f values and the migration of the dyes.

Therefore, prior to the exact determination of the R_f values, the influence of the conditions affecting substantivity had to be examined. These are:

Table I

The examined dyes

No.	Dye	Manufacturer	Colour-Index Number (1956)	Type	Structural formula
1.	Azorubin S (C. I. Acid Red 14)	Chemapol	14720	Monoazo	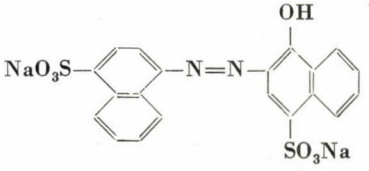
2.	Viktoriarubin O (C. I. Acid Red 27)	Chemapol	16185	Monoazo	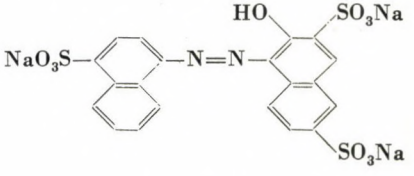
3.	Cochenillerot A (C. I. Acid Red 18)	Chemapol	16255	Monoazo	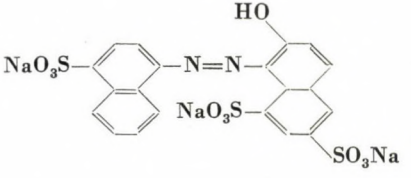
4.	Benzoechtrot F (C. I. Direct Red 1)	Bayer	22310	Disazo	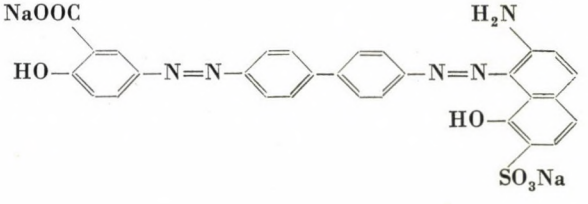

5.	Benzobraun M (C. I. Direct Brown2)	Bayer	22311	Disazo	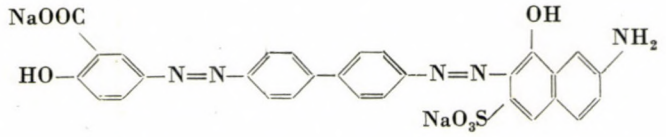
6.	Benzo-Bordeaux (C. I. Direct Red 13)	Bayer	22155	Disazo	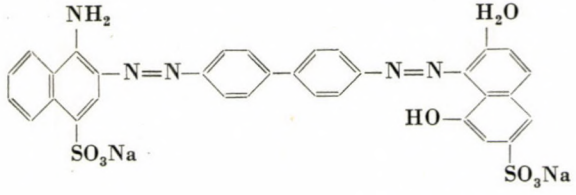
7.	Direct Grün B (C. I. Direct Green 6)	CIBA	30295	Trisazo	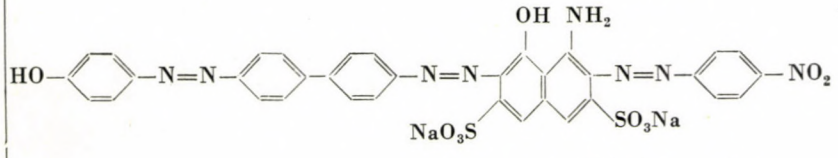
8.	Benzogrün GN (C. I. Direct Green 9)	Bayer	30310	Trisazo	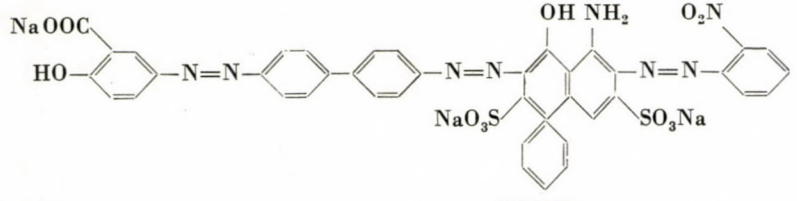
9.	Columbiagrün G (C. I. Direct Green 8)	Wolfen	30315	Trisazo	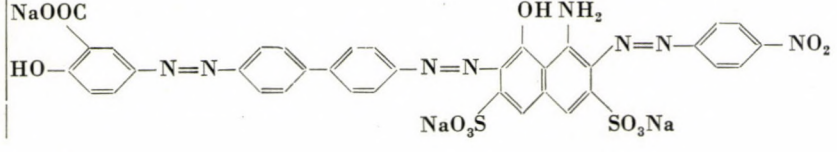

Table II

R_f values in function of the quantity of dyes used

(Developing solvent: phenol saturated with water)

No.	Dye	Quantity, in γ					
		1	2.5	5	10	25	50
2.	C. I. Acid Red 27	0.137	0.130	0.133	0.137	0.146	0.145
6.	C. I. Direct Red 13	0.213	0.206	0.210	0.210	0.160	0.097
8.	C. I. Direct Green 9	0.146	0.127	0.123	0.130	0.133	0.133

1. the concentration and
2. the effect of salts.

These investigations were made at room temperature because only relative values were needed.

When developed with the water-phenol mixture, also used for separation, the R_f values of the dyes did not show any dependence on concentration (in case of 1 γ — 25 γ drops). This was proved by the chromatograms of C.I. Acid Red 27 (monoazo), C.I. Direct Red 13 (disazo) and the C.I. Direct Green 9 (trisazo dye). The corresponding R_f values are shown in Table II. When experimenting with C.I. Direct Red 13, the application of 50 γ revealed definite dependence on the concentration. The R_f values with 50 γ of C.I. Acid Red 27 and C.I. Direct Green 9 deviated from the results obtained with smaller quantities only within the standard limits, so no dependence on concentration was found. The results show that the R_f values of the chosen dyes are independent of the concentration within a wide range. However, as in case of applying drops containing more than 5 γ the shape of the spots became indistinct and thus the possibility of evaluation was decreased (Figs. 19—21), in subsequent experiments 5 γ of each dye was applied.

To clarify the salt effect, the dependence of the R_f values of the dyes C.I. Acid Red 27, C.I. Direct Red 13 and C.I. Direct Green 9 in the presence of salt was determined. For this purpose 0.1—12.5 g/l of sodium chloride was added to a salt-free, 10 g/l solution of the pure dye investigated. Different behaviour was observed with the studied mono-, dis-, and trisazo-dyes. As to be seen from Fig. 22, even the smallest salt addition caused a decrease of the R_f value. At salt concentrations between 0.1 and 2.5 g/l, however, no relative change of the R_f values could be observed. A salt concentration of 12.5 g/l caused further decrease of the R_f value, and instead of spots, zones were obtained.

The R_f values of C.I. Direct Red 13 were not altered by salt addition, but the tendency for striped development was enhanced. Furthermore, a second or even a third centre appeared within the same zone (Fig. 23). The R_f value

of C.I. Direct Green 9 was increased even by the smallest salt addition. However, the R_f values were relatively constant again in the 0.1—2.5 g/l range of salt concentration. At salt concentrations of 12.5 g/l or higher, the spots became quite blurred and so the R_f values could not be determined (Fig. 24).

On the basis of the above results, the R_f values of the investigated dyes showed a marked dependence on salt concentration.

Considering the results of these preliminary experiments, the optimal conditions for chromatography during the systematic investigation were selected as follows:

Chromatographically purified, salt-free dyes were used which had been separated from other components. The sample was applied to the paper from an aqueous solution of 10 g/l concentration by means of a 10 μl micropipette having 0.1 μl graduation. 1/2 μl was applied in each case corresponding to 5 γ of the dye. During the procedure of applying the solutions, the Schleicher and Schüll 2043/b Gl paper (24×50.5 cm) was heated from below by an infrared lamp of 250 W. The starting spots were 6 cm far from the lower end of the paper and at a distance of at least 4.5 cm from the edge. Distance between the lamp and the paper was 5 cm. The starting points were placed 4 cm apart. The paper was subjected to the vapours of the moving phase solvent for 8 hours, then developed with phenol saturated with water using the ascending technique in a Chropa 001—1—2 apparatus (Fig. 25).

In each case freshly distilled phenol and freshly saturated mixture was applied. To ensure the required vapour tension, a trough containing water was placed at the bottom of the chamber during development.

The procedure lasted, in general, for 18 hours at 22 $\pm$ 1° C; ascension of the solvent front amounted to 200—220 mm. The developed chromatograms were dried with an infrared lamp.

For checking the results, twenty parallel runs were made with each purified dye, and the R_f value of each spot was determined separately. Using the equation

$$v = \frac{100 \sqrt{\Sigma \Delta_i^2}}{\bar{x} \cdot n}$$

the standard deviations of the R_f values of each dye were also determined.

(Δ_i = deviation from the arithmetic average of the results of measurements,
n = number of measurements,
v = percentage deviation,
$\bar{x}$ = arithmetic average of the results.)

The deviations were generally within the limit of 0.01—0.2 R_f units, which corresponds to 4.9% standard deviation. The maximum deviation was 9.6%.

Using the given method, unambiguous chromatograms of the investigated purified dyes could be obtained, which gave well defined R_f values.

Results and their evaluation

The arithmetical means of the R_f values of the dyes mentioned in Table I, determined by the above mentioned method, were taken as the basis of evaluation. The data are shown in Table III, constructed from Figs. 26—28.

Table III

R_f and R_m values of the purified dyes

No.	Dye	Type	Number of Colour Index	R_f value	R_m value
1.	C. I. Acid Red 14	monoazo	14720	0.450	+0.086
2.	C. I. Acid Red 27	monoazo	16185	0.190	+0.630
3.	C. I. Acid Red 18	monoazo	16255	0.230	+0.525
4.	C. I. Direct Red 1	disazo	22310	0.320	+0.327
5.	C. I. Direct Brown 2	disazo	22311	0.150	+0.753
6.	C. I. Direct Red 13	disazo	22155	0.230	+0.525
7.	C. I. Direct Green 6	trisazo	30295	0.400	+0.176
8.	C. I. Direct Green 9	trisazo	30310	0.240	+0.500
9.	C. I. Direct Green 8	trisazo	30315	0.230	+0.525

It appears that in case of the chosen dyes the R_f values do not depend primarily on the number of azo groups present. No other relationship between the structure and R_f value of the dyes could be detected.

Therefore, the corresponding R_m values were calculated from the R_f values:

$$R_m \equiv \log \frac{R_f}{1 - R_f}$$

According to REICHL [20] the final R_m value of a given molecule is built up from the partial R_m values, as the molecule is composed of groups. Every group corresponds to a partial R_m value and the sum of these makes up the final R_m value of the molecule, proving the R_m to be an additive quantity.

Table III shows the R_m values of the 9 dyes examined. On the basis of the R_m values of these dyes, the following correlations may be stated:

Monoazo dyes

1. The increase of the R_m value by 0.544 units of C.I. Acid Red 27 in comparison with C.I. Acid Red 14 may be attributed to three factors:
   a) The azo coupling is in α-position instead of β-position.
   b) An additional sulphonic acid substituent is attached to the non-coupling ring of naphthalene.
   c) The sulphonic acid group is in *o*-position instead of *p*-position in the coupled ring.
2. The transfer of a sulphonic acid group from position 3 to position 8 of the naphthalene ring results in the decrease of the R_m values by 0.105 (C.I. Acid Red 27 and C.I. Acid Red 18).

Disazo dyes

1. The transfer of the point of azo coupling from position 1 to position 7 causes 0.426 increase of the R_m value (C.I. Direct Red 1 and C.I. Direct Brown 2).
2. Considerable difference can be observed also between the R_m values of the dyes C.I. Direct Brown 2 and C.I. Direct Red 13. Since the substituents of the trisubstituted naphthalene rings are identical in both molecules, and they differ only in the coupling position, the difference in the R_m values can primarily be attributed to the fact that the salicylic acid molecule fragments of C.I. Direct Brown 2 has been replaced by a naphthylamine sulphonic acid radical.

Trisazo dyes

1. Introduction of one more carboxylic group results in an increase by 0.324 of the R_m value (C.I. Direct Green 6 and Direct Green 9).
2. The transfer of a nitro group from *p*-position to *o*-position (C.I. Direct Green 8 and C.I. Direct Green 9) results in a decrease of the R_m value by 0.025, which is within the limits of error, thus indicating that this structural change does not cause any observable difference in the R_m value. The chosen 9 dyes do not enable us to determine regular correlations between R_m values and the structures of the dyes. Therefore we intend to carry out further experiments to establish the influence of different groups and positions of substitution on the R_m values in a greater number of dyes.

An attempt was made to find relationship between the colour fastness of direct dyes, and their R_f or R_m values. The results are shown in Table IV. As it is seen from Table IV, the water and alkali fastness of the dyes varies reversely with the R_f values, but parallel with the R_m values.

Table IV

Correlation between some properties of dye fastness and the R_f and R_m values of the dyes

No.	Dye	No. of Colour Index	R_f value	R_m value	Water fastness*	Alkali fastness*
4.	C. I. Direct Red 1	22310	0.320	+0.327	2	4
4.	C. I. Direct Brown 2	22311	0.150	+0.753	4.5	4
6.	C. I. Direct Red 13	22155	0.230	+0.525	3.5	4
7.	C. I. Direct Green 6	30295	0.400	+0.176	1	1
8.	C. I. Direct Green 9	30310	0.240	+0.500	2	4
9.	C. I. Direct Green 8	30315	0.230	+0.525	4	5

* The given values were taken from the appropriate colour-cards.

SUMMARY

1. A procedure has been evolved for the purification of some azo dyes.

2. By means of a suitable developing agent, mono-, dis-, and trisazo dyes (3 of each type) were examined.

3. The R_f values of the nine purified azo dyes were determined, and the R_m values were calculated from the data.

4. Possible correlations were examined between the R_f and R_m values of the azo dyes, the structures and fastness values.

REFERENCES

1. KITAHARA, S., MANABE, O., HIYAMA, H.: J. Chem. Soc. Japan Ind. Chem. Sect. **58,** 675 (1955).
2. ZALOKAR, M.: J. Am. Chem. Soc. **74,** 4213 (1952).
3. MUZIK, F., ALLAN, Z. J.: Coll. Czechoslov. Chem. Communs. **20,** 623 (1955).
4. GRASSMAN, W., HÜBNER, L: Das Leder **5,** 49 (1956).
5. NISHIYAMA, K.: Kagaku ro Sosa **11,** 45 (1958).
6. ZAHN, H.: Textil Praxis **6,** 127 (1951).
7. ŠRÁMEK, J.: J. Chrom. **9,** 476 (1962).
8. JAX, P., AUST, H.: Milchwiss. Ber. **89,** 145 (1953).
9. MÜLLER, K., TEUFEL, K.: Ernährungsforsch. **1,** 354 (1956).
10. LINDBERG, W.: Z. Lebensm. Untersuch. u. Forsch. **103,** 1 (1956).
11. ELLIOT, K., TELESZ, L. A.: J. Soc. Dyers and Col. **78,** 8 (1957).
12. TILDEN, D. H.: J. Assoc. Offic. Agr. Chemists **35,** 423 (1952).
13. KOLSCHEK, J.: Chem. Ztg. **83,** 478 (1959).
14. VALENCIANO, O. A., IBARRA, A.: Rev. Assoc. bioquim. agr. **21,** 141 (1956); ibid. **24,** 121 (1959).
15. RAO, V. K. M., SARMA, P. S. N.: J. Sci. Ind. Research (India) **21D,** 61 (1962).
16. THALER, H., SOMMER, G.: Z. Lebensm. Untersuch. u. Forsch. **97,** 345 (1953).
17. GORE, T. S., UNNI, M. K., VENKATARAMAN, K.: J. Sci. Ind. Research (India) **15B,** 618 (1956).
18. THALER, H., SOMMER, G.: Z. Lebensm. Untersuch. u. Forsch. **97,** 441 (1953).
19. JASCHIK, S., KRAMMER, M.: Magy. Kém. Foly. **57,** 140 (1951).
20. REICHL, E. R.: Mh. Chem. **86,** 69 (1955).

Zusammenhänge zwischen den R_f- bzw. R_m- Werten von Azofarbstoffen und ihrer Struktur

A. LŐRINC, F. PÉTER und O. DOBOZY

Zusammenfassung. 1. Es wurde für einige Azofarbstoffe ein Reinigungsverfahren ausgearbeitet.

2. Unter Verwendung eines geeigneten Laufmittels wurden je 3 Mono-, Dis- und Trisazofarbstoffe untersucht.

3. Die R_f-Werte der 9 gereinigten Farbstoffe wurden bestimmt und aus diesen die R_m-Werte berechnet.

4. Es wurden Zusammenhänge zwischen den R_f- bzw. R_m-Werten der untersuchten Farbstoffe und ihrer Struktur bzw. gewisser Farbechtheitswerte festgestellt.

Зависимости между структурой и бумагохроматографическими величинами R_f и R_m азо-красителей

А. ЛЁРИНЦ, Ф. ПЕТЕР и О. ДОБОЗИ

Резюме. 1. Разработан способ очистки некоторых азо-красителей.

2. С помощью соответствующих пробегных агентов исследовались 3—3 моно-, дис- и трисазо-красители.

3. Для 9 очищенных красителей определены величины R_f, и из последних рассчитаны величины R_m.

4. Авторы искали зависимости между R_f- или R_m-величинами и структурой или отдельными величинами светостойкости исследованных азо-красителей.

Andor LŐRINC
Ferenc PÉTER
Ottó DOBOZY
Budapest IV., Váci út 71.

Fig. 13. Benzoechtrot F *(Bayer)* Developing solvent: 25% pyridine + 75% water

Fig. 14. Benzobraun M *(Bayer)* Developing solvent: 25% pyridine + 75% water

Fig. 15. Benzobordeaux B *(Bayer (*Developing solvent: 25% pyridine + 75% water

Fig. 16. Direktgrün B *(CIBA)* Developing solvent: 25% pyridine + 75% water

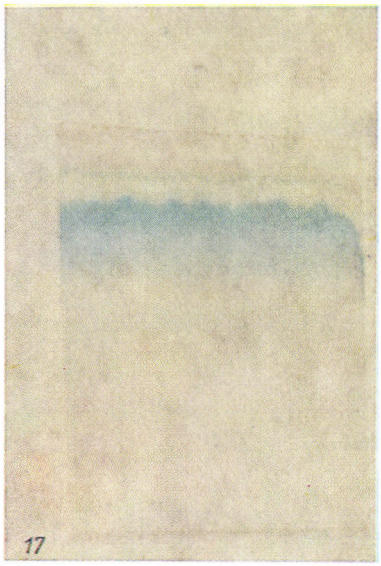

Fig. 17. Benzogrün GN *(Bayer)* Developing solvent: 25% pyridine + 75% water

Fig. 18. Columbiagrün G *(Wolfen)* Developing solvent: 25% pyridine + 75% water

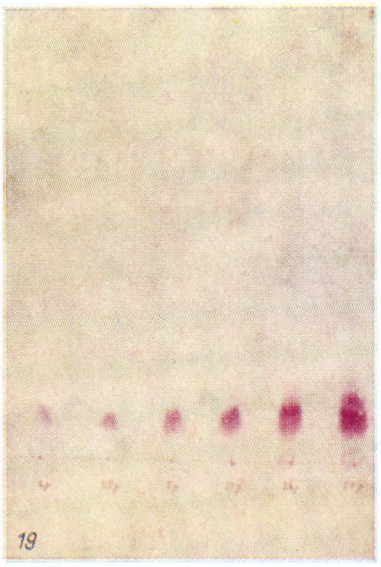

Fig. 19. Viktoriarubin O *(Chemapol)*, purified C. I. Acid Red 27

Effect of dye concentration, developing solvent: phenol saturated with water

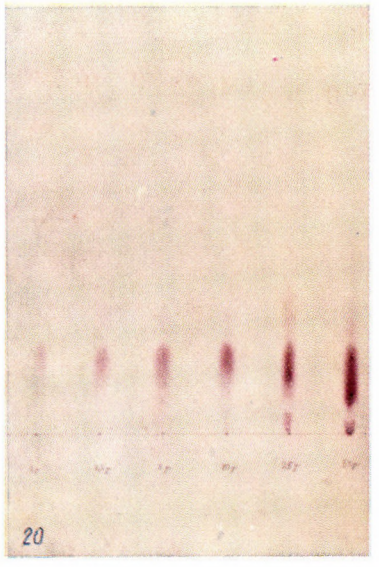

Fig. 20. Benzobordo B *(Bayer)*, purified C. I. Direct Red 13

Effect of dye concentration, developing solvent: phenol saturated with water

Fig. 21. Benzogrün GN *(Bayer)*, purified C. I. Direct Green 9
Effect of dye concentration, developing solvent: phenol saturated with water

Fig. 22. Viktoriarubin O *(Chemapol)*, purified C. I. Acid Red 27
Effect of salt (NaCl) concentration, developing solvent: phenol saturated with water

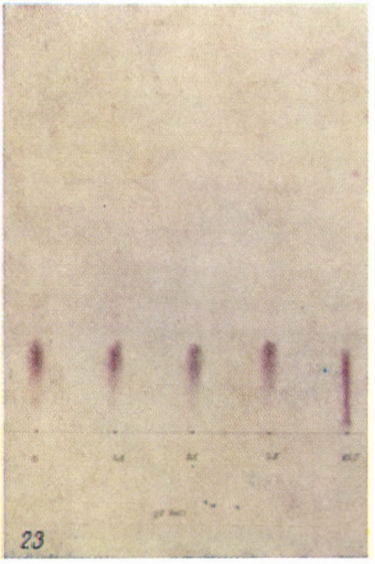

Fig. 23. Benzobordeaux B *(Bayer)*, purified C. I. Direct Red 13
Effect of salt (NaCl) concentration, developing solvent: phenol saturated with water

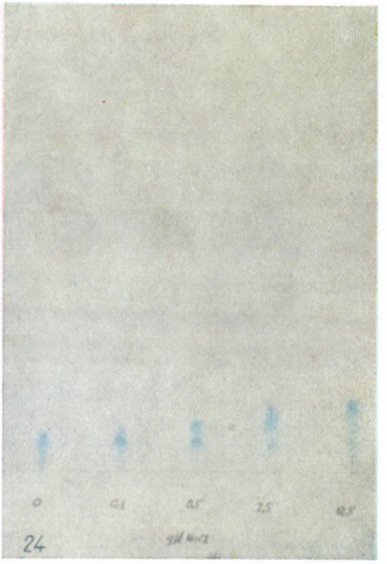

Fig. 24. Benzogrün GN *(Bayer)*, purified C. I. Direct Green 9
Effect of salt (NaCl) concentration, developing solvent: phenol saturated with water

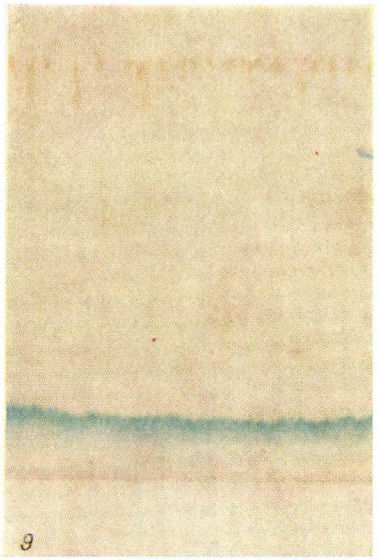

Fig. 9. Columbiagrün G *(Wolfen)* Developing solvent: phenol saturated with water

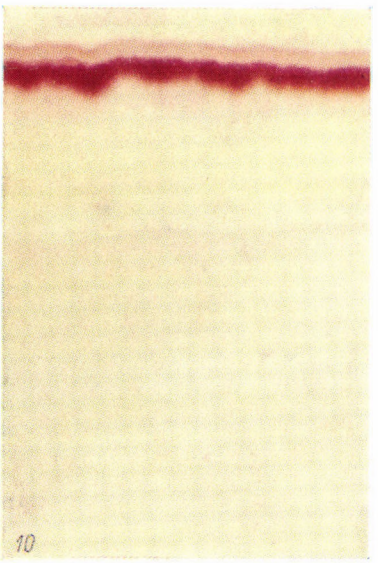

Fig. 10. Azorubin S *(Chemapol)* Developing solvent: 25% pyridine + 75% water

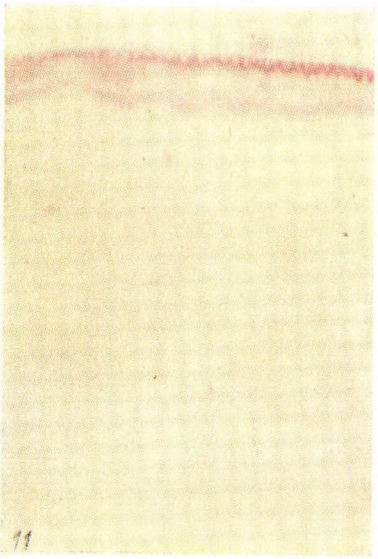

Fig. 11. Viktoriarubin O *(Chemapol)* Developing solvent: 25% pyridine + 75% water

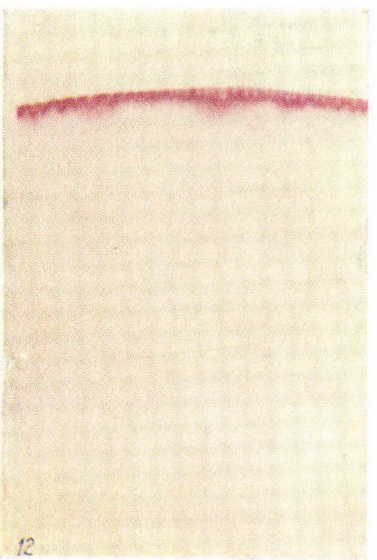

Fig. 12. Cochenillerot A *(Chemapol)* Developing solvent: 25% pyridine + 75% water

Fig. 5. Benzobraun M *(Bayer)* Developing solvent: phenol saturated with water

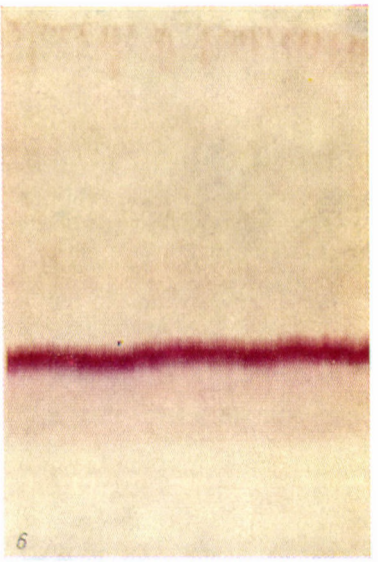

Fig. 6. Benzobordeaux B *(Bayer)* Developing solvent: phenol saturated with water

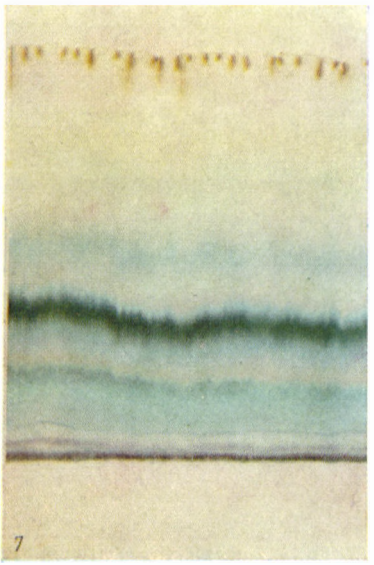

Fig. 7. Direktgrün G *(CIBA)* Developing solvent: phenol saturated with water

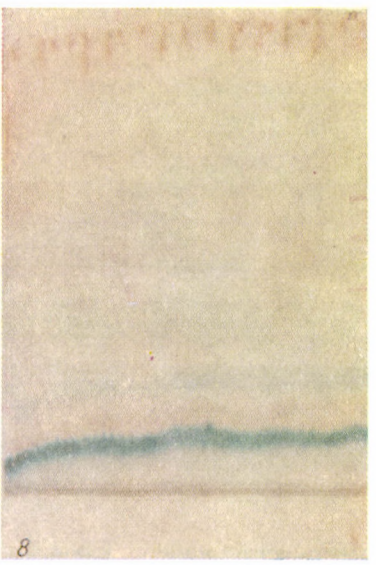

Fig. 8. Benzogrün GN *(Bayer)* Developing solvent: phenol saturated with water

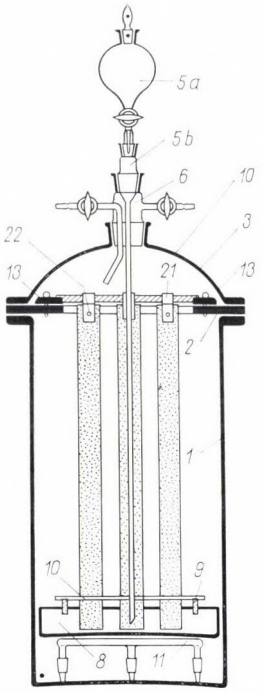

1. Glass cylinder
1/a Lid
2. Glass insert plate
3. Supporting glass rod
5/a Dropping funnel
5/b Inlet pipe
6. Gas inlet
8. Tray for developing solvent
9—10. Control of paper strip distance
11. Tray support
13. Plate for the glass rods
21. Clamp for mixing the paper strips
22. Glass nail

Fig. 25. Chropa 001-1-2 type apparatus

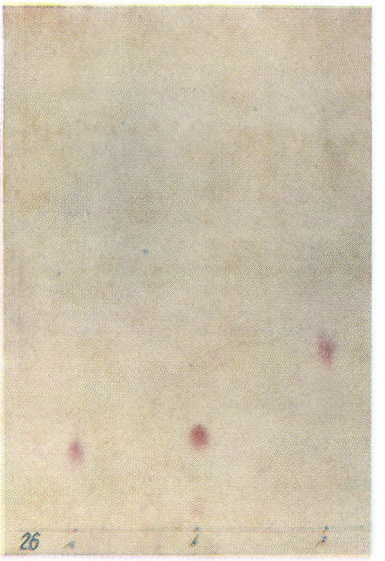

Fig. 26. a) Azorubin S *(Chemapol)*, purified C. I. Acid Red 14. *b)* Viktoriarubin O *(Chemapol)*, purified C. I. Acid Red 27. *c)* Cochenillerot A *(Chemapol)*, purified C. I. Acid Red 18. Developing solvent: phenol saturated with water

Fig. 27. a) Benzoechtrot F *(Bayer)*, purified C. I. Direct Red 1. *b)* Benzobraun M *(Bayer)*, purified C. I. Direct Brown 2. *c)* Benzobordeaux B *(Bayer)*, purified C. I. Direct Red 13. Developing solvent: phenol saturated with water

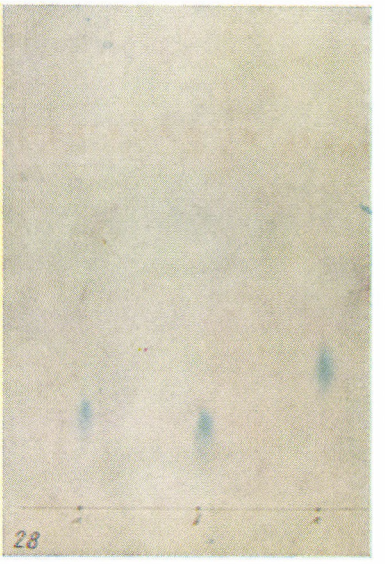

Fig. 28. a) Direktgrün B *(CIBA)*, purified C. I. Direct Green 6. *b)* Benzogrün GN *(Bayer)*, purified C. I. Direct Green 9. *c)* Columbiagrün G *(Wolfen)*, purified C. I. Direct Green 8. Developing solvent: phenol saturated with water

Fig. 1. Azorubin S *(Chemapol)* Developing solvent: phenol saturated with water

Fig. 2. Viktoriarubin O *(Chemapol)* Developing solvent: phenol saturated with water

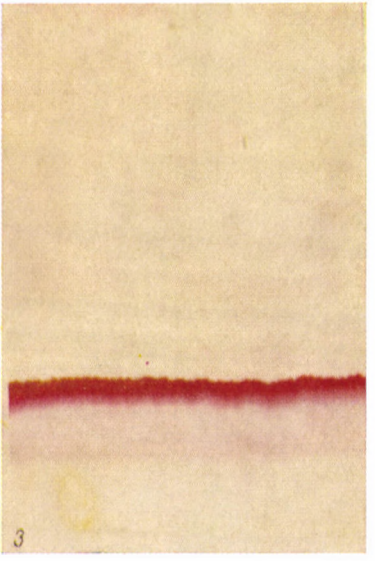

Fig. 3. Cochenillerot A *(Chemapol)* Developing solvent: phenol saturated with water

Fig. 4. Benzoechtrot F *(Bayer)* Developing solvent: phenol saturated with water

UNTERSUCHUNG DER VERÄNDERUNGEN VON SULFITABLAUGEN WÄHREND DER VERHEFUNG

B. Tóth

(Gerbstoffabrik, Budapest)

Eingegangen am 24. Mai 1965

Unter den zuckerhaltigen Nährstoffen der biologischen Proteinsynthese spielt die bei der Zellstoffherstellung anfallende Sulfitzellstoffablauge eine immer wichtigere Rolle [1]. Zu ihrer Verwertung wurden erfolgreiche Versuche bereits auch in Ungarn durchgeführt [2]. Die während der Verhefung eintretende Veränderung der Zusammensetzung ist jedoch noch immer nicht genügend geklärt [3]. Die Durchführung wissentschaftlicher Untersuchungen auf diesem Gebiete schien daher notwendig zu sein.

Die chemische Zusammensetzung der Sulfitablauge ist in erster Linie eine Funktion der Art der Zellstoffgewinnung [4, 5]. In letzter Zeit haben sich in Ungarn nicht nur in der Methode des Aufschlusses, sondern auch auf dem Gebiete des Ausgangsmaterials Veränderungen eingestellt [6]. Alldies hat zu einer Veränderung der Zusammensetzung der anfallenden Sulfitablauge geführt. Als Ergebnis der gegenwärtig angewandten, hohe Ausbeuten liefernden Zellstoffegewinnungsverfahren hat der Kohlehydratgehalt der Sulfitablaugen wesentlich abgenommen. (Im weiteren werden die Sulfitablaugen der normalen und »hochausbeute« Zellstoffgewinnungsverfahren, der Einfachheit halber, normale bzw. Hochausbeute-Sulfitablaugen genannt.) Die Umstellung von Nadelhölzern auf Laubhölzer hat zu einer Erhöhung des Pentosegehaltes — gegenüber den Hexosen — geführt [7, 8, 9], wie dies auch aus Tab. I und II ersichtlich ist.

Beschreibung der Verhefungsversuche

Zu den Versuchen der biologischen Proteinsynthese auf ungarischer Sulfitablaugenbasis standen uns die aus dem Forschungsinstitut für die Gärungsindustrie stammenden Torula utilis 21 und Candida mycoderma 257 Stämme zur Verfügung [10], die in der Folge an mehreren Stellen nur TU—21 bzw. CM—257 genannt werden. Für beide Stämme ist die große Wuchskräftigkeit kennzeichnend und ihre geringe Empfindlichkeit schwefliger Säure (Sulfit) gegenüber [11]. Trotzdem hat der hohe Schwefeldioxydgehalt der ursprünglichen, rohen Sulfitablauge ziemliche Schwierigkeiten bereitet. Der Hefehemm-

Tabelle I

Chemische Zusammensetzung des Trockensubstanzgehaltes der Sulfitablaugen

Komponenten	Hochausbeute Pappel-	Normale Fichten-
	Sulfitablauge	
Ligninsulfonsäure	40,5	54,9
Hexosezucker	4,8	18,0
Pentosezucker	15,8	5,5
Organische Säuren	6,1	2,8
Zuckerderivate*	10,0	6,2
Harze, Extraktstoffe	2,5	3,5
Asche	20,3	9,1
	100,0%	100,0%

* Z. B. Aldonsäuren, Saccharobisulfit usw.

stoff Schwefeldioxyd lag einesteils an Aldehyde gebunden, anderenteils in freier Form (als absorbiertes SO_2) vor. Seine Elimination gelang mittels längerer Belüftung [12], wodurch der freie Schwefeldioxydgehalt in der verdünnten Würze bis unter 0,03% gesenkt werden konnte. Die Enzymdestruktorwirkung des Schwefeldioxyds war in dieser Verdünnung nicht mehr wahrnehmbar [13].

Der Belüftung folgte die Filtration der Sulfitablaugelösung, zwecks Entfernung eventuell vorhandener Zellstoff-Fasern, die das Hefewachstum gestört hätten [14].

Tabelle II

Wichtigere Zuckerarten in der Sulfitablauge

Monosaccharide	Hochausbeute Pappel-	Normale Fichten-
	Sulfitablauge	
Hexosen %	4,8	18,0
Mannose %	0	10,0
Galactose %	4,7	3,0
Glucose %	0,1	5,0
Pentosen %	15,8	5,5
Xylose %	12,4	4,4
Arabinose %	3,4	1,1

Im Zuge der Verhefungsversuche wurde die Wirkung der folgenden Parameter untersucht:

a) Herkunft der Sulfitablauge
b) Stellhefe [15]
c) Dauer der Verhefung
d) pH-Wert während der Verhefung [16].

Die Rolle der Belüftung wurde auch schon von ungarischen Autoren eingehend untersucht [17, 18], daher schien uns die Untersuchung dieses Parameters überflüssig zu sein.

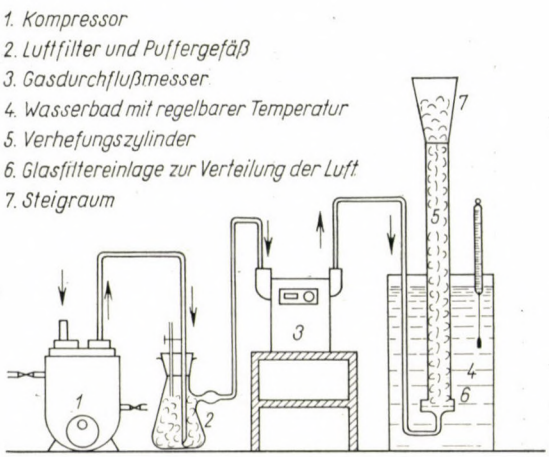

Abb. 1

Die Versuchsbedingungen der Laboruntersuchungen waren folgende (die Versuchseinrichtung ist auf Abb. 1 gezeigt):

Volumen der Sulfitablauge	400—600 ml
pH-Wert der Sulfitablauge	4,5—6,0
Stellhefe zur Beimpfung:	Torula utilis 21 und Candida mycoderma 257
Trockensubstanzgehalt der Stellhefe	0,64%
Superphosphat	0,57%
Ammoniumsulfat	0,58%
Belüftung	100 $m^3/m^2/h$

Die Versuchsbedingungen und die erhaltenen Ergebnisse sind in den Tab. III und IV zusammengefaßt.

Acta Chimica Academiae Scientiarum Hungaricae 47, 1966.

Tabelle III

Auf Fichten-Sulfitablauge erreichte Hefeausbeuten mit einzelnen Rassen und ihren Gemischen
(Ausgangsvolumen: 400 ml)

Nr.	Art der Sulfitablauge	Dauer Std.	pH	Stellhefe		Red. Zuckergeh. %	Endvolumen ml	Hefetrockensubstanzgehalt g				Hefewachstum g/Lit.	Zuckerverwertungsquotient
								Brutto	Stellhefe	Netto	Brutto in 100 ml		
		der Verhefung		TU-21	CM-257	der Sulfitablauge		im Gesamtvolumen					
1.	Normale Fichten-Sulfitablauge	9	4,5	100	—	1,9	460	3,79	2,56	1,23	0,8239	3,08	16,2
2.		9	4,5	80	20	1,9	520	4,46	2,56	1,90	0,8577	4,75	25,0
3.		9	6,0	20	80	1,9	530	4,72	2,56	2,16	0,8905	5,40	28,4
4.		9	6,0	—	100	1,9	530	4,29	2,56	1,73	0,8094	4,32	22,8
5.		12	4,5	100	—	1,9	536	4,17	2,56	1,61	0,7798	4,02	21,2
6.		12	4,5	80	20	1,9	555	4,94	2,56	2,38	0,8901	5,95	31,3
7.		12	6,0	20	80	1,9	536	5,44	2,56	2,88	1,0149	7,20	37,9
8.		12	6,0	—	100	1,9	542	4,82	2,56	2,26	0,8893	5,65	29,7
9.		12	4,5	80	20	2,72	530	5,27	2,56	2,71	0,9943	6,78	24,9
10.		12	5,0	50	50	2,72	550	6,68	2,56	4,12	1,2145	10,3	37,9
11.		12	6,0	20	80	2,72	540	7,17	2,56	4,61	1,3277	11,5	32,4

Tabelle IV

Auf Hochausbeute-Pappel- und Fichten-Pappel-Sulfitablauge erreichte Hefeausbeuten mit einzelnen Rassen und ihren Gemischen
(Ausgangsvolumen: 400 ml)

Nr	Art der Sulfitablauge	pH der Verhefung	Stellhefe		Red. Zuckergeh. %	Endvolumen ml	Hefetrockensubstanzgehalt g				Hefewachstum g/Lit.	Zuckerverwertungsquotient
							Brutto	Stellh.	Netto	Brutto im 100 ml		
			TU-21	CM 257	der Sulfitablauge		im Gesamtvolumen					
1.	Hochausbeute-	4,5	100	—	1,81	470	3,70	2,56	1,14	0,7872	2,85	15,7
2.	Pappel-Sulfitablauge	4,5	80	20	1,81	490	3,16	2,56	0,60	0,6449	1,50	8,3
3.		6,0	20	80	1,81	530	6,36	2,56	3,80	1,2000	9,50	52,5
4.		6,0	—	100	1,25	540	4,86	2,56	2,30	0,9000	5,75	46,0
5.		6,0	20	80	1,25	530	4,20	2,56	1,64	0,7924	4,10	32,8
6.		5,0	—	100	1,25	545	4,70	2,56	2,14	0,8624	5,35	42,8
7.	1 : 1 Gemisch aus Pappel-	5,0	100	—	2,21	460	4,43	2,56	1,87	0,9630	4,68	21,2
8.	und Fichten-Sulfitablauge	5,0	—	100	2,21	560	4,33	2,56	1,77	0,7732	4,43	20,1
9.		5,0	50	50	2,21	556	4,62	2,56	2,06	0,8309	5,15	23,3

Auf Grund der Versuchsergebnisse kann folgendes festgestellt werden:

1. Das geringe Hefewachstum zu Beginn der Verhefung kann auf die Inhibitorwirkung der vorhandenen Ligninsulfonsäure zurückgeführt werden. Infolge der eintretenden Adaptation stieg bei verlängerter Wachstumszeit auch die Ausbeute. An dieser Stelle sei bemerkt, daß mit entsprechend adaptierten Hefearten die Verhefungsdauer von 12 Stunden bis auf 6 Stunden reduziert werden konnte.

2. Die Versuche wurden bei den pH-Werten 4,5, 5,0 und 6,0, d. h. also innerhalb eines pH-Intervalls von 1,5 pH-Einheiten durchgeführt. Außerhalb

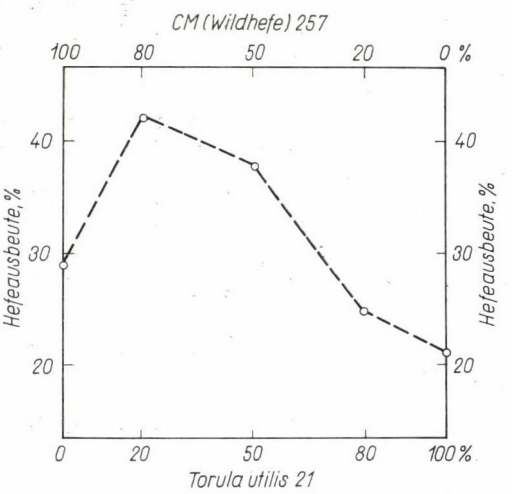

Abb. 2

dieses Intervalls trat entweder eine wesentliche Abnahme der Ausbeute oder die Gefahr von Infektionen auf [19].

3. Die auf Fichtensulfitablauge-Nährboden durchgeführten Untersuchungen haben gezeigt, daß die günstigsten Hefeausbeuten — sowohl bei neunstündiger als auch bei zwölfstündiger Verweilzeit — mit einem Gemisch aus 20% TU—21 und 80% CM—257 erreicht werden können. Die nächstgünstigste Zusammensetzung war vom Gesichtspunkte der Ausbeute 50% TU—21 und 50% CM—257. Weniger günstig vermehrte sich die Zusammensetzung 20% CM—257 und 80% TU—21, während die niedrigsten Ausbeuten mit den einzelnen Stämmen allein erzielt werden konnten. Die mit den beiden untersuchten Heferassen und mit ihren Gemischen erreichten Ausbeuten auf Fichtensulfitablauge veranschaulicht das Diagramm auf Abb. 2.

Wie aus der Abbildung hervorgeht, kann zwischen den beiden Stämmen eine deutliche synergistische Wirkung beobachtet werden.

4. Sowohl die normale Fichten- als auch die Hochausbeute-Pappel-Sulfitablauge kann verheft werden. Bei der letzteren ist der Schwefeldioxyd-

gehalt jedoch höher und muß daher sorgfältiger ausgetrieben werden [20]. Ein weiterer Unterschied zwischen den beiden erwähnten Sulfitablaugen ist, daß der absolute Ertrag an Erntehefe bei der Pappelsulfitablauge infolge des niedrigeren Zuckergehaltes geringer ist.

Im Zuge der nach den oben beschriebenen Prinzipien durchgeführten Verhefungsversuche ließen sich bei den Sulfitablaugen gut definierbare Veränderungen feststellen. Die Ergebnisse dieser Untersuchungen, die mit filtrierten, faserfreien Lösungen durchgeführt wurden, sind nachstehend beschrieben.

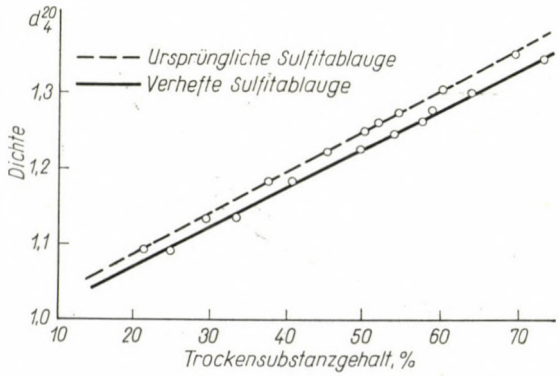

Abb. 3

Veränderungen einiger Merkmale der Sulfitablaugen während der Verhefung

1. *Änderungen der physikalischen Merkmale* (Dichte, Viskosität, Brechungsindex)

Auf den gleichen Trockensubstanzgehalt bezogen, hatte die Verhefung eine meßbare Abnahme des spezifischen Gewichtes zur Folge. Zwischen der Dichte der ursprünglichen und der verheften Sulfitablauge und dem Trockensubstanzgehalt konnte eine lineare Korrelation nachgewiesen werden. Wie aus dem auf Abb. 3 gezeigten Diagramm hervorgeht, waren diese Abweichungen jedoch bei der ursprünglichen und verheften Sulfitablauge verschieden.

Ähnlich nahm während der Verhefung auch die Viskosität ab. Zwischen dem Logarithmus der in Centipoise ausgedrückten Viskosität und dem Trokkensubstanzgehalt konnte ein nahezu exponentieller Zusammenhang festgestellt werden ($y = 2^x$) (Abb. 4).

Diese Feststellung über die Abnahme der Viskosität steht im Einklang mit den durch BUEWSKOI und SAPOTNITZKI beschriebenen Versuchsergebnissen [21].

Die Tatsache, daß die Dichte und Viskosität der verheften Sulfitablauge — bei gleichem Trockensubstanzgehalt — abnimmt, findet ihre Erklärung darin, daß die infolge der Assimilation verbrauchten Monosaccharide eine höhere Dichte und Viskosität besitzen, als die zurückgebliebene Ligninsulfonsäure.

Bezüglich der Viskosität der Sulfitablauge konnte auch festgestellt werden, daß diese mit steigender Temperatur stark abnahm. Zwischen den drei Parametern: Viskosität, Temperatur und Trockensubstanzgehalt konnte

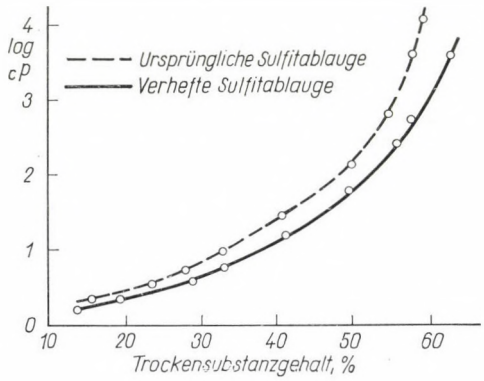

Abb. 4

ein Zusammenhang festgestellt werden, der sich mit folgender Gleichung ausdrücken läßt

$$\eta_t = (ax + b)\, t + cx + d$$

in dieser ist

η_t die Viskosität,
x der Trockensubstanzgehalt,
t die Temperatur,

während a, b, c, d Konstanten sind.

Von den Konstanten a und b hat mindestens eine einen negativen Wert, zumal die Viskosität mit der Temperatur abnimmt.

Mit der Untersuchung des Brechungsindexes der Sulfitablaugen (mit einem Zeiss-Refraktometer) konnte festgestellt werden, daß dieser mit dem Trockensubstanzgehalt (über 25%) einen gut definierten Zusammenhang zeigt. Der Brechungsindex der verheften Sulfitablauge war — im Gegensatz zu den Parametern Dichte und Viskosität — nach der Verhefung größer als vor dieser. Die Erklärung dieses interessanten Ergebnisses liegt darin, daß der Brechungsindex der Monosaccharide niedriger ist, als jener der Ligninsulfonsäure.

2. Änderung und Rolle des Schwefeldioxydgehaltes

Der in der ursprünglichen Sulfitablauge vorhandene, verhältnismäßig hohe Schwefeldioxydgehalt liegt in den folgenden drei Formen vor:

a) An Lignin gebunden [22].

b) An Aldohexose und Aldopentose additioniert [23].

c) In freier Form.

Von besonderer Bedeutung sind die diesbezüglichen Untersuchungen deshalb, weil das Schwefeldioxyd die Gärungsprozesse hemmt [24].

Ich habe bei diesen Untersuchungen den Begriff »SO_2-Quotient« eingeführt, mit welchem das Verhältnis des gesamten und des freien SO_2-Gehaltes definiert werden kann. Bei den normalen Sulfitablaugen ist dieser Wert 1,5—3,0mal größer, als bei der Hochausbeute-Sulfitablauge. Die Tab. V und VI zeigen die im SO_2-Gehalt bei normaler Fichten- und Hochausbeute-Pappel-Sulfitablauge während der unter verschiedenen Bedingungen durchgeführten Verhefung eintretenden Änderungen. Aus den Daten dieser Tabellen ergeben sich nachstehende Schlußfolgerungen:

a) Der gesamte und freie SO_2-Gehalt ändert sich bei den Sulfitablaugen verschiedener Herkunft nicht in der gleichen Weise. Der auch ursprünglich schon höhere Schwefeldioxydgehalt der Hochausbeute-Pappel-Sulfitablauge nimmt nämlich viel stärker ab, als der Schwefeldioxydgehalt der normalen Fichten-Sulfitablauge. Da sich der Schwefeldioxydgehalt der beiden Sulfitablaugen verschiedener Herkunft während der Verhefung sowohl in relativem als auch in absolutem Sinn unterschiedlich verhält, wird die ursprüngliche Differenz zwischen den beiden Werten viel geringer.

b) Vom Gesichtspunkte des in Aldehydbindung vorliegenden SO_2-Gehaltes konnte zwischen den beiden verschiedenen Sulfitablaugen kein eindeutiger Unterschied festgestellt werden, da die Differenz zwischen den auf die Trockensubstanz bezogenen Werten nicht groß war. Hierzu sei bemerkt, daß jener Teil des in Aldehydbindung vorliegenden Schwefeldioxyds, der nicht an Zuckeraldehyd gebunden ist, eine geringere Hemmwirkung auf die Verhefung ausübt als das an die Monosaccharide gebundene Schwefeldioxyd. Die letztere sogenannte Saccharobisulfitverbindung hemmte sogar die Vergärung der freien Monosaccharide [23].

3. Aziditätsverhältnisse in der ursprünglichen und verhefteten Sulfitablauge

Bei der Sulfitablauge haben wir es mit einer solchen Lösung zu tun, die 0,75—1,5% schwefelige Säure und 0,3—0,6% schwache organische Säure enthält. Der erste Wert entspricht einer 0,1—0,2 normalen H_2SO_3-Lösung, der letztere einer 0,05—0,1 normalen Essigsäurelösung.

Tabelle V

Schwefeldioxydverhältnisse bei normaler Fichten-Sulfitablauge nach der Verhefung

(Bezogen auf den Trockentubstanzgehalt)

(Nach 12stündiger Verhefung)

Bedingungen der Verhefung	Urspr. Sulfit-ablauge	20% Torula utilis 21+80% Candida mycoderma 257		
		pH = 6	pH = 5	pH = 4,5
Gesamt-SO_2 %	3,02	1,68	1,73	1,83
Gesamt-SO_2 in % des ursprüngl. Gesamt SO_2 %	100	55,6	57,3	60,6
Freies SO_2 %	0,86	0,25	0,26	0,25
Freies SO_2 in % des ursprüngl. gesamten freien SO_2 %	100	29,1	30,2	29,1
SO_2-Quotient	3,5	1,43	1,47	1,58
SO_2 in Aldehydbindung %	2,16	1,43	1,47	1,58
SO_2 in Ald-Bdg. in % des ursprüngl. SO_2 in Ald.-Bdg. %	100	66,2	68,0	73,1

Die Untersuchungen der Aziditätsverhältnisse [25, 26] erstreckten sich mit der Feststellung des Säuregrades einesteils auf die »Titrations-« oder »Totalazidität«, anderenteils wurde durch die Bestimmung des pH-Wertes die »aktive« Azidität ausgedrückt.

Tabelle VI

Schwefeldioxydverhältnisse bei Hochausbeute-Pappel-Sulfitablauge nach der Verhefung

(Bezogen auf den Trockensubstanzgehalt)

(Nach 12stüdingen Verhefung)

Bedingungen der Verhefung	Urspr. Sulfit-ablauge	Candida mycoderma 257		20% TU-21 80% CM-257
		pH = 6	pH = 5	pH = 6
Gesamt SO_2 %	16,1	1,6	1,34	1,5
Gesamt-SO_2 in % des ursprüngl. Gesamt SO_2 %	100	9,9	8,3	9,3
Freies SO_2 %	13,1	0,36	0,37	0,34
Freies SO_2 in % des ursprüngl. gesamten freien SO_2 %	100	2,7	2,8	2,6
SO_2-Quotient	1,2	4,4	3,6	4,4
SO_2 in Aldehydbindung %	3,0	1,24	0,97	1,16
SO_2 in Ald.-Bdg. in % des ursprüngl. SO_2 in Ald.-Bdg.	100	41,3	32,3	38,6

Tab. VII zeigt die Aziditätsverhältnisse einiger Sulfitablaugen.

Tabelle VII

Aziditätsverhältnisse von normaler Fichten- und Hochausbeute-Pappel-Sulfitablauge

(Bezogen auf die Trockensubstanz)

Nr.	Sulfitablauge Art	Säuregrad	Org. Säure %	pH-Wert	Schwefeldioxyd %	
					insges.	frei
1.	Normal-Fichte	63	2,6	3,1	5,0	1,6
13.	Normal-Fichte	72	2,8	2,9	5,5	1,8
15.	Normal-Fichte	79	3,3	2,6	6,1	1,9
5.	Hochausbeute-Pappel	166	5,5	3,9	8,9	5,9
14.	Hochausbeute-Pappel	233	7,6	3,4	16,1	13,1
16.	Hochausbeute-Pappel	212	6,2	3,2	11,5	7,2

Aus den Untersuchungsergebnissen kann festgestellt werden, daß die mit dem pH-Wert ausgedrückten Wasserstoffionen außer den anorganischen Säuren auch aus den in der Sulfitablauge vorhandenen und weniger dissoziierenden organischen Säuren stammen. Besonders war dies bei der aus dem Hochausbeute-Aufschluß stammenden Sulfitablauge der Fall.

Während der Verhefung werden die schwachen organischen Säuren von den Hefepilzen assimiliert, die also auch selbst an der Beeinflussung der Aziditätsverhältnisse teilnehmen. Dies trat in der Erhöhung des pH-Wertes und in der Abnahme des Säuregrades in Erscheinung. Im Hefewachstum spielt die sogenannte aktive Azidität eine größere Rolle als die Titrationsazidität.

4. Änderung der Menge der Ligninsulfonsäure

Die Bestimmung der Ligninsulfonsäure, der mengenmäßig wichtigsten Komponente der Sulfitablauge [27] konnte nicht nur mit der Naphthylaminmethode [28], sondern auch auf Grund der Salzbildungsreaktion der Ligninsulfonsäure mit Kollagen [29] erfolgreich bestimmt werden. Die Grundlage dieser Methode war die Feststellung, daß es in saurem Medium zwischen der kationischen Aminogruppe des Kollagens und dem anionischen Sulforadikal der Ligninsulfonsäure zu einer stöchiometrischen Bindung kommt (Abb. 5).

Auf Grund der Untersuchungen konnte festgestellt werden, daß der Ligninsulfonsäuregehalt in der normalen Fichten-Sulfitablauge wesentlich höher ist, als in der Hochausbeute-Pappel-Sulfitablauge. Während der Ver-

hefung nahm der Unterschied nur noch zu, was mit der stärkeren Kohlehydratassimilation in der Fichten-Sulfitablauge zusammenhing. Aus alldem folgt, daß für die Verwendungen, die auf der Ligninsulfonsäure als aktiven Stoff beruhen, (z. B. oberflächenaktive und Dispergiermittel) in erster Linie die verhefte Fichten-Sulfitablauge in Frage kommt.

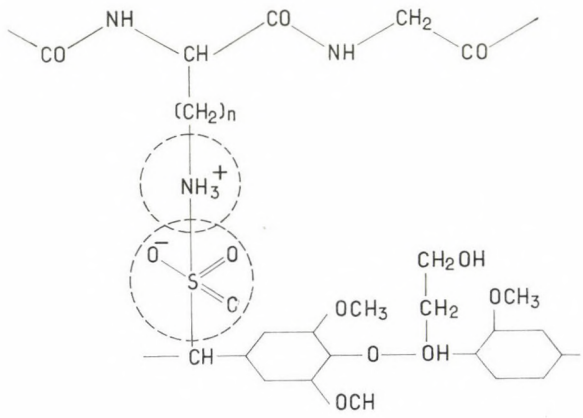

Abb. 5

5. Sauerstoffbedarf bei der ursprünglichen und verhefteten Sulfitablauge

Die Bestimmung der sauerstoffentziehenden Eigenschaften der Sulfitablauge bzw. ihres biologischen Sauerstoffbedarfes in Flußwasser ist von großer Bedeutung [30]. Im Laufe der diesbezüglichen Untersuchungen konnte ich feststellen, daß diese charakteristische Eigenschaft durch die Bestimmung der Kaliumpermanganatzahl gut ausgedrückt werden kann [31].

Zum Vergleich bestimmte ich den $KMnO_4$-Verbrauch einiger organischer Verbindungen. Die erhaltenen Ergebnisse sind in Tab. VIII zusammengefaßt.

Die Sulfitablauge und besonders ihre Zuckerkomponenten zeigen in dieser Zusammenstellung verhältnismäßig hohe Werte, die nur von einigen Verbindungen mit phenolischen Hydroxylgruppen übertroffen werden.

Der Sauerstoffbedarf der normalen Fichten-Sulfitablauge ist erheblich größer als der Sauerstoffbedarf der Hochausbeute-Pappel-Sulfitablauge. Nach der Verhefung nahm der Sauerstoffbedarf beider Sulfitablaugen ab, jedoch nicht in gleichem Maße. Die Abnahme war bei der Pappel-Sulfitablauge größer. Der Zusammenhang zwischen dem Gehalt an reduzierenden Stoffen und der $KMnO_4$-Zahl bei verhefter Sulfitablauge ist auf Abb. 6 veranschaulicht.

Tabelle VIII

$KMnO_4$-Verbrauch von 1 g verschiedener organischer Stoffe

(Bezogen auf die Trockensubstanz)

Stoff	$KMnO_4$— Verbr. g	Stoff	$KMnO_4$ Verbr. g
Resorcin	20,54	Fichten-Sulfitabl.	4,70
Pyrocatechin	18,36	Pappel-Sulfitabl.	3,60
Carbolsäure	9,85	Gallussäure	3,50
D-Glucose	6,15	Gelatine	2,23
DL-Xylose	6,04	Milchsäure	0,97
D-Galactose	5,77	Äthylenglykol	0,47
L-Arabinose	5,66	Carbamid	0,008
Tannin	5,37	Essigsäure	0,005

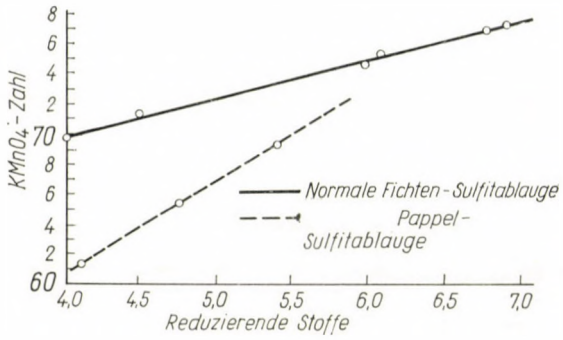

Abb. 6

Aus den Versuchsergebnissen konnte festgestellt werden, daß die Hochausbeute-Pappel-Sulfitablauge sowohl in ihrer ursprünglichen, als auch in der verheften Form eine geringere Gefahr führ die Lebewesen in den Flüssen bedeutet, als die Fichten-Sulfitablauge.

6. Gestaltung des Zuckergehaltes (der Menge der Monosaccharide)

Für die papierchromatographisch bestimmten Monosaccharide [32, 33, 34, 35, 36] ergab sich die folgende mengenmäßig abnehmende Reihenfolge:

Normale Fichten-Sulfitablauge: D-Mannose, D-Glucose, D-Xylose, D-Galactose und L-Arabinose.

Hochausbeute-Pappel-Sulfitablauge: D-Xylose, D-Galactose, L-Arabinose und D-Glucose.

Abb. 7 zeigt das Chromatogramm der Fichten-Sulfitablauge im ursprünglichen Zustand sowie nach Verhefung und Alkoholgärung.

Abb. 8 zeigt die Chromatogramme eines Fichten-Pappel-Gemisches im ursprünglichen bzw. im verheften Zustand.

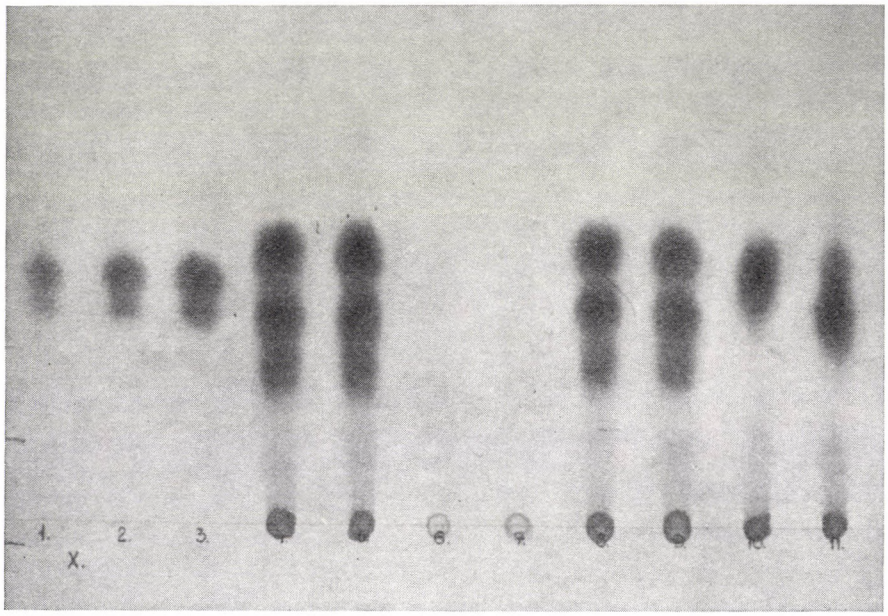

Abb. 7

7. Untersuchung der weiteren Verwendbarkeit der verheften Sulfitablauge

Diese Versuchsserie hatte das Ziel, festzustellen, inwieweit die von Kohlehydraten befreite Sulfitablauge als Komponente von Gerb- sowie Kleb- und Plastifiziermitteln verwendet werden kann [37, 38].

7.1 *Gerbmittel.* Vom Gesichtspunkte der Gerbwirkung ist der Ligninsulfonsäuregehalt der Sulfitablaugen die wirksame Komponente, während die übrigen Anteile nur Ballaststoffe bedeuten. Da jedoch die Ligninsulfonsäure allein als Gerbmittel nicht angewandt werden kann, wird ihre Gerbfähigkeit mit aromatischen Polykondensaten verbessert. In Ungarn wird die Ligninsulfonsäure hauptsächlich zur Herstellung von zwei Gerbhilfsmitteln angewandt und zwar des Lignotan und des Syntanol extra OP. Chemisch ist das Lignotan ein mit Al^{3+} gebildetes gemeinsames Salz eines Naphthalin-

sulfonsäure-Formaldehyd-Kondensats und der Ligninsulfonsäure, während das Syntanol extra OP ein Kondensat von Diphenolnovolak mit Ligninsulfonsäure ist [29]. Die Strukturformeln dieser beiden Verbindungen sind auf Abb. 9 gezeigt.

Zur Herstellung der oben erwähnten beiden Gerbmittel versuchte ich die Anwendung von eingedickter Sulfitablauge unter vollkommen gleichen

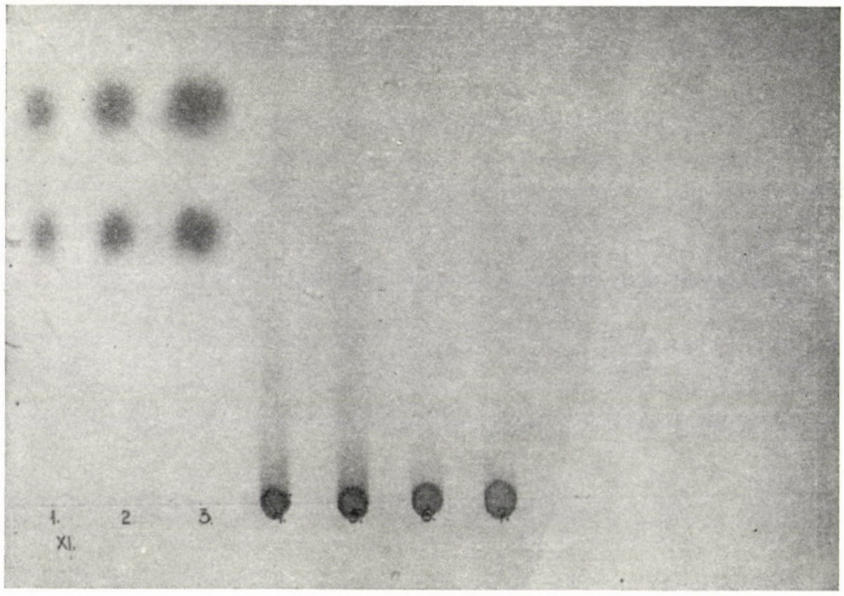

Abb. 8

Versuchsbedingungen parallel, vor und nach der Verhefung. Die vom Gesichtspunkte des Gerbeffektes wichtigen Angaben der erhaltenen beiden Gerbmittel sind in Tab. IX gezeigt.

Die Daten der Tabelle beweisen, daß das mit kohlehydratfreier, d. h. also verhefter Sulfitablauge hergestellte Syntanen die vorteilhafteren Eigenschaften besitzt. Es verfügt über ein besseres Gerbsäureverhältnis und einen niedrigeren CaO-Gehalt. Nur der Aschegehalt war — der ursprünglichen Sulfitablauge gegenüber — weniger günstig.

7.2 *Binde-(Klebe-)mittel.* Es mußte entschieden werden, ob die ursprüngliche oder verhefte Sulfitablauge die bessere Adhäsion besitzt. Die Untersuchung hatte gleichzeitig auch die Feststellung dessen zum Ziel, ob die Adhäsion auf den Zuckergehalt [39] oder auf die Ligninsulfonsäuren von verschiedenen Polymerisationsgraden zurückzuführen ist. Die mit dem Schopperschen Apparat auf faseriger Oberfläche gemessene Adhäsion der beiden verschiedenen Sulfitablaugen zeigt Tabelle X.

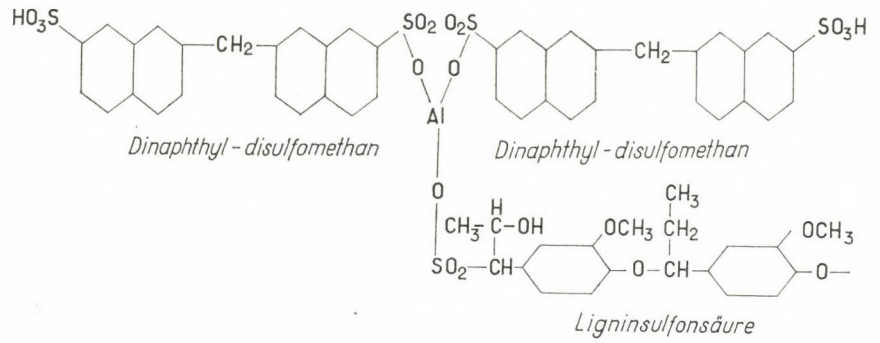

LIGNOTAN

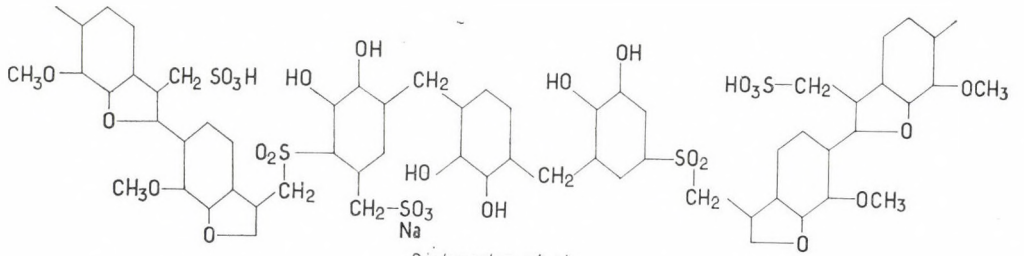

SYNTANOL extra OP

Abb. 9

Tabelle IX

Untersuchungsergebnisse der synthetischen Gerbstoffe Lignotan und Syntanol extra OP, hergestellt mit Sulfitablauge vor und nach der Verhefung

Untersuchte Werte	Lignotan		Syntanol extra OP	
	hergestellt mit Sulfitablauge			
	ursprüngl.	verheft	ursprüngl.	verheft
Lösliche Anteile %	58,5	58,7	50,3	50,1
Unlösliche Anteile %	0	0	0	0
Nicht gerbende Stoffe %	23,5	22,5	18,6	18,0
Gerbsäure %	35,0	36,2	31,7	32,1
Qualitäts(Anteil) Zahl	59,8	61,7	63,0	64,1
pH-Wert	3,2	3,2	3,4	3,4
Aschegehalt %	3,1	3,7	6,2	7,4
CaO-Gehalt %	1,9	1,4	0,82	0,69

Tabelle X

Untersuchung der Adhäsion der ursprünglichen und verheften, eingedickten Sulfitablauge

Trockensubstanzgehalt der zum Kleben verwendeten Sulfitablauge	Ursprüngliche eingedickte Sulfitablauge	Verhefte eingedickte Sulfitablauge
	Haftfestigkeit g/10 mm	
0,75 g/dm²	0	0
1,50 „	25	10
3,00 „	87,5	78
6,00 „	645	125
12,00 „	460	118
18,00 „	250	113

Auf Grund der Ergebnisse der Untersuchungen konnte festgestellt werden, daß die adhäsive Eigenschaft in erster Linie auf den Zuckergehalt zurückzuführen ist, da sie bei der durch Verhefung entzuckerten Sulfitablauge in bedeutendem Maße abnimmt.

7.3 *Plastifizierwirkung.* Die Versuche hatten das Ziel, die Plastifizierwirkung der ursprünglichen und durch Verhefung entzuckerten Sulfitablauge festzustellen. Die Ergebnisse der Untersuchung des unter Zugabe von 0,4% des Konzentrats hergestellten Betons sind in Tab. XI zusammengefaßt.

Aus den Daten dieser Tabelle geht eindeutig hervor, daß mit dem verhefteten Konzentrat eine bessere Plastifizierwirkung erzielt werden kann, als mit dem zuckerhaltigen [40].

Abschließend kann festgestellt werden, daß der Zuckergehalt der in Ungarn anfallenden Sulfitablaugen durch Verhefung — bei Anwendung entsprechender Heferassen — sehr gut verwertet werden kann. Die mikrobiologische Verwertung verursacht in der chemischen Zusammensetzung und in

Tabelle XI

Untersuchung der festigkeitssteigernden und plastifizierenden Wirkung von Sulfitablauge vor und nach der Verhefung

Plastifikator	Verdünnungswasser, Liter	Druckfestigkeit nach 28 Tagen kg/cm²	Plastifizierwirkung %	Festigkeitssteigerung %
—	7,5	253	—	—
Ursprüngliche eingedickte Sulfitablauge	6,5	315	13,3	24,5
Verhefte eingedickte Sulfitablauge	6,5	425	13,3	68,0

den physikalischen Eigenschaften der Sulfitablauge eine bedeutende Änderung. Diese Änderung ist bei den normalen Fichten-Sulfitablaugen und den Hochausbeute-Pappel-Sulfitablaugen nicht immer die gleiche. Es wurde auch festgestellt, daß das durch Verhefung entzuckerte Produkt zur Herstellung des synthetischen Gerbstoffes vorteilhafter angewandt werden kann, ebenso auch als Plastifikator, jedoch eine verminderte Adhäsion aufweist.

ZUSAMMENFASSUNG

Es wurde die Verhefbarkeit der Pentosen und Hexosen der normalen Fichten- und Hochausbeute-Pappel-Sulfitablaugen ungarischer Herkunft untersucht. Die Änderungen der Viskosität, des Brechungsindexes, der Dichte, des Sulfitgehaltes, der Aziditätsverhältnisse, des Ligninsulfonsäuregehaltes, des Sauerstoffbedarfes und des Monosaccharidgehaltes nach der Verhefung wurden festgestellt. Die Möglichkeiten der Weiterverarbeitung der entzuckerten Sulfitablauge wurden untersucht.

LITERATUR

1. Inskeep, H., Gordon, C., Wiley A.: Tappi **34,** No 10., 20 (1951).
2. Tóth, B., Sárkány, I.: Szeszipar **11,** 64 (1963).
3. Vogel, H.: Sulfitzellstoff-Ablaugen, Wepf et Co., Basel, 1948.
4. Wise, L.: Wood chemistry, Reinhold, New York, 1952.
5. Forss, K.: The Composition of spent spruce sulfite liquor, Tryckeri et Tidnings, Borga, 1961.
6. Lengyel, P.: Papíripar **3,** 17 (1962).
7. Nikitin, N.: Chimija drevessinü, Isdatelstwo Akademii Nauk, Moskwa—Leningrad, 1951.
8. West, C.: Nature of chemical component of wood, Techn. Assoc., Pulp Paper Ind. No 6. 1948.
9. Görög, J.: Kandidaturarbeit, Budapest, 1961.
10. Pelc, A.: Az élesztők élettana. Mérnöktovábbképző Int., No 2880, 1954.
11. Winter, R.: Wochenblatt für Papierfabrikation. **86,** 949 (1948).
12. Pelc, A.: Levegő jelentősége az élesztőgyártásban. Mérnöktovábbképző Int. No 2932, 1954.
13. Telegdy Kovács, L.—Holló, J.: Élelmezési iparok I. Budapest, Tankönyvkiadó, 1957.
14. Stich, E.: Beiträge zur Technik der Hefeerzeugung, Berlin, Springer Verlag, 1940.
15. Görög, J.: Mezőgazdasági kémia, Budapest, Jegyzetellátó V., 1957.
16. Kretschmar, G.: Zellstoff und Papier, **4,** No 2., 35 (1955).
17. Pelc, A., Szép, I.-né: Erjedésipari Kutató Intézet Évkönyve, 1959., p. 31,
18. Pelc, A., Simek, F.: Erjedésipari Kutató Intézet Évkönyve (Jahrbuch des Forschungsinstituts für die Gärungsindustrie), p. 44, 1951—52.
19. Winter, R.: Chem. Techn. **8,** No. 3., 145 (1956).
20. Vas, K.: Mezőgazdasági Ipar, **3,** No. 9., 19, (1949).
21. Buewszkoi, A., Sapotnitzki, Sz.: Szvoistwo lignosulfonwooi kisloty i jeje szolei. Szbornyik Trudov Tom IV. 35, Goszleszbumizdat, 1952.
22. Gierer, I.: Holz als Roh- und Werkstoff, B. 16. **7,** 251 (1958)
23. Sapotnitzki, A., Moskalewa, A.: Swoistwo sacharobisulfitnüch Soedineni, Goslesbumisdat, Moskwa—Leningrad, 1956.
24. Vas, K.: Magy. Kém. Lapja, **7,** 280 (1952).
25. Borisek, R.: Papír a Cellulosa **5,** No. 9., 113,
26. Vas, K.: Élelmezési ipar, **5,** 345 (1951).
27. Kjurschner, K.: Shurnal Prikladnoi Chimii, **6,** 629 (1955).
28. Stather, F., Reich, G.: Das Leder **10,** No. 1. 1 (1959).
29. Tóth, B.: Kolorisztikai Értesítő **3,** No. 5. 249 (1961).
30. Meinck, F.: Das Papier **9,** No. 13, 372 (1955).
31. Rogger, P.: Tappi **32,** No. 11, 481 (1949).
32. V. Vigyázó, L.: Papírkromatográfia és alkalmazása az erjesztőiparban (Die Papierchromatographie und ihre Anwendung in der Gärungsindustrie). Mérnöktovábbképző Int. 1954.

33. YAYME, G.: Quantitative papierchromatographische Zuckerbestimmung, I. Eucepa-Symposium **27,** 303 (1958).
34. HAJDUCZKY, G.: Doktorarbeit. Budapest, 1962.
35. SHAW, A.: Pulp and Paper Magazine of Canada, **58,** 170 (1957).
36. GAD, C., FÜRSTENAU, E.: Das Papier **7,** No. 7., 127 (1953).
37. TÓTH, B.: Magy. Kém. Lapja, **17,** 540 (1962).
38. MIHALIC, G., RADEJ, Z., KRIZANOVA, M.: Papír a Cellulose **16,** 15 (1961).
39. WILEY, A., WITHMORE, L., BROGGS, A.: Tappi, **42,** 5 (1949).
40. Ung. Pat. No. 149717.

Investigation of Changes Occurring During the Yeast Fermentation of Waste Sulfite Liquors

B. TÓTH

Summary. The yeastifying ability of the C_5 and C_6 sugars in Hungarian waste sulfite liquors originating from normal pines and high-yield polar poplar was investigated. The changes in density, viscosity, refraction index, sulfite content, acidity, oxygen demand, ligninsulfanic acid and monosaccharide contents were studied in the yeast-fermented sulfite liquor. Possibilities for further processing of the sulfite liquor free from carbohydrates were examined.

Исследование изменений, наступающих в ходе дрожжевания использованных сульфитных щелочей

Б. ТОТ

Резюме. Изучалась возможность дрожжевания 5 и 6 С-атомных сахаров сульфитной щелочи, происходящей из отечественной нормальной сосны и высокопродуктивного тополя. Далее, исследовались изменения плотности, вязкости, показателя преломления, условий кислотности и потребности в кислороде сульфитной щелочи после дрожжевания, а также, изменение содержания в ней сульфита, количества лигнинсульфоновой кислоты и содержание моносахаридов. Наконец, изучалась возможность дальнейшей переработки сульфитной щелочи, освобожденной от углеводов.

Dr. Béla TÓTH, Budapest XXI., Csepel, Zsák Hugó u. 22.

E. JUCKER: *Fortschritte der Arzneimittelforschung* Bd. 8. Birkhäuser Verlag, Basel und Stuttgart, 1965. 530 Seiten

Die von E. JUCKER herausgegebenen Fortschritte der Arzneimittelforschung erwarben sich in kurzer Zeit großes internationales Ansehen und ungeteilte Anerkennung. Dank ihrer ausgezeichneten Beiträge, wurde diese Serie zu einem unentbehrlichen Handbuch der sich in der Arzneimittelforschung Betätigenden. Der jetzt erschienene Band 8 steigerte noch den Wert dieser Serie. In diesem Band werden dem Leser 6 selbständige Abschnitte über die neueren Fortschritte in der Arzneimittelforschung geboten.

G. WOOLFE schrieb über die Chemotherapie der Amöbiasis einen zusammenfassenden Artikel von etwa 40 Seiten Umfang. Er behandelt kurz die Untersuchungsmethodik, und die mit Emetin und verwandten Derivaten, sowie die mit Verbindungen von antibiotischer Wirkung erzielten Resultate. Verständlicherweise vermittelt die Arbeit am eingehendsten die mit verschiedenen synthetischen Arzenimitteln, mit *Biallylamicol*, *Entobex*, *Mantomid*, *Diloxanid* und *Mebinol* erhaltenen Laboratoriumsergebnisse und klinischen Erfolge. Ein besonderer Verdienst dieses Abschnittes ist, daß die im Laboratorium und an der Klinik erzielten Resultate in strenger Einheit behandelt werden, so daß die Arbeit tatsächlich über die auf diesem Gebiet erzielten Fortschritte eine ausgezeichnete Auskunft gibt. Die Literaturangaben beschränken sich auch fast ausschließlich auf die in den letzten Jahren erschienene Literatur.

Eines der längsten Abschnitte des Bandes ist der Beitrag eines ungarischen Autors: L. DÉCSI berichtet auf etwa 140 Seiten über die Biochemie der auf das zentrale Nervensystem wirkenden Arzneimitteln. Die Bedeutung der chemischen Transmittelstoffe und ihre Biochemie werden behandelt, sodann in separaten Kapiteln die biochemische Wirkung der das zentrale Nervensystem reizenden und dämpfenden Verbindungen diskutiert. Dieser Abschnitt ist auch in Weltmaßstab eine der besten Zusammenfassungen dieses Themakreises, wobei 1841 Literaturzitate aufgearbeitet wurden.

H. UEHLKE befaßt sich in einer Arbeit von etwa 70 Seiten Umfang mit der biologischen Oxidation von aromatischen Amino- und Nitroverbindungen und ihrer Umwandlung im Organismus. Die Arbeit ist besonders vom Gesichtspunkt der theoretischen Pharmakologie von Bedeutung.

S. ARCHER und L. S. HARRIS befassen sich in ihrer Arbeit von etwa 50 Seiten Umfang mit den Antagonisten der Narkotika. Sie berichten unter hohen chemischen Anforderungen über Resultate auf dem Gebiet der Chemie des Morphins und Morphinans, ferner der Verbindungen mit Benzomorphanstruktur, über die Pharmakologie dieser Verbindungen und über die klinischen Eigenschaften des sich unter diesen Arzneimitteln in der Praxis am besten bewährten Nalorphins, Levallorphans und Benzomorphans. Die ausgezeichnete Arbeit bringt 220 Literaturanführungen.

Die sich auf über 100 Seiten erstreckende und 404 Literaturangaben enthaltende Arbeit von M. W. WHITEHOUSE beschäftigt sich mit wohl einem der wichtigsten Kapiteln der gegenwärtigen Arzneimittelforschung, mit den biochemischen und pharmakologischen Eigenschaften der entzündungshemmenden Arzneimitteln. Die Arbeit gibt eine ausgezeichnete Zusammenfassung der sich am besten bewährten Untersuchungsmethoden, der biochemischen Eigenschaften der entzündungshemmenden Pharmaka und behandelt die Eigenschaften und die Zusammenhänge zwischen Wirkung und Struktur der verschiedenen Antiphlogistica (Phenolderivate, Pyrazolonderivate, Steroide usw.). Lobenswert ist die Bestrebung des Autors, eine einheitliche Betrachtung über die Biologie der Entzündung und die Pharmakologie der Antiphlogistika zu geben bzw. die Zusammenhänge zwischen diesen beiden großen Gebieten zu klären.

Der letzte, etwa 70 Seiten betragende Abschnitt des Buches ist von J. A. MONTGOMERY abgefaßt und beschäftigt sich mit der Chemotherapie des Krebses. Für einen jeden wird es

offensichtlich sein, wie schwierig es ist, über dieses Problem eine kurze, jedoch übersichtliche Monographie zu schreiben, in der die erzielten Resultate gegen unzählige, auf diesem Gebiet durchgeführte Versuche abgeschätzt werden. Diese Aufgabe wurde vom Autor sehr erfolgreich gelöst, und es kann ruhig behauptet werden, daß die Arbeit eine in ausgezeichneter moderner Auffassung geschriebene Zusammenfassung dieser komplexen Frage darstellt. Natürlich kommt bei solchen Umfang eine detaillierte Diskussion nicht in Frage, vielmehr kann von einem proportionierten und gut gegliederten Bild gesprochen werden. Die Arbeit enthält 496 Literaturangaben.

Der Band wird durch ein Inhaltsverzeichnis ergänzt, das detaillierter als jeden der vorangehenden Bände ist. Außerdem wird auch über den Inhalt der vorangehenden Bände eine tabellarische Übersicht gegeben. Unter den 6 Abschnitten sind 5 in englischer Sprache abgefaßt, eine in deutscher Sprache. Ausführung, Druck und Abbildungen des Buches kommen jeder Anforderung nach.

K. NÁDOR

CHR. KLIXBÜLL JØRGENSEN: *Inorganic Complexes*

Academic Press, London and New York, 1963. 220 pp. Price: 42 sh

In the last two decades our knowledge on inorganic complexes has been enlarged extraordinarily. Thousands of important papers have been published in this field, and a critical survey evidently presents an enormous task. CHR. K. JØRGENSEN, after writing two books on the theoretical problems of coordination chemistry, undertook to write a concise account on the experimental facts of the field. The material of the book, arranged in ten chapters,where the basis of classification is the concept of inorganic chromophores, gives a vast amount of information. The bibliography amounts to 29 pages and contains 1176 references.

The greatest shortcoming of the book is the almost complete neglect of reaction kinetical results. Nowadays the reaction kinetical study of inorganic reactions gives so much profound information on the chemistry of complexes that disregarding them considerably lessens the value of such a general treatment. The structure of the book is a bit unbalanced. Such trivialities as the problems of nomenclature and preparation of ethylenediamine are thoroughly discussed, complexes very dear to the author are extensively described, while important classes of compounds — such as oxygen-containing complexes — are only superficially mentioned if at all. There are a number of erroneous statements. E. g., on p. 49 it is said that a halide already attached to another metalloid element does not seem to form complexes, whereas ANDREWS and KEEFER discovered such an effect in 1951. Sometimes conclusions concerning the composition of a species in solution from that in solid state do not seem to be quite correct. From the fact that aluminium chloride crystallizes from an aqueous solution as $[Al(H_2O)_6]Cl_3$, it does not follow that only hexaaquo ions exist in solution. The role of lattice energy also has to be considered.

It is an interesting and helpful feature of the book that the author makes many predictions; one of them, namely the formation of adducts between XeF_4 and fluorides of non-metals has already been proved.

The advantageous features overcompensate the shortcomings, and the book is warmly recommended to every critically minded reader interested in inorganic chemistry.

M. T. BECK

ELIEL, E. L., ALLINGER, N. L., ANGYAL, S. J. and MORISSON, G. A.: *Conformational Analysis*

Interscience Publishers, New York, London, Sidney. 1965. p. XIII + 524.

Conformational analysis is one of the most important chapters of modern organic chemistry. The explosion-like development and spreading of this branch of chemistry is known to be initiated some fifteen years ago by a fundamental treatise of D. H. R. BARTON. Since then, conformational analysis has become an indispensable tool in many fields of organic chemical research. Beginning with the chemistry of acyclic compounds and simple cyclohexane

derivatives, continued with the chemistry of the more complicated carbo- and heterocyclic compounds, steroids, triterpenoids, alkaloids and carbohydrates, recently including protein chemistry, conformational analysis flooded into and stimulated the most various fields of organic chemical research. Consequently, though several excellent reviews have been published in this domain, writing of a monograph on conformational analysis was very timely. The present book was written by a team of four authors of undisputable reputation; all of them are well-known scientists who have made important contributions to the various fields of application of conformational analysis, and to stereochemistry, in general.

The book fully comes up to the expectations based on the personal qualifications of the authors. The reader is guided systematically and with crystal-clear logic from the simplest to the most complex problems. Care is taken throughout to use accurate definitions and precise nomenclature, and occasional unsolved problems are pointed out with proper criticism. In this way, the attention of chemists who may newly take up research in this field is directed immediately in the right direction.

In this respect, the reviewer has only remark as criticism; in the subchapter 2—2c, the WINSTEIN-HOLNESS kinetic method for the determination of conformational equilibria is discussed in detail. This method, as it is known, has been subjected to severe criticism, particularly by professor W. HÜCKEL. Though the authors mention this criticism, the problem is not discussed further. However, if the authors do not agree with the objections (and in the opinion of the reviewer they do not), the lack of their remarks on the criticism is regrettable.

In addition to a short preface and introduction, the work consists of seven chapters. In the first chapter (35 pages) the confirmation of acyclic molecules, while in the second chapter (91 pages) the fundamental principles of conformational analysis are discussed, cyclohexane and its substituted derivatives serving as examples. Some characteristic subtitles in this chapter are as follows: chair and flexible forms, chemical equilibria, conformation and reactivity, cyclohexane derivatives containing a trigonal carbon atom, deformation of cyclohexane rings.

Physical methods of conformational analysis are summarized in 60 pages of the third chapter. Some subtitles of this chapter are: X-ray and electron diffraction, thermodynamical methods, spectroscopical methods, dipole moments, rotatory power, Kerr constants, acoustical methods, mass spectra and kinetical methods. It may be seen from this list that the material discussed in the book is quite up-to-date.

Chapter 4 (67 pages) deals with the extension of conformational analysis from the cyclohexane ring to other, relatively simple systems, such as cyclopentane, small, medium-sized, and large-rings, condensed skeletons, and heterocycles. Chapter 5 (95 pages) is actually the continuation of Chapter 4 in which the principles and correlations discussed so far are applied to particular groups of compounds of prominent significance, *e. g.* steroids, triterpenoids and alkaloids.

Chapter 6 (82 pages) is similarly devoted to a special domain, the conformational analysis of carbohydrates. In view of the fact that yclitols are also polyhydroxy compounds, their discussion is included in this chapter. One of the authors has gained distinction as an outstanding worker in the field of conformational analysis of these compounds.

Though the conformational analysis of carbohydrates has so far been restricted mainly to qualitative statements, it has led to significant results; the authors attempt now to approach the problem also from a quantitative point of view. As the writers of the book themselves confess, this approach naturally could not be made without using much more speculative considerations than in the preceding chapters. Still, this endeavour of the authors is to be appreciated as a significant pioneering work.

The last chapter (52 pages) presents data and problems which, for some reasons, were not treated by the authors in the preceding chapters, *e. g.*, the problem of boat conformations or the *a priori* calculation of comformational energies. Of the contents of this chapter, the table of comformational energies deserves special mentioning which summarizes the literature data concerning the substituents of the cyclohexane ring.

The volume is concluded with the conventional indexes.

The layout and printing of the book are agreeable, the figures are good and instructive. However, in Fig. 6 (p. 201) in the semi-chair form of cyclopentane the directions of the exocyclic valences of the carbon atoms are missing.

Summarily, the reviewed book is an excellent work. Its study will certainly be useful not only to experts in stereochemistry, but also to the majority of organic chemists.

K. LEMPERT

K. ABRESCH and I. CLAASSEN: *Coulometric Analysis*
Translated by L. L. LEVESON
Chapman and Hall, London, 1965. 275 pp. 66 figures and 3 tables. Price 36 shillings net

Coulometric analysis is one of the most important methods of modern analytical chemistry. It has not only been used reliably in all fields of volumetric analysis, but there are problems which are easier to solve by the coulometric method than by the classical one. Moreover it makes possible to discover new fields by way of investigating primary and secondary anodic and cathodic processes. Owing to the possibility of measuring coulombs with high accuracy, the method is applicable not only for determinations on the submicro scale, but also for reaction kinetic measurements and for the kinetic investigation of chemical processes.

This monograph was first published in German by *Verlag Chemie* in 1961. It is the first book to deal specifically with the subject, intended also as an introduction to the theory and practice of potentiostatic coulometry and constant current coulometry (coulometric titration).

The book is divided into two parts. Part I deals with the theory, apparatus and instrumentation, Part II with the analytical applications of coulometric analysis. In Part I the authors summarize the fundamentals of electrochemistry, and discuss the principles of coulometry.

They deal with the coulometry (a) at controlled constant potential, (b) at uncontrolled potential and constant current, (c) at constant potential and constant current and (d) at continuously varying potential.

After an interpretation of current efficiency, the authors deal with end-point detection of various kinds. The conditions of colorimetric, spectrophotometric and electrometric (potentiometric, amperometric) end-point detection methods are discussed. The theoretical discussion of the coulometric method is completed by the interpretation of current-voltage curves.

The following Chapters describe the apparatus for electrolysis. Electrodes, diaphragams and electrolysis cells used for various measurements, and coulometers of various types are listed. In a separate chapter the control of potential (potentiostat) is discussed and examples are given ranging from simple potentiostats to the most complicated electronic controlled-potential coulometric titrators.

The ease with which the generation circuit can be controlled at any magnitude of current makes possible automatic coulometric titrations. Such titrations may be performed using a combination of an automatic titrator and a coulometer. Descriptions of automatic titrators based on various principles, continuous titrators, and the conditions suitable for electrometric automatic end-point detection are also presented. Part I of the book is completed by a short description of pulse coulometry.

Part II is introduced by a theoretical treatment of direct and indirect methods of potentiostatic coulometry. In a comprehensive table the conditions of the potentiostatic-coulometric determination of various inorganic and organic substances are summarized.

Volumetric methods are the most important among coulometric determinations. Numerous examples illustrate the procedures which have been introduced in the field of acid-base, redox, precipitation and complexometric titrations. The survey of volumetric determinations is considerable facilitated by a comprehensive table of 40 pages, at the end of the chapter.

The final chapter of the book summarizes other analytical applications of coulometry, such as determination of film thickness, voltammetry (anodic dissolution with continuously changing potential, chronopotentiometry), determination of polarographic n-values, internal electrolysis, determination of oxygen and of water, reaction kinetics and other methods. Experimental details, range, accuracy and references are given for each entry. Over 500 references complete this very remarkable work.

In general, the book is an excellent example of a monograph in which theoretical and practical problems of coulometric analysis are presented to the reader. It will for certain considerably promote the development of this very interesting and excellent method.

I. BUZÁS

Radiation Chemistry. Proceedings of the Tihany Symposium, Ed. by J. Dobó. Akadémiai Kiadó. (Publishing House of the Hungarian Academy of Sciences.) Budapest, 1964. 482 pp.

The book presents in English the text of fifty lectures and discussions of the Tihany Symposium (Hungary) organized in September 1962. The list of authors participating in the Symposium comprises eminent experts in radiation chemistry, such as Swallow, Charlesby and Chapiro, who contributed by fundamental monographs to the systematization of the achievements of this young branch of sciences, excellent representatives of world-known Soviet and French schools, such as Voevodsky, Bach and Haissinsky. A great number of papers were submitted by younger scientists of the German Democratic and Federal Republics, Czechoslovakia, Rumania and Poland as well. Consequently, the Symposium was capable of presenting a wide survey of the trends of development in radiation chemistry and of the up-to-date methods of investigation.

In addition to the international character of the Symposium, a notable feature of the book is that the first report is given here on the researches into radiation chemistry started in Hungary only a few years ago.

The material pertaining to nearly all fields of radiation chemistry is divided into four parts in the book.

The first part contains papers dealing with the radiation chemistry of organic compounds. In summarizing lectures a review is given on the researches carried out in two important scientific institutions of the United Kingdom, *Imperial College* and *Wantage Research Laboratory*. A number of other papers deal with problems of radiation chemistry of interest from the aspect of applications in organic chemical industry. Such as radiation-induced chlorination, oxidation and sulfoxidation of hydrocarbons, the radiation-stability of certain types of hydrocarbons and of their haloid derivatives, and the radiation chemistry of acetonic solutions. The lectures discussing the ionic mechanism of radiation-chemical reactions of unsaturated hydrocarbons and the theory of the radiolysis of solid compounds based on free radical investigations are a prominent merit of the book.

The greatest number of lectures are contained by the second part devoted to polymeric systems. Some of these papers deal with radiation-induced co-polymerizations, such as the graft polymerization of styrene on polytetrafluoroethylene *(Teflon)*, of various monomers on polypropylene, of vinylpyridine on polyvinyl chloride fibres, and with the co-polymerization of acrylamide and methacrylamide. The problem of vulcanisation of rubber by radiation is discussed in several papers. Many new results are presented in the papers reporting the achievements of theoretical and experimental investigations of low-temperature polymerization processes in the solid phase. In addition to the papers mentioned above, interesting studies deal with the kinetics of radiation-induced polymerization and with the comparison of the effects of α-rays, γ-rays and ultraviolet radiation on polyethylene.

The third part embraces lectures in an already almost classical field, the radiation chemistry of aqueous solutions. Topics discussed by papers in this part comprise, among others, the processes which take place in concentrated and in alkaline aqueous solutions, the effect on electrode processes of products formed on irradiation, the radiolysis of the aqueous solutions of aliphatic amino acids and of some sulfur compounds, oxidation processes of chain-mechanism, and the after-effects of radiation chemistry. Some papers reporting direct observations made during irradiation, and presenting the results obtained by employing water-soluble free radicals are of outstanding interest from the point of view of experimental technique.

In the fourth part of the book, papers devoted to problems of dosimetry, and communications outside the fields discussed in the previous parts were compiled by the editor.

An outstanding advantage of the book is that the material of discussions, which frequently cleared up differences between the views of the various schools and which raised many new ideas and problems, is given immediately after each paper.

The excellent and extremely careful editorial work, together with the first-class printing are in line with the contents of this volume.

I. Kiss

E. PUNGOR: *Oscillometry and Conductometry*. Translated by T. DOMOKOS. Translation edited by A. TOWNSHEND
Pergamon Press, Oxford—London 1965. 239 pp., 122 figures and 28 tables.

Oscillometry, the "electrodeless" version of conductometry is one of the most modern methods of instrumental analysis. The principle of the method can be used not only to develop new volumetric methods, but also for the determination of liquids in closed systems, for chromatographic indication, furthermore for the measurement of dielectric constants of liquids.

This monograph first published in Hungarian in 1963, deals specifically with theoretical and practical aspects of conductometry and oscillometry. It gives a thorough survey of apparatuses and instruments used for measuring conductivity, high-frequency and dielectric constants.

The author has selected the most important and characteristic types of the great number of methods and instruments published in the field of high frequency and conductometry.

In the first part of the monograph Prof. PUNGOR explains the theoretical interpretation and the fundamentals of determination of conductivity, using many mathematical relations and diagrams.

Numerous figures illustrate the measuring cells and instruments of various kinds: simple and special high frequency capacitive and inductive measuring cells and cells for the determination of dielectric constant of liquids.

The constructions of many devices used for high frequency titrations and for the determination of dielectric constants are presented with circuit diagrams and block diagrams.

The conductivity of solutions can be used to determine the end-point of various titrations. In the second part of the book the author presents, on the basis of a most modern view, the theoretical interpretation of changes taking place during the titrations. Equations and relations are given for the construction of titration curves and for the calculation of end-points. Separate chapters deal with the titration of mono- and multivalent acids and bases, with displacement titrations, with acid-base titrations in non-aqueous media, finally with the titrations based on precipitation, complex formation and oxidation-reduction reactions.

The author presents to the practical chemists several examples showing the advantages of conductometry and oscillometry, and illustrates the accuracy of these methods in tables. Various titrations are described by way of practical examples and titration curves.

In the last part other applications of conductometry and oscillometry are summarized, such as applications to kinetic studies, to chromatographic analysis, in establishing phase diagrams, the direct determination of concentrations, and of water. Nearly 400 references complete this very remarkable work.

In general, the book is an excellent monograph in which the theoretical and practical problems of conductometry and oscillometry are very ingeniously represented to the reader. It may be well assumed that it will be of great interest for chemists working in modern analytical laboratories.

I. BUZÁS

I. N. BUTLER: *Ionic Equilibrium; A Mathematical Approach*
Addison-Wesley Publishing Co., 1964.

As stated in the preface by the author, this book is intended primarily as a handbook in the teaching of Analytical Chemistry, and accordingly, most of the concluded examples are relevant to analytical applications. In addition, the book will be useful as a source of examples and as reference material to chapters dealing with ionic equilibria in the teaching of General Chemistry and Physical Chemistry.

The treatment of the subject requires from its users basic knowledge in general chemistry and in mathematics. In its design, the book starts from fundamental principles, and proceeds step by step to a higher level, enabling the reader to study monographs and the research literature in this field of knowledge.

In this sense, the book may be considered a university text book. The more than 500 examples included are very helpful in accomplishing this aim. Some of the examples are fully worked out, while for others either the approach to a solution or the results are given.

Two chapters are devoted to acid-base, solubility, complex formation, and redox equilibria; two chapters treat mathematical methods used in the calculation of equilibria; one chapter deals with the measuring methods of equilibrium constants and corrections due to non-ideal behaviour.

At the end of each chapter, copious reference, involving papers and books up to 1963, is given. It should be emphasized that these references are not limited to bibliographic data, but include a short critical annotation on the cited work.

The above review implies also my full appreciation of the aims of the book, of the applied methods, and of the mode of treatment of the subject. However, two points may be commented:

1. In my estimation, the chapter dealing with the measuring methods of equilibrium constants is relatively short, as compared to the whole volume of the book, and I miss the description of modern methods, *e.g.*, that of radioactive tracer technique applicable for the solving of tasks of this type.

2. The author discusses corrections, due to non-ideal behaviour, in the last chapter of the book. I would have considered it more to purpose to treat this problem in the introductory chapter. Errors caused in certain cases by the neglect of corrections could have been pointed out with the aid of a few worked out examples. In the knowledge of the order of magnitude of these errors, corrections could have been deliberately omitted during the further discussion of the subject, or alternatively, attention could have been drawn to cases, where the neglecting of corrections is inadmissible.

Notwithstanding these remarks, I consider the book very useful and particularly suitable to accomplish the aims stated in the preface.

E. JUHÁSZ

J. L. KAVANAU: *Structure and function in biological membranes* Vol. I—II. Holden-Day Inc., San Francisco, 1965, pp. 760.

Professor KAVANAU's work is the first monographic discussion devoted entirely to the structure and function of biological membranes, and at the same time containing a detailed analysis of his own theories concerning certain aspects of the function of the membranes.

His theories which have been published in several preliminary papers since 1962 can be summed up as follows: the biological membranes are dynamic and highly labile structural elements which, while operating, are varying between various states, the two extreme cases of which are the open and closed configurations. In the open configuration the medium layer of the membrane would be composed of $80 \times 180 - 200$ Å cylindrical lipid micelles of a regular hexagonal arrangement, with water phase matrix between them. Both ends of the cylindrical micelles would be bound by relatively stable polar and non-polar bonds to the protein monolayers of 10—15 Å thickness bordering the membrane.

The closed configuration recalls in many respects the traditional pattern of biological membranes which, on the basis of the sketches outlined by DANIELLI and DAWSON (1935), has come to be known as "unit-membrane" (ROBERTSON, 1960) in recent years. In the "unit-membrane" a continuous bimolecular lipid layer, 50—60 Å thick, is sandwiched between the protein layers. The main difference between KAVANAU's closed membrane and the unit-membrane is that he suggests that the lipid layer is composed of sub-units. These disk-like units are supposed to be joined to one another more or less closely, with pores remaining between them, or to be merged with one another more or less intimately. The disks of the closed configuration would be formed from the pillar lipid micelles of the open membrane so that the matrix would be pumped out of the membrane. The transformation of the two membrane states would be induced by the replacement of monovalent and divalent cations. In KAVANAU's view this transformation may take place gradually and in a cyclical manner on the surface membranes of the cells and organelles, and by pumping the matrix out it could be responsible for protoplasmic streaming, the independent movements of the cell organelles, the streaming of the content of the organelles, and finally for amoeboid locomotion.

Professor KAVANAU's work, as he points out himself in the preface, consists of heterogenous chapters elaborated to varying extents. Chapter 3 entitled "On gross aspects of membrane transformations" discusses a part of the author's theory. It would have been advisable to concentrate this in Chapter 5 (The structure of biological membranes). Likewise, the author would have been better advised to remove the disproportionately lengthy section (extending to over 80 pages) on water structure from this Chapter, because it has nothing to do with

the subject discussed here. Perhaps it would have been better to begin the book with this section as an independent Chapter. This could have been followed by the present second (Micelle formation and transformations) and fourth Chapters (Properties of pure mixed monolayers and bilayers). These two Chapters are the most excellently elaborated parts of the book.

Volume II begins again with two highly problematic Chapters. Chapter 6 discusses on a total of two pages the factors inducing matrix movements, while Chapter 7 considers transformations between the open and closed configurations over a similarly short span of space. Chapter 11 also fails to come up to what is promised in its title (The effects of pressure and temperature on protoplasms). The most valuable parts of Volume II are Chapters 8—10 which review the various protoplasm and membrane movements.

One of the most important membrane functions, transport through the membrane, is discussed on slightly over 20 pages (Chapter 12). This Chapter also contains some pages on the conduction of electric impulse. In the reviewer's opinion, this part fails to reflect the present state of the problem of transport, nor does it make clear the extent to which the author's theories are compatible with the huge mass of data available about permeability and transport phenomena.

The last Chapter discusses some results of the electronmicroscopic studies of the membrane, with particular attention paid to preparations proving hexagonal sub-structures. The reviewer is not particularly familiar with electronmicroscopy, but he has the impression that these are rather evidence for the occurrence of a macromolecular membrane component than the author's miceilar membranes.

The book is supplied with a detailed index and a list of literature containing well over 2,000 references.

All in all, the reviewer wants to stress that a unified discussion of membrane structures and functions and the establishment of their molecular biological and bio-physico-chemical basis is imperative. This requirement could only be met by the author, obviously because of lack of data in the literature. The chapters discussing the physico-chemical basis of the biological membrane phenomena, such as micelle formation, mono- and bilayers, can be considered most useful. To read these chapters is very profitable for biologists even if a physico-chemist may regret the absence of a mathematical analysis. It seems desirable to complete the chapters on biology (for instance, Chapters 5 and 12). Similarly, the book should be completed by at least one chapter on the structure and operation of special organelle membranes (mitochondria, chloroplasts). Such an additional chapter would be all the more desirable since research in this area is most intensive, and the author's theoretical membrane model could be compared most favourably with physiological and biochemical data in this field.

Z. BÖSZÖRMÉNYI

P. CRABBÉ: *Optical Rotatory Dispersion and Circural Dichroism in Organic Chemistry*

Holden-Day, San-Francisco—London—Amsterdam, 1965, 378 pp.

Specialization is by necessity an inevitable consequence of the development of science and technology. Organic chemistry as a science is no exception to this rule. The organic chemist intensively occupied in scientific research is actually a specialist mainly in the methods of organic chemistry, whether he is concerned with synthesis, selective extraction, or structural research. However, he has to realize that his work increasingly demands the use also of other methods which offer indispensable help in his routine work. The significance of physical methods of investigation in the elucidation of the structure of organic molecules is great and constantly growing. An increasing number of books are being published, pointing out the practical aspects of physical methods based on complicated theoretical principles and applied to the everyday work of the organic chemist.

The book by PIERRE CRABBÉ, presenting the potential uses of optical rotatory dispersion and circular dichroism in solving the structural problems of organic chemistry, is sincerely welcome in this series. CRABBÉ's work does not go deeply into the discussion of theoretical fundamentals; the mode of presentation is rather practical, *i.e.* the book offers direct help in putting the method to independent use. A great many references are given at the end of each chapter, partly for readers who are interested in the theoretical background, and partly for those looking for analogies to concrete problems.

By studying the changes in rotatory power with the variation of the wavelength, *i.e.* by examining the rotatory dispersion, it is possible to establish the structural correlations of molecules to an extent much deeper than by determining the rotatory power at a given stable wavelength. For the measurement of rotatory dispersion a great number of commercial instruments are in use. Recently also devices suitable for the direct measurement of circular dichroism, the phenomenon responsible for the rotatory power, are available.

Today, the systematics of the correlations between structure and rotatory dispersion or circular dichroism have been developped to such an extent that this topic has afforded ample material to be chosen by CRABBÉ as the detailed subject of his monograph.

The book comprises the following chapters:

1. Optical activity.
2. Theoretical considerations.
3. Technical considerations.
4. Applications of optical rotatory dispersion and circular dichroism in structural problems.
5. Plain rotatory dispersion curves in stereochemistry.
6. Cotton-effect of carbonyl containing saturated compounds.
7. Vicinal effects in saturated ketones.
8. Inherently dissymmetric chromophores.
9. Unsaturated ketones.
10. Optically active dienes.
11. Asymmetrically perturbed symmetric chromophores other than ketones.
12. Polypeptides, proteins and nucleic acids.

The practical nature of the book is proved by the fact that the first three chapters occupy only 9% of the total volume. The way of presentation is characterized by the predominance of practical aspects, *e.g.*, though the definition of the octant rule is given and examples of its application are presented, the theoretical interpretation of the rule is omitted. As a valuable appendix, the automated programming of the data of circular dichroism is described. In the opinion of CRABBÉ, this is necessary because most of the spectrometers marketed for the time being are capable of automatic recording. However, for the evaluation of the data certain corrections are required, namely the values are to be converted into molar ellipticity. On the other hand, the values of rotatory power measured by planimetry and their changes with the variation of temperature may yield further structural informations of potential importance. Lastly, on subjecting the data to statistical analysis, the errors of measurements can be estimated, i.e., the presentation of data can be made more concrete.

It is hoped that, in addition to the above-discussed features, also the attractive appearance of the book will encourage organic chemists to confirm the results of their researches also by this up-to-date, useful, and productive method.

GY. VARSÁNYI

INDEX

PHYSIKALISCHE CHEMIE – PHYSICAL CHEMISTRY – ФИЗИЧЕСКАЯ ХИМИЯ

TÖRÖK, F. and HUN, B. GY.: On the Vibrational Spectrum of the Trimethylsilyl Group... 329

FODOR-CSÁNYI, P. and LÉVAY, B.: The Significance of Phosphorescence in the Measurement of Low Energy Beta Isotopes with Liquid Scintillator and Single-Channel Counter 343

GYARMATI, I.: Relations between the Integral Principle of Thermodynamics and the Hamilton Principle 367

KISS, I., JÁKLY, G. and ILLY, H.: Vapour Pressure of Solid D_2O 379

NÉMETH, A. and SZALAY, O.: New Method for the Quantitative Analysis of Combustion Processes with Toepler's Parallel Beam Schlieren Apparatus 385

ORGANISCHE CHEMIE – ORGANIC CHEMISTRY – ОРГАНИЧЕСКАЯ ХИМИЯ

LEMPERT, K. and ZAUER, K.: Hydantoins, Thiohydantoins and Glycocyamidines. XXIII Quaternization of 2,5-bis(methylthio)-4,4-diphenyl-4*H*-imidazole and the Reaction of the Quaternary Derivative with Nucleophilic Agents 391

DOLESCHALL, G., LÁNG, L. and LEMPERT, K.: Imidazoquinazolinediones, IV. Structure and Ultraviolet Spectra of Some Potentially Tautomeric Imidazoquinazolinediones and Related 4-Quinazolinones 405

LŐRINC, A., PÉTER, F. and DOBOZY, O.: Correlation between the Paper Chromatographic R_f and R_m-values and the Structure of Azo Dyes 419

CHEMISCHE TECHNOLOGIE – CHEMICAL TECHNOLOGY – ХИМИЧЕСКАЯ ТЕХНОЛОГИЯ

TÓTH, B.: Untersuchung der Veränderungen von Sulfitablaugen während der Verhefung 431

Buchesprechungen – Book Reviews – Рецензии книг 451

Printed in Hungary

A kiadásért felel az Akadémiai Kiadó igazgatója. Műszaki szerkesztő: Farkas Sándor

A kézirat nyomdába érkezett: 1966. I. 31. — Terjedelem: 11,75 (A/5) ív, 77 ábra (27 színes), 1 melléklet

66.61899 Akadémiai Nyomda, Budapest — Felelős vezető: Bernát György

The Acta Chimica publish papers on chemistry, in English, German, French and Russian.

The Acta Chimica appears in volumes consisting of four parts of varying size, 4 volumes being published a year.

Manuscripts should be addressed to

Acta Chimica
Budapest 502, Postafiók 32

Correspondence with the editors should be sent to the same address.

The rate of subscription is 110 forints a volume. Orders may be placed with "*Kultúra*" Foreign Trade Company for Books and Newspapers (Budapest I., Fő utca 32. Account No. 43-790-057-181) or with representatives abroad.

Les Acta Chimica paraissent en français, allemand, anglais et russe et publient des mémoires du domaine des sciences chimiques.

Les Acta Chimica sont publiés sous forme de fascicules. Quatre fascicules seront réunis en un volume (4 volumes par an).

On est prié d'envoyer les manuscrits destinés à la rédaction à l'adresse suivante:

Acta Chimica
Budapest 502, Postafiók 32

Toute correspondance doit être envoyée à cette même adresse.

Le prix de l'abonnement est de 110 forints par volume.

On peut s'abonner à l'Entreprise pour le Commerce Extérieur de Livres et Journaux «*Kultúra*» (Budapest I., Fő utca 32. Compte-courant No. 43-790-057-181) ou à l'étranger chez tous les représentants ou dépositaires.

«*Acta Chimica*» издают трактаты из области химической науки на русском, французском, английском и немецком языках.

«*Acta Chimica*» выходят отдельными выпусками разного объема. 4 выпуска составляют один том. 4 тома публикуются в год.

Предназначенные для публикации рукописи следует направлять по адресу:

Acta Chimica
Budapest 502, Postafiók 32

По этому же адресу направлять всякую корреспонденцию для редакции.

Подписная цена «*Acta Chimica*» — 110 форинтов за том. Заказы принимает предприятие по внешней торговле книг и газет «*Kultúra*» (Budapest I., Fő utca 32. Текущий счет № 43-790-057-181) или его заграничные представительства и уполномоченные.

36,— Ft

All the reviews of the Hungarian Academy of Sciences may be obtained among others from the following bookshops:

ALBANIA

Ndermarja Shtetnore e Botimeve
Tirana

AUSTRALIA

A. Keesing
Box 4886, GPO
Sidney

AUSTRIA

Globus Buchvertrieb
Salzgries 16
Wien I.

BELGIUM

Office International de Librairie
30, Avenue Marnix
Bruxelles 5
Du Monde Entier
5, Place St. Jean
Bruxelles

BULGARIA

Raznoiznos
1Tzar Assen
S fia

CANADA

Pannonia Books
2 Spadina Road
Toronto 4, Ont.

CHINA

Waiwen Shudian
Peking
P. O. B. Nr. 88.

CZECHOSLOVAKIA

Artia A. G.
Ve Smeckách 30
Praha II.
Postova Novinova Sluzba
Dovoz tisku
Vinohradska 46
Praha 2
Postova Novinova Sluzba
Dovoz tlace
Leningradska 14
Bratislava

DENMARK

Ejnar Munksgaard
Nörregade 6
Kopenhagen

FINLAND

Akateeminen Kirjakauppa
Keskuskatu 2
Helsinki

FRANCE

Office International de Documentation et Librairie
48, rue Gay Lussac
Paris 5

GERMAN DEMOCRATIC REPUBLIC

Deutscher Buch-Export und Import
Leninstraße 16.
Leipzig C. I.
Zeitungsvertriebsamt
Clara Zetkin Straße 62.
Berlin N. W.

GERMAN FEDERAL REPUBLIC

Kunst und Wissen
Erich Bieber
Postfach 46
7 Stuttgart S.

GREAT BRITAIN

Collet's' Subscription Dept.
44—45 Museum Street
London W. C. I.
Robert Maxwell and Co. Ltd.
Waynflete Bldg. The Plain
Oxford

HOLLAND

Swetz and Zeitlinger
Keizersgracht 471—487
Amsterdam C.
Martinus Nijhof
Lange Voorhout 9
The Hague

INDIA

Current Technical Literature
Co. Private Ltd.
Head Office:
India House OPP.
GPO Post Box 1374
Bombay I.

ITALY

Santo Vanasia
71 Via M. Macchi
Milano
Libreria Commissionaria Sansoni
Via La Marmora 45
Firenze

JAPAN

Nauka Ltd.
2 Kanada-Zimbocho 2-chome
Chiyoda-ku
Tokyo
Maruzen and Co. Ltd.
P. O. Box 605
Tokyo
Far Eastern Booksellers
Kanada P. O. Box 72
Tokyo

KOREA

Chulpanmul
Korejskoje Obshchestvo po Exportu i Importu Prozvedenij Pechati
Phenjan

NORWAY

Johan Grundt Tanum
Karl Johansgatan 43
Oslo

POLAND

Export und Import Unternehmen
RUCH
ul. Wilcza 46.
Warszawa

ROUMANIA

Cartimex
Str. Aristide Briand 14—18.
Bucuresti

SOVIET UNION

Mezhdunarodnaja Kniga
Moscow
G—200

SWEDEN

Almquist and Wiksell
Gamla Brogatan 26
Stockholm

USA

Stechert Hafner Inc.
31 East 10th Street
New York 3 N. Y.
Walter J. Johnson
111 Fifth Avenue
New York 3. N. Y.

VIETNAM

Xunhasaba
Service d'Export et d'Import des Livres et Périodiques
19, Tran Quoc Toan
Hanoi

YUGOSLAVIA

Forum
Vojvode Misica broj 1.
Novi Sad
Jugoslovenska Kniga
Terazije 27.
Beograd

5. V. 1966 Index: 26.007